DOKTORSAVHANDLINGAR
VID
CHALMERS TEKNISKA HÖGSKOLA
Nr 30

+ 10 bilagor

ON HYDRODYNAMIC LUBRICATION WITH SPECIAL REFERENCE TO CAVITATION IN BEARINGS

BY

LEIF FLOBERG

GÖTEBORG 1961

ON HYDRODYNAMIC LUBRICATION WITH SPECIAL REFERENCE TO CAVITATION IN BEARINGS

AV

LEIF FLOBERG

teknologie licentiat

AKADEMISK AVHANDLING

SOM MED TILLSTÅND AV CHALMERS TEKNISKA HÖGSKOLA FÖR TEKNOLOGIE DOKTORSGRADS VINNANDE TILL OFFENTLIG GRANSKNING FRAMLÄGGES Å FÖRELÄSNINGSSALEN FÖR FYSIK, GIBRALTARGATAN 5 B, GÖTEBORG, LÖRDAGEN DEN 13 MAJ 1961 KL. 10

GÖTEBORG
ELANDERS BOKTRYCKERI AKTIEBOLAG
1961

DOKTORSAVHANDLINGAR
VID
CHALMERS TEKNISKA HÖGSKOLA

ON HYDRODYNAMIC LUBRICATION WITH SPECIAL REFERENCE TO CAVITATION IN BEARINGS

by

LEIF FLOBERG

AKADEMIFÖRLAGET-GUMPERTS, *Göteborg*
GYLDENDALSKE BOGHANDEL/NORDISKA FORLAG, *København*
AKATEEMINEN KIRJAKAUPPA/AKADEMISKA
BOKHANDELN, *Helsingfors*
WILLIAM HEINEMANN LTD, *London, Melbourne, Toronto*

GÖTEBORG
ELANDERS BOKTRYCKERI AKTIEBOLAG
1961

The following papers are included in this dissertation:

1. "The Infinite Journal Bearing, Considering Vaporization." LEIF FLOBERG. Transactions of Chalmers University of Technology, No 189, 1957.
2. "The Finite Journal Bearing, Considering Vaporization." The chapters 4; 5,17 and 5,27. BENGT JAKOBSSON and LEIF FLOBERG. Transactions of Chalmers University of Technology, No 190, 1957.
3. "Experimental Investigation of Power Loss in Journal Bearings, Considering Cavitation." LEIF FLOBERG. Transactions of Chalmers University of Technology, No 215, 1959.
4. "Lubrication of a Rotating Cylinder on a Plane Surface, Considering Cavitation." LEIF FLOBERG. Transactions of Chalmers University of Technology, No 216, 1959.
5. "Boundary Conditions of Cavitation Regions in Journal Bearings." LEIF FLOBERG. American Society of Lubrication Engineers, Annual Meeting, 1960.
6. "The Optimum Thrust Tilting-pad Bearing." LEIF FLOBERG. Transactions of Chalmers University of Technology, No 231, 1960.
7. "The Two-groove Journal Bearing, Considering Cavitation." LEIF FLOBERG. Transactions of Chalmers University of Technology, No 232, 1960.
8. "Lubrication of Two Cylindrical Surfaces, Considering Cavitation." LEIF FLOBERG. Transactions of Chalmers University of Technology, No 234, 1961.
9. "Attitude-Eccentricity Curves and Stability Conditions of the Infinite Journal Bearing." LEIF FLOBERG. Transactions of Chalmers University of Technology, No 235, 1961.
10. "Experimental Investigation of Cavitation Regions in Journal Bearings." LEIF FLOBERG. Transactions of Chalmers University of Technology, No 238, 1961.

Preface

This work is the result of five years lubrication research, 1955—1960. It was made at the Institute of Machine Elements, Chalmers University of Technology, Göteborg, Sweden. Research leader was the head of the Institute, Professor BENGT JAKOBSSON. The work was sponsored by the Swedish Technical Research Council and it has resulted in thirteen published reports of which ten are included here.

I wish to express my sincere thanks to Professor BENGT JAKOBSSON, who gave the impulse to this work and put me on this interesting field for research work. His large interest and capability of inspiring enthusiasm have been of invaluable help in the preparation of my reports.

I thank the Swedish Technical Research Council for their kind sponsorship.

I thank the following assistents: BERTIL BJÖRKMAN, AXEL BRING, GÖSTA CEDERIN, RALPH CRAFOORD, THOMAS HAAGEN, TORE HALLÉN, VEIKKO HYTTINEN, BENGT HÅKANSSON, LARS JOHANSSON, LEIF LACHONIUS, ÅKE LINDH, REIMER SIEBENFREUND, BERTIL ÅBERG, and STURE ÖSTLUND, who have made numerical calculations, drawings, experimental investigations, and prepared programs for digital computers.

I also thank Dr. Phil. C. E. LATOURN and Mr. ERIC ELLIOT, who have read the English.

Introduction

Hydrodynamic lubrication is a field, which is paid more and more interest. Modern machines with higher and higher speeds of rotating parts need carefully designed bearings in order to avoid wear, heating and vibrations. It is important to know what happens within the carrying oil film between the shaft and the bearing.

The bearing is one of the oldest and most used machine elements. All rotating machine parts are mounted either in journal bearings or in rolling bearings. The latter operate in the rolling points after similar principles but with thinner oil films and less oil flow. The lubrication of ball and roller bearings is thus very simple. They are filled with grease only once for several years. The hydrodynamically lubricated bearings need a more careful lubrication and a frequent service, but are in spite of that used in several bearing applications, e. g. when a dividable bearing is needed, for silent-running machines, and for machines which, under non-operating periods, are subjected to vibrations.

The research on hydrodynamic lubrication was started in the 1880's when the railroads were growing up. The heavily loaded locomotive bearings gave problems. TOWER (39) published in 1883 his discovery that the maximum oil film pressure was about twice the average pressure. It had earlier been thought that the pressure was constant. He also showed that the pressure varied in the axial direction after a curve of parabolic form. The same year PETROFF (31) published a formula to determine the power loss in the bearing assuming the shaft and bearing concentric. This formula is still an acceptable approximation.

In 1886, REYNOLDS (34) presented his hydrodynamic oil film theory, which is the base for all calculations on bearing quantities. He combined the equilibrium and continuity conditions for a small oil element and gave the equation which determines the pressure build-up in a thin oil film between two moving surfaces. REYNOLDS solved this equation for an infinitely wide plane pad bearing and

made an approximate solution for the infinitely wide journal bearing. He showed that a shaft can carry a load swimming on an oil film without touching the bearing. A correctly designed bearing shall thus run without any wear. The exact solution of the infinitely wide journal bearing was given in 1904 by SOMMERFELD (36). His solution has been strongly criticized as it seems to include negative pressures in the oil film. SOMMERFELD, however, was fully aware of this shortage and defined the validity range of his theory.

In the year 1905, MICHELL (27) succeeded in solving REYNOLDS' equation for the plane pad bearing of finite width. The pressure at a certain point of the bearing area was given as the sum of an infinite series and the load was derived by numerical integration. In recent years REYNOLDS' equation has also been solved for the finite journal bearing case after several different methods, exact as well as numerical. The exact solutions are built upon infinite series and the approximate numerical calculations are usually made on digital computers in order to get good accuracy.

A field in the hydrodynamic lubrication theory which has been given little interest is cavitation and related problems. In journal bearings cavitation nearly always occurs and it is thus not correct to neglect that problem when investigating the quantities needed for journal bearing design. In this work great interest is paid to cavitation and the behaviour of the oil in a cavitation region. It has been possible to derive the boundary conditions of cavitation regions, thereby obtaining solutions to problems, hitherto unsolved. This has made it feasible to prepare tables and charts for bearing design. The usual assumptions of constant viscosity, constant load and rigid surfaces are made.

Hydrodynamic Lubrication and Cavitation

Bearings carry loads on lubricating films in which pressures are built up hydrostatically or hydrodynamically. Lubricants are oils, water, air, etc. In hydrostatic bearings the pressure is supplied by a pump. These are not treated here. In the hydrodynamic bearing the pressure is built up by shearing forces from the moving surfaces. These forces give rise to the power losses. It is thus the viscosity which is used to create the carrying effect and also gives loss. This fact was shown theoretically by REYNOLDS in 1886 when he derived the following equation which determines the pressure distribution in a lubricating film

$$\frac{d}{dx}\left(h^3\frac{dp}{dx}\right)+\frac{d}{dz}\left(h^3\frac{dp}{dz}\right)=6\eta\left\{(U_0+U_1)\frac{dh}{dx}+2V_1\right\}$$

where

p = pressure
h = film thickness
x, z = coordinates
η = absolute viscosity
U_0, U_1, V_1 = surface velocities

It is remarkable to find how REYNOLDS in his pioneer work finds a solution, which is fully correct in all respects.

If a bearing consists of converging wedges only, the pressure is positive in the whole bearing and the pressure distribution is derived from REYNOLDS' equation using as the only boundary conditions the pressure at the bearing boundaries. If there are diverging wedges in a bearing we usually get cavitation, while REYNOLDS' equation then falls out with negative pressures. In this case the REYNOLDS' equation solution is wrong *for the whole bearing* and we need other conditions to determine the pressure distribution.

This work treats hydrodynamic lubrication with cavitation. The boundary conditions of cavitation regions, which are derived here, make it possible to determine the bearing quantities for every steady state bearing case.

The Infinite Journal Bearing

When studying hydrodynamic lubrication it is suitable to start with the case of infinite width for which simple exact solutions are obtainable. The infinitely wide journal bearing is treated in Part 1. The full SOMMERFELD pressure curve with positive pressure all around the journal has been rejected in literature due to experimental evidence. This curve, which is theoretically possible if an oil groove is located at the minimum pressure point, has here been experimentally verified, see fig. 1. The test is made with a bearing with tight side seals making the side leakage negligible. The bearing width is thus practically infinite and the agreement with theory is quite satisfactory. The fact that the full SOMMERFELD curve earlier has been rejected is due to tests made with bearings of finite width. Two different

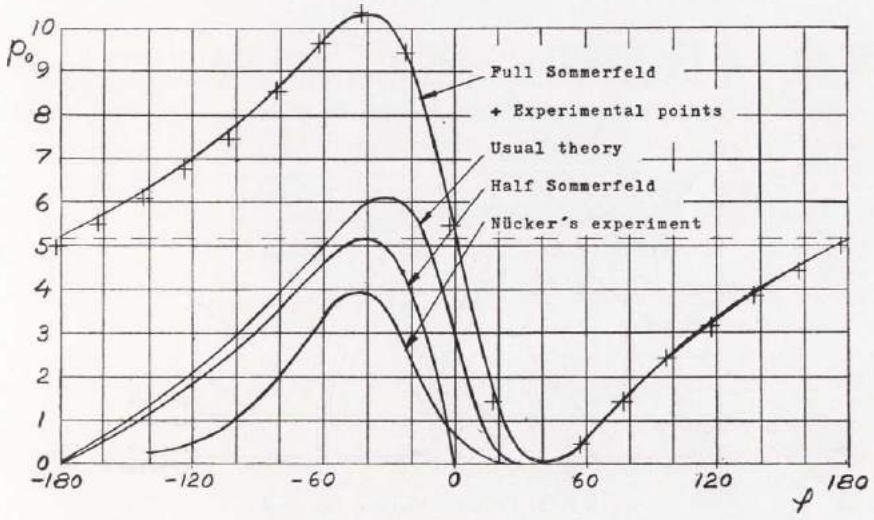

Fig. 1. Pressure Curves for $\varepsilon = 0{,}60$
(Compare CAMERON-WOOD fig. 2)
(Part 1: 40.1)

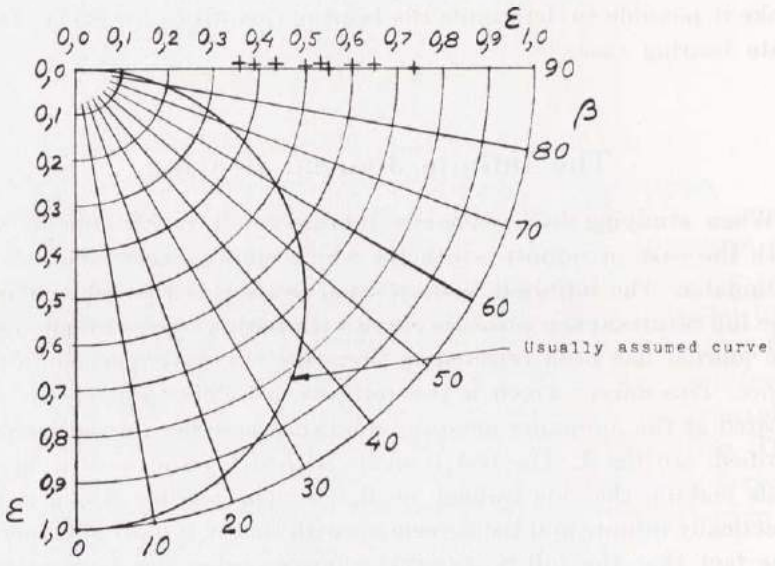

Fig. 2. Attitude-Eccentricity Curves
+Experimental points
(Compare CAMERON-WOOD fig. 3)
(Part 1: 40.2)

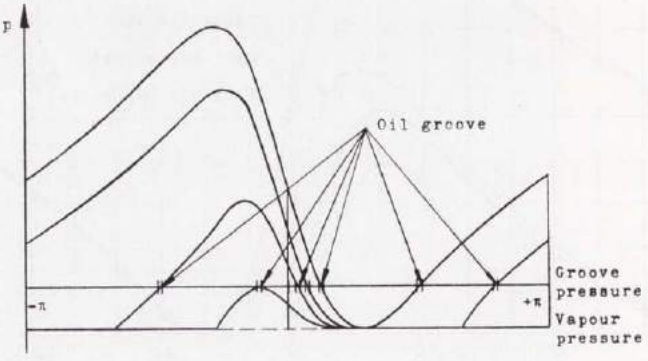

Fig. 3. Pressure Curves for $\varepsilon = 0{,}5$
(Part 1: 42.1)

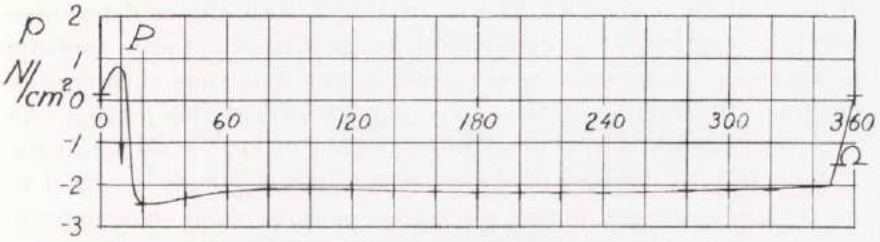

Fig. 4. Experimental Pressure Curve
(Part 1: 63.2)

bearing cases have thus been compared and incorrect conclusions have been drawn. The full SOMMERFELD pressure curves give a horizontal attitude-eccentricity line for the shaft centre location, which, however, has been regarded as impossible. CAMERON-WOOD (4) wrote in 1949: "In the full SOMMERFELD solution the resultant of pressure round the journal has no component along the line of centres, and the attitude is always at 90 deg. to the load line. It has been clear for a a considerable time that all the experimental evidence was against this straight line centre locus." Fig. 2 shows that SOMMERFELD was right.

When cavitation occurs in an infinitely wide journal bearing the continuity of flow gives zero pressure derivative at the film break as shown in Part 1, page 41. This gives for a certain eccentricity a group of pressure curves shown in fig. 3. The vapour pressure is now

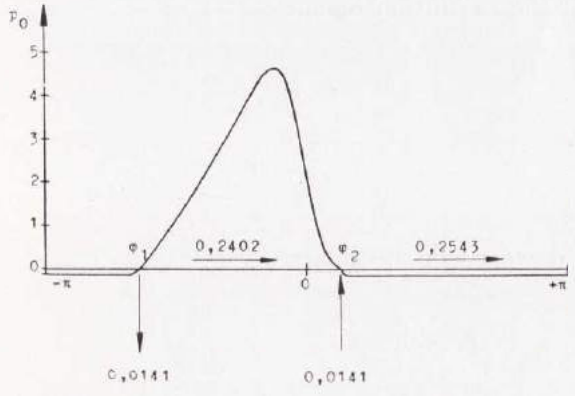

Fig. 5. Pressure Curves and Oil Flows
(Part 1: 70.2)

called cavitation pressure. The location of the oil groove determines which pressure curve is derived. In practice the cavitation pressure is usually close to the groove pressure and it is thus theoretically possible to derive a cavitation region all around the journal. An experimental curve with a cavitation region of 350° is shown in fig. 4. In literature the rate of the oil film region is usually assumed to be 180°. Such an assumption has no real background as shown above, where it is established that the cavitation region can vary from zero degrees to almost the full circumference.

In literature the low pressure part of the bearing has been shown very little interest, but many calculations have been made for the oil film part of the bearing with arbitrarily chosen boundary conditions. The risk with such a calculation is demonstrated in fig. 5. ten BOSCH (3) considers the oil film part only and obtains for the case chosen an oil flow of 0,2402 entering the bearing at φ_1 and leaving at φ_2. If the low pressure cavitation part is taken into account, an oil flow of 0,0141 will enter at φ_2 and leave at φ_1.

The Finite Journal Bearing

All practical bearings have considerable side flow. It is thus necessary to take this into account when calculating the bearing quantities. The three-dimensional oil flow case is studied in Part 2. It is theoretically demonstrated that the boundary conditions are, at the upstream boundary of the cavitation region

$$p = p_c$$

$$\frac{\partial p}{\partial x} = 0$$

and at the downstream boundary

$$p = p_c$$

$$\frac{Uh^*}{2} = \frac{Uh}{2} - \frac{h^3}{12\eta}\left[\frac{\partial p}{\partial x} - \frac{\partial p}{\partial z}\frac{dx}{dz}\right]$$

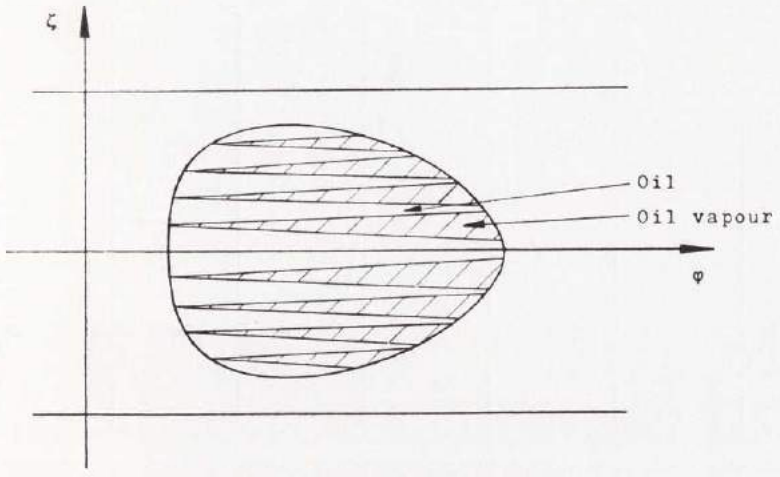

Fig. 6. Sketch of a Cavitation Region
(Part 2: 36.1)

where

p_c = cavitation pressure
U = surface velocity
h^* = oil film thickness at film rupture

The last condition has not earlier been presented in literature. A sketch of a cavitation region derived from this condition is shown in fig. 6. The oil flows in streamlets through the region. The shear stress, taking the air strips into account, is shown to be

$$\tau = \frac{\eta U h^*}{h^2}$$

Some authors assume a full oil film in the cavitation region and others an air region when calculating the power loss, but both methods violate the continuity condition and give incorrect results.

A theoretically determined pressure field with a cavitation zone is shown in fig. 18. For the same case a comparison between the theoretically determined pressure curves and experimental points is made in fig. 7, where

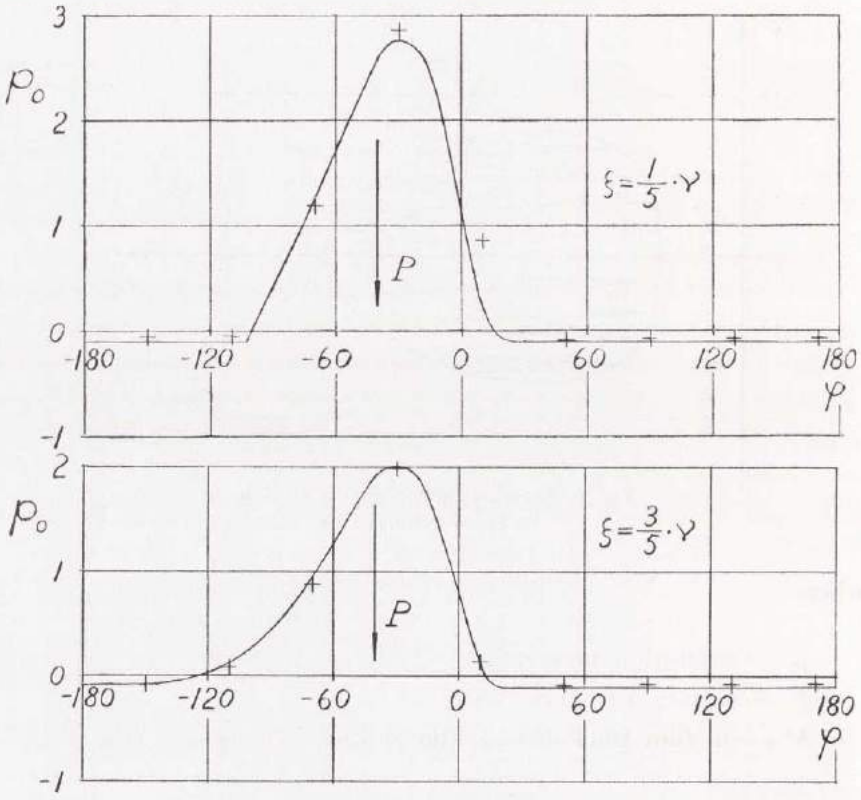

Fig. 7. Theoretical Curves for
$\nu = 1$; $\varepsilon = 0{,}6$ and $p_{c0} = -0{,}1$
+Experimental points
(Part 2: 71.1)

φ, ζ = coordinates
ν = width-diameter ratio
ε = eccentricity ratio
p_0 = non-dimensional pressure
p_{c0} = non-dimensional cavitation pressure

The agreement is quite satisfactory.

In Part 5 the behaviour of the oil at cavitation is discussed. Two numerical calculations are made on cases treated in a paper by RAIMONDI (33). He does not satisfy the continuity of flow at the downstream boundary of the cavitation regions, and in Part 5 this boundary is adjusted due to the continuity condition.

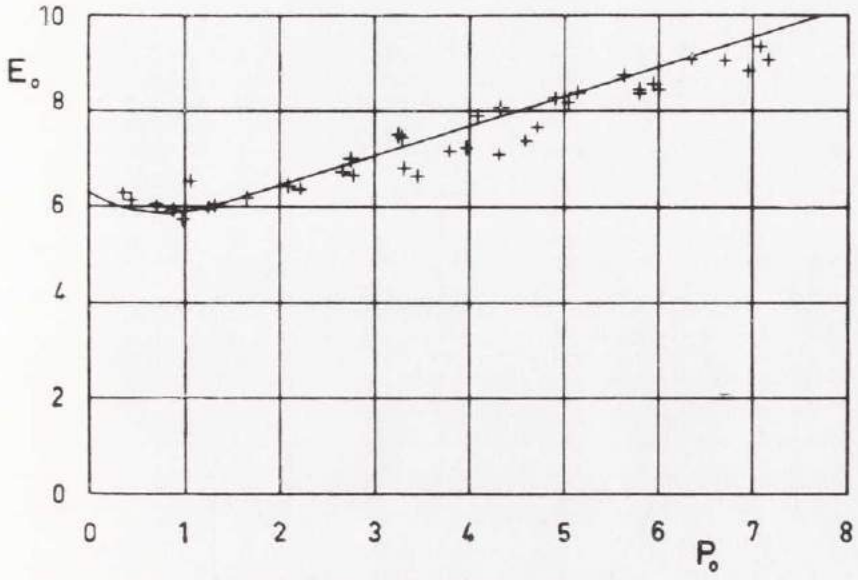

Fig. 8. Theoretical Power Loss
+Experimental points
(Part 3: 14.1)

Experimental Investigation of Power Loss in Journal Bearings

Part 3 represents an experimental investigation of the power loss in a 360° journal bearing with an oil groove 90° before the load line. The theoretical power loss is calculated taking the air strips in the cavitation region into account, and theory and tests are compared, see fig. 8. The experimental power loss is derived through measurements of journal torque and rotational speed. All the test apparatus is put on a cradle and therefore the journal torque is the same as the cradle torque. This method requires no calibrations and gives quite good results.

Lubrication of Cylindrical Surfaces

Part 4 treats hydrodynamic lubrication of a cylinder and a plane and Part 8 the two cylinder case. These two cases have earlier been treated by KNESCHKE (26) and GATCOMBE (18) but they have used arbitrarily chosen boundary conditions violating the continuity of flow. In the Parts 4 and 8 the continuity of flow is satisfied in every

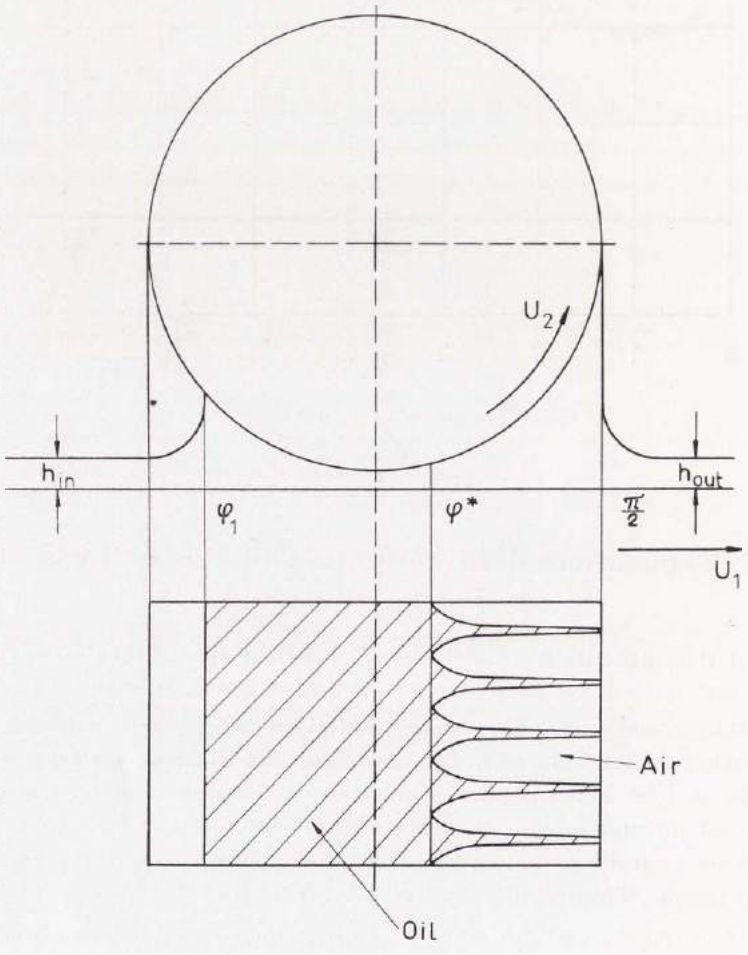

Fig. 9. Theoretical Film Break
(Part 4: 25.1)

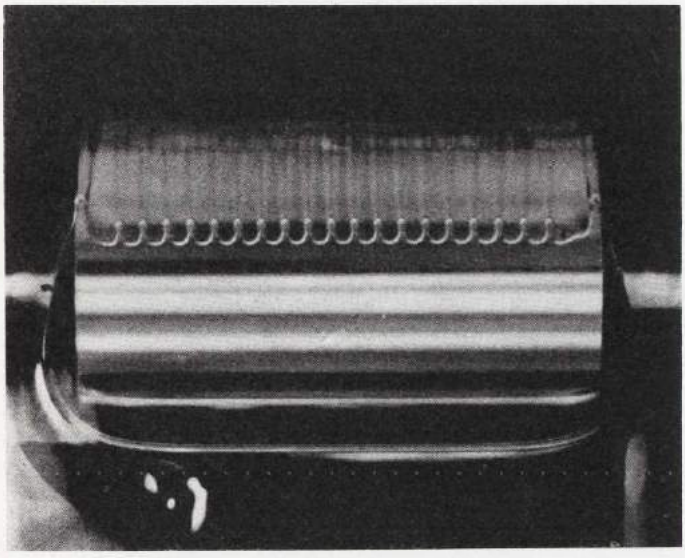

Fig. 10. Experimental Film Break
(Part 8: 32.1)

section of the oil wedge. KNESCHKE and GATCOMBE have the film break as a straight line in axial direction, but here it is theoretically shown that the oil will divide into streamlets and this behaviour is verified by tests, see the figs. 9 and 10.

Design of Thrust Tilting-pad Bearings

Part 6 treats the thrust tilting-pad bearing. It is shown how to choose the number of pads which gives minimum power loss at given values of load capacity, angular velocity and minimum permissible oil film thickness. Tables and charts for design calculation are given and a diagram for design of optimum thrust tilting-pad bearings is made.

Design of Journal Bearings

Part 7 treats the two-groove journal bearing. Tables and charts for design of ring- or pressure-lubricated journal bearings are given and it is shown how to design optimum bearings with minimum power loss at given values of load capacity, angular velocity and minimum permissible oil film thickness.

Stability Conditions

Part 9 is an extension of Part 1, treating the infinite journal bearing. The level of the cavitation pressure is studied and it is shown that it is just below that pressure where air or gases are in contact with the oil under a considerable time. Hitherto it has been normally believed that cavitation occurs just below the atmospheric pressure. Fig. 11 shows cavitating oil at atmospheric pressure in a test tube which earlier was put under higher pressure (6 atm g).

In Part 1 the continuity of the oil flow was studied and solutions were made starting with fixed locations of the shaft centre and the oil groove relative to the bearing. Those solutions are thus true if the shaft centre is forced to stay in that position. In practice, however, a certain load is applied at a certain angle, and the corresponding shaft centre position is only derived if that position is stable. In Part 9 the stability of the infinite journal bearing is treated both theoretically and experimentally. STIEBER (37) has theoretically treated the infinite journal bearing but has not considered the stability conditions. SWIFT (38) has studied a special infinite journal bearing case, but his calculation method satisfies neither the con-

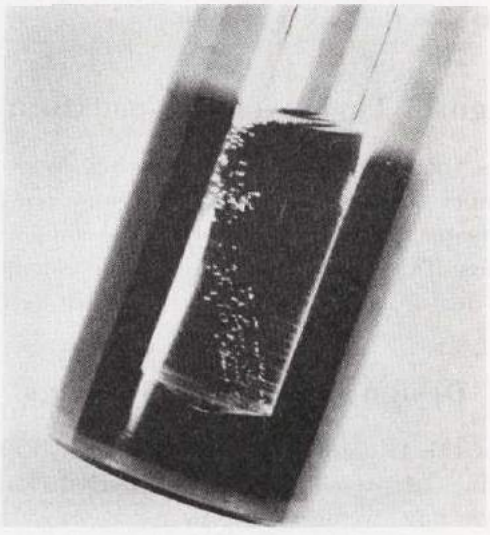

Fig. 11. Cavitation at Atmospheric Pressure
(Part 9: 11.1)

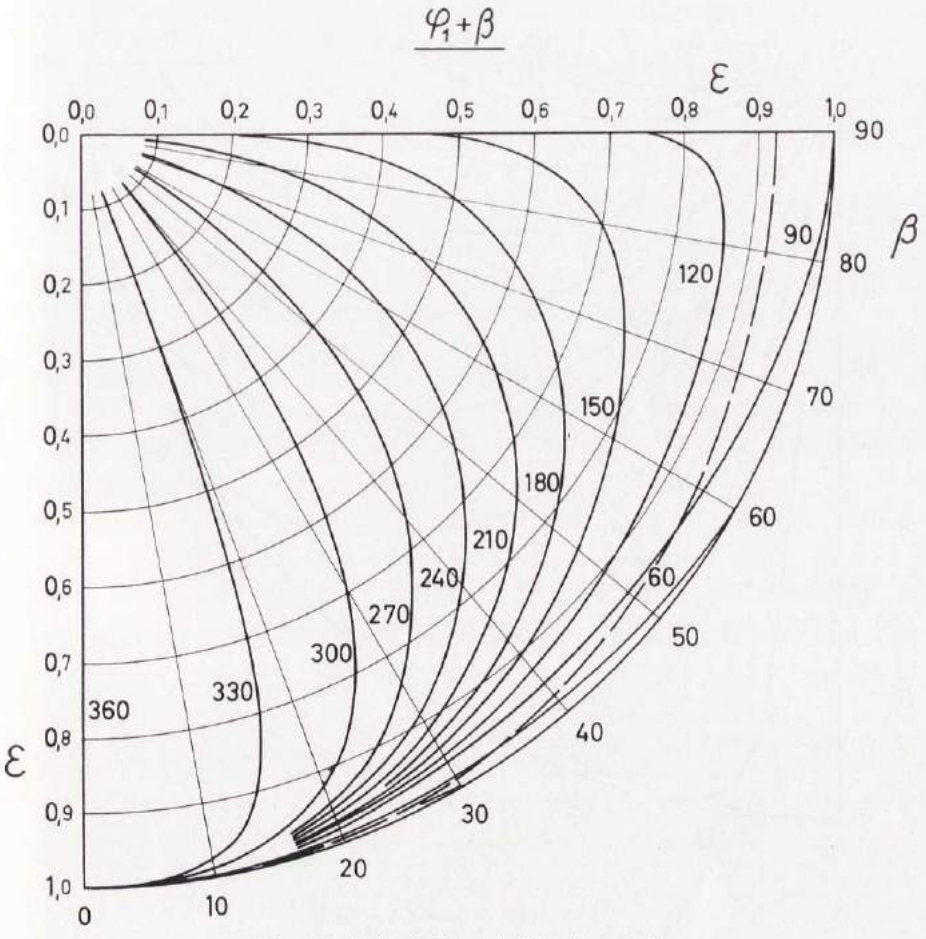

Fig. 12. Attitude-Eccentricity Curves for Different Groove Locations
(Part 9: 14.1)

tinuity condition nor the stability condition, but his work is, in spite of this, often referred to in literature.

Here the boundaries between stable and unstable regions are derived, see figs. 12 and 13. The regions to the left of the dotted lines are stable and those to the right are unstable. Fourteen test series have been made and the agreement with theory is good.

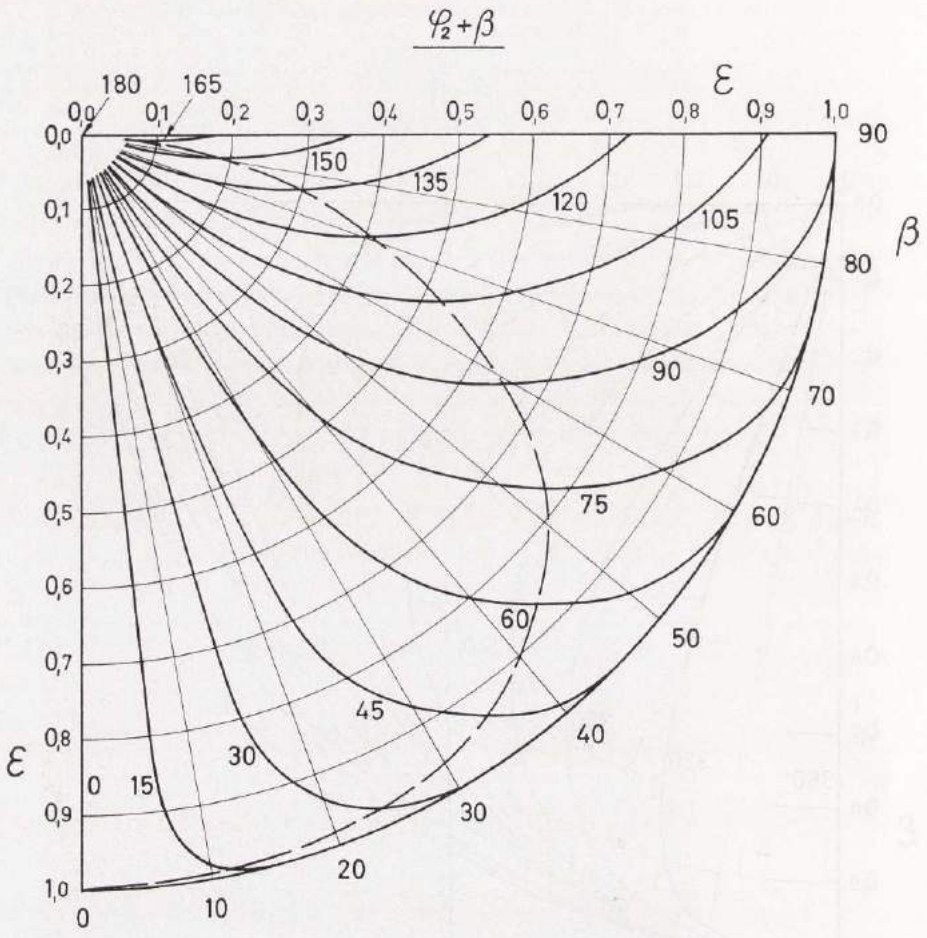

Fig. 13. Attitude-Eccentricity Curves for Different Groove Locations (Part 9: 15.1)

Experimental Investigation of Cavitation Regions

Part 10 represents an experimental investigation of cavitation regions in journal bearings of finite width. Tests are made with thin plastic bearings in order to photograph the regions and with thick plastic bearings to measure the region locations. The grooveless bearing case and the case with an oil groove 90° before the load line are studied.

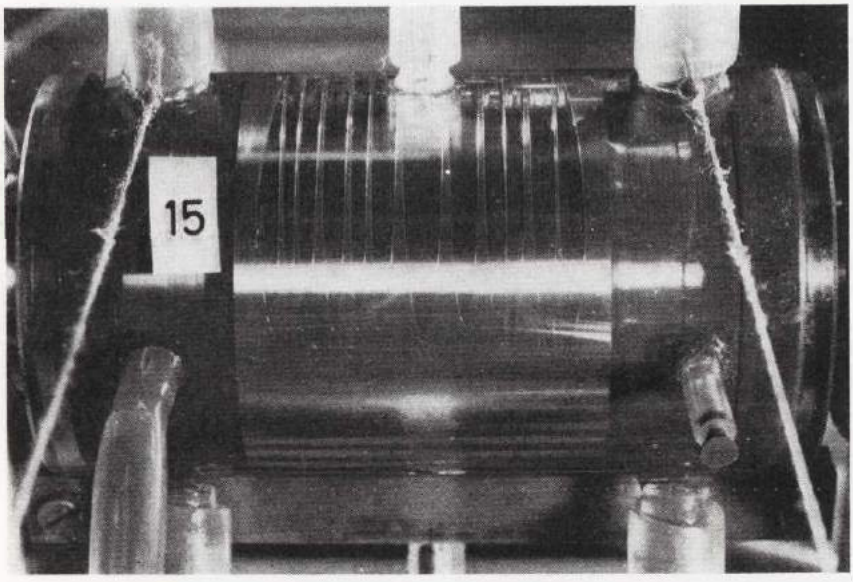

Fig. 14. Upstream Part of the Cavitation Region
($\nu=1$, $\varepsilon=0{,}6$ and $p_{c0}=-0{,}1$)
(Part 10: 17.1)

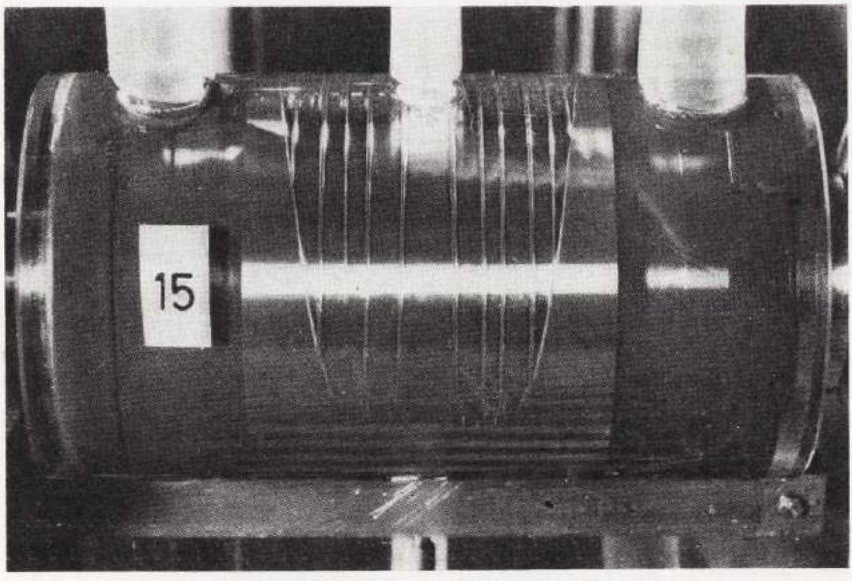

Fig. 15. Downstream Part of the Cavitation Region
($\nu=1$, $\varepsilon=0{,}6$ and $p_{c0}=-0{,}1$)
(Part 10: 17.2)

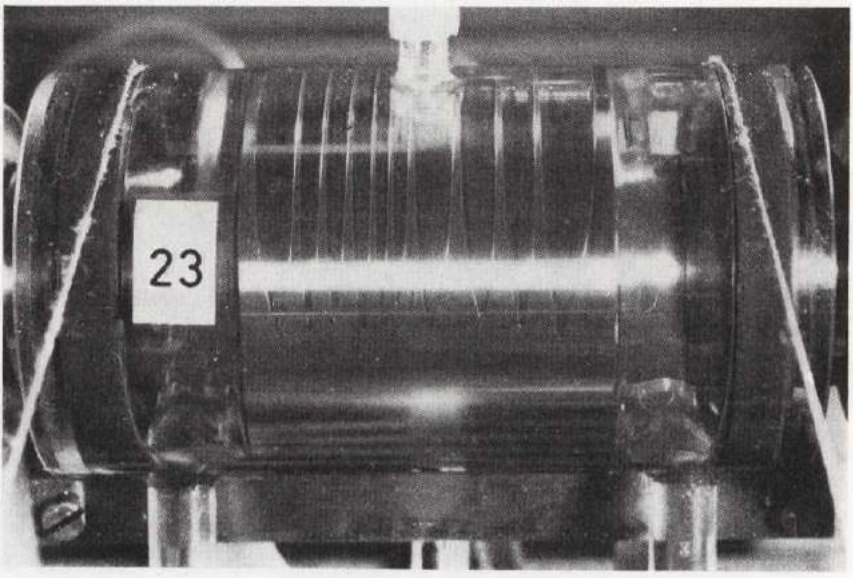

Fig. 16. Upstream Part of the Cavitation Region
($\nu=1$ and $\varepsilon=0,6$)
(Part 10: 23.1)

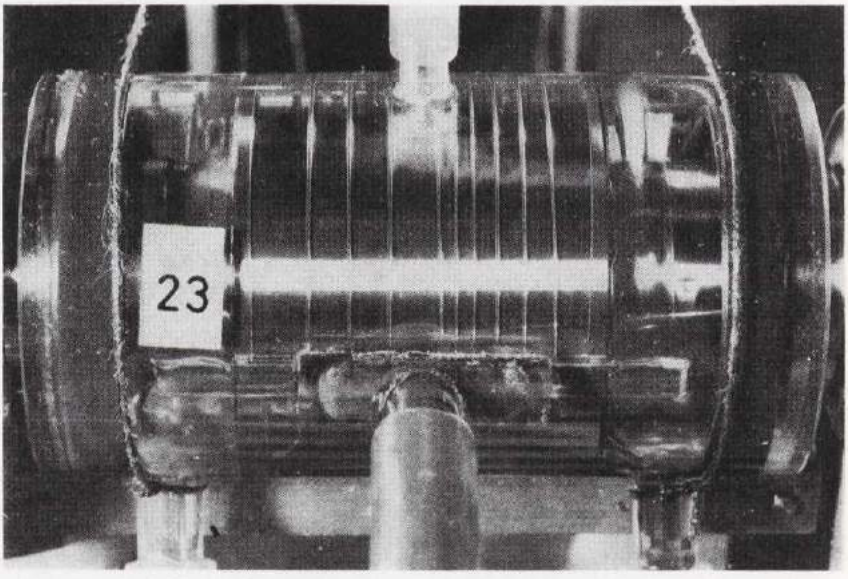

Fig. 17. Downstream Part of the Cavitation Region
($\nu=1$ and $\varepsilon=0,6$)
(Part 10: 23.2)

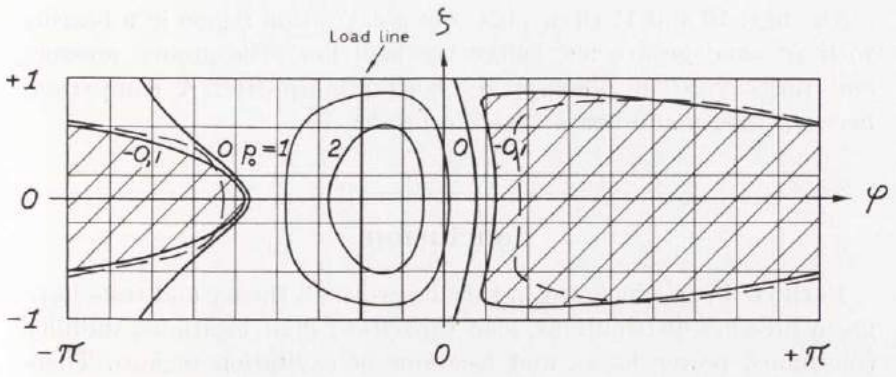

Fig. 18. Theoretical Cavitation Region for
$\nu = 1$, $\varepsilon = 0{,}6$ and $p_{c0} = -0{,}1$
The dotted line represents the experimental boundary
(Part 10: 19.2)

Figs. 14 and 15 show photos of a cavitation region in a bearing without axial oil grooves. There are peripheral grooves at the bearing sides with oil of higher pressure than the cavitation pressure. The oil flows into the bearing where the pressure is lower than the groove pressure and out from the bearing where the pressure is higher than that pressure. A comparison between the theoretical and experimental boundaries of the cavitation region is shown in fig. 18.

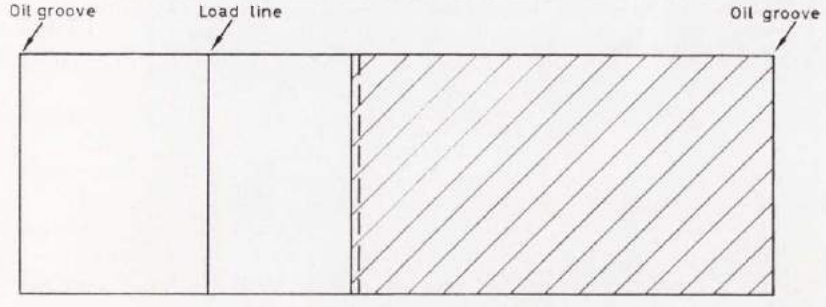

Fig. 19. Theoretical Cavitation Region for
$\nu = 1$ and $\varepsilon = 0{,}6$
The dotted line represents the experimental boundary
(Part 10: 24.2)

The figs. 16 and 17 show photos of a cavitation region in a bearing with an axial groove 90° before the load line. The groove pressure and the cavitation pressure are both atmospheric. A comparison between theory and test is given in fig. 19.

Conclusion

In the ten parts included in this dissertation, theory and tests have given pressure distributions, load capacities, shaft locations, stability conditions, power losses and locations of cavitation regions. There is in all cases close agreement between theory and tests.

References

1. Bickley, W. G.: Formulae for Numerical Integration. Math. Gazette, XXIII, pp. 352—359, Oct. 1939.
2. Bickley, W. G.: Formulae for Numerical Differentiation. Math. Gazette, XXV, pp. 19—27, Febr. 1941.
3. ten Bosch, M.: Berechnung der Maschinenelemente. Berlin, 1951.
4. Cameron, A. and Wood, W. L.: The Full Journal Bearing. Proc. Instn Mech. Engrs, vol. 161, p. 59, 1949.
5. Christopherson, D. G.: A New Mathematical Method for the Solution of Film Lubrication Problems. Proc. Instn Mech. Engrs, Lond., vol. 146, p. 126, 1941.
6. Cole, J. A. and Hughes, C. J.: Oil Flow and Film Extent in Complete Journal Bearings. Proc. Instn Mech. Engrs, vol. 170, p. 499, 1956.
7. Dowson, D.: Investigation of Cavitation in Lubricating Films Supporting Small Loads. Proceedings of The Conference on Lubrication and Wear, held by The Institution of Mechanical Engineers in London, 1957.
8. Floberg, L.: The Infinite Journal Bearing, Considering Vaporization. Göteborg, 1957.
9. Floberg, L.: Experimental Investigation of Power Loss in Journal Bearings, Considering Cavitation. Göteborg, 1959.
10. Floberg, L.: Lubrication of a Rotating Cylinder on a Plane Surface, Considering Cavitation. Göteborg, 1959.
11. Floberg, L.: Boundary Conditions of Cavitation Regions in Journal Bearings. American Society of Lubrication Engineers, Annual Meeting, 1960.
12. Floberg, L.: The Optimum Thrust Tilting-pad Bearing. Göteborg, 1960.
13. Floberg, L.: The Two-groove Journal Bearing, Considering Cavitation. Göteborg, 1960.
14. Floberg, L.: Lubrication of Two Cylindrical Surfaces, Considering Cavitation. Göteborg, 1961.
15. Floberg, L.: Attitude-Eccentricity Curves and Stability Conditions of the Infinite Journal Bearing. Göteborg, 1961.
16. Floberg, L.: Experimental Investigation of Cavitation Regions in Journal Bearings. Göteborg, 1961.
17. Fränkel, A.: Berechnung von zylindrischen Gleitlagern. Zürich, 1944.
18. Gatcombe, E. K.: Lubrication Characteristics of Involute Spur Gears. Trans. Am. Soc. Mech. Engrs, vol. 67, p. 177, 1945.
19. Grubin, A. N.: Fundamentals of the Hydrodynamic Theory of Lubrication of Heavily Loaded Cylindrical Surfaces. Moscow, 1949 (Translation from Russian).

20. GÜMBEL, L. and EVERLING, E.: Reibung und Schmierung im Maschinenbau. Berlin, 1925.
21. HAYS, D. F.: Plane Sliders of Finite Width. Trans. Am. Soc. Lubr. Engrs, Vol. 1, No 2, 1958.
22. JAKOBSSON, B. and FLOBERG, L.: The Finite Journal Bearing, Considering Vaporization. Göteborg, 1957.
23. JAKOBSSON, B. and FLOBERG, L.: The Partial Journal Bearing. Göteborg, 1958.
24. JAKOBSSON, B. and FLOBERG, L.: The Rectangular Plane Pad Bearing. Göteborg, 1958.
25. JAKOBSSON, B. and FLOBERG, L.: The Centrally Loaded Partial Journal Bearing. Göteborg, 1959.
26. KNESCHKE, A.: Rollreibung auf spurbildender Fahrbahn. Ingenieur-Archiv XXV. Band, 1957.
27. MICHELL, A. G. M.: The Lubrication of Plane Surfaces. Z. Math. Phys., vol. 52, p. 123, 1905.
28. MICHELL, A. G. M.: Lubrication. London, 1950.
29. NÜCKER, W.: Über den Schmiervorgang im Gleitlager. VDI-Forschungsheft 352, 1932.
30. OTT, H. H.: Zylindrische Gleitlager bei instationärer Belastung. Zürich, 1948.
31. PETROFF, N. P.: Friction in Machines and the Effect of the Lubricant. Engineering Journal, St. Petersburg, 1883, No 1, pp. 71—140; No 2, pp. 228—279; No 3, pp. 377—436; No 4, pp. 535—564.
32. RAIMONDI, A. A. and BOYD, J.: A Solution for the Finite Journal Bearing and its Application to Analysis and Design: III. Trans. Am. Soc. Lubr. Engrs, Vol. 1, No 1, 1958.
33. RAIMONDI, A. A.: A Theoretical Study of the Effect of Offset Loads on the Performance of a 120° Partial Journal Bearing. Trans. Am. Soc. Lubr. Engrs, Vol. 2, No 1, 1959.
34. REYNOLDS, O.: On the Theory of Lubrication and its Application to Mr. Beauchamp Tower's Experiments, including an Experimental Determination of the Viscosity of Olive Oil. Phil. Trans. Roy. Soc., vol. 177, p. 157, 1886.
35. SASSENFELD, H. and WALTHER, A.: Gleitlagerberechnungen. VDI-Forschungsheft 441, 1954.
36. SOMMERFELD, A.: Zur hydrodynamischen Theorie der Schmiermittelreibung. Z. Math. Phys., vol. 50, p. 97, 1904.
37. STIEBER, W.: Das Schwimmlager. Hydrodynamische Theorie des Gleitlagers. Berlin, 1933.
38. SWIFT, H. W.: The Stability of Lubricating Films in Journal Bearings. Proc. Instn Civ. Engrs, vol. 233, p. 267, 1932.
39. TOWER, B.: First Report on Friction Experiments. Proc. Instn Mech. Engrs, vol. 34, p. 632, 1883.
40. TOWER, B.: Second Report on Friction Experiments. Proc. Instn Mech. Engrs, vol. 36, p. 58, 1885.
41. WILCOCK, D. F. and ROSENBLATT, M.: Oil Flow, Key Factor in Sleeve-Bearing Performance. Trans. Am. Soc. Mech. Engrs, vol. 74, p. 849, 1952.
42. VOGELPOHL, G.: Beiträge zur Kenntnis der Gleitlagerreibung. VDI-Forschungsheft 386, 1937.
43. VOGELPOHL, G.: Zur Integration der Reynoldsschen Gleichung für das Zapfenlager endlicher Breite. Ingenieur-Archiv XIV. Band, 1943.

GÖTEBORG
ELANDERS BOKTRYCKERI AKTIEBOLAG
1961

CHALMERS TEKNISKA HÖGSKOLAS HANDLINGAR
TRANSACTIONS OF CHALMERS UNIVERSITY OF TECHNOLOGY GOTHENBURG, SWEDEN
Nr 189 (Avd. Maskinteknik 9) 1957

THE INFINITE JOURNAL BEARING, CONSIDERING VAPORIZATION

(Das Gleitlager von unendlicher Breite mit Verdampfung)

BY

LEIF FLOBERG

REPORT No. 2 FROM THE INSTITUTE OF MACHINE ELEMENTS
CHALMERS UNIVERSITY OF TECHNOLOGY
GOTHENBURG, SWEDEN
1957

GUMPERTS FÖRLAG
GÖTEBORG

Av Chalmers Tekniska Högskolas Handlingar hava tidigare utkommit:

Fullständig förteckning över Chalmers Tekniska Högskolas Handlingar lämnas av Chalmers Tekniska Högskolas Bibliotek, Göteborg.

101. Rydbeck, Olof E. H., *The theory of magneto ionic triple splitting.* 40 s. 1951. Kr. 4:50. (Avd. Elektroteknik. 17.)
102. Rydbeck, Olof E. H., and Forsgren, Sven K. H., *On the theory of electron wave tubes.* 31 s. 1951. Kr. 3: 50. (Avd. Elektroteknik. 18.)
103. Lindquist, Rune, *Polar blackouts recorded at the Kiruna Observatory.* 25 s. 1951. Kr. 3: —. (Avd. Elektroteknik. 19.)
104. Forsgren, Sven K. H., *Some calculations of ray paths in the ionosphere.* 23 s. 1951. Kr. 3: —. (Avd. Elektroteknik. 20.)
105. Agdur, Bertil N., *Experimental observation of double-stream amplification.* 13 s. 1951. Kr. 1: 50. (Avd. Elektroteknik. 21.)
106. Agdur, Bertil N., and Åsdal, Carl-Gösta L., *Noise measurements on a traveling wave tube.* 9 s. 1951. Kr. 1: 50. (Avd. Elektroteknik. 22.)
107. Forsgren, Sven K. H., and Perers, Olof F., *Vertical recording of rain by radar.* 19 s. 1951. Kr. 2: 50. (Avd. Elektroteknik. 23.)
108. Perers, Olof F., Stjernberg, Bo K. E., and Forsgren, Sven K. H., *Microwave propagation in the optical range.* 20 s. 1951. Kr. 3: —. (Avd. Elektroteknik. 24.)
109. Lindquist, Rune, *A 16 kW panoramic ionospheric recorder.* 41 s. 1951. Kr. 4: 50. (Avd. Elektroteknik. 25.)
110. Lindblad, Anders, *Some experiments with selfpropelled models of twin screw ships.* 24 s. 1951. Kr. 4: 50. (Avd. Skeppsbyggeri. 4.)
111. Beskow, Gunnar, *Amerikansk och svensk jordklassifikation. Speciellt för vägar och flygfält.* 48 s. 1951. Kr. 2: —. (Avd. Väg- och Vattenbyggnad. Byggnadsteknik. 18.)
112. Dahr, Konstantin, *On the mathematical analysis of an idealized multiplex electromagnetic machine.* 116 s. 1951. Kr. 17: —. (Avd. Elektroteknik. 26.)
113. Troedsson, Carl Birger, *Two standpoints towards modern architecture. Wright and Le Corbusier.* 22 s. 1951. Kr. 4: —. (Avd. Arkitektur. 1.)
114. Stranski, I. N., *Die Vorgänge an Kristalloberflächen.* 21 s. 1951. Kr. 3: —. (Avd. Kemi och Kemisk Teknologi. 24.)
115. *Mitteilungen aus dem Institut für organische Chemie. VII.* Von Erik Larsson. 31 s. 1951. Kr. 4: —. (Avd. Kemi och Kemisk Teknologi. 25.)
116. Ekelöf, Stig, *Les machines mathématiques en Suède.* 26 s. 1951. Kr. 5: —. (Avd. Elektroteknik. 27.)
117. Möller, Torsten, *En ny metod för beräkning av spikförband.* 77 s. 1951. Kr. 7: —. (Avd. Väg- och Vattenbyggnad. Byggnadsteknik. 19.)
118. Hedvall, J. Arvid, Jagitsch, Robert und Olson, Gillis, *Über das Problem der Zerstörung antiker Gläser. II.* 15 s. 1951. Kr. 2: 50. (Institutionen för Silikatkemisk Forskning. 28.)
119. Ahlberg, R., *A contribution to the methods of measuring the plasticity of clays.* 25 s. 1951. Kr. 5: —. (Institutionen för Silikatkemisk Forskning. 29.)
120. Ekelöf, S., Bengtson, L., Kihlberg, G., and Leithammel, P., *An integrating amplifier for the oscillographic recording of magnetic flux.* 23 s. 1951. Kr. 5: —. (Avd. Elektroteknik. 28.)
121. *Mitteilungen aus dem Institut für organische Chemie. VIII.* Von Erik Larsson. 17 s. 1951. Kr. 2: 50. (Avd. Kemi och Kemisk Teknologi. 26.)
122. Karlson, K. G., *Sur le frein à sabots extérieurs articulés.* 31 s. 1951. Kr. 5: —. (Avd. Maskinteknik. 6.)
123. Ambjörn, Gustaf, *Släpförsök med fartygsmodeller i sned och tvär ställning mot körriktningen samt resultatens tillämpning på ett intressant sjörättsfall.* 31 s. 1952. Kr. 5: —. (Avd. Skeppsbyggeri. 5.)
124. Berne, Eric, *Studies on radioactive bromine.* 46 s. 1952. Kr. 6: —. (Avd. Allmänna Vetenskaper. 8.)
125. Nilsson, Ingvar, *A scaler using dekatron scaling tubes. — Note on the cross section of the reaction* $^{31}P(n,p)^{31}Si$. 8 s. 1952. Kr. 2: —. (Avd. Allmänna Vetenskaper. 9.)
126. Hedvall, J. A., and Liljegren, B., *An investigation of the reaction* $2\ CaCO_3 + SiO_2$ *at high temperatures.* 12 s. 1952. Kr. 2: 50. (Institutionen för Silikatkemisk Forskning. 30.)
127. Saretok, Vitold, *Tillsatsmedel till betong.* 67 s. 1952. Kr. 5: —. (Avd. Väg- och Vattenbyggnad. Byggnadsteknik. 20.)

Forts. å omsl. 3:dje sida.

CHALMERS TEKNISKA HÖGSKOLAS
HANDLINGAR

TRANSACTIONS OF CHALMERS UNIVERSITY OF TECHNOLOGY
GOTHENBURG, SWEDEN

Nr 189 (Avd. Maskinteknik 9) 1957

THE INFINITE JOURNAL BEARING, CONSIDERING VAPORIZATION

(Das Gleitlager von unendlicher Breite mit Verdampfung)

BY

LEIF FLOBERG

REPORT No. 2 FROM THE INSTITUTE OF MACHINE ELEMENTS
CHALMERS UNIVERSITY OF TECHNOLOGY
GOTHENBURG, SWEDEN
1957

GÖTEBORG 1957
ELANDERS BOKTRYCKERI AKTIEBOLAG

Preface

The aim of this treatise is to study the effect of vaporization on the properties of a journal bearing of infinite width. In practice, there is no infinitely wide journal bearing, but a correct theory for this should be a basis for the study of the finite. However, there are practical cases which are approximately infinite. Several errors in the oil film theory are due to confusion in regard to infinite and finite bearing width. In the case of an infinite journal, it is possible to give exact solutions for the equations.

The subject was put forward during lubrication research work under leadership of professor B. JAKOBSSON, at the Institute of Machine Elements, Chalmers University of Technology, Gothenburg, Sweden, and sponsored by Statens Tekniska Forskningsråd. The experimental investigation has been made at the laboratory of the institute.

I wish to express my gratitude to those who have helped me in this work.

Leif Floberg

Contents

Page

Preface 3

1. Introduction 7

2. Notation 8

3. Fundamental Oil Film Theory 10

3,1. The Pressure in the Oil Film 10
3,2. Load Capacity 14
3,3. Oil Flow 16
3,4. Friction Force 17
3,5. Friction Torque 18
3,6. Power Loss 19
3,7. Temperature Rise 20

4. The 360° Bearing without Vapour Regions 21

4,1. Infinitesimal Compression and Boundary Conditions 21
4,2. Pressure Curves 23
4,3. Load Capacity 25
4,4. Oil Flow 27
4,5. Friction Force, Friction Torque, and Power Loss 28
4,6. Temperature Rise 29
4,7. Coefficient of Friction and Relative Power Loss 30
4,8. Experimental Investigation 33

5. The 360° Bearing with Vapour Regions 41

5,1. Vapour Regions and Boundary Conditions 41
5,2. Pressure Curves 43
5,3. Load Capacity 46
5,4. Oil Flow 52
5,5. Oil Volume in the Bearing 53
5,6. Friction Force, Friction Torque, and Power Loss 54
5,7. Temperature Rise 55
5,8. Coefficient of Friction and Relative Power Loss 55
5,9. Experimental Investigation 59

6. The Optimum 360° Bearing 64

6,1. General Considerations 64
6,2. Load per Unit Projected Area 65
6,3. The Ratio of Maximum Pressure to Load per Unit Projected Area 66

Page

6,4. Schedule for Calculation 66
6,5. Example 67

7. Bearings with Two Oil Grooves 68
7,1. General Considerations 68
7,2. ten Bosch's Solution 69
7,3. Example 70

8. The 180° Bearing with Minimum Film Thickness at the Trailing Edge 72

9. The Optimum 180° Bearing with Minimum Film Thickness at the Trailing Edge 76
9,1. General Considerations 76
9,2. Schedule for Calculation 77

10. Vogelpohl's Solution for an Infinitely Wide Partial Journal Bearing with Oil Inlet 90° before the Load Line 78

11. Conclusion 80

12. Zusammenfassung 81

13. References 83

1. Introduction

The first mathematical treatment of the pressure in the oil film in a bearing was made by REYNOLDS (7) in 1886. He combined continuity and equilibrium for the flow of an incompressible, viscous fluid and derived the differential equation for the pressure. For the infinite slider bearing he gave an exact solution, and for the infinite journal bearing an approximate solution. SOMMERFELD (8) succeeded in getting an exact solution for a journal bearing of infinite width in 1904. If the pressure distribution is known, load, load direction, power loss, and oil flow can be determined.

REYNOLDS and SOMMERFELD, however, have not treated the case with vaporized oil. SOMMERFELD writes: »Sehr bedenklich muss für die Stichhaltigkeit unserer Theorie das Auftreten negativen Druckes erscheinen. . . . Zerreisst nämlich die Ölschicht an der Stelle beginnenden negativen Druckes, so werden die Voraussetzungen hinfällig, . . .» Several authors, among them GÜMBEL (5), FRÄNKEL (4), TEN BOSCH (1), and OTT (6), have tried to determine the pressure distribution when the oil is vaporized in parts of the bearing, but no satisfactory treatment has been made hitherto. This case, with constant pressure vapour or air regions in the bearing, is discussed in this paper. Experiments confirm the theoretical results for bearings without and with constant pressure regions.

2. Notation

A, C = Constants of integration

c = Specific heat of oil

E = Power loss per unit width

$E_0 = \dfrac{E\,\psi}{\eta\,U^2}$ = Non-dimensional power loss per unit width

e = Eccentricity of journal relative to bearing

F_b = Friction force on bearing per unit width

F_j = Friction force on journal per unit width

$F_{j0} = \dfrac{F_j\,\psi}{\eta\,U}$ = Non-dimensional friction force on journal per unit width

$f = \dfrac{E}{P}$ = Relative power loss

$H = \dfrac{h}{\Delta r}$ = Film thickness/radial clearance

h = Oil film thickness

M_b = Friction torque on bearing per unit width

M_j = Friction torque on journal per unit width

$M_{j0} = \dfrac{M_j\,\psi}{\eta\,U\,r}$ = Non-dimensional friction torque on journal per unit width

P = Load per unit width

$P_0 = \dfrac{P\,\psi^2}{\eta\,U}$ = Non-dimensional load per unit width

p = Pressure

$p_0 = \dfrac{p\,\psi^2}{\eta\,\omega}$ = Non-dimensional pressure

q = Oil flow per unit width

$q_0 = \dfrac{q}{U\Delta r}$ = Non-dimensional oil flow per unit width

R = Radius of bearing

r = Radius of journal

$\Delta r = R - r$ = Radial clearance

Δt = Temperature rise

$\Delta t_0 = c\,\varrho \cdot \dfrac{\Delta t\,\psi^2}{\eta\,\omega}$ = Non-dimensional temperature rise

$U = r\,\omega$ = Velocity of journal surface

$u,\ v$ = Velocities of a fluid particle in the x- and y-directions respectively

V = Volume of oil per unit width

$V_0 = \dfrac{V}{r\,\Delta r}$ = Non-dimensional volume of oil per unit width

$x,\ y,\ z$ = Rectangular coordinates

β = Angle between load line and line of centres

γ = Angle

$\varepsilon = \dfrac{e}{\Delta r}$ = Eccentricity/radial clearance

η = Viscosity of the oil

μ = Coefficient of friction

ϱ = Density of the oil

τ = Shear stress

$\varphi = \dfrac{x}{r}$ = Angular coordinate

$\psi = \dfrac{\Delta r}{r}$ = Radial clearance/journal radius

Ω = Angular coordinate measured from the oil groove

ω = Angular velocity

Indices

a = Average

b = Bearing

e = Experimental

j = Journal

t = Theoretical

o = Non-dimensional

3. Fundamental Oil Film Theory

3,1. The Pressure in the Oil Film

For the pressure in a thin oil film between two surfaces, which are moved relative to each other, REYNOLDS (7) obtained the partial differential equation

$$\frac{\partial}{\partial x}\left(h^3 \frac{\partial p}{\partial x}\right) + \frac{\partial}{\partial z}\left(h^3 \frac{\partial p}{\partial z}\right) = 6\,\eta\,U\,\frac{\partial h}{\partial x} \quad \ldots\ldots 10.1$$

where x, z = rectangular coordinates
p = oil film pressure
h = oil film thickness
η = absolute viscosity
U = surface velocity

The viscosity is assumed to be constant.

The equation has the form as in 10.1, in the cases of 10.2.

If the direction of the velocities is changed, as in 11.1, the right-hand term in the equation changes its sign. The positive x-direction is to the right.

For a bearing of infinite width the second term of 10.1 disappears, and therefore

$$\frac{d}{dx}\left(h^3 \frac{dp}{dx}\right) = 6\,\eta\,U\,\frac{dh}{dx}$$

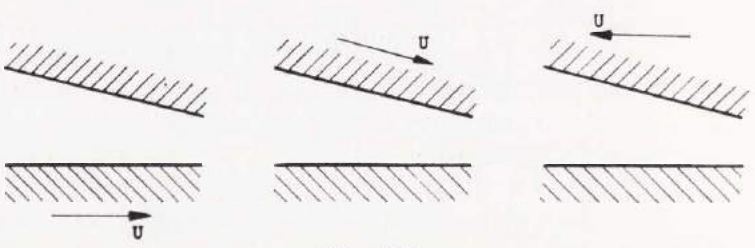

Fig. 10.2

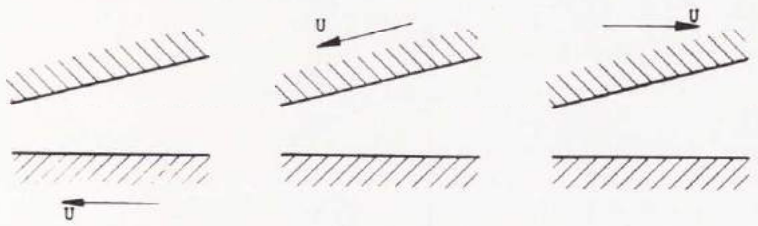

Fig. 11.1

Integration with respect to x gives

$$h^3 \frac{dp}{dx} = 6 \eta U h + C$$

$$\frac{dp}{dx} = \frac{6 \eta U}{h^2} + \frac{C}{h^3}$$

If $\frac{dp}{dx} = 0$ for $h = h^*$ $\qquad C = -6 \eta U h^*$

and

$$\frac{dp}{dx} = \frac{6 \eta U}{h^3} (h - h^*) \quad \ldots\ldots\ldots\ldots \quad 11.2$$

For the journal bearing, as in 12.1, the oil film thickness is

$$h = \Delta r - e \cos \varphi = \Delta r \, (1 - \varepsilon \cos \varphi)$$

where Δr = radial clearance
e = eccentricity of journal relative to bearing
$\varepsilon = \frac{e}{\Delta r}$ = non-dimensional eccentricity

and with journal radius r

$$x = r \varphi \qquad dx = r \, d\varphi$$

Then 11.2 becomes

$$\frac{dp}{d\varphi} = \frac{6 \eta \omega}{\psi^2} \left[\frac{1}{(1 - \varepsilon \cos \varphi)^2} - \frac{1 - \varepsilon \cos \varphi^*}{(1 - \varepsilon \cos \varphi)^3} \right] \ldots . \quad 11.3$$

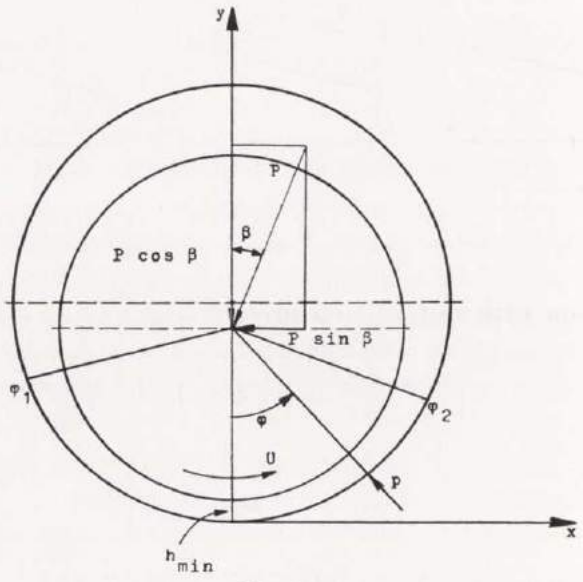

Fig. 12.1

where $\omega =$ angular velocity

$$\psi = \frac{\Delta r}{r} = \text{non-dimensional clearance}$$

Integrate from φ_1 to φ, assuming p_1 to be zero.

$$p = \frac{6\,\eta\,\omega}{\psi^2} \int_{\varphi_1}^{\varphi} \left[\frac{1}{(1 - \varepsilon \cos \varphi)^2} - \frac{1 - \varepsilon \cos \varphi^*}{(1 - \varepsilon \cos \varphi)^3} \right] d\varphi$$

or non-dimensionally

$$p_0 = \frac{p\,\psi^2}{\eta\,\omega} = 6 \int_{\varphi_1}^{\varphi} \left[\frac{1}{(1 - \varepsilon \cos \varphi)^2} - \frac{1 - \varepsilon \cos \varphi^*}{(1 - \varepsilon \cos \varphi)^3} \right] d\varphi$$

To solve this integral, introduce

$$\cos \varphi = \frac{\cos \gamma + \varepsilon}{1 + \varepsilon \cos \gamma}$$

$$d\varphi = \frac{\sqrt{1-\varepsilon^2}}{1+\varepsilon\cos\gamma}\,d\gamma$$

The solution is

$$j_1 = \int_{\varphi_1}^{\varphi} \frac{d\varphi}{1-\varepsilon\cos\varphi} = \frac{\gamma-\gamma_1}{\sqrt{1-\varepsilon^2}}$$

$$j_2 = \int_{\varphi_1}^{\varphi} \frac{d\varphi}{(1-\varepsilon\cos\varphi)^2} = \frac{(\gamma-\gamma_1)+\varepsilon(\sin\gamma-\sin\gamma_1)}{\sqrt{(1-\varepsilon^2)^3}}$$

$$j_3 = \int_{\varphi_1}^{\varphi} \frac{d\varphi}{(1-\varepsilon\cos\varphi)^3} =$$

$$= \frac{\left(1+\frac{\varepsilon^2}{2}\right)(\gamma-\gamma_1)+2\varepsilon(\sin\gamma-\sin\gamma_1)+\frac{\varepsilon^2}{4}(\sin 2\gamma-\sin 2\gamma_1)}{\sqrt{(1-\varepsilon^2)^5}}$$

and

$$p_0 = 6\,[j_2 - (1-\varepsilon\cos\varphi^*)\,j_3]$$

This solution was first obtained by SOMMERFELD.

If at φ_2, p_2 is assumed to be zero, three different cases can be treated:

I. φ_1 and φ_2 are known, then $\varphi^* = f(\varphi_1, \varphi_2, \varepsilon)$.

II. φ_1 is known, and $\varphi_2 = \varphi^*$, then $\varphi^* = f(\varphi_1, \varepsilon)$.

III. A complete 360° oil film, $\varphi_1 = -\pi$ and $\varphi_2 = \pi$, then $\varphi^* = f(\varepsilon)$.

I. $p = 0$ for $\varphi = \varphi_1$ and $\varphi = \varphi_2$

$$j_2(\varphi_2) = (1-\varepsilon\cos\varphi^*)\,j_3(\varphi_2)$$

$$1+\varepsilon\cos\gamma^* =$$

$$= \frac{\left(1+\frac{\varepsilon^2}{2}\right)(\gamma_2-\gamma_1)+2\varepsilon(\sin\gamma_2-\sin\gamma_1)+\frac{\varepsilon^2}{4}(\sin 2\gamma_2-\sin 2\gamma_1)}{(\gamma_2-\gamma_1)+\varepsilon(\sin\gamma_2-\sin\gamma_1)}$$

This expression holds for the angle between φ_1 and φ_2.

II. $p = 0$ for $\varphi = \varphi_1$ and $\varphi = \varphi_2 = \varphi^*$

In this case, there is no negative pressure between φ_1 and φ_2.

$$1 + \varepsilon \cos \gamma^* =$$

$$= \frac{\left(1 + \frac{\varepsilon^2}{2}\right)(\gamma^* - \gamma_1) + 2\,\varepsilon\,(\sin \gamma^* - \sin \gamma_1) + \frac{\varepsilon^2}{4}(\sin 2\,\gamma^* - \sin 2\,\gamma_1)}{(\gamma^* - \gamma_1) + \varepsilon\,(\sin \gamma^* - \sin \gamma_1)}$$

which holds for the angle between φ_1 and φ_2.

III. $p = 0$ for $\varphi_1 = -\pi$ and $\varphi_2 = \pi$

This gives

$$1 + \varepsilon \cos \gamma^* = \frac{\left(1 + \frac{\varepsilon^2}{2}\right) 2\pi}{2\pi} = 1 + \frac{\varepsilon^2}{2}$$

$$\cos \gamma^* = \frac{\varepsilon}{2}$$

and

$$\cos \varphi^* = \frac{3\,\varepsilon}{2 + \varepsilon^2} \quad \ldots\ldots\ldots\ldots\ldots\ldots \quad 14.1$$

In this case $p = 0$ for $\varphi = 0$

3,2. **Load Capacity**

The load components are from 12.1

$$P_x = P \sin \beta = -\int_{\varphi_1}^{\varphi_2} p \sin \varphi\, r\, d\varphi$$

$$P_y = P \cos \beta = \int_{\varphi_1}^{\varphi_2} p \cos \varphi\, r\, d\varphi$$

The integrals are transformed into

$$P_x = -\int_{\varphi_1}^{\varphi_2} \frac{dp}{d\varphi} \cos\varphi \, r \, d\varphi$$

$$P_y = -\int_{\varphi_1}^{\varphi_2} \frac{dp}{d\varphi} \sin\varphi \, r \, d\varphi$$

With

$$J_1 = j_1(\varphi_2) = \int_{\varphi_1}^{\varphi_2} \frac{d\varphi}{1 - \varepsilon\cos\varphi} = \frac{\gamma_2 - \gamma_1}{\sqrt{1-\varepsilon^2}}$$

$$J_2 = j_2(\varphi_2)$$

$$J_3 = j_3(\varphi_2)$$

the load components can be written

$$P_x = \frac{6\,\eta\,U}{\psi^2} \cdot \frac{J_1 - \frac{J_2^2}{J_3}}{\varepsilon}$$

$$P_y = \frac{6\,\eta\,U}{\psi^2} \left(I_2 - \frac{J_2}{J_3} \cdot I_3 \right)$$

where

$$I_2 = \int_{\varphi_1}^{\varphi_2} \frac{\sin\varphi\, d\varphi}{(1 - \varepsilon\cos\varphi)^2} = \frac{\cos\gamma_2 - \cos\gamma_1}{1 - \varepsilon^2}$$

$$I_3 = \int_{\varphi_1}^{\varphi_2} \frac{\sin\varphi\, d\varphi}{(1 - \varepsilon\cos\varphi)^3} =$$

$$= \frac{(\cos\gamma_2 - \cos\gamma_1) + \frac{\varepsilon}{4}(\cos 2\gamma_2 - \cos 2\gamma_1)}{(1-\varepsilon^2)^2}$$

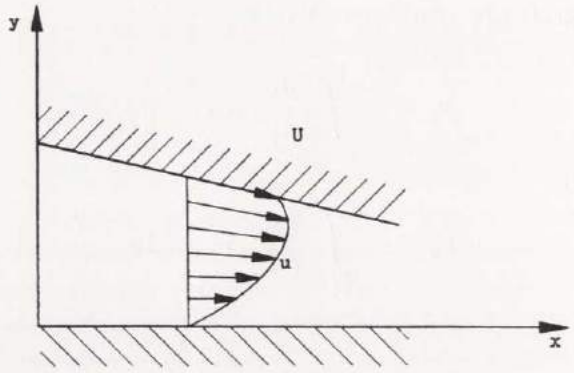

Fig. 16.1

The non-dimensional load components are

$$P_{x0} = \frac{P_x \psi^2}{\eta U} = \frac{6}{\varepsilon}\left(J_1 - \frac{J_2^2}{J_3}\right)$$

$$P_{y0} = \frac{P_y \psi^2}{\eta U} = 6\left(I_2 - \frac{J_2}{J_3} \cdot I_3\right)$$

The angle β between the load line and the line of centres is calculated from

$$\tan \beta = \frac{P_x}{P_y}$$

3,3. Oil Flow

The vertical velocity component can be neglected beside the horizontal component. Fig. 16.1 shows the velocity distribution.

For an oil element

$$\tau = \eta \frac{du}{dy} \quad \ldots\ldots\ldots\ldots\ldots\ldots \quad 16.2$$

and

$$\frac{d\tau}{dy} = \frac{dp}{dx}$$

τ = shear stress.

This gives

$$u = \frac{1}{2\,\eta} \cdot \frac{dp}{dx}\,(y^2 - hy) + \frac{U}{h} \cdot y \quad \ldots\ldots\ldots \quad 17.1$$

The oil flow per unit width is

$$q = \int_0^h u\, dy$$

$$q = \frac{Uh}{2} - \frac{h^3}{12\,\eta} \cdot \frac{dp}{dx} \quad \ldots\ldots\ldots\ldots \quad 17.2$$

With the non-dimensional expressions

$$H = \frac{h}{\Delta r} = 1 - \varepsilon \cos \varphi$$

$$p_0 = \frac{p\,\psi^2}{\eta\,\omega}$$

we can write

$$q_0 = \frac{q}{U \Delta r} = \frac{H}{2} - \frac{H^3}{12} \cdot \frac{dp_0}{d\varphi}$$

3,4. **Friction Force**

The shear stress is obtained from 16.2 and 17.1

$$\tau = \frac{1}{2} \cdot \frac{dp}{dx}\,(2\,y - h) + \eta \cdot \frac{U}{h}$$

With the indices j for journal and b for bearing

$$y = h \qquad \tau_j = \frac{h}{2} \cdot \frac{dp}{dx} + \eta \cdot \frac{U}{h}$$

$$y = 0 \qquad \tau_b = -\frac{h}{2} \cdot \frac{dp}{dx} + \eta \cdot \frac{U}{h}$$

τ is the shear stress on an oil element.

The friction forces per unit bearing length

$$F_j = \int_{\varphi_1}^{\varphi_2} \tau_j \, r \, d\varphi$$

$$F_b = \int_{\varphi_1}^{\varphi_2} \tau_b \, r \, d\varphi$$

and

$$F_j = \int_{\varphi_1}^{\varphi_2} \left(\frac{h}{2} \cdot \frac{dp}{dx} + \eta \cdot \frac{U}{h} \right) r \, d\varphi$$

$$F_b = \int_{\varphi_1}^{\varphi_2} \left(-\frac{h}{2} \cdot \frac{dp}{dx} + \eta \cdot \frac{U}{h} \right) r \, d\varphi$$

or non-dimensionally

$$F_{j0} = \frac{F_j \, \psi}{\eta \, U} = \int_{\varphi_1}^{\varphi_2} \left(\frac{4}{H} - \frac{3 \, H^*}{H^2} \right) d\varphi \quad \ldots\ldots\ldots \quad 18.1$$

$$F_{b0} = \frac{F_b \, \psi}{\eta \, U} = \int_{\varphi_1}^{\varphi_2} \left(\frac{3 \, H^*}{H^2} - \frac{2}{H} \right) d\varphi$$

or

$$F_{j0} = 4 \, J_1 - 3 \, H^* \, J_2$$

$$F_{b0} = 3 \, H^* \, J_2 - 2 \, J_1$$

3,5. Friction Torque

The friction torques for journal and bearing per unit length are

$$M_j = F_j r = \frac{\eta \, U}{\psi} \cdot F_{j0} r$$

$$M_b = F_b r = \frac{\eta \, U}{\psi} \cdot F_{b0} r$$

Non-dimensionally

$$M_{j0} = \frac{M_j \psi}{\eta U r} = F_{j0}$$

$$M_{b0} = \frac{M_b \psi}{\eta U r} = F_{b0}$$

The relation between these two is derived through equilibrium condition for the oil film in fig. 12.1.

$$M_j = M_b + P e \sin \beta$$

With non-dimensional expressions

$$M_{j0} \cdot \frac{\eta U r}{\psi} = M_{b0} \cdot \frac{\eta U r}{\psi} + P_0 \cdot \frac{\eta U}{\psi^2} \cdot \varepsilon \Delta r \sin \beta$$

now

$$\psi = \frac{\Delta r}{r}$$

and

$$M_{j0} = M_{b0} + P_0 \varepsilon \sin \beta$$

3,6. Power Loss

The power loss per unit length of the rotating shaft is

$$E = F_j U = \frac{\eta U}{\psi} \cdot F_{j0} U$$

$$\therefore E = \frac{\eta U^2}{\psi} \cdot F_{j0}$$

The non-dimensional expression for the power loss then becomes

$$E_0 = \frac{E \psi}{\eta U^2} = F_{j0}$$

It is interesting to note that the non-dimensional expressions for friction force, friction torque, and power loss per unit length have the same value.

3,7. **Temperature Rise**

Between the two points φ_1 and φ_2, with the same pressure, the temperature rise is Δt. The total power loss is assumed to heat the oil, conduction being neglected.

Then the energy equation gives

$$F_j U = c \varrho q \Delta t$$

where c = specific heat of oil
ϱ = density of oil

$$\therefore \quad \Delta t = \frac{F_j U}{c \varrho q}$$

Since

$$F_j = \frac{\eta U}{\psi} \cdot F_{j0}$$

and

$$q = U \Delta r q_0$$

$$\Delta t = \frac{1}{c \varrho} \cdot \frac{\eta \omega}{\psi^2} \cdot \frac{F_{j0}}{q_0}$$

The non-dimensional temperature rise then becomes

$$\Delta t_0 = c \varrho \cdot \frac{\Delta t \psi^2}{\eta \omega} = \frac{F_{j0}}{q_0} = \frac{E_0}{q_0}$$

4. The 360° Bearing without Vapour Regions

4,1. Infinitesimal Compression and Boundary Conditions

Consider an infinitely wide journal bearing with given radius, clearance, and eccentricity. The space between journal and bearing is filled with oil, and this space is assumed to be completely separated from the atmosphere. In the beginning, the shaft does not rotate, and the pressure in the oil film is equal to an arbitrary initial pressure. The shaft starts rotating, and the speed is increased very slowly, so that the oil film is not influenced by the acceleration. At a certain speed, the pressure curve has the form shown in 21.1.

This curve is antisymmetrical with respect to the angle of minimum film thickness. The pressure is higher than the initial pressure in the convergent part, and lower in the divergent part of the oil flow. If the oil is assumed to be infinitesimally compressible in proportion to the pressure increase, the increase of the volume at an angle φ is equal to the decrease at $-\varphi$; therefore, the average pressure is the same as the initial pressure.

There are no problems at increasing rotational speed until the pressure curve reaches the vapour pressure. When this occurs, vaporization will appear. There is, however, no space for a volume increase, and therefore the average pressure must increase, while the pressure gradient of 11.3 is not influenced.

The increase in average pressure is assumed to give the oil an infinitesimal compression. This balances an infinitesimal vaporization. The new pressure curve is shown in 22.1.

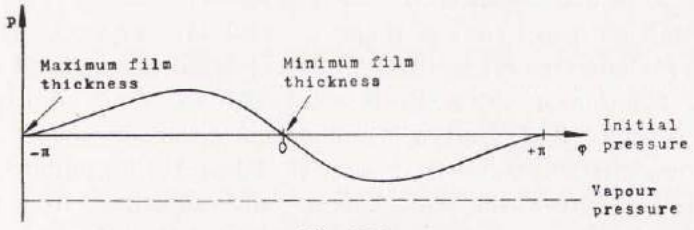

Fig. 21.1

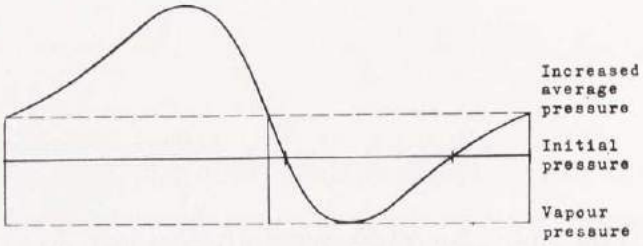

Fig. 22.1

If now the rotational speed is reduced, the average pressure decreases to the initial average pressure, and when the journal has come to a standstill, the pressure is again constant.

According to this theory, the full SOMMERFELD conditions are theoretically possible. It is, however, not possible to have a bearing with the same oil all the time, because of the temperature rise. Consequently, it is necessary to change the oil. This can be done through an axial groove at an arbitrary angle, if the oil pressure in the groove coincides with the pressure in the oil film at this angle. In this theoretical treatise, the oil groove is assumed to be a straight line, having no width in peripheral direction. If the changed quantity of oil is equal to the oil flow $q = \frac{Uh^*}{2}$ in the bearing, the temperature rise Δt is the same as that in the oil film. If now the changed quantity is nq, the temperature rise of the oil for the cooling system is $\frac{\Delta t}{n}$; but in the oil film the rise is still Δt.

The full SOMMERFELD conditions are realized if an oil reservoir with arbitrary pressure is connected with the bearing at an angle between the points φ' and φ'' in 23.1, where the pressure curve with the vapour pressure as a tangent crosses the reservoir pressure.

An infinite bearing could perform without changing the oil if a coolant were introduced in the bearing metal.

Several authors, among them GÜMBEL (5), FRÄNKEL (4), TEN BOSCH (1), and OTT (6) treat the infinite journal bearing and use the theory for this as given by SOMMERFELD (8); but unfortunately all refer to the finite bearing in maintaining that air comes in from the sides. In the theoretical case of a bearing of infinite width, nothing comes from the sides; but air can be dissolved from the oil. It is obviously not correct to mix the theory of the infinite and finite

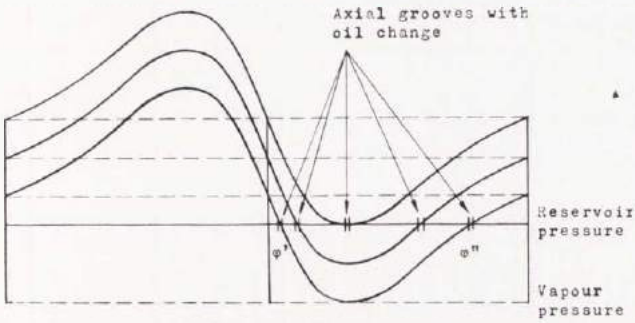

Fig. 23.1

bearings. The infinite bearing must be thought of as a finite one with ideally tight side-packings.

In his paper »Berechnung von zylindrischen Gleitlagern» FRÄNKEL (4) writes: »Da SOMMERFELD seine Berechnungen unter Berücksichtigung dieser negativen Drücke durchführte, hat er Ergebnisse erhalten, welche mit der Wirklichkeit nicht übereinstimmten (z. B. horizontale Verlagerungskurve des Wellenmittelpunktes), und deshalb wenig beachtet wurden.» SOMMERFELD's calculations are made for an infinite bearing and are completely correct. For vertical bearing load, the attitude-eccentricity curve is a straight horizontal line because of the antisymmetrical pressure curve. The main problem, since 1904, has been the boundary conditions. Authors who have treated this problem have assumed one or both of the boundary conditions and have no satisfactory solution for the region with pressure lower than atmospheric pressure. They have avoided negative pressures, putting $p = p_{\text{atm}}$ as the lowest oil film pressure. The pressure curve, however, can, as shown, be strictly treated, the negative pressure region giving no special difficulty.

4,2. Pressure Curves

The pressure curve is antisymmetrical with respect to the minimum film thickness, and equal to the average pressure at $\varphi = 0$ and $\varphi = \pm \pi$. We assume that the oil groove is located at the point of minimum film pressure and put this equal to zero.

Then the expression for the pressure becomes

$$p_0 = p_{0a} - \frac{6\,\varepsilon}{2 + \varepsilon^2} \cdot \sin\varphi \left[\frac{1}{1 - \varepsilon\cos\varphi} + \frac{1}{(1 - \varepsilon\cos\varphi)^2} \right] \qquad 23.2$$

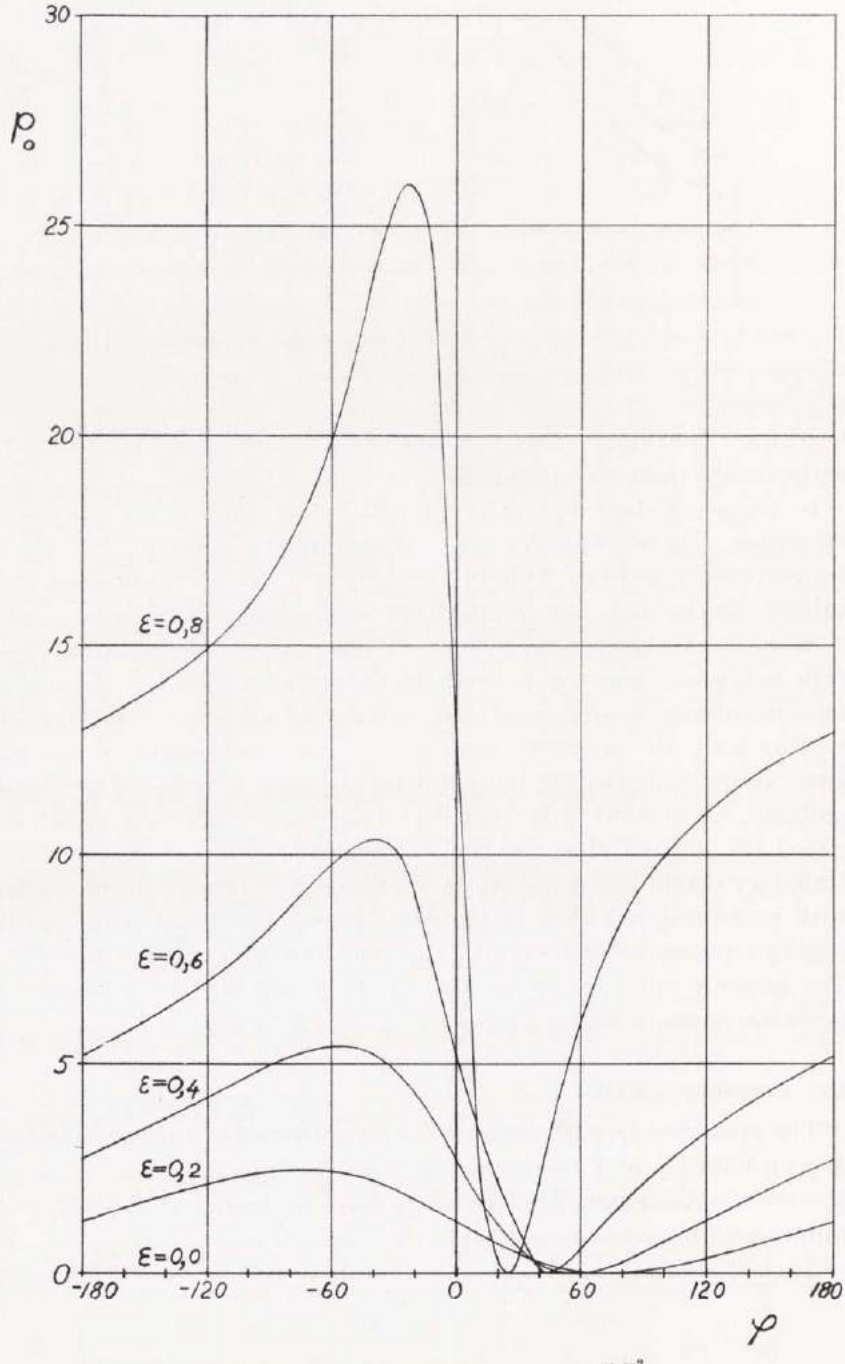

Fig. 24.1. Pressure Curves $p_0 = \frac{p\,\psi^2}{\eta\,\omega}$

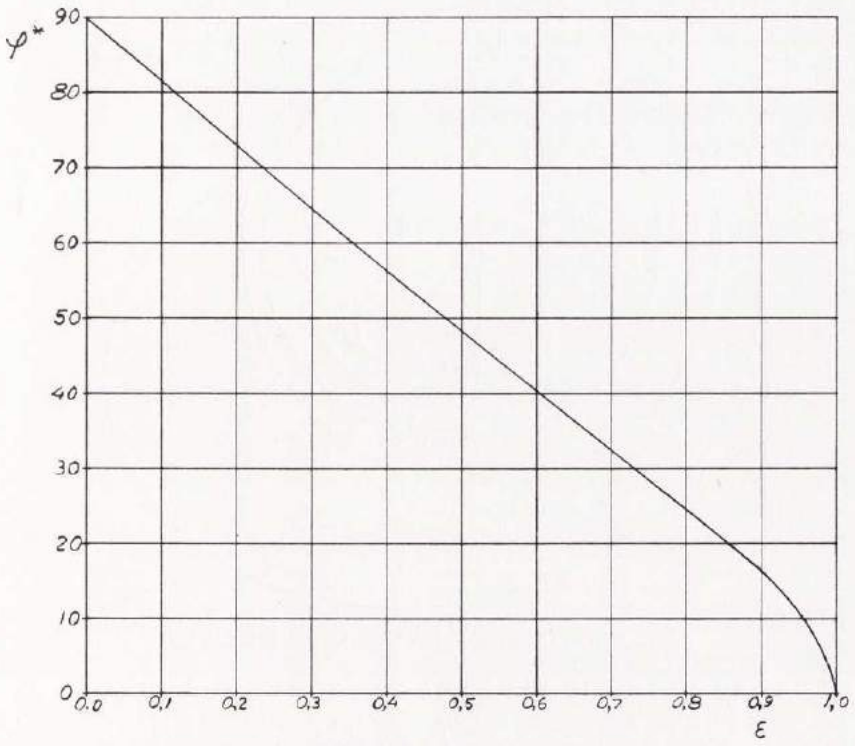

Fig. 25.1. $\varphi^* = f(\varepsilon)$

where

$$p_{0a} = \frac{3\,\varepsilon}{2\,(2+\varepsilon^2)} \sqrt{\left(\frac{4-\varepsilon^2}{1-\varepsilon^2}\right)^3} \qquad \text{25.2}$$

p_0 is drawn as a function of φ for different ε in 24.1. Fig. 25.1 gives φ^* as a function of ε. Fig. 26.1 shows an infinite journal bearing with vertical load and operating with an eccentricity of 0,6. The oil groove with the pressure equal to zero is located at $\varphi = 40{,}3°$ from the horizontal line of centres. The pressure is positive all around the circumference.

4,3. **Load Capacity**

From 3,2 we have

$$P_{x0} = \frac{6}{\varepsilon}\left(J_1 - \frac{J_2^2}{J_3}\right)$$

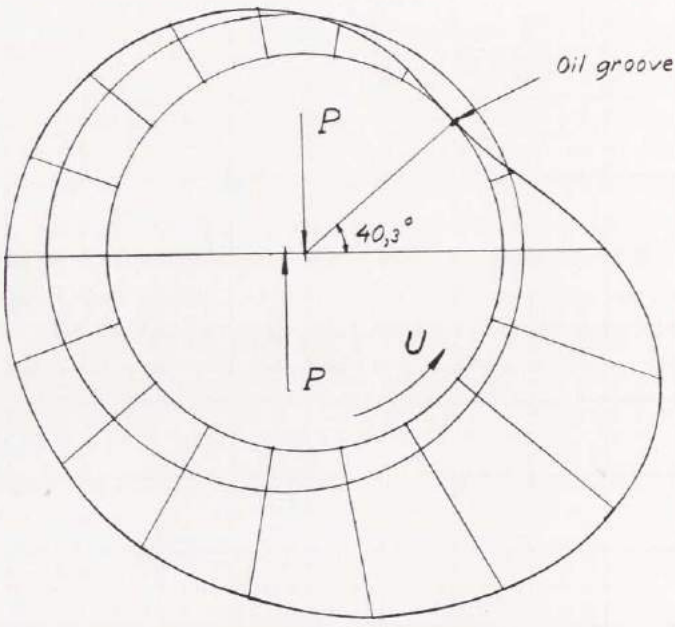

Fig. 26.1. Theoretical Pressure Curve for $\varepsilon = 0{,}6$

$$P_{y0} = 6\left(I_2 - \frac{J_2}{J_3} \cdot I_3\right)$$

Now

$$\gamma_1 = -\pi \qquad \gamma_2 = \pi$$

and

$$P_{x0} = \frac{12\,\pi\,\varepsilon}{(2+\varepsilon^2)\sqrt{1-\varepsilon^2}}$$

$$P_{y0} = 0$$

The non-dimensional load capacity per unit length and the attitude angle then become

$$P_0 = \frac{P\,\psi^2}{\eta\,U} = \frac{12\,\pi\,\varepsilon}{(2+\varepsilon^2)\sqrt{1-\varepsilon^2}}$$

$$\beta = 90^\circ$$

P_0 is shown as function of ε in 27.1.

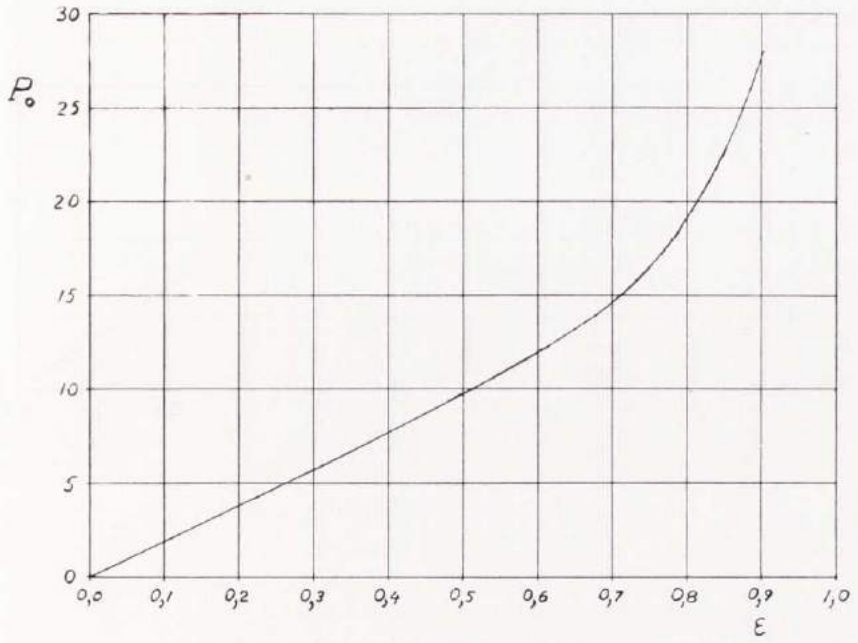

Fig. 27.1. Load Capacity $P_0 = \dfrac{P\,\psi^2}{\eta\,U}$

4,4. Oil Flow

For the oil flow per unit width we have from 17.2 the expression

$$q = \frac{Uh}{2} - \frac{h^3}{12\,\eta} \cdot \frac{dp}{dx} = \frac{Uh^*}{2} = \text{const}$$

Non-dimensionally

$$q_0 = \frac{q}{U\Delta r} = \frac{H^*}{2} = \frac{1 - \varepsilon \cos \varphi^*}{2}$$

but

$$\cos \varphi^* = \frac{3\,\varepsilon}{2 + \varepsilon^2}$$

and then

$$q_0 = \frac{q}{U\Delta r} = \frac{1 - \varepsilon^2}{2 + \varepsilon^2}$$

which is shown in 28.1.

The oil volume in the bearing is $Q = 2\,\pi\,r\,\Delta r$ per unit width.

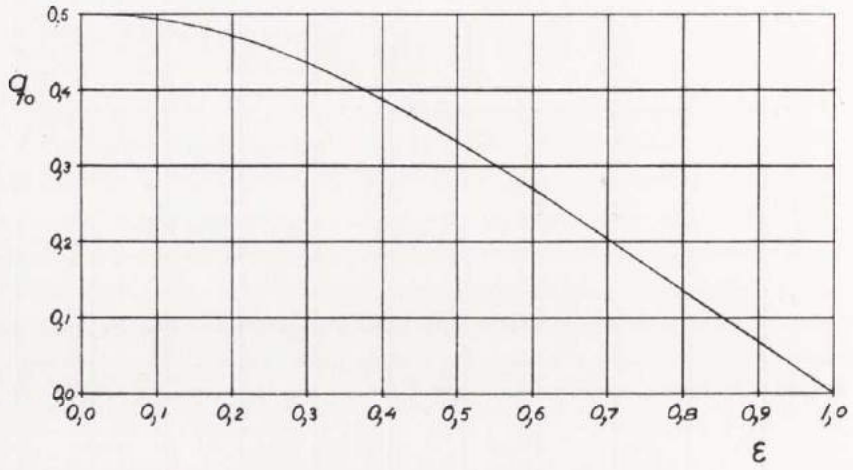

Fig. 28.1. Oil Flow per Unit Width $q_0 = \frac{q}{U \Delta r}$

4,5. Friction Force, Friction Torque, and Power Loss

From 18.1

$$F_{j0} = M_{j0} = E_0 = \int_{\varphi_1}^{\varphi_2} \left(\frac{4}{H} - \frac{3\, H^*}{H^2} \right) d\varphi$$

Integration between $-\pi$ and π gives the non-dimensional expression for friction force, friction torque, and power loss per unit width.

$$F_{j0} = \frac{F_j\, \psi}{\eta\, U} =$$

$$= M_{j0} = \frac{M_j\, \psi}{\eta\, U\, r} =$$

$$= E_0 = \frac{E\, \psi}{\eta\, U^2} = \frac{4\, \pi\, (1 + 2\, \varepsilon^2)}{(2 + \varepsilon^2)\, \sqrt{1 - \varepsilon^2}}$$

This function is drawn in 29.1.

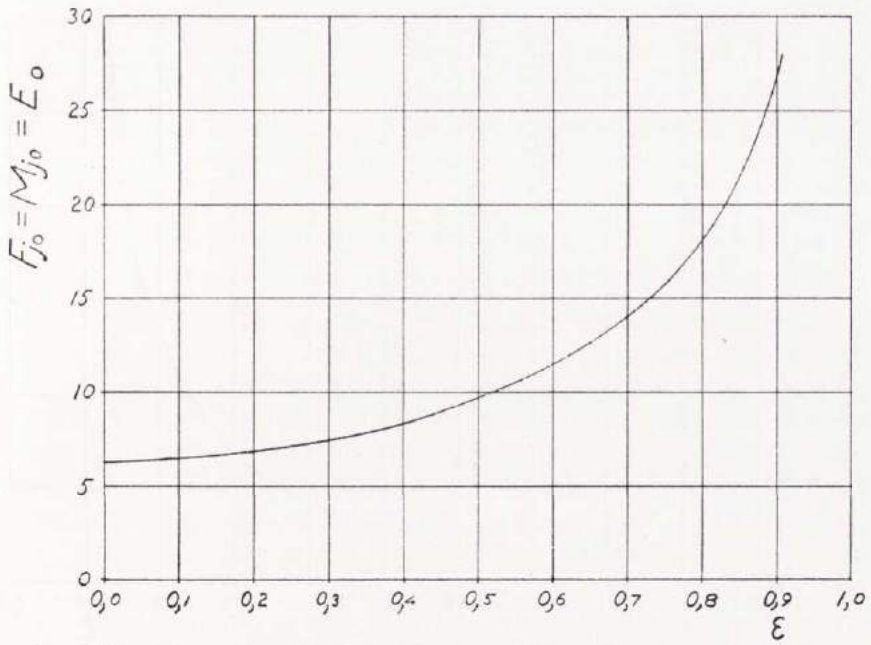

Fig. 29.1. Friction Force, Friction Torque, and Power Loss per Unit Width

$$F_{j0} = \frac{F_j\,\psi}{\eta\,U} = M_{j0} = \frac{M_j\,\psi}{\eta\,U\,r} = E_0 = \frac{E\,\psi}{\eta\,U^2}$$

4,6. Temperature Rise

Assume that no conduction exists and all the power generated is supplied to the oil. Then the non-dimensional temperature rise for an angle of $2\,\pi$ is

$$\Delta t_0 = c\,\varrho \cdot \frac{\Delta t\,\psi^2}{\eta\,\omega} = \frac{E_0}{q_0} = \frac{4\,\pi\,(1 + 2\,\varepsilon^2)}{\sqrt{(1 - \varepsilon^2)^3}}$$

which is shown in 30.1.

The temperature rise between the angle of minimum film thickness and an arbitrary angle is

$$\int_0^{\varphi} \Delta t_0 = \frac{1}{\sqrt{(1 - \varepsilon^2)^3}} \cdot \frac{1}{2 + \varepsilon^2}\,[2\,(2 + \varepsilon^2)\,(1 + 2\,\varepsilon^2)\,\gamma - 12\,\varepsilon^3 \sin\,\gamma +$$

$$+ 3\,\varepsilon^2 \sin 2\,\gamma]$$

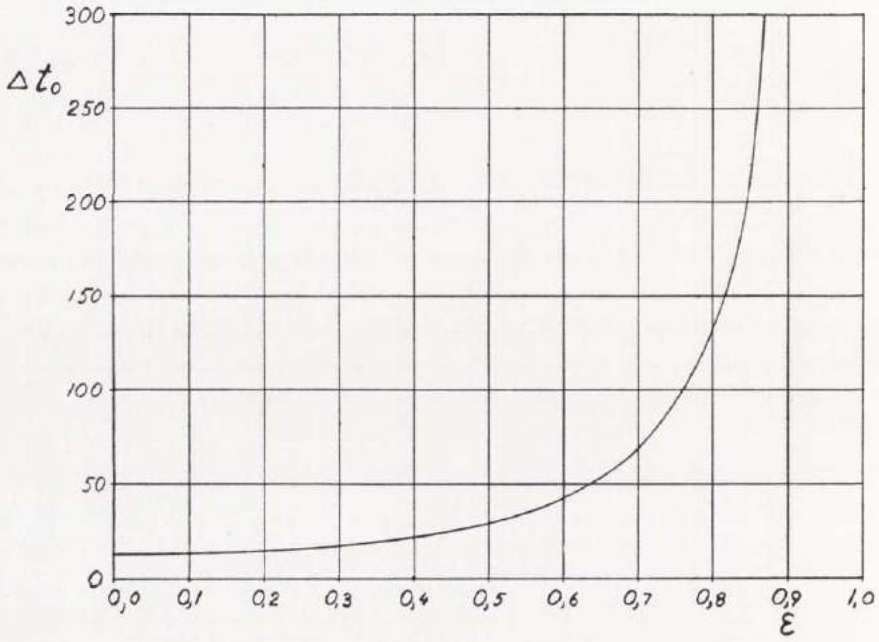

Fig. 30.1. Temperature Rise $\Delta t_0 = c \cdot \varrho \cdot \frac{\Delta t \cdot \psi^2}{\eta \cdot \omega}$

where

$$\gamma = \text{arc cos} \frac{\cos \varphi - \varepsilon}{1 - \varepsilon \cos \varphi}$$

4,7. Coefficient of Friction and Relative Power Loss

The coefficient of friction is defined as friction force per unit load

$$\mu = \frac{F_j}{P}$$

or

$$\mu = \frac{\psi (1 + 2 \varepsilon^2)}{3 \varepsilon} \quad \ldots\ldots\ldots\ldots\ldots\ldots \quad 30.2$$

The definition of the relative power loss, as introduced here, is power loss per unit load; and this is the most important value for

a bearing. A practical condition is that the power loss for a given load capacity is as low as possible. This means that the relative power loss will have an optimum value.

$$f = \frac{E}{P}$$

or

$$f = \frac{\omega \, \Delta r \, (1 + 2 \, \varepsilon^2)}{3 \, \varepsilon} \quad \ldots\ldots\ldots\ldots \quad 31.1$$

If ψ is constant in the coefficient of friction, and ω and Δr are constant in the relative power loss, the non-dimensional expressions for those two are the same.

From 30.2 and 31.1 we find

$$\frac{\mu}{\psi} = \frac{f}{\omega \, \Delta r} = \frac{1 + 2 \, \varepsilon^2}{3 \, \varepsilon} \quad \ldots\ldots\ldots\ldots \quad 31.2$$

The minimum of 31.2 is

$$\frac{\mu_{\min}}{\psi} = \frac{f_{\min}}{\omega \, \Delta r} = \frac{2 \sqrt{2}}{3} = 0,9428$$

for

$$\varepsilon = \frac{\sqrt{2}}{2} = 0,7071$$

The variation of $\frac{\mu}{\psi}$ and $\frac{f}{\omega \, \Delta r}$ for $0,5 < \varepsilon < 1$ is very small

$0,9428 < \frac{\mu}{\psi} < 1$.

Above ψ and Δr were constant. Assume now the minimum film thickness $h_{\min}$ to have a given constant value, as $h_{\min}$ is an important design parameter.

The film thickness is

$$h = \Delta r \, (1 - \varepsilon \cos \varphi)$$

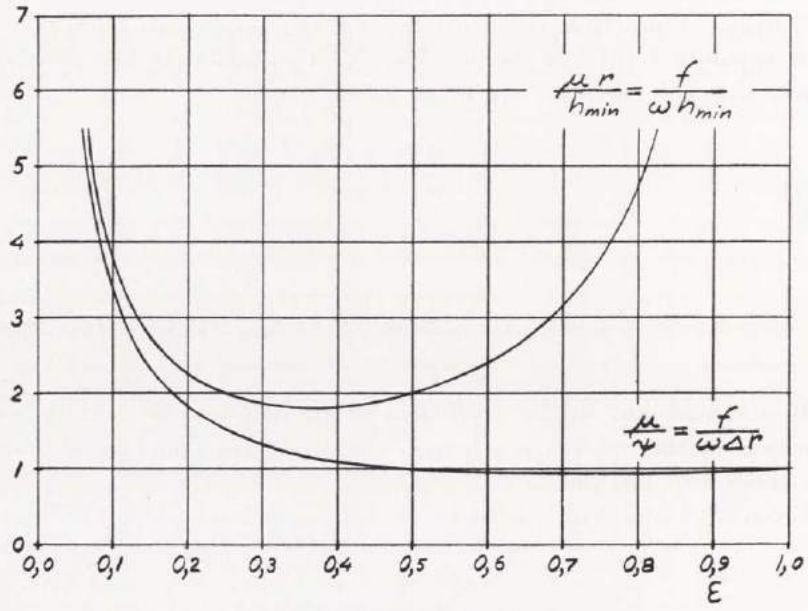

Fig. 32.1. Coefficient of Friction and Relative Power Loss

and then

$$h_{\min} = \Delta r\,(1 - \varepsilon)$$

$$\because\ \Delta r = \frac{h_{\min}}{1 - \varepsilon}$$

Substitute this for Δr.

$$\frac{\mu\, r}{h_{\min}} = \frac{f}{\omega\, h_{\min}} = \frac{1 + 2\,\varepsilon^2}{3\,\varepsilon\,(1 - \varepsilon)} \qquad \ldots\ldots\ldots\ldots\ldots\ 32.2$$

Through derivation

$$\frac{\mu_{\min}\, r}{h_{\min}} = \frac{f_{\min}}{\omega\, h_{\min}} = \frac{2\left(\sqrt{3} + 1\right)}{3} = 1{,}821$$

for

$$\varepsilon = \frac{\sqrt{3} - 1}{2} = 0{,}3660$$

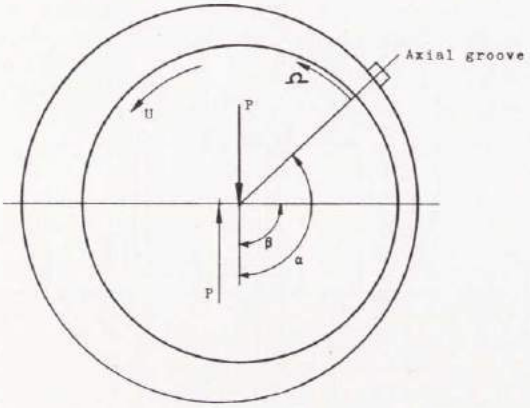

Fig. 33.1

As seen from 32.1, the curve of 32.2 has a more pronounced minimum than 31.2, showing that correct design is important.

4,8. Experimental Investigation

The data for the experimental journal bearing were:

$$r = 50 \text{ mm}$$
$$\psi = 0{,}00825$$

The bearing had a width of 135 mm, and there were seals at the sides with axial clearance of about 0,02 mm and radial length of about 20 mm. The oil was exchanged at about atmospheric pressure at an axial groove, the angle of which relative to the load could be varied. The pressures were measured at 18 points in the middle of the bearing, with intervals of 20°, by means of a mercury manometer with 18 glass tubes. Simultaneous readings were taken from photos of the manometer. Maximum allowable pressure was about 3 atm g. Fig. 33.1 gives the principle of the test bearing, and a sketch over the rig is shown in 34.1.

The journal was carried by two ball bearings; and the load was vertically directed. The angle Ω is measured from the oil groove in rotational direction. The rotational speed was varied from 450 to 1500 rpm.

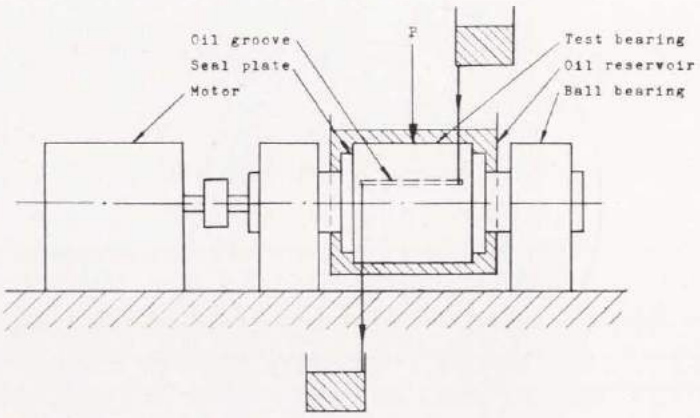

Fig. 34.1

From the experiments we see that it is possible to have a bearing operating with positive pressure all around the circumference, as in 35.1 and 37.1. There is evidently not atmospheric pressure at the maximum film thickness, which is a usual assumption. If the average pressure is drawn in 35.1, we find the locations of minimum and maximum film thickness. For φ^* we can read the value 40°, and from 14.1 $\varepsilon = 0{,}60$. The angle between load line and line of centres is 92°. The theory gives 90°.

The experimental pressure curve in 38.1 should be compared with the theoretical curve in 26.1. In both cases: $\varepsilon = 0{,}60$, and the pressures are non-dimensional.

In 39.1 and 39.2, the theoretical curves for nondimensional pressure are shown together with the experimental points.

Two experiments are analysed in detail:

1) Fig. 35.1 and 39.1

$\eta = 0{,}0161\ \mathrm{Ns/m^2}$

$\omega = 47{,}3\ \mathrm{1/s}$

$\alpha = 130°$

$\varphi^* = 40°$

$\varepsilon = 0{,}60$

$\beta = 91°$

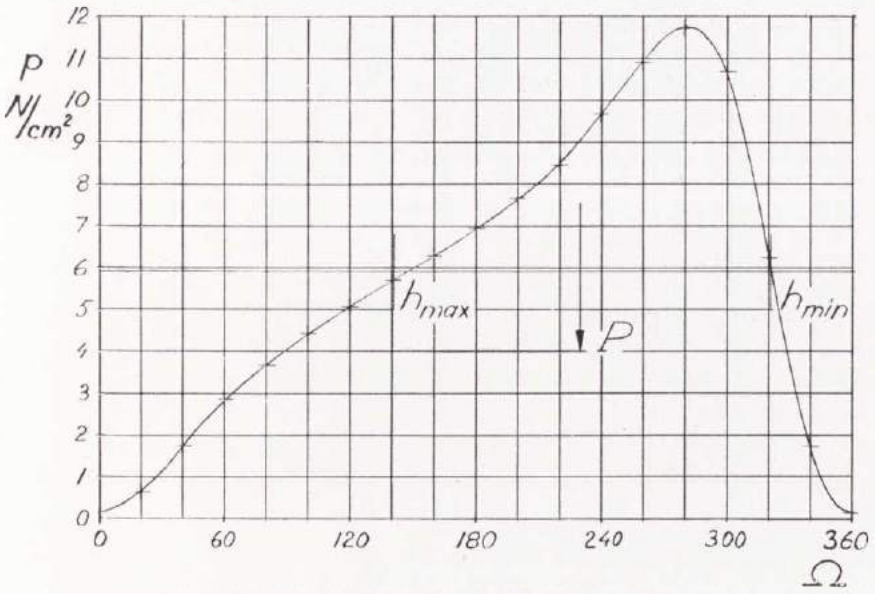

Fig. 35.1. Experimental Pressure Curve for $\varepsilon = 0{,}60$

Experimental maximum pressure

$$p_e = 11{,}6 \text{ N/cm}^2$$

$$p_{0e} = \frac{p_e \psi^2}{\eta \omega} = \frac{11{,}6 \cdot 10^4 \cdot 0{,}00825^2}{0{,}0161 \cdot 47{,}3}$$

$$p_{0e} = 10{,}4$$

Theoretical maximum pressure from 25.2

$$p_{0t} = 2 \cdot 5{,}17265 = 10{,}345$$

Ratio $$\frac{p_{0e}}{p_{0t}} = \frac{10{,}4}{10{,}345} = 101\ \%$$

Experimental load capacity

$$p_e = 6750 \text{ N/m}$$

$$p_{0e} = \frac{P_e \psi^2}{\eta U} = \frac{6750 \cdot 0{,}00825^2}{0{,}0161 \cdot 0{,}05 \cdot 47{,}3}$$

$$P_{0e} = 12{,}1$$

Theoretical load capacity

$$P_{0t} = 11{,}981$$

Ratio $$\frac{P_{0e}}{P_{0t}} = \frac{12{,}1}{11{,}981} = 101\ \%$$

2) Fig. 37.1 and 39.2

$\eta = 0{,}0161\ \mathrm{Ns/m^2}$

$\omega = 63{,}8\ \mathrm{1/s}$

$\alpha = 150^\circ$

$\varphi^* = 56^\circ$

$\varepsilon = 0{,}40$

$\beta = 92^\circ$

Experimental maximum pressure

$$p_e = 8{,}05\ \mathrm{N/cm^2}$$

$$p_{0e} = \frac{8{,}05 \cdot 10^4 \cdot 0{,}00825^2}{0{,}0161 \cdot 63{,}8} = 5{,}33$$

Theoretical maximum pressure from 25.2

$$p_{0t} = 2 \cdot 2{,}715 = 5{,}430$$

Ratio $$\frac{p_{0e}}{p_{0t}} = \frac{5{,}33}{5{,}430} = 98\ \%$$

Experimental load capacity

$$P_e = 5670\ \mathrm{N/m}$$

$$P_{0e} = \frac{5670 \cdot 0{,}00825^2}{0{,}0161 \cdot 0{,}05 \cdot 63{,}8} = 7{,}51$$

Theoretical load capacity

$$P_{0t} = 7{,}617$$

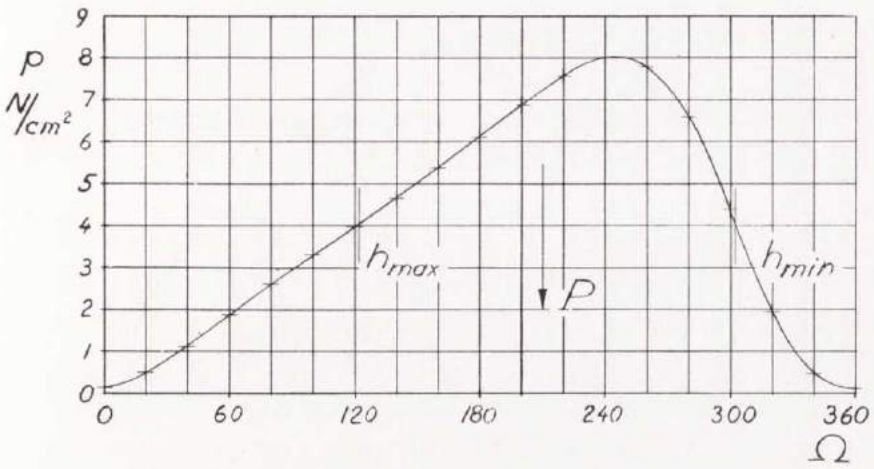

Fig. 37.1. Experimental Pressure Curve for $\varepsilon = 0{,}40$

Ratio $$\frac{P_{0e}}{P_{0t}} = \frac{7{,}51}{7{,}617} = 99\ \%$$

In the two experiments the difference between the theoretical and experimental values is less than the measurement accuracy.

Theoretical loads from the paper »The Full Journal Bearing» by CAMERON and WOOD (2) for infinite width are

ε	P_0
0,6	8,17
0,4	4,97

compared to the test values here

ε	P_0
0,6	12,1
0,4	7,51

The experimental load on this bearing with side seals is thus about 50 % greater than the usually used theoretical load for an infinitely wide bearing, where the oil film pressure starts at the maximum space and has zero derivative at the end.

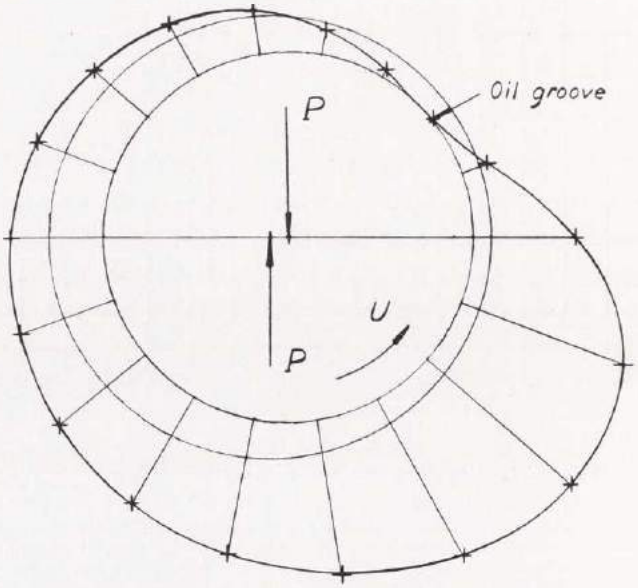

Fig. 38.1. Experimental Pressure Curve for $\varepsilon = 0{,}60$

Fig. 40.1 and 40.2 should be compared with those by CAMERON-WOOD (2), where these problems are discussed. According to experiments by NÜCKER whose pressure curve is considerably lower than that marked with »usual theory» in fig. 40.1, they use this theory based upon the boundary conditions $p = 0$ at $\varphi = -\pi$ and where $\frac{dp}{d\varphi} = 0$. From the experimental points, taken from 39.1, it is evident that their conditions have no theoretical background but are arbitrarily chosen.

The usual attitude-eccentricity ratio curve for the finite bearing, and often for the infinite bearing, too, is a semicircle, as in fig. 40.2. From 4,3 this curve should be a straight horizontal line. CAMERON-WOOD write: »In the full Sommerfeld solution the resultant of pressure round the journal has no component along the line of centres, and the attitude is always at 90 deg. to the load line. It has been clear for a considerable time that all the experimental evidence was against this straight line centre locus.» As shown in 40.2, the experiments, however, have a very close agreement to the horizontal attitude-eccentricity curve.

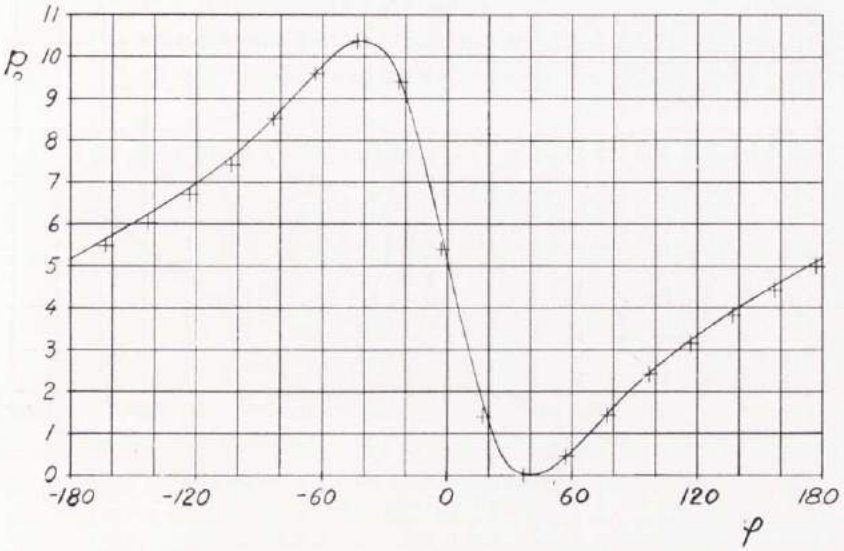

Fig. 39.1. Theoretical Pressure Curve for $\varepsilon = 0{,}60$ $\quad p_0 = \dfrac{p\,\psi^2}{\eta\,\omega}$
+ Experimental points

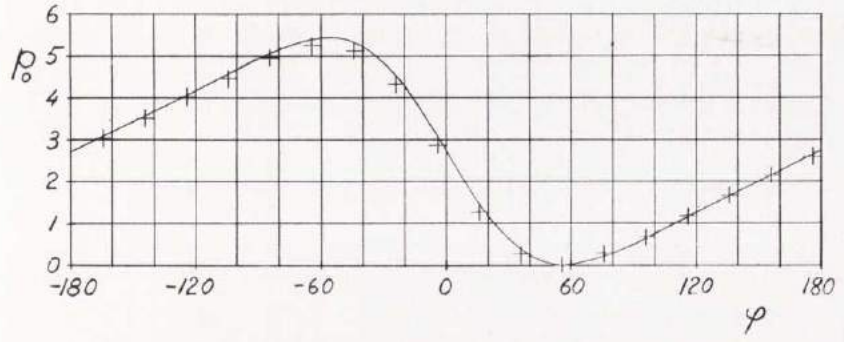

Fig. 39.2. Theoretical Pressure Curve for $\varepsilon = 0{,}40$ $\quad p_0 = \dfrac{p\,\psi^2}{\eta\,\omega}$
+ Experimental points

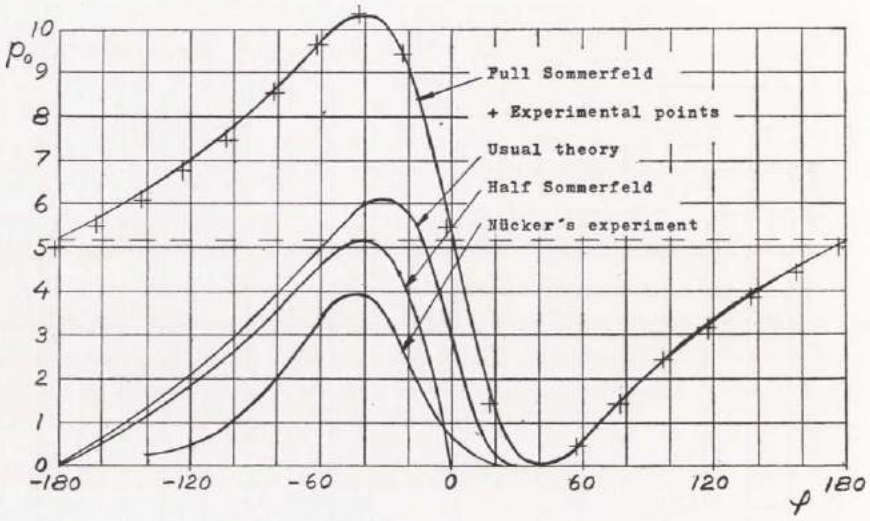

Fig. 40.1. Pressure curves for $\varepsilon = 0{,}60$.
(Compare Cameron-Wood fig. 2)

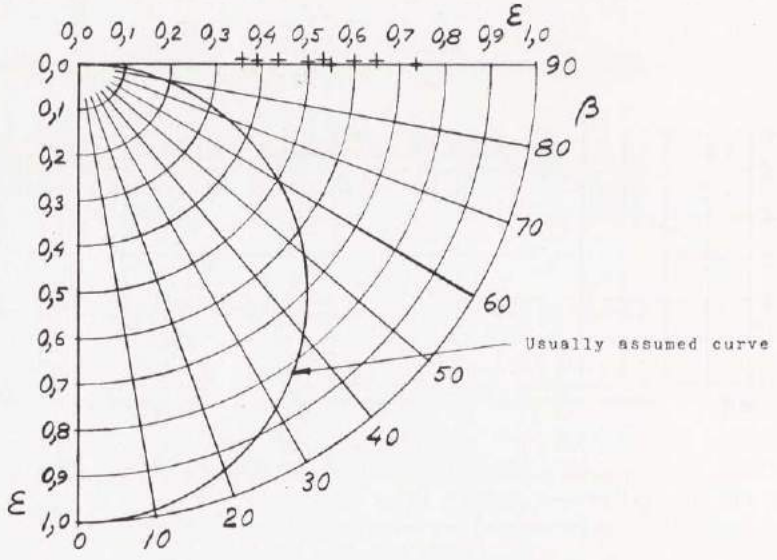

Fig. 40.2. Attitude-Eccentricity Ratio Curves
+ Experimental points.
(Compare Cameron-Wood fig. 3)

5. The 360° Bearing with Vapour Regions

5,1. Vapour Regions and Boundary Conditions

The assumptions are:

The lowest possible oil film pressure value is the vapour pressure. In a vapour region the pressure is constant and equal to this vapour pressure.

This hypothesis holds for an ideal oil. In many cases there is, however, air dissolved in the oil, and in this case the vapour pressure is replaced by the higher value of the »air expulsion pressure of the oil»; but the same theory can still be applied.

Now we will discuss the boundary condition for the pressure at the beginning of a vapour region. The derivative of the pressure cannot be positive, because there is no pressure below the vapour pressure; therefore it must be, as in 41.1, negative or zero.

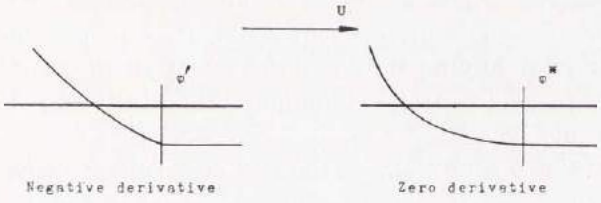

Fig. 41.1

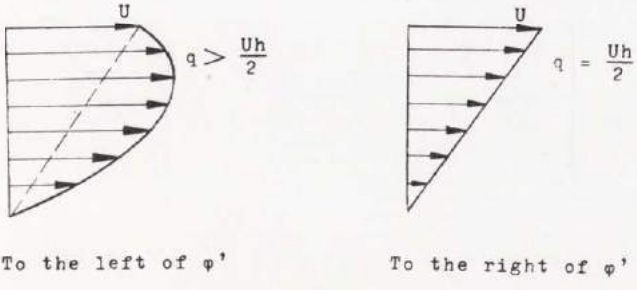

Fig. 41.2

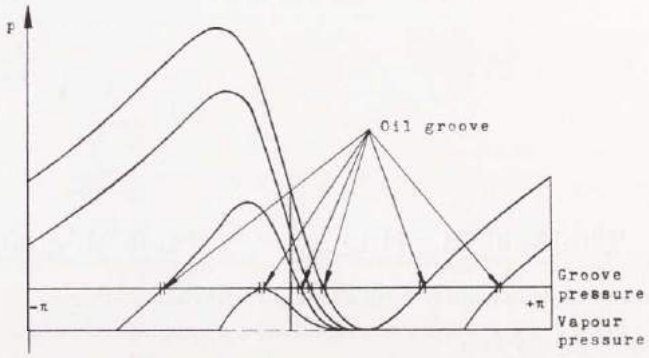

Fig. 42.1. Pressure curves for variable φ^* at $\varepsilon = 0{,}5$

The velocity distribution for negative pressure derivative is shown in 41.2.

The conditions of 41.2 violate the continuity condition, which is fulfilled only if the derivative at the beginning of the vapour region is zero.

The pressure curve is completely determined by ε and φ^*, see 42.1. In practice, the pressure has a given value at a given angle by connection of an oil groove to the bearing. Then φ^* can be computed from this condition. For every oil groove angle there is one, and only one, pressure distribution.

It is possible to get an oil film all around the circumference (SOMMERFELD's solution), and it would also be possible to get a vapour region all around the circumference if an oil groove at vapour pressure were placed at the minimum film thickness. In this case the load would be zero.

The continuity conditions at the end of a vapour region shall now be discussed. The velocity distributions are shown in 42.2.

Fig. 42.2

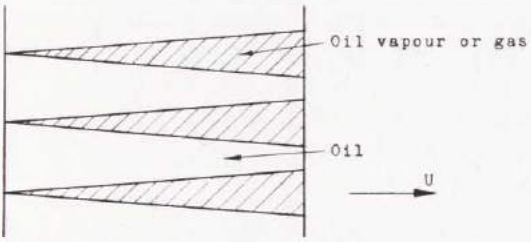

Fig. 43.1

From 42.2 it is clear that the left distribution gives a greater oil flow per unit width than the right one. There is, however, in the vapour region only oil flow over parts of the width, and so the continuity is fulfilled. Thus, a vapour region should look like 43.1, which can be found on photos by COLE-HUGHES (3).

An infinite number of strips is assumed. It is not necessary for the gas to move in rotational direction because of its low viscosity.

If

$$q = \frac{Uh}{2} - \frac{h^3}{12\,\eta} \cdot \frac{dp}{dx} = 0$$

$$\frac{dp}{dx} = \frac{6\,\eta\,U}{h^2}$$

where η is the low vapour or gas viscosity.

This derivative can be neglected beside that for the oil.

5,2. **Pressure Curves**

The general expression for the pressure is

$$p_2 - p_1 = \frac{\eta\,\omega}{\psi^2} \cdot 6 \int_{\varphi_1}^{\varphi_2} \left[\frac{1}{(1 - \varepsilon \cos \varphi)^2} - \frac{1 - \varepsilon \cos \varphi^*}{(1 - \varepsilon \cos \varphi)^3} \right] d\varphi$$

This integral is solved in 3,1.

Putting $\varphi_1 = 0$ at minimum film thickness gives

$$p_2 - p_1 = \frac{\eta\,\omega}{\psi^2} \cdot \frac{6}{\sqrt{(1-\varepsilon^2)^3}} \left[\left(1 - H^* \cdot \frac{2+\varepsilon^2}{2\,(1-\varepsilon^2)} \right) \arccos \left(\frac{\cos\varphi - \varepsilon}{H} \right) + \right.$$

$$+ \left(\varepsilon - H^* \cdot \frac{2\,\varepsilon}{1-\varepsilon^2} \right) \frac{\sin\varphi \sqrt{1-\varepsilon^2}}{H} -$$

$$\left. - H^* \cdot \frac{\varepsilon^2}{2\,(1-\varepsilon^2)} \cdot \frac{\cos\varphi - \varepsilon}{H} \cdot \frac{\sin\varphi \sqrt{1-\varepsilon^2}}{H} \right]$$

where

$$H = 1 - \varepsilon \cos\varphi$$

$$H^* = 1 - \varepsilon \cos\varphi^*$$

In the following figures the pressure is measured from vapour pressure (= 0).

The curves are valid for every vapour pressure; and the line for non-dimensional atmospheric pressure can be drawn afterwards. Pressure curves are drawn for $\varepsilon = 0{,}2$; $0{,}4$; $0{,}6$ and $0{,}8$ in 44.1, 45.1, 45.2, and 46.1.

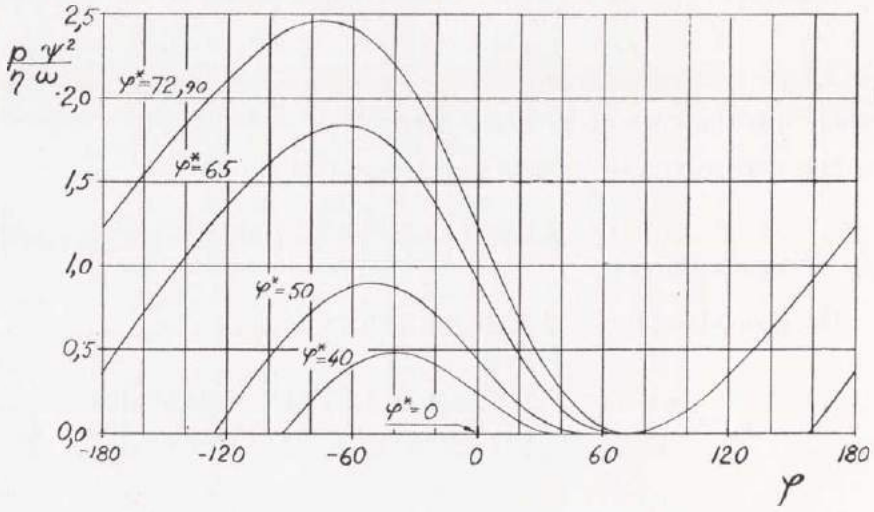

Fig. 44.1. Pressure Curves for $\varepsilon = 0{,}2$ $\qquad p_0 = \frac{p\,\psi^2}{\eta\,\omega}$

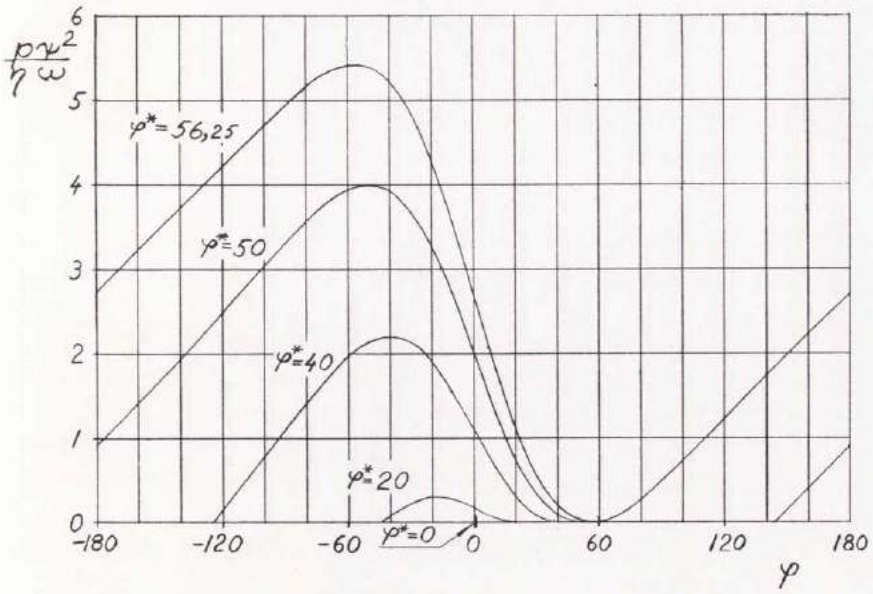

Fig. 45.1. Pressure Curves for $\varepsilon = 0{,}4$ $\qquad p_0 = \dfrac{p\,\psi^2}{\eta\,\omega}$

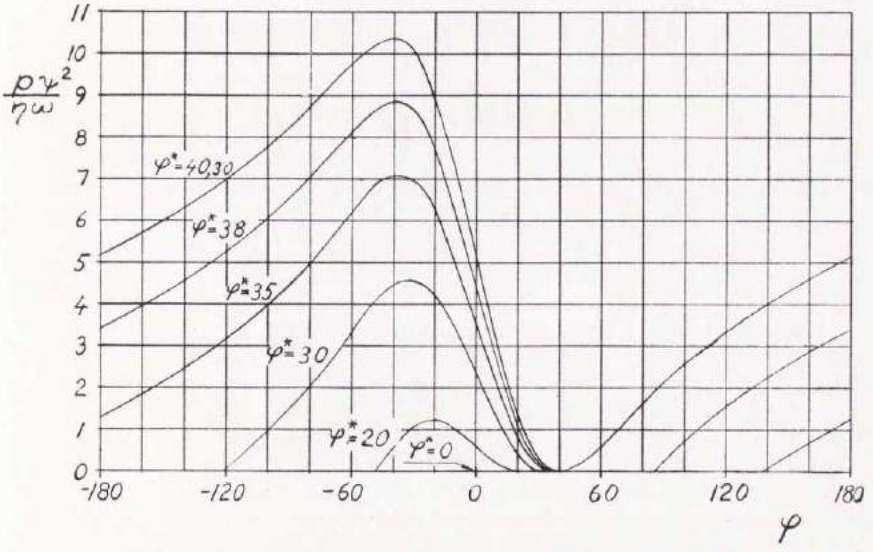

Fig. 45.2. Pressure Curves for $\varepsilon = 0{,}6$ $\qquad p_0 = \dfrac{p\,\psi^2}{\eta\,\omega}$

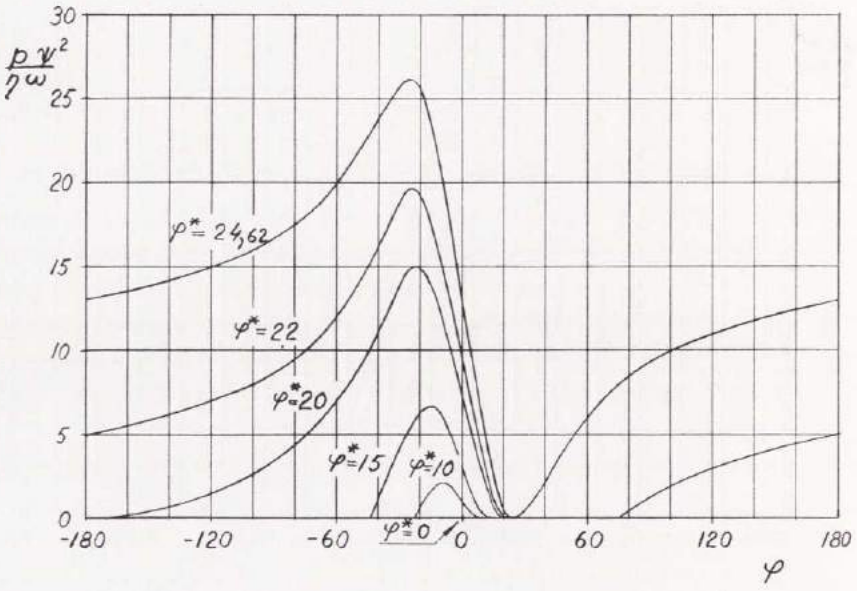

Fig. 46.1. Pressure Curves for $\varepsilon = 0{,}8$ $\qquad p_0 = \dfrac{p\,\psi^2}{\eta\,\omega}$

5,3. **Load Capacity**

For the load components we have

$$P_x = \frac{\eta\, U}{\psi^2} \cdot \frac{6}{\varepsilon}\left(J_1 - \frac{J_2^2}{J_3}\right)$$

$$P_y = \frac{\eta\, U}{\psi^2} \cdot 6\left(I_2 - \frac{J_2}{J_3} \cdot I_3\right)$$

The quantities I and J are introduced in 3,2.

$$P = \sqrt{P_x^2 + P_y^2}$$

$$\tan\,\beta = \frac{P_x}{P_y}$$

Curves over P_0 and β are shown in 47.1 and 48.1 as functions of ε and φ^*.

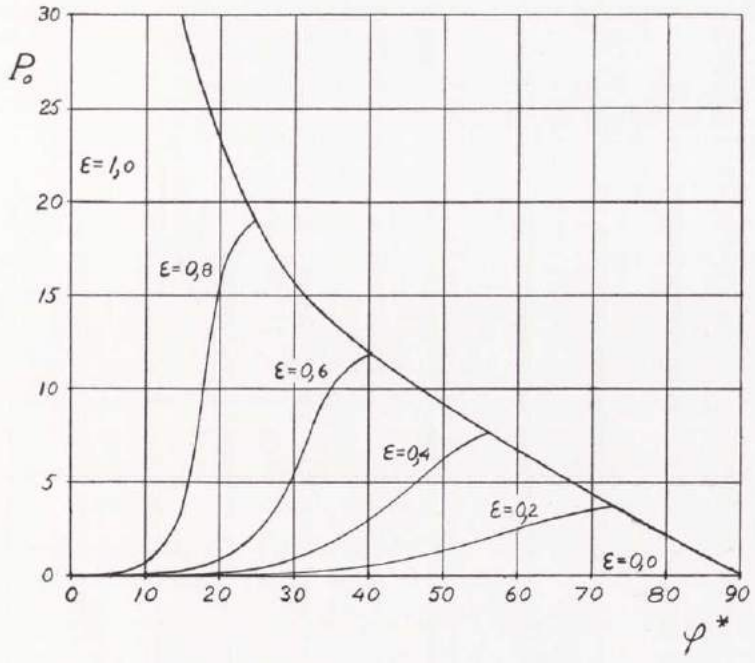

Fig. 47.1. Load Capacity $P_0 = \frac{P \psi^2}{\eta U}$

Attitude-eccentricity curves for various values of the angle between the load and the beginning of the oil film are shown in 50.1. Attitude-eccentricity curves for various values of the angle between the load and the end of the oil film are drawn in 51.1. When the centre is moving through changing rotational speed or load, the curves in both diagrams must be studied for angles between 90° and 180°. Curves for constant non-dimensional load capacity are shown in 49.1.

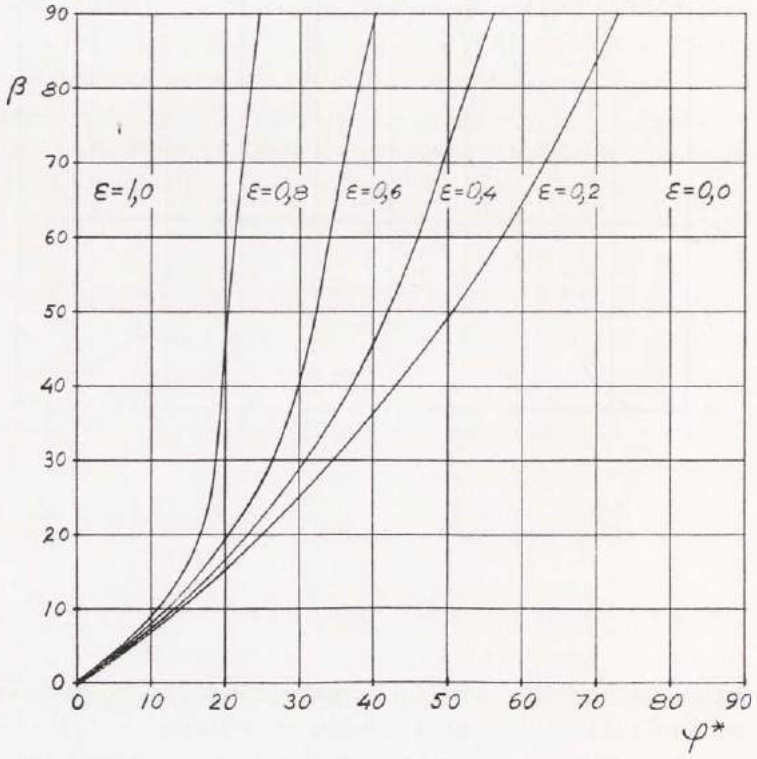

Fig. 48.1. Angle between Load Line and Line of Centres

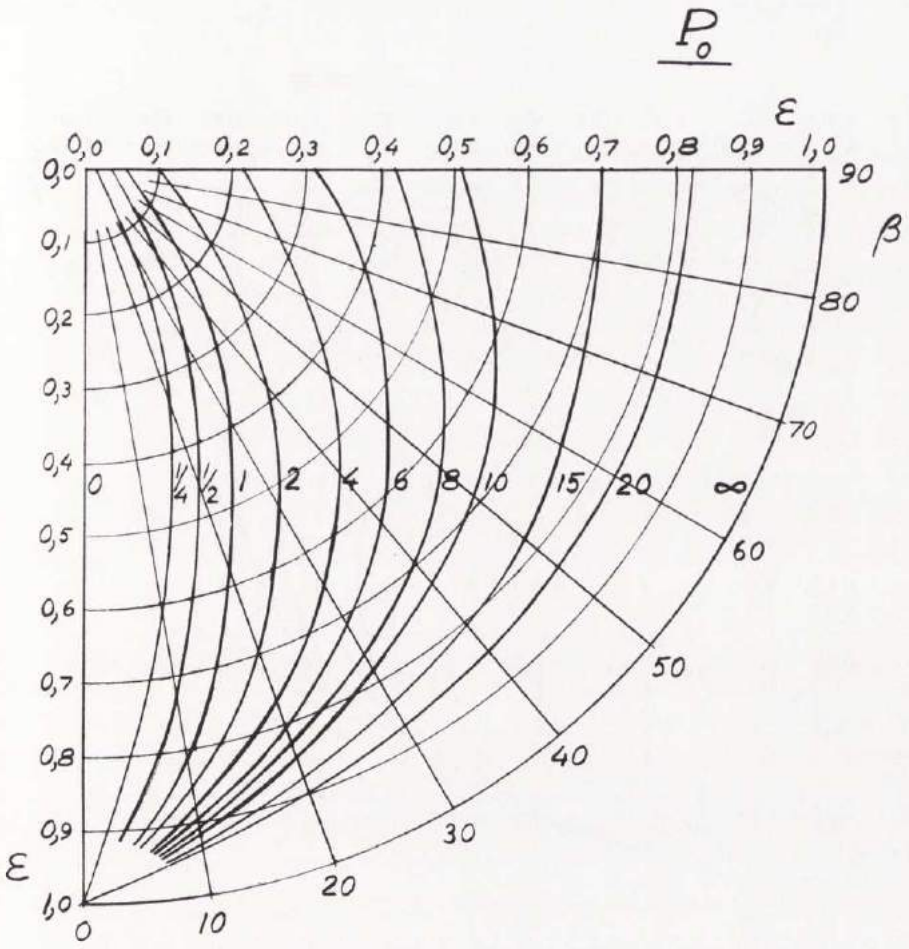

Fig. 49.1. Attitude-Eccentricity Curves for Different Load Capacity

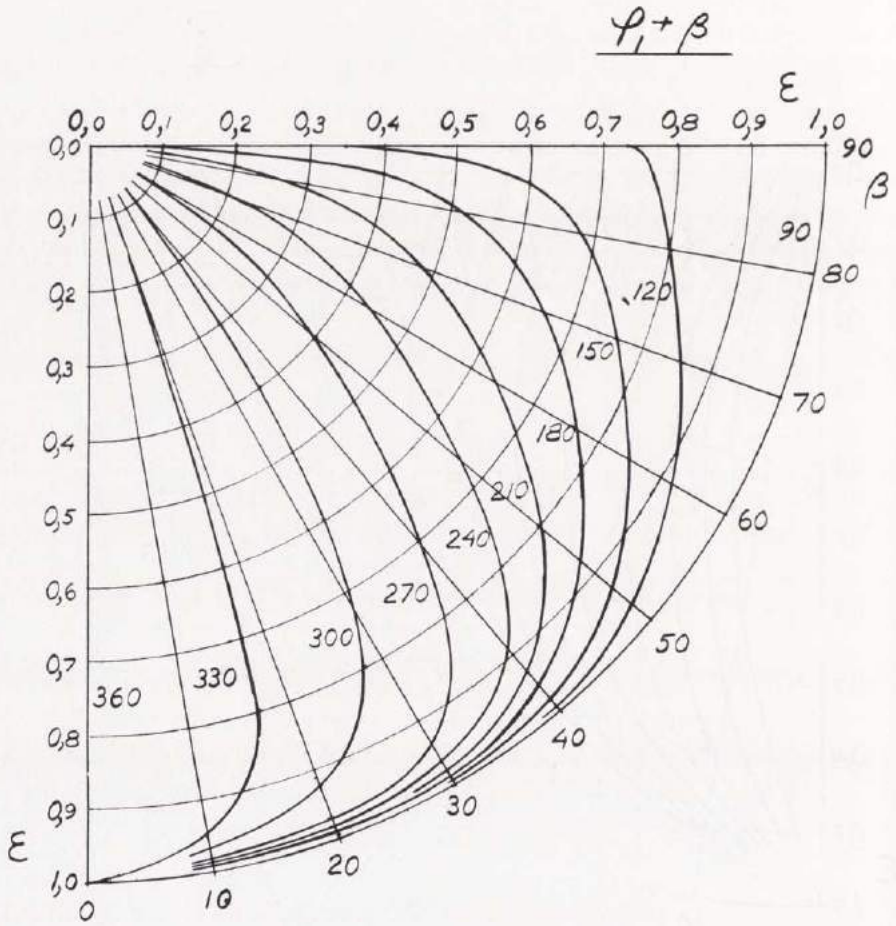

Fig. 50.1. Attitude-Eccentricity Curves for Various Values of the Angle between the Load and the Beginning of the Oil Film

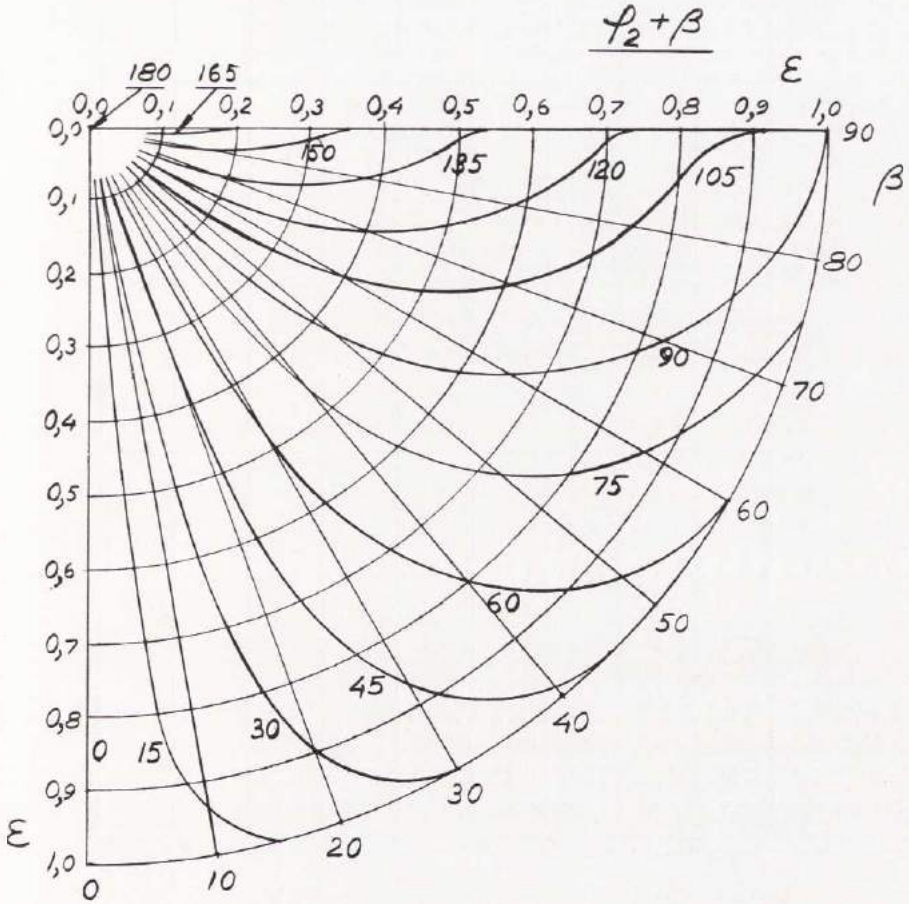

Fig. 51.1. Attitude-Eccentricity Curves for Various Values of the Angle between the Load and the End of the Oil Film

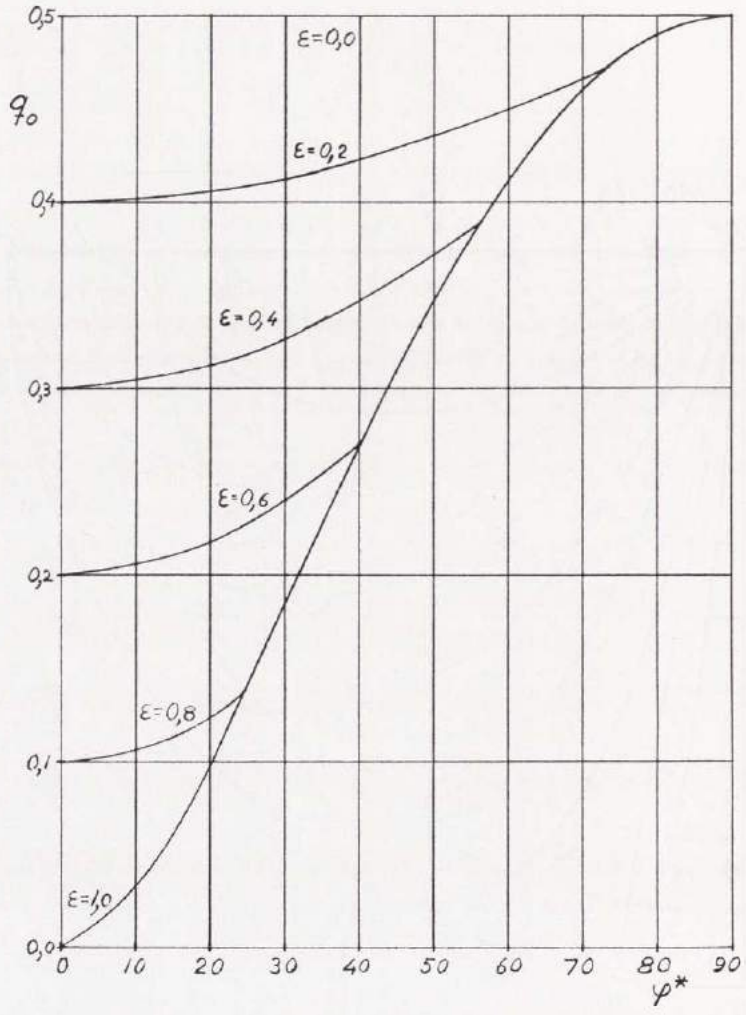

Fig. 52.1. Oil Flow per Unit Width $q_0 = \dfrac{q}{U\,\Delta r}$

5,4. Oil Flow

The oil flow per unit width is

$$q = \frac{Uh^*}{2} = \frac{U\,\Delta r}{2}\,(1 - \varepsilon \cos \varphi^*)$$

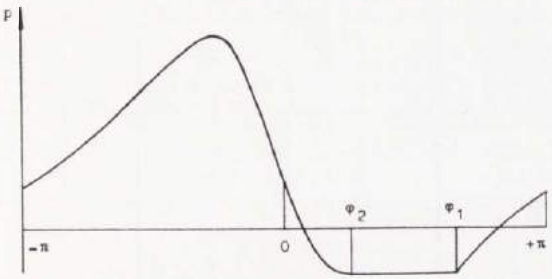

Fig. 53.1

or non-dimensionally

$$q_0 = \frac{q}{U \Delta r} = \frac{1 - \varepsilon \cos \varphi^*}{2}$$

which is shown in 52.1.

5,5. Oil Volume in the Bearing

Assume the pressure curve in 53.1.

Between φ_1 and φ_2 the bearing is filled with oil, and between φ_2 and φ_1 there is a mixture of oil and oil vapour, or air. In every section of the last region there is the same oil area.

Oil volume in the bearing per unit width

$$V = \int_{\varphi_1 - 2\pi}^{\varphi_2} h r \, d\varphi + h_2 r (\varphi_1 - \varphi_2)$$

Vapour volume

$$V_v = \int_{\varphi_2}^{\varphi_1} h r \, d\varphi - h_2 r (\varphi_1 - \varphi_2)$$

The dimensionless volumes are

$$V_0 = \frac{V}{r \Delta r} = \int_{\varphi_1 - 2\pi}^{\varphi_2} (1 - \varepsilon \cos \varphi) \, d\varphi + H_2 (\varphi_1 - \varphi_2)$$

$$V_{v0} = \frac{V_v}{r \Delta r} = \int_{\varphi_2}^{\varphi_1} (1 - \varepsilon \cos \varphi) \, d\varphi - H_2 (\varphi_1 - \varphi_2)$$

Then

$$V_0 = 2\pi + (1 - H_2)(\varphi_2 - \varphi_1) - \varepsilon (\sin \varphi_2 - \sin \varphi_1)$$

which is shown in 54.1.

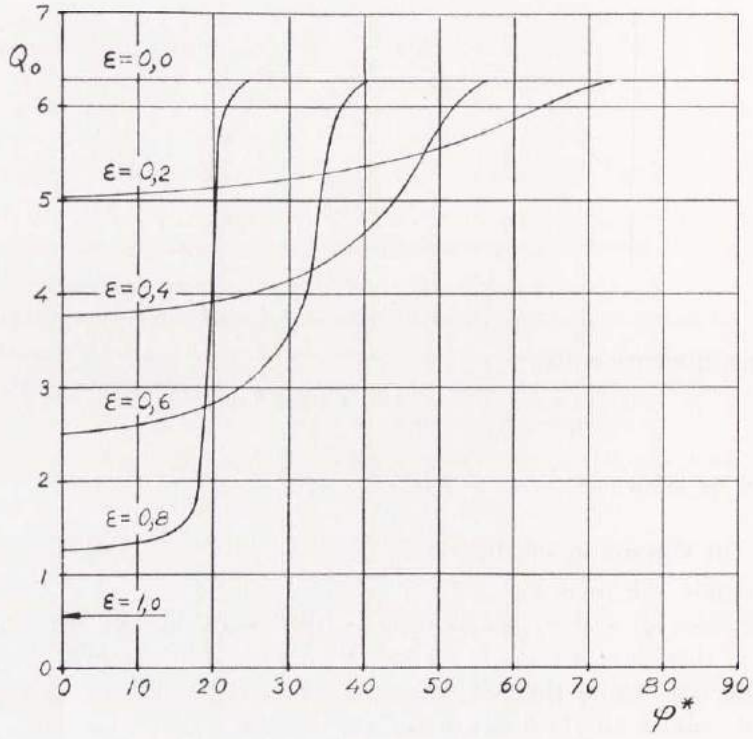

Fig. 54.1. Oil Volume in the Bearing per Unit Width $V_0 = \dfrac{V}{r\,\Delta r}$

5,6. Friction Force, Friction Torque, and Power Loss

The velocity distribution in a vapour region is a straight line. When the film thickness h increases, the width of an oil strip Δb decreases, see 55.1.

The continuity gives

$$h^* \, \Delta b^* = h \, \Delta b$$

The mean shear stress becomes

$$\tau = \frac{\Delta b}{\Delta b^*} \cdot \eta \cdot \frac{U}{h} = \frac{h^*}{h} \cdot \eta \cdot \frac{U}{h}$$

$$\therefore \tau = \frac{\eta \, U \, h^*}{h^2}$$

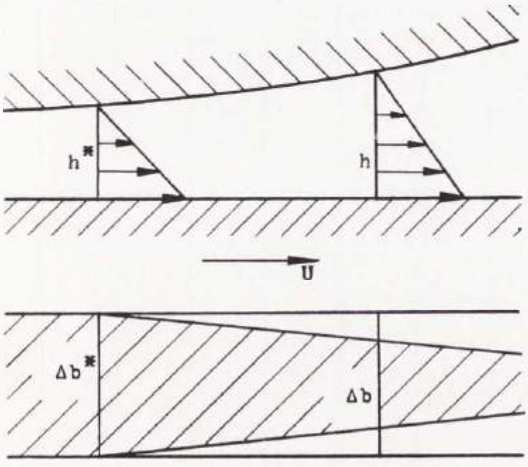

Fig. 55.1

Now the dimensionless friction force, shown in 56.1, is

$$F_{j0} = \int_{\varphi_1 - 2\pi}^{\varphi_2} \left(\frac{4}{H} - \frac{3\,H^*}{H^2} \right) d\varphi + \int_{\varphi_2}^{\varphi_1} \frac{H^*}{H^2}\, d\varphi = 4 \int_{\varphi_1 - 2\pi}^{\varphi_2} \left(\frac{1}{H} - \frac{H^*}{H^2} \right) d\varphi + \int_{0}^{2\pi} \frac{H^*}{H^2}\, d\varphi$$

From 3,5 and 3,6

$$F_{j0} = M_{j0} = E_0$$

5,7. Temperature Rise

As in 3,7

$$\Delta t_0 = c\,\varrho \cdot \frac{\Delta t\,\psi^2}{\eta\,\omega} = \frac{E_0}{q_0}$$

which is shown in 57.1.

5,8. Coefficient of Friction and Relative Power Loss

The coefficient of friction

$$\mu = \frac{F_j}{P} = \psi \cdot \frac{F_{j0}}{P_0}$$

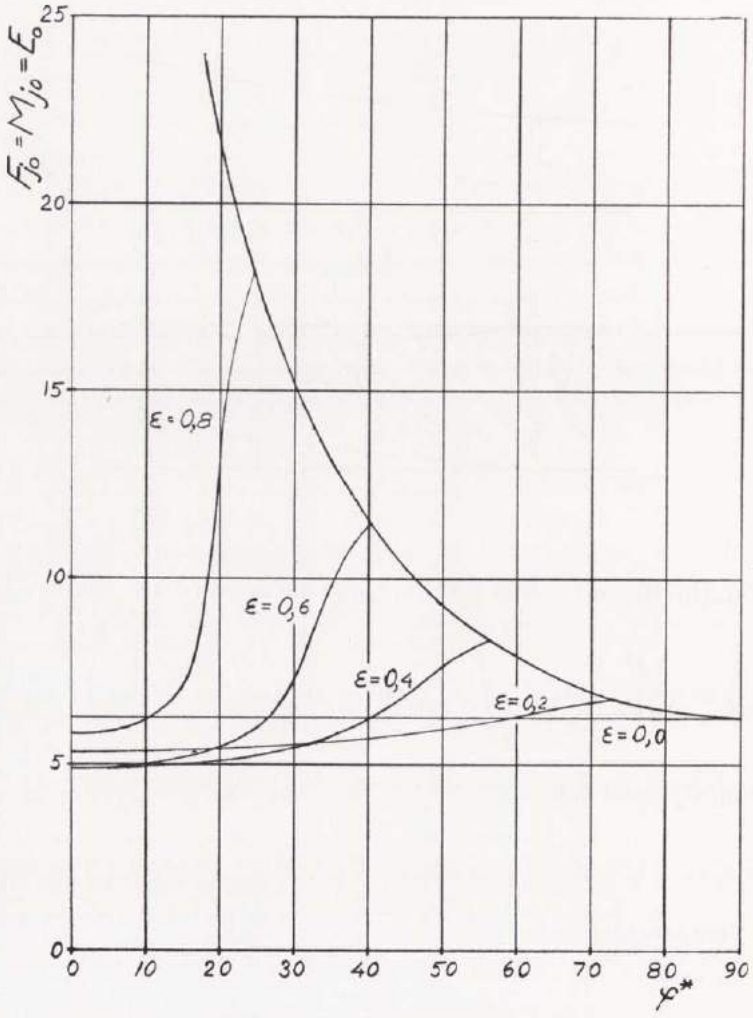

Fig. 56.1. Friction Force, Friction Torque, and Power Loss

$$F_{j0} = \frac{F_j \psi}{\eta U} = M_{j0} = \frac{M_j \psi}{\eta U r} = E_0 = \frac{E \psi}{\eta U^2}$$

$$\frac{\mu}{\psi} = \frac{F_{j0}}{P_0}$$

The relative power loss

$$f = \frac{E}{P} = \omega \Delta r \cdot \frac{E_0}{P_0}$$

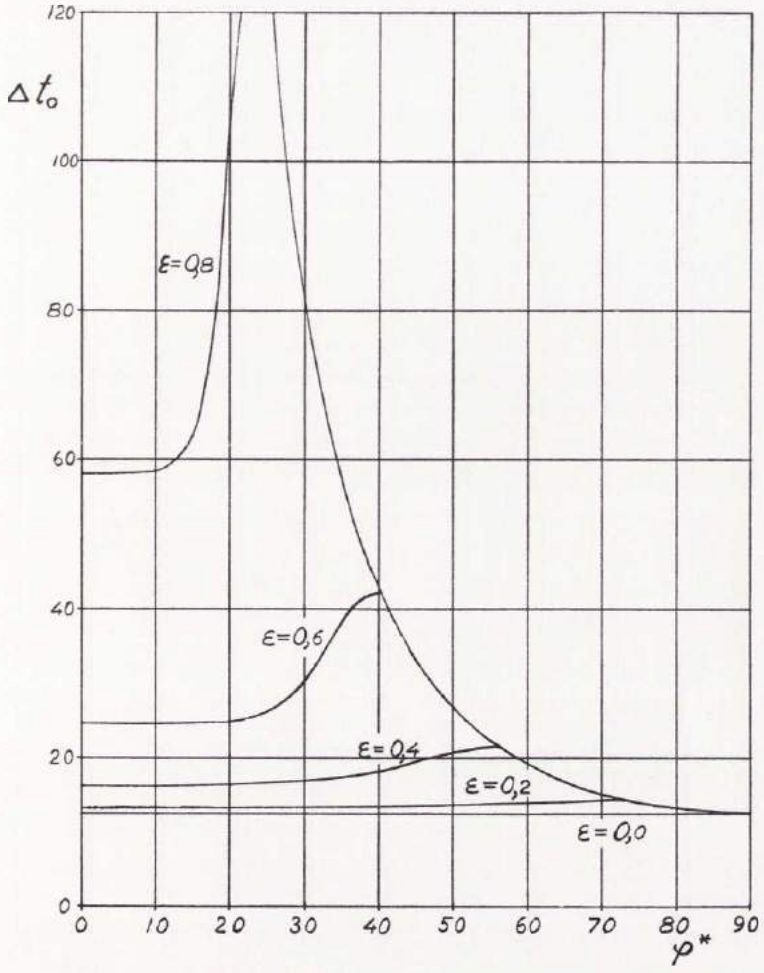

Fig. 57.1. Temperature Rise $\Delta t_0 = c\,\varrho\,.\,\frac{\Delta t\,\psi^2}{\eta\,\omega}$

$$\frac{f}{\omega\,\Delta r} = \frac{E_0}{P_0}$$

$$\because \frac{\mu}{\psi} = \frac{f}{\omega\,\Delta r} = \frac{F_{j0}}{P_0}$$

which is shown in 58.1.

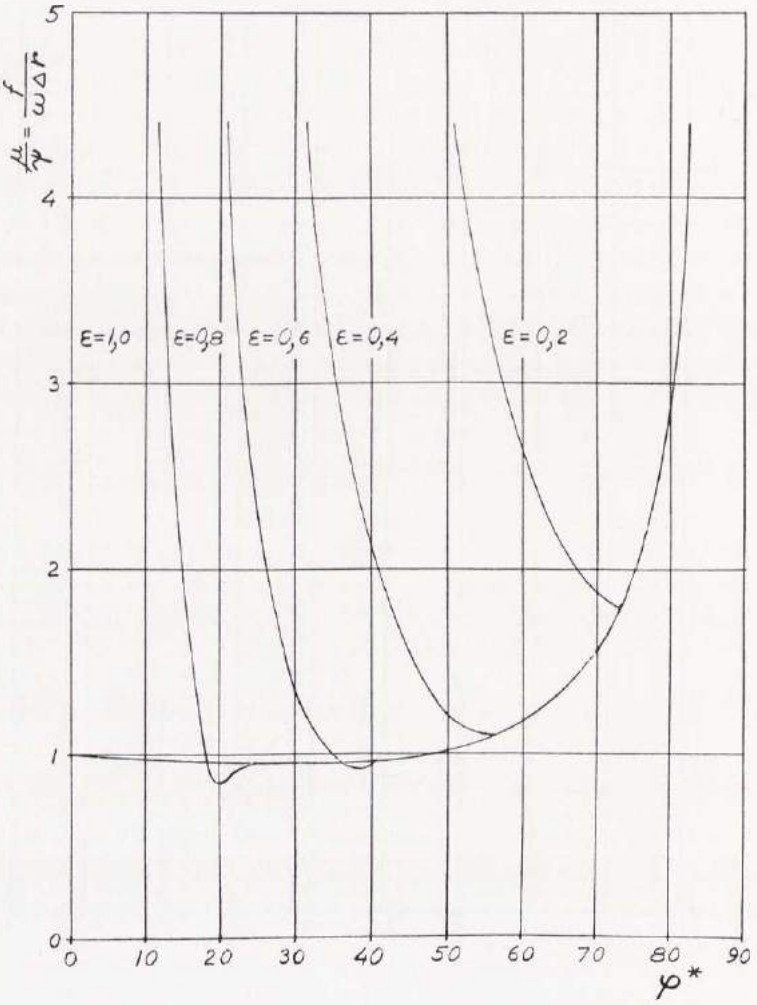

Fig. 58.1. Coefficient of Friction and Relative Power Loss for given ψ, Δr and ω

Here ψ, Δr and ω are constants. If $h_{\min}$ is a given constant,

$$\Delta r = \frac{h_{\min}}{1 - \varepsilon}$$

$$\frac{\mu r}{h_{\min}} = \frac{f}{\omega h_{\min}} = \frac{F_{j0}}{P_0 (1 - \varepsilon)}$$

which is shown in 59.1.

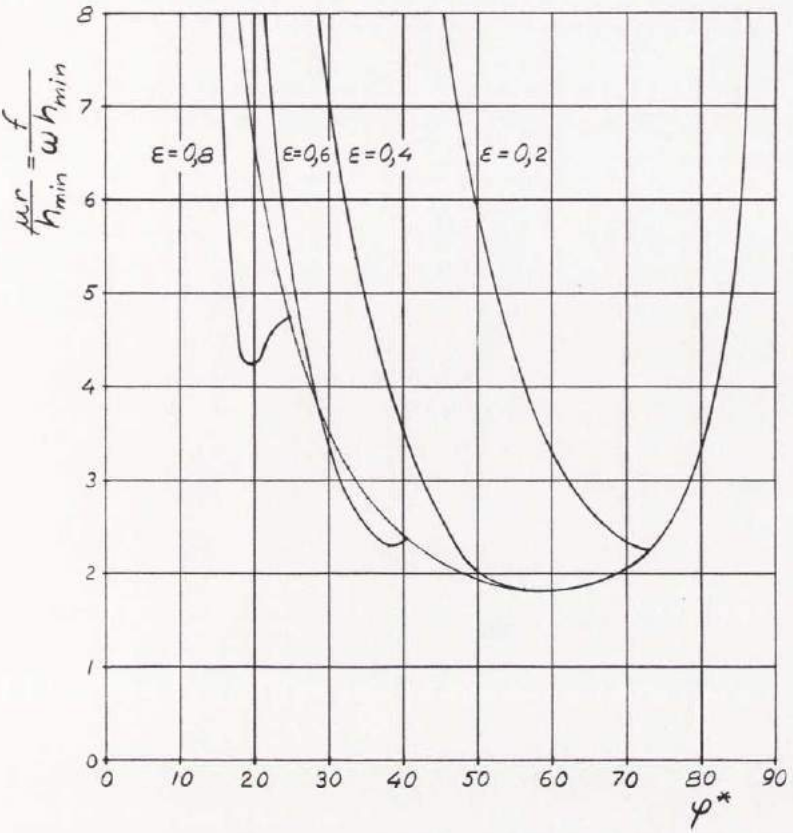

Fig. 59.1. Coefficient of Friction and Relative Power Loss for given $h_{\min}$ and ω

5,9. Experimental Investigation

The same bearing as in 4,8 was used. The groove with about atmospheric pressure is at $\Omega = 0$.

The experiments coincide very closely with the theory. Fig. 63.2 shows that it is possible to have a negative pressure region almost all around the circumference.

For an ideal oil without dissolved gases the vapour pressure is about absolute vacuum. In practice, one finds that this low pressure is impossible to reach. When an experiment starts, the vapour pressure is considerably low (about $-0,7$ atm g), depending on the amount of gases in the oil, but after some hours this pressure has arisen to about $-0,01$ atm g.

Three experiments are analysed in detail:

1) Fig. 61.1

$$\eta = 0{,}0161 \text{ Ns/m}^2$$
$$\omega = 64{,}4 \text{ 1/s}$$
$$\varphi_1 + \beta = 191°$$
$$\varphi_2 + \beta = 121°$$

Experimental load capacity

$$P_e = 7100 \text{ N/m}$$
$$P_{0e} = \frac{P_e \psi^2}{\eta U} = \frac{7100 \cdot 0{,}00825^2}{0{,}0161 \cdot 0{,}05 \cdot 64{,}4}$$
$$P_{0e} = 9{,}3$$

Experimental load angle

$$\beta_e = 81°$$

From diagram 50.1 and 51.1

$$\varepsilon = 0{,}51$$
$$\beta_t = 76°$$

Theoretical load capacity from diagram 49.1

$$P_{0t} = 9{,}0$$

Ratio $$\frac{P_{0e}}{P_{0t}} = \frac{9{,}3}{9{,}0} = 103\ \%$$

2) Fig. 61.2

$$\eta = 0{,}0161 \text{ Ns/m}^2$$
$$\omega = 64{,}4 \text{ 1/s}$$
$$\varphi_1 + \beta = 209°$$
$$\varphi_2 + \beta = 109°$$

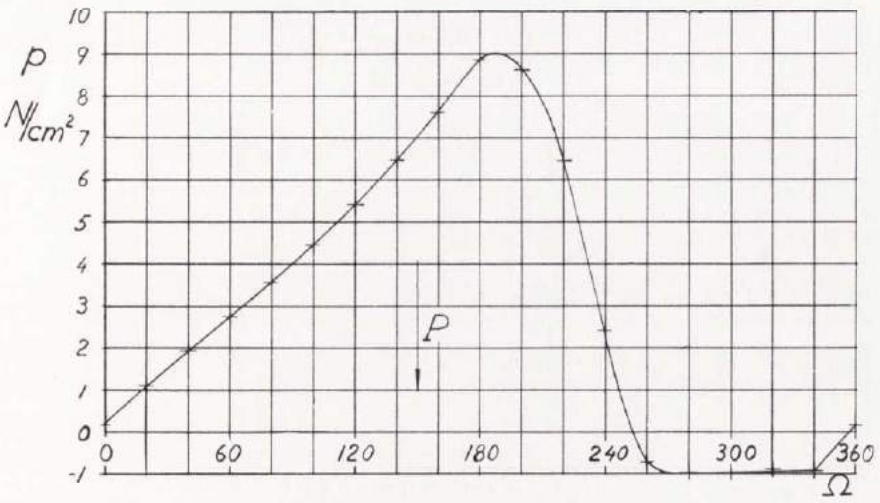

Fig. 61.1. Experimental Pressure Curve

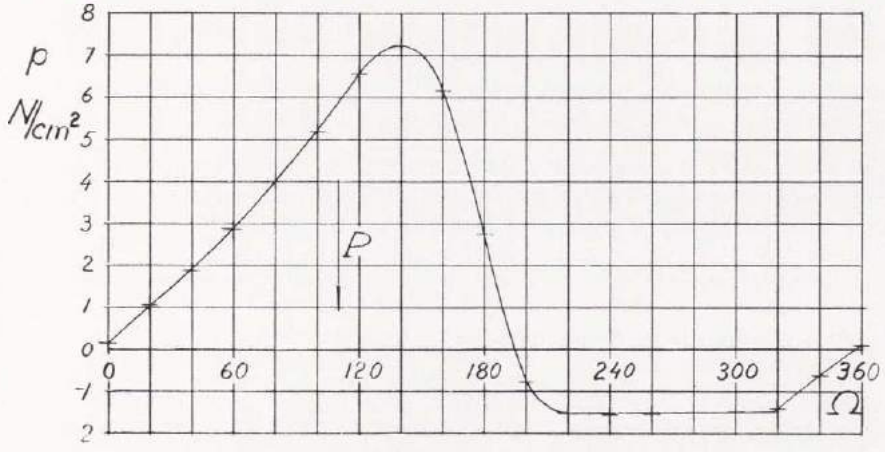

Fig. 61.2. Experimental Pressure Curve

Experimental load capacity

$$P_e = 6400 \text{ N/m}$$

$$P_{0e} = \frac{6400 \cdot 0{,}00825^2}{0{,}0161 \cdot 0{,}05 \cdot 64{,}4} = 8{,}4$$

Experimental load angle

$$\beta_e = 69^\circ$$

From diagram 50.1 and 51.1

$$\varepsilon = 0{,}53$$

$$\beta_t = 68^\circ$$

Theoretical load capacity from diagram 49.1

$$P_{0t} = 8{,}5$$

Ratio $$\frac{P_{0e}}{P_{0t}} = \frac{8{,}4}{8{,}5} = 99\ \%$$

3) Fig. 63.1

$$\eta = 0{,}0161 \text{ Ns/m}^2$$

$$\omega = 64{,}4 \text{ 1/s}$$

$$\varphi_1 + \beta = 263^\circ$$

$$\varphi_2 + \beta = 69^\circ$$

Experimental load capacity

$$P_e = 6400 \text{ N/m}$$

$$P_{0e} = 8{,}4$$

Experimental load angle

$$\beta_e = 44^\circ$$

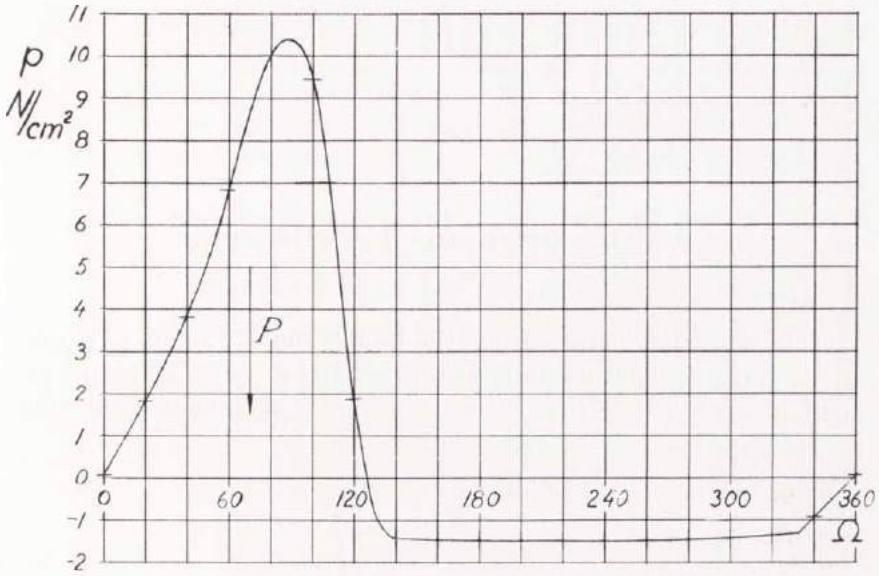

Fig. 63.1. Experimental Pressure Curve

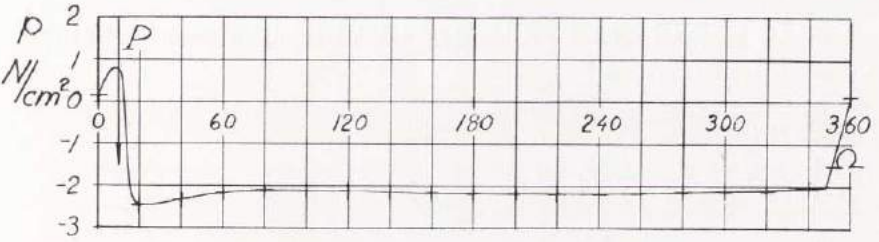

Fig. 63.2. Experimental Pressure Curve

From diagram 50.1 and 51.1

$$\varepsilon = 0{,}69$$

$$\beta_t = 43^\circ$$

Theoretical load capacity from diagram 49.1

$$P_{0t} = 8{,}5$$

Ratio $$\frac{P_{0e}}{P_{0t}} = \frac{8{,}4}{8{,}5} = 99\ \%$$

6. The Optimum 360° Bearing

6,1. General Considerations

When dimensioning a bearing, the load P and the angular velocity ω are normally known. It is also necessary to have values of the minimum permissible film thickness and the maximum permissible temperature rise.

Values to be calculated are:

Eccentricity ratio	ε
Radial clearance	Δr
Radius	r
Absolute viscosity	η

To determine these unknowns, we must have four conditions. These are chosen to be

1. P is given
2. f shall be a minimum
3. $h_{\min} = \Delta r\,(1 - \varepsilon)$
4. $p \leq p_{\max}$ and $\Delta t \leq \Delta t_{\max}$

From 59.1 we see that the full bearing has the lowest relative power loss.

Then

$$f_{\min} = \frac{2\,(\sqrt{3} + 1)}{3} \cdot \omega\, h_{\min} = 1{,}821 \cdot \omega\, h_{\min}$$

for

$$\varepsilon = \frac{\sqrt{3} - 1}{2} = 0{,}3660$$

Then becomes

$$\Delta r = \frac{h_{\min}}{1-\varepsilon} = \frac{3+\sqrt{3}}{3} \cdot h_{\min} = 1{,}577 \cdot h_{\min}$$

From 1 and 4, if the temperature condition is chosen:

$$\left.\begin{aligned} \frac{P\,\psi^2}{\eta\,U} &= \frac{12\,\pi\,\varepsilon}{(2+\varepsilon^2)\sqrt{1-\varepsilon^2}} \\ \frac{\eta\,\omega}{\psi^2} \cdot \frac{1}{c\,\varrho} \cdot \frac{4\,\pi\,(1+2\,\varepsilon^2)}{\sqrt{(1-\varepsilon^2)^3}} &= \Delta t \le \Delta t_{\max} \end{aligned}\right\}$$

or

$$\left.\begin{aligned} \eta\,r^3 &= \frac{P\,\Delta r^2\,(2+\varepsilon^2)\sqrt{1-\varepsilon^2}}{12\,\pi\,\varepsilon\,\omega} \\ \eta\,r^2 &= c\,\varrho \cdot \frac{\Delta r^2}{\omega} \cdot \frac{\sqrt{(1-\varepsilon^2)^3}}{4\,\pi\,(1+2\,\varepsilon^2)} \cdot \Delta t \end{aligned}\right\}$$

This gives

$$r = \frac{(2+\varepsilon^2)\,(1+2\,\varepsilon^2)}{3\,\varepsilon\,(1-\varepsilon^2)} \cdot \frac{1}{c\,\varrho} \cdot \frac{P}{\Delta t}$$

or

$$r = \frac{2\,(6-\sqrt{3})}{3} \cdot \frac{1}{c\,\varrho} \cdot \frac{P}{\Delta t} = 2{,}845 \cdot \frac{P}{c\,\varrho\,\Delta t}$$

and

$$\eta = \frac{\sqrt[4]{3}\,(101+59\sqrt{3})}{3872\sqrt{2}\,\pi} \cdot \frac{(c\,\varrho\,\Delta t)^3}{P^2\,\omega} \cdot h_{\min}^2 =$$

$$= 0{,}01554 \cdot \frac{(c\,\varrho\,\Delta t)^3}{P^2\,\omega} \cdot h_{\min}^2$$

6,2. Load per Unit Projected Area

$$p_p = \frac{P}{2\,r} = \frac{c\,\varrho}{2 \cdot 2{,}845} \cdot \Delta t$$

If

$$c = 2000 \text{ Nm/kg } ^\circ\text{C}$$

$$\varrho = 900 \text{ kg/m}^3$$

$$p_p \left(\frac{N}{\text{cm}^2} \right) = 31{,}6 \, \Delta t \, (^\circ\text{C})$$

6,3. The Ratio of Maximum Pressure to Load per Unit Projected Area

$$\frac{p_m}{p_p} = \frac{\sqrt{(4 - \varepsilon^2)^3}}{2\pi (1 - \varepsilon^2)}$$

If

$$\varepsilon = \frac{\sqrt{3} - 1}{2}$$

$$\frac{p_m}{p_p} = \frac{\sqrt{6 \left(6 + \sqrt{3}\right)^3}}{12\pi} = 1{,}397$$

6,4. Schedule for Calculation

$$\varepsilon = 0{,}3660$$

$$r = 2{,}845 \cdot \frac{P}{c \, \varrho \, \Delta t}$$

$$\eta = 0{,}01554 \cdot \frac{(c \, \varrho \, \Delta t)^3 \, h_{\min}^2}{P^2 \, \omega}$$

$$\Delta r = 1{,}577 \cdot h_{\min}$$

$$\psi = \frac{\Delta r}{r}$$

$$f = 1{,}821 \cdot \omega \, h_{\min}$$

$$\mu = 1{,}821 \cdot \frac{h_{\min}}{r}$$

$$E = fP$$

6,5. **Example**

Given is

$$P = 50000 \text{ N/m}$$

$$\omega = 100 \text{ rad/s}$$

$$c\,\varrho = 18 \cdot 10^5 \text{ Nm/m}^3\,^\circ\text{C}$$

The journal ought to have a diameter of 50 mm from strength considerations.

Minimum film thickness $h_{\min} = 0{,}025$ mm.

$$\varepsilon = 0{,}366$$

$$0{,}025 = \frac{2{,}845 \cdot 50000}{18 \cdot 10^5 \cdot \Delta t}$$

$$\Delta t = 3{,}16^\circ \text{ C}$$

$$\eta = \frac{0{,}01554 \cdot (18 \cdot 10^5 \cdot 3{,}16)^3 \cdot 0{,}000025^2}{50000^2 \cdot 100}$$

$$\eta = 0{,}0072 \text{ Ns/m}^2$$

$$\Delta r = 1{,}577 \cdot 0{,}025 = 0{,}039 \text{ mm}$$

$$\psi = \frac{0{,}039}{25} = 1{,}58\,{}^\circ/_{\circ\circ}$$

$$f = 1{,}821 \cdot 100 \cdot 0{,}000025 = 0{,}00455 \text{ Nm/sN}$$

$$\mu = \frac{1{,}821 \cdot 0{,}000025}{0{,}025} = 0{,}0018$$

$$E = 0{,}00455 \cdot 50000 = 228 \text{ Nm/sm} = 228 \text{ W/m}$$

If this oil should seem to be too thin, $h_{\min}$ must be increased and then f increases.

7. Bearings with Two Oil Grooves

7,1. General Considerations

Assume a bearing with given ε and with the pressure equal to zero at two given oil groove angles φ_1 and φ_2, see 68.1.

The pressure derivative

$$\frac{dp}{d\varphi} = f(\varepsilon, \varphi^*, \varphi)$$

The pressure

$$p = F(\varepsilon, \varphi^*, \varphi) + A$$

Four different pressure curves exist:

I. Boundary conditions

$$\left.\begin{aligned} p &= 0 \\ \varphi &= \varphi_1 \end{aligned}\right\} \qquad \left.\begin{aligned} p &= 0 \\ \varphi &= \varphi_2 \end{aligned}\right\}$$

Equations to determine the two constants φ_I^* and A_I:

$$\left.\begin{aligned} 0 &= F(\varepsilon, \varphi_I^*, \varphi_1) + A_I \\ 0 &= F(\varepsilon, \varphi_I^*, \varphi_2) + A_I \end{aligned}\right\}$$

II. $$\left.\begin{aligned} p &= 0 \\ \varphi &= \varphi_2 \end{aligned}\right\} \qquad \left.\begin{aligned} p &= p_e \\ \varphi &= \varphi_{II}^* \end{aligned}\right\}$$

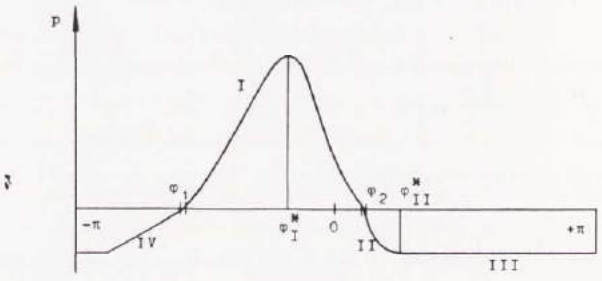

Fig. 68.1

$$\left.\begin{aligned} 0 &= F(\varepsilon, \varphi_{II}^*, \varphi_2) + A_{II} \\ p_v &= F(\varepsilon, \varphi_{II}^*) + A_{II} \end{aligned}\right\}$$

III. $$p = p_v$$

A straight horizontal line.

IV. $$\left.\begin{aligned} p &= 0 \\ \varphi &= \varphi_1 \end{aligned}\right\}$$

Because of the continuity, φ_{IV}^* has the same value as φ_{II}^*.

$$0 = F(\varepsilon, \varphi_{II}^*, \varphi_2) + A_{IV}$$

The oil flows become:

$$q_I = \frac{Uh_I^*}{2}$$

$$q_{II} = q_{III} = q_{IV} = \frac{Uh_{II}^*}{2}$$

In 68.1 $h_{II}^* > h_I^*$, which means that $(q_{II} - q_I)$ is introduced at φ_2, and the same quantity is removed at φ_1. This oil quantity takes care of the generated friction power.

7,2. ten Bosch's Solution

TEN BOSCH (1) assumes as boundary conditions

$$\left.\begin{aligned} p &= 0 \\ \varphi &= \varphi_1 \end{aligned}\right\} \qquad \left.\begin{aligned} p &= 0 \\ \frac{dp}{d\varphi} &= 0 \\ \varphi &= \varphi_2 = \varphi_I^* \end{aligned}\right\}$$

TEN BOSCH has oil inlet at φ_1, and oil outlet at $\varphi_2 = \varphi^*$, see 70.1. The curves II and IV, however, have a greater h^* than curve I, and therefore a greater oil flow. This gives oil inlet at φ_2, and oil outlet at φ_1. TEN BOSCH gives the oil flow $q_I = \frac{Uh_I^*}{2}$, which is for a partial bearing; but the real oil change is the difference between the two flows q_{II} and q_I equal to $\frac{Uh_{II}^*}{2} - \frac{Uh_I^*}{2}$. The »air expulsion pressure of the oil» is just below atmospheric pressure, and therefore

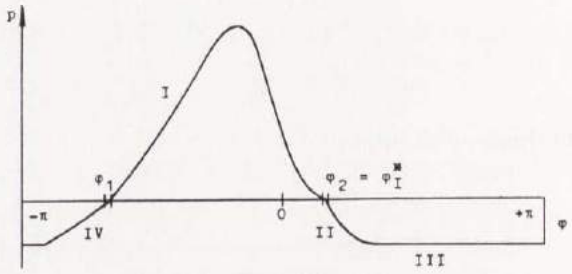

Fig. 70.1

h_{II}^* is nearly equal to h_I^*. The oil change is thus very small compared with TEN BOSCH's value.

TEN BOSCH's bearing is therefore only a partial bearing, and the theory may give dangerous conclusions if used for a 360° bearing.

7,3. Example

For the pressure curve in 70.2, the given values are:

$$\varepsilon = 0,6$$

$$\varphi_2 = \varphi_I^* = 30°$$

If $\varphi_{II}^* = 35°$, the corresponding vapour pressure is $p_{v0} = -0,10$.

This means that the maximum pressure is about 50 times the vapour pressure. In practice this is a low value, because the vapour pressure is normally some hundredths of an atm.

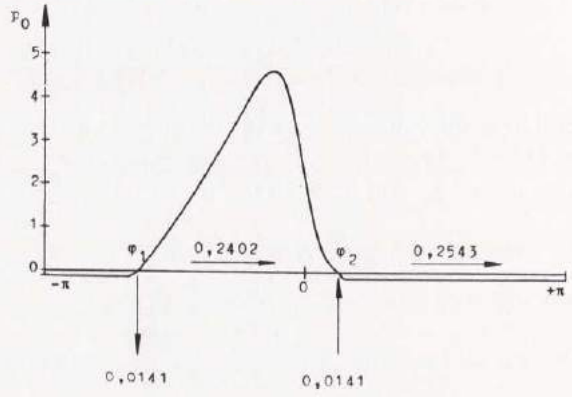

Fig. 70.2

The oil flow between φ_1 and φ_2

$$\frac{q_{12}}{U\Delta r} = \frac{1 - 0{,}6 \cos 30^\circ}{2} = 0{,}2402$$

and between φ_2 and φ_1

$$\frac{q_{21}}{U\Delta r} = \frac{1 - 0{,}6 \cos 35^\circ}{2} = 0{,}2543$$

$$\frac{q_{21} - q_{12}}{U\Delta r} = 0{,}0141$$

If the temperature rise is calculated from the non-dimensional oil flow 0,0141, it will be 17 times higher than if the calculation is based upon the flow 0,2402. The load carrying capacity is very little influenced by the vapour pressure, but from the above we see that a temperature rise calculation based upon the circulating oil has no real background and might be dangerous.

8. The 180° Bearing with Minimum Film Thickness at the Trailing Edge

The maximum film thickness is chosen to be located at $\varphi = -\pi$ and the minimum at $\varphi = 0$. The boundary conditions then are $p = 0$ for $\varphi = -\pi$ and $p = 0$ for $\varphi = 0$, see 73.1. An infinite number of 180° bearings exists.

The pressure in the oil film from 23.2 becomes

$$p_0 = \frac{p\,\psi^2}{\eta\,\omega} = -\frac{6\,\varepsilon}{2+\varepsilon^2} \cdot \sin\varphi \left[\frac{1}{1-\varepsilon\cos\varphi} + \frac{1}{(1-\varepsilon\cos\varphi)^2}\right]$$

The load components from 3,2

$$P_{x0} = \frac{P_x\,\psi^2}{\eta\,U} = \frac{6\,\pi\,\varepsilon}{(2+\varepsilon^2)\,\sqrt{1-\varepsilon^2}}$$

$$P_{y0} = \frac{P_y\,\psi^2}{\eta\,U} = \frac{12\,\varepsilon^2}{(2+\varepsilon^2)\,(1-\varepsilon^2)}$$

Then

$$P_0 = \frac{6\,\varepsilon\,\sqrt{\pi^2-\varepsilon^2\,(\pi^2-4)}}{(2+\varepsilon^2)\,(1-\varepsilon^2)}$$

$$\tan\beta = \frac{\pi\,\sqrt{1-\varepsilon^2}}{2\,\varepsilon}$$

The circulating oil is the same as in 4,4.

$$q_0 = \frac{q}{U\,\Delta r} = \frac{1-\varepsilon^2}{2+\varepsilon^2}$$

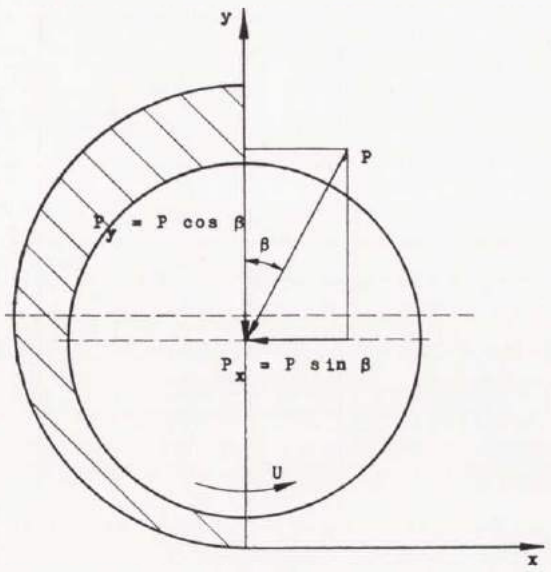

Fig. 73.1

The non-dimensional value of friction force, friction torque, and power loss is half the value in 4,5

$$F_{j0} = \frac{F_j\,\psi}{\eta\,U} = M_{j0} = \frac{M_j\,\psi}{\eta\,U\,r} = E_0 = \frac{E\,\psi}{\eta\,U^2} = \frac{2\,\pi\,(1+2\,\varepsilon^2)}{(2+\varepsilon^2)\,\sqrt{1-\varepsilon^2}}$$

Temperature rise

$$\Delta t_0 = c\,\varrho\cdot\frac{\Delta t\,\psi^2}{\eta\,\omega} = \frac{2\,\pi\,(1+2\,\varepsilon^2)}{\sqrt{(1-\varepsilon^2)^3}}$$

For the coefficient of friction and the relative power loss, we then get

$$\frac{\mu}{\psi} = \frac{f}{\omega\,\Delta r} = \frac{\pi\,(1+2\,\varepsilon^2)\sqrt{1-\varepsilon^2}}{3\,\varepsilon\sqrt{\pi^2-\varepsilon^2\,(\pi^2-4)}}$$

if ψ, ω and Δr are constant, and

$$\frac{\mu\,r}{h_{\min}} = \frac{f}{\omega\,h_{\min}} = \frac{\pi\,(1+2\,\varepsilon^2)\sqrt{1-\varepsilon^2}}{3\,\varepsilon\,(1-\varepsilon)\sqrt{\pi^2-\varepsilon^2\,(\pi^2-4)}}$$

if r, ω and $h_{\min}$ are constant.

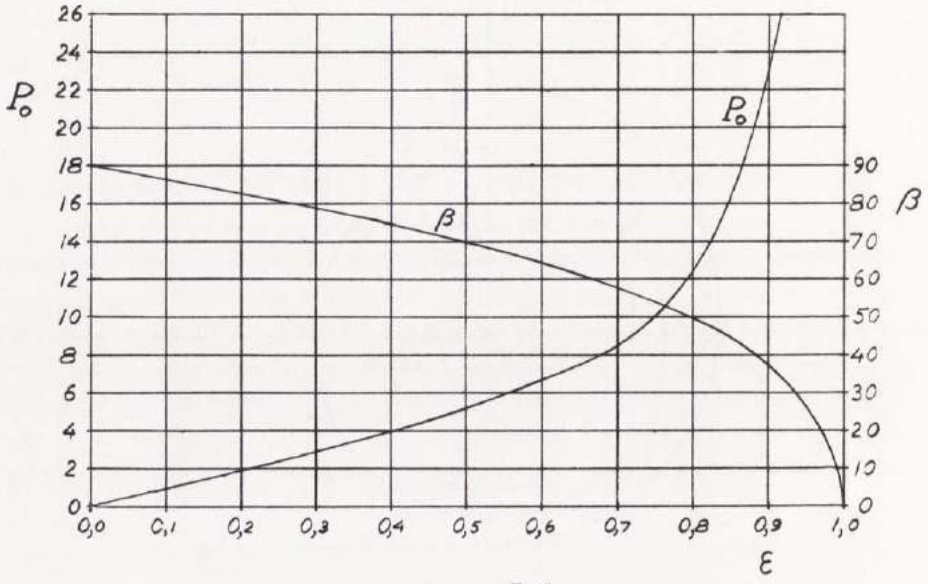

Fig. 74.1. Load Capacity $P_0 = \dfrac{P\,\psi^2}{\eta\,U}$ and Load Angle β

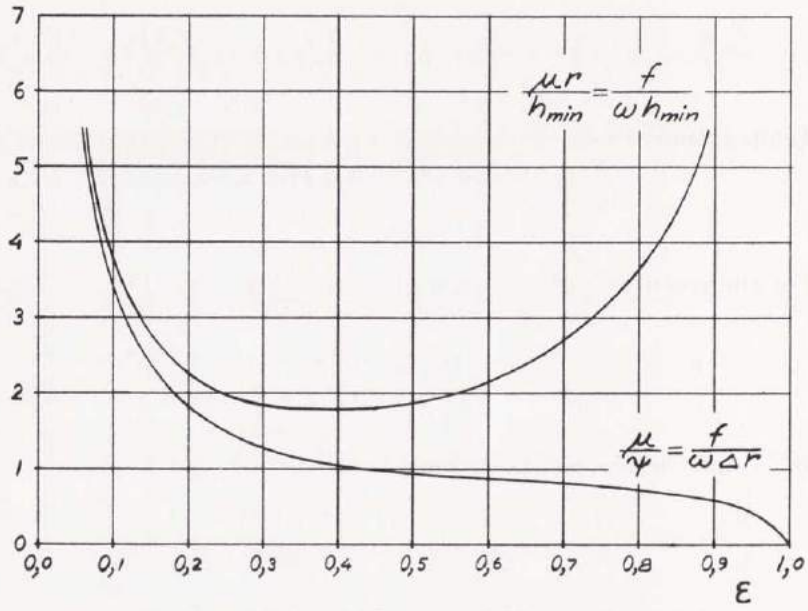

Fig. 74.2. Coefficient of Friction and Relative Power Loss

This expression has minimum for

$$2\,(\pi^2-4)\,\varepsilon^5+4\,(\pi^2-2)\,\varepsilon^4-(\pi^2+4)\,\varepsilon^3-(5\,\pi^2-8)\,\varepsilon^2-\pi^2\,\varepsilon+\pi^2=0$$

which gives

$$\frac{\mu_{\min}\,r}{h_{\min}}=\frac{f_{\min}}{\omega\,h_{\min}}=1{,}764\;\ldots\ldots\ldots\ldots\;75.1$$

for

$$\varepsilon=0{,}3835$$

The decrease in power loss is thus very small, compared with the 360° bearing (3,1 %).

Fig. 74.1 gives the load capacity, and the angle between the load line and the line of centres. The coefficient of friction and the relative power loss are shown in 74.2.

The angle between the load and the trailing edge is β, according to the chosen conditions.

9. The Optimum 180° Bearing with Minimum Film Thickness at the Trailing Edge

9,1. General Considerations

The case of chap. 8 is studied.
The load P and the angular velocity ω are assumed to be known.
ε, Δr, r and η are unknown.
The four conditions are the same as in 6,1.

1. P is given
2. f shall be a minimum
3. $h_{\min} = \Delta r\,(1 - \varepsilon)$
4. $p \leq p_{\max}$ and $\Delta t \leq \Delta t_{\max}$

From 2, according to 75.1

$$f_{\min} = 1{,}764 \cdot \omega\, h_{\min}$$

for

$$\varepsilon = 0{,}3835$$

If the temperature condition is chosen, 1 and 4 give

$$\left.\begin{aligned} \frac{P\,\psi^2}{\eta\,U} &= \frac{6\,\varepsilon\,\sqrt{\pi^2 - \varepsilon^2\,(\pi^2 - 4)}}{(2 + \varepsilon^2)\,(1 - \varepsilon^2)} \\ \frac{\eta\,\omega}{\psi^2} \cdot \frac{1}{c\,\varrho} \cdot \frac{2\,\pi\,(1 + 2\,\varepsilon^2)}{\sqrt{(1 - \varepsilon^2)^3}} &= \Delta t \leq \Delta t_{\max} \end{aligned}\right\}$$

or

$$\left.\begin{aligned} \eta\,r^3 &= \frac{P\,\Delta r^2\,(2 + \varepsilon^2)\,(1 - \varepsilon^2)}{6\,\omega\,\varepsilon\,\sqrt{\pi^2 - \varepsilon^2\,(\pi^2 - 4)}} \\ \eta\,r^2 &= c\,\varrho \cdot \frac{\Delta r^2}{\omega} \cdot \frac{\sqrt{(1 - \varepsilon^2)^3}}{2\,\pi\,(1 + 2\,\varepsilon^2)} \cdot \Delta t \end{aligned}\right\}$$

This gives

$$r = \frac{(2 + \varepsilon^2)\,(1 + 2\,\varepsilon^2)\,\pi}{3\,\varepsilon\,\sqrt{1 - \varepsilon^2}\,\sqrt{\pi^2 - \varepsilon^2\,(\pi^2 - 4)}} \cdot \frac{1}{c\,\varrho} \cdot \frac{P}{\Delta t}$$

or

$$r = 2{,}738 \cdot \frac{P}{c\,\varrho\,\Delta t}$$

and

$$\eta = \frac{9\,\varepsilon^2\,\sqrt{(1 - \varepsilon^2)^5}\,[\pi^2 - \varepsilon^2\,(\pi^2 - 4)]}{2\,\pi^3\,(1 + 2\,\varepsilon^2)^3\,(2 + \varepsilon^2)^2\,(1 - \varepsilon)^2} \cdot \frac{(c\,\varrho\,\Delta t)^3}{P^2\,\omega} \cdot h_{\min}^2$$

or

$$\eta = 0{,}03401 \cdot \frac{(c\,\varrho\,\Delta t)^3}{P^2\,\omega} \cdot h_{\min}^2$$

9,2. Schedule for Calculation

$$\varepsilon = 0{,}3835$$

$$r = 2{,}738 \cdot \frac{P}{c\,\varrho\,\Delta t}$$

$$\eta = 0{,}03401 \cdot \frac{(c\,\varrho\,\Delta t)^3}{P^2\,\omega} \cdot h_{\min}^2$$

$$\Delta r = 1{,}622 \cdot h_{\min}$$

$$\psi = \frac{\Delta r}{r}$$

$$f = 1{,}764 \cdot \omega\,h_{\min}$$

$$\mu = 1{,}764 \cdot \frac{h_{\min}}{r}$$

$$E = fP$$

10. Vogelpohl's Solution for an Infinitely Wide Partial Journal Bearing with Oil Inlet 90° before the Load Line

In his paper »Zur Integration der Reynoldsschen Gleichung», VOGELPOHL (10) assumes oil inlet at $\varphi_1 = -(90 + \beta)$, and oil outlet at $\varphi_2 = \varphi^*$, or if $\varphi^* \geq 90 - \beta$ at $\varphi_2 = 90 - \beta$, see 78.1. These boundary conditions give the coefficient of friction and the relative power loss shown in 79.1. If a parabola is drawn through the three lowest points of the relative power loss curve, the minimum is

$$\frac{\mu_{\min} r}{h_{\min}} = \frac{f_{\min}}{\omega h_{\min}} = 2{,}147$$

for

$$\varepsilon = 0{,}3849$$

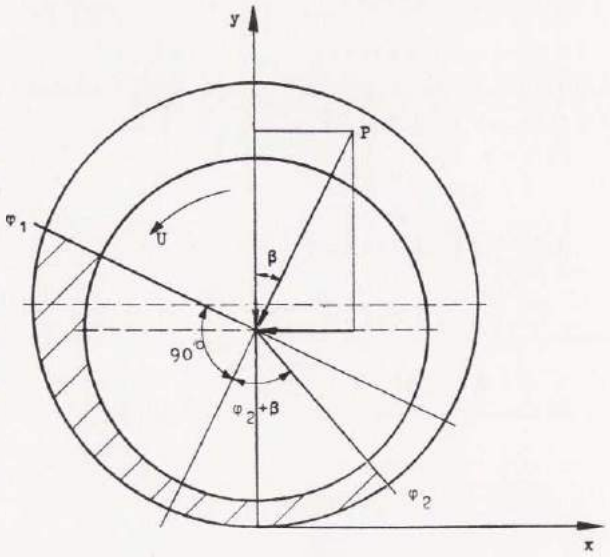

Fig. 78.1

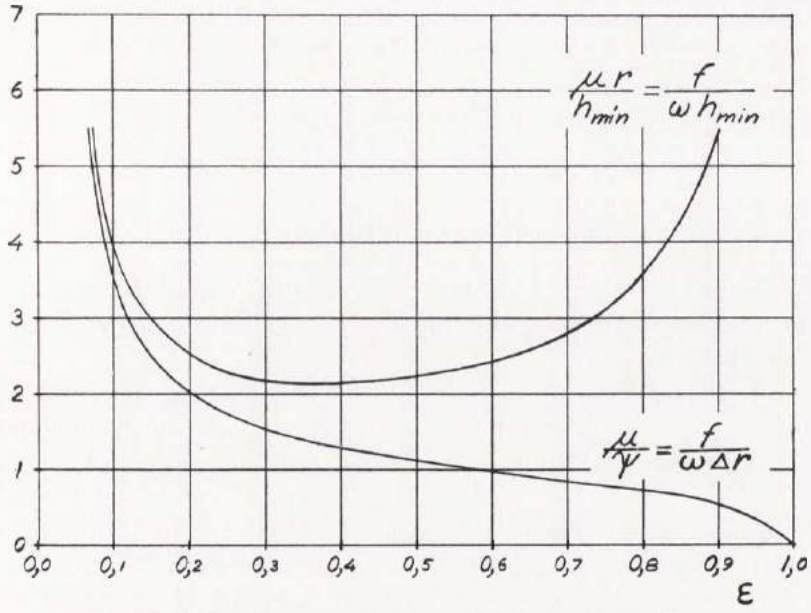

Fig. 79.1. Coefficient of Friction and Relative Power Loss

The power loss is thus 18 % greater than the value 1,821 for the 360° bearing, and 22 % greater than the value 1,764 for the 180° bearing with minimum film thickness at the trailing edge.

11. Conclusion

This treatise deals with the 360° infinite journal bearing, both theoretically and experimentally. The behaviour of vaporized regions is specially studied.

It is shown that it is possible to have a bearing operating with positive pressure all around the circumference. This means no vapour region in the bearing and horizontal attitude-eccentricity curve. Experiments verify the reality of this horizontal line, which is usually thought to be impossible. It is also shown that a bearing can operate with negative pressure all around the circumference.

The experimental investigations show a very good agreement with the theory, and confirm REYNOLD's equation for the pressure in the oil film.

A theory for vaporization is put forward, and for different locations of the oil groove relative to the load line, diagrams are drawn on load capacity, oil flow, friction force, power loss, temperature rise, coefficient of friction, and relative power loss. Here is described how to design an optimum infinitely wide journal bearing which should have the eccentricity 0,37.

In this study the assumption of infinite width is rigorously followed; and there is no flow of either oil or air in axial direction. No arbitrary boundary conditions are used, but the continuity of flow at the boundaries of a vapour region is strictly treated.

Calculations are also made for an 180° infinite journal bearing with maximum oil film thickness at the leading edge and minimum oil film thickness at the trailing edge. Here, too, the optimum power loss conditions are determined. The optimum value for the eccentricity is 0,38.

12. Zusammenfassung

Die vorliegende Arbeit gibt eine theoretische und experimentelle Behandlung des 360° radialen Gleitlagers mit unendlicher Breite. Dabei wird das Auftreten negativer Drücke studiert und die Randbedingungen für die Druckentwicklung an den Grenzen einer Öldampfzone diskutiert.

Es wird gezeigt, dass ein radiales Gleitlager mit positiven Drücken auf dem ganzen Umkreis arbeiten kann. Dann ist die Verlagerungskurve des Wellenmittelpunktes eine horizontale Linie. Diese Behauptung, hier mit Experimenten bestätigt, ist vielfach als falsch betrachtet worden. In seiner Arbeit »Berechnung von zylindrischen Gleitlagern» schreibt FRÄNKEL: »Da Sommerfeld seine Berechnungen unter Berücksichtigung dieser negativen Drücke durchführte, hat er Ergebnisse erhalten, welche mit der Wirklichkeit nicht übereinstimmten (z. B. horizontale Verlagerungskurve des Wellenmittelpunktes), und deshalb wenig beachtet wurden.» Die Experimente zeigen, dass die horizontale Verlagerungskurve sehr gut mit der Wirklichkeit übereinstimmt (Bild 40.2). REYNOLDS' Differentialgleichung für die Druckentwicklung im Ölfilm ist in den Bildern 39.1 und 39.2 bestätigt, wo die Kurven die Theorie und die Punkte die experimentellen Werte vertreten.

Diagramme für Tragkraft, Ölfluss, Reibungskraft, Verlustleistung, Temperatursteigerung, Reibungskoeffizient und relative Verlustleistung sind für verschiedene Winkel zwischen der Richtung der Tragkraft und dem Ölspalte gegeben. Es wird gezeigt, wie ein ideelles 360° radiales Gleitlager ausgelegt sein soll.

In dieser Arbeit ist die Voraussetzung, dass man unendliche Breite hat, streng beachtet. Es gibt keinen Fluss von Öl oder Luft in achsialer Richtung. Man muss die Theorien für unendliche und endliche Breite von einander trennen. Eine Vernachlässigung dieser Trennung ist ein gewöhnlicher Fehler.

Berechnungen für ein 180° radiales Gleitlager mit unendlicher Breite und minimaler Filmdicke an dem Ende des Druckberges sind für optimale Bedingungen ausgeführt.

13. References

1. TEN BOSCH, M.: Berechnung der Maschinenelemente. Springer-Verlag, 1951.
2. CAMERON, A. and WOOD, W. L.: The Full Journal Bearing. Proc. Instn Mech. Engrs, vol. 161, p. 59, 1949.
3. COLE, J. A. and HUGHES, C. J.: Oil Flow and Film Extent in Complete Journal Bearings. The Engineer, March 16, 1956.
4. FRÄNKEL, A.: Berechnung von zylindrischen Gleitlagern. Zürich, 1944.
5. GÜMBEL, L. and EVERLING, E.: Reibung und Schmierung im Maschinenbau. Berlin, 1925.
6. OTT, H. H.: Zylindrische Gleitlager bei instationärer Belastung. Zürich, 1948.
7. REYNOLDS, O.: On the Theory of Lubrication . . . Phil. Trans. Roy. Soc., vol. 177, p. 157, 1886.
8. SOMMERFELD, A.: Zur hydrodynamischen Theorie der Schmiermittelreibung. Zeitschrift für Mathematik und Physik, vol. 50, p. 97, 1904.
9. VOGELPOHL, G.: Beiträge zur Kenntnis der Gleitlagerreibung. VDI-Forschungsheft 386, 1937.
10. VOGELPOHL, G.: Zur Integration der Reynoldsschen Gleichung für das Zapfenlager endlicher Breite. Ingenieur-Archiv XIV. Band, 1943.

Forts. fr. omsl. 2:dra sida.

128. LAVEMARK, SVEN, *The treatment of the load in electric power-system. Stability studies.* 53 s. 1952. Kr. 9: —. (Avd. Elektroteknik. 29.)
129. LINDBLAD, BERTIL-ANDERS, *A radar investigation of the delta aquarid meteor shower of 1950.* 27 s. 1952. Kr. 5: —. (Avd. Elektroteknik. 30.)
130. HELLGREN, GÖSTA, *The propagation of electromagnetic waves along a conical helix with variable pitch.* 13 s. 1953. Kr. 3: —. (Avd. Elektroteknik. 31.)
131. RYDBECK, O. E. H., *On the excitation of different space charge wave modes in travelling wave tubes.* 15 s. 1953. Kr. 5: —. (Avd. Elektroteknik. 32.)
132. WALLMAN, HENRY, *A wideband searching automatic frequency control circuit of new type.* 21 s. 1953. Kr. 5: —. (Avd. Elektroteknik. 33.)
133. SANDFORD, FOLKE, und FRANSSON, STIG, *Über die Entmischung von grobzerkleinertem Quarz.* 24 s. 1953. Kr. 5: —. (Institutionen för Silikatkemisk Forskning. 31.)
134. EKELÖF, STIG, *The magnetic circuit of telephone relays.* 32 s. 1953. Kr. 5: —. (Avd. Elektroteknik. 34.)
135. YHLAND, C.-H., *Application of the similarity theory on radiation in furnaces.* 31 s. 1953. Kr. 5: —. (Avd. Maskinteknik. 7.)
136. SJÖSTRÖM, EERO, *Über die Verwendung von Ionenaustauschern für die Sorption und Trennung von Ketonen.* 50 s. 1953. Kr. 8:—. (Avd. Kemi och Kemisk Teknologi. 27.)
137. HELLERSTEDT, LARS-MAGNUS, *Wideband amplifiers for bandwidths up to 200 MHz.* 36 s. 1954. Kr. 7: —. (Avd. Elektroteknik. 35.)
138. RYDBECK, O. E. H., and AGDUR, B., *The propagation of electronic space charge waves in periodic structures.* 20 s. 1954. Kr. 5: —. (Avd. Elektroteknik. 36.)
139. AGDUR, N. BERTIL, *Experimental investigation of noise reduction in traveling wave tubes.* 12 s. 1954. Kr. 3: —. (Avd. Elektroteknik. 37.)
140. AGDUR, N. BERTIL, *Amplification measurements on a velocity step tube.* 10 s. 1954. Kr. 2: 50. (Avd. Elektroteknik. 38.)
141. EKELÖF, STIG, *Theory of electromagnetically delayed telephone relays.* 88 s. 1954. Kr. 13: —. (Avd. Elektroteknik. 39.)
142. EKELÖF, S., and KIHLBERG, G., *Theory of the thermistor as an electric circuit element.* 36 s. 1954. Kr. 6: 50. (Avd. Elektroteknik. 40.)
143. SMITH, BENGT, *Peat-gasoline.* 38 s. 1954. Kr. 6: 50. (Avd. Kemi och Kemisk Teknologi. 28.)
144. LEDEN, N., and SCHÖÖN, N.-H., *The solubility of silver azide and the formation of complexes between silver and azide ions.* 17 s. 1954. Kr. 4: —. (Avd. Kemi och Kemisk Teknologi. 29.)
145. *Basorganisation för forskning vid de tekniska högskolorna.* 154 s. + 6 tabellbilagor. 1954. Kr. 12: —. (Not for exchange.)
146. TROEDSSON, CARL BIRGER, *Transportation and city-building.* 30 s. 1954. Kr. 6: —. (Avd. Arkitektur 2.)
147. SANDFORD, FOLKE, and FRANSSON, STIG, *The refractoriness of some types of quartz and quartzite. I.* 28 s. 1954. Kr. 6: —. (Avd. Kemi och Kemisk Teknologi. 30.)
148. CARLSSON, ORVAR, *Porstorlek och frostbeständighet hos tegelmaterial.* 64 s. 1954. Kr. 9: —. (Avd. Kemi och Kemisk Teknologi. 31.)
149. RYDBECK, O. E. H., and WILHELMSSON, H., *A theoretical investigation of the ionospheric electron density variation during a total solar eclipse.* 22 s. 1954. Kr. 3: 50. (Avd. Elektroteknik. 41.)
150. SMITH, BENGT, *Quantitative analysis of mixtures of hydrogen sulfide and sulfur dioxide.* 19 s. 1954. Kr. 4: —. (Avd. Kemi och Kemisk Teknologi. 32.)
151. HEDVALL, J. A., *Reactions with activated solids.* 23 s. 1954. Kr. 5: —. (Institutionen för Silikatkemisk Forskning. 32.)
152. SMITH, CYRIL STANLEY, *The microstructure of polycrystalline materials.* 49 s. 1954. Kr. 9: 50. (Institutionen för Silikatkemisk Forskning. 33.)
153. SELBERG, ARNE, *Norske erfaringer fra bygging av små hengebroer.* 20 s. 1954. Kr. 4: —. (Avd. Väg- och Vattenbyggnad. Byggnadsteknik. 21.)
154. GRANHOLM, HJALMAR, *Armerat trä.* 96 s. 1954. Kr. 9: —. (Avd. Väg- och Vattenbyggnad. Byggnadsteknik. 22.)
155. WILHELMSSON, HANS, *The interaction between an obliquely incident plane electromagnetic wave and an electron beam. I.* 31 s. 1954. Kr. 7: —. (Avd. Elektroteknik. 42.)
156. OLVING, SVEN, *Electromagnetic wave propagation on helical conductors imbedded in dielectric medium.* 14 sid. 1955. Kr. 3: —. (Avd. Elektroteknik. 43.)
157. OLVING, SVEN, *Amplification of the traveling wave tube at high beam current. I.* 11 s. 1955. Kr. 3: —. (Avd. Elektroteknik. 44.)
158. HEDVALL, J. A., NORDENGREN, SVEN, und LILJEGREN, B., *Über die thermische Zersetzung von Kalziumsulfat bei niedrigen Temperaturen.* 18 s. 1955. Kr. 5: —. (Institutionen för Silikatkemisk Forskning. 34.)
159. DAHLGREN, SVEN-ERIC, *On the break-down of thixotropic materials.* 18 s. 1955. Kr. 3: 50. (Institutionen för Silikatkemisk Forskning. 35.)

Forts. å omsl. 4:de sida.

Forts. fr. omsl. 3:dje sida.

160. SANDFORD, FOLKE, och LILJEGREN, BERNE, *Torkningen av råtegel och dennas inverkan på teglets frostbeständighet.* 22 s. 1955. Kr. 3: —. (Institutionen för Silikatkemisk Forskning. 36.)
161. WALLMAN, HENRY, *Automatic noise-factor meter.* 17 s. 1955. Kr. 3: —. (Avd. Elektroteknik. 45.)
162. SANDFORD, FOLKE and FRANSSON, STIG, *The refractoriness of some types of quartz and quartsite.* 24 s. 1955. Kr. 5: —. (Institutionen för Silikatkemisk Forskning. 37.)
163. LINDBLAD, ANDERS, *Konstruktion av linjer för moderna handelsfartyg.* 176 s. 1955. Kr. 20:—. (Avd. Skeppsbyggeri. 6.)
164. SVARTHOLM, NILS, *Two problems in the theory of the slowing down of neutrons by collisions with atomic nuclei.* 15 s. 1955. Kr. 5:—. (Avd. Allmänna Vetenskaper. 10.)
165. PERSSON, PER, *Bostadsvaneundersökning utförd i hyreslägenheter byggda 1947 i Göteborg, Torpaområdet.* 86 s. 1955. Kr. 12: —. (Avd. Arkitektur. 3.)
166. HANSSON, P. R., *Undersökning av mullitbildning i keramiska produkter.* 29 s. 1955. Kr. 6: —. (Institutionen för Silikatkemisk Forskning. 38.)
167. EKELÖF, STIG, *Die Temperaturverteilung in einem gleichstromdurchflossenen langen Metallzylinder mit kreisförmigem Querschnitt.* 38 s. 1955. Kr. 10: —. (Avd. Elektroteknik. 46.)
168. WILHELMSSON, HANS, *On the reflection of electromagnetic waves from a dielectric cylinder.* 17 s. 1955. Kr. 4:50. (Avd. Elektroteknik. 47.)
169. BJÖRK, N., and DAVIDSON, R., *Small signal behaviour of directly heated thermistors.* 43 s. 1955. Kr. 11: —. (Avd. Elektroteknik. 48.)
170. FORESTIER, H., *Tendances actuelles dans la formation de l'ingenieur chimiste: selection, orientation, specialisation; amelioration de son efficience.* 13 s. 1956. Kr. 2: 50. (Avd. Kemi och Kemisk Teknologi. 33.)
171. WAX, NELSON, *On the ring current hypothesis.* 32 s. 1956. Kr. 7: —. (Avd. Elektroteknik. 49.)
172. ELGESKOG, ERIK, *Photoformer analysis and design.* 40 s. 1956. Kr. 8: 50. (Avd. Elektroteknik. 50.)
173. ANZELIUS, ADOLF, *Bimolekulare Reaktion von zwei in Mischung vorliegenden Substanzen mit einer dritten Substanz.* 8 s. 1956. Kr. 5: —. (Avd. Allm. vetenskaper. 11.)
174. REINIUS, ERLING, *Model studies for the extension of the harbour of Gothenburg.* 38 s. 1956. Kr. 6: —. (Avd. Väg- och Vattenbyggnad. Byggnadsteknik. 23.)
175. ZIMEN, K. E., *Diffusion von Edelgasatomen die durch Kernreaktion in festen Stoffen gebildet werden.* 7 s. 1956. Kr. 2: —. (Institutionen för Kärnkemi. 1.)
176. INTHOFF, W., und ZIMEN, K. E., *Kinetik der Diffusion radioaktiver Edelgase aus festen Stoffen nach Bestrahlung.* 16 s. 1956. Kr. 4: —. (Institutionen för Kärnkemi. 2.)
177. GRANHOLM, HJALMAR, *Puts och lättbetong.* 45 s. 1956. Kr. 3: —. (Avd. Väg- och Vattenbyggnad. Byggnadsteknik. 24.)
178. OLVING, SVEN, *A new method for space charge wave interaction studies. I.* 12 s. 1956. Kr. 3: —. (Avd. Elektroteknik. 51.)
179. HANSBO, SVEN, *The critical load of rectangular frames analysed by convergence methods.* 47 s. 1956. Kr. 11: —. (Avd. Väg- och Vattenbyggnad. Byggnadsteknik. 25.)
180. WESTBERG, VIDOR, *Measurements of noise radiation at 10 cm from glow lamps. Preliminary report.* 14 s. 1956. Kr. 4: 50. (Avd. Elektroteknik. 52.)
181. SVENSSON, S. I., HELLGREN, G. and PERERS, O., *The Swedish radioscientific solar eclipse expedition to Italy, 1952. Preliminary report.* 30 s. 1956. Kr. 8: —. (Avd. Elektroteknik. 53.)
182. WAX, NELSON, *A note on design considerations for a proposed auroral radar.* 16 s. 1957. Kr. 3: —. (Avd. Elektroteknik. 54.)
183. JOSHI, G. H., *The electromagnetic interaction between two crossing electron streams. Part I.* 31 s. 1957. Kr. 8: —. (Avd. Elektroteknik. 55.)
184. SMITH, BENGT, *Dry methods for removing hydrogen sulphide from gases.* 65 s. 1957. Kr. 15: —. (Avd. Kemi och Kemisk Teknologi. 34.)
185. EKELÖF, S., BJÖRK, N. and DAVIDSON, R., *Large signal behaviour of directly heated thermistors.* 31 s. 1957. Kr. 8: —. (Avd. Elektroteknik. 56).
186. CARLSSON, BENGT und LARSSON, HANS, *Wirkungsgrad und Selbsthemmung einfacher Umlaufgetriebe.* 48 s. 1957. Kr. 9: —. (Avd. Maskinteknik. 8.)
187. AURELL, CARL G., *The equivalent transmission line of a linear four-terminal network. Calculations with cascade-connected four-terminal networks.* 39 s. 1957. Kr. 6: —. (Avd. Elektroteknik. 57.)
188. LUNDHOLM, R., *Induced overvoltage-surges on transmission lines and their bearing on the lightning performance at medium voltage networks.* 117 s. 1957. Kr. 19: —. (Avd. Elektroteknik. 58.)

Pris kronor 13:—

ELANDERS BOKTRYCKERI AKTIEBOLAG
GÖTEBORG 1957

CHALMERS TEKNISKA HÖGSKOLAS
HANDLINGAR

TRANSACTIONS OF CHALMERS UNIVERSITY OF TECHNOLOGY
GOTHENBURG, SWEDEN

Nr 190 (Avd. Maskinteknik 10) 1957

THE FINITE JOURNAL BEARING, CONSIDERING VAPORIZATION

(Das Gleitlager von endlicher Breite mit Verdampfung)

BY

BENGT JAKOBSSON and LEIF FLOBERG

REPORT No. 3 FROM THE INSTITUTE OF MACHINE ELEMENTS
CHALMERS UNIVERSITY OF TECHNOLOGY
GOTHENBURG, SWEDEN
1957

GUMPERTS FÖRLAG
GÖTEBORG

Av Chalmers Tekniska Högskolas Handlingar hava tidigare utkommit:

Fullständig förteckning över Chalmers Tekniska Högskolas Handlingar lämnas av Chalmers Tekniska Högskolas Bibliotek, Göteborg.

101. Rydbeck, Olof E. H., *The theory of magneto ionic triple splitting.* 40 s. 1951. Kr. 4:50. (Avd. Elektroteknik. 17.)
102. Rydbeck, Olof E. H., and Forsgren, Sven K. H., *On the theory of electron wave tubes.* 31 s. 1951. Kr. 3: 50. (Avd. Elektroteknik. 18.)
103. Lindquist, Rune, *Polar blackouts recorded at the Kiruna Observatory.* 25 s. 1951. Kr. 3: —. (Avd. Elektroteknik 19.)
104. Forsgren, Sven K. H., *Some calculations of ray paths in the ionosphere.* 23 s. 1951. Kr. 3: —. (Avd. Elektroteknik. 20.)
105. Agdur, Bertil N., *Experimental observation of double-stream amplification.* 13 s. 1951. Kr. 1: 50. (Avd. Elektroteknik. 21.)
106. Agdur, Bertil N., and Åsdal, Carl-Gösta L., *Noise measurements on a traveling wave tube.* 9 s. 1951. Kr. 1: 50. (Avd. Elektroteknik. 22.)
107. Forsgren, Sven K. H., and Perers, Olof F., *Vertical recording of rain by radar.* 19 s. 1951. Kr. 2: 50. (Avd. Elektroteknik. 23.)
108. Perers, Olof F., Stjernberg, Bo K. E., and Forsgren, Sven K. H., *Microwave propagation in the optical range.* 20 s. 1951. Kr. 3: —. (Avd. Elektroteknik. 24.)
109. Lindquist, Rune, *A 16 kW panoramic ionospheric recorder.* 41 s. 1951. Kr. 4: 50. (Avd. Elektroteknik. 25.)
110. Lindblad, Anders, *Some experiments with selfpropelled models of twin screw ships.* 24 s. 1951. Kr. 4: 50. (Avd. Skeppsbyggeri. 4.)
111. Beskow, Gunnar, *Amerikansk och svensk jordklassifikation. Speciellt för vägar och flygfält.* 48 s. 1951. Kr. 2: —. (Avd. Väg- och Vattenbyggnad. Byggnadsteknik. 18.)
112. Dahr, Konstantin, *On the mathematical analysis of an idealized multiplex electromagnetic machine.* 116 s. 1951. Kr. 17: —. (Avd. Elektroteknik. 26.)
113. Troedsson, Carl Birger, *Two standpoints towards modern architecture. Wright and Le Corbusier.* 22 s. 1951. Kr. 4: —. (Avd. Arkitektur. 1.)
114. Stranski, I. N., *Die Vorgänge an Kristalloberflächen.* 21 s. 1951. Kr. 3: —. (Avd. Kemi och Kemisk Teknologi. 24.)
115. *Mitteilungen aus dem Institut für organische Chemie. VII.* Von Erik Larsson. 31 s. 1951. Kr. 4: —. (Avd. Kemi och Kemisk Teknologi. 25.)
116. Ekelöf, Stig, *Les machines mathématiques en Suède.* 26 s. 1951. Kr. 5: —. (Avd. Elektroteknik. 27.)
117. Möller, Torsten, *En ny metod för beräkning av spikförband.* 77 s. 1951. Kr. 7: —. (Avd. Väg- och Vattenbyggnad. Byggnadsteknik. 19.)
118. Hedvall, J. Arvid, Jagitsch, Robert und Olson, Gillis, *Über das Problem der Zerstörung antiker Gläser. II.* 15 s. 1951. Kr. 2: 50. (Institutionen för Silikatkemisk Forskning. 28.)
119. Ahlberg, R., *A contribution to the methods of measuring the plasticity of clays.* 25 s. 1951. Kr. 5: —. (Institutionen för Silikatkemisk Forskning. 29.)
120. Ekelöf, S., Bengtson, L., Kihlberg, G., and Leithammel, P., *An integrating amplifier for the oscillographic recording of magnetic flux.* 23 s. 1951. Kr. 5: —. (Avd. Elektroteknik. 28.)
121. *Mitteilungen aus dem Institut für organische Chemie. VIII.* Von Erik Larsson. 17 s. 1951. Kr. 2: 50. (Avd. Kemi och Kemisk Teknologi. 26.)
122. Karlson, K. G., *Sur le frein à sabots extérieurs articulés.* 31 s. 1951. Kr. 5: —. (Avd. Maskinteknik. 6.)
123. Ambjörn, Gustaf, *Släpförsök med fartygsmodeller i sned och tvär ställning mot körriktningen samt resultatens tillämpning på ett intressant sjörättsfall.* 31 s. 1952. Kr. 5: —. (Avd. Skeppsbyggeri. 5.)
124. Berne, Eric, *Studies on radioactive bromine.* 46 s. 1952. Kr. 6: —. (Avd. Allmänna Vetenskaper. 8.)
125. Nilsson, Ingvar, *A scaler using dekatron scaling tubes. — Note on the cross section of the reaction* $^{31}P(n,p)^{31}Si$. 8 s. 1952. Kr. 2: —. (Avd. Allmänna Vetenskaper. 9.)
126. Hedvall, J. A., and Liljegren, B., *An investigation of the reaction 2* $CaCO_3 + SiO_2$ *at high temperatures.* 12 s. 1952. Kr. 2: 50. (Institutionen för Silikatkemisk Forskning. 30.)
127. Saretok, Vitold, *Tillsatsmedel till betong.* 67 s. 1952. Kr. 5: —. (Avd. Väg- och Vattenbyggnad. Byggnadsteknik. 20.)

Forts. å omsl. 3:dje sida.

CHALMERS TEKNISKA HÖGSKOLAS
HANDLINGAR

TRANSACTIONS OF CHALMERS UNIVERSITY OF TECHNOLOGY
GOTHENBURG, SWEDEN

Nr 190 (Avd. Maskinteknik 10) 1957

THE FINITE JOURNAL BEARING, CONSIDERING VAPORIZATION

(Das Gleitlager von endlicher Breite mit Verdampfung)

BY

BENGT JAKOBSSON and LEIF FLOBERG

REPORT No. 3 FROM THE INSTITUTE OF MACHINE ELEMENTS
CHALMERS UNIVERSITY OF TECHNOLOGY
GOTHENBURG, SWEDEN
1957

GÖTEBORG 1957
ELANDERS BOKTRYCKERI AKTIEBOLAG

Preface

In recent years, lubrication research has been carried out at the Institute of Machine Elements, Chalmers University of Technology, Gothenburg, Sweden. Since 1955, the sponsorship of Statens Tekniska Forskningsråd has allowed me to keep Mr L. FLOBERG, M. Sc. as full-time research assistant working on journal bearings.

When starting my work I felt that the works by REYNOLDS and SOMMERFELD could be interpreted in a better way. I was not convinced that their equations were so far from right in practice as has hitherto been said. The apparent lack of agreement between theory and practice could be due to the lack of rigorous similarity in oil film boundary conditions.

We have regarded constant pressure vapour zones and have satisfied the equation of continuity rigorously for all of the bearing. Our theoretical results have been verified experimentally.

In report No. 2 from the Institute, L. FLOBERG (6) has treated the infinite journal bearing with vaporization.

In this report, journal bearings of finite width are discussed.

Instead of *vaporization* some authors use the term *cavitation*.

I am very glad to thank Mr L. FLOBERG for very clever work on this treatise.

I wish to express my sincere thanks to Statens Tekniska Forskningsråd for their invaluable help.

Bengt Jakobsson

Professor, Dr.Sc. (Eng)
Head of the Institute of
Machine Elements

Contents

Page

Preface 3

1. Introduction 6

2. Notation 8

3. Oil Film Theory 11

3,1. The Differential Equation for the Pressure in the Oil Film 11

3,2. Numerical Solution of the Differential Equation for the Pressure Distribution 15

3,3. Load Capacity 17

3,4. Oil Flow 19

3,5. Friction Force, Friction Torque, and Power Loss 21

3,6. Temperature Rise 24

3,7. Coefficient of Friction and Relative Power Loss 26

4. Theory for Vaporization 28

4,1. Boundary Conditions for a Vapour Region 28

4,2. Friction Force, Friction Torque, and Power Loss for a Vapour Region 34

4,3. Temperature Rise 37

5. The 360° Bearing with No Oil Grooves 39

5,1. The 360° Bearing with No Oil Grooves and without Vapour Regions 39

5,11. Pressure Distribution 39

5,12. Load Capacity 41

5,13. Oil Flow 42

5,14. Power Loss 44

5,15. Average Temperature Rise 45

5,16. Coefficient of Friction and Relative Power Loss 46

5,17. Experimental Investigation 47

5,2. The 360° Bearing with No Oil Grooves and with Vapour Regions 54

5,21. Pressure Distribution 54

5,22. Load Capacity 57

5,23. Oil Flow 59

5,24. Power Loss 60

5,25. Average Temperature Rise 64

5,26. Coefficient of Friction and Relative Power Loss 64

5,27. Experimental Investigation 64

5,3. The Optimum 360° Bearing without Oil Grooves 66

Page

6. The 180° Bearing with Minimum Film Thickness at the Trailing Edge 73
   6,1. Pressure Distribution 73
   6,2. Load Capacity 74
   6,3. Oil Flow 74
   6,4. Power Loss 77
   6,5. Average Temperature Rise 77
   6,6. Coefficient of Friction and Relative Power Loss 78
   6,7. Optimum Analysis 78
   6,8. Schedule for Calculation 80
   6,9. Examples 81

7. The 360° Bearing with an Oil Groove at the Maximum Film Thickness, and a Vapour Region at Atmospheric Pressure 83
   7,1. General Considerations 83
   7,2. Optimum Analysis 88
   7,3. Schedule for Calculation 89
   7,4. Examples 90

8. The 180° Centrally Loaded Bearing with a Vapour Region at Atmospheric Pressure 92
   8,1. General Considerations 92
   8,2. Optimum Analysis 94

9. The 360° Bearing with an Oil Groove 90° before the Load Line, and a Vapour Region at Atmospheric Pressure 96
   9,1. General Considerations 96
   9,2. Optimum Analysis 96

10. Superposition of Solutions 98
   10,1. Superposition of Pressure Distributions 98
   10,2. Load Capacity 99
   10,3. Oil Flow 100
   10,4. Power Loss 101

11. Conclusion 102

12. Zusammenfassung 103

13. Appendix: Tables of Calculated Values 104

14. References 117

1. Introduction

TOWER (11, 12) was the first to show that in a journal bearing the shaft is completely separated from the bearing by a thin carrying oil film. He measured an oil film pressure which was higher than the average pressure. This was at that time very important. His reports on these experiments were published in 1883 and 1885.

These problems were treated theoretically by REYNOLDS (8) in his classical work published in 1886, in which he derived the well-known differential equation for the pressure in a thin oil film. This equation considers flow in axial direction.

The first problem to be discussed was the infinitely wide bearing. REYNOLDS solved the equation exactly for the slider bearing and approximately for the journal bearing. The exact solution for the latter case was given by SOMMERFELD (10) in 1904.

It was early emphasized that the vapour pressure of the lubricant represented a limit for the oil film pressure. The journal bearing with vaporization has been treated recently by FLOBERG (6), who has verified the theoretical analysis by experiments.

The bearings of greatest interest, however, are those of finite width where axial oil flow occurs. In practice, there is usually side leakage; therefore the theory for infinite width cannot be used.

The primary problem in the theory of lubrication is to solve REYNOLDS' partial differential equation. MICHELL (7) succeeded to give a solution for the plain bearing of finite width in 1905. The pressure for a point in the bearing is given as an infinite series. A numerical or graphical integration gives the load capacity. Another way to solve the differential equation is the relaxation method which gives only an approximate pressure distribution, but the pressure can be determined at a sufficient number of points to give satisfactory values for load capacity, oil flow, and power loss.

The big problem, already stressed in 1904 by SOMMERFELD, has been the vaporization. Because the vapour pressure for oil is usually close to the atmospheric pressure, there is no practical 360° journal bearing without oil vapour or air. Several authors have treated

this case, but no satisfactory treatment has been given. The usual error is the lack of correct boundary conditions for the vapour region.

Vaporization will be treated in this paper. The theory has strict boundary conditions. The locations of the vapour regions are not assumed, but are determined by calculation. There is a good agreement between theory and experiments.

Other authors have assumed that the vapour pressure is zero, i. e. atmospheric pressure, and that the oil film pressure curve in a 360° bearing begins at maximum film thickness and ends with zero derivative. CAMERON-WOOD (3) have given a solution based upon these assumptions.

In this treatise is shown that the condition with beginning oil film at the maximum film thickness is arbitrarily chosen. This is confirmed by experiments. For a bearing with an axial oil groove at the maximum oil film thickness, however, CAMERON-WOOD give approximately correct load capacity; but their assumption that a vapour region is filled with oil, could not give correct values for the power loss. In this paper a method for calculation of power loss in a vapour region is put forward; and it is shown how to design an optimum bearing in the different cases.

Calculations are made for width-diameter ratios 1; 0,5 and 0,25 for some 360° and some 180° partial bearings. All calculations are made for constant viscosity.

2. Notation

b = Bearing width

c = Specific heat of oil

D = Diameter of bearing

d = Diameter of journal

E = Power loss per unit width

E_{tot} = Total power loss

$E_0 = \frac{E\,\psi}{\eta\,U^2}$ = Non-dimensional power loss per unit width

e = Eccentricity of journal relative to bearing

F_b = Friction force on bearing per unit width

F_j = Friction force on journal per unit width

$F_{j0} = \frac{F_j\,\psi}{\eta\,U}$ = Non-dimensional friction force on journal per unit width

$f = \frac{E}{P} = \frac{E_{tot}}{P_{tot}}$ = Relative power loss

$H = \frac{h}{\Delta r}$ = Non-dimensional film thickness

h = Oil film thickness

k = Oil supply pressure

M_b = Friction torque on bearing per unit width

M_j = Friction torque on journal per unit width

$M_{j0} = \frac{M_j\,\psi}{\eta\,U\,r}$ = Non-dimensional friction torque on journal per unit width

P = Load capacity per unit width

P_{tot} = Total load capacity

$P_0 = \frac{P\,\psi^2}{\eta\,U}$ = Non-dimensional load capacity per unit width

p = Pressure

p_v = Vapour pressure

$p_0 = \frac{p\,\psi^2}{\eta\,\omega}$ = Non-dimensional pressure

Q = Oil flow

$Q_0 = \frac{Q}{r\,U\,\Delta r}$ = Non-dimensional oil flow

q = Oil flow per unit width

$q_0 = \frac{q}{U\,\Delta r}$ = Non-dimensional oil flow per unit width

R = Radius of bearing

r = Radius of journal

$\Delta r = R - r$ = Radial clearance

t = Temperature

Δt = Temperature rise

$\Delta t_0 = c\,\varrho \cdot \frac{\Delta t\,\psi^2}{\eta\,\omega}$ = Non-dimensional temperature rise

U, V = Surface velocities in the x- and y-directions respectively

u, v, w = Velocities of a fluid particle in the x-, y- and z-directions respectively

x, y, z = Rectangular coordinates

β = Angle between load line and line of centres

γ = Angle

$\varepsilon = \frac{e}{\Delta r}$ = Non-dimensional eccentricity

$\zeta = \frac{z}{r}$ = Non-dimensional coordinate

η = Viscosity of the oil

Θ = Angle measured from the load line in positive direction

$\mu = \frac{F_j}{P}$ = Coefficient of friction

$\nu = \frac{b}{d}$ = Ratio width-diameter

ϱ = Density of oil

τ = Shear stress

$\varphi = \frac{x}{r}$ = Angular coordinate

$\psi = \frac{\Delta r}{r}$ = Radial clearance/journal radius

ω = Angular velocity

Indices

a = Average

b = Bearing

e = Experimental

j = Journal

t = Theoretical

0 = Non-dimensional

3. Oil Film Theory

3,1. The Differential Equation for the Pressure in the Oil Film

To derive the differential equation for the pressure, the following assumptions are made:

The oil film is considered so thin that there are no variations in pressure or temperature throughout its thickness.

The viscosity is constant.

The oil is incompressible.

Inertia terms and hydrostatic pressure can be neglected.

The flow is laminar.

Consider an oil element with the sides dx, dy and dz.

The equilibrium gives

$$\left.\begin{aligned} \frac{\partial p}{\partial x} &= \frac{\partial \tau_x}{\partial y} \\ \frac{\partial p}{\partial z} &= \frac{\partial \tau_z}{\partial y} \end{aligned}\right\} \quad \ldots\ldots\ldots\ldots\ldots\ldots \quad 11.1$$

where

p = oil film pressure
τ_x, τ_z = shear stresses in the x- and z-directions respectively
x, y, z = rectangular coordinates

Due to the continuity we have

$$\frac{\partial u}{\partial x} + \frac{\partial v}{\partial y} + \frac{\partial w}{\partial z} = 0 \quad \ldots\ldots\ldots\ldots\ldots \quad 11.2$$

where

u, v, w = velocities of a fluid particle in the x-, y- and z-directions respectively

The shear stresses are obtained from NEWTON's law for laminar viscous flow.

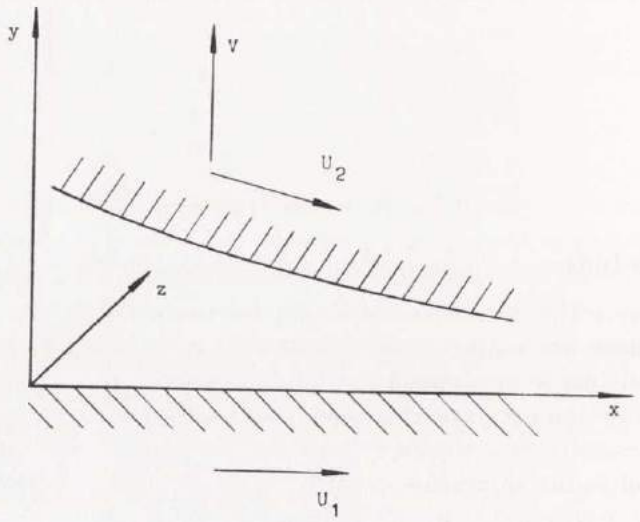

Fig. 12.1

$$\left.\begin{aligned} \tau_x &= \eta \frac{\partial u}{\partial y} \\ \tau_z &= \eta \frac{\partial w}{\partial y} \end{aligned}\right\} \quad \ldots\ldots\ldots\ldots\ldots\ldots \quad 12.2$$

where

η = oil viscosity

Eq. 11.1 and 12.2 give

$$\left.\begin{aligned} \frac{\partial^2 u}{\partial y^2} &= \frac{1}{\eta} \cdot \frac{\partial p}{\partial x} \\ \frac{\partial^2 w}{\partial y^2} &= \frac{1}{\eta} \cdot \frac{\partial p}{\partial z} \end{aligned}\right\} \quad \ldots\ldots\ldots\ldots\ldots\ldots \quad 12.3$$

Since the viscosity is assumed to be constant, and there is no variation in the pressure over the oil film thickness, these two equations can be integrated. With the boundary conditions from 12.1

$y = 0$	$y = h$
$u = U_1$	$u = U_2$
$w = 0$	$w = 0$

where h is the oil film thickness, the equations 12.3 give

$$\left.\begin{aligned} u &= \frac{1}{2\eta} \cdot \frac{\partial p}{\partial x} (y^2 - hy) + \frac{U_2 - U_1}{h} \cdot y + U_1 \\ w &= \frac{1}{2\eta} \cdot \frac{\partial p}{\partial z} (y^2 - hy) \end{aligned}\right\} \quad \ldots\ldots \text{13.1}$$

Integrate the continuity equation 11.2 with respect to y between $y = 0$ and $y = h$ with the expressions for u and w from 13.1. The boundary conditions for v are

$$\begin{aligned} y &= 0 & y &= h \\ v &= 0 & v &= V + U_2 \frac{\partial h}{\partial x} \end{aligned}$$

Then

$$\frac{\partial}{\partial x}\left(h^3 \frac{\partial p}{\partial x}\right) + \frac{\partial}{\partial z}\left(h^3 \frac{\partial p}{\partial z}\right) = 6\eta (U_1 + U_2) \frac{\partial h}{\partial x} + 12\eta V$$

This is the partial differential equation for the pressure in a bearing.

Usually for a journal bearing

$$U_1 = V = 0$$

$$U_2 = U = r\omega$$

where

r = journal radius

ω = angular velocity

The equation is then simplified to

$$\frac{\partial}{\partial x}\left(h^3 \frac{\partial p}{\partial x}\right) + \frac{\partial}{\partial z}\left(h^3 \frac{\partial p}{\partial z}\right) = 6\eta U \frac{\partial h}{\partial x} \quad \ldots\ldots \text{13.2}$$

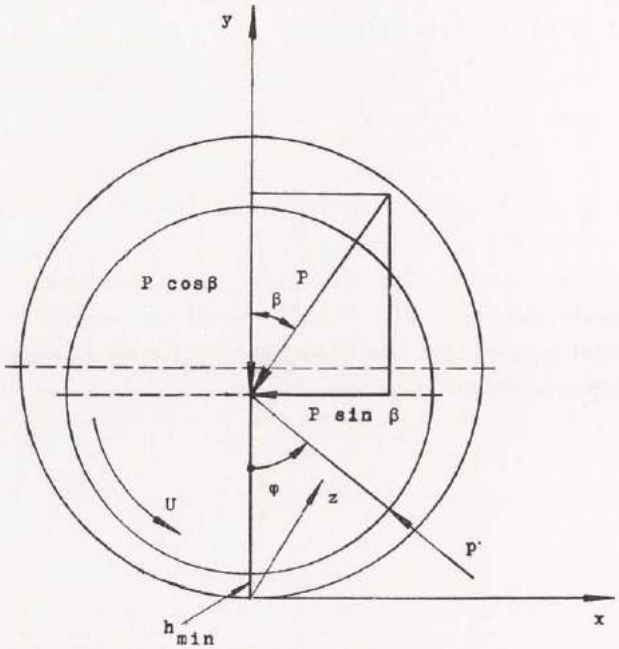

Fig. 14.1

The oil film thickness for a journal bearing with parallel journal and bearing axes is

$$h = \Delta r - e \cos \varphi = \Delta r \, (1 - \varepsilon \cos \varphi)$$

where

Δr = radial clearance

e = eccentricity of journal relative to bearing

$\varepsilon = \dfrac{e}{\Delta r}$ = non-dimensional eccentricity

Introduce now the non-dimensional expressions

$$\varphi = \frac{x}{r}$$

$$\zeta = \frac{z}{r}$$

$$H = \frac{h}{\Delta r} = 1 - \varepsilon \cos \varphi$$

Then eq. 13.2 becomes

$$\frac{\partial}{\partial \varphi}\left(H^3 \frac{\partial p}{\partial \varphi}\right) + \frac{\partial}{\partial \zeta}\left(H^3 \frac{\partial p}{\partial \zeta}\right) = \frac{\eta \omega}{\psi^2} \cdot 6 \frac{\partial H}{\partial \varphi} \quad \ldots \quad 15.1$$

where

$$\psi = \frac{\Delta r}{r}$$

With the non-dimensional expression for the pressure

$$p_0 = \frac{p \psi^2}{\eta \omega}$$

eq. 13.2 can be simplified to

$$\frac{\partial}{\partial \varphi}\left(H^3 \frac{\partial p_0}{\partial \varphi}\right) + \frac{\partial}{\partial \zeta}\left(H^3 \frac{\partial p_0}{\partial \zeta}\right) = 6 \frac{\partial H}{\partial \varphi} \quad \ldots\ldots \quad 15.2$$

3,2. Numerical Solution of the Differential Equation for the Pressure Distribution

Hitherto, it has not been possible to give an exact solution for the equation 15.2. Hence, it is necessary to solve it by approximate methods. One suitable way is to use the relaxation method by which the pressure in a number of points over the bearing area is determined. From the pressure values further calculations give the load, the oil flow, the power loss and related quantities.

When using the relaxation method, the differential equation is transformed into a difference equation. For this purpose the unfolded bearing area is divided into a rectangular network with the panel sides $\Delta\varphi$ and $\Delta\zeta$, as in 15.3 where $v = b/d =$ width/diameter ratio.

Consider five neighbouring points of 15.3 as shown in 16.1.

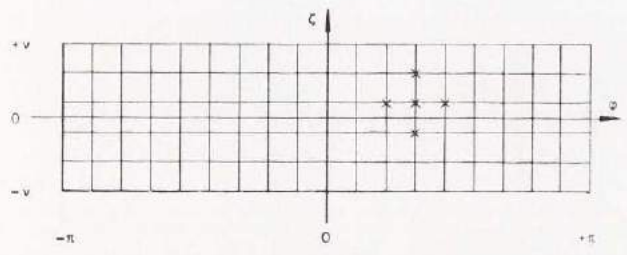

Fig. 15.3

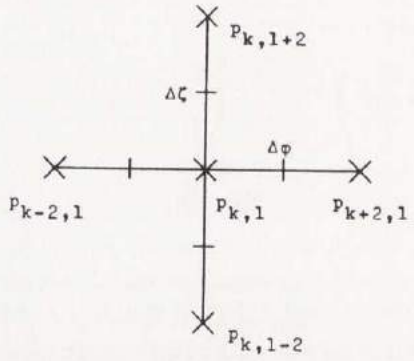

Fig. 16.1

The first two terms in 15.1 can be transformed in the following manner for the point (k, l)

$$\frac{\partial}{\partial \varphi}\left(H^3 \frac{\partial p}{\partial \varphi}\right) = \frac{\left(H^3 \frac{\partial p}{\partial \varphi}\right)_{k+1,l} - \left(H^3 \frac{\partial p}{\partial \varphi}\right)_{k-1,l}}{\Delta\varphi} =$$

$$= H^3_{k+1,l} \cdot \frac{p_{k+2,l} - p_{k,l}}{\Delta\varphi^2} - H^3_{k-1,l} \cdot \frac{p_{k,l} - p_{k-2,l}}{\Delta\varphi^2}$$

$$\frac{\partial}{\partial \zeta}\left(H^3 \frac{\partial p}{\partial \zeta}\right) = \frac{\left(H^3 \frac{\partial p}{\partial \zeta}\right)_{k,l+1} - \left(H^3 \frac{\partial p}{\partial \zeta}\right)_{k,l-1}}{\Delta\zeta} =$$

$$= H^3_{k,l+1} \cdot \frac{p_{k,l+2} - p_{k,l}}{\Delta\zeta^2} - H^3_{k,l-1} \cdot \frac{p_{k,l} - p_{k,l-2}}{\Delta\zeta^2}$$

For non-dimensional pressure, eq. 15.2, we get the same transformation. The right-hand term in 15.2 can be exactly calculated at every point. The difference equation then becomes

$$\frac{H^3_{k+1,l}}{\Delta\varphi^2} \cdot (p_0)_{k+2,l} + \frac{H^3_{k,l-1}}{\Delta\zeta^2} \cdot (p_0)_{k,l-2} +$$

$$+ \frac{H^3_{k-1,l}}{\Delta\varphi^2} \cdot (p_0)_{k-2,l} + \frac{H^3_{k,l+1}}{\Delta\zeta^2} \cdot (p_0)_{k,l+2} -$$

$$- \left[\frac{H^3_{k+1,l}}{\Delta\varphi^2} + \frac{H^3_{k,l-1}}{\Delta\zeta^2} + \frac{H^3_{k-1,l}}{\Delta\varphi^2} + \frac{H^3_{k,l+1}}{\Delta\zeta^2}\right] (p_0)_{k,l} -$$

$$- 6\left(\frac{\partial H}{\partial \varphi}\right)_{k,l} = 0 \quad \ldots\ldots\ldots\ldots\ldots\ldots\ldots\ldots\ldots\ldots \quad 16.2$$

This equation shall be satisfied in all points. The number of equations is equal to the number of unknowns. This gives a system of equations which is very tedious to solve exactly. An easier method is to guess a pressure distribution and then adjust the pressure values successively until all eqs. 16.2 are approximately satisfied.

The calculations in this work are made with

$$\Delta\varphi = \frac{\pi}{9} \text{ and } \Delta\zeta = \frac{2\,r}{5}$$

This division of the bearing area gives in chap. 5 a number of unknowns equal to 16.

CHRISTOPHERSON (4) has derived a relaxation method in which he makes further approximations. Instead of using the H^3-values between the pressure points, he uses an average value. His solution gives a result which is not as accurate as that of the above method. For a bearing of infinite width, it is possible to integrate 15.2. Thus the two approximate solutions can be compared with the exact one. For example, with the eccentricity $\varepsilon = 0{,}9$ and $\Delta\varphi = \frac{\pi}{5}$. CHRISTOPHERSON'S method gives an error 4 times greater than the method described above.

The solution of the equation system is advantageously performed by an electronic mathematical machine. In such a fast machine it is possible to use a larger number of unknowns, which gives greater accuracy.

3,3. Load Capacity

The load capacity $P_{tot} = Pb$, where P is load per unit width and b the bearing width, is derived through integration of the pressure over the bearing area. From 14.1 the load components become

$$\left.\begin{aligned} P_x b = Pb \sin\beta &= -\int_{\zeta_1}^{\zeta_2}\int_{\varphi_1}^{\varphi_2} p \sin\varphi\, r\, d\varphi\, r\, d\zeta \\ P_y b = Pb \cos\beta &= \int_{\zeta_1}^{\zeta_2}\int_{\varphi_1}^{\varphi_2} p \cos\varphi\, r\, d\varphi\, r\, d\zeta \end{aligned}\right\} \quad \ldots\ldots \quad 17.1$$

Then the load and the load angle can be determined.

$$\left.\begin{aligned} P &= \sqrt{P_x^2 + P_y^2} \\ \tan\beta &= \frac{P_x}{P_y} \end{aligned}\right\} \quad \ldots\ldots\ldots\ldots\ldots\ldots \quad 18.1$$

Introduce now the non-dimensional expression for the pressure

$$p_0 = \frac{p\,\psi^2}{\eta\,\omega}$$

and $b = 2\,r\,r$

Then the load components are

$$P_x = -\frac{\eta\,U}{\psi^2} \cdot \frac{1}{2\,r} \int_{\zeta_1}^{\zeta_2} \int_{\varphi_1}^{\varphi_2} p_0 \sin\varphi\, d\varphi\, d\zeta$$

$$P_y = \frac{\eta\,U}{\psi^2} \cdot \frac{1}{2\,r} \int_{\zeta_1}^{\zeta_2} \int_{\varphi_1}^{\varphi_2} p_0 \cos\varphi\, d\varphi\, d\zeta$$

or non-dimensionally

$$\left.\begin{aligned} P_{x0} &= \frac{P_x\,\psi^2}{\eta\,U} = -\frac{1}{2\,r} \int_{\zeta_1}^{\zeta_2} \int_{\varphi_1}^{\varphi_2} p_0 \sin\varphi\, d\varphi\, d\zeta \\ P_{y0} &= \frac{P_y\,\psi^2}{\eta\,U} = \frac{1}{2\,r} \int_{\zeta_1}^{\zeta_2} \int_{\varphi_1}^{\varphi_2} p_0 \cos\varphi\, d\varphi\, d\zeta \end{aligned}\right\} \quad \ldots \quad 18.2$$

The non-dimensional expressions for the load and the load angle are

$$\left.\begin{aligned} P_0 &= \frac{P\,\psi^2}{\eta\,U} = \sqrt{P_{x0}^2 + P_{y0}^2} \\ \tan\beta &= \frac{P_{x0}}{P_{y0}} \end{aligned}\right\} \quad \ldots\ldots\ldots\ldots \quad 18.3$$

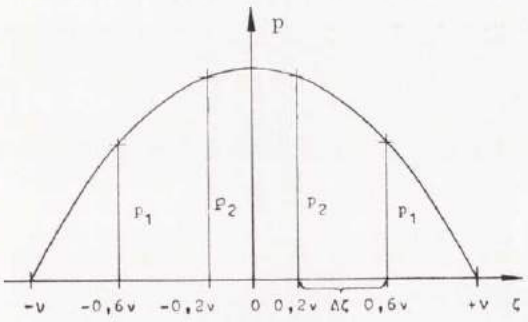

Fig. 19.1

To solve the integrals 18.2, it is convenient to use two different methods in the φ- and ζ-directions respectively. As the pressure curves in the ζ-direction are nearly parabolas, which is assumed by some authors when integrating the differential equation for the pressure, numerical integrations of polynoms through the calculated pressure values give very good results. Numerical integration has been treated by BICKLEY (1). As an example the method is described for five intervals in the ζ-direction.

A third degree curve for $\zeta \geq 0$ going through p_1 and p_2 with zero derivative at $\zeta = 0$ gives for the average pressure in the ζ-direction the value

$$p_a = \frac{275\, p_1 + 200\, p_2}{552}$$

In peripheral direction the numerical integration by polynoms cannot be recommended due to the variations in the derivative.

Thus the best value seems to be obtained by a planimeter.

3,4. Oil Flow

From 13.1 if $U_2 = U$ and $U_1 = 0$

$$\left.\begin{aligned} u &= \frac{1}{2\eta} \cdot \frac{\partial p}{\partial x} (y^2 - hy) + \frac{U}{h} \cdot y \\ w &= \frac{1}{2\eta} \cdot \frac{\partial p}{\partial z} (y^2 - hy) \end{aligned}\right\} \quad \ldots\ldots\ldots 19.2$$

Since $\frac{\partial p}{\partial x}$ and $\frac{\partial p}{\partial z}$ are independent of y, the two velocities can be integrated with respect to this variable.

The oil flows per unit width in the x- and z-directions respectively are

$$q_x = \int_0^h u \, dy$$

$$q_z = \int_0^h w \, dy$$

or integrated

$$\left.\begin{aligned} q_x &= \frac{Uh}{2} - \frac{h^3}{12\eta} \cdot \frac{\partial p}{\partial x} \\ q_z &= -\frac{h^3}{12\eta} \cdot \frac{\partial p}{\partial z} \end{aligned}\right\} \quad \ldots\ldots\ldots\ldots\ldots \quad 20.1$$

Introduce the non-dimensional expressions

$$H = \frac{h}{\Delta r} = 1 - \varepsilon \cos \varphi$$

$$p_0 = \frac{p \, \psi^2}{\eta \, \omega}$$

$$\varphi = \frac{x}{r}$$

$$\zeta = \frac{z}{r}$$

Then

$$q_x = U \Delta r \left[\frac{H}{2} - \frac{H^3}{12} \cdot \frac{\partial p_0}{\partial \varphi} \right]$$

$$q_z = U \Delta r \left[-\frac{H^3}{12} \cdot \frac{\partial p_0}{\partial \zeta} \right]$$

and

$$\left.\begin{aligned} q_{x0} &= \frac{q_x}{U \Delta r} = \frac{H}{2} - \frac{H^3}{12} \cdot \frac{\partial p_0}{\partial \varphi} \\ q_{z0} &= \frac{q_z}{U \Delta r} = -\frac{H^3}{12} \cdot \frac{\partial p_0}{\partial \zeta} \end{aligned}\right\}$$

To evaluate the non-dimensional oil flow, the derivatives are calculated by numerical methods. If a great number of pressure points are known, a good method is to draw a parabola through three points.

For the curve in 19.1 the third degree polynome gives

$$\left(\frac{\partial p}{\partial \zeta}\right)_{\zeta=\nu} = -\frac{140\, p_1 - 55\, p_2}{46\, \Delta\zeta}$$

Numerical differentiation has been treated by BICKLEY (2).

The oil flow entering the bearing must be equal to the flow leaving the bearing from the continuity condition. The oil flow can then be calculated either as the integral over the oil flow per unit width entering the bearing, or as the integral over the flow per unit width leaving the bearing. This oil flow Q is the changed oil quantity per unit time.

The non-dimensional oil flow becomes

$$Q_0 = \frac{Q}{r\, U\, \Delta r} \qquad \ldots\ldots\ldots\ldots\ldots\ldots \quad 21.1$$

where Q_0 is equal to the integral over the non-dimensional oil flow per unit width in non-dimensional coordinates.

3,5. Friction Force, Friction Torque, and Power Loss

Newton's law gives the shear stress for an oil element

$$\tau_x = \eta \frac{\partial u}{\partial y}$$

where $\dfrac{\partial u}{\partial y}$ is derived from 19.2 and

$$\tau_x = \frac{1}{2} \cdot \frac{\partial p}{\partial x} (2\, y - h) + \eta \cdot \frac{U}{h}$$

and

$$(\tau_x)_{y=h} = \frac{h}{2} \cdot \frac{\partial p}{\partial x} + \eta \cdot \frac{U}{h}$$

The friction force is

$$F_j b = \int_{\zeta_1}^{\zeta_2}\int_{\varphi_1}^{\varphi_2} (\tau_x)_{y=h}\, r\, d\varphi\, r\, d\zeta = \int_{\zeta_1}^{\zeta_2}\int_{\varphi_1}^{\varphi_2} \left[\frac{h}{2}\cdot\frac{\partial p}{\partial x} + \eta\cdot\frac{U}{h}\right] r^2\, d\varphi\, d\zeta \quad 22.1$$

where F_j is friction force per unit width.

Non-dimensionally

$$F_{j0} = \frac{F_j\,\psi}{\eta\, U} = \frac{1}{4\,r}\int_{\zeta_1}^{\zeta_2}\int_{\varphi_1}^{\varphi_2} H\,\frac{\partial p_0}{\partial \varphi}\, d\varphi\, d\zeta + \frac{1}{2\,r}\int_{\zeta_1}^{\zeta_2}\int_{\varphi_1}^{\varphi_2}\frac{1}{H}\, d\varphi\, d\zeta \quad \ldots\ 22.2$$

where $H = 1 - \varepsilon\cos\varphi$

The friction torque per unit width becomes

$$M_j = F_j r = \frac{\eta\, U}{\psi}\cdot F_{j0}\, r$$

and

$$M_{j0} = \frac{M_j\,\psi}{\eta\, U\, r} = F_{j0}$$

Then the power loss per unit width

$$E = M_j\,\omega = \frac{\eta\, U\, r}{\psi}\cdot M_{j0}\,\omega$$

and

$$E_0 = \frac{E\,\psi}{\eta\, U^2} = M_{j0}$$

Thus the non-dimensional expressions for friction force, friction torque and power loss are the same.

$$F_{j0} = \frac{F_j\,\psi}{\eta\, U} = M_{j0} = \frac{M_j\,\psi}{\eta\, U\, r} = E_0 = \frac{E\,\psi}{\eta\, U^2}$$

In evaluating 22.2 it is suitable to transform the first integral.

$$\int_{\zeta_1}^{\zeta_2}\left[\int_{\varphi_1}^{\varphi_2} H\,\frac{\partial\, p_0}{\partial\,\varphi}\,d\varphi\right]d\zeta = \int_{\zeta_1}^{\zeta_2}\left[\overline{\int_{\varphi_1}^{\varphi_2}} Hp_0\right]d\zeta -$$

$$-\int_{\zeta_1}^{\zeta_2}\int_{\varphi_1}^{\varphi_2} p_0\,\varepsilon\,\sin\varphi\,d\varphi\,d\zeta$$

as $\dfrac{\partial\, H}{\partial\,\varphi} = \varepsilon\,\sin\varphi$

The last integral in 22.2 can be solved exactly. H is a function of φ only.

$$\int_{\zeta_1}^{\zeta_2}\int_{\varphi_1}^{\varphi_2}\frac{1}{H}\,d\varphi\,d\zeta = \int_{\zeta_1}^{\zeta_2}\int_{\varphi_1}^{\varphi_2}\frac{d\varphi}{1-\varepsilon\cos\varphi}\,d\zeta$$

Substitute

$$\left.\begin{aligned}\cos\varphi &= \frac{\cos\gamma+\varepsilon}{1+\varepsilon\cos\gamma}\\ d\varphi &= \frac{\sqrt{1-\varepsilon^2}}{1+\varepsilon\cos\gamma}\,d\gamma\end{aligned}\right\} \quad \ldots\ldots\ldots\ldots\ 23.1$$

Then we get

$$\int_{\varphi_1}^{\varphi_2}\frac{d\varphi}{1-\varepsilon\cos\varphi} = \frac{\gamma_2-\gamma_1}{\sqrt{1-\varepsilon^2}}$$

where

$$\gamma = \arccos\frac{\cos\varphi-\varepsilon}{1-\varepsilon\cos\varphi}$$

Eq. 22.2 can now be written

$$F_{j0} = M_{j0} = E_0 =$$

$$= \frac{1}{4\,\nu}\int_{\zeta_1}^{\zeta_2}\left[\overline{\int_{\varphi_1}^{\varphi_2}} Hp_0\right]d\zeta - \frac{\varepsilon}{4\,\nu}\int_{\zeta_1}^{\zeta_2}\int_{\varphi_1}^{\varphi_2} p_0\,\sin\varphi\,d\varphi\,d\zeta +$$

$$+\frac{1}{2\,\nu}\int_{\zeta_1}^{\zeta_2}\frac{\gamma_2-\gamma_1}{\sqrt{1-\varepsilon^2}}\,d\zeta \quad \ldots\ldots\ldots\ldots\ 23.2$$

If $\zeta_1 = -\nu$ $\varphi_1 = -\pi$

$\zeta_2 = +\nu$ $\varphi_2 = +\pi$

$$E_0 = \frac{\varepsilon}{2} \cdot P_{x0} + \frac{2\pi}{\sqrt{1-\varepsilon^2}} \quad \ldots\ldots\ldots\ldots \quad 24.1$$

If $\zeta_1 = -\nu$ $\varphi_1 = -\pi$

$\zeta_2 = +\nu$ $\varphi_2 = 0$

$$E_0 = \frac{\varepsilon}{2} \cdot P_{x0} + \frac{\pi}{\sqrt{1-\varepsilon^2}} \quad \ldots\ldots\ldots\ldots \quad 24.2$$

The power loss for the 180° bearing is half the value of the power loss for the 360° bearing.

3,6. Temperature Rise

The determination of the average temperature rise in the oil is based on the assumption that all the power loss heats the oil, i. e. no conduction exists. The energy equation gives

$$E_{tot} = Eb = c\,\varrho\,Q\,\Delta t$$

where

c = specific heat of oil

ϱ = density of oil

t = temperature

Δt = temperature rise

From 22.2 and 21.1

$$E = \frac{\eta\,U^2}{\psi} \cdot E_0$$

$$Q = r\,U\,\Delta r\,Q_0$$

Then

$$\Delta t = \frac{1}{c\,\varrho} \cdot \frac{\eta\,\omega}{\psi^2} \cdot \frac{2\,\nu\,E_0}{Q_0}$$

Non-dimensionally

$$\Delta t_0 = c\,\varrho \cdot \frac{\Delta t\,\psi^2}{\eta\,\omega} = \frac{2\,r\,E_0}{Q_0} \quad \ldots\ldots\ldots\ldots \quad 25.1$$

The equation 25.1 gives a value for the average temperature rise of the oil passing the bearing. In order to determine the temperature in every point in the bearing, consider a small oil element with the sides dx, dy and dz. The power transmitted to this element is

$$d^3E_{\text{tot}} = \left[\frac{\partial}{\partial y}(\tau_x u + \tau_z w) - u\frac{\partial p}{\partial x} - w\frac{\partial p}{\partial z}\right] dx\,dy\,dz =$$

$$= \left[\frac{\partial \tau_x}{\partial y}u + \tau_x\frac{\partial u}{\partial y} + \frac{\partial \tau_z}{\partial y}w + \tau_z\frac{\partial w}{\partial y} - \right.$$

$$\left. - u\frac{\partial p}{\partial x} - w\frac{\partial p}{\partial z}\right] dx\,dy\,dz$$

Now from 11.1

$$\frac{\partial p}{\partial x} = \frac{\partial \tau_x}{\partial y} \qquad \frac{\partial p}{\partial z} = \frac{\partial \tau_z}{\partial y}$$

The expression then becomes

$$d^3E_{\text{tot}} = \left[\tau_x\frac{\partial u}{\partial y} + \tau_z\frac{\partial w}{\partial y}\right] dx\,dy\,dz$$

From 12.2

$$\tau_x = \eta\frac{\partial u}{\partial y} \qquad \tau_z = \eta\frac{\partial w}{\partial y}$$

and

$$d^3E_{\text{tot}} = \eta\left[\left(\frac{\partial u}{\partial y}\right)^2 + \left(\frac{\partial w}{\partial y}\right)^2\right] dx\,dy\,dz$$

The derivatives are obtained from 19.2, and integration with respect to y gives

$$d^2E_{\text{tot}} = \left[\frac{\eta\,U^2}{h} + \frac{h^3}{12\,\eta}\left(\frac{\partial p}{\partial x}\right)^2 + \frac{h^3}{12\,\eta}\left(\frac{\partial p}{\partial z}\right)^2\right] dx\,dz$$

This power increases the temperature of the oil. Consider a small element with the sides dx, dz and the oil film thickness h.

$$d^2E_{\text{tot}} = c\,\varrho \left[\frac{\partial}{\partial x}(q_x t) + \frac{\partial}{\partial z}(q_z t) \right] dx\,dz =$$

$$= \left[\frac{\eta U^2}{h} + \frac{h^3}{12\,\eta} \left(\frac{\partial p}{\partial x} \right)^2 + \frac{h^3}{12\,\eta} \left(\frac{\partial p}{\partial z} \right)^2 \right] dx\,dz$$

As from the continuity

$$\frac{\partial q_x}{\partial x} + \frac{\partial q_z}{\partial z} = 0,$$

the equation for the temperature distribution in the oil film becomes

$$q_x \frac{\partial t}{\partial x} + q_z \frac{\partial t}{\partial z} = \frac{1}{c\,\varrho} \left\{ \frac{\eta U^2}{h} + \frac{h^3}{12\,\eta} \left[\left(\frac{\partial p}{\partial x} \right)^2 + \left(\frac{\partial p}{\partial z} \right)^2 \right] \right\}$$

3,7. Coefficient of Friction and Relative Power Loss

The coefficient of friction is the ratio of friction force to load capacity

$$\mu = \frac{F_j}{P} \qquad \ldots\ldots\ldots\ldots\ldots\ldots \quad 26.1$$

The relative power loss is defined as power loss per unit load

$$j = \frac{E}{P} \qquad \ldots\ldots\ldots\ldots\ldots\ldots \quad 26.2$$

With the non-dimensional expressions

$$F_{j0} = \frac{F_j\,\psi}{\eta\,U} = E_0 = \frac{E\,\psi}{\eta\,U^2}$$

$$P_0 = \frac{P\,\psi^2}{\eta\,U}$$

the expressions 26.1 and 26.2 can be written

$$\frac{\mu}{\psi} = \frac{f}{\omega \, \Delta r} = \frac{E_0}{P_0} \quad \ldots\ldots\ldots\ldots\ldots \quad 27.1$$

By introducing

$$\psi = \frac{\Delta r}{r}$$

$$h_{\min} = \Delta r \, (1 - \varepsilon)$$

eq. 27.1 becomes

$$\frac{\mu \, r}{h_{\min}} = \frac{f}{\omega \, h_{\min}} = \frac{E_0}{P_0 \, (1 - \varepsilon)} \quad \ldots\ldots\ldots\ldots \quad 27.2$$

When designing an optimum bearing, the relative power loss shall have a minimum. If we assume that the angular velocity ω and the minimum oil film thickness have given constant values, the expression 27.2 shall be a minimum.

4. Theory for Vaporization

4,1. Boundary Conditions for a Vapour Region

Two assumptions are made:

The lowest possible oil film pressure value is the vapour pressure.

In a vapour region the pressure is constant and equal to this vapour pressure.

The vapour pressure for an ideal oil is nearly absolute vacuum. In practical cases, however, there are air or gases dissolved in the oil, which are expelled at a higher pressure than the vapour pressure. The theory is still valid, but the vapour pressure must be replaced by the »air expulsion pressure» of the oil.

Fig. 28.1 shows a strip in peripheral direction of the vapour region and

$$\Delta z_1 = \Delta z_2 = \Delta z$$

The flows per unit width for an oil region are from 20.1

$$q_x = \frac{Uh}{2} - \frac{h^3}{12\eta} \cdot \frac{\partial p}{\partial x}$$

$$q_z = -\frac{h^3}{12\eta} \cdot \frac{\partial p}{\partial z}$$

The terms containing pressure derivatives may be called *pressure flows.* In the vapour region there is no pressure flow, since the pressure is constant.

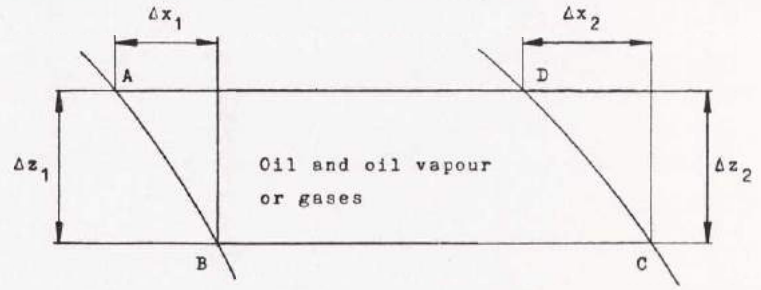

Fig. 28.1

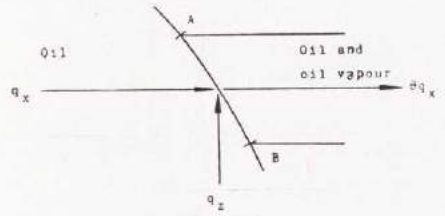

Fig. 29.1

Consider now the beginning of the vapour region as in 29.1.

The oil flow entering the vapour region over the small strip width Δz is for the oil region

$$\left[\frac{Uh}{2} - \frac{h^3}{12\,\eta} \cdot \frac{\partial p}{\partial x}\right] \Delta z - \frac{h^3}{12\,\eta} \cdot \frac{\partial p}{\partial z}\, \Delta x$$

and for the vapour region

$$\Theta \cdot \frac{Uh}{2} \cdot \Delta z$$

where $0 \leq \Theta \leq 1$, because it is not clear that the oil covers the complete width of the strip.

The two flows must be equal.

Thus

$$(1 - \Theta)\, \frac{Uh}{2} \cdot \Delta z - \frac{h^3}{12\,\eta} \cdot \frac{\partial p}{\partial x}\, \Delta z - \frac{h^3}{12\,\eta} \cdot \frac{\partial p}{\partial z}\, \Delta x = 0$$

Δx and Δz are positive

$\frac{\partial p}{\partial x}$ and $\frac{\partial p}{\partial z}$ must be negative or zero, because there is no pressure below vapour pressure.

Then the equation represents a sum equal to zero of three positive terms. The equation is satisfied only if all three terms are zero.

Thus

$$\Theta = 1 \qquad \frac{\partial p}{\partial x} = \frac{\partial p}{\partial z} = 0$$

At the beginning of a vapour region there is oil over the whole width of the peripheral strips, and the boundary conditions are

$$\frac{\partial p}{\partial x} = \frac{\partial p}{\partial z} = 0 \quad \ldots\ldots\ldots\ldots\ldots\ldots \quad 29.2$$

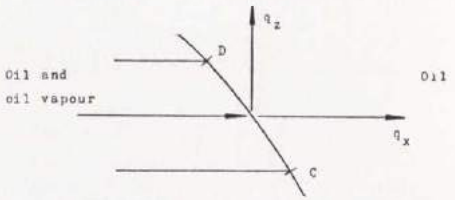

Fig. 30.1

Since the pressure derivative $\frac{\partial p}{\partial s}$ along the boundary is zero, it is only nessessary to control that one of the derivatives in 29.2 is zero. If the pressure derivative is zero in two different directions, it is zero in every direction.

Consider now the end of the vapour region, see 30.1.

Since there is no pressure flow in the vapour region, there is no flow over the lines AD and BC in 28.1. The oil flow entering the vapour region over AB is thus equal to the flow leaving over CD. This flow is

$$\frac{Uh^*}{2} \cdot \Delta z$$

where h^* = oil film thickness at the beginning of the vapour region.

The flow leaving the strip is for the oil region

$$\left[\frac{Uh}{2} - \frac{h^3}{12\eta} \cdot \frac{\partial p}{\partial x}\right] \Delta z - \frac{h^3}{12\eta} \cdot \frac{\partial p}{\partial z} \Delta x$$

These two expressions must be equal to fulfil the continuity.

$$\frac{Uh^*}{2} \cdot \Delta z = \frac{Uh}{2} \cdot \Delta z - \frac{h^3}{12\eta}\left[\frac{\partial p}{\partial x} \Delta z + \frac{\partial p}{\partial z} \Delta x\right] \ldots 30.2$$

With non-dimensional expressions, the condition 30.2 can be transformed into

$$\frac{H^*}{2} \cdot \Delta\zeta = \frac{H}{2} \cdot \Delta\zeta - \frac{H^3}{12}\left[\frac{\partial p_0}{\partial \varphi} \Delta\zeta + \frac{\partial p_0}{\partial \zeta} \Delta\varphi\right] \ldots 30.3$$

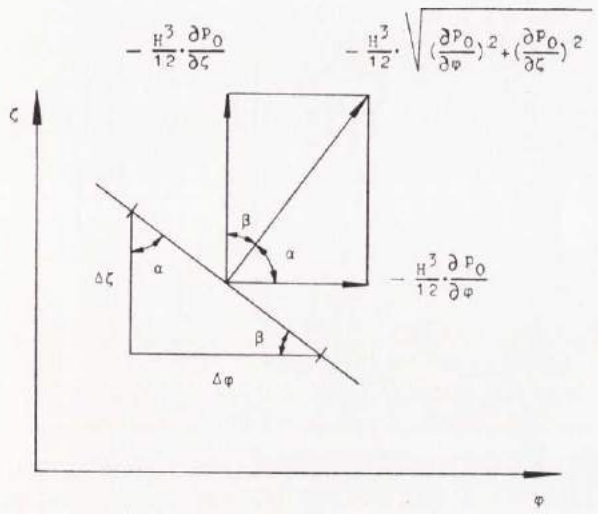

Fig. 31.1

Now as $\Delta\varphi$ and $\Delta\zeta$ are positive

$$\lim_{\Delta\zeta\to 0}\frac{\Delta\varphi}{\Delta\zeta}=-\frac{d\varphi}{d\zeta}$$

and 30.3 is therefore transformed into

$$H^*=H-\frac{H^3}{6}\cdot\frac{\partial p_0}{\partial \varphi}\left[1-\frac{\frac{\partial p_0}{\partial \zeta}}{\frac{\partial p_0}{\partial \varphi}}\cdot\frac{d\varphi}{d\zeta}\right]\ldots\ldots 31.2$$

The pressure flows over the rear boundary of a vapour region are shown in 31.1. The resultant of the pressure flows per unit width in the φ- and ζ-directions is directed perpendicularly to the boundary.

From 31.1

$$\lim_{\Delta\zeta\to 0}\frac{\Delta\varphi}{\Delta\zeta}=-\frac{d\varphi}{d\zeta}=\frac{\frac{\partial p_0}{\partial \zeta}}{\frac{\partial p_0}{\partial \varphi}}=\operatorname{tg}\alpha$$

Then 31.2 can be written in three different ways:

$$\left.\begin{aligned} H^* &= H - \frac{H^3}{6} \cdot \frac{\partial p_0}{\partial \varphi}\left[1 + \left(\frac{d\varphi}{d\zeta}\right)^2\right] \\ H^* &= H + \frac{H^3}{6} \cdot \frac{\partial p_0}{\partial \zeta}\left[\frac{d\zeta}{d\varphi} + \frac{d\varphi}{d\zeta}\right] \\ H^* &= H - \frac{H^3}{6} \cdot \frac{\left(\frac{\partial p_0}{\partial \varphi}\right)^2 + \left(\frac{\partial p_0}{\partial \zeta}\right)^2}{\frac{\partial p_0}{\partial \varphi}} \end{aligned}\right\} \quad \ldots\ldots\ldots \text{32.1}$$

The expressions 32.1 are not convenient for control of the location of the boundary. For this purpose the following equations are more suitable

$$\left.\begin{aligned} \frac{H^*}{2} \cdot \Delta\zeta &= \frac{H}{2} \cdot \Delta\zeta - \frac{H^3}{12} \cdot \frac{\partial p_0}{\partial \varphi} \cdot \frac{\Delta\zeta}{\cos^2 \alpha} \\ \frac{H^*}{2} \cdot \Delta\zeta &= \frac{H}{2} \cdot \Delta\zeta - \frac{H^3}{12} \cdot \frac{\partial p_0}{\partial \zeta} \cdot \frac{\Delta\varphi}{\cos^2 \beta} \\ \frac{H^*}{2} \cdot \Delta\zeta &= \frac{H}{2} \cdot \Delta\zeta - \frac{H^3}{12} \cdot \sqrt{\left(\frac{\partial p_0}{\partial \varphi}\right)^2 + \left(\frac{\partial p_0}{\partial \zeta}\right)^2} \cdot \frac{\Delta\zeta}{\cos \alpha} \end{aligned}\right\}$$

or

$$\left.\begin{aligned} H^* &= H - \frac{H^3}{6} \cdot \frac{\partial p_0}{\partial \varphi} \cdot \frac{1}{\cos^2 \alpha} \\ H^* &= H - \frac{H^3}{3} \cdot \frac{\partial p_0}{\partial \zeta} \cdot \frac{1}{\sin 2\beta} \\ H^* &= H - \frac{H^3}{6} \cdot \sqrt{\left(\frac{\partial p_0}{\partial \varphi}\right)^2 + \left(\frac{\partial p_0}{\partial \zeta}\right)^2} \cdot \frac{1}{\cos \alpha} \end{aligned}\right\}$$

Each one of these three expressions corresponds to the continuity equation 31.2. In actual calculations the most suitable form is chosen.

The problem now to be solved is a very difficult one. REYNOLD's equation which has no known exact solution shall be solved approximately, satisfying some conditions on the known boundaries $\varphi = \pm \pi$, $\zeta = \pm r$; and satisfying on the vapour region boundary, the position of which is unknown, the conditions

$$\frac{\partial p_0}{\partial \varphi} = \frac{\partial p_0}{\partial \zeta} = 0 \quad \ldots\ldots\ldots\ldots\ldots\ldots \quad 33.1$$

at the beginning and

$$H^* = H - \frac{H^3}{6} \cdot \frac{\left(\frac{\partial p_0}{\partial \varphi}\right)^2 + \left(\frac{\partial p_0}{\partial \zeta}\right)^2}{\frac{\partial p_0}{\partial \varphi}} \quad \ldots\ldots\ldots \quad 33.2$$

at the end of the vapour region.

The solution can be obtained in the following manner: Guess a vapour region. Determine the pressure distribution by relaxation. Check the boundary conditions 33.1 and 33.2. From this check a better boundary can be »guesstimated». The new boundary gives a new pressure field. This gives a new check, and so on. The procedure is repeated until a satisfactory result is reached. At the sides of the vapour region a finer network is used for the relaxation.

The two boundary conditions for the vapour region in connection with the boundary condition $p_0 = 0$ for $\zeta = \pm r$ completely determine the pressure distribution for the classical case of a finite 360° journal bearing with oil supply at the sides and without axial oil grooves.

CAMERON-WOOD (3) have treated this case, but they have not given the boundary condition for the end of the vapour region. Their conditions are

$$p = 0$$

at maximum film thickness and

$$p = 0$$

$$\frac{\partial p}{\partial \varphi} = 0$$

at the end of the continuous oil film.

The first of these two conditions is arbitrarily chosen. The zero isobar at the beginning of the oil film is always located in the convergent part of the bearing. The location is dependent on the ratio width/diameter, the non-dimensional eccentricity, and the non-dimensional vapour pressure.

CAMERON-WOOD wrote in reply to the discussion that they were dealing with the classical problem of a rotating circular shaft, in a circular bearing with no oil grooves, which was surrounded entirely by a perfect Newtonian fluid. In the paper, however, they write: »In the finite bearing, air is sucked into this expanding part of the film from the sides to compensate for the side leakage, which itself precludes the continuous SOMMERFELD film.» There is a contradiction in these assumptions, because the first one says that the bearing is surrounded by a Newtonian fluid, and the second one that there is air surrounding the bearing. Furthermore, the leakage from the positive pressure region cannot be compensated by air, as it is impossible to have an oil flow from the bearing and an air flow into the bearing and still retain the oil in it. If we had a finite bearing without axial oil grooves working at a given eccentricity and the vapour pressure equal to zero, there would be an oil flow from the bearing as long as there is positive pressure in it; but there could not be any flow into the bearing, because there was no negative pressure. Thus stationary conditions would not be reached until the pressure were zero in all of the bearing. In this case the load would be zero, too.

CAMERON-WOOD's arbitrarily chosen boundary condition for the beginning of the complete oil film is correct if an oil groove is located at the maximum oil film thickness. For actual oils the »air expulsion pressure» is not far below atmospheric pressure. For this case their solution gives very good values for the pressure and the load capacity. If the groove is not exactly at, but quite near to, the maximum film thickness, the change in load is very small because of the low pressure derivatives near this section.

4,2. Friction Force, Friction Torque, and Power Loss for a Vapour Region

The behaviour of the oil in a vapour region must be further discussed. As the pressure is constant, there is no pressure flow. There exists no flow in axial direction; and the velocity distribution for the peripheral flow is a straight line.

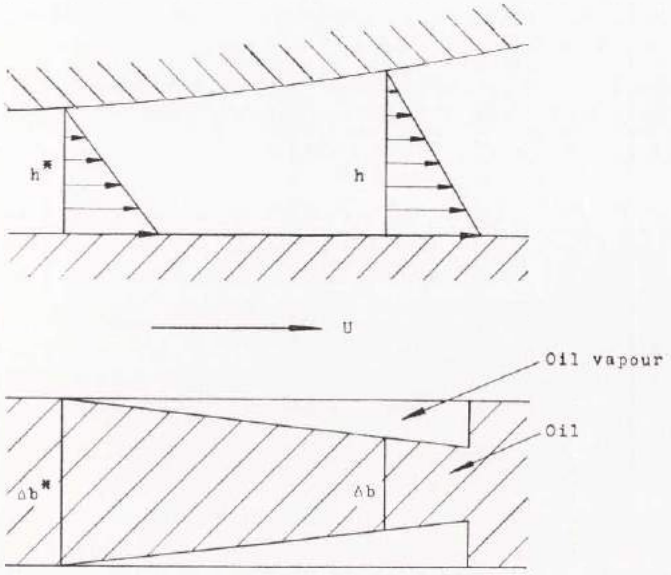

Fig. 35.1

The left velocity distribution in 35.1 represents the beginning of a vapour region, and there is no oil vapour. It is clear that the right velocity distribution gives a greater oil flow per unit width than the left one. For the continuity to be fulfilled, there must be a decrease in the width of the strip. An infinite number of strips is assumed.

From 35.1

$$\frac{Uh^*}{2} \cdot \Delta b^* = \frac{Uh}{2} \cdot \Delta b$$

$$h^* \, \Delta b^* = h \, \Delta b$$

Then the shear stress becomes

$$\tau = \frac{\Delta b}{\Delta b^*} \cdot \eta \cdot \frac{U}{h} = \frac{h^*}{h} \cdot \eta \cdot \frac{U}{h}$$

$$\tau = \frac{\eta \, U \, h^*}{h^2} \qquad \ldots\ldots\ldots\ldots\ldots\ldots\ldots\ldots \quad 35.2$$

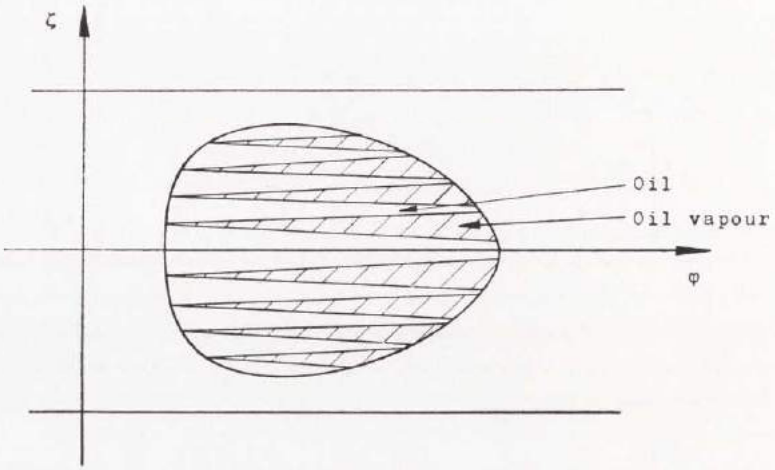

Fig. 36.1

The appearance of a vapour region is shown in 36.1. Such regions are found on photos published in papers by VOGELPOHL (13) and COLE-HUGHES (5). In practice there is a finite number of strips because of the cohesive forces in the oil.

The friction force for the vapour region is

$$F_j b = \int_{\zeta_1}^{\zeta_2} \int_{\varphi_1}^{\varphi_2} \tau \, r \, d\varphi \, r \, d\zeta$$

and with 35.2

$$F_j b = \int_{\zeta_1}^{\zeta_2} \int_{\varphi_1}^{\varphi_2} \frac{\eta \, U \, h^*}{h^2} \, r \, d\varphi \, r \, d\zeta$$

or non-dimensionally

$$F_{j0} = \frac{F_j \psi}{\eta \, U} = \frac{1}{2 \, r} \int_{\zeta_1}^{\zeta_2} \int_{\varphi_1}^{\varphi_2} \frac{H^*}{H^2} \, d\varphi \, d\zeta \quad \ldots\ldots\ldots \quad 36.2$$

where H^* is the non-dimensional oil film thickness at the beginning of the vapour region. H^* is thus a function of ζ for given values of the ratio width/diameter, the non-dimensional eccentricity, and the non-dimensional vapour pressure.

From chap. 3,5

$$F_{j0} = \frac{F_j \psi}{\eta U} = M_{j0} = \frac{M_j \psi}{\eta U r} = E_0 = \frac{E \psi}{\eta U^2}$$

When the boundary for the vapour region is known, the integral 36.2 can be exactly solved in peripheral direction.

$$I = \int_{\varphi_1}^{\varphi_2} \frac{H^*}{H^2} \, d\varphi = \int_{\varphi_1}^{\varphi_2} \frac{H^*}{(1 - \varepsilon \cos \varphi)^2} \, d\varphi$$

The substitution from 23.1 is used.

Then

$$I = H^* \cdot \frac{(\gamma_2 - \gamma_1) + \varepsilon (\sin \gamma_2 - \sin \gamma_1)}{\sqrt{(1 - \varepsilon^2)^3}} \quad \ldots\ldots\ 37.1$$

where

$$\gamma = \arccos \frac{\cos \varphi - \varepsilon}{1 - \varepsilon \cos \varphi}$$

In axial direction we must use numerical integration.

When determining the power loss for a vapour region in a journal bearing, other authors often assume that there is only air or only oil in this region. The first assumption gives too small power loss, and the second one too high power loss.

CAMERON-WOOD's solution, discussed in 4,1, gives very good values for the load capacity if oil grooves are located at the maximum film thickness; but their power loss is too large, because of the assumption that the vapour or zero pressure region is filled with oil which has a linear velocity distribution. If the power loss were adjusted and a minimum analysis were made for the function 27.2, their calculations would be very suitable for practical design of journal bearings, as the vapour pressure is near the atmospheric pressure. This is further discussed in chap. 7.

4,3. Temperature Rise

The average temperature rise for a bearing with a vapour region is derived from 25.1.

Now we will study the temperature distribution in a vapour region.

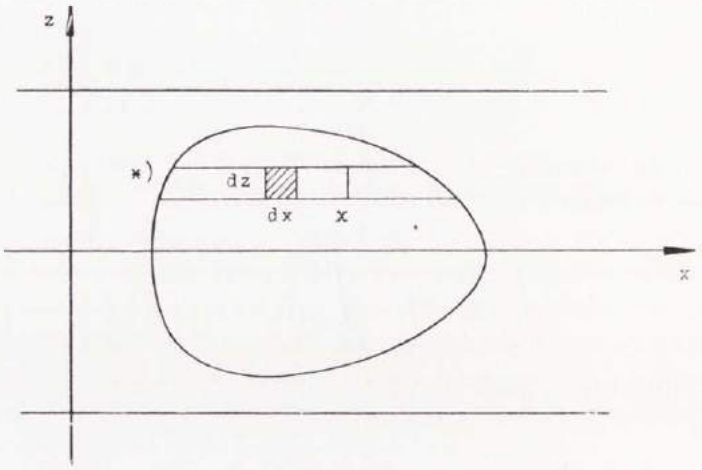

Fig. 38.1

For the small element dx, dz in 38.1 the power equation gives

$$\tau\, U\, dx\, dz = c\, \varrho\, q_x \frac{\partial\, t}{\partial\, x}\, dx\, dz$$

where

$$\tau = \frac{\eta\, U\, h^*}{h^2}$$

$$q_x = \frac{U\, h^*}{2}$$

Then we get

$$\frac{\partial\, t}{\partial\, x} = \frac{2\, \eta\, U}{c\, \varrho} \cdot \frac{1}{h^2}$$

Integration with respect to x gives

$$t_x - t^* = \frac{2\, \eta\, U}{c\, \varrho} \int_{x^*}^{x} \frac{dx}{h^2}$$

The expression represents the temperature rise between the beginning of the vapour region and the point x in 38.1. Introduce non-dimensional quantities.

$$t_{x\,0} - t_0^* = c\, \varrho \cdot \frac{(t_x - t^*)\, \psi^2}{\eta\, \omega} = 2 \int_{\varphi^*}^{\varphi} \frac{d\varphi}{H^2}$$

5. The 360° Bearing with No Oil Grooves

5,1. The 360° Bearing with No Oil Grooves and without Vapour Regions

5,11. Pressure Distribution

The bearing is thought to be completely submerged in oil, and the pressure at the bearing sides is a assumed to be zero, i. e. atmospheric pressure. This latter assumption means no limit to the theory, because if the oil pressure at the bearing sides were increased to another constant value, the pressure in all of the bearing would be increased by the same amount. As the bearing shall have no vapour region, the vapour pressure p_v must be lower than the lowest oil film pressure $p_{\min}$.

The unfolded thin oil film area from the bearing in 41.1 is shown in 39.1. The boundary condition is now

$$p = 0 \quad \text{for} \quad \zeta = \pm r$$

$$p_{\varphi=-\pi} = p_{\varphi=\pi}$$

The oil film thickness is symmetrical and the derivative for this is antisymmetrical with respect to $\varphi = 0$. Therefore the pressure

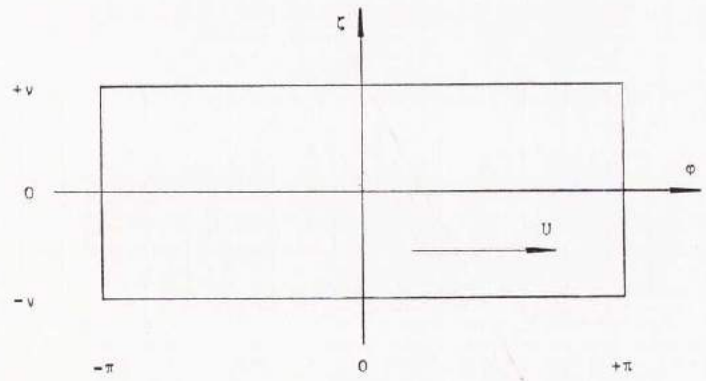

Fig. 39.1

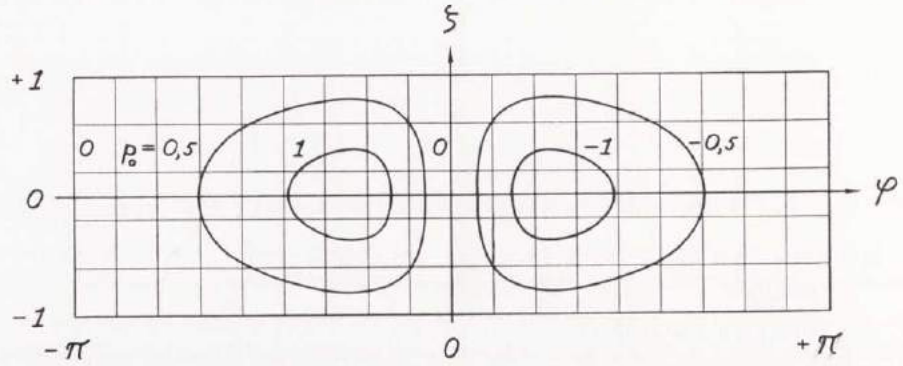

Fig. 40.1. Theoretical Pressure Distribution for $\nu = 1$, $\varepsilon = 0{,}4$ and $p_{v\,0} < p_{\min,\,0}$

distribution from 16.2 is antisymmetrical with respect to the angle of minimum film thickness $\varphi = 0$. The pressure is positive in the convergent part and negative in the divergent part of the bearing. The pressure is symmetrical with respect to the φ-axis and therefore it is only necessary to calculate the pressure distribution for one fourth of the bearing area.

The different cases which are numerically analysed in this treatise are tabulated in Appendix, chap. 13.

Fig. 40.1 shows the theoretical pressure distribution for $\nu = 1$ and $\varepsilon = 0{,}4$. For 40.2 holds: $\nu = 1$, $\varepsilon = 0{,}6$. The curves shown are isobars. The rotational direction is to the right.

This solution is of theoretical interest only, because the vapour pressure in practice is very close to atmospheric. Bearings are not

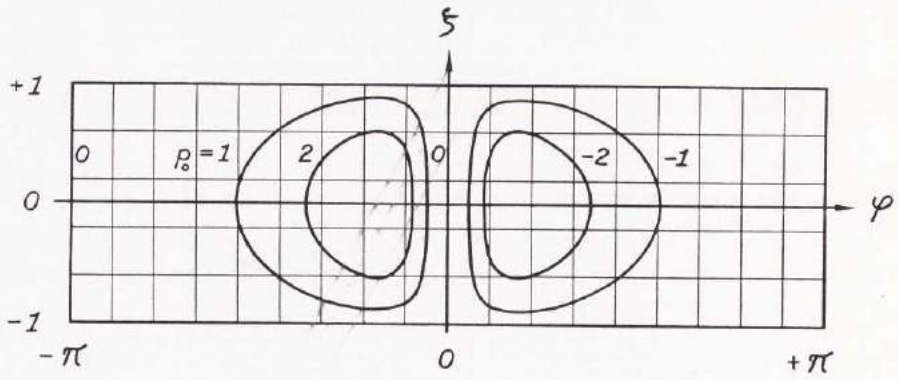

Fig. 40.2. Theoretical Pressure Distribution for $\nu = 1$, $\varepsilon = 0{,}6$ and $p_{v\,0} < p_{\min,\,0}$

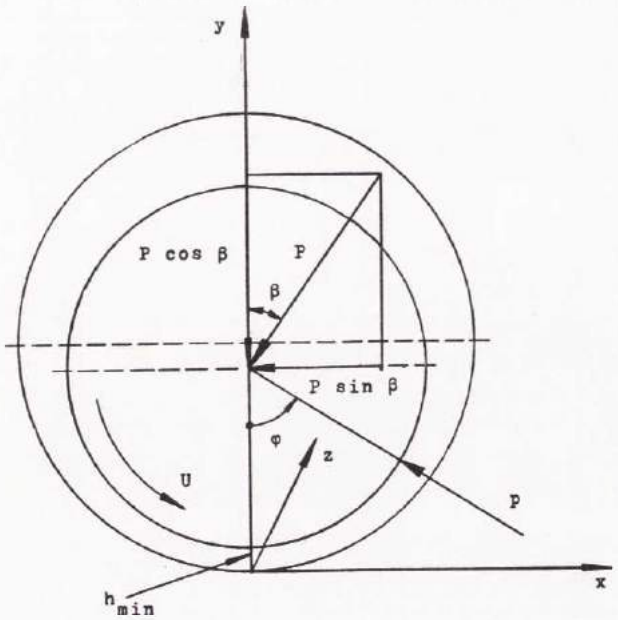

Fig. 41.1

used at such low pressures. If the oil had no air or gases dissolved in it, the minimum pressure would be close to absolute vacuum, and the maximum pressure 1 atm g, which would give some load capacity. But even if the oil holds gases, it takes some time before these are expelled. Therefore, when a lightly loaded bearing is started, the above described pressure distribution exists. This is verified by the experiments in chap. 5,17. But after a few minutes testing, the gases were expelled, the vapour pressure became higher, and a vapour region was formed.

VOGELPOHL (13), in 1937, published photos of bearings operating with a full oil film all around the circumference.

5,12. Load Capacity

When the pressure is known at a number of points, the load can be numerically evalutated.

Now the pressure is positive in the convergent part and negative in the divergent part of the bearing, but the absolute values are the same. Thus the load component in the y-direction is zero.

From 18.2

$$P_{x0} = \frac{P_x \psi^2}{\eta U} = -\frac{1}{2\nu} \int_{-\nu}^{+\nu} \int_{-\pi}^{+\pi} p_0 \sin\varphi \, d\varphi \, d\zeta =$$

$$= -\frac{1}{\nu} \int_{-\nu}^{+\nu} \int_{-\pi}^{0} p_0 \sin\varphi \, d\varphi \, d\zeta$$

$$P_{y0} = \frac{P_y \psi^2}{\eta U} = 0$$

Then

$$P_0 = \frac{P \psi^2}{\eta U} = P_{x0}$$

$$\beta = 90°$$

The attitude-eccentricity curve is thus a straight horizontal line.

Fig. 43.1 shows the load capacity as a function of the eccentricity for different values of the ratio width/diameter.

5,13. **Oil Flow**

The bearing has no oil groove and therefore all the oil change occurs over the borders of the bearing as shown in 43.2.

The oil is leaving the bearing in the convergent part with positive pressure and entering at the divergent part with negative pressure. These two flows are equal. The oil flow Q takes care of the generated heat.

From 20.1 the side leakage per unit width becomes

$$q_z = -\frac{h^3}{12\eta} \left(\frac{\partial p}{\partial z} \right)_{\zeta = \nu}$$

and

$$Q = -2 \int_{-\pi}^{0} \frac{h^3}{12\eta} \left(\frac{\partial p}{\partial z} \right)_{\zeta = \nu} r \, d\varphi$$

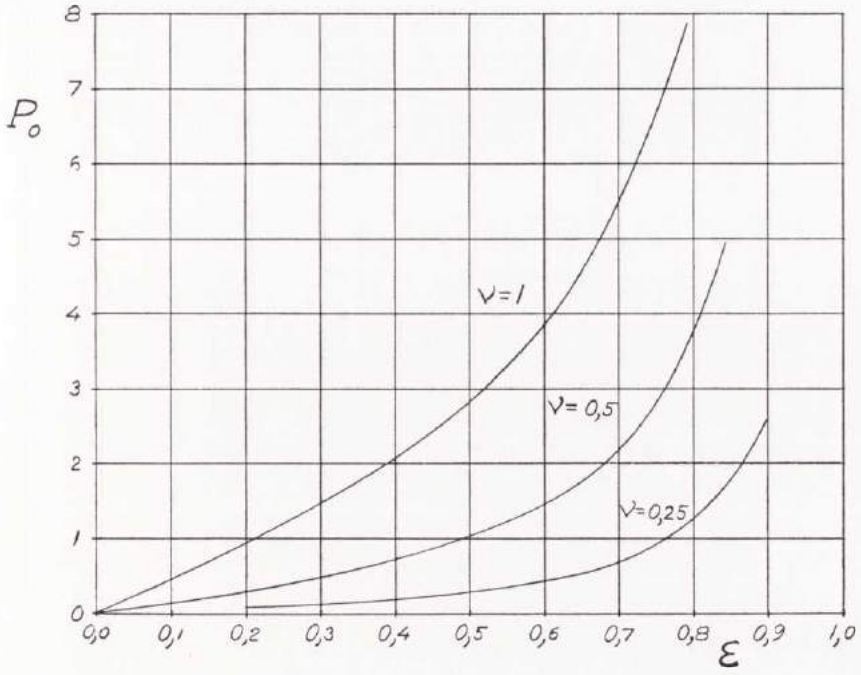

Fig. 43.1. Load Capacity $P_0 = \dfrac{P\,\psi^2}{\eta\,U}$

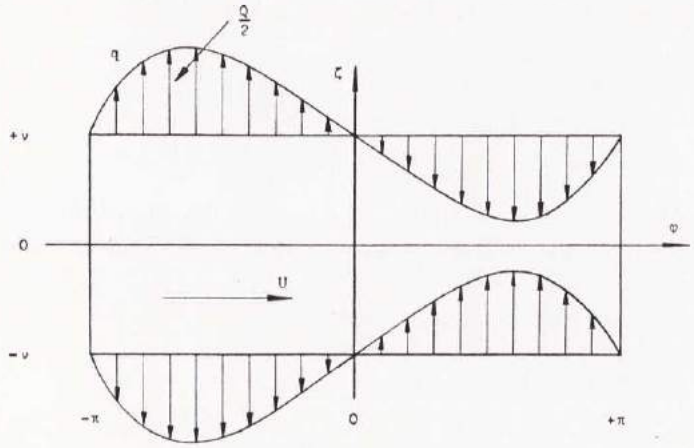

Fig. 43.2

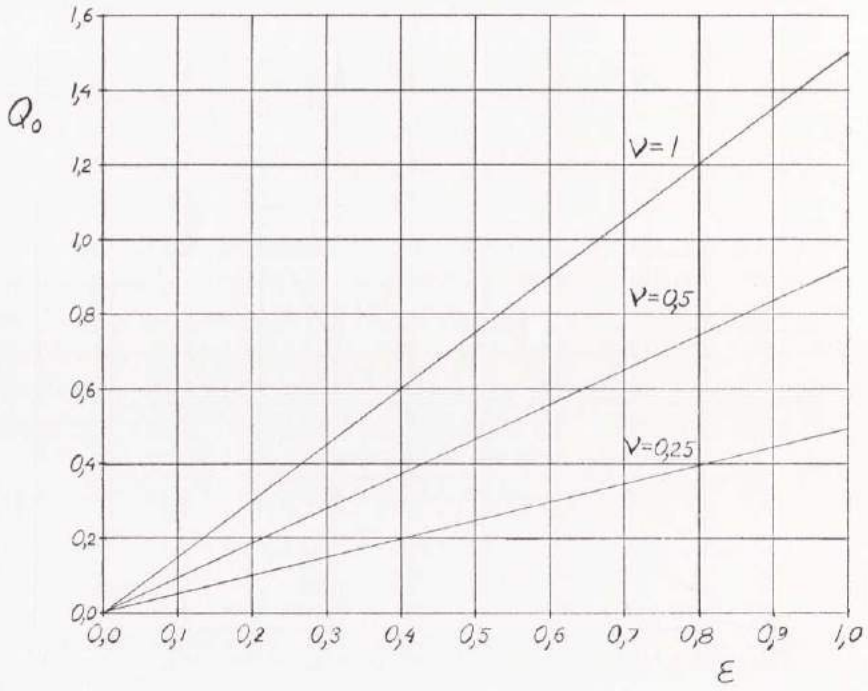

Fig. 44.1. Oil Flow $\quad Q_0 = \dfrac{Q}{r\,U\,\Delta r}$

The non-dimensional expressions are

$$q_{z0} = \frac{q_z}{U\,\Delta r} = -\frac{H^3}{12}\left(\frac{\partial\, p_0}{\partial\, \zeta}\right)_{\zeta=\nu}$$

and

$$Q_0 = \frac{Q}{r\,U\,\Delta r} = -2\int_{-\pi}^{0} \frac{H^3}{12}\left(\frac{\partial\, p_0}{\partial\, \zeta}\right)_{\zeta=\nu} d\varphi$$

Fig. 44.1 shows the changed oil quantity per unit time as a function of the eccentricity for different values of the ratio width/diameter.

5,14. Power Loss

The power loss is from 24.1

$$E_0 = \frac{E\,\psi}{\eta\,U^2} = \frac{\varepsilon}{2}\cdot P_{x0} + \frac{2\,\pi}{\sqrt{1-\varepsilon^2}}$$

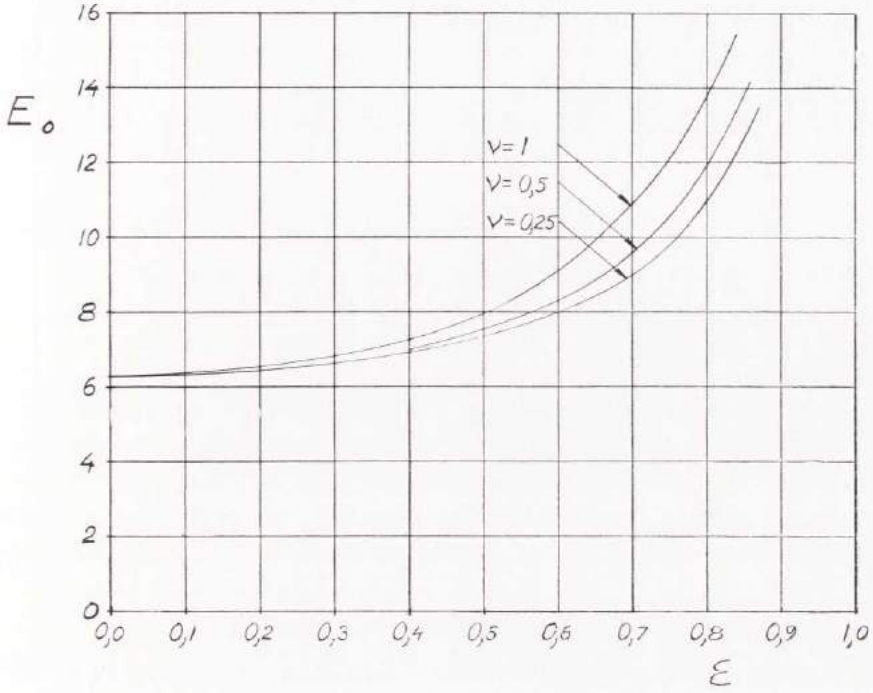

Fig. 45.1. Power Loss $E_0 = \dfrac{E\,\psi}{\eta\,U^2}$

When P_{x0} is known, the expression can be directly calculated.
The non-dimensional power loss is drawn in 45.1.

5,15. Average Temperature Rise

The temperature rise is based upon the assumption that all the power generated in the oil film is taken up by the oil expelled over the bearing sides.

From 25.1

$$\Delta t_0 = c\,\varrho \cdot \frac{\Delta t\,\psi^2}{\eta\,\omega} = \frac{2\,\nu\,E_0}{Q_0}$$

This function is drawn in 46.1.

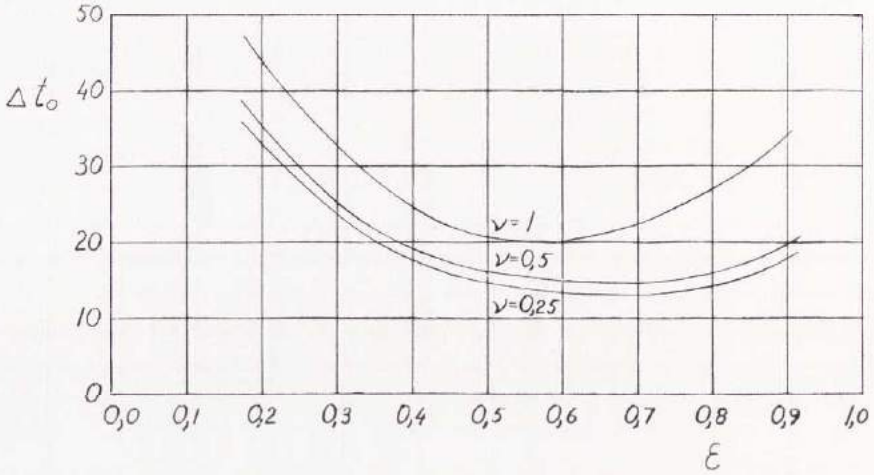

Fig. 46.1. Average Temperature Rise $\Delta t_0 = c\,\varrho \cdot \frac{\Delta t\,\psi^2}{\eta\,\omega}$

5,16. **Coefficient of Friction and Relative Power Loss**

The general expressions for the coefficient of friction and the relative power loss are from 27.1 and 27.2

$$\frac{\mu}{\psi} = \frac{f}{\omega\,\Delta r} = \frac{E_0}{P_0}$$

$$\frac{\mu\,r}{h_{\min}} = \frac{f}{\omega\,h_{\min}} = \frac{E_0}{P_0\,(1-\varepsilon)} \quad \ldots\ldots\ldots\ldots \quad 46.2$$

where

$$\mu = \frac{F_j}{P} \qquad\qquad f = \frac{E}{P}$$

A bearing operates with a minimum power loss for a given load, angular velocity, and minimum oil film thickness, if the expression 46.2 is a minimum. The function 46.2 is drawn in 47.1. The infinitely wide journal bearing has the lowest power loss for a given load. This is due to the fact that the load capacity decreases faster than the power loss when the bearing is shortened.

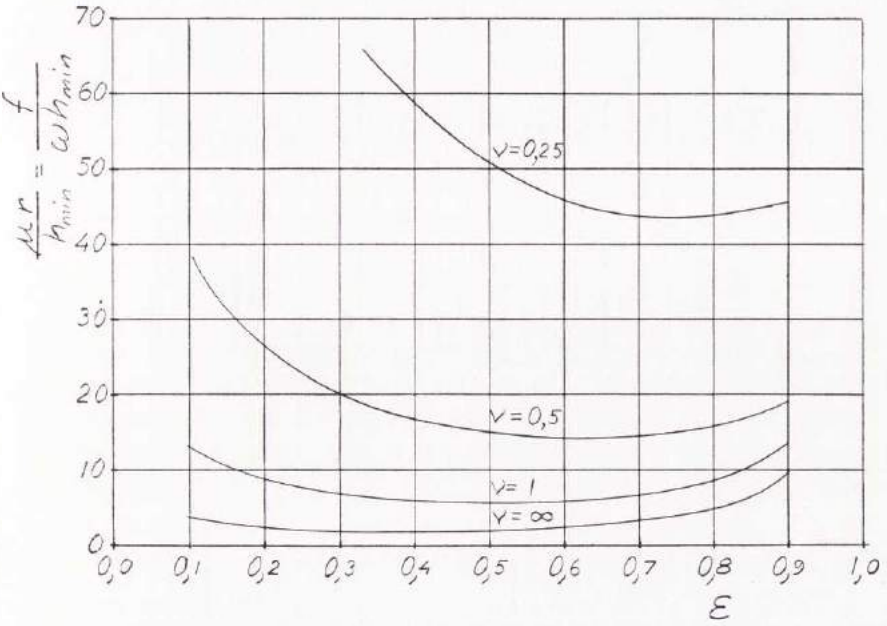

Fig. 47.1. Coefficient of Friction and Relative Power Loss

5,17. Experimental Investigation

The test apparatus consisted of a journal carried by two ball bearings and driven by an electric motor. Two different bearings were tested.

A principle sketch of the arrangement is shown in 47.2. The journal had a diameter of 100 mm and the data for the two bearings combined with the journal were:

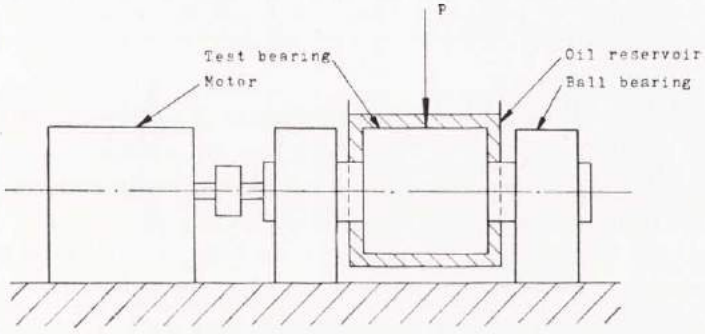

Fig. 47.2

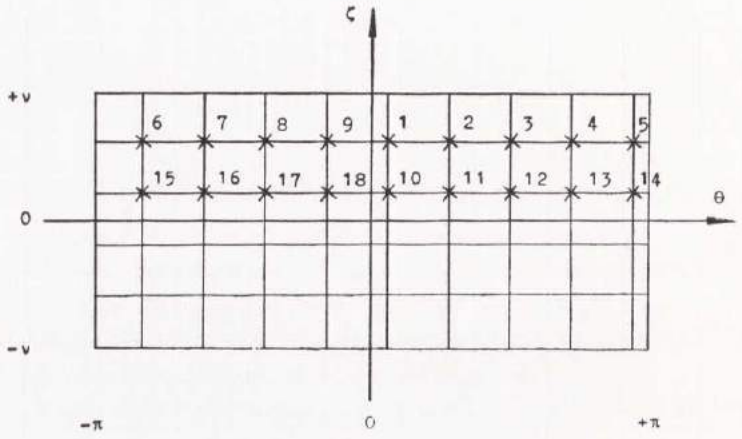

Fig. 48.1

$$\left.\begin{aligned} r &= \frac{4}{3} \\ \psi &= 0{,}00291 \end{aligned}\right\} \qquad \left.\begin{aligned} r &= 1 \\ \psi &= 0{,}00364 \end{aligned}\right\}$$

For the measurement of the pressure the bearing area was divided into 45 panels in the same way as in the calculations. There were 5 panels over the bearing width and 9 panels around the periphery.

The pressure was measured at 18 points by means of a mercury manometer with 18 glass tubes. The distribution of the points is shown in 48.1 ,where $\Theta = 0$ represents the position of the load. The angle between the load line and the two points 1 and 10 was 10°. The pressure was thus measured with intervals of 40°. If the bearing was turned 20°, we got another 18 pressure values. Thus two tests gave 36 measured pressure values with intervals of 20°, which was the used relaxation interval. The bearings had no oil grooves and were submerged in oil.

From the experiments it is found that a bearing can operate with a full oil film all around the circumference if the load is low and there is no air dissolved in the oil. When an experiment starts, a considerable low pressure can be reached; but gradually air is dissolved from the oil and a constant pressure region is formed. In 51.1 it is verified that the pressure distribution is antisymmetrical with respect to the minimum oil film thickness ($\varphi = 0$). This test, however, does not correspond to practice, because so lightly loaded bearings are hardly ever used. Further, normal oils have air dissolved in them,

which is expelled at a pressure just below atmospheric. It is, however, interesting that the curves do exist. The experiments give a check on the theory for an oil film region. It is also found that the attitude-eccentricity curve is a straight horizontal line.

Two experiments are analysed in detail:

1) Fig. 50.1 and 51.1.

$$r = \frac{4}{3}$$

$$\psi = 0{,}00291$$

$$\eta = 0{,}0153 \text{ Ns/m}^2$$

$$\omega = 47{,}1 \text{ 1/s}$$

The experimental load capacity

$$P_e b = 680 \text{ N}$$

gives

$$P_{0e} = \frac{P_e \psi^2}{\eta U} = \frac{680 \cdot 3 \cdot 0{,}00291^2}{2 \cdot 4 \cdot 0{,}05 \cdot 0{,}0153 \cdot 0{,}05 \cdot 47{,}1}$$

$$P_{0e} = 1{,}20$$

From the theoretical calculations this load is found to correspond to

$$\varepsilon = 0{,}18$$

The calculated pressure curves for this value of ε are shown in 51.1. The agreement between theory and test is very good.

2) Fig. 52.1 and 53.1.

$$r = 1$$

$$\psi = 0{,}00364$$

$$\eta = 0{,}0164 \text{ Ns/m}^2$$

$$\omega = 48{,}1 \text{ 1/s}$$

Experimental load capacity

$$P_e b = 620 \text{ N}$$

$$P_{0e} = \frac{P_e \psi^2}{\eta U} = \frac{620 \cdot 0{,}00364^2}{2 \cdot 0{,}05 \cdot 0{,}0164 \cdot 0{,}05 \cdot 48{,}1}$$

$$P_{0e} = 2{,}08$$

This corresponds to $\varepsilon = 0{,}40$ which was aimed at. Here, too, the agreement is good.

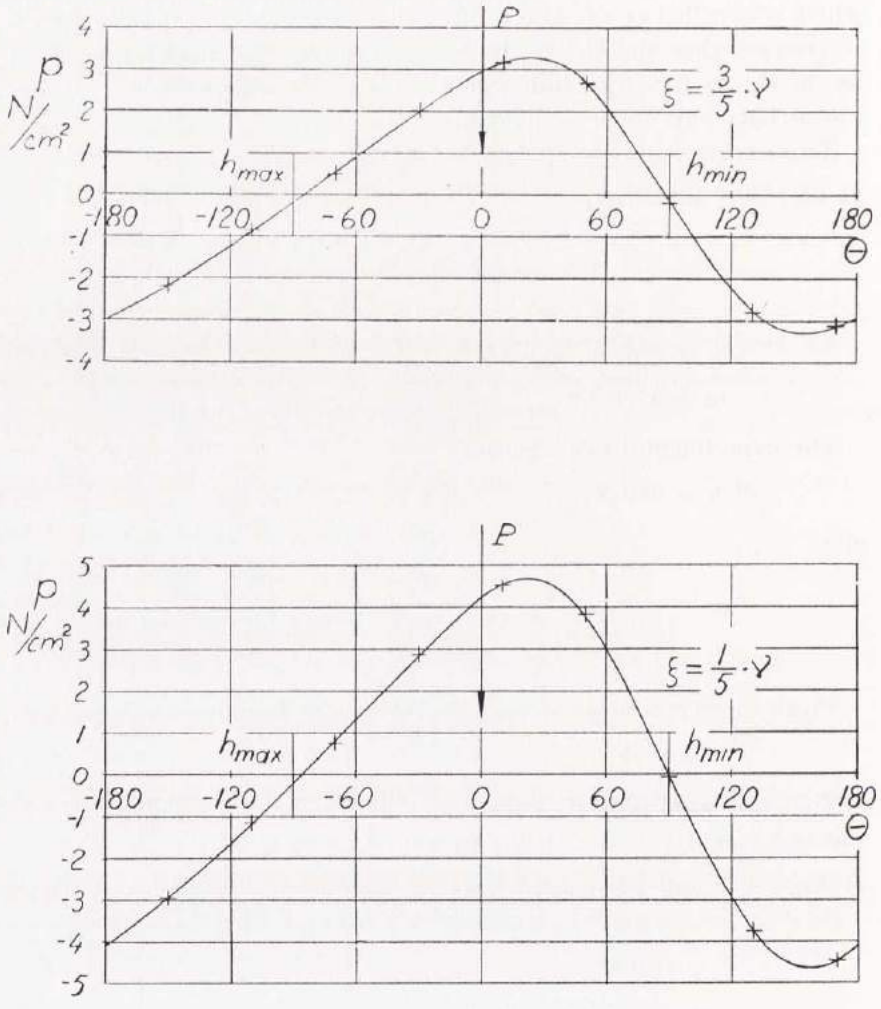

Fig. 50.1. Experimental Curves for $\nu = \frac{4}{3}$ and $\varepsilon = 0{,}18$

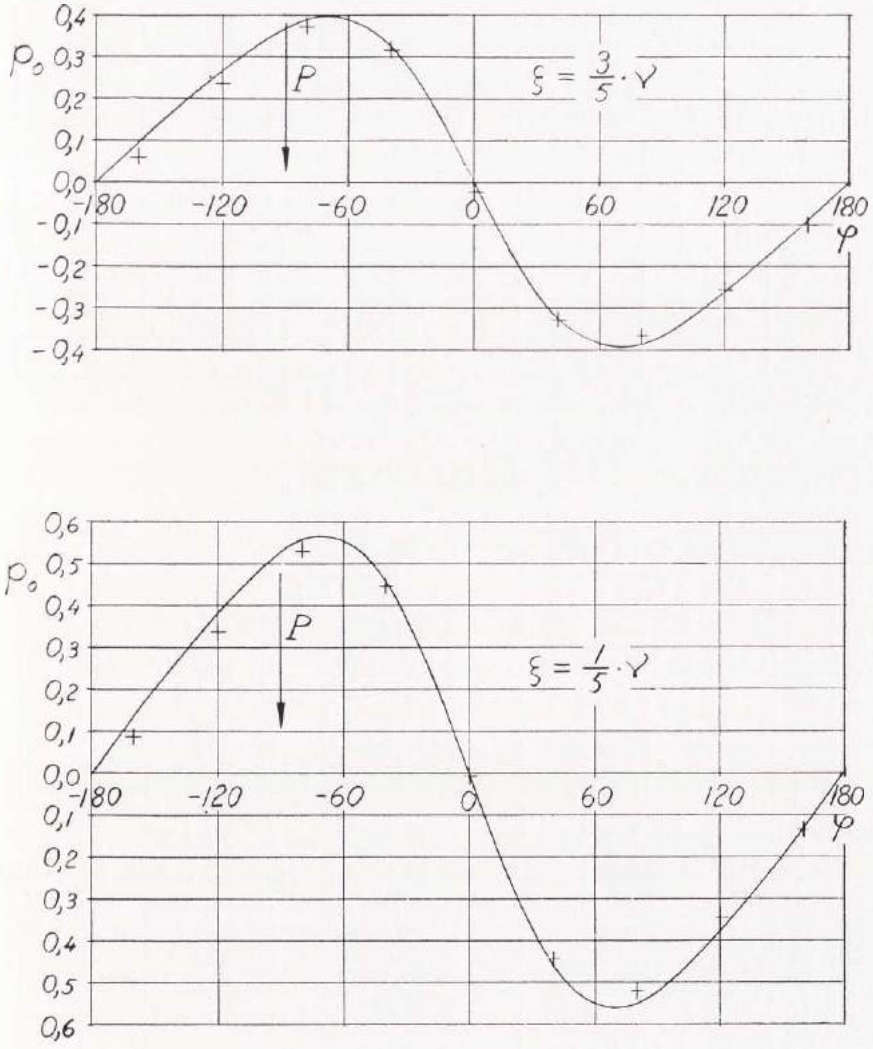

Fig. 51.1. Theoretical Curves for $\nu = \frac{4}{3}$ and $\varepsilon = 0{,}18$
+ Experimental Points

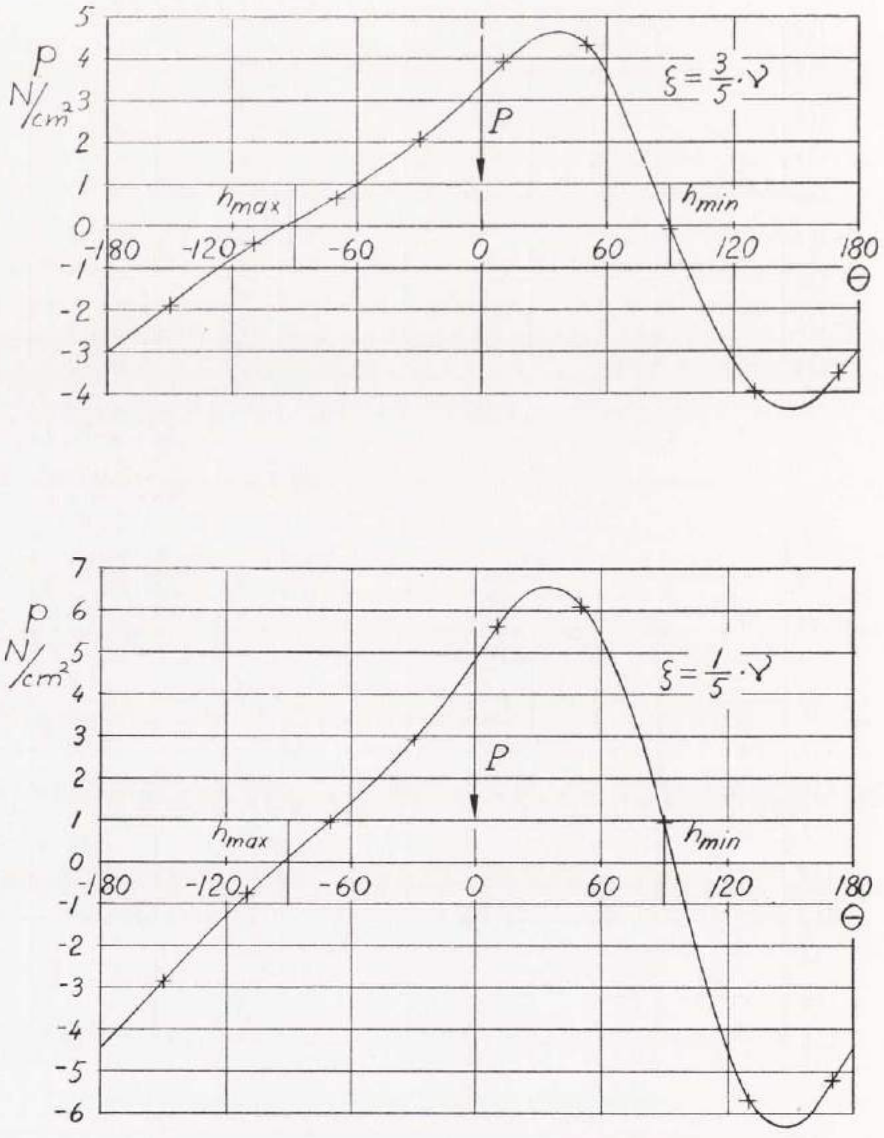

Fig. 52.1. Experimental Curves for $\nu = 1$ and $\varepsilon = 0{,}4$

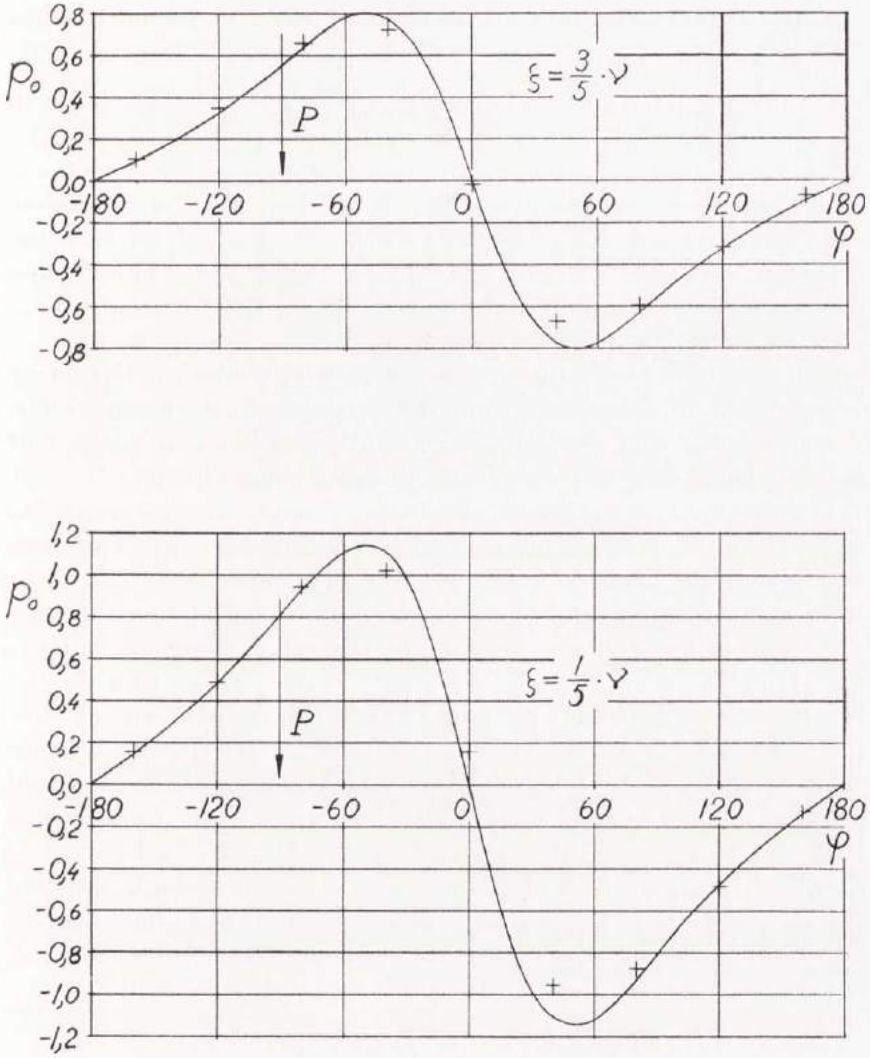

Fig. 53.1. Theoretical Curves for $\nu = 1$ and $\varepsilon = 0{,}4$
+ Experimental Points

5,2. The 360° Bearing with No Oil Grooves and with Vapour Regions

5,21. Pressure Distribution

Consider a bearing without oil grooves, and submerged in oil. This is the classical case which has not hitherto been solved. The solution requires a vapour pressure or »air expulsion pressure» lower than the pressure in the surrounding oil. If the vapour pressure were exactly the same as the pressure in the surrounding oil, no oil would be sucked into the bearing. Thus in the stationary case with a given eccentricity, the pressure would be zero in all of the bearing, giving no load capacity.

Our tests have shown that it is possible to have a bearing operating without any oil grooves and with oil supply only at the bearing sides. A bearing with the width/diameter ratio 4/3 was tested under load for four hours and was completely self-supplying with oil.

The working principle for bearings without oil grooves is as follows: The oil is flowing out from the bearing in the positive pressure region and into the bearing in the negative pressure region. Streamlines are shown on photos by VOGELPOHL (13). The smaller the difference is between the pressure in the surrounding oil and the vapour pressure, the larger is the vapour region needed to make the bearing self-supporting with oil. (Spherical journal bearings after this principle are for the present produced by H. DESCH, Neheim-Hüsten, Germany.) It is, however, somewhat uncertain to design journal bearings without axial grooves, as it is difficult to guarantee that the vapour pressure is low enough. Actual oils have gases dissolved in them which are expelled at a higher pressure than the vapour pressure. If there were no gases, the bearings would operate very well without grooves when supplied with oil at the sides.

To determine the pressure in the oil region 15.2 is used.

$$\frac{\partial}{\partial \varphi}\left(H^3 \frac{\partial p_0}{\partial \varphi}\right) + \frac{\partial}{\partial \zeta}\left(H^3 \frac{\partial p_0}{\partial \zeta}\right) = 6 \frac{\partial H}{\partial \varphi}$$

The boundary conditions are (see 55.1):

for the bearing sides

$$p_0 = 0 \quad \text{for} \quad \zeta = \pm r$$

at the maximum film thickness

$$(p_0)_{\varphi=-\pi} = (p_0)_{\varphi=\pi}$$

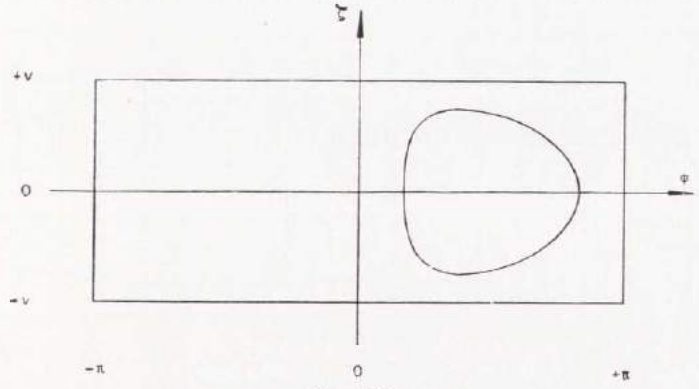

Fig. 55.1

for the beginning of the vapour region from 29.2

$$\frac{\partial p_0}{\partial \varphi} = 0 \quad \text{or} \quad \frac{\partial p_0}{\partial \zeta} = 0$$

for the end of the vapour region from 33.2

$$H^* = H - \frac{H^3}{6} \cdot \frac{\left(\frac{\partial p_0}{\partial \varphi}\right)^2 + \left(\frac{\partial p_0}{\partial \zeta}\right)^2}{\frac{\partial p_0}{\partial \varphi}}$$

where H^* is the oil film thickness at the beginning, and H the thickness at the end of the region.

In 55.2 the calculated pressure distribution for a bearing with $\nu = 1$, $\varepsilon = 0{,}4$ and $p_{v0} = -1$ is shown. The curves represent isobars.

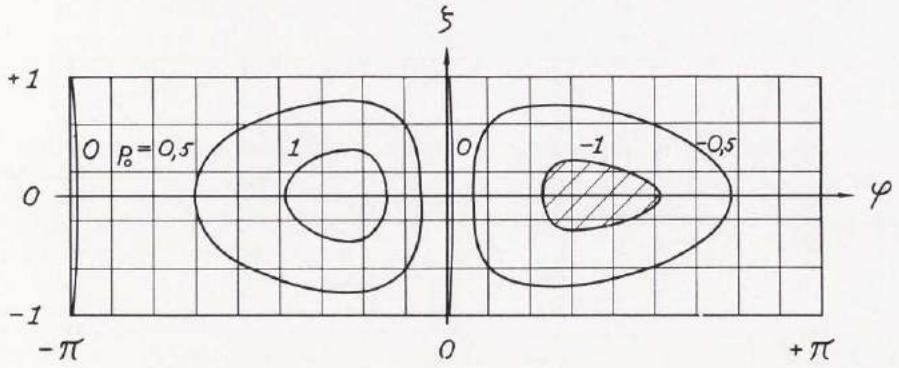

Fig. 55.2. Theoretical Pressure Distribution for $\nu = 1$, $\varepsilon = 0{,}4$ and $p_{v0} = -1$

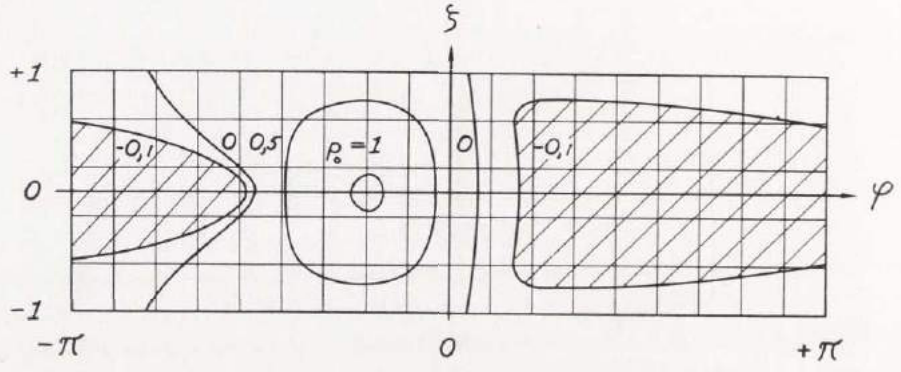

Fig. 56.1. Theoretical Pressure Distribution for $\nu = 1$, $\varepsilon = 0{,}4$ and $p_{c0} = -0{,}1$

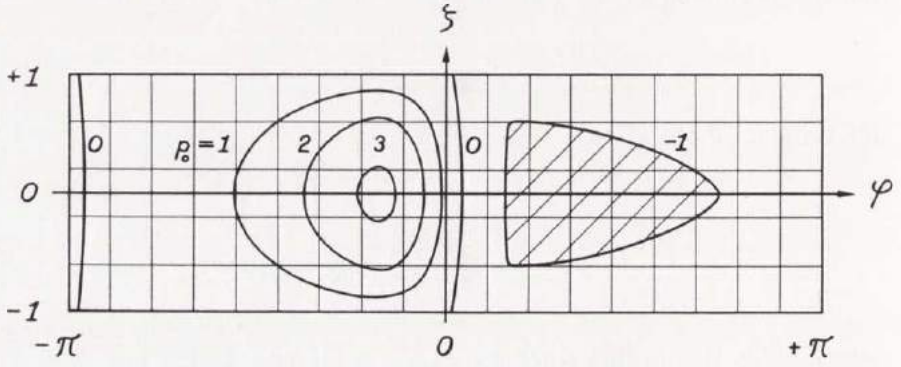

Fig. 56.2. Theoretical Pressure Distribution for $\nu = 1$, $\varepsilon = 0{,}6$ and $p_{c0} = -1$

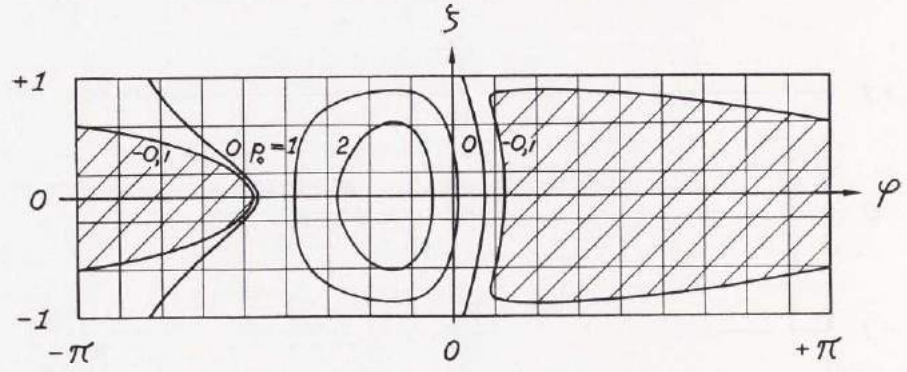

Fig. 56.3. Theoretical Pressure Distribution for $\nu = 1$, $\varepsilon = 0{,}6$ and $p_{c0} = -0{,}1$

Fig. 56.1 shows the same bearing operating with $p_{v0} = -0{,}1$. It is obvious that the vapour region does not end at the maximum film thickness $\varphi = \pi$. The higher the vapour pressure is, the more the region moves into the convergent part. Thus the area of the vapour region can vary between zero and the whole bearing area $4\,\pi\,r\,r^2$. The figs 56.2 and 56.3 show the same cases as described above, but with $\varepsilon = 0{,}6$.

5,22. Load Capacity

The expression for the load capacity is not changed, even though there is a vapour region. Thus from 18.2

$$P_{x0} = \frac{P_x\,\psi^2}{\eta\,U} = -\frac{1}{2\,r}\int_{-\nu}^{+\nu}\int_{-\pi}^{+\pi} p_0 \sin\varphi\; d\varphi\; d\zeta$$

$$P_{y0} = \frac{P_y\,\psi^2}{\eta\,U} = \frac{1}{2\,r}\int_{-\nu}^{+\nu}\int_{-\pi}^{+\pi} p_0 \cos\varphi\; d\varphi\; d\zeta$$

The resultant load and the angle between the load line and the line of centres are from 18.3

$$P_0 = \frac{P\,\psi^2}{\eta\,U} = \sqrt{P_{x0}^2 + P_{y0}^2}$$

$$\tan\beta = \frac{P_{x0}}{P_{y0}}$$

The results obtained for $p_{v0} = -1$ and $p_{v0} = -0{,}1$ are found in 58.1 and 59.1.

Attitude-eccentricity curves are usually drawn. For a bearing without vapour regions, this curve is the same for increasing load and increasing speed. For the bearings with a vapour region described above, we get two different curves for these two variations.

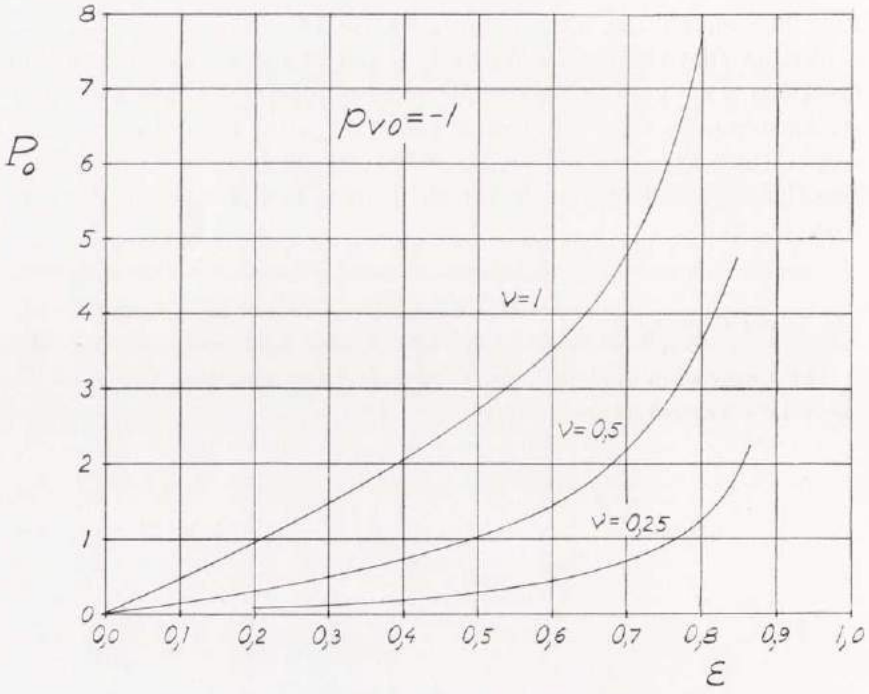

Fig. 58.1. Load Capacity $P_0 = \dfrac{P\,\psi^2}{\eta\,U}$

1. Varying load

For the non-dimensional vapour pressure we have

$$p_{v0} = \frac{p_v \psi^2}{\eta\,\omega}$$

For constant p_v, ψ, η and ω, the value p_{v0} is constant. It is thus possible to draw attitude-eccentricity curves for constant non-dimensional vapour pressure, which are valid for varying load.

2. Varying angular velocity

For the vapour pressure and the load we have

$$p_{v0} = \frac{p_v \psi^2}{\eta\,\omega}$$

$$P_0 = \frac{P\,\psi^2}{\eta\,U}$$

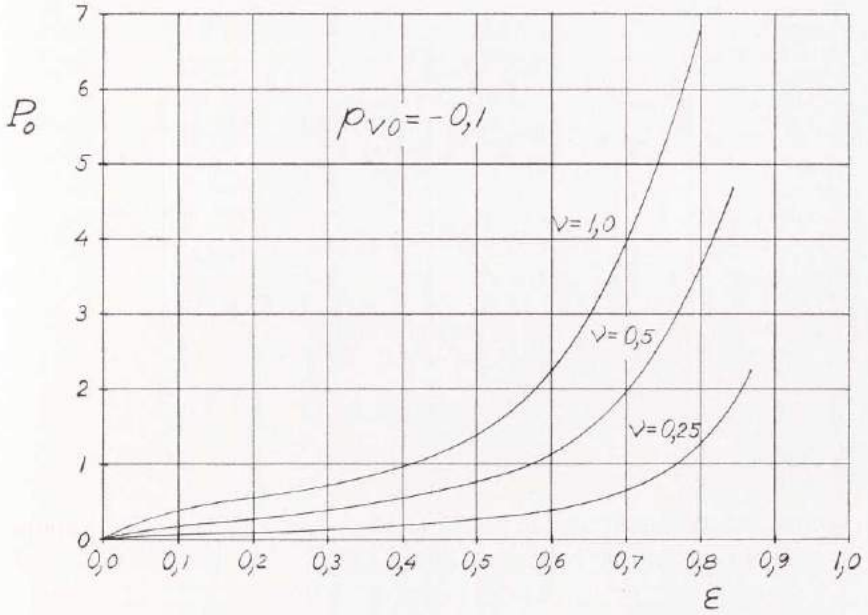

Fig. 59.1. Load Capacity $P_0 = \dfrac{P\,\psi^2}{\eta\,U}$

Then

$$\frac{P_0}{p_{v0}} = \frac{P}{p_v r} = \text{const}$$

from which the attitude-eccentricity curves for varying speed can be determined.

5,23. **Oil Flow**

The oil quantity per unit time passing over the edges of the bearing takes care of the generated heat. From the continuity condition, the flow leaving the bearing is equal to that entering the bearing. The best value for the changed oil is derived from the side leakage, because the pressure derivatives in the positive pressure region can be calculated with greater accuracy. This is due to the fact that the location of the vapour region is derived through approximate relaxation methods.

The oil flow is shown in 60.1. When there is no vapour region, the isobars $p_0 = 0$ are located at $\varphi = 0$ and $\varphi = \pm\pi$. If a vapour

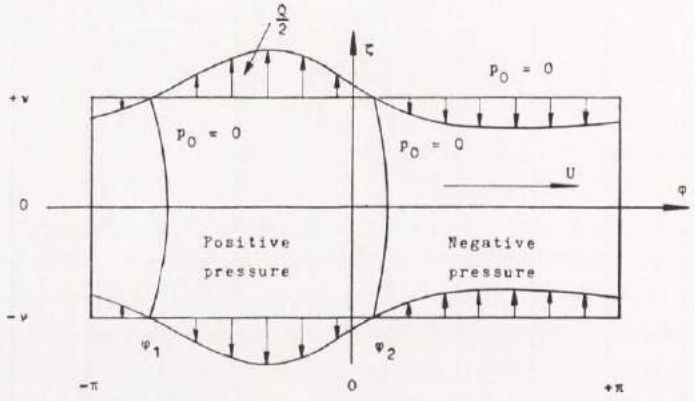

Fig. 60.1

region exists, they are moved to the right. When the vapour pressure has the limit value zero, both of them are located at $\varphi = 0$, and there is zero pressure all around the journal.

The oil flow in 60.1 for a bearing with a vapour region is from 20.1

$$Q = 2 \int_{\varphi_1}^{\varphi_2} q_z \, r \, d\varphi = -2 \int_{\varphi_1}^{\varphi_2} \frac{h^3}{12\,\eta} \left(\frac{\partial p}{\partial z} \right)_{z=\frac{b}{2}} r \, d\varphi$$

or non-dimensionally

$$Q_0 = \frac{Q}{r\,U\,\Delta r} = -2 \int_{\varphi_1}^{\varphi_2} \frac{H^3}{12} \left(\frac{\partial p_0}{\partial \zeta} \right)_{\zeta=\nu} d\varphi$$

The calculated oil flow is given in 61.1 and 61.2.

5,24. Power Loss

The power loss for a bearing with a vapour region is rather complicated to evaluate, because there are two expressions for it, one for the oil region and one for the vapour region. The difference is due to the vapour or gas strips in the vapour region, as discussed in chap. 4,2. Another complication in evaluating the power loss is that the boundary of the vapour region φ_1 and φ_2 are functions of ζ, which are numerically determined.

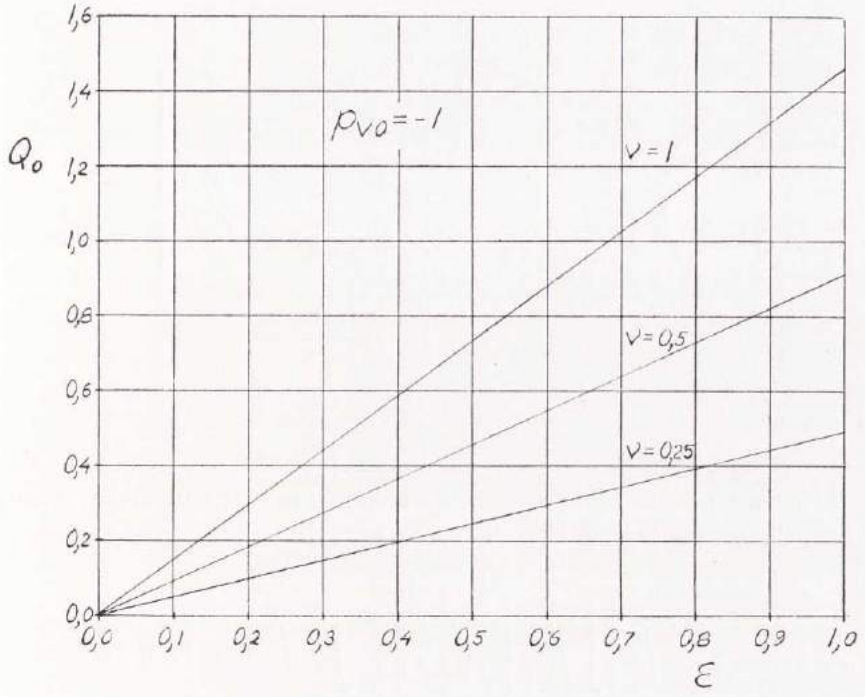

Fig. 61.1. Oil Flow $Q_0 = \dfrac{Q}{r\,U\,\Delta r}$

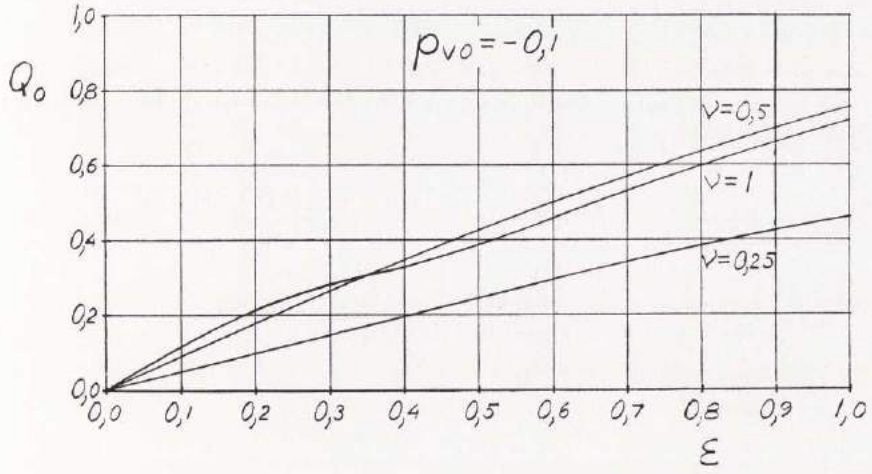

Fig. 61.2. Oil Flow $Q_0 = \dfrac{Q}{r\,U\,\Delta r}$

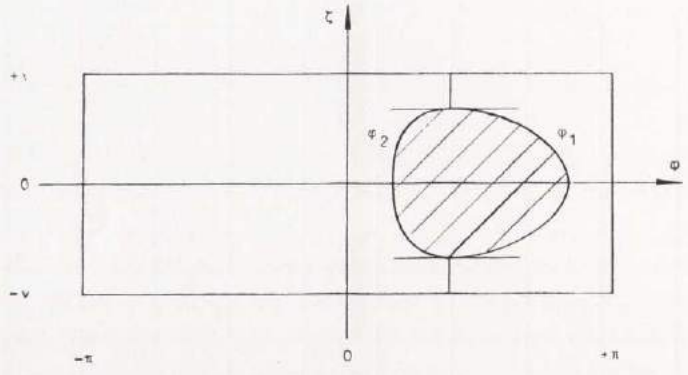

Fig. 62.1

The unfolded bearing area in 62.1 shows the vapour zone. From 23.2 the power loss in the oil region is

$$E_0' = \frac{1}{4\,r} \int_{-\nu}^{+\nu} \left[\int_{\varphi_1}^{\varphi_2} H p_0 \right] d\zeta - \frac{\varepsilon}{4\,r} \int_{-\nu}^{+\nu} \int_{\varphi_1}^{\varphi_2} p_0 \sin\varphi \, d\varphi \, d\zeta +$$

$$+ \frac{1}{2\,r} \int_{-\nu}^{+\nu} \frac{\gamma_2 - \gamma_1}{\sqrt{1-\varepsilon^2}} \, d\zeta$$

The power loss in the vapour region becomes from 36.2 and 37.1

$$E_0'' = \frac{1}{2\,r} \int_{-\nu}^{+\nu} H^* \cdot \frac{(\gamma_1 - \gamma_2) + \varepsilon\,(\sin\gamma_1 - \sin\gamma_2)}{\sqrt{(1-\varepsilon^2)^3}} \, d\zeta$$

Thus the total power loss for the bearing is

$$E_0 = \frac{E\,\psi}{\eta\,U^2} = E_0' + E_0''$$

which is shown in 63.1 and 63.2.

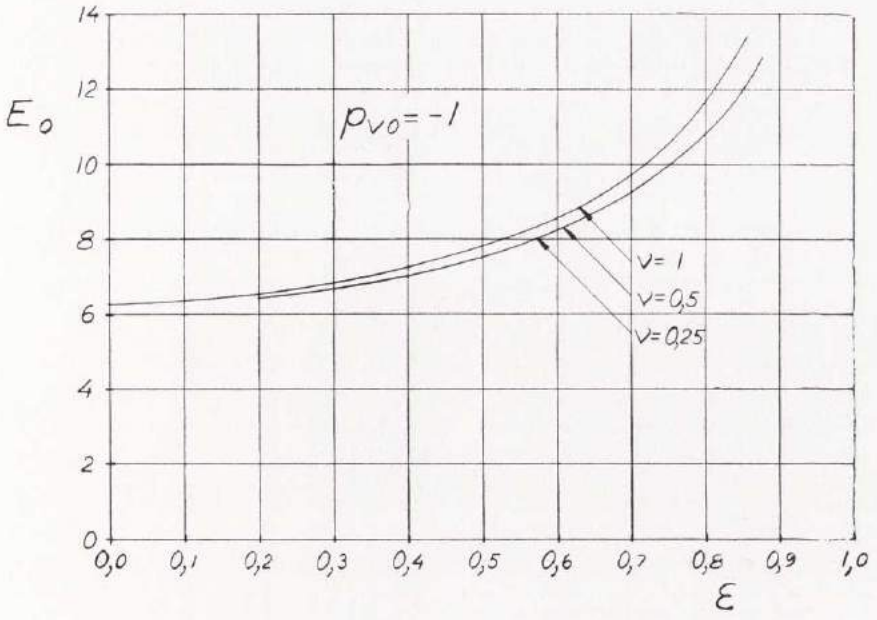

Fig. 63.1. Power Loss $E_0 = \dfrac{E\,\psi}{\eta\,U^2}$

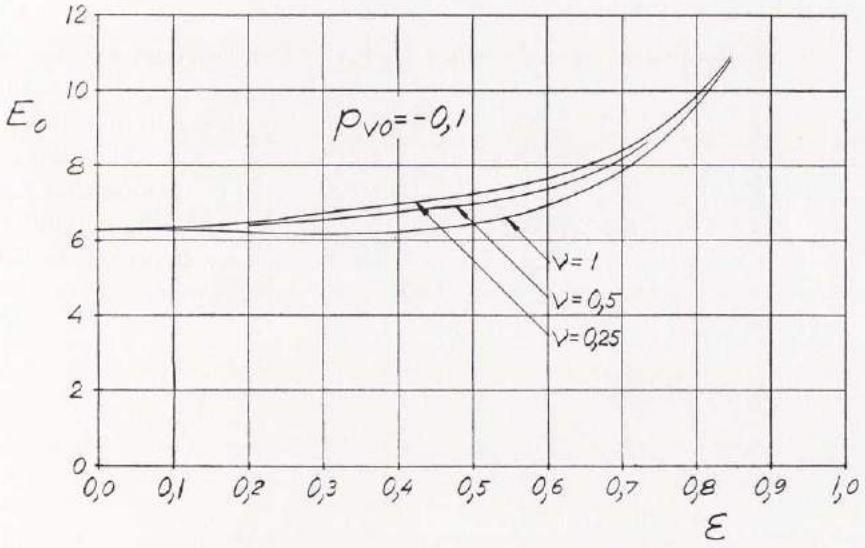

Fig. 63.2. Power Loss $E_0 = \dfrac{E\,\psi}{\eta\,U^2}$

5,25. **Average Temperature Rise**

The average temperature rise is derived as in 3,6.

$$\Delta t_0 = c\,\varrho \cdot \frac{\Delta t\,\psi^2}{\eta\,\omega} = \frac{2\,\nu\,E_0}{Q_0}$$

where Q_0 and E_0 are known from chap. 5,23 and 5,24 respectively.

5,26. **Coefficient of Friction and Relative Power Loss**

As in 3,7 we have

$$\frac{\mu}{\psi} = \frac{f}{\omega\,\Delta r} = \frac{E_0}{P_0}$$

or

$$\frac{\mu\,r}{h_{\min}} = \frac{f}{\omega\,h_{\min}} = \frac{E_0}{P_0\,(1-\varepsilon)} \quad \ldots\ldots\ldots \quad 64.1$$

Curves over 64.1 are given in 65.1 and 65.2.

5,27. **Experimental Investigation**

The test apparatus is described in 5,17. The bearings had no oil grooves and had oil supply only at the bearing sides, due to the surrounding oil. The tests were made at two different non-dimensional vapour pressures $p_{v0} = -1$ and $p_{v0} = -0{,}1$. The experiments show good agreement with the theory. It is obvious that the assumption that the positive oil film pressure begins at the maximum oil film thickness is wrong. When a bearing has a vapour region the positive pressure always starts in the convergent part.

Two experiments are analysed in detail:

1. Fig. 68.1 and 69.1

$$\nu = \frac{4}{3}$$

$$\psi = 0{,}00291$$

$$\eta = 0{,}0127 \text{ Ns/m}^2$$

$$\omega = 48{,}1 \text{ 1/s}$$

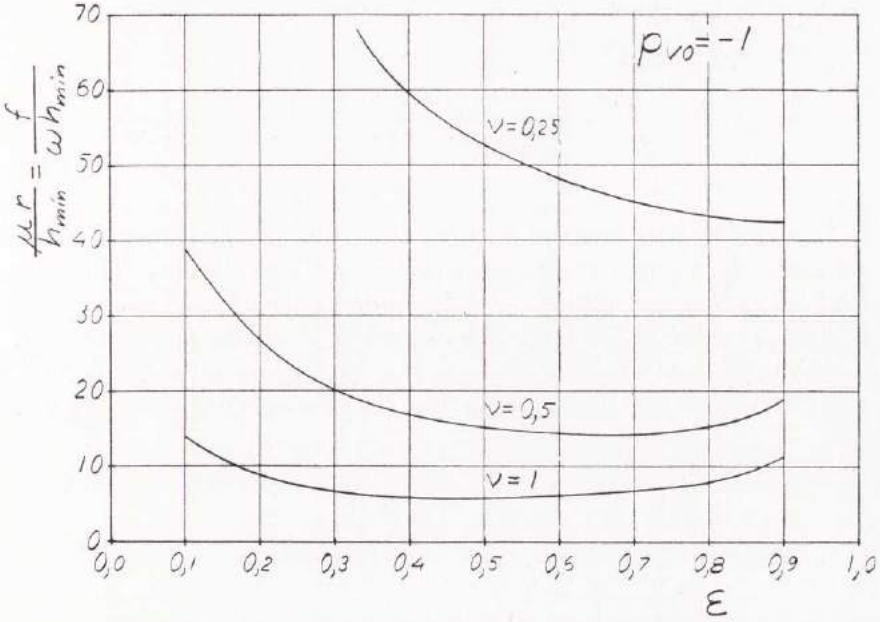

Fig. 65.1. Coefficient of Friction and Relative Power Loss

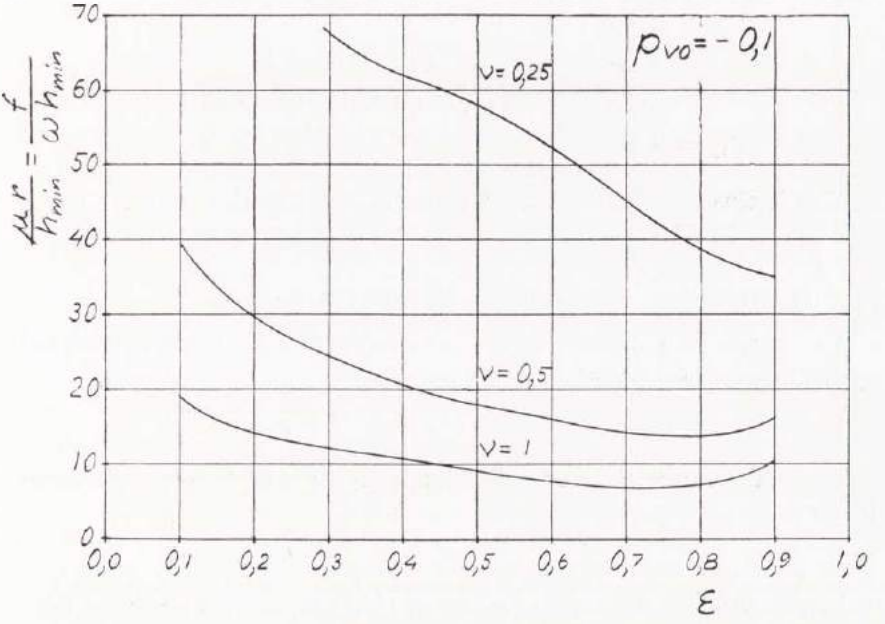

Fig. 65.2. Coefficient of Friction and Relative Power Loss

Experimental load capacity

$$P_e b = 2\,250 \text{ N}$$

$$P_{0e} = \frac{P_e \psi^2}{\eta U} = \frac{2\,250 \cdot 3 \cdot 0{,}00291^2}{2 \cdot 4 \cdot 0{,}05 \cdot 0{,}0127 \cdot 0{,}05 \cdot 48{,}1}$$

$$P_{0e} = 4{,}68$$

The aim was to test the bearing at $\varepsilon = 0{,}6$ and $p_{v0} = -1$. The angular velocity was varied until $p_{v0} = -1$ was reached. Then the load 2 250 N was applied to get a non-dimensional load close to the theoretical value $P_{0t} = 4{,}46$. The value of P_{0e} corresponds to $\varepsilon \approx 0{,}61$.

The experimental pressure is shown in 68.1 and 69.1. In 69.1, the test points are compared to the theoretical curves for $\varepsilon = 0{,}6$.

2. Fig. 70.1 and 71.1.

$$\nu = 1 \qquad p_{v0} = -0{,}1$$

$$\psi = 0{,}00364$$

$$\eta = 0{,}0153 \text{ Ns/m}^2$$

$$\omega = 48{,}6 \text{ l/s}$$

Experimental load capacity

$$P_e b = 620 \text{ N}$$

$$P_{0e} = \frac{P_e \psi^2}{\eta U} = \frac{620 \cdot 0{,}00364^2}{2 \cdot 0{,}05 \cdot 0{,}0153 \cdot 0{,}05 \cdot 48{,}6}$$

$$P_{0e} = 2{,}21$$

This is close to the calculated value $P_{0t} = 2{,}26$ at $\varepsilon = 0{,}6$. Curves are shown in 71.1.

5,3. The Optimum 360° Bearing without Oil Grooves

The three parameters, which determine all the non-dimensional quantities for a journal bearing, are

$$\nu \qquad \varepsilon \qquad p_{v0}$$

The real quantities can be derived from the non-dimensional, if we know

$$\Delta r \qquad r \qquad \eta$$

In the above statements is assumed that the basic quantities, load capacity P_{tot} and angular velocity ω, are given.

The problem is now to determine the six unknowns, so that the power loss is as small as possible. This is reached when f is a minimum.

$$f = \frac{E}{P} = \frac{E_0}{P_0 (1 - \varepsilon)} \cdot \omega h_{\min} \quad \ldots\ldots\ldots\ldots \quad 67.1$$

From the expression 67.1 we see that $h_{\min}$ shall have the lowest permissible value. This value depends upon manufacture. Now we have to find minimum for the function

$$\frac{f}{\omega h_{\min}} = \frac{E_0}{P_0 (1 - \varepsilon)}$$

From 65.1 and 65.2 we can see that the relative power loss is lower for a wide bearing than for a narrow one. For every width/diameter ratio it is possible to get optimum values for ε and p_{v0}. This minimum analysis gives three of the unknowns. Now Δr, r and η remain to be determined. This requires three conditions. These are:

1. A given load
2. A given vapour pressure
3. A minimum permissible oil film thickness

These conditions give

$$P_0 = \frac{P \psi^2}{\eta U} = \frac{P \Delta r^2}{\eta \omega r^3}$$

$$p_{v0} = \frac{p_v \psi^2}{\eta \omega} = \frac{p_v \Delta r^2}{\eta \omega r^2}$$

$$h_{\min} = \Delta r (1 - \varepsilon)$$

and from these equations

$$\Delta r = \frac{h_{\min}}{1 - \varepsilon}$$

$$r = \frac{P p_{v0}}{P_0 p_v}$$

$$\eta = \frac{P_0 p_v^2 \Delta r^2}{P p_{v0}^2 r \omega}$$

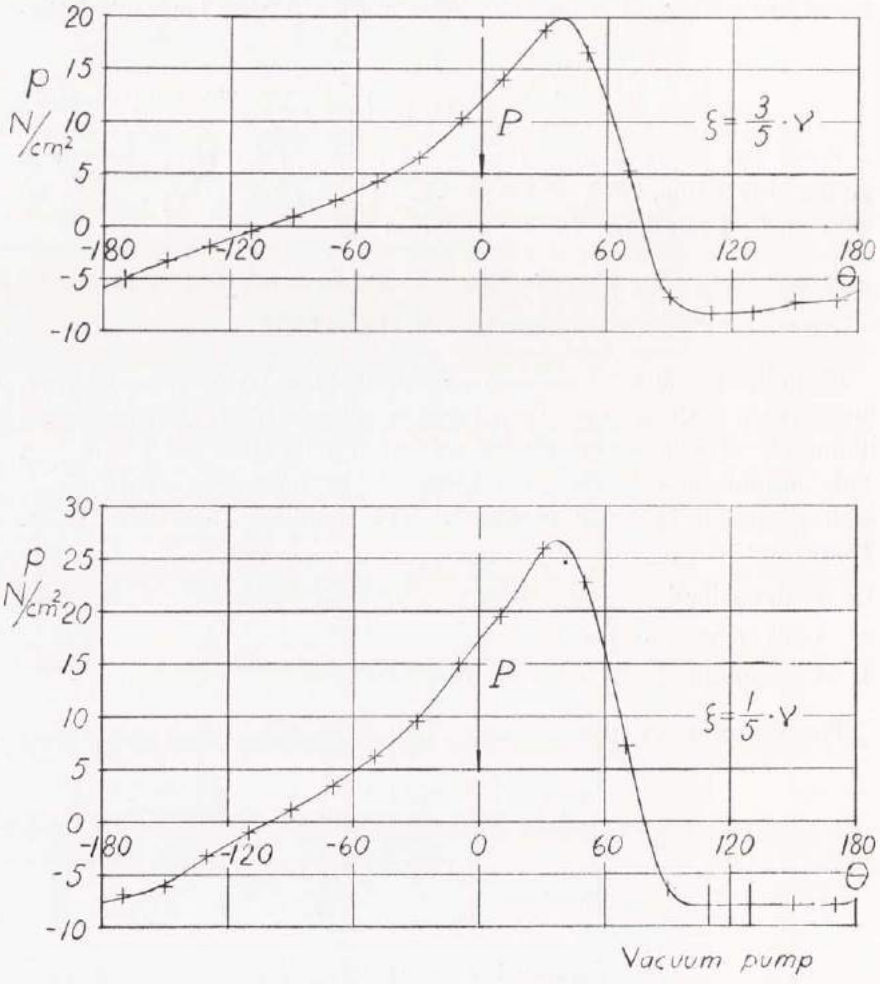

Fig. 68.1. Experimental Curves for $\nu = \frac{4}{3}$; $\varepsilon = 0{,}6$ and $p_{v0} = -1$

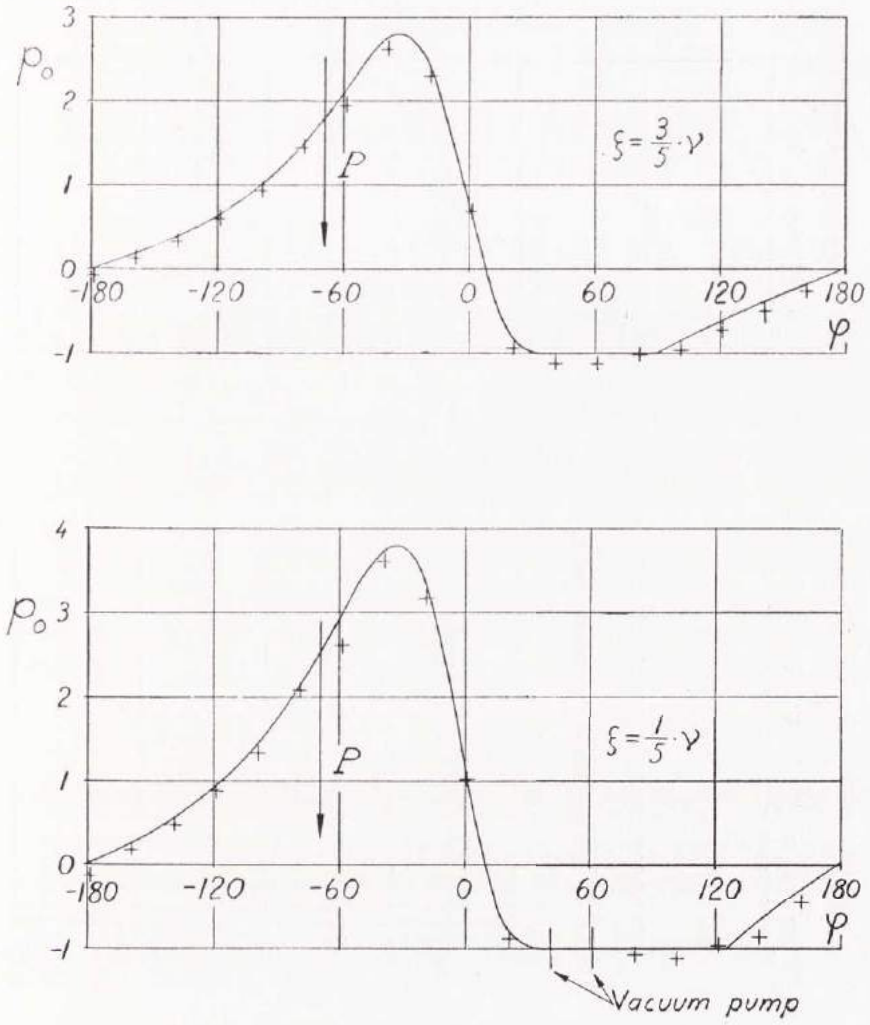

Fig. 69.1. Theoretical Curves for $\nu = \frac{4}{3}$; $\varepsilon = 0{,}6$ and $p_{\nu 0} = -1$
+ Experimental Points

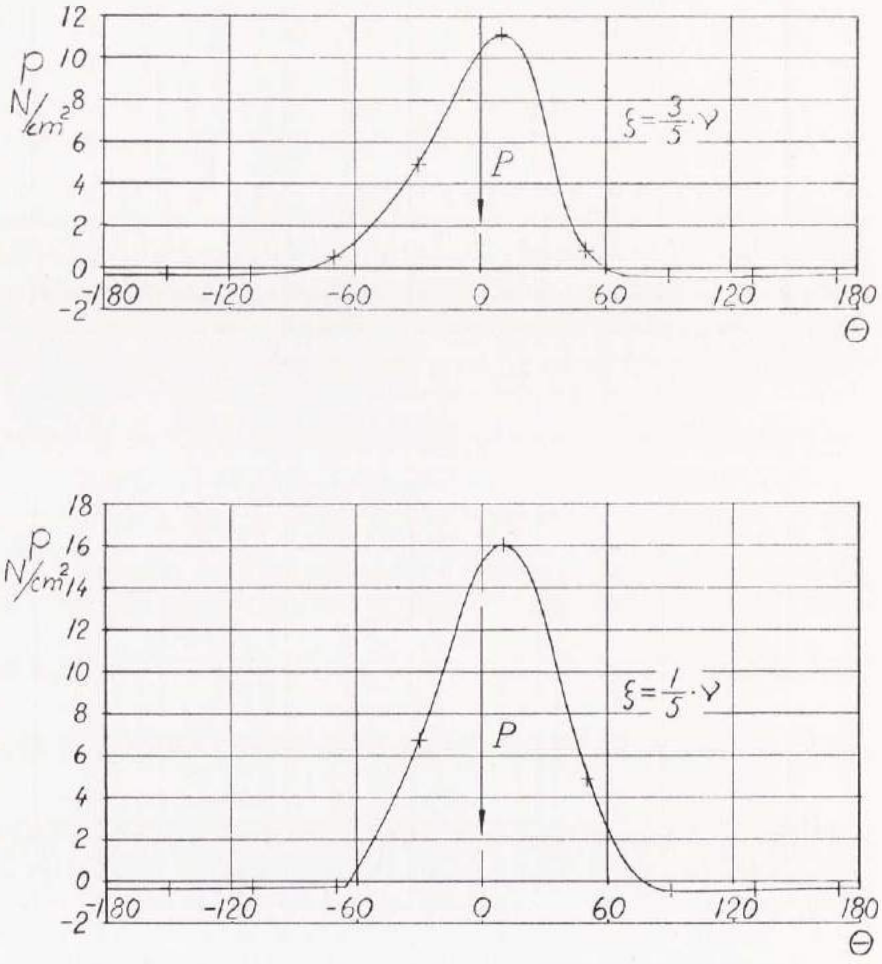

Fig. 70.1. Experimental Curves for $\nu = 1$; $\varepsilon = 0{,}6$ and $p_{\xi 0} = -0{,}1$

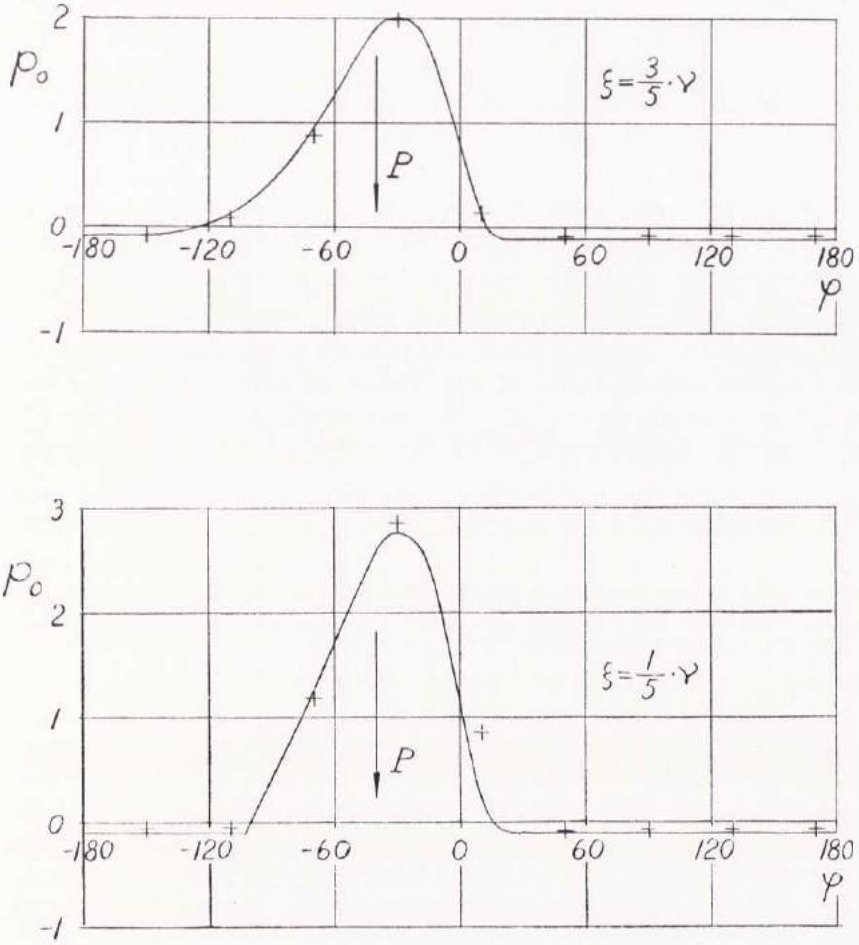

Fig. 71.1. Theoretical Curves for $\nu = 1$; $\varepsilon = 0{,}6$ and $p_{v0} = -0{,}1$
+ Experimental Points

Now the bearing is completely determined, but the result may be impossible to use. For instance, there must exist an incompressible medium with the derived viscosity. The radius r must be large enough from strength considerations. These two conditions can make it necessary to renounce the optimum condition of the lubrication theory. Sometimes an optimum bearing would have a lubricant viscosity lower than that of air. But if air were used, one must consider that the medium is compressible, and this theory does not hold. It should be pointed out that we must have the suggested vapour pressure if the bearing is to be self-supporting with oil.

6. The 180° Bearing with Minimum Film Thickness at the Trailing Edge

6,1. Pressure Distribution

A partial bearing without vapour regions will now be discussed. If a 180° partial journal bearing shall have no vapour region for every ε, it is necessary to have a convergent part only. This means that the oil film begins at maximum oil film thickness and ends at minimum oil film thickness. Such a bearing is not centrally loaded. The bearing must be turned relative to the load line according to 73.1.

The differential equation for the pressure in the oil film is from 3,1

$$\frac{\partial}{\partial \varphi}\left(H^3 \frac{\partial p_0}{\partial \varphi}\right) + \frac{\partial}{\partial \zeta}\left(H^3 \frac{\partial p_0}{\partial \zeta}\right) = 6 \frac{\partial H}{\partial \varphi}$$

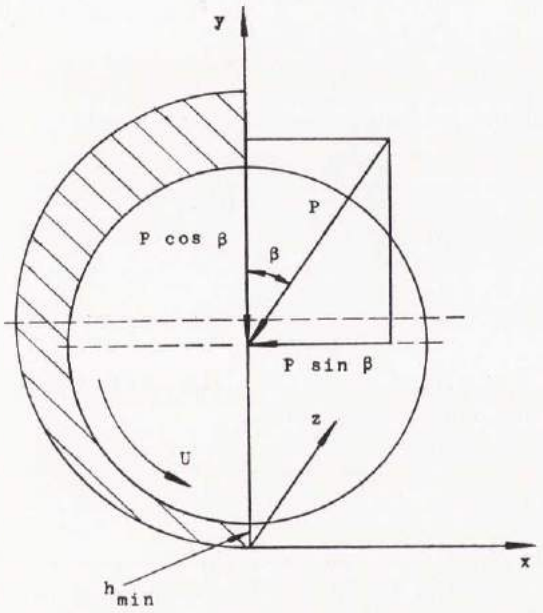

Fig. 73.1

The boundary conditions are

$$p_0 = 0 \text{ for } \zeta = \pm \nu$$

$$p_0 = 0 \text{ for } \varphi = -\pi \text{ and } \varphi = 0$$

The solution gives positive pressure in all of the bearing. Accordingly, the only boundary condition to be kept in practice is that sufficient oil at zero pressure is present at the beginning of the bearing, because there is no flow into the bearing at the sides.

The pressure distributions in this case are exactly the same as in positive pressure parts of the bearings in chap. 5,1.

6,2. Load Capacity

From 3,3 the load components are

$$P_{x0} = \frac{P_x \psi^2}{\eta U} = -\frac{1}{2\nu} \int_{-\nu}^{+\nu} \int_{-\pi}^{0} p_0 \sin \varphi \, d\varphi \, d\zeta$$

$$P_{y0} = \frac{P_y \psi^2}{\eta U} = \frac{1}{2\nu} \int_{-\nu}^{+\nu} \int_{-\pi}^{0} p_0 \cos \varphi \, d\varphi \, d\zeta$$

and the resultant load and the load angle become

$$P_0 = \frac{P \psi^2}{\eta U} = \sqrt{P_{x0}^2 + P_{y0}^2}$$

$$\tan \beta = \frac{P_{x0}}{P_{y0}}$$

Curves of load capacity and load angle as functions of the eccentricity are drawn in 75.1 and 75.2.

6,3. Oil Flow

The oil flow is determined from 20.1.

The oil entering the bearing at the leading edge leaves the bearing at the sides and at the trailing edge, see 76.1.

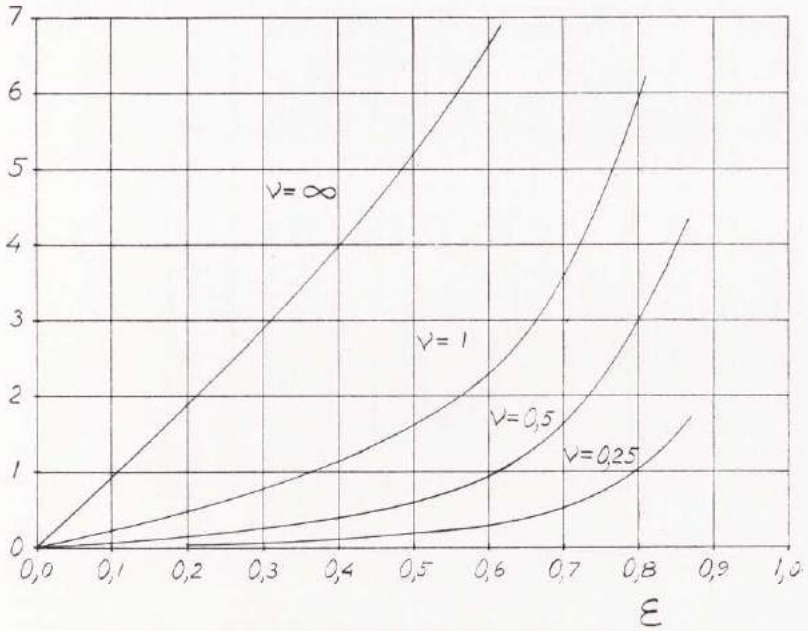

Fig. 75.1. Load Capacity $P_0 = \frac{P \psi^2}{\eta U}$

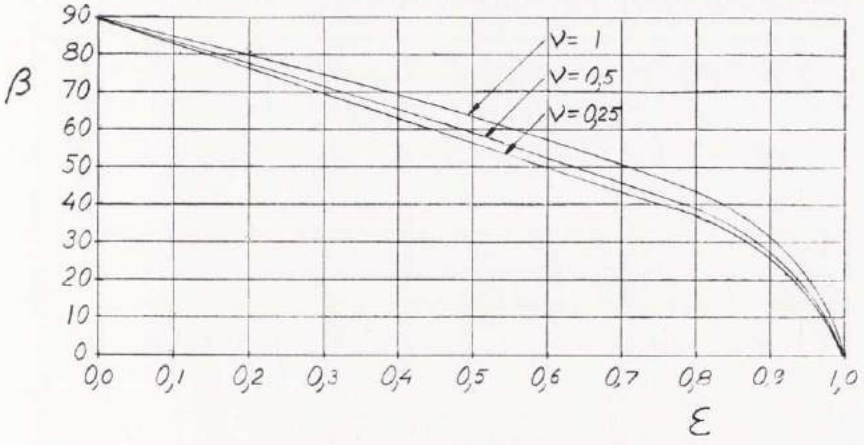

Fig. 75.2. Load Angle

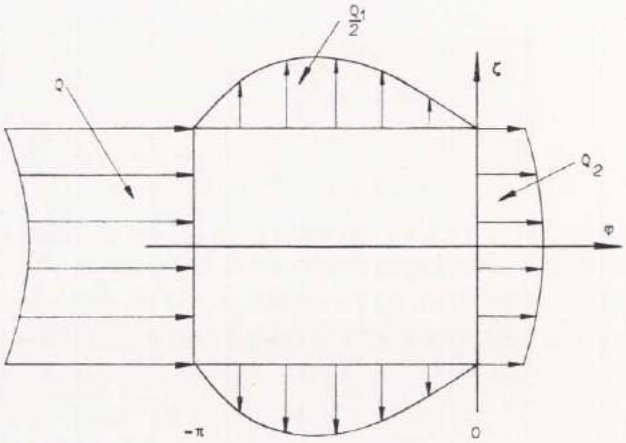

Fig. 76.1

Thus

$$Q = Q_1 + Q_2$$

Q is the changed oil quantity per unit time, and for this we have

$$Q = \int_{-\frac{b}{2}}^{+\frac{b}{2}} (q_x)_{\varphi=-\pi}\, dz$$

or with non-dimensional expressions

$$\frac{Q}{r\, U\, \Delta r} = \int_{-\nu}^{+\nu} \left(\frac{H}{2} - \frac{H^3}{12} \cdot \frac{\partial\, p_0}{\partial\, \varphi} \right)_{\varphi=-\pi} d\zeta$$

For $\varphi = -\pi$ $H = 1 + \varepsilon$

and thus

$$Q_0 = \frac{Q}{r\, U\, \Delta r} = \nu\,(1+\varepsilon) - \frac{(1+\varepsilon)^3}{12} \int_{-\nu}^{+\nu} \left(\frac{\partial\, p_0}{\partial\, \varphi} \right)_{\varphi=-\pi} d\zeta$$

Q_0 is given as a function of ε in 77.1.

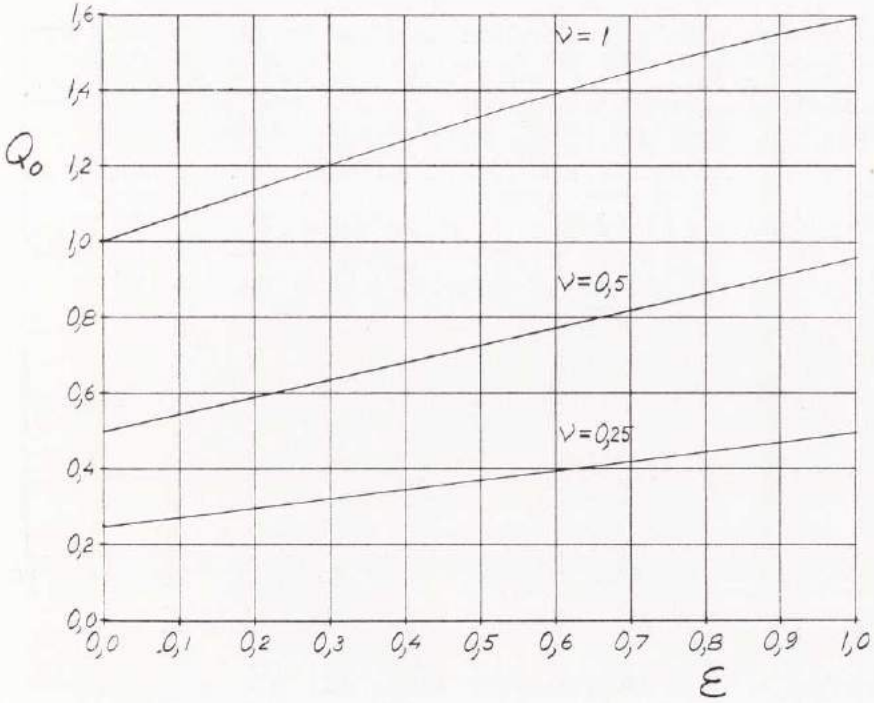

Fig. 77.1. Oil Flow $Q_0 = \dfrac{Q}{r\,U\,\Delta r}$

6,4. Power Loss

The power loss for this bearing is already derived in chap. 3,5 eq. 24.2.

$$E_0 = \frac{\varepsilon}{2} \cdot P_0 \sin \beta + \frac{\pi}{\sqrt{1-\varepsilon^2}}$$

After the load component in the x-direction is calculated, the power loss for a bearing without vapour regions can be determined without further approximations.

Curves of E_0 are drawn in 78.1.

6,5. Average Temperature Rise

The temperature rise is from 3,6

$$\Delta t_0 = c\,\varrho \cdot \frac{\Delta t\,\psi^2}{\eta\,\omega} = \frac{2\,\nu\,E_0}{Q_0}$$

where Q_0 and E_0 are known from chap. 6,3 and 6,4 respectively.

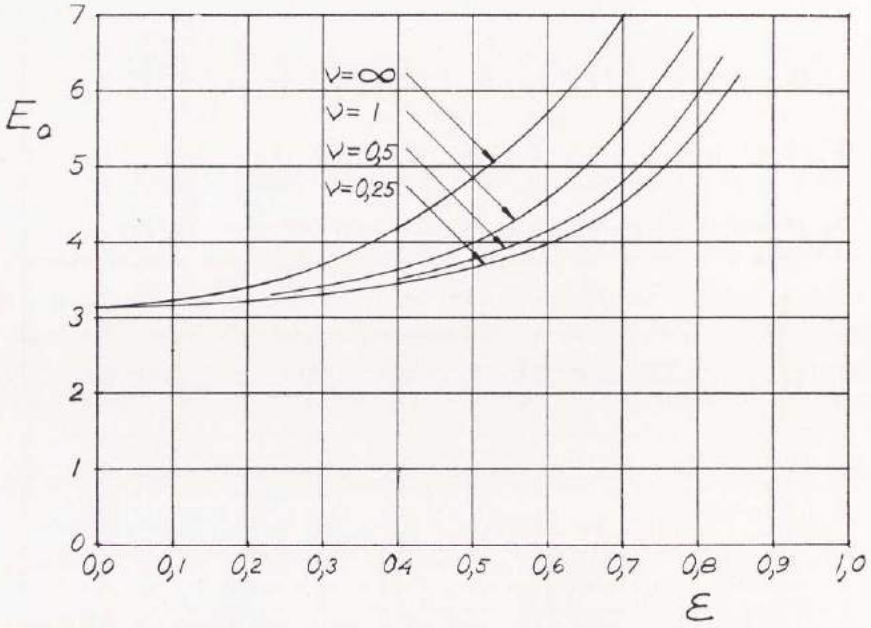

Fig. 78.1. Power Loss $E_0 = \dfrac{E\,\psi}{\eta\,U^2}$

6,6. Coefficient of Friction and Relative Power Loss

The equations are analogous to the equations of chap. 5,26 and the curves for the relative power loss are shown in 79.1.

6,7. Optimum Analysis

As we have no vapour region in this case, there are now two parameters to determine the non-dimensional quantities, viz.

$$\nu \qquad \varepsilon$$

The real quantities are then derived from the values

$$\Delta r \qquad r \qquad \eta$$

When dimensioning a journal bearing, we know the load capacity P_{tot}, the angular velocity ω, and assume a minimum permissible value for the minimum film thickness h_{min}, which does not cause failure.

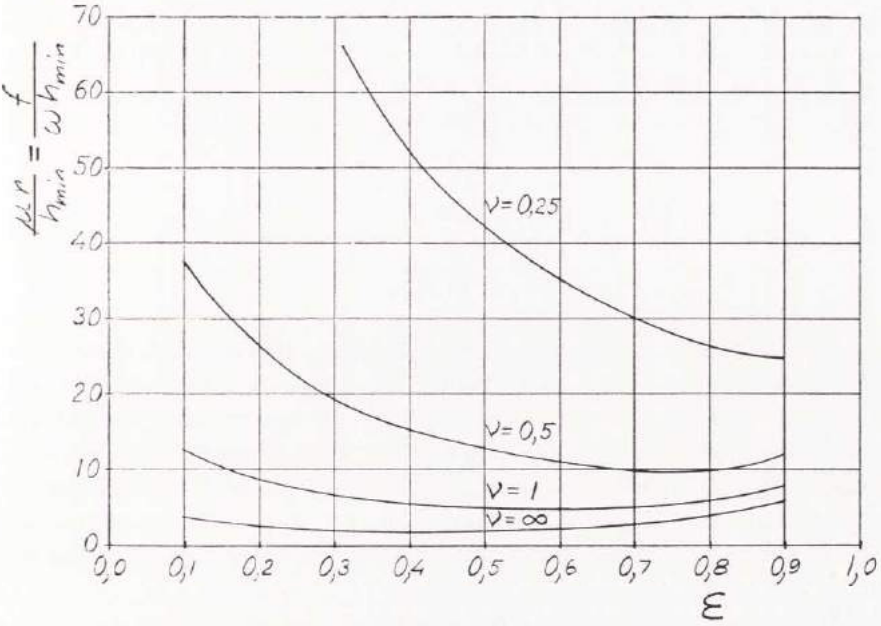

Fig. 79.1. Coefficient of Friction and Relative Power Loss

From 79.1 it is clear that a wide bearing has always lower power loss than a narrow one for a given P_{tot}, ω and h_{min}. For every ν there is an optimum value for the non-dimensional eccentricity ε. Then minimum for the function

$$\frac{f}{\omega h_{min}} = \frac{E_0}{P_0 (1 - \varepsilon)}$$

determines ν and ε. Now the determination of Δr, r and η remains. For this we need three conditions:

1. A given load capacity
2. Strength considerations for the journal
3. A minimum permissible oil film thickness

Condition 3 gives

$$h_{min} = \Delta r (1 - \varepsilon)$$

$$\Delta r = \frac{h_{min}}{1 - \varepsilon}$$

From 2 we get a value for the shaft radius. The power loss is not dependent on the value of r. An increase in radius corresponds to a decrease in viscosity. From the first condition we have

$$P_0 = \frac{P \psi^2}{\eta U}$$

or

$$\eta = \frac{P \Delta r^2}{P_0 \omega r^3} = \frac{P h_{\min}^2}{P_0 \omega (1 - \varepsilon)^2 r^3}$$

If there is no oil with as low viscosity as the derived value, the optimum condition must be abandoned. Then the oil with the lowest existing viscosity is chosen, and the optimum condition for this oil is determined. This optimum is reached by increasing ε at constant value of $h_{\min}$. This oil can also be used for the same ε at a higher value of $h_{\min}$; but the power loss is larger in this case. Sometimes, however, it is necessary to use the latter way, because ε otherwise gets too high value.

For the temperature rise we have

$$\Delta t = \frac{2 \nu E_0}{Q_0} \cdot \frac{1}{c \varrho} \cdot \frac{\eta \omega}{\psi^2}$$

but now

$$P_0 = \frac{P \psi^2}{\eta U}$$

or

$$\frac{\eta \omega}{\psi^2} = \frac{P}{P_0 r}$$

which gives

$$\Delta t = \frac{2 \nu E_0}{Q_0 P_0} \cdot \frac{1}{c \varrho} \cdot \frac{P}{r}$$

6,8. Schedule for Calculation

ν is chosen as large as possible

ε is chosen so that the function $\frac{f}{\omega h_{\min}}$ in diagram 79.1 is minimum

r is derived from strength considerations

$$\eta = \frac{P h_{\min}^2}{P_0 \omega (1 - \varepsilon)^2 r^3}$$

$$\Delta r = \frac{h_{\min}}{1 - \varepsilon}$$

$$\psi = \frac{\Delta r}{r}$$

$$f = \frac{E_0}{P_0 (1 - \varepsilon)} \cdot \omega h_{\min}$$

$$E_{\text{tot}} = f P_{\text{tot}}$$

β is determined from 75.2.

$$Q = Q_0 r U \Delta r$$

$$\Delta t = \frac{2 r E_0}{Q_0 P_0} \cdot \frac{1}{c \varrho} \cdot \frac{P}{r}$$

6,9. Examples

1. Design a 180° partial bearing with load capacity 5000 N, rotational speed 3000 r/m and minimum oil film thickness 0,025 mm. Because of strength considerations the shaft shall have a minimum diameter of 70 mm. Ratio width-diameter 1.

From diagram 79.1 the eccentricity $\varepsilon = 0,5$

$$\eta = \frac{5000 \cdot 0,000025^2}{2 \cdot 0,035 \cdot 1,6 \cdot 314 \cdot 0,5^2 \cdot 0,035^3}$$

$$\eta = 0,0083 \text{ Ns/m}^2$$

$$\Delta r = \frac{0,025}{0,5} = 0,050 \text{ mm}$$

$$\psi = \frac{0,050}{35} = 1,43 \text{ }^0/_{00}$$

$$f = \frac{4,0}{1,6 \cdot 0,5} \cdot 314 \cdot 0,000025 = 0,039 \text{ m/s}$$

$$E_{\text{tot}} = 0,039 \cdot 5000 = 195 \text{ Nm/s} = 195 \text{ W}$$

From diagram 75.2

$$\beta = 63^\circ$$

which represents the angle between the load line and the trailing edge.

$$Q = 1{,}33 \cdot 0{,}035^2 \cdot 314 \cdot 0{,}000050$$

$$Q = 25{,}6 \cdot 10^{-6}\ \mathrm{m^3/s}$$

If

$$c = 2000\ \mathrm{Nm/kg^\circ C}$$

$$\varrho = 900\ \mathrm{kg/m^3}$$

$$\Delta t = \frac{2 \cdot 4{,}0}{1{,}33 \cdot 1{,}6} \cdot \frac{1}{2000 \cdot 900} \cdot \frac{5000}{2 \cdot 0{,}035^2}$$

$$\Delta t = 4{,}3^\circ\ \mathrm{C}$$

2. Design an optimum 180° bearing for a load capacity 10000 N, rotational speed 1500 r/m and minimum oil film thickness 0,03 mm. Shaft diameter 100 mm and ratio width-diameter 0,5.

From diagram 79.1 the eccentricity is chosen to be $\varepsilon = 0{,}7$.

$$\eta = \frac{10000 \cdot 0{,}00003^2}{0{,}05 \cdot 1{,}6 \cdot 157 \cdot 0{,}3^2 \cdot 0{,}05^3}$$

$$\eta = 0{,}064\ \mathrm{Ns/m^2}$$

$$\Delta r = \frac{0{,}03}{0{,}3} = 0{,}10\ \mathrm{mm}$$

$$\psi = \frac{0{,}10}{50} = 2\ {}^0/_{00}$$

$$f = \frac{4{,}8}{1{,}6 \cdot 0{,}3} \cdot 157 \cdot 0{,}00003 = 0{,}0471\ \mathrm{m/s}$$

$$E_{\mathrm{tot}} = 0{,}0471 \cdot 10000 = 471\ \mathrm{Nm/s} = 471\ \mathrm{W}$$

From diagram 75.2

$$\beta = 46^\circ$$

$$Q = 0{,}82 \cdot 0{,}050^2 \cdot 157 \cdot 0{,}00010$$

$$Q = 32 \cdot 10^{-6}\ \mathrm{m^3/s}$$

$$\Delta t = \frac{4{,}8}{0{,}82 \cdot 1{,}6} \cdot \frac{1}{2000 \cdot 900} \cdot \frac{10000}{0{,}050^2}$$

$$\Delta t = 8{,}1^\circ\ \mathrm{C}$$

7. The 360° Bearing with an Oil Groove at the Maximum Film Thickness, and a Vapour Region at Atmospheric Pressure

7,1. General Considerations

In their paper »The Full Journal Bearing», CAMERON-WOOD (3) treat the case of finite journal bearings without oil grooves and surrounded by oil, which is already discussed to some extent in chap. 4,1. Their boundary condition for the beginning of the oil film, which states that the pressure curve starts at maximum oil film thickness is only correct if there is an oil groove with zero pressure at the maximum oil film thickness. The condition for the end of the oil film, which states that the oil film pressure would reach zero at zero derivative is not completely correct, because the vapour pressure is not exactly zero. This, however, can be regarded as a good approximation if the maximum pressure is large in comparison with the vapour pressure, and there is air at the bearing sides.

Their load capacities are, under the conditions described above, approximately right. In this case, approximate does not mean the numerical solution method. On this account, all solutions for finite bearing width are approximate. The values for the power loss given by CAMERON-WOOD are not correct. They assume that there is a full oil film with straight line velocity distribution in the vapour region, which is impossible, because the oil film thickness is increasing, and there is no oil flow in axial direction. Here a better expression for the power loss is derived.

The connection between our symbols and those of Cameron-Wood is:

$$\varepsilon = c$$

$$\nu = \frac{1}{B}$$

$$P_0 = \Delta$$

$$\beta = \psi$$

$$Q_0 = \frac{1}{B} \cdot f(\Theta)$$

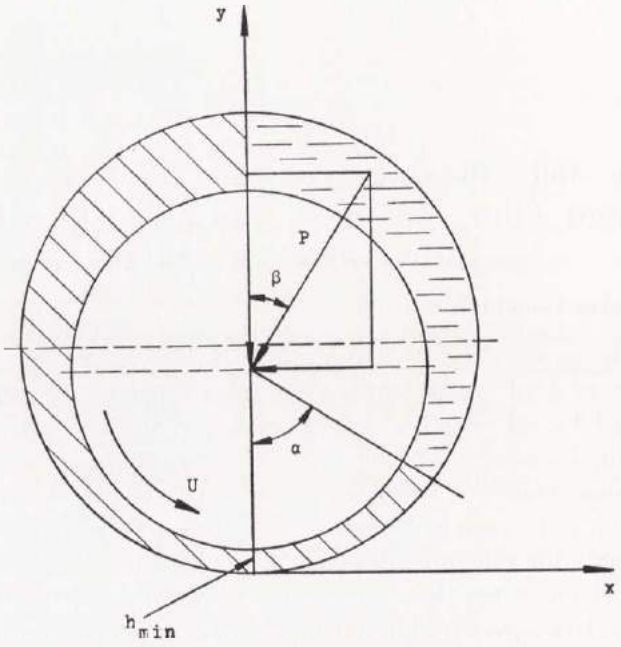

Fig. 84.1

The oil region begins at $\varphi = -\pi$ and ends at $\varphi = \alpha$, see 84.1. The expression 23.2 gives the power loss for the oil region

$$E_0' = \frac{\varepsilon}{2} \cdot P_0 \sin \beta + \frac{\gamma_2 - \gamma_1}{\sqrt{1 - \varepsilon^2}}$$

Now

$$\gamma_1 = -\pi \quad \text{and} \quad \gamma_2 = \gamma_\alpha$$

where

$$\cos \gamma_\alpha = \frac{\cos \alpha - \varepsilon}{1 - \varepsilon \cos \alpha}$$

Thus

$$E_0' = \frac{\varepsilon}{2} \cdot P_0 \sin \beta + \frac{\gamma_\alpha + \pi}{\sqrt{1 - \varepsilon^2}}$$

The expression for the power loss in the vapour region is derived from 36.2 and 37.1

$$E_0'' = H^* \cdot \frac{(\gamma_2 - \gamma_1) + \varepsilon\,(\sin\gamma_2 - \sin\gamma_1)}{\sqrt{(1-\varepsilon^2)^3}}$$

where

$$H^* = 1 - \varepsilon\cos\alpha$$

$$\gamma_1 = \gamma_\alpha$$

$$\gamma_2 = \pi$$

and thus

$$E_0'' = (1 - \varepsilon\cos\alpha)\,\frac{(\pi - \gamma_\alpha) - \varepsilon\sin\gamma_\alpha}{\sqrt{(1-\varepsilon^2)^3}}$$

The total power loss is the sum of the two above derived

$$E_0 = \frac{E\,\psi}{\eta\,U^2} = E_0' + E_0''$$

Curves of load capacity, load angle, oil flow, power loss, and relative power loss are drawn in the diagrams 86.1—88.1. The calculations are based upon the values given by CAMERON-WOOD. The coefficient of friction from CAMERON-WOOD for $r = 1$; $\varepsilon = 0{,}8$ is 1,72, and from the above equations 1,44. The difference is thus 19 %. For $r = 0{,}25$; $\varepsilon = 0{,}8$ the values are 8,90 and 7,07 respectively. This difference is 26 %.

Owing to the above discussion, the attitude-eccentricity curves drawn in fig. 3 in their paper are of limited value. From the diagram one can get values for the load angle, but the shaft centre does not follow these curves when the speed or the load is slowly varied. To get such curves at constant values of the angle between the load line and the oil groove, calculations must be made for various locations of the groove, and then the attitude-eccentricity curves can be drawn.

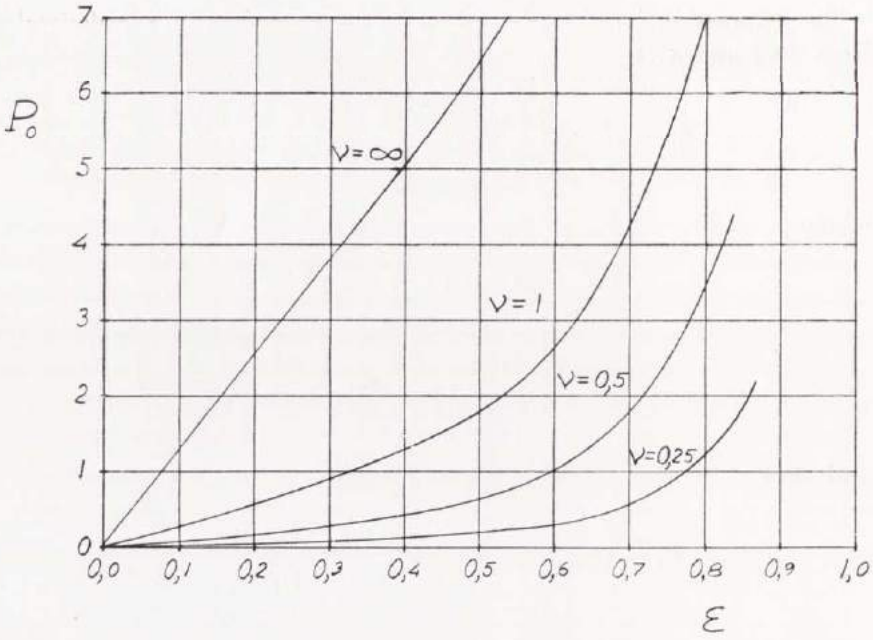

Fig. 86.1. Load Capacity $P_0 = \dfrac{P\,\psi^2}{\eta\,U}$

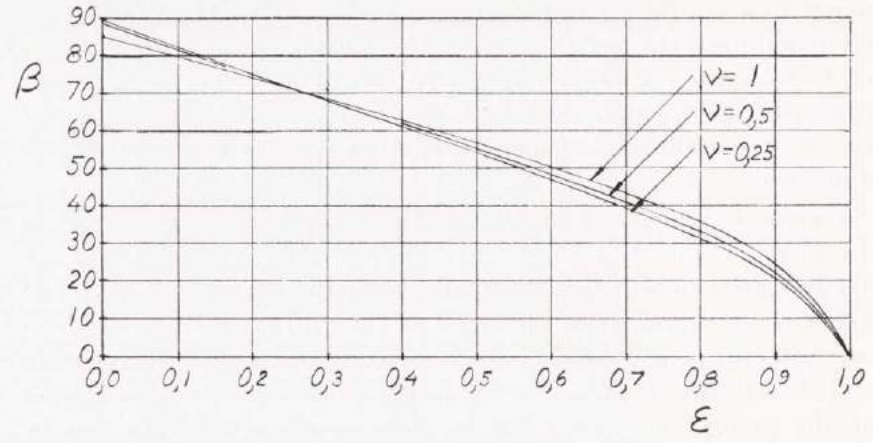

Fig. 86.2. Load Angle

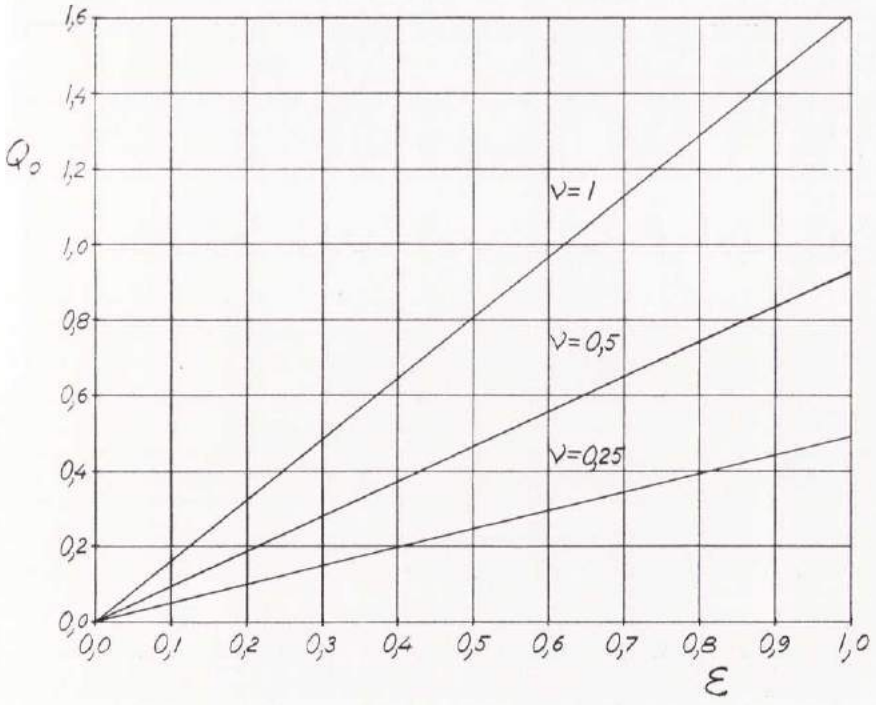

Fig. 87.1. Oil Flow $\quad Q_0 = \dfrac{Q}{r\,U\,\Delta r}$

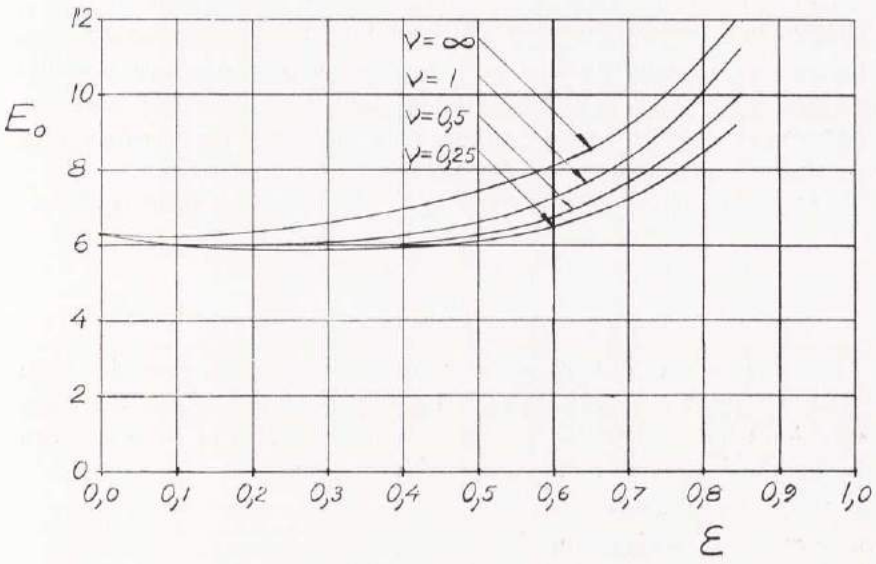

Fig. 87.2. Power Loss $\quad E_0 = \dfrac{E\,\psi}{\eta\,U^2}$

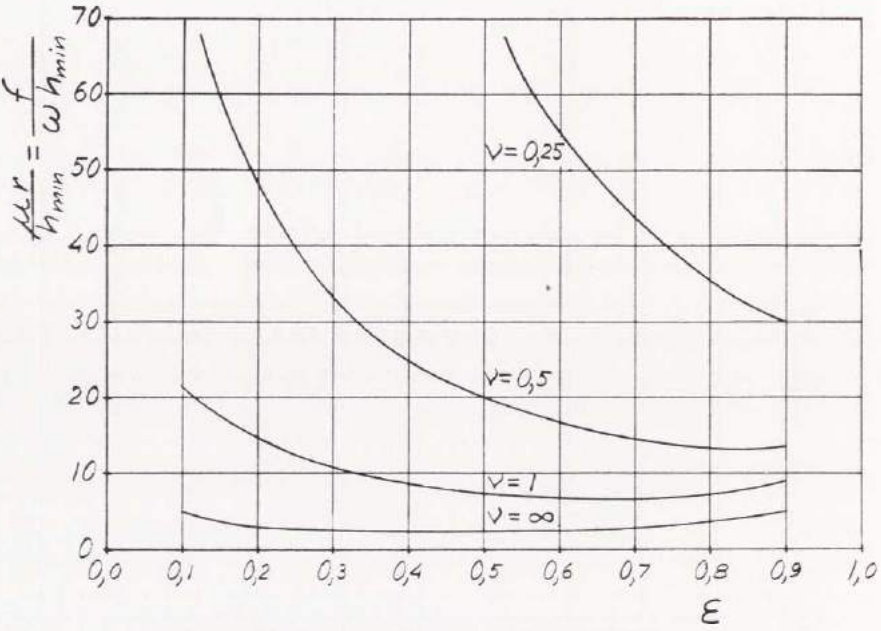

Fig. 88.1. Coefficient of Friction and Relative Power Loss

7,2. Optimum Analysis

The optimum conditions are analysed after the lines of chap. 6,7. The vapour pressure is now considered to be approximately zero. To get the optimum conditions for this zero vapour pressure, it would be necessary to vary the location of the oil groove. But with the material here presented, optimum conditions only for bearings with a groove at the maximum film thickness can be considered.

For constant values of ω and $h_{\min}$, the optimum bearing should have a minimum for the function

$$\frac{f}{\omega\, h_{\min}} = \frac{E_0}{P_0\,(1-\varepsilon)}$$

From diagram 88.1 it is clear that even in this case the ratio width-diameter ν should be as large as possible. For every ν-value we get an optimum value for the eccentricity ε. Now it remains to determine Δr, r and η. These are derived from

1. The load capacity
2. Strength considerations for the shaft
3. The minimum permissible oil film thickness

From 1 and 3 we get

$$h_{\min} = \Delta r\,(1 - \varepsilon)$$

$$P_0 = \frac{P\,\psi^2}{\eta\,U}$$

or

$$\Delta r = \frac{h_{\min}}{1 - \varepsilon}$$

$$\eta = \frac{P\,h_{\min}^2}{P_0\,\omega\,(1 - \varepsilon)^2\,r^3}$$

For the temperature rise we have

$$\Delta t = \frac{2\,r\,E_0}{Q_0} \cdot \frac{1}{c\,\varrho} \cdot \frac{\eta\,\omega}{\psi^2} = \frac{2\,r\,E_0}{Q_0\,P_0} \cdot \frac{1}{c\,\varrho} \cdot \frac{P}{r}$$

7,3. Schedule for Calculation

r is chosen as large as possible

ε is chosen so that the function $\dfrac{f}{\omega h_{\min}}$ in 88.1 is minimum

r is derived from strength considerations

$$\eta = \frac{P h_{\min}^2}{P_0\,\omega\,(1 - \varepsilon)^2\,r^3}$$

$$\Delta r = \frac{h_{\min}}{1 - \varepsilon}$$

$$\psi = \frac{\Delta r}{r}$$

$$f = \frac{E_0}{P_0\,(1 - \varepsilon)} \cdot \omega h_{\min}$$

$$E_{\text{tot}} = f P_{\text{tot}}$$

The oil groove shall be located at the angle $(180 - \beta)$ before the load line, where β is derived from 86.2.

$$Q = Q_0 \, r \, U \, \Delta r$$

$$\Delta t = \frac{2 \, r \, E_0}{Q_0 \, P_0} \cdot \frac{1}{c \, \varrho} \cdot \frac{P}{r}$$

7,4. Examples

1. Design an optimum 360° journal bearing with an oil groove at the maximum oil film thickness and vapour pressure equal to zero. Load capacity 7000 N, rotational speed 750 r/m and minimum oil film thickness 0,02 mm. The shaft shall have a diameter of 80 mm and the ratio width-diameter is 1.

From diagram 88.1 $\varepsilon = 0,6$

$$\eta = \frac{7000 \cdot 0,00002^2}{2 \cdot 0,04 \cdot 2,60 \cdot 78,5 \cdot 0,4^2 \cdot 0,04^3}$$

$$\eta = 0,0167 \text{ Ns/m}^2$$

$$\Delta r = \frac{0,02}{0,4} = 0,05 \text{ mm}$$

$$\psi = \frac{0,05}{40} = 1,25 \, {}^0/_{00}$$

$$f = \frac{7,2}{2,60 \cdot 0,4} \cdot 78,5 \cdot 0,00002 = 0,0109 \text{ m/s}$$

$$E_{\text{tot}} = 0,0109 \cdot 7000 = 76 \text{ Nm/s} = 76 \text{ W}$$

The location of the oil groove is 130° before the load line.

$$Q = 0,96 \cdot 0,040^2 \cdot 78,5 \cdot 0,00005$$

$$Q = 0,0000060 \text{ m}^3\text{/s} = 0,0060 \text{ l/s}$$

$$\Delta t = \frac{2 \cdot 7,2}{0,96 \cdot 2,60} \cdot \frac{1}{2000 \cdot 900} \cdot \frac{7000}{2 \cdot 0,040^2}$$

$$\Delta t = 7,0^\circ \text{ C}$$

2. Design an optimum 360° journal bearing with an oil groove at the maximum oil film thickness and vapour pressure equal to zero. Load capacity 3000 N, rotational speed 1500 r/m, and minimum oil film thickness 0,02 mm. Shaft diameter 50 mm, and $r = 0,5$.

$$\varepsilon = 0,8 \text{ from diagram 88.1}$$

$$\eta = \frac{3000 \cdot 0,00002^2}{0,025 \cdot 3,44 \cdot 157 \cdot 0,2^2 \cdot 0,025^3}$$

$$\eta = 0,142 \text{ Ns/m}^2$$

$$\Delta r = \frac{0,02}{0,2} = 0,10 \text{ mm}$$

$$\psi = \frac{0,10}{25} = 4 \text{ }^0/_{00}$$

$$f = \frac{9,10}{3,44 \cdot 0,2} \cdot 157 \cdot 0,00002 = 0,0415 \text{ m/s}$$

$$E_{tot} = 0,0415 \cdot 3000 = 125 \text{ Nm/s} = 125 \text{ W}$$

The location of the oil groove is 148° before the load line.

$$Q = 0,74 \cdot 0,025^2 \cdot 157 \cdot 0,00010$$

$$Q = 0,0000073 \text{ m}^3/\text{s} = 0,0073 \text{ l/s}$$

$$\Delta t = \frac{9,10}{0,74 \cdot 3,44} \cdot \frac{1}{2000 \cdot 900} \cdot \frac{3000}{0,025^2}$$

$$\Delta t = 9,5^\circ \text{ C}$$

8. The 180° Centrally Loaded Bearing with a Vapour Region at Atmospheric Pressure

8,1. General Considerations

SASSENFELD-WALTHER (9) have made a solution for the 360° journal bearing, which corresponds to that by CAMERON-WOOD (3), but the calculations cover a larger range.

They have also treated the centrally loaded 180° bearing, which will now be discussed here.

Such a bearing has sometimes a vapour region before the trailing edge. They assumed the condition

$$p_0 = 0 \qquad \text{for} \qquad \frac{\partial p_0}{\partial \varphi} = 0$$

for the beginning of the vapour region which is the same as CAMERON-WOOD's assumption. The vapour pressure is assumed to be zero, and therefore the load capacity is somewhat approximate. But SASSENFELD-WALTHER's power losses are not correct, as they assume that there is only oil in a vapour region for the 360° bearing, and that there is only air in a vapour region for the 180° bearing.

The oil film extent can be seen in 93.1

$$\varphi_1 = -(90 + \beta)$$

$$\varphi_2 = 90 - \beta$$

The connections between the symbols used here and those of SASSENFELD-WALTHER are:

$$\varepsilon = \chi$$

$$\nu = \frac{B}{D}$$

$$P_0 = 2\,S_0$$

$$\beta = \alpha$$

$$\delta = \gamma - \alpha$$

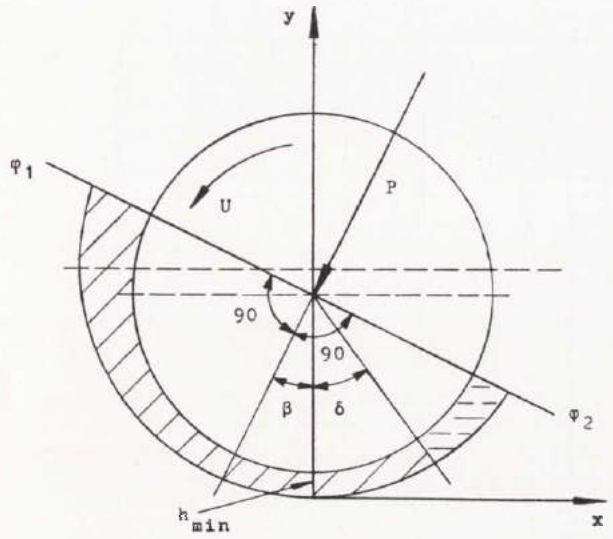

Fig. 93.1

The end of the oil region is here approximated to a straight line, which is also made by SASSENFELD-WALTHER.

The power loss for the oil region is derived from expression 23.2

$$E_0' = \frac{\varepsilon}{2} \cdot P_0 \sin \beta + \frac{(\gamma_2 - \gamma_1)}{\sqrt{1 - \varepsilon^2}}$$

where

$$\gamma_2 = \gamma_\delta$$

$$\gamma_1 = \gamma_{-(90+\beta)}$$

Thus

$$E_0' = \frac{\varepsilon}{2} \cdot P_0 \sin \beta + \frac{[\gamma_\delta + \gamma_{(90+\beta)}]}{\sqrt{1 - \varepsilon^2}} \quad \ldots\ldots\ldots \quad 93.2$$

The power loss for the vapour region is derived from 36.2 and 37.1

$$E_0'' = (1 - \varepsilon \cos \delta) \frac{[\gamma_{(90-\beta)} - \gamma_\delta] + \varepsilon [\sin \gamma_{(90-\beta)} - \sin \gamma_\delta]}{\sqrt{(1 - \varepsilon^2)^3}} \quad 93.3$$

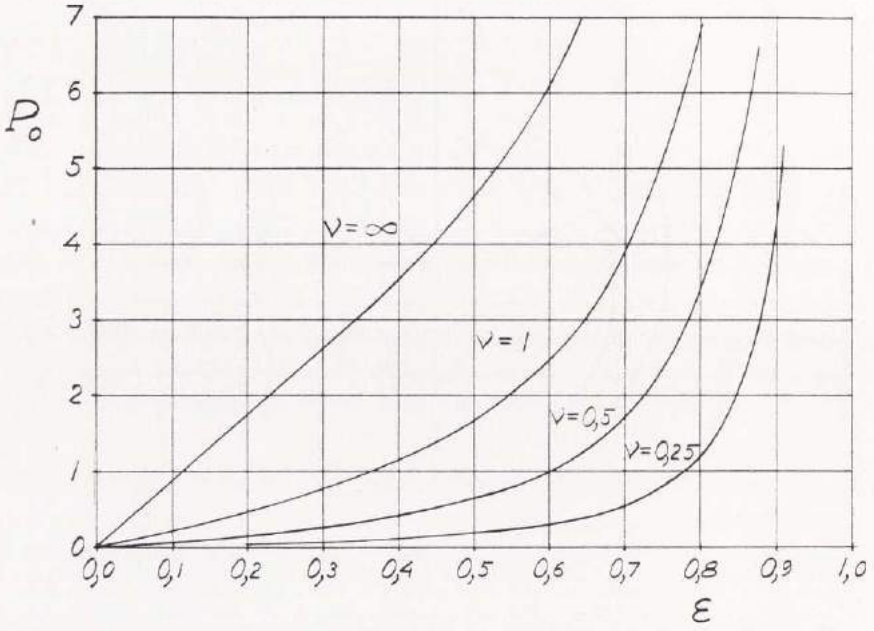

Fig. 94.1. Load Capacity $P_0 = \dfrac{P\,\psi^2}{\eta\,U}$

The total power loss

$$E_0 = E_0' + E_0''$$

The coefficient of friction from SASSENFELD-WALTHER for $\nu = 1$; $\varepsilon = 0{,}8$ is 1,11, and from the above equations 1,30. The difference is thus 15 %. For $\nu = 0{,}25$; $\varepsilon = 0{,}8$ the values are 4,7 and 6,28 respectively. The difference is here 25 %.

Curves of load capacity, power loss, and relative power loss are shown in 94.1—95.2.

8,2. Optimum Analysis

An optimum bearing is designed in the same way as in chap. 6,7 after the schedule of chap. 6,8.

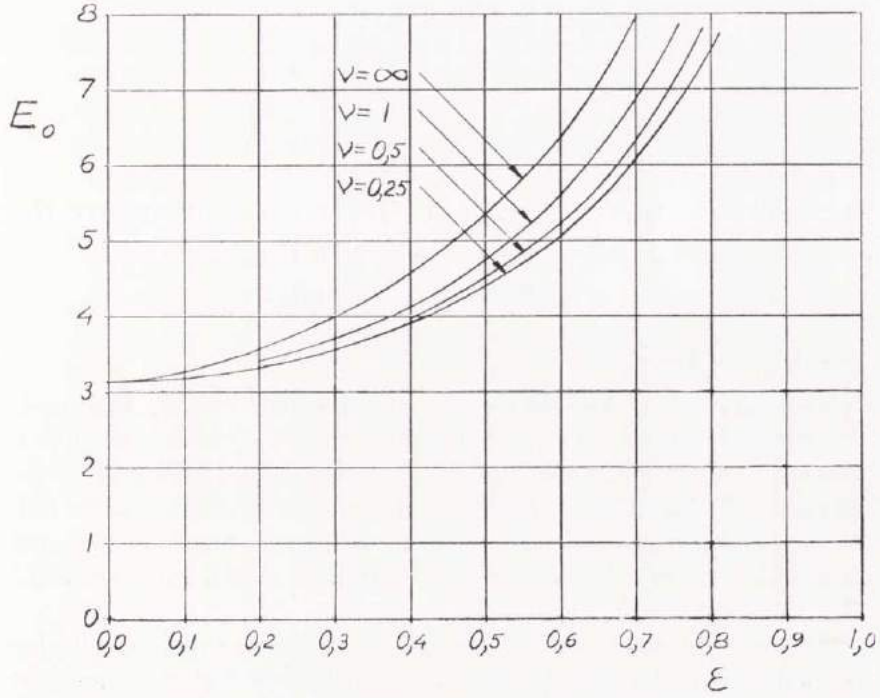

Fig. 95.1. Power Loss $E_0 = \dfrac{E\,\psi}{\eta\,U^2}$

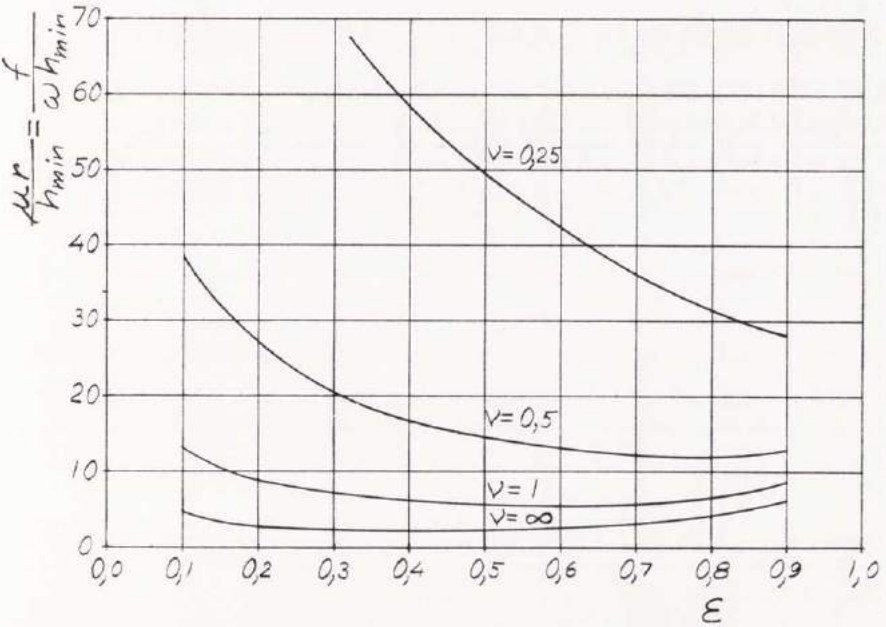

Fig. 95.2. Coefficient of Friction and Relative Power Loss

9. The 360° Bearing with an Oil Groove 90° before the Load Line, and a Vapour Region at Atmospheric Pressure

9,1. General Considerations

The calculations for the centrally loaded 180° bearing can easily be adjusted to represent a 360° bearing with an oil groove 90° before the load line if the beginning of the vapour region is located within the 180° bearing. Such a 360° bearing gets the same load as the 180° bearing, as the pressure is zero over the added angle. The power loss 93.2 for the oil region is the same, but in the expression 93.3 for the vapour region $\gamma'_{(90-\beta)}$ must be changed to $\gamma'_{(270-\beta)}$.

A 360° bearing with an oil groove 90° before the load line has a lower power loss than the bearing with a groove at the maximum film thickness, see chap. 7; but the difference is only a few per cent.

Curves of power loss and relative power loss are shown in 97.1 and 97.2.

9,2. Optimum Analysis

The optimum problem is solved as in chap. 6,7 and 6,8.

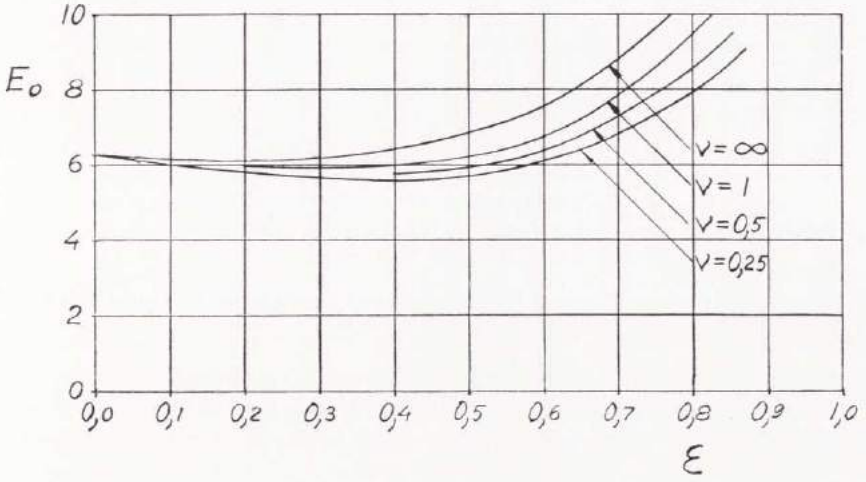

Fig. 97.1. Power Loss $E_0 = \dfrac{E\,\psi}{\eta\,U^2}$

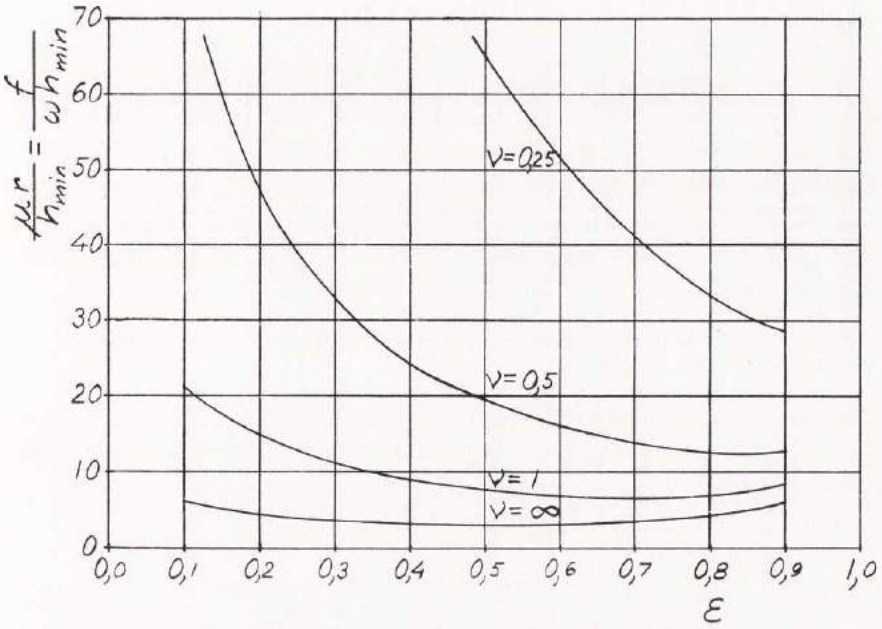

Fig. 97.2 Coefficient of Friction and Relative Power Loss

10. Superposition of Solutions

10,1. Superposition of Pressure Distributions

A bearing without vaporized oil is assumed. Consider the differential equation for the pressure in the oil film

$$\frac{\partial}{\partial x}\left(h^3\frac{\partial p}{\partial x}\right)+\frac{\partial}{\partial z}\left(h^3\frac{\partial p}{\partial z}\right)=6\,\eta\,U\frac{\partial h}{\partial x}$$

If a bearing, for instance, has an oil groove, it would be very advantageous if a pressure distribution proportional to the supply pressure could be added to the hydrodynamic solution. This is possible if we can satisfy the differential equation and the boundary conditions.

Try a solution $p = p_1 + kp_2$, which is substituted in the differential equation.

$$\frac{\partial}{\partial x}\left[h^3\frac{\partial\,(p_1+kp_2)}{\partial x}\right]+\frac{\partial}{\partial z}\left[h^3\frac{\partial\,(p_1+kp_2)}{\partial z}\right]=6\,\eta\,U\frac{\partial h}{\partial x}$$

This is transformed to

$$\frac{\partial}{\partial x}\left(h^3\frac{\partial p_1}{\partial x}\right)+\frac{\partial}{\partial z}\left(h^3\frac{\partial p_1}{\partial x}\right)+$$

$$+k\left[\frac{\partial}{\partial x}\left(h^3\frac{\partial p_2}{\partial x}\right)+\frac{\partial}{\partial z}\left(h^3\frac{\partial p_2}{\partial z}\right)\right]=6\,\eta\,U\frac{\partial h}{\partial x}$$

This equation is satisfied if the following two equations are satisfied

$$\frac{\partial}{\partial x}\left(h^3\frac{\partial p_1}{\partial x}\right)+\frac{\partial}{\partial z}\left(h^3\frac{\partial p_1}{\partial z}\right)=6\,\eta\,U\frac{\partial h}{\partial x}$$

$$\frac{\partial}{\partial x}\left(h^3\frac{\partial p_2}{\partial x}\right)+\frac{\partial}{\partial z}\left(h^3\frac{\partial p_2}{\partial z}\right)=0$$

As the equations are written, p_1 represents the hydrodynamic pressure distribution for zero supply pressure and rotational speed ω. Let kp_2 be the solution for the supply pressure k at zero rotational speed. The distribution p_2 is conveniently calculated for the supply pressure equal to 1. In the term kp_2, k is a non-dimensional scale factor.

The differential equation is satisfied by

$$p = p_1 + kp_2$$

which also fulfils the boundary conditions if p_1 and p_2 do this.

10,2. Load Capacity

The pressure distribution has the form $p = p_1 + kp_2$. Substitute this in the expressions 17.1

$$P_x b = -\int_{\zeta_1}^{\zeta_2}\int_{\varphi_1}^{\varphi_2} (p_1 + kp_2) \sin\varphi \, r\, d\varphi \, r\, d\zeta$$

$$P_y b = \int_{\zeta_1}^{\zeta_2}\int_{\varphi_2}^{\varphi_2} (p_1 + kp_2) \cos\varphi \, r\, d\varphi \, r\, d\zeta$$

Introduce the following notation

$$P_{x1} b = -\int\int p_1 \sin\varphi \, r\, d\varphi \, r\, d\zeta$$

$$P_{x2} b = -\int\int p_2 \sin\varphi \, r\, d\varphi \, r\, d\zeta$$

$$P_{y1} b = \int\int p_1 \cos\varphi \, r\, d\varphi \, r\, d\zeta$$

$$P_{y2} b = \int\int p_2 \cos\varphi \, r\, d\varphi \, r\, d\zeta$$

Thus

$$P_x = P_{x1} + kP_{x2}$$

$$P_y = P_{y1} + kP_{y2}$$

The equations 18.1 give

$$P = \sqrt{(P_{x1} + kP_{x2})^2 + (P_{y1} + kP_{y2})^2}$$

$$\tan\beta = \frac{P_{x1} + k\,P_{x2}}{P_{y1} + k\,P_{y2}}$$

In the x- and y-directions the components are algebraically summarized, and then the x- and y-components are geometrically summarized.

10,3. Oil Flow

Substitution $p = p_1 + kp_2$ in 20.1 gives

$$q_x = \frac{U\,h}{2} - \frac{h^3}{12\,\eta} \cdot \frac{\partial\,(p_1 + kp_2)}{\partial\,x}$$

$$q_z = -\frac{h^3}{12\,\eta} \cdot \frac{\partial\,(p_1 + kp_2)}{\partial\,z}$$

Introduce the notation

$$q_{x1} = \frac{U\,h}{2} - \frac{h^3}{12\,\eta} \cdot \frac{\partial\,p_1}{\partial\,x}$$

$$q_{x2} = -\frac{h^3}{12\,\eta} \cdot \frac{\partial\,p_2}{\partial\,x}$$

$$q_{z1} = -\frac{h^3}{12\,\eta} \cdot \frac{\partial\,p_1}{\partial\,z}$$

$$q_{z2} = -\frac{h^3}{12\,\eta} \cdot \frac{\partial\,p_2}{\partial\,z}$$

Then

$$q_x = q_{x1} + kq_{x2}$$

$$q_z = q_{z1} + kq_{z2}$$

For the oil flow over a given boundary we have

$$Q = \int_{s_1}^{s_2} q\,ds$$

and thus

$$Q = Q_1 + k\,Q_2$$

To determine the oil flow for two superposed pressure distributions, the flows in the two cases are to be directly summarized.

10,4. **Power Loss**

The pressure $p = p_1 + kp_2$ is substituted as above in 22.1.

$$F_j b = \int_{\zeta_1}^{\zeta_2} \int_{\varphi_1}^{\varphi_2} \left[\frac{h}{2} \cdot \frac{\partial (p_1 + kp_2)}{\partial x} + \eta \cdot \frac{U}{h} \right] r \, d\varphi \, r \, d\zeta$$

If now

$$F_{j1} b = \int_{\zeta_1}^{\zeta_2} \int_{\varphi_1}^{\varphi_2} \left[\frac{h}{2} \cdot \frac{\partial p_1}{\partial x} + \eta \cdot \frac{U}{h} \right] r \, d\varphi \, r \, d\zeta$$

$$F_{j2} b = \int_{\zeta_1}^{\zeta_2} \int_{\varphi_1}^{\varphi_2} \frac{h}{2} \cdot \frac{\partial p_2}{\partial x} \cdot r \, d\varphi \, r \, d\zeta$$

we have

$$F_j = F_{j1} + k F_{j2}$$

It is thus possible to summarize the power losses for the two superposed solutions.

11. Conclusion

This work treats journal bearings of finite width with due consideration to all boundary conditions and negative pressure vapour zones. It succeeds an earlier work by FLOBERG (6) on journal bearings of infinite width. A theory for vaporization is put forward where the conditions are strictly treated all around the periphery. The boundary conditions for the beginning and the end of a vapour region are derived from the continuity. The continuity is fulfilled in all of the bearing. It is described how to determine the power loss for a vapour region.

The problem with vaporized regions in journal bearings is hitherto very unsatisfactorily treated in literature. Usually the boundary conditions are arbitrarily chosen, which gives approximate solutions for pressure distributions and load capacities. When calculating the power loss, wrong assumptions are made for the vapour regions.

This work treats first the 360° journal bearing without vaporized oil. This case is of very little practical interest. Then solutions for finite journal bearings with vapour regions and without oil grooves are given. It is shown how these bearings operate if there is oil at the bearing sides. Tests have confirmed that this method of lubrication is practically plausible.

The solution by CAMERON-WOOD (3) with an oil groove at the maximum film thickness and zero vapour pressure is discussed, and a correction to their power loss values is made.

Calculations are made for 180° partial journal bearings with maximum film thickness at the leading edge, and minimum film thickness at the trailing edge. Such a bearing has no negative pressure, and therefore no vapour zone. Also treated are 180° centrally loaded bearings and 360° bearings with oil grooves 90° before the load line.

For the different cases, optimum conditions are discussed. The optimum is reached when for a given load, angular velocity, and minimum permissible oil film thickness the power loss is a minimum.

Diagrams show load capacity, load angle, oil flow, power loss, and relative power loss for three different width-diameter ratios as functions of the eccentricity.

Experimental investigations show a very close agreement with the vaporization theory.

12. Zusammenfassung

Diese Arbeit behandelt das Auftreten von Öldampfzonen in radialen Gleitlagern von endlicher Breite. Gleitlager von unendlicher Breite sind schon von FLOBERG (6) behandelt worden.

Die Randbedingungen für den Anfang und das Ende einer Öldampfzone werden aufgestellt. Die Kontinuität des Ölflusses liegt im ganzen Lager vor. Die Theorie ist durch Experimente bestätigt.

Keine genügende Behandlung dieser Probleme ist bisher erfolgt. Manchmal sind beliebige Bedingungen für den positiven Druckberg gewählt worden. Die Verlustleistung einer Öldampfzone ist vorher nicht korrekt berechnet worden. Entweder rechnet man mit Öl allein oder mit Luft allein in einer solchen Zone. In der Praxis aber tritt eine Mischung von beiden auf.

Die vorliegende Arbeit behandelt das 360° Gleitlager ohne achsiale Ölkanäle mit Ölzufuhr nur an den Seiten des Gleitlagers. Es wird gezeigt, wie sich ein solches Gleitlager mit Öl versieht. Das 180° partiale Gleitlager mit minimaler Filmdicke am Ende des Druckberges wird auch behandelt.

Die Arbeit »The Full Journal Bearing» von CAMERON-WOOD (3) wird diskutiert. Sie rechnen mit einer beliebig gewählten Randbedingung für den Anfang des Druckberges. Wenn das Lager mit einem Ölkanal an dieser Stelle versehen ist, ist ihre Lösung approximativ richtig. Ihre Werte für die Verlustleistung sind indessen zu gross. Sie rechnen mit einem ganzen Ölfilm in der Öldampfzone, aber dort ist eine Mischung von Öl und Luft. Korrigierte Werte für die Verlustleistung werden hier gegeben.

SASSENFELD-WAHLTER (9) haben das 180° Partiallager mit zentrischer Belastung behandelt. Sie rechnen in der Dampfzone nur mit Luft. Ihr Fall, sowie das 360° Lager mit einer Ölspalte 90° vor der Lastlinie, wird hier behandelt.

Es wird gezeigt, wie für die verschiedenen Fälle optimale Gleitlager konstruiert werden sollen. Die optimalen Verhältnisse sind erreicht, wenn bei gegebener Last, gegebener Winkelgeschwindigkeit und gegebener mindestzulässiger Ölfilmdicke, die Verlustleistung am kleinsten ist.

Für die oben beschriebenen Fälle sind Diagramme für Tragkraft, Ölfluss, Verlustleistung und relative Verlustleistung gegeben.

13. Appendix: Tables of Calculated Values

The following non-dimensional expressions are used:

$$r = \frac{b}{d}$$

$$\varepsilon = \frac{e}{\Delta r}$$

$$p_{v0} = \frac{p_v \psi^2}{\eta \omega}$$

$$P_0 = \frac{P \psi^2}{\eta U}$$

$$Q_0 = \frac{Q}{r U \Delta r}$$

$$E_0 = \frac{E \psi}{\eta U^2}$$

$$\Delta t_0 = c \varrho \cdot \frac{\Delta t \psi^2}{\eta \omega}$$

$$\frac{\mu}{\psi} = \frac{f}{\omega \Delta r} = \frac{E_0}{P_0}$$

$$\frac{\mu r}{h_{\min}} = \frac{f}{\omega h_{\min}} = \frac{E_0}{P_0 (1 - \varepsilon)}$$

360° Bearings with No Oil Grooves and without Vapour Regions (chap. 5,1)

$\nu = 1{,}0$

ε	0,0	0,2	0,4	0,6	0,8	1,0
P_0	0	0,934	2,07	3,87	8,11	∞
β	90	90	90	90	90	90
Q_0	0	0,299	0,601	0,899	1,20	—
E_0	6,28	6,51	7,27	9,12	13,8	∞
Δt_0	∞	43,5	24,2	20,3	27,0	∞
$\frac{f}{\omega \Delta r}$	∞	6,96	3,51	2,35	1,70	1
$\frac{f}{\omega h_{\min}}$	∞	8,70	5,84	5,88	8,50	∞

$\nu = 0{,}5$

ε	0,0	0,2	0,4	0,6	0,8	1,0
P_0	0	0,301	0,704	1,47	3,77	∞
β	90	90	90	90	90	90
Q_0	0	0,184	0,369	0,554	0,745	—
E_0	6,28	6,44	7,00	8,29	11,9	∞
Δt_0	∞	35,1	19,0	15,0	16,0	∞
$\frac{f}{\omega \Delta r}$	∞	21,4	9,93	5,66	3,17	1
$\frac{f}{\omega h_{\min}}$	∞	26,7	16,6	14,2	15,7	∞

$\nu = 0{,}25$

ε	0,0	0,2	0,4	0,6	0,8	1,0
P_0	0	0,0811	0,196	0,435	1,25	∞
β	90	90	90	90	90	90
Q_0	0	0,0980	0,196	0,296	0,392	—
E_0	6,28	6,42	6,90	7,98	11,0	∞
Δt_0	∞	32,8	17,6	13,5	14,0	∞
$\frac{f}{\omega\, \Delta r}$	∞	79,1	35,2	18,4	8,78	∞
$\frac{f}{\omega h_{\min}}$	∞	98,8	58,6	45,0	43,9	∞

360° Bearings with No Oil Grooves and with Vapour Regions at $p_{v0} = -1$ (chap. 5,2)

$\nu = 1{,}0$

ε	0,0	0,2	0,4	0,6	0,8	1,0
P_0	0	0,934	2,07	3,52	7,76	∞
β	90	90	90	71,4	46,6	0
Q_0	0	0,299	0,601	0,870	1,18	—
E_0	6,28	6,51	7,27	8,55	11,7	∞
Δt_0	∞	43,5	24,2	19,7	19,8	∞
$\frac{f}{\omega\, \Delta r}$	∞	6,96	3,51	2,43	1,51	0
$\frac{f}{\omega h_{\min}}$	∞	8,70	5,84	6,07	7,54	∞

$\nu = 0{,}5$

ε	0,0	0,2	0,4	0,6	0,8	1,0
P_0	0	0,301	0,704	1,43	3,61	∞
β	90	90	90	86,9	51,0	0
Q_0	0	0,184	0,369	0,535	0,726	—
E_0	6,28	6,44	7,00	8,27	10,8	∞
Δt_0	∞	35,1	19,0	14,9	14,9	∞
$\frac{f}{\omega \Delta r}$	∞	21,4	9,93	5,79	3,01	0
$\frac{f}{\omega h_{\min}}$	∞	26,7	16,6	14,5	15,0	∞

$\nu = 0{,}25$

ε	0,0	0,2	0,4	0,6	0,8	1,0
P_0	0	0,0811	0,196	0,435	1,25	∞
β	90	90	90	90	71,4	0
Q_0	0	0,0980	0,196	0,296	0,392	—
E_0	6,28	6,45	7,01	8,37	10,8	∞
Δt_0	∞	32,9	17,9	14,1	13,7	∞
$\frac{f}{\omega \Delta r}$	∞	79,4	35,8	19,2	8,61	0
$\frac{f}{\omega h_{\min}}$	∞	99,2	59,6	48,1	43,1	∞

360° Bearings with No Oil Grooves and with Vapour Regions at $p_{v0} = -0{,}1$(chap. 5,2)

$\nu = 1{,}0$

ε	0,0	0,2	0,4	0,6	0,8	1,0
P_0	0	0,549	0,960	2,26	6,77	∞
β	90	62,9	47,0	39,8	30,9	0
Q_0	0	0,212	0,323	0,459	0,595	—
E_0	6,28	6,22	6,21	6,94	9,61	∞
Δt_0	∞	57,7	38,5	30,3	32,3	∞
$\frac{f}{\omega \Delta r}$	∞	11,3	6,47	3,08	1,42	0
$\frac{f}{\omega h_{\min}}$	∞	14,2	10,8	7,70	7,10	∞

$\nu = 0{,}5$

ε	0,0	0,2	0,4	0,6	0,8	1,0
P_0	0	0,272	0,547	1,13	3,62	∞
β	90	87,1	68,4	51,3	34,2	0
Q_0	0	0,183	0,343	0,502	0,637	—
E_0	6,28	6,44	6,73	7,38	9,89	∞
Δt_0	∞	35,1	19,7	14,7	15,5	∞
$\frac{f}{\omega \Delta r}$	∞	23,7	12,3	6,50	2,73	0
$\frac{f}{\omega h_{\min}}$	∞	29,6	20,5	16,1	13,7	∞

$\nu = 0{,}25$

ε	0,0	0,2	0,4	0,6	0,8	1,0
P_0	0	0,0811	0,189	0,362	1,27	∞
β	90	90	90	66,6	37,0	0
Q_0	0	0,0980	0,196	0,294	0,381	—
E_0	6,28	6,45	7,01	7,61	9,85	∞
Δt_0	∞	32,9	17,9	12,9	12,9	∞
$\frac{f}{\omega\, \Delta r}$	∞	79,4	37,2	21,0	7,75	0
$\frac{f}{\omega h_{\min}}$	∞	99,2	62,0	52,5	38,7	∞

180° Bearings with Minimum Film Thickness at the Trailing Edge (chap. 6)

$\nu = \infty$

ε	0,0	0,2	0,4	0,6	0,8	1,0
P_0	0	1,90	3,95	6,64	12,5	∞
β	90	82,6	74,5	64,5	49,7	0
E_0	3,14	3,39	4,19	5,72	9,04	∞
$\frac{f}{\omega\, \Delta r}$	∞	1,79	1,06	0,862	0,724	0
$\frac{f}{\omega h_{\min}}$	∞	2,23	1,77	2,15	3,62	∞

$\nu = 1$

ε	0,0	0,2	0,4	0,6	0,8	1,0
P_0	0	0,474	1,13	2,30	5,94	∞
β	90	80,2	68,8	57,2	43,1	0
Q_0	1,00	1,14	1,27	1,39	1,50	—
E_0	3,14	3,25	3,64	4,56	6,89	∞
Δt_0	6,28	5,69	5,72	6,54	9,22	∞
$\frac{f}{\omega \Delta r}$	∞	6,86	3,21	1,98	1,16	0
$\frac{f}{\omega h_{\min}}$	∞	8,57	5,35	4,95	5,80	∞

$\nu = 0{,}5$

ε	0,0	0,2	0,4	0,6	0,8	1,0
P_0	0	0,153	0,387	0,925	3,00	∞
β	90	77,7	65,4	52,4	39,0	0
Q_0	0,500	0,591	0,683	0,774	0,865	—
E_0	3,14	3,22	3,50	4,15	5,97	∞
Δt_0	6,28	5,45	5,13	5,36	6,90	∞
$\frac{f}{\omega \Delta r}$	∞	21,1	9,03	4,48	1,99	0
$\frac{f}{\omega h_{\min}}$	∞	26,3	15,1	11,2	9,96	∞

$r = 0{,}25$

ε	0,0	0,2	0,4	0,6	0,8	1,0
P_0	0	0,0417	0,110	0,284	1,04	∞
β	90	76,8	62,8	50,0	37,0	0
Q_0	0,250	0,299	0,348	0,397	0,447	—
E_0	3,14	3,21	3,45	3,99	5,48	∞
Δt_0	6,28	5,37	4,95	5,03	6,14	∞
$\frac{f}{\omega\, \Delta r}$	∞	77,1	31,3	14,0	5,28	0
$\frac{f}{\omega h_{\min}}$	∞	96,3	52,1	35,1	26,4	∞

360° Bearings with Oil Grooves at Maximum Film Thickness and Vapour Regions at $p_{v0} = 0$ (chap. 7)

$r = \infty$

ε	0,0	0,2130	0,3204	0,4289	0,5383	0,6479	0,8660	1,0
P_0	0	2,73	4,02	5,44	7,09	9,26	21,4	∞
β	71,0	60,3	52,3	44,4	37,1	29,9	15,7	0
E_0	6,28	6,37	6,65	7,07	7,68	8,52	12,7	∞
$\frac{f}{\omega\, \Delta r}$	∞	2,33	1,66	1,30	1,08	0,920	0,593	0
$\frac{f}{\omega h_{\min}}$	∞	2,96	2,44	2,28	2,34	2,61	4,42	∞

$\nu = 1{,}0$

ε	0,0	0,2	0,5	0,8	1,0
P_0	0	0,507	1,78	7,05	∞
β	85	74,5	56,5	36	0
Q_0	0	0,32	0,79	1,30	—
E_0	6,28	6,01	6,60	10,1	∞
Δt_0	∞	37,6	16,7	15,6	∞
$\frac{f}{\omega \Delta r}$	∞	11,9	3,72	1,44	0
$\frac{f}{\omega h_{\min}}$	∞	14,8	7,44	7,18	∞

$\nu = 0{,}5$

ε	0,0	0,2	0,4	0,6	0,8	1,0
P_0	0	0,156	0,405	0,997	3,44	∞
β	88,5	75	62	48	33	0
Q_0	0	0,185	0,375	0,560	0,740	—
E_0	6,28	5,96	6,01	6,71	9,10	∞
Δt_0	∞	32,2	16,0	12,0	12,3	∞
$\frac{f}{\omega \Delta r}$	∞	38,2	14,8	6,73	2,65	0
$\frac{f}{\omega h_{\min}}$	∞	47,8	24,7	16,8	13,2	∞

$r = 0{,}25$

ε	0,0	0,2	0,4	0,6	0,8	1,0
P_0	0	0,0419	0,112	0,295	1,20	∞
β	89,5	75	61	47	31	0
Q_0	0	0,100	0,198	0,295	0,393	—
E_0	6,28	5,89	5,92	6,49	8,49	∞
Δt_0	∞	29,5	14,9	11,0	10,8	∞
$\frac{f}{\omega \Delta r}$	∞	141	52,8	22,0	7,07	0
$\frac{f}{\omega h_{\min}}$	∞	176	88,0	55,0	35,4	∞

180° Centrally Loaded Bearings with Vapour Regions at $p_{v0} = 0$ (chap. 8)

$r = \infty$

ε	0,0	0,2	0,4	0,6	0,8	1,0
P_0	0	1,76	3,54	6,09	12,6	∞
β	90	61	50	43	33	0
E_0	3,14	3,56	4,57	6,38	10,3	∞
$\frac{f}{\omega \Delta r}$	∞	2,02	1,29	1,05	0,816	0
$\frac{f}{\omega h_{\min}}$	∞	2,53	2,15	2,63	4,08	∞

$\nu = 1$

ε	0,0	0,2	0,4	0,6	0,8	1,0
P_0	0	0,480	1,14	2,47	6,89	∞
β	90	68	56	45	32	0
E_0	3,14	3,41	4,14	5,60	8,99	∞
$\frac{f}{\omega\, \Delta r}$	∞	7,10	3,63	2,27	1,30	0
$\frac{f}{\omega h_{\min}}$	∞	8,88	6,05	5,68	6,50	∞

$\nu = 0{,}5$

ε	0,0	0,2	0,4	0,6	0,8	1,0
P_0	0	0,155	0,400	0,989	3,42	∞
β	90	71	58	45	31	0
E_0	3,14	3,36	3,98	5,23	8,10	∞
$\frac{f}{\omega\, \Delta r}$	∞	21,7	9,95	5,29	2,37	0
$\frac{f}{\omega h_{\min}}$	∞	27,1	16,6	13,2	11,9	∞

$\nu = 0{,}25$

ε	0,0	0,2	0,4	0,6	0,8	1,0
P_0	0	0,0420	0,112	0,298	1,20	∞
β	90	74	59	45	31	0
E_0	3,14	3,32	3,91	5,06	7,53	∞
$\frac{f}{\omega\, \Delta r}$	∞	79,1	34,9	17,0	6,28	0
$\frac{f}{\omega h_{\min}}$	∞	98,9	58,2	42,4	31,4	∞

360° Bearings with Oil Grooves 90° before the Load and Vapour Regions at $p_{v0} = 0$ (chap. 9)

$r = \infty$

ε	0,0	0,4	0,6	0,8	1,0
P_0	0	3,54	6,09	12,6	∞
β	71	50	43	33	0
E_0	6,28	6,41	7,55	10,6	∞
$\frac{f}{\omega \Delta r}$	∞	1,81	1,24	0,844	0
$\frac{f}{\omega h_{\min}}$	∞	3,02	3,10	4,22	∞

$r = 1$

ε	0,0	0,4	0,6	0,8	1,0
P_0	0	1,14	2,47	6,89	∞
β	85	56	45	32	0
E_0	6,28	5,97	6,78	9,50	∞
$\frac{f}{\omega \Delta r}$	∞	5,23	2,74	1,38	0
$\frac{f}{\omega h_{\min}}$	∞	8,72	6,86	6,89	∞

$\nu = 0{,}5$

ε	0,0	0,2	0,4	0,6	0,8	1,0
P_0	0	0,155	0,400	0,989	3,42	∞
β	89	71	58	45	31	0
E_0	6,28	5,83	5,79	6,34	8,57	∞
$\frac{f}{\omega \Delta r}$	∞	37,6	14,5	6,41	2,51	0
$\frac{f}{\omega h_{\min}}$	∞	47,0	24,1	16,0	12,5	∞

$\nu = 0{,}25$

ε	0,0	0,2	0,4	0,6	0,8	1,0
P_0	0	0,0420	0,112	0,298	1,20	∞
β	90	74	59	45	31	0
E_0	6,28	5,81	5,58	6,13	7,97	∞
$\frac{f}{\omega \Delta r}$	∞	138	49,8	20,6	6,64	0
$\frac{f}{\omega h_{\min}}$	∞	173	83,0	51,4	33,2	∞

14. References

1. Bickley, W. G.: Formulae for Numerical Integration. Math. Gazette, XXIII, pp. 352—359, Oct. 1939.
2. Bickley, W. G.: Formulae for Numerical Differentiation. Math. Gazette, XXV, pp. 19—27, Febr. 1941.
3. Cameron, A. and Wood, W. L.: The Full Journal Bearing. Proc. Instn Mech. Engrs, vol. 161, p. 59, 1949.
4. Christopherson, D. G.: A New Mathematical Method for the Solution of Film Lubrication Problems. Proc. Instn Mech. Engrs, Lond., vol. 146, p. 126, 1941.
5. Cole, J. A. and Hughes, C. J.: Oil Flow and Film Extent in Complete Journal Bearings. The Engineer, March 16, 1956.
6. Floberg, L.: The Infinite Journal Bearing, Considering Vaporization. Gothenburg 1957.
7. Michell, A. G. M.: Lubrication. London 1950.
8. Reynolds, O.: On the Theory of Lubrication . . . Phil. Trans. Roy. Soc., vol. 177, p. 157, 1886.
9. Sassenfeld, H. and Walther, A.: Gleitlagerberechnungen. VDI-Forschungsheft 441, 1954.
10. Sommerfeld, A.: Zur hydrodynamischen Theorie der Schmiermittelreibung. Z. Math. Phys., vol. 50, p. 97, 1904.
11. Tower, B.: First Report on Friction Experiments. Proc. Instn Mech. Engrs, vol. 34, p. 632, 1883.
12. Tower, B.: Second Report on Friction Experiments. Proc. Instn Mech. Engrs, vol. 36, p. 58, 1885.
13. Vogelpohl, G.: Beiträge zur Kenntnis der Gleitlagerreibung. VDI-Forschungsheft 386, 1937.

Forts. fr. omsl. 2:dra sida.

128. LAVEMARK, SVEN, *The treatment of the load in electric power-system. Stability studies.* 53 s. 1952. Kr. 9: —. (Avd. Elektroteknik. 29.)
129. LINDBLAD, BERTIL-ANDERS, *A radar investigation of the delta aquarid meteor shower of 1950.* 27 s. 1952. Kr. 5: —. (Avd. Elektroteknik. 30.)
130. HELLGREN, GÖSTA, *The propagation of electromagnetic waves along a conical helix with variable pitch.* 13 s. 1953. Kr. 3: —. (Avd. Elektroteknik. 31.)
131. RYDBECK, O. E. H., *On the excitation of different space charge wave modes in travelling wave tubes.* 15 s. 1953. Kr. 5: —. (Avd. Elektroteknik. 32.)
132. WALLMAN, HENRY, *A wideband searching automatic frequency control circuit of new type.* 21 s. 1953. Kr. 5: —. (Avd. Elektroteknik. 33.)
133. SANDFORD, FOLKE, und FRANSSON, STIG, *Über die Entmischung von grobzerkleinertem Quarz.* 24 s. 1953. Kr. 5: —. (Institutionen för Silikatkemisk Forskning. 31.)
134. EKELÖF, STIG, *The magnetic circuit of telephone relays.* 32 s. 1953. Kr. 5: —. (Avd. Elektroteknik. 34.)
135. YHLAND, C.-H., *Application of the similarity theory on radiation in furnaces.* 31 s. 1953. Kr. 5: —. (Avd. Maskinteknik. 7.)
136. SJÖSTRÖM, EERO, *Über die Verwendung von Ionenaustauschern für die Sorption und Trennung von Ketonen.* 50 s. 1953. Kr. 8:—. (Avd. Kemi och Kemisk Teknologi. 27.)
137. HELLERSTEDT, LARS-MAGNUS, *Wideband amplifiers for bandwidths up to 200 MHz.* 36 s. 1954. Kr. 7: —. (Avd. Elektroteknik. 35.)
138. RYDBECK, O. E. H., and AGDUR, B., *The propagation of electronic space charge waves in periodic structures.* 20 s. 1954. Kr. 5: —. (Avd. Elektroteknik. 36.)
139. AGDUR, N. BERTIL, *Experimental investigation of noise reduction in traveling wave tubes.* 12 s. 1954. Kr. 3: —. (Avd. Elektroteknik. 37.)
140. AGDUR, N. BERTIL, *Amplification measurements on a velocity step tube.* 10 s. 1954. Kr. 2: 50. (Avd. Elektroteknik. 38.)
141. EKELÖF, STIG, *Theory of electromagnetically delayed telephone relays.* 88 s. 1954. Kr. 13: —. (Avd. Elektroteknik. 39.)
142. EKELÖF, S., and KIHLBERG, G., *Theory of the thermistor as an electric circuit element.* 36 s. 1954. Kr. 6: 50. (Avd. Elektroteknik. 40.)
143. SMITH, BENGT, *Peat-gasoline.* 38 s. 1954. Kr. 6: 50. (Avd. Kemi och Kemisk Teknologi. 28.)
144. LEDEN, N., and SCHÖÖN, N.-H., *The solubility of silver azide and the formation of complexes between silver and azide ions.* 17 s. 1954. Kr. 4: —. (Avd. Kemi och Kemisk Teknologi. 29.)
145. *Basorganisation för forskning vid de tekniska högskolorna.* 154 s. + 6 tabellbilagor. 1954. Kr. 12: —. (Not for exchange.)
146. TROEDSSON, CARL BIRGER, *Transportation and city-building.* 30 s. 1954. Kr. 6: —. (Avd. Arkitektur 2.)
147. SANDFORD, FOLKE, and FRANSSON, STIG, *The refractoriness of some types of quartz and quartzite. I.* 28 s. 1954. Kr. 6: —. (Avd. Kemi och Kemisk Teknologi. 30.)
148. CARLSSON, ORVAR, *Porstorlek och frostbeständighet hos tegelmaterial.* 64 s. 1954. Kr. 9: —. (Avd. Kemi och Kemisk Teknologi. 31.)
149. RYDBECK, O. E. H., and WILHELMSSON, H., *A theoretical investigation of the ionospheric electron density variation during a total solar eclipse.* 22 s. 1954. Kr. 3: 50. (Avd. Elektroteknik. 41.)
150. SMITH, BENGT, *Quantitative analysis of mixtures of hydrogen sulfide and sulfur dioxide.* 19 s. 1954. Kr. 4: —. (Avd. Kemi och Kemisk Teknologi. 32.)
151. HEDVALL, J. A., *Reactions with activated solids.* 23 s. 1954. Kr. 5: —. (Institutionen för Silikatkemisk Forskning. 32.)
152. SMITH, CYRIL STANLEY, *The microstructure of polycrystalline materials.* 49 s. 1954. Kr. 9: 50. (Institutionen för Silikatkemisk Forskning. 33.)
153. SELBERG, ARNE, *Norske erfaringer fra bygging av små hengebroer.* 20 s. 1954. Kr. 4: —. (Avd. Väg- och Vattenbyggnad. Byggnadsteknik. 21.)
154. GRANHOLM, HJALMAR, *Armerat trä.* 96 s. 1954. Kr. 9: —. (Avd. Väg- och Vattenbyggnad. Byggnadsteknik. 22.)
155. WILHELMSSON, HANS, *The interaction between an obliquely incident plane electromagnetic wave and an electron beam. I.* 31 s. 1954. Kr. 7: —. (Avd. Elektroteknik. 42.)
156. OLVING, SVEN, *Electromagnetic wave propagation on helical conductors inbedded in dielectric medium.* 14 sid. 1955. Kr. 3: —. (Avd. Elektroteknik. 43.)
157. OLVING, SVEN, *Amplification of the traveling wave tube at high beam current. I.* 11 s. 1955. Kr. 3: —. (Avd. Elektroteknik. 44.)
158. HEDVALL, J. A., NORDENGREN, SVEN, und LILJEGREN, B., *Über die thermische Zersetzung von Kalziumsulfat bei niedrigen Temperaturen.* 18 s. 1955. Kr. 5: —. (Institutionen för Silikatkemisk Forskning. 34.)
159. DAHLGREN, SVEN-ERIC, *On the break-down of thixotropic materials.* 18 s. 1955. Kr. 3: 50. (Institutionen för Silikatkemisk Forskning. 35.)

Forts. å omsl. 4:de sida.

Forts. fr. omsl. 3:dje sida.

160. SANDFORD, FOLKE, och LILJEGREN, BERNE, *Torkningen av råtegel och dennas inverkan på teglets frostbeständighet.* 22 s. 1955. Kr. 3: —. (Institutionen för Silikatkemisk Forskning. 36.)
161. WALLMAN, HENRY, *Automatic noise-factor meter.* 17 s. 1955. Kr. 3: —. (Avd. Elektroteknik. 45.)
162. SANDFORD, FOLKE and FRANSSON, STIG, *The refractoriness of some types of quartz and quartsite.* 24 s. 1955. Kr. 5: —. (Institutionen för Silikatkemisk Forskning. 37.)
163. LINDBLAD, ANDERS, *Konstruktion av linjer för moderna handelsfartyg.* 176 s. 1955. Kr. 20:—. (Avd. Skeppsbyggeri. 6.)
164. SVARTHOLM, NILS, *Two problems in the theory of the slowing down of neutrons by collisions with atomic nuclei.* 15 s. 1955. Kr. 5:—. (Avd. Allmänna Vetenskaper. 10.)
165. PERSSON, PER, *Bostadsvaneundersökning utförd i hyreslägenheter byggda 1947 i Göteborg, Torpaområdet.* 86 s. 1955. Kr. 12: —. (Avd. Arkitektur. 3.)
166. HANSSON, P. R., *Undersökning av mullitbildning i keramiska produkter.* 29 s. 1955. Kr. 6: —. (Institutionen för Silikatkemisk Forskning. 38.)
167. EKELÖF, STIG, *Die Temperaturverteilung in einem gleichstromdurchflossenen langen Metallzylinder mit kreisförmigem Querschnitt.* 38 s. 1955. Kr. 10: —. (Avd. Elektroteknik. 46.)
168. WILHELMSSON, HANS, *On the reflection of electromagnetic waves from a dielectric cylinder.* 17 s. 1955. Kr. 4:50. (Avd. Elektroteknik. 47.)
169. BJÖRK, N., and DAVIDSON, R., *Small signal behaviour of directly heated thermistors.* 43 s. 1955. Kr. 11: —. (Avd. Elektroteknik. 48.)
170. FORESTIER, H., *Tendances actuelles dans la formation de l'ingenieur chimiste: selection, orientation, specialisation; amelioration de son efficience.* 13 s. 1956. Kr. 2: 50. (Avd. Kemi och Kemisk Teknologi. 33.)
171. WAX, NELSON, *On the ring current hypothesis.* 32 s. 1956. Kr. 7: —. (Avd. Elektroteknik. 49.)
172. ELGESKOG, ERIK, *Photoformer analysis and design.* 40 s. 1956. Kr. 8: 50. (Avd. Elektroteknik. 50.)
173. ANZELIUS, ADOLF, *Bimolekulare Reaktion von zwei in Mischung vorliegenden Substanzen mit einer dritten Substanz.* 8 s. 1956. Kr. 5: —. (Avd. Allm. vetenskaper. 11.)
174. REINIUS, ERLING, *Model studies for the extension of the harbour of Gothenburg.* 38 s. 1956. Kr. 6: —. (Avd. Väg- och Vattenbyggnad. Byggnadsteknik. 23.)
175. ZIMEN, K. E., *Diffusion von Edelgasatomen die durch Kernreaktion in festen Stoffen gebildet werden.* 7 s. 1956. Kr. 2: —. (Institutionen för Kärnkemi. 1.)
176. INTHOFF, W., und ZIMEN, K. E., *Kinetik der Diffusion radioaktiver Edelgase aus festen Stoffen nach Bestrahlung.* 16 s. 1956. Kr. 4: —. (Institutionen för Kärnkemi. 2.)
177. GRANHOLM, HJALMAR, *Puts och lättbetong.* 45 s. 1956. Kr. 3: —. (Avd. Väg- och Vattenbyggnad. Byggnadsteknik. 24.)
178. OLVING, SVEN, *A new method for space charge wave interaction studies. I.* 12 s. 1956. Kr. 3: —. (Avd. Elektroteknik. 51.)
179. HANSBO, SVEN, *The critical load of rectangular frames analysed by convergence methods.* 47 s. 1956. Kr. 11: —. (Avd. Väg- och Vattenbyggnad. Byggnadsteknik. 25.)
180. WESTBERG, VIDOR, *Measurements of noise radiation at 10 cm from glow lamps. Preliminary report.* 14 s. 1956. Kr. 4: 50. (Avd. Elektroteknik. 52.)
181. SVENSSON, S. I., HELLGREN, G. and PERERS, O., *The Swedish radioscientific solar eclipse expedition to Italy, 1952. Preliminary report.* 30 s. 1956. Kr. 8: —. (Avd. Elektroteknik. 53.)
182. WAX, NELSON, *A note on design considerations for a proposed auroral radar.* 16 s. 1957. Kr. 3: —. (Avd. Elektroteknik. 54.)
183. JOSHI, G. H., *The electromagnetic interaction between two crossing electron streams. Part I.* 31 s. 1957. Kr. 8: —. (Avd. Elektroteknik. 55.)
184. SMITH, BENGT, *Dry methods for removing hydrogen sulphide from gases.* 65 s. 1957. Kr. 15: —. (Avd. Kemi och Kemisk Teknologi. 34.)
185. EKELÖF, S., BJÖRK, N. and DAVIDSON, R., *Large signal behaviour of directly heated thermistors.* 31 s. 1957. Kr. 8: —. (Avd. Elektroteknik. 56).
186. CARLSSON, BENGT und LARSSON, HANS, *Wirkungsgrad und Selbsthemmung einfacher Umlaufgetriebe.* 48 s. 1957. Kr. 9: —. (Avd. Maskinteknik. 8.)
187. AURELL, CARL G., *The equivalent transmission line of a linear four-terminal network. Calculations with cascade-connected four-terminal networks.* 39 s. 1957. Kr. 6: —. (Avd. Elektroteknik. 57.)
188. LUNDHOLM, R., *Induced overvoltage-surges on transmission lines and their bearing on the lightning performance at medium voltage networks.* 117 s. 1957. Kr. 19: —. (Avd. Elektroteknik. 58.)
189. FLOBERG, LEIF, *The infinite journal bearing, considering vaporization.* 83 s. 1957. Kr. 13: —. (Avd. Maskinteknik. 9.)

Pris kronor 19:50

ELANDERS BOKTRYCKERI AKTIEBOLAG
GÖTEBORG 1957

CHALMERS TEKNISKA HÖGSKOLAS HANDLINGAR

TRANSACTIONS OF CHALMERS UNIVERSITY OF TECHNOLOGY GOTHENBURG, SWEDEN

Nr 215 (Avd. Maskinteknik 15.) 1959

EXPERIMENTAL INVESTIGATION OF POWER LOSS IN JOURNAL BEARINGS, CONSIDERING CAVITATION

BY

LEIF FLOBERG

REPORT NO. 8 FROM THE INSTITUTE OF MACHINE ELEMENTS
CHALMERS UNIVERSITY OF TECHNOLOGY
GOTHENBURG, SWEDEN
1959

GUMPERTS FÖRLAG
GÖTEBORG

Av Chalmers Tekniska Högskolas Handlingar hava tidigare utkommit:

Fullständig förteckning över Chalmers Tekniska Högskolas Handlingar lämnas av Chalmers Tekniska Högskolas Bibliotek, Göteborg.

126. Hedvall, J. A., and Liljegren, B., *An investigation of the reaction* $2\ CaCO_3 + SiO_2$ *at high temperatures.* 12 s. 1952. Kr. 2: 50. (Institutionen för Silikatkemisk Forskning. 30.)
127. Saretok, Vitold, *Tillsatsmedel till betong.* 67 s. 1952. Kr. 5: —. (Avd. Väg- och Vattenbyggnad. Byggnadsteknik. 20.)
128. Lavemark, Sven, *The treatment of the load in electric power-system. Stability studies.* 53 s. 1952. Kr. 9: —. (Avd. Elektroteknik. 29.)
129. Lindblad, Bertil-Anders, *A radar investigation of the delta aquarid meteor shower of 1950.* 27 s. 1952. Kr 5: —. (Avd. Elektroteknik. 30.)
130. Hellgren, Gösta, *The propagation of electromagnetic waves along a conical helix with variable pitch.* 13 s. 1953. Kr. 3: —. (Avd. Elektroteknik. 31.)
131. Rydbeck, O. E. H., *On the excitation of different space charge wave modes in travelling wave tubes.* 15 s. 1953. Kr. 5: —. (Avd. Elektroteknik. 32.)
132. Wallman, Henry, *A wideband searching automatic frequency control circuit of new type.* 21 s. 1953. Kr. 5: —. (Avd. Elektroteknik. 33.)
133. Sandford, Folke, und Fransson, Stig, *Über die Entmischung von grobzerkleinertem Quarz.* 24 s. 1953. Kr. 5: —. (Institutionen för Silikatkemisk Forskning. 31.)
134. Ekelöf, Stig, *The magnetic circuit of telephone relays.* 32 s. 1953. Kr. 5: —. (Avd. Elektroteknik. 34.)
135. Yhland, C.-H., *Application of the similarity theory on radiation in furnaces.* 31 s. 1953. Kr. 5: —. (Avd. Maskinteknik. 7.)
136. Sjöström, Eero, *Über die Verwendung von Ionenaustauschern für die Sorption und Trennung von Ketonen.* 50 s. 1953. Kr 8: —. (Avd. Kemi och Kemisk Teknologi. 27.)
137. Hellerstedt, Lars-Magnus, *Wideband amplifiers for bandwidths up to 200 MHz.* 36 s. 1954. Kr 7: —. (Avd. Elektroteknik. 35.)
138. Rydbeck, O. E. H., and Agdur, B., *The propagation of electronic space charge waves in periodic structures.* 20 s. 1954. Kr. 5: —. (Avd. Elektroteknik. 36.)
139. Agdur, N. Bertil, *Experimental investigation of noise reduction in traveling wave tubes.* 12 s. 1954. Kr 3: —. (Avd. Elektroteknik. 37.)
140. Agdur, N. Bertil, *Amplification measurements on a velocity step tube.* 10 s. 1954. Kr. 2: 50. (Avd. Elektroteknik. 38.)
141. Ekelöf, Stig, *Theory of electromagnetically delayed telephone relays.* 88 s. 1954. Kr. 13:— (Avd. Elektroteknik. 39.)
142. Ekelöf, S., and Kihlberg, G., *Theory of the thermistor as an electric circuit element.* 36 s. 1954. Kr. 6: 50. (Avd. Elektroteknik. 40.)
143. Smith, Bengt, *Peat-gasoline.* 38 s. 1954. Kr. 6: 50. (Avd. Kemi och Kemisk Teknologi. 28.)
144. Leden, N., and Schöön, N.-H., *The solubility of silver azide and the formation of complexes between silver and azide ions.* 17 s. 1954. Kr. 4: —. (Avd. Kemi och Kemisk Teknologi. 29.)
145. *Basorganisation för forskning vid de tekniska högskolorna.* 154 s. + 6 tabellbilagor. 1954. Kr. 12: —. (Not for exchange.)
146. Troedsson, Carl Birger, *Transportation and city-building.* 30 s. 1954. Kr. 6: —. (Avd. Arkitektur 2.)
147. Sandford, Folke, and Fransson, Stig, *The refractoriness of some types of quartz and quartzite. I.* 28 s. 1954. Kr. 6: —. (Avd. Kemi och Kemisk Teknologi. 30.)
148. Carlsson, Orvar, *Porstorlek och frostbeständighet hos tegelmaterial.* 64 s. 1954. Kr. 9: —. (Avd. Kemi och Kemisk Teknologi. 31.)
149. Rydbeck, O. E. H., and Wilhelmsson, H., *A theoretical investigation of the ionospheric electron density variation during a total solar eclipse.* 22 s. 1954. Kr. 3: 50. (Avd. Elektroteknik. 41.)
150. Smith, Bengt, *Quantitative analysis of mixtures of hydrogen sulfide and sulfur dioxide.* 19 s. 1954. Kr. 4: —. (Avd. Kemi och Kemisk Teknologi. 32.)
151. Hedvall, J. A., *Reactions with activated solids.* 23 s. 1954 Kr. 5: —. (Institutionen för Silikatkemisk Forskning. 32.)
152. Smith, Cyril Stanley, *The microstructure of polycrystalline materials.* 49 s. 1954. Kr. 9: 50 (Institutionen för Silikatkemisk Forskning. 33.)
153. Selberg, Arne, *Norske erfaringer fra bygging av små hengebroer.* 20 s. 1954. Kr. 4: —. (Avd. Väg- och Vattenbyggnad. Byggnadsteknik. 21.)

Forts. å omsl. 3:dje sida.

CHALMERS TEKNISKA HÖGSKOLAS
HANDLINGAR

TRANSACTIONS OF CHALMERS UNIVERSITY OF TECHNOLOGY
GOTHENBURG, SWEDEN

Nr 215 (Avd. Maskinteknik 15.) 1959

EXPERIMENTAL INVESTIGATION OF POWER LOSS IN JOURNAL BEARINGS, CONSIDERING CAVITATION

BY

LEIF FLOBERG

REPORT NO. 8 FROM THE INSTITUTE OF MACHINE ELEMENTS
CHALMERS UNIVERSITY OF TECHNOLOGY
GOTHENBURG, SWEDEN
1959

GÖTEBORG 1959
ELANDERS BOKTRYCKERI AKTIEBOLAG

Manuscript received by the Publications Committee,
Chalmers University of Technology May 8th, 1959

Preface

During lubrication research at the Institute of Machine Elements, Chalmers University of Technology, Gothenburg, Sweden, under the leadership of the head of the institute, professor B. JAKOBSSON, the basic theory of oil films at constant viscosity has been studied. Earlier five reports, (1), (2), (3), (4), and (5), are published. For journal bearings cavitation was treated, and the performance for cavitation zone bearings was calculated. In the reports (1) and (2), tests have verified the accuracy of the present cavitation theory as far as pressure distribution and load capacity are concerned.

The present report compares the experimental power loss in a journal bearing with the theoretical value. In theory the power loss was calculated with consideration to cavitation regions.

I wish to express my gratitude to the Swedish Technical Research Council for their sponsorship. I also thank Mr REIMER SIEBENFREUND, who has participated in the investigations.

Leif Floberg
Tekn. lic.

Contents

Page

Preface 3

1. Introduction 5

2. Notation 6

3. Experimental Investigation 7

3,1. Theory Used 7
3,2. Test Method 8
3,3. Comparison between Theory and Experiments 10

4. Conclusion 15

5. References 16

1. Introduction

Hitherto no acceptable agreement between theory and experiments for power loss determination in journal bearings has been shown in literature. As late as in 1956, VOGELPOHL (7) published diagrams, in which the power loss values varied between boundaries with the ratio 1: 2. His diagrams represent theoretical and experimental results from a large number of authors.

When calculating the power loss in a bearing, the problem is how to determine the loss for the cavitation region. Some authors assume a full oil film, others that there is only air in this region. Neither method is correct, as there are oil and air strips in it. Due to the low viscosity of air, the air strips give negligible power loss. Therefore the extension of the oil strips in the cavitation region must be accurately considered. This has been done recently in ref. (2) and is mentioned by WILCOCK-ROSENBLATT (8).

Moreover, the bad agreement between experiments and theory often depends on differences between the cases compared. The boundary conditions must be the same in theory and test to give a correct comparison.

In this work these conditions are rigorously followed and the tests show that then a good agreement with theory is reached.

2. Notation

a = Length of lever

b = Bearing width

D = Bearing diameter

d = Journal diameter

E = Power loss per unit width

E_{tot} = Total power loss

$E_0 = \dfrac{E\psi}{\eta U^2}$ = Non-dimensional power loss per unit width

e = Eccentricity of journal relative to bearing

$f = \dfrac{E}{P} = \dfrac{E_{tot}}{P_{tot}}$ = Relative power loss

g = Acceleration due to gravity

h = Oil film thickness

m = Weight

P = Load capacity per unit width

P_{tot} = Total load capacity

$P_0 = \dfrac{P\psi^2}{\eta U}$ = Non-dimensional load capacity per unit width

r = Journal radius

Δr = Radial clearance

t = Temperature

U = Surface velocity

β = Angle between load and line of centres

$\varepsilon = \dfrac{e}{\Delta r}$ = Non-dimensional eccentricity

η = Viscosity of the oil

$\nu = \dfrac{b}{d}$ = Ratio width-diameter

$\psi = \dfrac{\Delta r}{r}$ = Radial clearance/journal radius

ω = Angular velocity

3. Experimental Investigation

3,1. Theory Used

The aim of this work is to give a comparison between theory and experiment for the 360° journal bearing with an oil groove 90° before the load line and a cavitation region at atmospheric pressure, see fig. 7.1. The width-diameter ratio $r = 1$. In theory the viscosity is assumed to be constant and an attempt is made to fulfil this condition also in the experiments. Therefore the test bearing is designed to give a low temperature rise.

The theoretical values given in table 8.1 are determined as in ref. (2), chap. 9, and based on values calculated for the centrally loaded 180° journal bearing by SASSENFELD-WALTHER (6). If the pressure ends with zero derivative within this bearing, an 180° zero pressure zone may be added as an upper half of the bearing. This has no effect on load capacity; but the power loss increases.

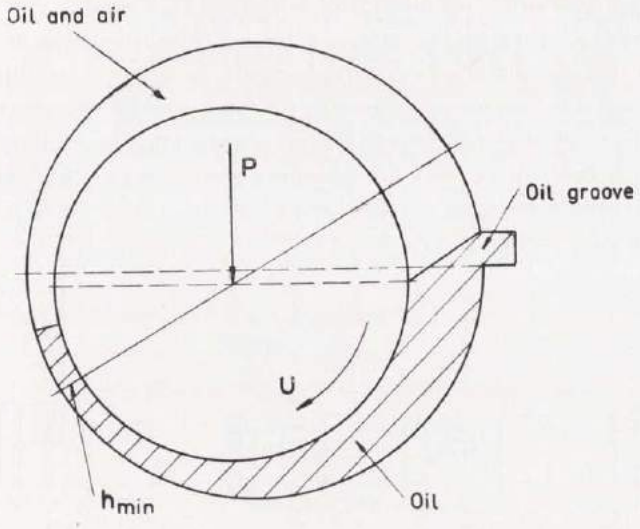

Fig. 7.1

Tab. 8.1. Theoretical Values for the 360° Journal Bearing with an Oil Groove 90° before the Load Line and $r=1$.

ε	0,0	0,3	0,4	0,5	0,6	0,7	0,8	0,9	1,0
P_0	0	0,76	1,14	1,67	2,47	3,90	6,89	16,4	∞
β	—	62	56	50	45	38	32	25	0
E_0	6,28	5,86	5,97	6,25	6,78	7,71	9,50	14,1	∞
$\frac{f}{\omega\, \Delta r}$	∞	7,71	5,23	3,74	2,74	1,98	1,38	0,857	0
$\frac{f}{\omega\, h_{\min}}$	∞	11,0	8,72	7,49	6,86	6,59	6,89	8,57	∞

3,2. Test Method

The power loss is derived as the product of journal torque and angular velocity. The torque cannot be measured at the bearing as this torque is not the same as that of the journal, due to the horisontal displacement of their centres. The test apparatus is shown in the figs 8.2, 9.1, and 9.2. The motor, as well as the journal shaft ball bearings, are placed on a cradle. The cradle torque is the journal torque and it is balanced and measured by weights on a scale. The bearing is assumed to work at the temperature of the oil leaving at the bearing sides. In the tests an attempt is made to keep the temperature rise low and the temperature as constant as possible to get the assumed condition of constant and known viscosity. The oil is introduced through two tubes into the axial oil groove which is drained by two other tubes, see fig. 8.3. By these means a large quantity of oil passes the groove and cools the bearing.

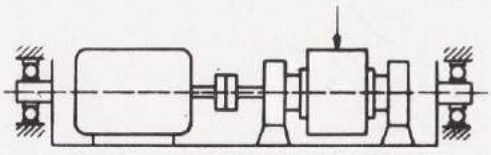

Fig. 8.2

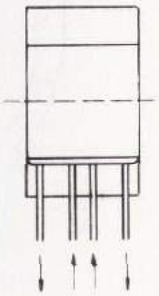

Fig. 8.3

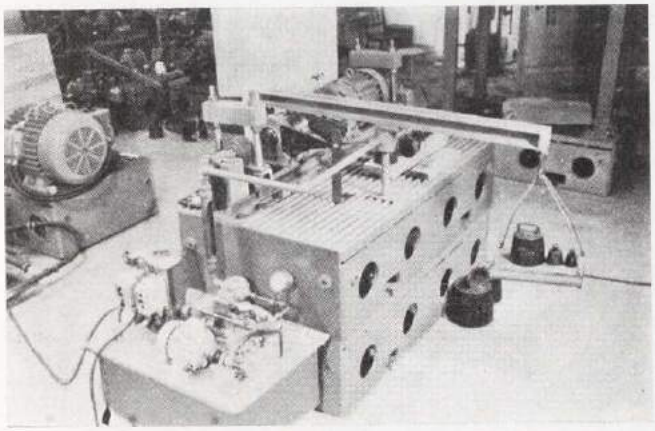

Fig. 9.1

The applied load must not give any torque on the cradle. Therefore the shaft and the cradle must have the same centre line. To compensate for any error that may occur, every experiment was made in both directions of rotation and the average value of the torques was used.

In theory the oil groove has an infinitely small width. In the experiments the width of it must be finite and, to give minimum error, the groove is placed at the end of the cavitation region, giving a 90° full oil film before the load. The rotational speed was varied between 300 and 1000 r/m.

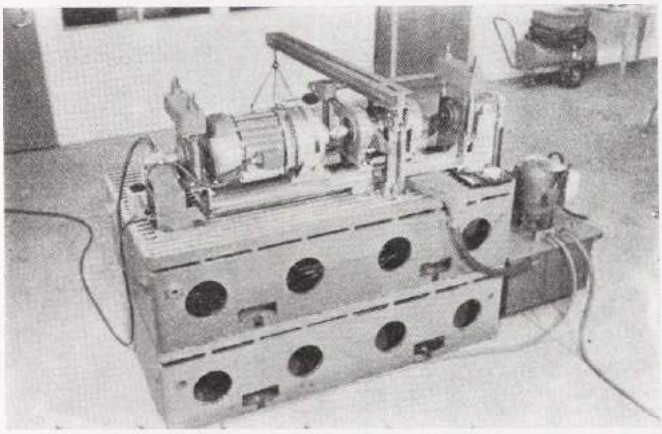

Fig. 9.2

3,3. Comparison between Theory and Experiments

Test bearing data:

Journal diameter	d	= 99,968 mm
Bearing diameter	D	= 100,430 mm
Non-dimensional clearance	$\psi = \frac{\Delta r}{r}$	= 4,62 $^{0}/_{00}$
Bearing width	b	= 100 mm

The oil quality was Velocite Oil No. 6 and the relation between viscosity and temperature was determined.

Measured quantities:

Load capacity	P_{tot}
Angular speed	ω
Oil temperature	t
Oil viscosity	η
Power loss	E_{tot}

The power loss is derived from the identity

$$E_{tot} = m\, g\, a\, \omega$$

where

m = weight on the scale
g = acceleration due to gravity (9,81 m/s²)
a = length of lever (here 0,25 m)

To explain the test evaluation, two experiments are given in detail.

1. P_{tot} = 1960 N (kgm/s²)
   ω = 31,4 1/s
   t = 23,8° C
   η = 0,0617 Ns/m²
   m = 0,345 kg

Now we have

$$P_0 = \frac{P\,\psi^2}{\eta\,U} = \frac{1960 \cdot 0{,}00462^2}{0{,}1 \cdot 0{,}0617 \cdot 0{,}050 \cdot 31{,}4} = 4{,}32$$

and

$$E_0 = \frac{E\,\psi}{\eta\,U^2} = \frac{0{,}345 \cdot 9{,}81 \cdot 0{,}25 \cdot 31{,}4 \cdot 0{,}00462}{0{,}1 \cdot 0{,}0617 \cdot 0{,}050^2 \cdot 31{,}4^2} = 8{,}06$$

2. $P_{tot} = 2940$ N
   $\omega = 62{,}8$ 1/s
   $t = 24{,}2°$ C
   $\eta = 0{,}0604$ Ns/m²
   $m = 0{,}570$ kg

Now

$$P_0 = \frac{2940 \cdot 0{,}00462^2}{0{,}1 \cdot 0{,}0604 \cdot 0{,}050 \cdot 62{,}8} = 3{,}31$$

and

$$E_0 = \frac{0{,}570 \cdot 9{,}81 \cdot 0{,}25 \cdot 62{,}8 \cdot 0{,}00462}{0{,}1 \cdot 0{,}0604 \cdot 0{,}050^2 \cdot 62{,}8^2} = 6{,}80$$

The tables 12.1 and 13.1 give the test results.

The figs 14.1 and 14.2 show the theoretical curve and the experimental points. In fig. 14.1 the journal speed is varied from 300 to 600 r/m, giving low loads and low temperature rises. This series of tests shows a good agreement with theory and the viscosity is approximately constant. In fig. 14.2 the speed is higher, 800—1000 r/m, which gives higher loads and higher temperature rises. This test series has a larger variation in viscosity, on account of which there is less agreement with theory. Thermoelements placed in the oil film within the bearing showed 2—3° C higher temperature than that measured at the bearing sides, which gives a 10—15 % lower viscosity, explaining the low experimental points.

Table 12.1. Table of Experimental Values. Rotational speed 300—600 r/m.

P_{tot}	ω	t	η	m	P_0	E_0
N	1/s	°C	Ns/m²	kg		
1230	31,4	24,1	0,0607	0,295	2,74	7,01
1470	31,4	23,8	0,0617	0,320	3,24	7,48
1960	31,4	23,8	0,0617	0,345	4,32	8,06
2940	31,4	25,4	0,0565	0,365	7,08	9,32
490	36,7	26,3	0,0538	0,285	1,06	6,55
981	36,7	25,9	0,0550	0,285	2,08	6,41
1960	36,7	24,2	0,0604	0,350	3,78	7,16
2940	36,7	25,2	0,0571	0,390	6,00	8,44
1960	41,9	24,0	0,0610	0,420	3,28	7,45
2940	41,9	24,0	0,0610	0,465	4,92	8,25
3920	41,9	24,4	0,0597	0,500	6,70	9,06
245	47,1	27,6	0,0502	0,320	0,442	6,13
490	47,1	27,6	0,0502	0,310	0,885	5,94
736	47,1	26,5	0,0532	0,330	1,25	5,96
981	47,1	26,3	0,0538	0,345	1,65	6,18
1960	52,4	24,3	0,0600	0,465	2,67	6,71
2940	52,4	24,7	0,0587	0,535	4,09	7,89
3920	52,4	25,3	0,0568	0,575	5,63	8,76
2940	57,6	27,5	0,0505	0,455	4,32	7,09
3430	57,6	27,5	0,0505	0,525	5,04	8,18
3920	57,6	27,6	0,0502	0,535	5,79	8,38
4410	57,6	27,1	0,0515	0,595	6,35	9,09
4900	57,6	27,4	0,0507	0,585	7,17	9,08
1960	60,2	27,6	0,0502	0,445	2,77	6,67
2450	60,2	27,5	0,0505	0,445	3,44	6,63
2940	60,2	26,7	0,0526	0,505	3,97	7,22
3430	60,2	27,1	0,0515	0,525	4,72	7,67
3920	60,2	26,2	0,0541	0,600	5,14	8,34
4410	60,2	26,7	0,0526	0,600	5,95	8,58
245	62,8	29,5	0,0458	0,400	0,364	6,30
490	62,8	29,2	0,0464	0,390	0,718	6,06
736	62,8	27,3	0,0510	0,405	0,980	5,73
981	62,8	27,3	0,0510	0,425	1,31	6,01
1960	62,8	24,3	0,0600	0,530	2,22	6,37
2940	62,8	24,2	0,0604	0,570	3,31	6,80
3920	62,8	24,9	0,0581	0,595	4,59	7,38
4900	62,8	25,1	0,0575	0,675	5,79	8,46
5880	62,8	25,1	0,0575	0,705	6,95	8,84

Table 13.1. Table of Experimental Values. Rotational speed 800—1000 r/m.

P_{tot}	ω	t	η	m	P_0	E_0
N	1/s	°C	Ns/m²	kg		
490	83,8	29,4	0,0460	0,495	0,543	5,82
736	83,8	28,0	0,0492	0,520	0,762	5,72
981	83,8	26,4	0,0535	0,560	0,934	5,66
1470	83,8	26,3	0,0538	0,560	1,39	5,63
1960	83,8	27,1	0,0515	0,575	1,94	6,04
2450	83,8	27,4	0,0507	0,585	2,46	6,24
2940	83,8	27,5	0,0505	0,605	2,97	6,48
3430	83,8	28,0	0,0492	0,615	3,55	6,76
3920	83,8	28,2	0,0488	0,640	4,10	7,09
4410	83,8	27,9	0,0495	0,670	4,54	7,32
490	94,2	29,3	0,0462	0,510	0,480	5,31
736	94,2	28,5	0,0480	0,545	0,694	5,46
981	94,2	27,5	0,0505	0,575	0,880	5,47
1470	94,2	27,6	0,0502	0,595	1,33	5,70
1960	94,2	26,9	0,0521	0,620	1,71	5,72
2450	94,2	26,7	0,0526	0,625	2,11	5,71
2940	94,2	26,1	0,0544	0,660	2,45	5,83
3430	94,2	27,5	0,0505	0,685	3,08	6,52
3920	94,2	27,9	0,0495	0,700	3,59	6,80
4410	94,2	28,6	0,0478	0,710	4,18	7,14
4900	94,2	29,2	0,0464	0,720	4,79	7,46
490	105	28,5	0,0480	0,550	0,416	4,96
736	105	30,0	0,0447	0,550	0,671	5,32
981	105	28,7	0,0476	0,590	0,840	5,36
1470	105	27,7	0,0500	0,635	1,20	5,49
1960	105	28,8	0,0474	0,630	1,69	5,75
2450	105	28,7	0,0476	0,650	2,10	5,91
2940	105	28,6	0,0478	0,675	2,51	6,11
3430	105	28,6	0,0478	0,690	2,93	6,25
3920	105	27,8	0,0497	0,745	3,22	6,49
4410	105	28,1	0,0490	0,760	3,67	6,71
4900	105	28,0	0,0492	0,765	4,06	6,73

Several authors calculate the power loss for the cavitation region as if there were oil with a straight line velocity distribution. This gives a power loss of 20—30 % higher than that in the figs 14.1 and 14.2, and a comparison between such a theory and the present tests would have led to wrong conclusions.

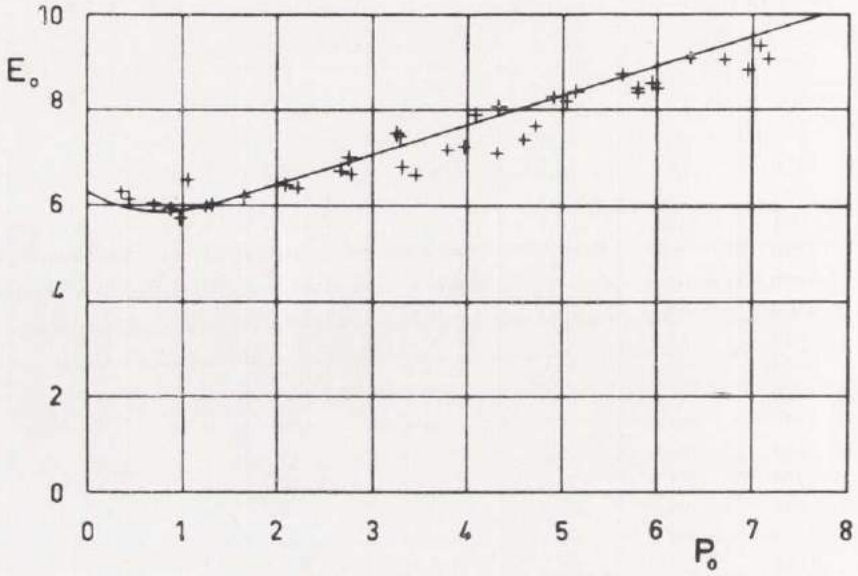

Fig. 14.1. Theoretical Power Loss Curve
+ Experimental points from tab. 12.1

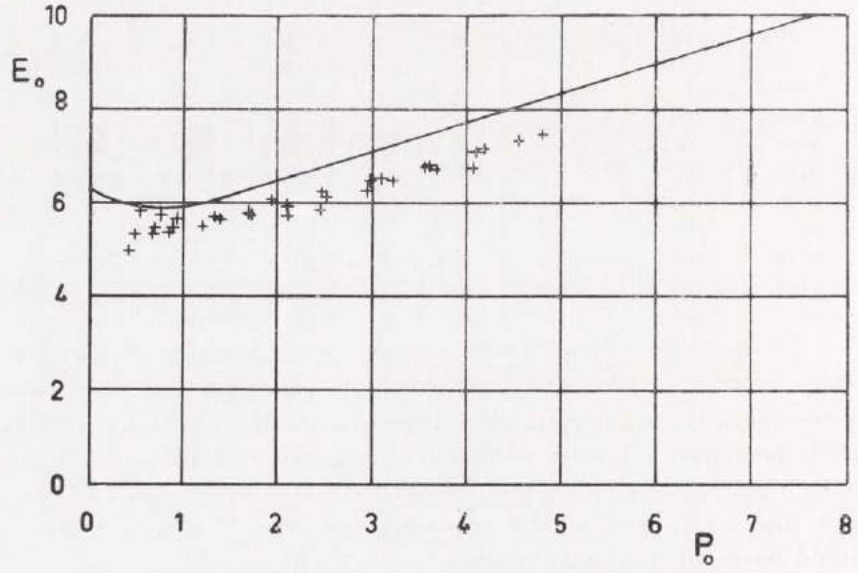

Fig. 14.2. Theoretical Power Loss Curve
+ Experimental points from tab. 13.1

4. Conclusion

This work represents a test report on the power loss in a 360° journal bearing with an oil groove 90° before the load. It is discussed how to calculate the power loss in a cavitation region.

The experiments show a very good agreement with theory when the temperature rise is low and they are made very close to the conditions that have been used in the theoretical deductions. To eliminate the power loss in ball bearings and thus keep the error in the measurements low, all the test apparatus are placed on a cradle and the loss is measured by mechanical means.

From this report and the refs (1) and (2), pressure distribution, load capacity, and power loss for constant viscosity bearings are shown to give full agreement between theory and test. Therefore it may be stated that the cavitation theory, as well as the bearing performance given in the refs (1), (2), (3), (4), and (5) for lubrication oil of constant viscosity, are reliable for technical use.

In practice, when the temperature rise cannot be neglected, an average value of the temperature may be used. A good average value is assumed to be had by adding the average temperature rise to the inlet oil temperature.

5. References

1. Floberg, L.: The Infinite Journal Bearing, Considering Vaporization. Gothenburg, 1957.
2. Jakobsson, B. and Floberg, L.: The Finite Journal Bearing, Considering Vaporization. Gothenburg, 1957.
3. Jakobsson, B. and Floberg, L.: The Partial Journal Bearing. Gothenburg, 1958.
4. Jakobsson, B. and Floberg, L.: The Rectangular Plane Pad Bearing. Gothenburg, 1958.
5. Jakobsson, B. and Floberg, L.: The Centrally Loaded Partial Journal Bearing. Gothenburg, 1959.
6. Sassenfeld, H. and Walther, A.: Gleitlagerberechnungen. VDI-Forschungsheft 441, 1954.
7. Vogelpohl, G.: Das Reibungsverhalten von Gleitlagern. Konstruktion, March 1956.
8. Wilcock, D. F. and Rosenblatt, M.: Oil Flow, Key Factor in Sleeve-Bearing Performance. Trans. Am. Soc. Mech. Engrs, vol. 74, p. 849, 1952.

Forts. fr. omsl. 2:dra sida.

154. GRANHOLM, HJALMAR, *Armerat trä.* 96 s. 1954. Kr. 9: — (Avd. Väg- och Vattenbyggnad. Byggnadsteknik. 22.)
155. WILHELMSSON, HANS, *The interaction between an obliquely incident plane electromagnetic wave and an electron beam. I.* 31 s. 1954. Kr. 7: —. (Avd. Elektroteknik. 42.)
156. OLVING, SVEN, *Electromagnetic wave propagation on helical conductors imbedded in dielectric medium.* 14 sid. 1955. Kr. 3: —. (Avd. Elektroteknik. 43.)
157. OLVING, SVEN, *Amplification of the traveling wave tube at high beam current. I.* 11 s. 1955. Kr. 3: —. (Avd. Elektroteknik. 44.)
158. HEDVALL, J. A., NORDENGREN, SVEN, und LILJEGREN, B., *Über die thermische Zersetzung von Kalziumsulfat bei niedrigen Temperaturen.* 18 s. 1955. Kr. 5: — (Institutionen för Silikatkemisk Forskning. 34.)
159. DAHLGREN, SVEN-ERIC, *On the break-down of thixotropic materials.* 18 s. 1955. Kr. 3: 50. (Institutionen för Silikatkemisk Forskning. 35.)
160. SANDFORD, FOLKE, och LILJEGREN, BERNE, *Torkningen av råtegel och dennas inverkan på teglets frostbeständighet.* 22 s. 1955. Kr. 3: —. (Institutionen för Silikatkemisk Forskning. 36.)
161. WALLMAN, HENRY, *Automatic noise-factor meter.* 17 s. 1955. Kr. 3: —. (Avd. Elektroteknik. 45.)
162. SANDFORD, FOLKE, and FRANSSON, STIG, *The refractoriness of some types of quartz and quartzite. II.* 24 s. 1955. Kr. 5: —. (Institutionen för Silikatkemisk Forskning. 37.)
163. LINDBLAD, ANDERS, *Konstruktion av linjer för moderna handelsfartyg.* 176 s. 1955 Kr. 20: —. (Avd. Skeppsbyggeri. 6.)
164. SVARTHOLM, NILS, *Two problems in the theory of the slowing down of neutrons by collisions with atomic nuclei.* 15 s. 1955. Kr. 5: —. (Avd. Allmänna Vetenskaper. 10.)
165. PERSSON, PER, *Bostadsvaneundersökning utförd i hyreslägenheter byggda 1947 i Göteborg, Torpaområdet.* 86 s. 1955. Kr. 12: —. (Avd. Arkitektur. 3.)
166. HANSSON, P. R., *Undersökning av mullitbildning i keramiska produkter.* 29 s. 1955. Kr. 6: —. (Institutionen för Silikatkemisk Forskning. 38.)
167. EKELÖF, STIG, *Die Temperaturverteilung in einem gleichstromdurchflossenen langen Metallzylinder mit kreisförmigem Querschnitt.* 38 s. 1955. Kr. 10: —. (Avd. Elektroteknik. 46.)
168. WILHELMSSON, HANS, *On the reflection of electromagnetic waves from a dielectric cylinder.* 17 s. 1955. Kr. 4: 50. (Avd. Elektroteknik. 47.)
169. BJÖRK, N., and DAVIDSON, R., *Small signal behaviour of directly heated thermistors.* 43 s. 1955. Kr. 11: —. (Avd. Elektroteknik. 48.)
170. FORESTIER, H., *Tendances actuelles dans la formation de l'ingenieur chimiste: selection, orientation, specialisation; amelioration de son efficience.* 13 s. 1956. Kr. 2: 50. (Avd. Kemi och Kemisk Teknologi. 33.)
171. WAX, NELSON, *On the ring current hypothesis.* 32 s. 1956. Kr. 7: —. (Avd. Elektroteknik. 49.)
172. ELGESKOG, ERIK, *Photoformer analysis and design.* 40 s. 1956. Kr. 8: 50. (Avd Elektroteknik. 50.)
173. ANZELIUS, ADOLF, *Bimolekulare Reaktion von zwei in Mischung vorliegenden Substanzen mit einer dritten Substanz.* 8 s. 1956. Kr. 5: —. (Avd. Allm. Vetenskaper. 11.)
174. REINIUS, ERLING, *Model studies for the extension of the harbour of Gothenburg.* 38 s. 1956. Kr. 6: —. (Avd. Väg- och Vattenbyggnad. Byggnadsteknik. 23.)
175. ZIMEN, K. E., *Diffusion von Edelgasatomen die durch Kernreaktion in festen Stoffen gebildet werden.* 7 s. 1956. Kr. 2: —. (Institutionen för Kärnkemi. 1.)
176. INTHOFF, W., und ZIMEN, K. E., *Kinetik der Diffusion radioaktiver Edelgase aus festen Stoffen nach Bestrahlung.* 16 s. 1956. Kr. 4: —. (Institutionen för Kärnkemi. 2.)
177. GRANHOLM, HJALMAR, *Puts och lättbetong.* 45 s. 1956. Kr. 3: —. (Avd. Väg- och Vattenbyggnad. Byggnadsteknik. 24.)
178. OLVING, SVEN, *A new method for space charge wave interaction studies. I.* 12 s. 1956. Kr. 3: —. (Avd. Elektroteknik. 51.)
179. HANSBO, SVEN, *The critical load of rectangular frames analysed by convergence methods.* 47 s. 1956. Kr. 11: —. (Avd. Väg- och Vattenbyggnad. Byggnadsteknik. 25.)
180. WESTBERG, VIDOR, *Measurements of noise radiation at 10 cm from glow lamps. Preliminary report.* 14 s. 1956. Kr. 4: 50. (Avd. Elektroteknik. 52.)
181. SVENSSON, S. I., HELLGREN, G. and PERERS, O., *The Swedish radioscientific solar eclipse expedition to Italy, 1952. Preliminary report.* 30 s. 1956. Kr. 8: —. (Avd. Elektroteknik. 53.)
182. WAX, NELSON, *A note on design considerations for a proposed auroral radar.* 16 s. 1957. Kr. 3: —. (Avd. Elektroteknik. 54.)
183. JOSHI, G. H., *The electromagnetic interaction between two crossing electron streams. I.* 31 s. 1957. Kr. 8: —. (Avd. Elektroteknik. 55.)

Forts. å omsl. 4:de sida.

Forts. fr. omsl. 3:dje sida.

184. Smith, Bengt, *Dry methods for removing hydrogen sulphide from gases.* 65 s. 1957. Kr. 15: —. (Avd. Kemi och Kemisk Teknologi. 34.)
185. Ekelöf, S., Björk, N., and Davidson, R., *Large signal behaviour of directly heated thermistors.* 31 s. 1957. Kr. 8: —. (Avd. Elektroteknik. 56.)
186. Carlsson, Bengt und Larsson, Hans, *Wirkungsgrad und Selbsthemmung einfacher Umlaufgetriebe.* 48 s. 1957. Kr. 9: —. (Avd. Maskinteknik. 8.)
187. Aurell, Carl G., *The equivalent transmission line of a linear four-terminal network. Calculations with cascade-connected four-terminal networks.* 39 s. 1957. Kr. 6: —. (Avd. Elektroteknik. 57.)
188. Lundholm, R., *Induced overvoltage-surges on transmission lines and their bearing on the lightning performance at medium voltage networks.* 117 s. 1957. Kr. 19: —. (Avd. Elektroteknik. 58.)
189. Floberg, Leif, *The infinite journal bearing, considering vaporization.* 83 s. 1957. Kr. 13: —. (Avd. Maskinteknik. 9.)
190. Jakobsson, Bengt, and Floberg, Leif, *The finite journal bearing, considering vaporization.* 117 s. 1957. Kr. 19: 50. (Avd. Maskinteknik. 10.)
191. Chako, Nicholas, *Characteristic curves on planes in the image space.* 49 s. 1957. Kr. 15: —. (Avd. Allmänna Vetenskaper. 12.)
192. Ekelöf, Stig, *The development and decay of the magnetic flux in a non-delayed telephone relay.* 50 s. 1957. Kr. 15: —. (Avd. Elektroteknik. 59.)
193. Björklund, Kjell, *Bestämning av porslins draghållfasthet.* 78 s. 1958. Kr. 15: —. (Institutionen för Silikatkemisk Forskning. 39.)
194. Granholm, Per, *Sound insulation of single leaf walls.* 48 s. 1958. Kr. 8: —. (Avd. Väg- och Vattenbyggnad. Byggnadsteknik. 26.)
195. Granholm, Hjalmar, *Om vattengenomslag i murade väggar med särskild hänsyn till tegel som fasadmaterial.* 172 s. 1958. Kr. 16: —. (Avd. Väg- och Vattenbyggnad. Byggnadsteknik. 27).
196. Meos, Johan, and Olving, Sven, *On the origin of radar echoes associated with auroral activity.* 20 s. 1958. Kr. 5: —. (Avd. Elektroteknik. 60.)
197. Joshi, G. H., *The electromagnetic interaction between two crossing electron streams. II.* 10 s. 1958. Kr. 3: 50. (Avd. Elektroteknik. 61.)
198. Wilhelmsson, Hans, *The interaction between an obliquely incident plane electromagnetic wave and an electron beam. II.* 32 s. 1958. Kr. 7: —. (Avd. Elektroteknik. 62.)
199. Kärrholm, Gunnar, *A method of iteration applied to beams resting on springs.* 50 s. 1958. Kr. 12: —. (Avd. Allm. Vetenskaper. 13.)
200. Jakobsson, Bengt, and Floberg, Leif, *The partial journal bearing.* 60 s. 1958. Kr. 14: —. (Avd. Maskinteknik. 11.)
201. Kärrholm, Gunnar, *Influence functions of elastic plates divided in strips.* 18 s. 1958. Kr. 4: 50. (Avd. Väg- och Vattenbyggnad. Byggnadsteknik. 28.)
202. Råde, Lennart, *Sampling planes for acceptance sampling by variables using the range.* 34 s. 1958. Kr. 9:50. (Avd. Allm. Vetenskaper. 14.)
203. Jakobsson, Bengt, and Floberg, Leif, *The rectangular plane pad bearing.* 44 s. 1958. Kr. 5: —. (Avd. Maskinteknik. 12.)
204. Asplund, Sven Olof, *Column-beams and suspension bridges analyzed by »Green's matrix».* 36 s. 1958. Kr. 7: —. (Avd. Väg- och Vattenbyggnad. Byggnadsteknik. 29.)
205. Wilhelmsson, Hans, *On the properties of the electron beam in the presence of an axial magnetic field of arbitrary strength.* 32 s. 1958. Kr. 7: 50. (Avd. Elektroteknik. 63.)
206. Wilhelmsson, Hans, *The interaction between an obliquely incident plane electromagnetic wave and an electron beam. III.* 17 s. 1958. Kr. 5:—. (Avd. Elektroteknik. 64.)
207. Hedvall, Arvid J., *On the influence of pre-treatment and transition processes on the adsorption capacity and the reactivity of various types of glass and silica.* 39 s. 1959. Kr. 8: —. (Institutionen för Silikatkemisk Forskning. 40.)
208. Kärrholm, Gunnar, *A flow problem solved by strip method.* 22 s. 1959. Kr. 4: 50. (Avd. Allm. Vetenskaper. 15.)
209. Granholm, Hjalmar, *Allmän teori för beräkning av armerad betong.* 228 s. 1959. Kr. 20:—. (Avd. Väg- och Vattenbyggnad. Byggnadsteknik. 30.)
210. Lars G. Lidin, *On helical-spring suspension.* 75 s. 1959. Kr. 15: —. (Avd. Maskinteknik. 13.)
211. Björk, Nils, *Theory of the indirectly heated thermistor.* 46 s. 1959. Kr. 10: —. (Avd. Elektroteknik. 65.)
212. Carlsson, Orvar, *The influence of submicroscopic pores on the resistance of bricks towards frost.* 13 s. 1959. Kr. 3:50—. (Institutionen för Silikatkemisk Forskning. 41.)
213. Granholm, Hjalmar, *KAM 40, KAM 60 och KAM 90.* 41 s. 1959. Kr. 3: 50. (Avd. Väg- och Vattenbyggnad. Byggnadsteknik. 31.)
214. Jakobsson, Bengt and Floberg, Leif, *The centrally loaded partial journal bearing.* Kr. 7: 50. 35 s. 1959. (Avd. Maskinteknik. 14.)

Pris kronor 3: 50

OMSLAGET TRYCKT HOS
ELANDERS BOKTRYCKERI AKTIEBOLAG
GÖTEBORG 1959

CHALMERS TEKNISKA HÖGSKOLAS
HANDLINGAR

TRANSACTIONS OF CHALMERS UNIVERSITY OF TECHNOLOGY
GOTHENBURG, SWEDEN

Nr 216 (Avd. Maskinteknik 16) 1959

LUBRICATION OF A ROTATING CYLINDER ON A PLANE SURFACE, CONSIDERING CAVITATION

BY

LEIF FLOBERG

REPORT NO. 9 FROM THE INSTITUTE OF MACHINE ELEMENTS
CHALMERS UNIVERSITY OF TECHNOLOGY
GOTHENBURG, SWEDEN
1959

GUMPERTS FÖRLAG
GÖTEBORG

Av Chalmers Tekniska Högskolas Handlingar hava tidigare utkommit:

Fullständig förteckning över Chalmers Tekniska Högskolas Handlingar lämnas av Chalmers Tekniska Högskolas Bibliotek, Göteborg.

151. HEDVALL, J. A., *Reactions with activated solids.* 23 s. 1954 Kr. 5: —. (Institutionen för Silikatkemisk Forskning. 32.)
152. SMITH, CYRIL STANLEY, *The microstructure of polycrystalline materials.* 49 s. 1954. Kr. 9: 50 (Institutionen för Silikatkemisk Forskning. 33.)
153. SELBERG, ARNE, *Norske erfaringer fra bygging av små hengebroer.* 20 s. 1954. Kr. 4: —. (Avd. Väg- och Vattenbyggnad. Byggnadsteknik. 21.)
154. GRANHOLM, HJALMAR, *Armerat trä.* 96 s. 1954. Kr. 9: — (Avd. Väg- och Vattenbyggnad. Byggnadsteknik. 22.)
155. WILHELMSSON, HANS, *The interaction between an obliquely incident plane electromagnetic wave and an electron beam. I.* 31 s. 1954. Kr. 7: —. (Avd. Elektroteknik. 42.)
156. OLVING, SVEN, *Electromagnetic wave propagation on helical conductors inbedded in dielectric medium.* 14 sid. 1955. Kr. 3: —. (Avd. Elektroteknik. 43.)
157. OLVING, SVEN, *Amplification of the traveling wave tube at high beam current. I.* 11 s. 1955. Kr. 3: —. (Avd. Elektroteknik. 44.)
158. HEDVALL, J. A., NORDENGREN, SVEN, und LILJEGREN, B., *Über die thermische Zersetzung von Kalziumsulfat bei niedrigen Temperaturen.* 18 s. 1955. Kr. 5: —. (Institutionen för Silikatkemisk Forskning. 34.)
159. DAHLGREN, SVEN-ERIC, *On the break-down of thixotropic materials.* 18 s. 1955. Kr. 3: 50. (Institutionen för Silikatkemisk Forskning. 35.)
160. SANDFORD, FOLKE, och LILJEGREN, BERNE, *Torkningen av råtegel och dennas inverkan på teglets frostbeständighet.* 22 s. 1955. Kr. 3: —. (Institutionen för Silikatkemisk Forskning. 36.)
161. WALLMAN, HENRY, *Automatic noise-factor meter.* 17 s. 1955. Kr. 3: —. (Avd. Elektroteknik. 45.)
162. SANDFORD, FOLKE, and FRANSSON, STIG, *The refractoriness of some types of quartz and quartzite. II.* 24 s. 1955. Kr. 5: —. (Institutionen för Silikatkemisk Forskning. 37.)
163. LINDBLAD, ANDERS, *Konstruktion av linjer för moderna handelsfartyg.* 176 s. 1955 Kr. 20: —. (Avd. Skeppsbyggeri. 6.)
164. SVARTHOLM, NILS, *Two problems in the theory of the slowing down of neutrons by collisions with atomic nuclei.* 15 s. 1955. Kr. 5: —. (Avd. Allmänna Vetenskaper. 10.)
165. PERSSON, PER, *Bostadsvaneundersökning utförd i hyreslägenheter byggda 1947 i Göteborg, Torpaområdet.* 86 s. 1955. Kr. 12: —. (Avd. Arkitektur. 3.)
166. HANSSON, P. R., *Undersökning av mullitbildning i keramiska produkter.* 29 s. 1955. Kr. 6: —. (Institutionen för Silikatkemisk Forskning. 38.)
167. EKELÖF, STIG, *Die Temperaturverteilung in einem gleichstromdurchflossenen langen Metallzylinder mit kreisförmigem Querschnitt.* 38 s. 1955. Kr. 10: —. (Avd. Elektroteknik. 46.)
168. WILHELMSSON, HANS, *On the reflection of electromagnetic waves from a dielectric cylinder.* 17 s. 1955. Kr. 4: 50. (Avd. Elektroteknik. 47.)
169. BJÖRK, N., and DAVIDSON, R., *Small signal behaviour of directly heated thermistors.* 43 s. 1955. Kr. 11: —. (Avd. Elektroteknik. 48.)
170. FORESTIER, H., *Tendances actuelles dans la formation de l'ingenieur chimiste: selection, orientation, specialisation; amelioration de son efficience.* 13 s. 1956. Kr. 2: 50. (Avd. Kemi och Kemisk Teknologi. 33.)
171. WAX, NELSON, *On the ring current hypothesis.* 32 s. 1956. Kr. 7: —. (Avd. Elektroteknik. 49.)
172. ELGESKOG, ERIK, *Photoformer analysis and design.* 40 s. 1956. Kr. 8: 50. (Avd Elektroteknik. 50.)
173. ANZELIUS, ADOLF, *Bimolekulare Reaktion von zwei in Mischung vorliegenden Substanzen mit einer dritten Substanz.* 8 s. 1956. Kr. 5: —. (Avd. Allm. Vetenskaper. 11.)
174. REINIUS, ERLING, *Model studies for the extension of the harbour of Gothenburg.* 38 s. 1956. Kr. 6: —. (Avd. Väg- och Vattenbyggnad. Byggnadsteknik. 23.)
175. ZIMEN, K. E., *Diffusion von Edelgasatomen die durch Kernreaktion in festen Stoffen gebildet werden.* 7 s. 1956. Kr. 2: —. (Institutionen för Kärnkemi. 1.)
176. INTHOFF, W., und ZIMEN, K. E., *Kinetik der Diffusion radioaktiver Edelgase aus festen Stoffen nach Bestrahlung.* 16 s. 1956. Kr. 4: —. (Institutionen för Kärnkemi. 2.)
177. GRANHOLM, HJALMAR, *Puts och lättbetong.* 45 s. 1956. Kr. 3: —. (Avd. Väg- och Vattenbyggnad. Byggnadsteknik. 24.)

Forts. å omsl. 3:dje sida.

CHALMERS TEKNISKA HÖGSKOLAS
HANDLINGAR

TRANSACTIONS OF CHALMERS UNIVERSITY OF TECHNOLOGY
GOTHENBURG, SWEDEN

Nr 216 (Avd. Maskinteknik 16) 1959

LUBRICATION OF A ROTATING CYLINDER ON A PLANE SURFACE, CONSIDERING CAVITATION

BY

LEIF FLOBERG

REPORT NO. 9 FROM THE INSTITUTE OF MACHINE ELEMENTS
CHALMERS UNIVERSITY OF TECHNOLOGY
GOTHENBURG, SWEDEN
1959

GÖTEBORG 1959
ELANDERS BOKTRYCKERI AKTIEBOLAG

Manuscript received by the Publications Committee,
Chalmers University of Technology June 26th, 1959

Preface

At the Institute of Machine Elements, Chalmers University of Technology, lubrication has been treated under the leadership of the head of the institute, Professor B. JAKOBSSON. The theory for hydrodynamic lubrication, considering cavitation in the oil film, has been studied, and experiments to verify the theory have been made. Six reports are published (1), (2), (4), (5), (6), and (7).

In this work the contact between a cylinder and a plane surface is hydrodynamically treated. The surfaces are here rigid, and the viscosity of oil is assumed to be constant.

I wish to express my gratitude to the Swedish Technical Research Council for their sponsorship. I also thank Mr. BENGT HÅKANSSON, M. Sc., who has made the evaluations at the electronic computer ALWAC III E.

Leif Floberg

Tekn. lic.

Contents

Page

Preface 3

1. Introduction 5

2. Notation 6

3. Lubrication of a Rotating Cylinder on a Plane Surface 8
   - 3,1. Hydrodynamic Pressure Distribution in the Oil Film 8
   - 3,2. Load Capacity 17
   - 3,3. Oil Flow 24
   - 3,4. Power Loss 27
   - 3,5. Temperature Rise 28
   - 3,6. Relative Power Loss 28

4. Some Applications 29
   - 4,1. Torqueless Cylinder 29
   - 4,2. The Plane Surface without Shear Force 30
   - 4,3. One Cylinder Driving Another One 30
   - 4,4. Determination of the Minimum Space 31
   - 4,5. Numerical Example 32

5. Conclusion 34

6. Appendix I: Solution of Integrals 35

7. Appendix II: Tables of Calculated Values 37

8. References 40

1. Introduction

The problem treated here has earlier been studied by KNESCHKE (8), in 1957. However, he uses wrong boundary conditions for the hydrodynamic oil film pressure, and gets no cavitation. At a contact such as that between a cylinder and a plane surface, there must always be a cavitation region due to the continuity condition. GATCOMBE (3) has studied a neighbouring problem, the contact between involute spur gears, and used an incorrect boundary condition at the end of the pressure build-up. Authors of lubrication papers often use arbitrarily chosen boundary conditions, neglecting the fact that these must satisfy the continuity condition.

In this paper the continuity is satisfied in every section of the oil wedge, and the cavitation is considered. The continuity prescribes zero pressure derivative at the beginning of a cavitation region, see ref. (1). The boundary at the starting point of the oil film is depending on the oil quantity supplied. When calculating the power loss, the air strips in the cavitation region are taken into account. The width of the cylinder is assumed to be infinite.

Ordinarily the circular surface is approximated to a parabolic surface. Here the original circle is used to get theoretically correct boundary conditions, which also in practice hold with very good accuracy. If a parabola is used, the two theoretical boundaries are located at infinity. The parabola method, however, is mathematically easier to use and gives very good results.

2. Notation

A = Constant to be calculated

C = Constant of integration

c = Specific heat of oil

E = Power loss per unit width

$E_0 = \dfrac{E}{\eta\,(U_1 + U_2)^2}$ = Non-dimensional power loss per unit width

F = Shear force per unit width

$F_0 = \dfrac{F}{\eta\,(U_1 + U_2)}$ = Non-dimensional shear force per unit width

$f = \dfrac{E}{P_y}$ = Relative power loss

$H = \dfrac{h}{h_{\min}}$ = Non-dimensional oil film thickness

h = Oil film thickness

$h_{\min}$ = Minimum oil film thickness

$k = \dfrac{U_2}{U_1}$ = Velocity ratio

P = Load per unit width

$P_0 = \dfrac{P}{\eta\,(U_1 + U_2)}$ = Non-dimensional load per unit width

p = Oil film pressure

$p_0 = \dfrac{p\,h_{\min}}{\eta\,(U_1 + U_2)}$ = Non-dimensional oil film pressure

q = Oil flow per unit width

$q_0 = \dfrac{q}{(U_1 + U_2)\,h_{\min}}$ = Non-dimensional oil flow per unit width

r = Radius of the cylinder

Δt = Temperature rise

$\Delta t_0 = c\,\varrho \cdot \dfrac{\Delta t\,h_{\min}}{\eta\,(U_1 + U_2)}$ = Non-dimensional temperature rise

U_1 = Velocity of the plane surface

U_2 = Velocity of the cylinder surface

u = Velocity of a fluid particle

x, y = Coordinates

β = Load angle

γ = Angle

$\varepsilon = \dfrac{\psi}{1 + \psi}$ = Ratio

η = Absolute viscosity

ϱ = Density of oil

τ = Shear stress

φ = Angular coordinate

$\psi = \dfrac{r}{h_{\min}}$ = Radius of cylinder / minimum oil film thickness

3. Lubrication of a Rotating Cylinder on a Plane Surface

3,1. Hydrodynamic Pressure Distribution in the Oil Film

When determining the pressure build-up in the oil film between the cylinder and the plane surface, REYNOLDS' continuity equation is used. This holds for laminar oil flow in thin oil films, so it is not fully correct to use in this case. Now the practically essential pressure build-up takes place where the oil film is thin and REYNOLDS' equation holds with good accuracy; but in regions where the oil film is thicker, and the continuity equation is therefore less accurate, the pressure increase has practically negligible values. Therefore REYNOLDS' equation is usually used in cases similar to that treated here.

In this paper the following usual assumptions are made:

The flow is laminar.
The oil adheres to the surfaces.
Weight and acceleration forces of the oil are negligible.
The viscosity is constant.
The surfaces are rigid.
The width is infinite.

The last assumption of infinite width holds very well also for rolling contacts occurring in practice. In journal bearings the side flow cannot be neglected. Here the minimum oil film thickness is only a fraction of that in a journal bearing, and as the oil flow is proportional to the cube of the oil film thickness, the side flow has very low values.

The problem is now the boundary conditions. Since REYNOLDS (9), in 1886, derived the continuity equation for the pressure determination in an oil film between two moving surfaces, the great problem has been the boundary conditions for the pressure curve and the behaviour of the oil in cavitation regions.

In the paper "Rollreibung auf spurbildender Fahrbahn" KNESCHKE (8) has treated the above problem. Referring to his fig. 1, also

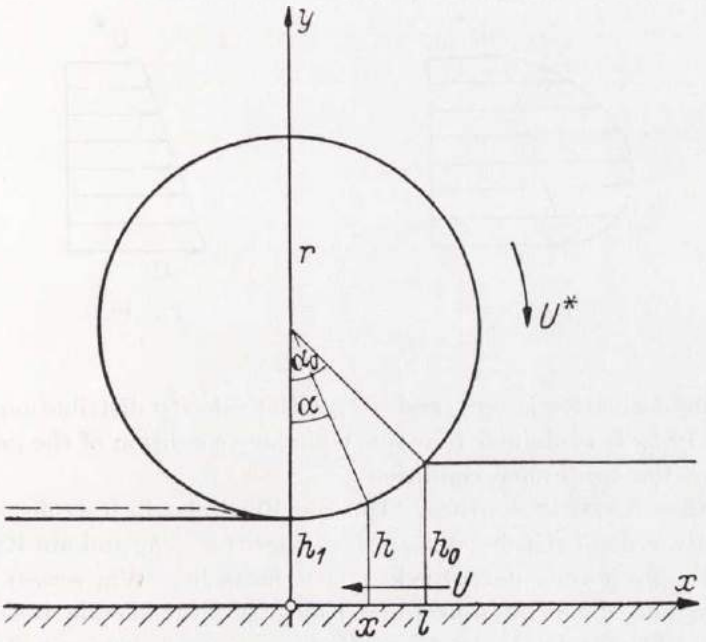

"Abb. 1. Rollspalt"
Fig. 9.1. From Kneschke

shown here as 9.1, KNESCHKE writes: "Die im Aufriß durch den Grenzwinkelbogen α_0 dargestellte obere Begrenzung des Rollspaltes ist durch die Eingrifftiefe $h_0 - h_1$ festgelegt, die im Spalt veränderliche Höhe h durch den Winkel α." This condition, with the pressure build-up beginning at the oil film thickness equal to the thickness of the oil layer at the plane surface, is not right, because it violates the oil flow continuity. The oil flow before the wedge is, using KNESCHKE's notation, $U\,h_0$. Within the wedge the flow is $0{,}5\;U\,h^*$, where $h^* < h_0$. There is thus an error of more than 50 % in continuity.

Concerning the extension of the oil wedge KNESCHKE writes: "Der Rollspalt selbst soll sich in allen weiteren Betrachtungen entsprechend Abb. 1 über das Intervall $h_1 \leqq h \leqq h_0$ erstrecken. Auch darin liegt eine die Rechnung vereinfachende Voraussetzung." Also this other boundary condition does not fulfil the continuity. The oil flow passing at the minimum space has the velocity distribution shown in fig. 10.1, as the pressure curve has a positive derivative at this point. At an infinitely small distance in the flow direction the

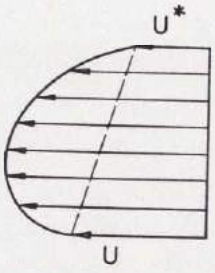

Fig. 10.1

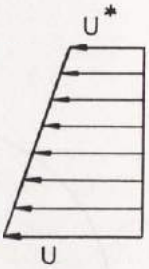

Fig. 10.2

pressure derivative is zero, and we get the velocity distribution given in fig. 10.2. It is obvious that this boundary condition of the pressure violates the continuity condition.

Further KNESCHKE writes: "Um die Fließscheide festzulegen, benutzen wir die Tatsache, daß am Radeingriff $h = h_0$ und am Radauslauf $h = h_1$ jeweils der Druck $p = 0$ herrscht. Wir setzen dabei voraus, daß die nicht durch den Rollspalt abströmende Restmasse der Schicht von der Dicke h_0 am Radeingriff nach beiden Seiten der eingreifenden Radbreite abströmt, ohne daß ein nennenswerter Staudruck dabei entsteht." This is a very usual error in literature to consider a bearing to be of alternatingly infinite and finite width As it is easier to calculate with infinite width, this is often done; but when there is too much oil in a section, this is supposed to vanish in axial direction assuming finite width. KNESCHKE's two arbitrarily chosen and incorrect boundary conditions, which have no real background, give a pressure lower than the correct value.

In the paper "Lubrication Characteristics of Involute Spur Gears" GATCOMBE (3) mathematically treats the lubricating-oil wedge separating the surfaces of involute straight spur gears. He writes:

"The wedging force, created by the pressure in the film which separates two rotating cylinders, is given by the integral of the pressure function $p\,(x)$ (see Fig. 4), between the limits $-\infty$ and $+\infty$. However, experiments show that lubricants are incapable of creating or sustaining the tension stresses indicated by that portion of the graph below the x-axis in Fig. 4.

Thus, the absolute pressure will be atmospheric for any point in the interval $-\infty$ to zero. The wedging force will then be obtained by integrating the pressure function over the interval $0 = x = \infty$ (see Fig. 5)."

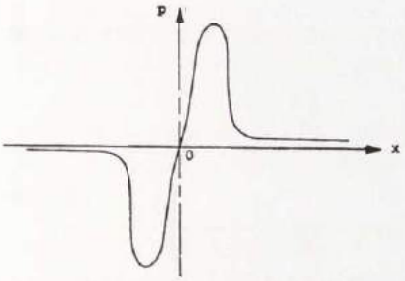

"Fig. 4. Hypothetical Pressure-Distribution Graph for Single Phase of Mating Period"

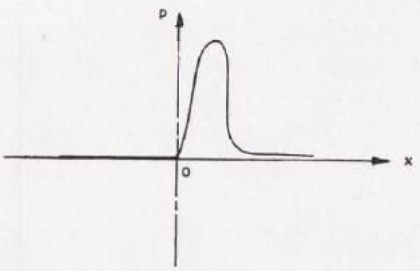

"Fig. 5. Theoretical Pressure-Distribution Graph for Single Phase of Mating Period"

Fig. 11.1. From Gatcombe

It is not correct to calculate as if negative pressure exists and then neglect the negative pressure zone and use a zero pressure zone, see fig. 11.1. Then the wrong condition is already used to get the positive pressure curve. The boundary condition is correct at the beginning of the wedge; but the pressure curve does not end at the minimum space, which does not fulfil the continuity, as shown above.

REYNOLDS' equation for infinite width and two surface velocities has the following form, see fig. 12.1

$$\frac{d}{dx}\left(h^3 \frac{dp}{dx}\right) = 6\,\eta\,(U_1 + U_2)\,\frac{dh}{dx} \quad \ldots\ldots\ldots \quad 11.2$$

where x = coordinate
h = oil film thickness
p = oil film pressure
η = absolute viscosity
U_1, U_2 = surface velocities

Integrated, the equation becomes

$$h^3 \frac{dp}{dx} = 6\,\eta\,(U_1 + U_2)\,h + C$$

or

$$\frac{dp}{dx} = 6\,\eta\,(U_1 + U_2)\,\frac{1}{h^2} + \frac{C}{h^3}$$

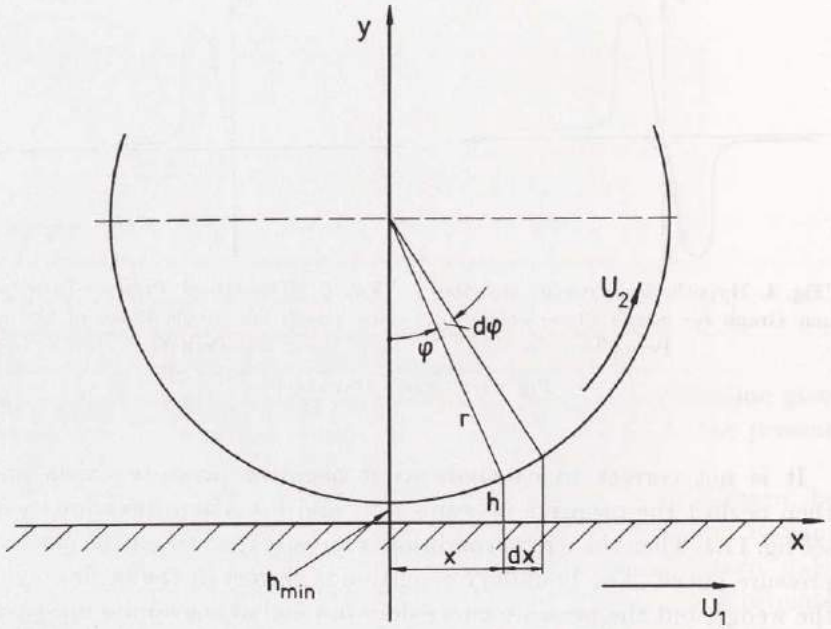

Fig. 12.1

where C is an integration constant.

If $\frac{dp}{dx} = 0$ corresponds to $h = h^*$

$$C = -6\,\eta\,(U_1 + U_2)\,h^*$$

and

$$\frac{dp}{dx} = 6\,\eta\,(U_1 + U_2)\,\frac{h - h^*}{h^3} \quad \ldots\ldots\ldots\ldots \quad 12.2$$

The oil film thickness is

$$h = h_{min} + r\,(1 - \cos\varphi)$$

where h_{min} = minimum oil film thickness

r = cylinder radius

φ = angular coordinate

and the non-dimensional thickness

$$H = \frac{h}{h_{\min}} = 1 + \psi\,(1 - \cos\varphi)$$

where

$$\psi = \frac{r}{h_{\min}}$$

Transform the expression in the following manner

$$\begin{aligned} H &= 1 + \psi\,(1 - \cos\varphi) = \\ &= 1 + \psi - \psi\cos\varphi = \\ &= (1 + \psi)\left(1 - \frac{\psi}{1 + \psi} \cdot \cos\varphi\right) \end{aligned}$$

or

$$H = (1 + \psi)\,(1 - \varepsilon\cos\varphi)$$

where

$$\varepsilon = \frac{\psi}{1 + \psi}$$

The connection between x and φ is

$$\begin{aligned} x &= r\sin\varphi \\ dx &= r\cos\varphi\,d\varphi \end{aligned}$$

Now

$$\frac{dp}{dx} = \frac{dp}{d\varphi} \cdot \frac{d\varphi}{dx} = \frac{1}{r\cos\varphi} \cdot \frac{dp}{d\varphi}$$

and eq. 12.2 may be written

$$\frac{1}{r\cos\varphi} \cdot \frac{dp}{d\varphi} = 6\,\eta\,(U_1 + U_2)\,\frac{H - H^*}{H^3\,h_{\min}^2}$$

Using the notation

$$p_0 = \frac{p\, h_{\min}}{\eta\,(U_1 + U_2)}$$

we get

$$\frac{dp_0}{d\varphi} = 6\,\psi \cdot \frac{H - H^*}{H^3} \cdot \cos\varphi \quad \ldots\ldots\ldots\ldots \quad 14.1$$

or

$$\frac{dp_0}{d\varphi} = \frac{6\,\psi}{(1+\psi)^2}\left[\frac{\cos\varphi}{(1-\varepsilon\cos\varphi)^2} - \frac{(1-\varepsilon\cos\varphi^*)\cos\varphi}{(1-\varepsilon\cos\varphi)^3}\right] \quad 14.2$$

To integrate this equation the boundary conditions must be known. These are dependent upon the oil flow through the wedge, and the flow is represented by H^* in eq. 14.1. If there is oil enough, and the weight of the oil is neglected, the pressure build-up begins at the beginning of the wedge, where $\varphi = -90°$, and ends at $\varphi = \varphi^*$ with zero derivative, which is the only condition that fulfils the continuity of the oil flow. In practice the pressure build-up will begin later because of the weight of the oil; but when the weight influences the pressure curve, the hydrodynamic pressure is negligible, and this behaviour of the oil has no effect on the calculated values. The cavitation pressure is approximately zero or atmospheric. Thus the boundary conditions for full oil film are

$$p = 0 \text{ at } \varphi = -90° = -\frac{\pi}{2}$$

$$p = 0 \text{ at } \varphi = \varphi^* \text{ where } \frac{dp}{d\varphi} = 0$$

If, now, the oil supply is less than above, the pressure curve begins later, and the value of φ^* decreases. The general boundary conditions become

$$p = 0 \text{ at } \varphi = \varphi_1 \text{ (negative angle)}$$

$$p = 0 \text{ at } \varphi = \varphi_2 = \varphi^* \text{ where } \frac{dp}{d\varphi} = 0$$

Tab. 15.1. Pressure Values at $\psi = 10000$

Curve No	φ_1	$\varphi_2 = \varphi^*$	φ	p_0
			−90	0
			−10	0,1442
			− 2	13,94
I	−90	0,3850	− 1	56,95
			−0,3850	107,9
			0	53,93
			0,3850	0
			−1,388	0
			−0,8	45,27
II	−1,388	0,35	−0,35	82,35
			0	41,18
			0,35	0
			−0,8705	0
			−0,30	53,18
III	−0,8705	0,30	0	26,59
			0,30	0
			−0,6230	0
			−0,25	31,47
IV	−0,6230	0,25	0	15,74
			0,25	0

The non-dimensional oil film pressure at the angle φ is

$$p_0 = \int_{\varphi_1}^{\varphi} \frac{dp_0}{d\varphi}\, d\varphi$$

and using eq. 14.2

$$p_0 = \frac{6\,\psi}{(1+\psi)^2}\left[\int_{\varphi_1}^{\varphi} \frac{\cos\,\varphi\; d\varphi}{(1-\varepsilon\,\cos\,\varphi)^2} - (1-\varepsilon\cos\varphi^*)\int_{\varphi_1}^{\varphi} \frac{\cos\,\varphi\, d\varphi}{(1-\varepsilon\,\cos\,\varphi)^3}\right] \quad 15.2$$

The solutions of the integrals are given in Appendix I, and thus we get

$$p_0 = \frac{6}{1+\psi}\left[-\int_{\varphi_1}^{\varphi}(j_1 - j_2) + (1-\varepsilon\cos\varphi^*)\int_{\varphi_1}^{\varphi}(j_2 - j_3)\right] \quad 15.3$$

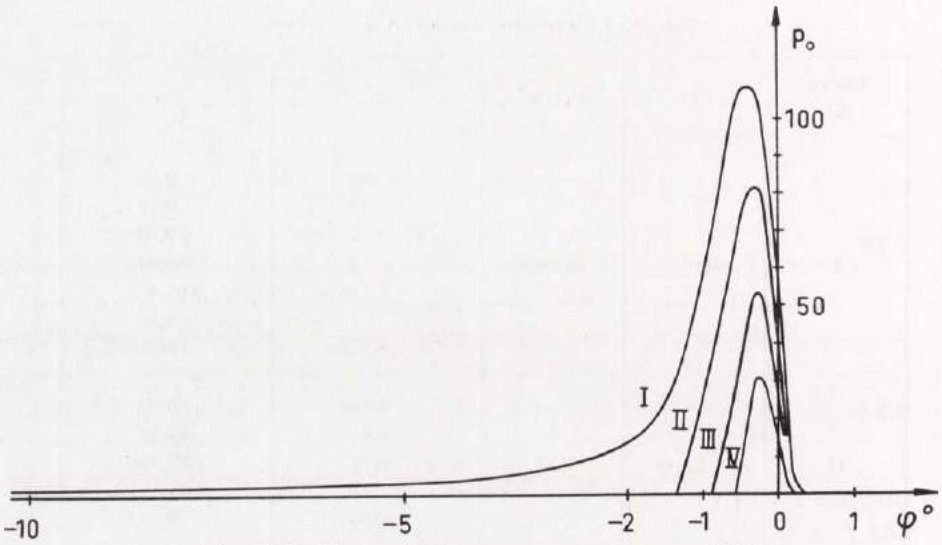

Fig. 16.1. Theoretical Pressure Curves at $\psi = 10000$

The table 15.1 gives theoretical pressure values for $\psi = 10000$. The curves are drawn in fig. 16.1. The pressure is shown to be concentrated to the closest approach. If the oil supply is enough to fill the wedge, we get curve I with the oil flow $q_0 = 0{,}6129$ and the load capacity $P_0 = 24430$. The other curves have smaller oil flows and smaller load capacities. If the oil flow is decreased to $q_0 = 0{,}5476$, we get curve IV with the load $P_0 = 2661$. A small decrease in the oil flow thus gives a large decrease in the load capacity at constant minimum oil film thickness. A starved bearing loses its load-carrying capacity.

It has been mentioned above that REYNOLDS' equation only holds for thin oil films and nearly parallel surfaces. As the equation is used here in all the space, this must be further analysed. In the interval $-10° < \varphi < 10°$ the equation holds with good accuracy. In the converging space at $\varphi < -10°$, the right hand term in eq. 11.2 gets too high values, giving too large pressure derivatives and pressure build-up. The pressure at $\varphi = -10°$ for the full solution is thus less than $p_0 = 0{,}14$, and is negligible besides the maximum pressure $p_0 = 107{,}9$. If thus REYNOLDS' equation is assumed to hold in all the interval $-90° < \varphi < \varphi^*$, this has very little influence on the calculated values. To give a further confirmation of this opinion, tab. 17.1 is calculated with the pressure build-up beginning at $\varphi_1 =$

Tab. 17.1. Theoretical Values at $\psi = 10000$

$\varphi_1{}^\circ$	-90	-60	-30	-10	-5	-3	-1	$-0{,}5$
$\varphi^{*\circ}$	0,3850	0,3850	0,3850	0,3848	0,3838	0,3800	0,3178	0,2151
P_{x_0}	444,9	443,7	434,8	391,2	326,4	248,4	47,85	4,829
P_{y_0}	24420	24420	24400	24070	22930	20680	7657	1416
P_0	24430	24430	24400	24070	22930	20680	7658	1416
β°	1,044	1,041	1,021	0,9313	0,8156	0,6884	0,3580	0,1954
p_0	0,6129	0,6129	0,6129	0,6128	0,6122	0,6099	0,5769	0,5352
A	346,4	346,2	344,7	337,4	326,1	311,4	248,6	195,4

$= -90^\circ$, -60°, -30°, -10°, -5°, -1°, and $-0{,}5^\circ$. In the first three cases φ^* has the same value and when φ_1 is changed from -90° to -30°, the load is decreased only 1 ‰. A change in φ_1 from -90° to -10° decreases the load 1,5 %. An incorrectness in the continuity equation at the widening space has therefore very little influence.

When $\varphi_1 = -90^\circ$ and $\varphi_2 = \varphi^* = 0{,}3850^\circ$, the maximum pressure from tab. 15.1 is $p_{0_{\max}} = 107{,}9$. If we use the boundary conditions

$$p_0 = 0 \text{ at } \varphi_1 = -90^\circ$$
$$p_0 = 0 \text{ at } \varphi_2 = 0^\circ$$

when $\psi = 10000$ as above

$$p_{0_{\max}} = 91{,}8 \text{ at } \varphi^* = -0{,}4678^\circ$$

The error in the last boundary condition gives 15 % decrease in maximum pressure.

3,2. Load Capacity

The load components from the pressure are per unit width

$$P_x = -\int_{-\frac{\pi}{2}}^{\frac{\pi}{2}} p \sin\varphi \, r \, d\varphi$$

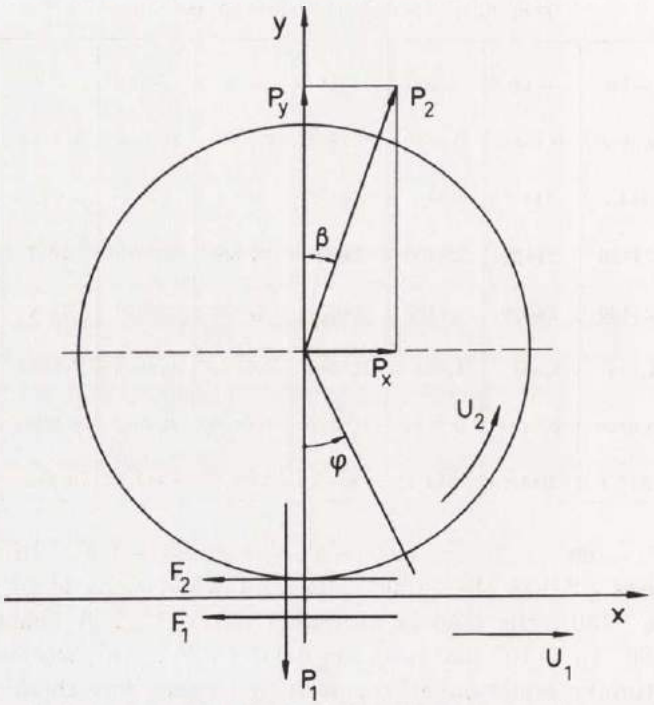

Fig. 18.1. Load Components from Pressure and Shear Stress in the Oil

$$P_y = \int_{-\frac{\pi}{2}}^{\frac{\pi}{2}} p \cos \varphi \, r \, d\varphi$$

$$P_1 = \int_{-\frac{\pi}{2}}^{\frac{\pi}{2}} p \cos \varphi \, r \, d\varphi = P_y$$

when p is derived from eq. 15.2 at $\varphi_1 < \varphi < \varphi^*$.

$$p = 0 \text{ at } \varphi < \varphi_1 \text{ and at } \varphi > \varphi^*.$$

Now we have for the load component in the x-direction

$$P_x = -\int_{\varphi_1}^{\varphi^*} p \sin \varphi \, r \, d\varphi = -\int \frac{\eta \, (U_1 + U_2)}{h_{\min}} \cdot p_0 \sin \varphi \, r \, d\varphi$$

Non-dimensionally

$$P_{x0} = \frac{P_x}{\eta\,(U_1 + U_2)} = -\,\psi \int p_0 \sin\varphi\, d\varphi =$$

$$= -\,\psi \,\Big|\, p_0\,(-\cos\varphi) + \psi \int (-\cos\varphi)\,\frac{dp_0}{d\varphi}\, d\varphi =$$

$$= -\,\psi \int \frac{dp_0}{d\varphi}\,\cos\varphi\, d\varphi =$$

$$= -\,\frac{6\,\psi^2}{(1+\psi)^2}\left[\int_{\varphi_1}^{\varphi^*} \frac{\cos^2\varphi\, d\varphi}{(1-\varepsilon\cos\varphi)^2} - (1-\varepsilon\cos\varphi^*)\int_{\varphi_1}^{\varphi^*} \frac{\cos^2\varphi\, d\varphi}{(1-\varepsilon\cos\varphi)^3}\right]$$

The solutions of the integrals are given in Appendix I and

$$P_{x0} = -\,6\,\Big|_{\varphi_1}^{\varphi^*} (\varphi - 2\,j_1 + j_2) + 6\,(1-\varepsilon\cos\varphi^*)\,\Big|_{\varphi_1}^{\varphi^*} (j_1 - 2\,j_2 + j_3)$$

From eq. 15.3 with $p_0 = 0$ at $\varphi = \varphi^*$

$$-\,\Big|_{\varphi_1}^{\varphi^*} (j_1 - j_2) + (1-\varepsilon\cos\varphi^*)\,\Big|_{\varphi_1}^{\varphi^*} (j_2 - j_3) = 0$$

and thus

$$P_{x0} = -\,6\,\Big|_{\varphi_1}^{\varphi^*} (\varphi - j_1) + 6\,(1-\varepsilon\cos\varphi^*)\,\Big|_{\varphi_1}^{\varphi^*} (j_1 - j_2)$$

The load component in the y-direction is

$$P_y = \int_{\varphi_1}^{\varphi^*} p\,\cos\varphi\, r\, d\varphi = \int_{\varphi_1}^{\varphi^*} \frac{\eta\,(U_1+U_2)}{h_{\min}} \cdot p_0\,\cos\varphi\, r\, d\varphi$$

or non-dimensionally

$$P_{y0} = \frac{P_y}{\eta\,(U_1+U_2)} = \psi \int p_0\,\cos\varphi\, d\varphi =$$

$$= \psi \left| p_0 \sin \varphi - \psi \int \sin \varphi \, \frac{dp_0}{d\varphi} \, d\varphi \right. =$$

$$= - \psi \int \frac{dp_0}{d\varphi} \sin \varphi \, d\varphi =$$

$$= - \frac{6 \psi^2}{(1+\psi)^2} \left[\int_{\varphi_1}^{\varphi^*} \frac{\sin \varphi \cos \varphi \, d\varphi}{(1 - \varepsilon \cos \varphi)^2} - (1 - \varepsilon \cos \varphi^*) \int_{\varphi_1}^{\varphi^*} \frac{\sin \varphi \cos \varphi \, d\varphi}{(1 - \varepsilon \cos \varphi)^3} \right]$$

In the same manner

$$P_{10} = \frac{P_1}{\eta \, (U_1 + U_2)} = P_{y0}$$

Solving the integrals we get

$$P_{y0} = P_{10} = 6 \left| \ln (1 - \varepsilon \cos \varphi) + \right.$$

$$+ 6 \left| \frac{1}{1 - \varepsilon \cos \varphi} + 6 (1 - \varepsilon \cos \varphi^*) \right| \frac{1}{1 - \varepsilon \cos \varphi} -$$

$$- 3 (1 - \varepsilon \cos \varphi^*) \left| \frac{1}{(1 - \varepsilon \cos \varphi)^2} \right.$$

For the numerical evaluations the electronic computer ALWAC III E was used. The load is shown in fig. 21.1.

When $\varphi_1 = -90°$ and $\varphi_2 = \varphi^* = 0{,}3850°$ at $\psi = 10000$, the load $P_{y0} = 24420$.

If the boundaries are $\varphi_1 = -90°$ and $\varphi_2 = 0°$, which corresponds to KNESCHKE's theory, $P_{y0} = 20060$. The decrease is 18 %.

The total load capacity from the pressure per unit width of the cylinder and the load angle are

$$P_{20} = \frac{P_2}{\eta \, (U_1 + U_2)} = \sqrt{P_{x0}^2 + P_{y0}^2}$$

$$\operatorname{tg} \beta = \frac{P_{x0}}{P_{y0}}$$

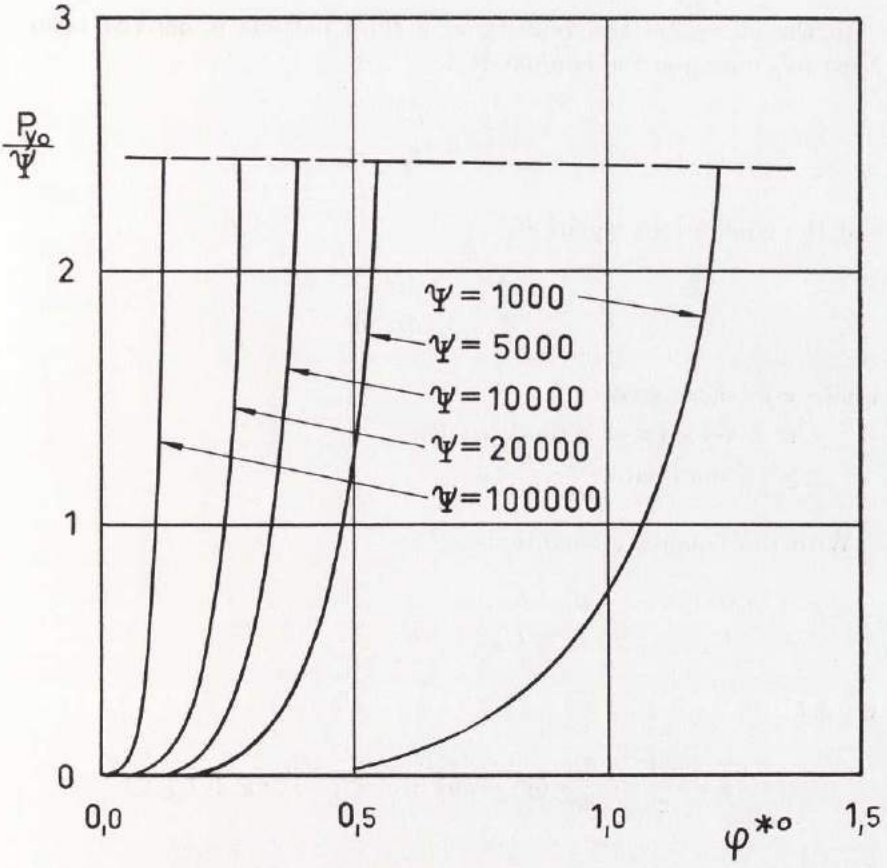

Fig. 21.1. Load Capacity

The load components from the shear stress of the oil are per unit width

$$F_1 = -\int_{-\frac{\pi}{2}}^{\frac{\pi}{2}} \tau_{y=0} \cos\varphi \; r \; d\varphi$$

$$F_2 = \int_{-\frac{\pi}{2}}^{\frac{\pi}{2}} \tau_{y=h} \cos\varphi \; r \; d\varphi$$

The component in the y-direction on the cylinder is negligible beside the pressure component.

In the oil region the velocity of a fluid particle is derived from Newton's equation for laminar flow

$$\tau = \eta \frac{du}{dy}$$

and the equilibrium equation

$$\frac{d\tau}{dy} = \frac{dp}{dx}$$

where τ = shear stress
u = velocity of a fluid particle
y = coordinate

With the boundary conditions

$y = 0$	$y = h$
$u = U_1$	$u = U_2$

we get

$$u = \frac{1}{2\eta} \cdot \frac{dp}{dx} (y^2 - hy) + \frac{U_2 - U_1}{h} \cdot y + U_1$$

and thus

$$\tau = \frac{1}{2} \cdot \frac{dp}{dx} (2y - h) - \eta \cdot \frac{U_1 - U_2}{h}$$

The shear stresses at the two surfaces are

$$\tau_{y=0} = -\frac{h}{2} \cdot \frac{dp}{dx} - \eta \cdot \frac{U_1 - U_2}{h}$$

$$\tau_{y=h} = \frac{h}{2} \cdot \frac{dp}{dx} - \eta \cdot \frac{U_1 - U_2}{h}$$

In the cavitation region there is a straight line velocity distribution, and considering the oil and air strips in the region, the mean shear stress can be written, compare ref. (1), p. 54

$$\tau = -\frac{h^*}{h} \cdot \eta \cdot \frac{U_1 - U_2}{h}$$

In the interval $-\frac{\pi}{2} < \varphi < \varphi_1$, there is no oil contact between the surfaces. In the interval $\varphi_1 < \varphi < \varphi^*$ there is an oil region, and in the last interval, $\varphi^* < \varphi < \frac{\pi}{2}$, there is a cavitation region with oil and air strips.

Now the component at the plane surface is

$$F_1 = \int_{\varphi_1}^{\varphi^*} \frac{h}{2} \cdot \frac{dp}{dx} \cos\varphi \, r \, d\varphi + \int_{\varphi_1}^{\varphi^*} \eta \cdot \frac{U_1 - U_2}{h} \cdot \cos\varphi \, r \, d\varphi +$$

$$+ \int_{\varphi^*}^{\frac{\pi}{2}} \frac{h^*}{h} \cdot \eta \cdot \frac{U_1 - U_2}{h} \cdot \cos\varphi \, r \, d\varphi =$$

$$= \eta \, (U_1 + U_2) \left[\frac{1}{2} \int_{\varphi_1}^{\varphi^*} H \frac{dp_0}{d\varphi} \, d\varphi + \frac{1-k}{1+k} \cdot \psi \int_{\varphi_1}^{\varphi^*} \frac{\cos\varphi \, d\varphi}{H} + \right.$$

$$\left. + \frac{1-k}{1+k} \cdot \psi \, H^* \int_{\varphi^*}^{\frac{\pi}{2}} \frac{\cos\varphi \, d\varphi}{H^2} \right]$$

where $k = \frac{U_2}{U_1}$.

The first term may be transformed in the following manner

$$\int H \frac{dp_0}{d\varphi} d\varphi = \Big| H \, p_0 - \int p_0 \, \psi \sin\varphi \, d\varphi$$

The first term at the right hand side is zero, and the second term is equal to P_{x0}. Thus

$$F_1 = \eta \, (U_1 + U_2) \left[\frac{P_{x0}}{2} + \frac{1-k}{1+k} \cdot \frac{\psi}{1+\psi} \int_{\varphi_1}^{\varphi^*} \frac{\cos\varphi \, d\varphi}{1 - \varepsilon \cos\varphi} + \right.$$

$$\left. + \frac{1-k}{1+k} \cdot \frac{\psi}{1+\psi} (1 - \varepsilon \cos\varphi^*) \int_{\varphi^*}^{\frac{\pi}{2}} \frac{\cos\varphi \, d\varphi}{(1 - \varepsilon \cos\varphi)^2} \right]$$

Non-dimensionally with solved integrals

$$F_{10}=\frac{F_1}{\eta\,(U_1+U_2)}=\frac{P_{x0}}{2}+\frac{1-k}{1+k}\left[-\int_{\varphi_1}^{\varphi^*}(\varphi-j_1)-(1-\varepsilon\cos\varphi^*)\int_{\varphi^*}^{\frac{\pi}{2}}(j_1-j_2)\right]$$

Calling the parenthesis A

$$F_{10}=\frac{F_1}{\eta\,(U_1+U_2)}=\frac{P_{x0}}{2}+\frac{1-k}{1+k}\cdot A$$

After the same lines the component on the cylinder is found to be

$$F_{20}=\frac{F_2}{\eta\,(U_1+U_2)}=\frac{P_{x0}}{2}-\frac{1-k}{1+k}\cdot A$$

Control now the equilibrium of the oil film in fig. 18.1. In the x- and y-directions respectively we have

$$F_1+F_2-P_x=0$$
$$P_1-P_y=0$$

If the expressions are introduced, we find that the two equations are exactly satisfied.

3,3. Oil Flow

As the width is infinite, there is no side flow, and the continuity gives constant oil flow in every section through the wedge. At $\varphi=\varphi^*$ and $h=h^*$, there is a straight line velocity distribution, and the oil flow per unit width is

$$q=\frac{(U_1+U_2)\,h^*}{2}$$

In fig. 25.1 the oil flow through the wedge is shown. The pressure build-up begins at φ_1 and ends at φ^*, where the cavitation starts. The continuity is satisfied in every section. In practice the weight of the oil will probably influence the theoretical boundary conditions giving a shorter oil wedge, which, however, has very little influence on the calculated quantities. In theory an infinite number of strips is assumed. In practice the number will be finite.

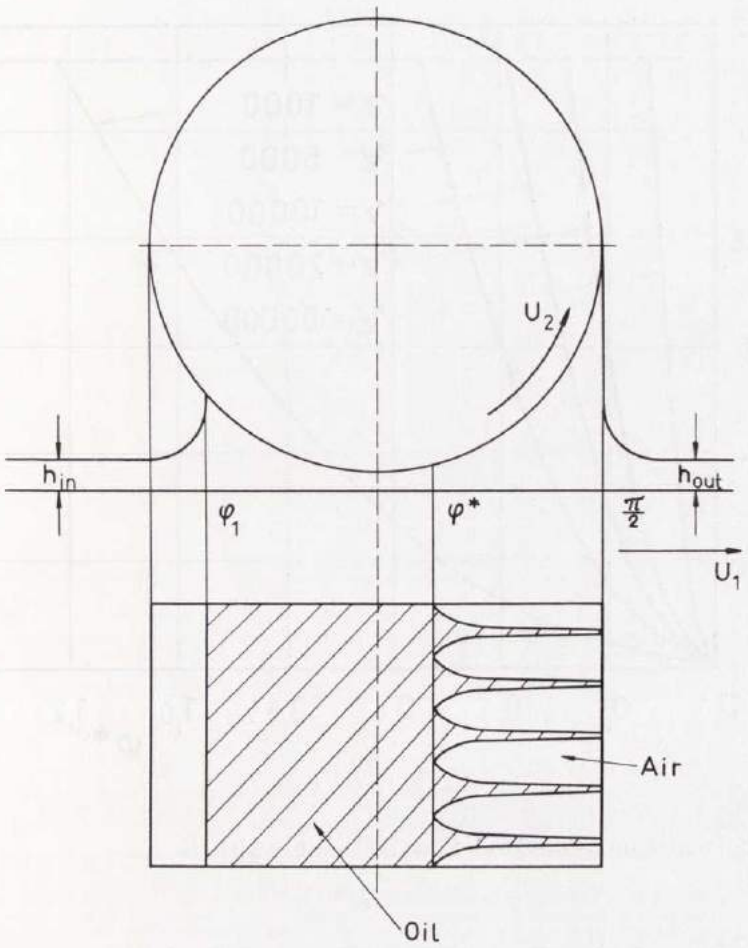

Fig. 25.1

The continuity gives, see fig. 25.1

$$q = U_1 h_{in} = \frac{(U_1 + U_2) h^*}{2} = U_1 h_{out}$$

and

$$h_{in} = h_{out} = \frac{1 + k}{2} \cdot h^*$$

If $U_1 = U_2$ giving $k = 1$, we get $h_{in} = h_{out} = h^*$. A very thin oil film layer is thus needed to fill the wedge.

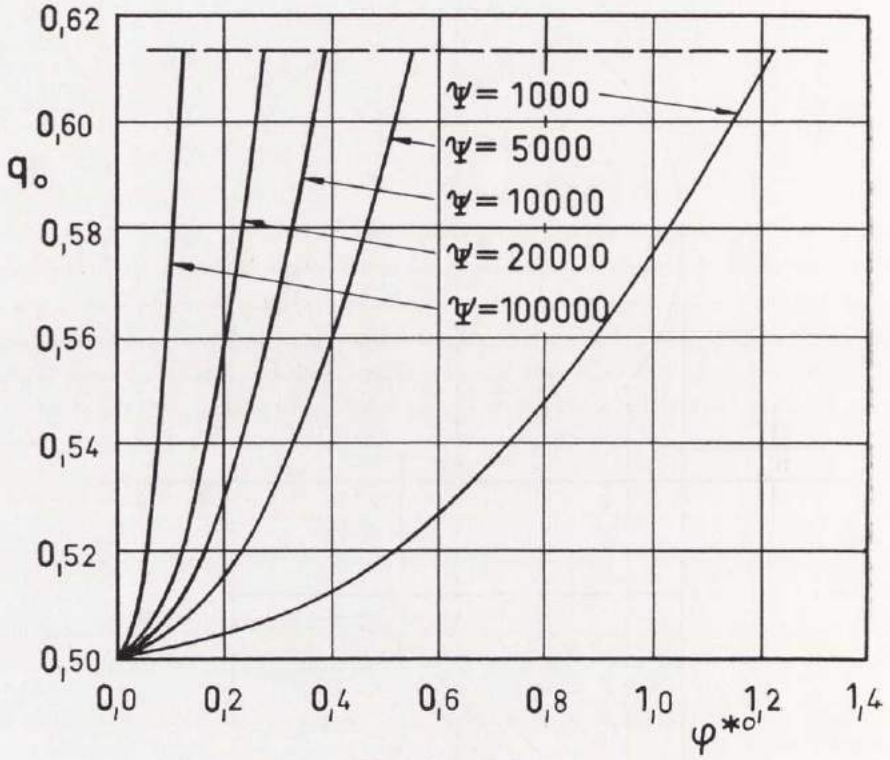

Fig. 26.1. Oil Flow

The non-dimensional oil flow per unit width is

$$q_0 = \frac{q}{(U_1 + U_2)\, h_{\min}} = \frac{H^*}{2}$$

where

$$H^* = 1 + \psi\,(1 - \cos\varphi^*) = (1 + \psi)\,(1 - \varepsilon \cos\varphi^*)$$

$$\varepsilon = \frac{\psi}{1 + \psi}$$

The non-dimensional oil film thickness may be written as an infinite series

$$H^* = 1 + \psi\left(\frac{\varphi^{*2}}{2!} - \frac{\varphi^{*4}}{4!} + \frac{\varphi^{*6}}{6!} - \ldots\ldots\right)$$

Curves of the oil flow are shown in fig. 26.1.

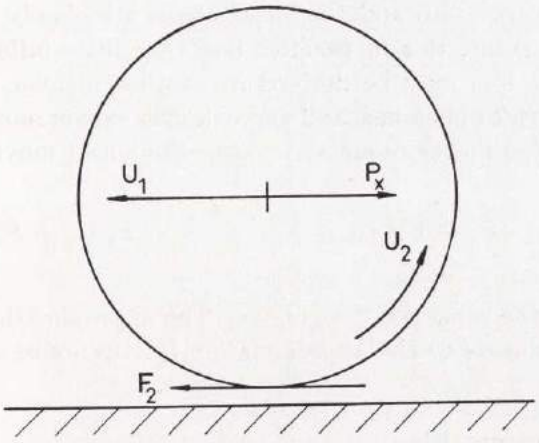

Fig. 27.1

3,4. Power Loss

The power loss in the oil per unit width is

$$E = F_1 U_1 + F_2 U_2 = \eta (U_1 + U_2)(F_{10} U_1 + F_{20} U_2) =$$

$$= \eta (U_1 + U_2)^2 \left(F_{10} \cdot \frac{U_1}{U_1 + U_2} + F_{20} \cdot \frac{U_2}{U_1 + U_2} \right) =$$

$$= \eta (U_1 + U_2)^2 \frac{1}{1 + k} (F_{10} + k F_{20})$$

where $k = \dfrac{U_2}{U_1}$.

Non-dimensionally

$$E_0 = \frac{E}{\eta (U_1 + U_2)^2} = \frac{1}{1 + k} (F_{10} + k F_{20})$$

Substitution gives

$$E_0 = \frac{P_{x0}}{2} + \left(\frac{1 - k}{1 + k} \right)^2 A$$

In the power loss calculation it is assumed that the force F_2 is located at the point of closest approach, which gives an approxima-

tion. As the pressure and the shear stress are closely concentrated around this point, this in practice has very little influence.

The power loss may be derived in another manner. In fig. 27.1 the plane surface is at rest and the cylinder axis is moving with the speed U_1. The power required to keep the wheel moving is

$$E = (P_x - F_2)\, U_1 + F_2\, r \cdot \frac{U_2}{r} = F_1\, U_1 + F_2\, U_2$$

which gives the same result as above. The approximation mentioned above corresponds to the approximation in REYNOLDS' equation.

3,5. Temperature Rise

If all the power generated heats the oil, the energy equation gives

$$E = c\, \varrho\, q\, \Delta t$$

and

$$\Delta t = \frac{E}{c\, \varrho\, q} = \frac{\eta\, (U_1 + U_2)^2\, E_0}{c\, \varrho\, (U_1 + U_2)\, h_{\min}\, q_0}$$

Non-dimensionally

$$\Delta t_0 = c\, \varrho \cdot \frac{\Delta t\, h_{\min}}{\eta\, (U_1 + U_2)} = \frac{E_0}{q_0}$$

3,6. Relative Power Loss

The relative power loss defined as power loss per unit load is

$$f = \frac{E}{P_y} = \frac{\eta\, (U_1 + U_2)^2\, E_0}{\eta\, (U_1 + U_2)\, P_{y0}}$$

or

$$\frac{f}{U_1 + U_2} = \frac{E_0}{P_{y0}}$$

4. Some Applications

4,1. Torqueless Cylinder

Consider a rotating cylinder at zero torque moved by the viscous stresses from the plane surface, which is moving at the speed U_1. The shear force F_2 in fig. 18.1 vanishes and

$$F_{20} = \frac{P_{x0}}{2} - \frac{1-k}{1+k} \cdot A = 0$$

Solving this equation we get

$$k = \frac{A - \frac{P_{x0}}{2}}{A + \frac{P_{x0}}{2}}$$

For full oil film, i. e. $\varphi_1 = -90°$, the following table gives k.

ψ	k
1000	0,245
5000	0,223
10000	0,218
20000	0,214
100000	0,209

For different values of φ^* at $\psi = 10000$ the following table gives the k-values.

φ^*	k
0,3850	0,218
0,35	0,694
0,30	0,871
0,25	0,949
0,20	0,983
0,15	0,996

4,2. The Plane Surface without Shear Force

Consider the case where the plane surface is moving without shear force. Thus the force F_1 in fig. 18.1 vanishes and we get

$$F_{10} = \frac{P_{x0}}{2} + \frac{1-k}{1+k} \cdot A = 0$$

which gives

$$k = \frac{A + \frac{P_{x0}}{2}}{A - \frac{P_{x0}}{2}}$$

The k-values from this equation are the reciprocals of the previous k-values.

4,3. One Cylinder Driving Another One

Two wheels are rolling on a wet surface, which is at rest see fig. 31.1. The right wheel has an applied torque, which gives the driving action. The left wheel is driven and has zero torque.

The radii of the wheels, the applied loads, the velocity U_1, and the oil viscosity is known. A full oil film is assumed.

The unknowns are ψ', ψ'', k', and k''.

As the left wheel is torqueless we have

$$F_2'(\psi', k') = 0$$

The equilibrium gives

$$F_2'' - P_x' - P_x'' = 0$$

or

$$F_1'(\psi', k') = F_1''(\psi'', k'')$$

The upward pressure resultant must be equal to the applied load and

$$P_y'(\psi', k') = P'$$

$$P_y''(\psi'', k'') = P''$$

From these four equations the four unknowns can be determined.

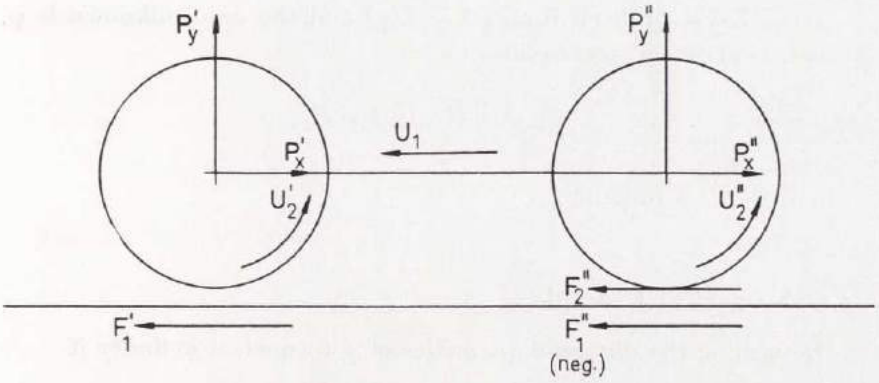

Fig. 31.1

4,4. Determination of the Minimum Space

In this case the load, the radius, the viscosity, the velocities, and the oil flow are given. Then the value of $h_{\min}$ has to be determined. The unknowns are ψ and φ^* using the definition

$$\psi = \frac{r}{h_{\min}}$$

The continuity gives

$$q = \frac{(U_1 + U_2)\, h^*}{2}$$

where h^* is a function of ψ and φ^*.

The equilibrium gives

$$P_y = \eta\, (U_1 + U_2)\, P_{y0}$$

where P_{y0} too is a function of ψ and φ^*. We now have two equations to determine the two unknowns.

It must be considered that φ^* at every ψ has an upper limit, see fig. 26.1, giving the condition

$$\frac{q}{(U_1 + U_2)\, h_{\min}} = q_0 < q_{0_{\lim}}\, (\approx 0{,}613)$$

If we have a full oil film, $\varphi^* = f(\psi)$ and the only unknown is ψ, which is given by the equation

$$P_y = \eta (U_1 + U_2) P_{y0}$$

where P_{y0} is a function of ψ.

4,5. Numerical Example

Determine the different quantities of a torqueless cylinder if

$$P_y = 10 \text{ N/cm}$$
$$r = 10 \text{ mm}$$
$$U_1 = 2 \text{ m/s}$$
$$h_{\min} = 0{,}001 \text{ mm}$$

We have

$$\psi = \frac{r}{h_{\min}} = \frac{10}{0{,}001} = 10000$$

As there is no torque applied at the cylinder $k = 0{,}218$, see chap. 4,1.

Now

$$P_y = \eta (U_1 + U_2) P_{y0}$$

and the viscosity

$$\eta = \frac{P_y}{P_{y0} (U_1 + U_2)} = \frac{1000}{24420 \cdot 2 \cdot 1{,}218} = 0{,}0168 \text{ Ns/m}^2$$

The component from the pressure in the x-direction is equal to the shear force and

$$P_x = F_1 = \eta (U_1 + U_2) P_{x0} =$$
$$= 0{,}0168 \cdot 2 \cdot 1{,}218 \cdot 444{,}9 = 18{,}2 \text{ N/m} = 0{,}182 \text{ N/cm}$$

The maximum pressure

$$p_{max} = \frac{\eta\,(U_1 + U_2)}{h_{min}} \cdot p_{0_{max}} = \frac{0{,}0168 \cdot 2 \cdot 1{,}218}{0{,}000001} \cdot 107{,}9 =$$

$$= 4{,}42 \cdot 10^6\ \mathrm{N/m^2} = 4{,}42\ \mathrm{N/mm^2}$$

The oil flow

$$q = (U_1 + U_2)\, h_{min}\, q_0 = 2 \cdot 1{,}218 \cdot 0{,}000001 \cdot 0{,}6129 =$$

$$= 0{,}00000149\ \mathrm{m^3/s\ m} = 0{,}000894\ \mathrm{l/min\ cm}$$

The non-dimensional power loss

$$E_0 = \frac{P_{x0}}{2} + \left(\frac{1-k}{1+k}\right)^2 A = \frac{444{,}9}{2} + \left(\frac{0{,}782}{1{,}218}\right)^2 346{,}4 = 365$$

The power loss

$$E = \eta\,(U_1 + U_2)^2\, E_0 = 0{,}0168 \cdot 2^2 \cdot 1{,}218^2 \cdot 365 = 36{,}4\ \mathrm{Nm/s\ m} =$$

$$= 0{,}364\ \mathrm{W/cm}$$

The temperature rise

$$\Delta t = \frac{1}{c\,\varrho} \cdot \frac{\eta\,(U_1 + U_2)}{h_{min}} \cdot \frac{E_0}{q_0} = \frac{1}{2000 \cdot 900} \cdot \frac{0{,}0168 \cdot 2 \cdot 1{,}218}{0{,}000001} \cdot \frac{365}{0{,}6129} =$$

$$= 13{,}5^\circ\ \mathrm{C}$$

5. Conclusion

In this work the hydrodynamic theory for the contact between a cylinder and a plane surface is studied. The boundary conditions of the pressure curves are discussed. The surfaces are assumed to be rigid and the calculations thus hold for light loads. The viscosity of the oil is constant. Due consideration is taken to cavitation in the oil film. The pressure build-up is found to take place in a narrow band around the point of closest approach. The width is assumed to be infinite. As in practice the oil film thickness is very thin, this represents a good approximation. When studying journal bearings on the other hand, calculations made for infinite width must not be used in the cases of finite width.

Values of load capacity, oil flow, and power loss are calculated and given in Appendix II. It is studied how these quantities are influenced when the oil supply is varied.

6. Appendix I: Solution of Integrals

$$j_1 = \int \frac{d\varphi}{1 - \varepsilon \cos \varphi} = \frac{\gamma}{\sqrt{1 - \varepsilon^2}}$$

$$j_2 = \int \frac{d\varphi}{(1 - \varepsilon \cos \varphi)^2} = \frac{\gamma + \varepsilon \sin \gamma}{\sqrt{(1 - \varepsilon^2)^3}}$$

$$j_3 = \int \frac{d\varphi}{(1 - \varepsilon \cos \varphi)^3} = \frac{\left(1 + \frac{\varepsilon^2}{2}\right)\gamma + 2\,\varepsilon \sin \gamma + \frac{\varepsilon^2}{4} \cdot \sin 2\gamma}{\sqrt{(1 - \varepsilon^2)^5}}$$

where

$$\cos \gamma = \frac{\cos \varphi - \varepsilon}{1 - \varepsilon \cos \varphi}$$

$$\int \frac{\sin \varphi \, d\varphi}{1 - \varepsilon \cos \varphi} = \frac{1}{\varepsilon} \cdot \ln (1 - \varepsilon \cos \varphi)$$

$$\int \frac{\sin \varphi \, d\varphi}{(1 - \varepsilon \cos \varphi)^2} = -\frac{1}{\varepsilon} \cdot \frac{1}{1 - \varepsilon \cos \varphi} = -\frac{\cos \gamma}{1 - \varepsilon^2}$$

$$\int \frac{\sin \varphi \, d\varphi}{(1 - \varepsilon \cos \varphi)^3} = -\frac{1}{2\,\varepsilon} \cdot \frac{1}{(1 - \varepsilon \cos \varphi)^2} = -\frac{\cos \gamma + \frac{\varepsilon}{4} \cdot \cos 2\gamma}{(1 - \varepsilon^2)^2}$$

$$\int \frac{\cos \varphi \, d\varphi}{1 - \varepsilon \cos \varphi} = -\frac{1}{\varepsilon} \int d\varphi + \frac{1}{\varepsilon} \int \frac{d\varphi}{1 - \varepsilon \cos \varphi} = -\frac{1}{\varepsilon} (\varphi - j_1)$$

$$\int \frac{\cos \varphi \, d\varphi}{(1 - \varepsilon \cos \varphi)^2} = -\frac{1}{\varepsilon} \int \frac{d\varphi}{1 - \varepsilon \cos \varphi} + \frac{1}{\varepsilon} \int \frac{d\varphi}{(1 - \varepsilon \cos \varphi)^2} =$$

$$= -\frac{1}{\varepsilon} (j_1 - j_2)$$

$$\int \frac{\cos\varphi\, d\varphi}{(1-\varepsilon\cos\varphi)^3} = -\frac{1}{\varepsilon}\int \frac{d\varphi}{(1-\varepsilon\cos\varphi)^2} + \frac{1}{\varepsilon}\int \frac{d\varphi}{(1-\varepsilon\cos\varphi)^3} =$$

$$= -\frac{1}{\varepsilon}(j_2 - j_3)$$

$$\int \frac{\sin\varphi\cos\varphi\, d\varphi}{1-\varepsilon\cos\varphi} = -\frac{1}{\varepsilon}\int \sin\varphi\, d\varphi + \frac{1}{\varepsilon}\int \frac{\sin\varphi\, d\varphi}{1-\varepsilon\cos\varphi} =$$

$$= \frac{1}{\varepsilon}\cdot\cos\varphi + \frac{1}{\varepsilon^2}\cdot\ln(1-\varepsilon\cos\varphi)$$

$$\int \frac{\sin\varphi\cos\varphi\, d\varphi}{(1-\varepsilon\cos\varphi)^2} = -\frac{1}{\varepsilon^2}\cdot\ln(1-\varepsilon\cos\varphi) - \frac{1}{\varepsilon^2}\cdot\frac{1}{1-\varepsilon\cos\varphi}$$

$$\int \frac{\sin\varphi\cos\varphi\, d\varphi}{(1-\varepsilon\cos\varphi)^3} = \frac{1}{\varepsilon^2}\cdot\frac{1}{1-\varepsilon\cos\varphi} - \frac{1}{2\varepsilon^2}\cdot\frac{1}{(1-\varepsilon\cos\varphi)^2}$$

$$\int \frac{\cos^2\varphi\, d\varphi}{1-\varepsilon\cos\varphi} = -\frac{1}{\varepsilon}\int \cos\varphi\, d\varphi + \frac{1}{\varepsilon}\int \frac{\cos\varphi\, d\varphi}{1-\varepsilon\cos\varphi} =$$

$$= -\frac{1}{\varepsilon}\cdot\sin\varphi - \frac{1}{\varepsilon^2}(\varphi - j_1)$$

$$\int \frac{\cos^2\varphi\, d\varphi}{(1-\varepsilon\cos\varphi)^2} = \frac{1}{\varepsilon^2}(\varphi - j_1) - \frac{1}{\varepsilon^2}(j_1 - j_2) = \frac{1}{\varepsilon^2}(\varphi - 2j_1 + j_2)$$

$$\int \frac{\cos^2\varphi\, d\varphi}{(1-\varepsilon\cos\varphi)^3} = \frac{1}{\varepsilon^2}(j_1 - j_2) - \frac{1}{\varepsilon^2}(j_2 - j_3) = \frac{1}{\varepsilon^2}(j_1 - 2j_2 + j_3)$$

7. Appendix II: Tables of Calculated Values

The following non-dimensional expressions are used:

$$\psi = \frac{r}{h_{\min}}$$

$$p_0 = \frac{p\, h_{\min}}{\eta\,(U_1 + U_2)}$$

$$P_0 = \frac{P}{\eta\,(U_1 + U_2)}$$

$$q_0 = \frac{q}{(U_1 + U_2)\, h_{\min}}$$

$\psi = 1000$

$\varphi^{*\circ}$	1,216	1,20	1,10	1,00	0,80	0,60
$\varphi_1{}^\circ$	−90,00	−9,299	−4,277	−3,124	−2,008	−1,343
P_{x0}	130,7	77,10	29,33	14,64	3,750	0,7764
P_{y0}	2411	2041	1193	748,6	289,0	84,55
P_0	2414	2043	1194	748,8	289,0	84,56
β°	3,104	2,163	1,408	1,120	0,7434	0,5261
q_0	0,6126	0,6097	0,5924	0,5762	0,5487	0,5274
A	107,8	98,10	85,46	78,28	67,37	58,23

$\psi = 5000$

φ^*	0,5444	0,50	0,45	0,39	0,35	0,30
$\varphi_1{}^\circ$	−90,00	−2,062	−1,420	−1,040	−0,8673	−0,6943
P_{x0}	310,2	75,67	34,12	13,83	7,387	3,146
P_{y0}	12190	6512	3853	2027	1275	669,2
P_0	12190	6513	3853	2027	1275	669,2
β°	1,458	0,6657	0,5074	0,3911	0,3320	0,2694
q_0	0,6129	0,5953	0,5772	0,5580	0,5467	0,5344
A	244,2	197,3	176,0	158,8	148,8	137,2

$\psi = 10000$

$\varphi^{*\circ}$	0,3850	0,35	0,30	0,25	0,20	0,15
$\varphi_1{}^\circ$	−90,00	−1,389	−0,8705	−0,6230	−0,4541	−0,3206
P_{x0}	444,9	98,12	32,83	11,11	3,274	0,7364
P_{y0}	24420	12340	5880	2661	1049	324,3
P_0	24430	12340	5881	2661	1049	324,3
β°	1,044	0,4557	0,3199	0,2391	0,1788	0,1301
q_0	0,6129	0,5933	0,5685	0,5476	0,5305	0,5171
A	346,4	272,1	237,9	211,7	188,7	167,6

$\psi = 20000$

$\varphi^{*\circ}$	0,2723	0,25	0,23	0,19	0,15
$\varphi_1{}^\circ$	−90,00	−1,030	−0,7542	−0,4964	−0,3470
P_{x0}	635,3	151,1	79,28	23,79	6,248
P_{y0}	48890	22420	16380	7238	2672
P_0	48900	22420	16380	7238	2672
β°	0,7489	0,3861	0,2774	0,1883	0,1338
q_0	0,6129	0,5952	0,5806	0,5550	0,5343
A	491,0	389,3	358,5	312,5	274,4

$\psi = 100000$

$\varphi^{*\circ}$	0,1218	0,11	0,10	0,08	0,06
$\varphi_1{}^\circ$	−90,00	−0,4264	−0,3118	−0,2005	−0,1340
P_{x0}	1439	293,1	145,4	37,02	7,375
P_{y0}	244600	119100	74650	27860	8371
P_0	244700	119100	74650	27860	8371
β°	0,3372	0,1410	0,1116	0,07614	0,05048
q_0	0,6130	0,5922	0,5762	0,5487	0,5274
A	1101	854,4	789,8	673,7	582,2

8. References

1. Floberg, L.: The Infinite Journal Bearing, Considering Vaporization. Gothenburg, 1957.
2. Floberg, L.: Experimental Investigation of Power Loss in Journal Bearings, Considering Cavitation. Gothenburg, 1959.
3. Gatcombe, E. K.: Lubrication Characteristics of Involute Spur Gears. Trans. Am. Soc. Mech. Engrs, vol. 67, p. 177, 1945.
4. Jakobsson, B. and Floberg, L.: The Finite Journal Bearing, Considering Vaporization. Gothenburg, 1957.
5. Jakobsson, B. and Floberg, L.: The Partial Journal Bearing. Gothenburg, 1958.
6. Jakobsson, B. and Floberg, L.: The Rectangular Plane Pad Bearing. Gothenburg, 1958.
7. Jakobsson, B. and Floberg, L.: The Centrally Loaded Partial Journal Bearing. Gothenburg, 1959.
8. Kneschke, A.: Rollreibung auf spurbildender Fahrbahn. Ingenieur-Archiv XXV. Band, 1957.
9. Reynolds, O.: On the Theory of Lubrication .... Phil. Trans. Roy. Soc., vol. 177, p. 157, 1886.

Forts. fr. omsl. 2:dra sida.

178. OLVING, SVEN, *A new method for space charge wave interaction studies. I.* 12 s. 1956. Kr. 3: —. (Avd. Elektroteknik. 51.)
179. HANSBO, SVEN, *The critical load of rectangular frames analysed by convergence methods.* 47 s. 1956. Kr. 11: —. (Avd. Väg- och Vattenbyggnad. Byggnadsteknik. 25.)
180. WESTBERG, VIDOR, *Measurements of noise radiation at 10 cm from glow lamps. Preliminary report.* 14 s. 1956. Kr. 4: 50. (Avd. Elektroteknik. 52.)
181. SVENSSON, S. I., HELLGREN, G. and PERERS, O., *The Swedish radioscientific solar eclipse expedition to Italy, 1952. Preliminary report.* 30 s. 1956. Kr. 8: —. (Avd. Elektroteknik. 53.)
182. WAX, NELSON, *A note on design considerations for a proposed auroral radar.* 16 s. 1957. Kr. 3: —. (Avd. Elektroteknik. 54.)
183. JOSHI, G. H., *The electromagnetic interaction between two crossing electron streams. I.* 31 s. 1957. Kr. 8: —. (Avd. Elektroteknik. 55.)
184. SMITH, BENGT, *Dry methods for removing hydrogen sulphide from gases.* 65 s. 1957. Kr. 15: —. (Avd. Kemi och Kemisk Teknologi. 34.)
185. EKELÖF, S., BJÖRK, N., and DAVIDSON, R., *Large signal behaviour of directly heated thermistors.* 31 s. 1957. Kr. 8: —. (Avd. Elektroteknik. 56.)
186. CARLSSON, BENGT und LARSSON, HANS, *Wirkungsgrad und Selbsthemmung einfacher Umlaufgetriebe.* 48 s. 1957. Kr. 9: —. (Avd. Maskinteknik. 8.)
187. AURELL, CARL G., *The equivalent transmission line of a linear four-terminal network. Calculations with cascade-connected four-terminal networks.* 39 s. 1957. Kr. 6: —. (Avd. Elektroteknik. 57.)
188. LUNDHOLM, R., *Induced overvoltage-surges on transmission lines and their bearing on the lightning performance at medium voltage networks.* 117 s. 1957. Kr. 19: —. (Avd. Elektroteknik. 58.)
189. FLOBERG, LEIF, *The infinite journal bearing, considering vaporization.* 83 s. 1957. Kr. 13: —. (Avd. Maskinteknik. 9.)
190. JAKOBSSON, BENGT, and FLOBERG, LEIF, *The finite journal bearing, considering vaporization.* 117 s. 1957. Kr. 19: 50. (Avd. Maskinteknik. 10.)
191. CHAKO, NICHOLAS, *Characteristic curves on planes in the image space.* 49 s. 1957. Kr. 15: —. (Avd. Allmänna Vetenskaper. 12.)
192. EKELÖF, STIG, *The development and decay of the magnetic flux in a non-delayed telephone relay.* 50 s. 1957. Kr. 15: —. (Avd. Elektroteknik. 59.)
193. BJÖRKLUND, KJELL, *Bestämning av porslins draghållfasthet.* 78 s. 1958. Kr. 15: —. (Institutionen för Silikatkemisk Forskning. 39.)
194. GRANHOLM, PER, *Sound insulation of single leaf walls.* 48 s. 1958. Kr. 8: —. (Avd. Väg- och Vattenbyggnad. Byggnadsteknik. 26.)
195. GRANHOLM, HJALMAR, *Om vattengenomslag i murade väggar med särskild hänsyn till tegel som fasadmaterial.* 172 s. 1958. Kr. 16: —. (Avd. Väg- och Vattenbyggnad. Byggnadsteknik. 27).
196. MEOS, JOHAN, and OLVING, SVEN, *On the origin of radar echoes associated with auroral activity.* 20 s. 1958. Kr. 5: —. (Avd. Elektroteknik. 60.)
197. JOSHI, G. H., *The electromagnetic interaction between two crossing electron streams. II.* 10 s. 1958. Kr. 3: 50. (Avd. Elektroteknik. 61.)
198. WILHELMSSON, HANS, *The interaction between an obliquely incident plane electromagnetic wave and an electron beam. II.* 32 s. 1958. Kr. 7: —. (Avd. Elektroteknik. 62.)
199. KÄRRHOLM, GUNNAR, *A method of iteration applied to beams resting on springs.* 50 s. 1958. Kr. 12: —. (Avd. Allm. Vetenskaper. 13.)
200. JAKOBSSON, BENGT, and FLOBERG, LEIF, *The partial journal bearing.* 60 s. 1958. Kr. 14: —. (Avd. Maskinteknik. 11.)
201. KÄRRHOLM, GUNNAR, *Influence functions of elastic plates divided in strips.* 18 s. 1958. Kr. 4: 50. (Avd. Väg- och Vattenbyggnad. Byggnadsteknik. 28.)
202. RÅDE, LENNART, *Sampling planes for acceptance sampling by variables using the range.* 34 s. 1958. Kr. 9:50. (Avd. Allm. Vetenskaper. 14.)
203. JAKOBSSON, BENGT, and FLOBERG, LEIF, *The rectangular plane pad bearing.* 44 s. 1958. Kr. 5: —. (Avd. Maskinteknik. 12.)
204. ASPLUND, SVEN OLOF, *Column-beams and suspension bridges analyzed by »Green's matrix».* 36 s. 1958. Kr. 7: —. (Avd. Väg- och Vattenbyggnad. Byggnadsteknik. 29.)
205. WILHELMSSON, HANS, *On the properties of the electron beam in the presence of an axial magnetic field of arbitrary strength.* 32 s. 1958. Kr. 7: 50. (Avd. Elektroteknik. 63.)
206. WILHELMSSON, HANS, *The interaction between an obliquely incident plane electromagnetic wave and an electron beam. III.* 17 s. 1958. Kr. 5:—. (Avd. Elektroteknik. 64.)
207. HEDVALL, ARVID J., *On the influence of pre-treatment and transition processes on the adsorption capacity and the reactivity of various types of glass and silica.* 39 s. 1959. Kr. 8: —. (Institutionen för Silikatkemisk Forskning. 40.)

Forts. å omsl. 4:de sida.

Forts. fr. omsl. 3:dje sida.

208. KÄRRHOLM, GUNNAR, *A flow problem solved by strip method.* 22 s. 1959. Kr. 4: 50. (Avd. Allm. Vetenskaper. 15.)
209. GRANHOLM, HJALMAR, *Allmän teori för beräkning av armerad betong.* 228 s. 1959. Kr. 20:—. (Avd. Väg- och Vattenbyggnad. Byggnadsteknik. 30.)
210. LARS G. LIDIN, *On helical-spring suspension.* 75 s. 1959. Kr. 15: —. (Avd. Maskinteknik. 13.)
211. BJÖRK, NILS, *Theory of the indirectly heated thermistor.* 46 s. 1959. Kr. 10: —. (Avd. Elektroteknik. 65.)
212. CARLSSON, ORVAR, *The influence of submicroscopic pores on the resistance of bricks towards frost.* 13 s. 1959. Kr. 3:50—. (Institutionen för Silikatkemisk Forskning. 41.)
213. GRANHOLM, HJALMAR, *KAM 40, KAM 60 och KAM 90.* 41 s. 1959. Kr. 3: 50. (Avd. Väg- och Vattenbyggnad. Byggnadsteknik. 31.)
214. JAKOBSSON, BENGT and FLOBERG, LEIF, *The centrally loaded partial journal bearing.* Kr. 7: 50. 35 s. 1959. (Avd. Maskinteknik. 14.)
215. FLOBERG, LEIF, *Experimental investigation of power loss in journal bearings, considering cavitation.* Kr. 3: 50. 16 s. 1959. (Avd. Maskinteknik. 15.)

Pris kronor 8:—

OMSLAGET TRYCKT HOS
ELANDERS BOKTRYCKERI AKTIEBOLAG
GÖTEBORG 1959

AMERICAN SOCIETY OF
LUBRICATION ENGINEERS

5 North Wabash Avenue Chicago 2, Illinois

Preprint No. 60AM 5A-1

BOUNDARY CONDITIONS OF CAVITATION REGIONS IN JOURNAL BEARINGS

by Leif Floberg,
Chalmers Institute of Technology,
Gothenburg, Sweden

Presented at the 15th ASLE Annual Meeting
April, 1960 in Cincinnati, Ohio

Price 75 cents per copy (50 cents to ASLE members)

Boundary Conditions of Cavitation Regions in Journal Bearings

By Leif Floberg*

The behaviour of the oil in a cavitation region is studied. Boundary conditions of the pressure distribution at the inlet and at the outlet border of such a region are given. Calculation of the power loss in a cavitated zone is demonstrated.

Introduction

For a long time there has been some confusion in the hydrodynamic theory regarding the cavitation occurring in divergent parts of the bearings. Often arbitrary boundary conditions are used to give the pressure build-up. However, it is not enough to have the continuity equation satisfied in the oil region. The continuity of flow must also be satisfied within the cavitation region and at the boundaries between the two regions. As cavitation influences the pressure build-up, it is not reasonable to do calculations in cases where cavitation occurs, before the behaviour of the oil in such a region is studied. Some authors treat the ruptured region as an oil region, others as an air region. None of these assumptions can be accepted, as they violate the continuity condition. The cavitation problem must be solved, before charts and tables for bearing design can be made.

In the chapter "Application" two partial journal bearing cases are numerically treated. These have the bearing angle 120° and diverging parts of 40° and 30° resp. at the leading edge.

*Research Assistant, Institute of Machine Elements,
Chalmers University of Technology, Gothenburg,
Sweden

Nomenclature

h	Oil film thickness
P	Load per unit width
$P_O = \frac{P\psi^2}{\mu U}$	Non-dimensional load per unit width
p	Pressure
$p_O = \frac{p\psi^2}{\mu \omega}$	Non-dimensional pressure
U, V	Surface velocities
x, z	Coordinates
α	Angle between leading edge and load line
β	Bearing angle
ε	Non-dimensional eccentricity
Θ_A	Angular coordinate of the leading edge
μ	Absolute viscosity
ν	Width-diameter ratio
τ	Shear stress
$\psi = \frac{C}{r}$	Radial clearance / journal radius
ω	Angular velocity

Oil Film Theory

The hydrodynamic pressure in a bearing is derived from the well-known Reynolds' equation. In its original form from 1886, ref. (11), it is written

$$\frac{d}{dx}\left(h^3 \frac{dp}{dx}\right) + \frac{d}{dz}\left(h^3 \frac{dp}{dz}\right) = 6\mu \left\{(U_O + U_1) \frac{dh}{dx} + 2 V_1\right\} \qquad (1)$$

If this equation gives positive pressure all over the bearing, the solution is the correct one. If, however, the solution gives sub-atmospheric pressures over parts of the bearing area, this means that the oil film will rupture and the solution must be rejected. Then further considerations are needed.

Cavitation Theory

Bearing tests show that film rupture produces cavitation zones of essentially constant pressure. The oil film can withstand sub-atmospheric pressures to some extent. When a bearing starts rotating, it is possible to measure 50 - 70% vacuum in a cavitated region. However, this condition is not stationary, as air is continuously expelled from the oil making the ruptured zone larger and increasing the pressure. After a quarter of an hour the vacuum may be 10 - 30%, and after some hours it is only about 2 - 4%. For practical bearing cases, it is thus correct to assume atmospheric pressure in the cavitation region.

To solve a bearing case where cavitation occurs it is necessary to have a theory for the behaviour of the oil at the boundaries of and within such a region. The location of the boundaries is also to be determined, which is another complication of the problem.

At the beginning of the ruptured oil film the continuity condition requires zero pressure derivative in the direction of motion, if the oil adheres to the surfaces and there are no pressures lower than the atmospheric pressure, and thus

$$p = \frac{\partial p}{\partial x} = 0 \qquad (2)$$

where zero is the atmospheric pressure.

This condition at the end of the pressure build-up is nowadays widely accepted. In the ruptured region the oil flow is divided into strips and between the strips is air, which is stationary. The appearance of a cavitation region is shown in fig. 1. The oil adheres to the surfaces and the section of the strips is approximately rectangular. This behaviour can be experimentally verified by using transparent bearing material. In theory an infinite number of strips is assumed; but in practice there will be a finite number of them giving insignificant deviation from the present theory. The oil and sir strips have been shown in experiments by Cole-Hughes (2). However, they used an oil hole for the lubricant supply, which is unsuitable, as the corresponding case has not been theoretically tabulated.

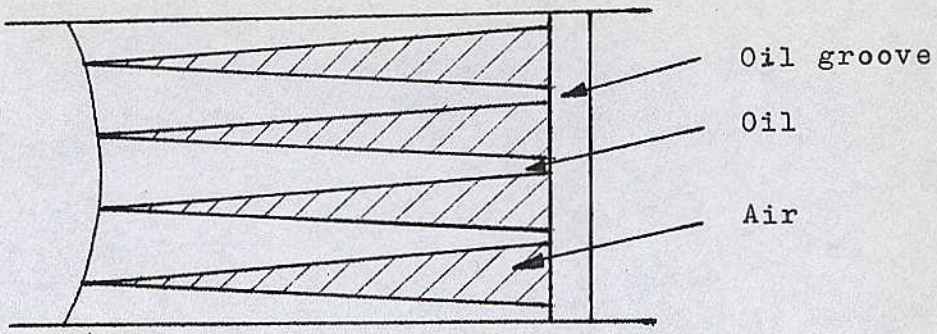

Fig. 1. Oil Strips in a Cavitation Region

In front of the cavitation region there is sometimes part of the pressure curve below the constant cavitation pressure. This part decreases with time and it may be assumed that eventually it vanishes. The appearance of a cavitation region, when we have such a slope of the pressure curve, is shown in fig. 2. Because of the very small sub-atmospheric pressures, the pressure build-up will be very slightly influenced and the difference between the areas of the air strips in the two cases is fully negligible. The location of the zero pressure derivative is in both cases approximately the same.

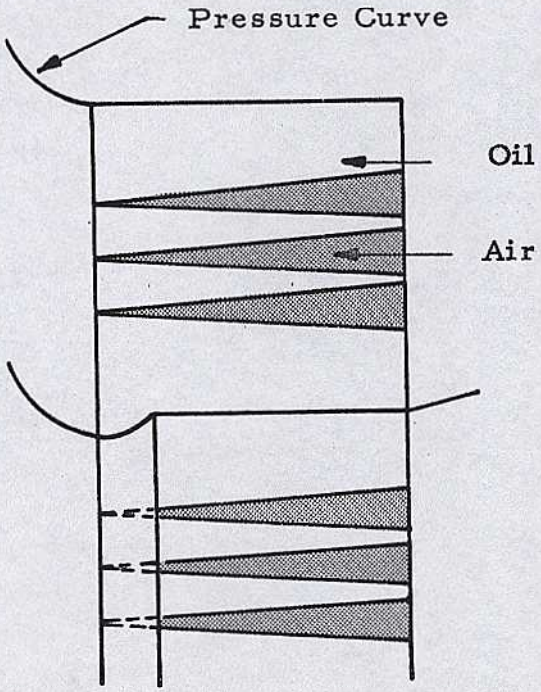

Fig. 2. The Form of the Air Strips in a Cavitation Region

In order to determine the location of the boundary at the end of the ruptured region, we must study the continuity of flow through this one. As the pressure is constant, there are no pressure flows and there is only flow in the x-direction, see fig. 3. The oil quantity entering the region over the width Δz at the inlet boundary must therefore leave over the same width at the outlet boundary. Thus the following equation must be satisfied

$$\frac{Uh^*}{2} \cdot \Delta z = \frac{Uh}{2} \cdot \Delta z - \frac{h^3}{12\mu} \left[\frac{\partial p}{\partial x} \Delta z + \frac{\partial p}{\partial z} \Delta x\right] \tag{3}$$

where h^* is the oil film thickness at the inlet boundary of the ruptured region. The above equation determines the location of the outlet boundary of this region.

As here $\lim_{\Delta z \to 0} \frac{\Delta x}{\Delta z} = -\frac{dx}{dz}$, i.e. the derivative of the border line, the equation becomes

$$\frac{Uh^*}{2} = \frac{Uh}{2} - \frac{h^3}{12\mu} \left[\frac{\partial p}{\partial x} - \frac{\partial p}{\partial z} \cdot \frac{dx}{dz}\right] \tag{4}$$

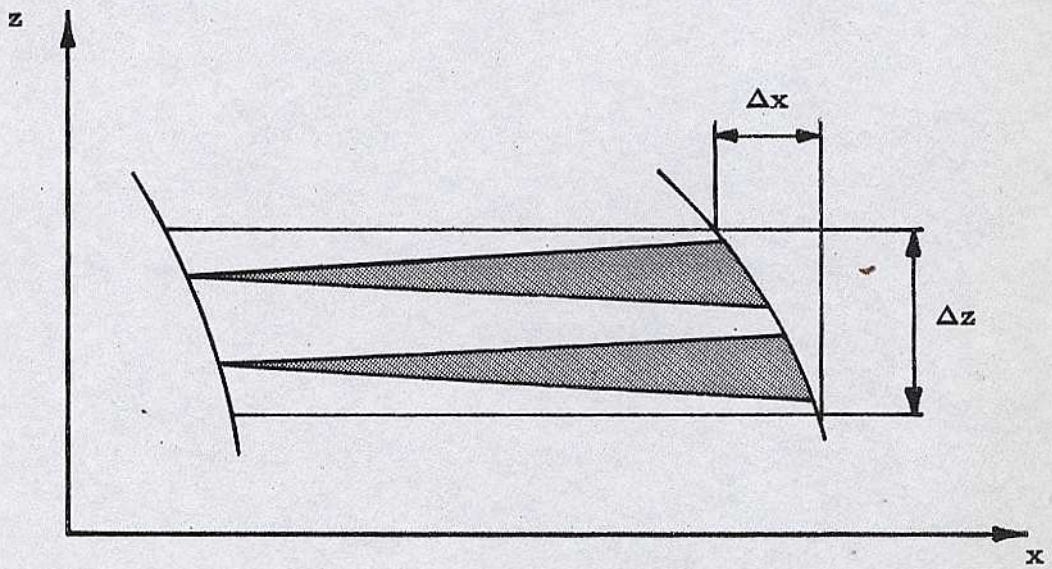

Fig. 3. Oil Continuity through a Cavitation Region

As eq. 1 is usually solved by the relaxation method, a probable boundary of the cavitation region is assumed and then adjusted until the eqs. 2 and 4 are satisfied everywhere along the border. Now the continuity of flow is satisfied both in the oil and in the cavitation region and also at the boundaries between the two regions and the solution is thus the desired one.

At the end of film rupture there is a jump in the pressure derivatives, as the viscosity value is changed from that of air to that of oil. This is the same sort of jump, as that in the derivative in vertical direction of the hydrostatic pressure at a water surface.

Power Loss at Cavitation

Several authors, among them Cameron-Wood (1), Sassenfeld-Walther (12), and Raimondi-Boyd (9), assume that there is a full oil film with a straight line velocity distribution in the cavitated region. This does not agree with the continuity condition, as the oil film thickness varies and the oil film is divided into strips. Thus they give too high values of the power loss in this region. The air strips must be taken into account. As the width of the strips is inversely proportional to the oil film thickness, the mean shear stress can be written

$$\tau = \frac{h^*}{h} \cdot \mu \cdot \frac{U}{h}$$

Strip flow in the cavitation region has earlier been treated by Wilcock-Rosenblatt (13). However, when calculating the reduced power loss, they assume that cavitation starts at the minimum space, and in the oil region they neglect the pressure flow term, which makes two approximations.

Application

In many journal bearing cases the oil groove will be located at the maximum space or in the converging part of the bearing. Then the pressure build-up will start at the groove and end with zero derivative. This case is widely used and needs no further discussion as long as pressure distribution and load capacity are concerned. However, there is still some confusion in literature due to the power loss calculation as treated above and also in the refs. (3), (4), (5), and (8).

Now a case with a cavitation region after the groove will be studied. The groove is then located in the diverging space. This case has recently been treated by Raimondi (10). However, he uses the boundary condition 2, which holds for the end of the pressure build-up, also at the inlet boundary of the pressure. This violates the continuity condition 4 and gives erroneous pressure distributions. As there is a straight line velocity distribution both at the inlet and outlet borders of the cavitation region, and the oil film thickness is not the same, it is obvious that the continuity is not satisfied.

Fig. 4 shows the pressure distribution derived by Raimondi for a 120° partial journal bearing at the eccentricity 0,8 and with a diverging part of 40° length at the leading edge. The width of the bearing is equal to its diameter. Fig. 5 shows the same case calculated after the above theory (eq. 4). There is an obvious deviation between the two pressure distributions. Raimondi gives the load number $P_0 = 0,134$ and the load location $\alpha/\beta = 0,676$. The above theory gives $P_0 = 0,108$ and $\alpha/\beta = 0,711$.

Raimondi's pressure distribution for the same case, but with a diverging part of 30° length at the leading edge is shown in fig. 6. The pressure distribution for the last case using the above theory is given in fig. 7. Also here there is a considerable move of the boundary. Raimondi gives $P_0 = 0,208$ and $\alpha/\beta = 0,655$. The above theory gives 0,200 and 0,652 resp. The diversity in bearing width is due to the fact that Raimondi uses different scales in the two directions.

The relaxation is here made with the network 5 x 12 shown in the figures, and therefore the solutions are somewhat approximate.

The two cases treated above are unpractical and the bearing quantities calculated by Raimondi are slightly affected by the above cavitation theory. Therefore the above discussion influences very little on Raimondi's extremely good work.

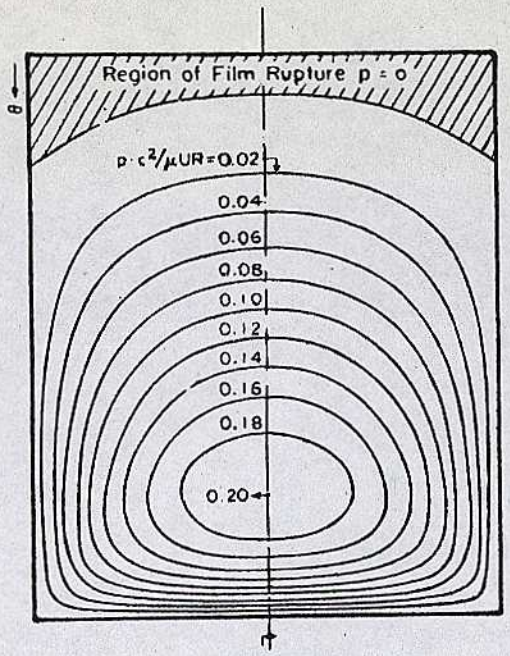

FIG. 3(c). Typical pressure distribution for diverging-converging film shape ($\epsilon = 0.8$, $\theta_A = -40°$, $\alpha/\beta = 0.676$).

Fig. 4. From Raimondi

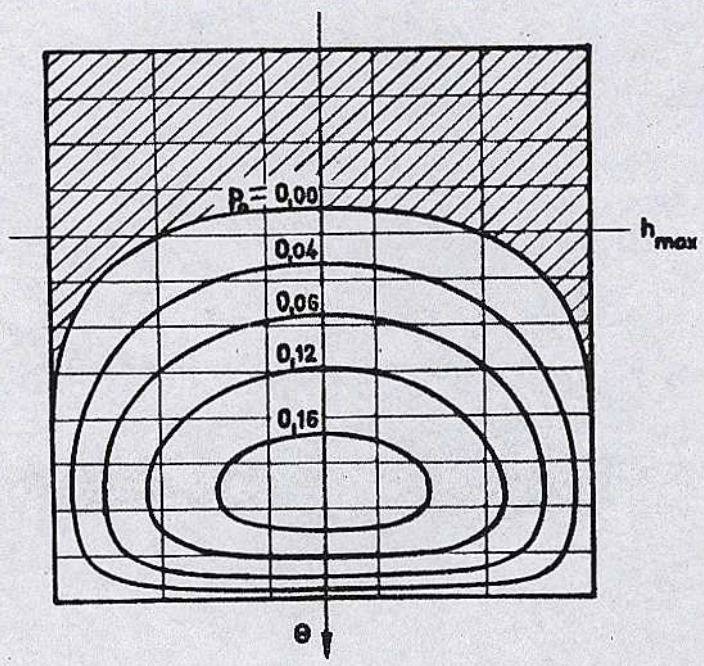

Fig. 5. Pressure Distribution ($\beta=120°$, $\nu=1$, $\varepsilon=0,8$, and $\Theta_A=-40°$)

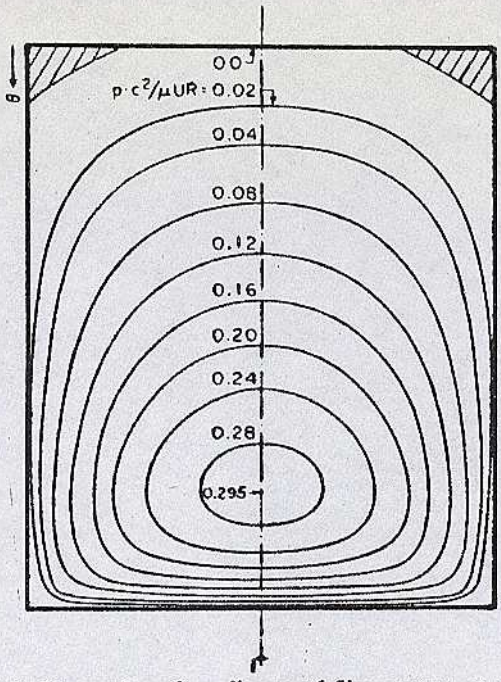

FIG. 3(d). Illustration of small area of film rupture at entrance ($\epsilon = 0.8$, $\theta_A = -30°$).

Fig. 6. From Raimondi

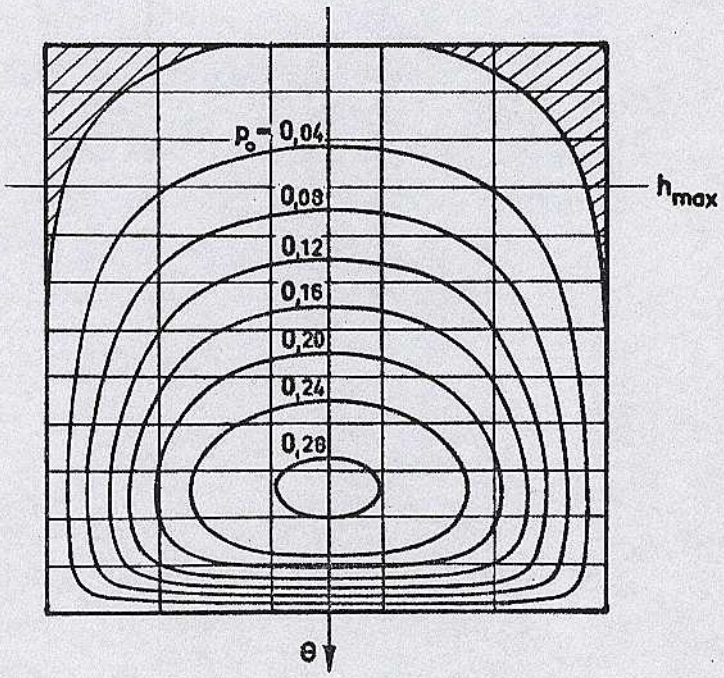

Fig. 7. Pressure Distribution ($\beta = 120°$, $\nu = 1$, $\varepsilon = 0,8$, and $\Theta_A = -30°$)

Acknowledgement

This paper has been produced during lubrication research at the Institute of Machine Elements, Chalmers University of Technology, Gothenburg, Sweden. Previous reports, see ref. (3) - (8).
I wish to express my thanks to Professor B. Jakobsson, head of the Institute, for his kind support. I should also like to thank the Swedish Technical Research Council for their sponsorship.

References

1. Cameron, A. and Wood, W. L.: The Full Journal Bearing. Proc. Instn. Mech. Engrs., vol. 161, p. 59, 1949.
2. Cole, J. A. and Hughes, C. J.: Oil Flow and Film Extent in Complete Journal Bearings. The Engineer, March 16, 1956.
3. Floberg, L.; The Infinite Journal Bearing Considering Vaporization. Gothenburg, 1957.
4. Floberg, L.: Experimental Investigation of Power Loss in Journal Bearings, Considering Cavitation. Gothenburg, 1959.
5. Jakobsson, B. and Floberg, L.: The Finite Journal Bearing, Considering Vaporization. Gothenburg, 1957.
6. Jakobsson, B. and Floberg, L.: The Partial Journal Bearing. Gothenburg, 1958.
7. Jakobsson, B. and Floberg, L.: The Rectangular Plane Pad Bearing. Gothenburg, 1958.
8. Jokobsson, B. and Floberg, L.: The Centrally Loaded Partial Journal Bearing. Gothenburg, 1959.
9. Raimondi, A. A. and Boyd, J.: A Solution for the Finite Journal Bearing and Its Application to Analysis and Design-III. Trans. Am. Soc. Lubr. Engrs., vol. 1, No. 1, 1958.
10. Raimondi, A. A.: A Theoretical Study of the Effect of Offset Loads on the Performance of a 120° Partial Journal Bearing. Trans. Am. Soc. Lubr. Engrs., vol. 2, No. 1, 1959.
11. Reynolds, O.: On the Theory of Lubrication.... Phil. Trans. Roy. Soc., vol. 177, p. 157, 1886.
12. Sassenfeld, H. and Walther, A.: Gleitlagerberechnungen. VDI-Forschungsheft 441, 1954.
13. Wilcock, D. F. and Rosenblatt, M.: Oil Flow, Key Factor in Sleeve Bearing Performance. Trans. Am. Soc. Mech. Engr., vol. 74, p. 849, 1952.

CHALMERS TEKNISKA HÖGSKOLAS HANDLINGAR
TRANSACTIONS OF CHALMERS UNIVERSITY OF TECHNOLOGY
GOTHENBURG, SWEDEN
Nr 231 (Avd. Maskinteknik 19) 1960

THE OPTIMUM THRUST TILTING-PAD BEARING

BY

LEIF FLOBERG

Report No. 12 from the Institute of Machine Elements
Chalmers University of Technology
Gothenburg, Sweden
1960

GUMPERTS FÖRLAG
GÖTEBORG

Av Chalmers Tekniska Högskolas Handlingar hava tidigare utkommit:

Fullständig förteckning över Chalmers Tekniska Högskolas Handlingar lämnas av Chalmers Tekniska Högskolas Bibliotek, Göteborg.

151. Hedvall, J. A., *Reactions with activated solids.* 23 s. 1954 Kr. 5: —. (Institutionen för Silikatkemisk Forskning. 32.)
152. Smith, Cyril Stanley, *The microstructure of polycrystalline materials.* 49 s. 1954. Kr. 9: 50 (Institutionen för Silikatkemisk Forskning. 33.)
153. Selberg, Arne, *Norske erfaringer fra bygging av små hengebroer.* 20 s. 1954. Kr. 4: —. (Avd. Väg- och Vattenbyggnad. Byggnadsteknik. 21.)
154. Granholm, Hjalmar, *Armerat trä.* 96 s. 1954. Kr. 9: — (Avd. Väg- och Vattenbyggnad. Byggnadsteknik. 22.)
155. Wilhelmsson, Hans, *The interaction between an obliquely incident plane electromagnetic wave and an electron beam. I.* 31 s. 1954. Kr. 7: —. (Avd. Elektroteknik. 42.)
156. Olving, Sven, *Electromagnetic wave propagation on helical conductors inbedded in dielectric medium.* 14 s. 1955. Kr. 3: —. (Avd. Elektroteknik. 43.)
157. Olving, Sven, *Amplification of the traveling wave tube at high beam current. I.* 11 s. 1955. Kr. 3: —. (Avd. Elektroteknik. 44.)
158. Hedvall, J. A., Nordengren, Sven, und Liljegren, B., *Über die thermische Zersetzung von Kalziumsulfat bei niedrigen Temperaturen.* 18 s. 1955. Kr. 5: — (Institutionen för Silikatkemisk Forskning. 34.)
159. Dahlgren, Sven-Eric, *On the break-down of thixotropic materials.* 18 s. 1955. Kr. 3: 50. (Institutionen för Silikatkemisk Forskning. 35.)
160. Sandford, Folke, och Liljegren, Berne, *Torkningen av råtegel och dennas inverkan på teglets frostbeständighet.* 22 s. 1955. Kr. 3: —. (Institutionen för Silikatkemisk Forskning. 36.)
161. Wallman, Henry, *Automatic noise-factor meter.* 17 s. 1955. Kr. 3: —. (Avd. Elektroteknik. 45.)
162. Sandford, Folke, and Fransson, Stig, *The refractoriness of some types of quartz and quartzite. II.* 24 s. 1955. Kr. 5: —. (Institutionen för Silikatkemisk Forskning. 37.)
163. Lindblad, Anders *Konstruktion av linjer för moderna handelsfartyg.* 176 s. 1955. Kr. 20: —. (Avd. Skeppsbyggeri. 6.)
164. Svartholm, Nils, *Two problems in the theory of the slowing down of neutrons by collisions with atomic nuclei.* 15 s. 1955. Kr. 5: —. (Avd. Allmänna Vetenskaper. 10.)
165. Persson, Per, *Bostadsvaneundersökning utförd i hyreslägenheter byggda 1947 i Göteborg, Torpaområdet.* 86 s. 1955. Kr. 12: —. (Avd. Arkitektur. 3.)
166. Hansson, P. R., *Undersökning av mullitbildning i keramiska produkter.* 29 s. 1955. Kr. 6: —. (Institutionen för Silikatkemisk Forskning. 38.)
167. Ekelöf, Stig, *Die Temperaturverteilung in einem gleichstromdurchflossenen langen Metallzylinder mit kreisförmigem Querschnitt.* 38 s. 1955. Kr. 10: —. (Avd. Elektroteknik. 46.)
168. Wilhelmsson, Hans, *On the reflection of electromagnetic waves from a dielectric cylinder.* 17 s. 1955. Kr. 4: 50. (Avd. Elektroteknik. 47.)
169. Björk, N., and Davidson, R., *Small signal behaviour of directly heated thermistors.* 43 s. 1955. Kr. 11: —. (Avd. Elektroteknik. 48.)
170. Forestier, H., *Tendances actuelles dans la formation de l'ingenieur chimiste: selection, orientution, specialisation; amelioration de son efficience.* 13 s. 1956. Kr. 2: 50. (Avd. Kemi och Kemisk Teknologi. 33.)
171. Wax, Nelson, *On the ring current hypothesis.* 32 s. 1956. Kr. 7: —. (Avd. Elektroteknik. 49.)
172. Elgeskog, Erik, *Photoformer analysis and design.* 40 s. 1956. Kr. 8:50. (Avd. Elektroteknik. 50.)
173. Anzelius, Adolf, *Bimolekulare Reaktion von zwei in Mischung vorliegenden Substanzen mit einer dritten Substanz.* 8 s. 1956. Kr. 5: —. (Avd. Allm. Vetenskaper. 11.)
174. Reinius, Erling, *Model studies for the extension of the harbour of Gothenburg.* 38 s. 1956. Kr. 6: —. (Avd. Väg- och Vattenbyggnad. Byggnadsteknik. 23.)
175. Zimen, K. E., *Diffusion von Edelgasatomen die durch Kernreaktion in festen Stoffen gebildet werden.* 7 s. 1956. Kr. 2: —. (Institutionen för Kärnkemi. 1.)
176. Inthoff, W., und Zimen, K. E., *Kinetik der Diffusion radioaktiver Edelgase aus festen Stoffen nach Bestrahlung.* 16 s. 1956. Kr. 4: —. (Institutionen för Kärnkemi. 2.)
177. Granholm, Hjalmar, *Puts och lättbetong.* 45 s. 1956. Kr. 3: —. (Avd. Väg- och Vattenbyggnad. Byggnadsteknik. 24.)

Forts. å omsl. 3:dje sida

CHALMERS TEKNISKA HÖGSKOLAS HANDLINGAR
TRANSACTIONS OF CHALMERS UNIVERSITY OF TECHNOLOGY
GOTHENBURG, SWEDEN
Nr 231 (Avd. Maskinteknik 19) 1960

THE OPTIMUM THRUST TILTING-PAD BEARING

BY

LEIF FLOBERG

Report No. 12 from the Institute of Machine Elements
Chalmers University of Technology
Gothenburg, Sweden
1960

GÖTEBORG 1960
ELANDERS BOKTRYCKERI AKTIEBOLAG

Manuscript received by the Publications Committee,
Chalmers University of Technology, Nov. 25th, 1959.

Preface

At the Institute of Machine Elements, Chalmers University of Technology, Sweden, hydrodynamic lubrication has been treated under the leadership of the head of the institute, Professor B. JAKOBSSON. The main problem has been cavitation in journal bearings and problems connected with it. Earlier seven reports, (1)—(3) and (5)—(8), have been published.

This work is an extension of an earlier work ref. (7) on plane pad bearings. It treats optimum conditions of a thrust bearing consisting of a number of pads.

I wish to express my thanks to the Swedish Technical Research Council for their sponsorship.

Leif Floberg
Tekn. lic.

Contents

Page

Preface 3

1. Introduction 5

2. Notation 6

3. Optimum Analysis 8

3,1. General Considerations 8

3,2. Influence of a Scale Factor 9

3,3. Influence of Width-Length Ratio and Number of Pads 10

3,4. Schedule for Calculation 14

3,5. Example 15

4. Charts of Bearing Quantities 16

5. Appendix: Tables of Bearing Quantities 18

6. Conclusion 22

7. References 23

1. Introduction

The hydrodynamic theory for the pressure build-up in the thin oil film of a bearing was given by REYNOLDS (10), in 1886. He derived the differential equation for the pressure and gave the solution for the infinitely wide pad bearing.

The solution method for the pad bearing of finite width was given by MICHELL (9), in 1905. He gave the pressure at a point in the bearing as an infinite series and solutions for some special bearing cases.

A more brief calculation was made in an earlier work by JAKOBSSON-FLOBERG (7), in 1958, on the digital computer BESK in Stockholm, using the difference equation method. The calculations were made for six different width-length ratios and eight oil film thickness ratios. A similar calculation was published at the same time by HAYS (4), who used Bessel functions for the solution. The agreement of the results of these two solution methods is very good.

The single rectangular pad bearing is under the normally used assumptions of laminar flow, constant viscosity, etc. treated well enough; but there is still a shortage of works treating the design of a thrust tilting-pad bearing consisting of a number of pads. In this work it is shown how to design a thrust bearing with a minimum power loss and how to choose the optimum number of pads.

2. Notation

b = Width of the pads

c = Specific heat of oil

E = Power loss per unit width for one pad

$E_0 = \frac{E\, h_{\min}}{\eta\, U^2\, l}$ = Non-dimensional power loss per unit width for one pad

E_{tot} = Total power loss for one pad

f = Relative power loss, i. e. power loss per unit load

$h_{\max}$ = Maximum oil film thickness

$h_{\min}$ = Minimum oil film thickness

$k = \frac{h_{\max} - h_{\min}}{h_{\min}}$ = Slope coefficient

l = Mean length of one of the pads

n = Number of pads

P = Load per unit width for one pad

$P_0 = \frac{P\, h_{\min}^2}{\eta\, U\, l^2}$ = Non-dimensional load per unit width for one pad

P_{tot} = Total load for one pad

Q = Oil flow for one pad

$Q_0 = \frac{Q}{U\, h_{\min}\, l}$ = Non-dimensional oil flow for one pad

q = Oil flow per unit width for one pad

$q_0 = \frac{q}{U\, h_{\min}}$ = Non-dimensional oil flow per unit width for one pad

r = Radius of rotation

Δt = Average temperature rise

U = Mean velocity

W = Load capacity of the thrust bearing

x_P = Load location

η = Absolute viscosity

λ = Scale factor

$r = \frac{b}{l}$ = Width-length ratio

ϱ = Density of the oil

$\xi_P = \frac{x_P}{l}$ = Non-dimensional load location

ω = Angular velocity

3. Optimum Analysis

3,1. General Considerations

The problem is how to design an optimum thrust tilting-pad bearing. Optimum means here minimum power loss. The radius of rotation, the width-length ratio of the pads, and the number of them are to be taken into account. Quantities assumed to be given are total load W, angular velocity ω, and minimum permissible oil film thickness $h_{\min}$. The calculation is based on the values determined for rectangular plane pads in ref. (7), also given here in the appendix. The rotational velocity U at the mean radius r is used as an average velocity, and the length l of the pads in rotational direction is also measured at this radius, see fig. 8.1. This makes an approximation, which, however, is insignificant for the practical design.

In the following it is assumed that the pads will fill 5 r of the total peripheral length $2\,\pi\,r$, and the rest consist of spaces between the pads. Thus the pads will fill 80 % of the periphery.

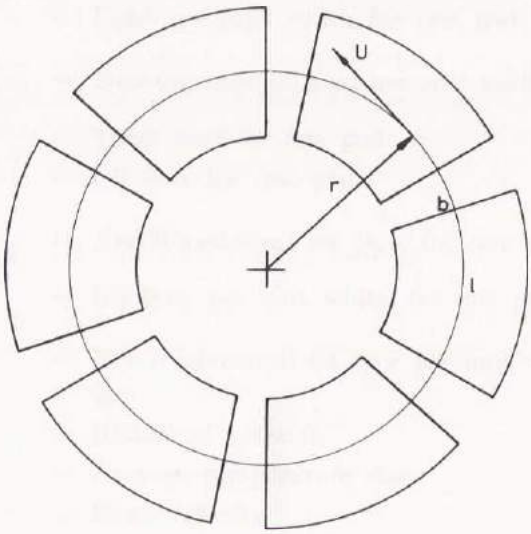

Fig. 8.1

3,2. Influence of a Scale Factor

Study the influence of a scale factor on the bearing quantities, if load capacity, angular velocity, and minimum permissible oil film thickness are constant. Using the schedule for design calculation given in ref. (7) page 33, the bearing quantities become

$$\eta_{\mathrm{I}} = \frac{W\, h_{\min}^2}{n\, b\, P_0\, r\, \omega\, l^2}$$

$$f_{\mathrm{I}} = \frac{E_0}{P_0} \cdot \frac{r\, \omega\, h_{\min}}{l}$$

$$n\, E_{\mathrm{tot_I}} = f_{\mathrm{I}}\, W$$

$$Q_{\mathrm{I}} = Q_0\, r\, \omega\, h_{\min}\, l$$

$$\Delta t_{\mathrm{I}} = \frac{r\, E_0}{Q_0\, P_0} \cdot \frac{1}{c\, \varrho} \cdot \frac{W}{n\, b\, l}$$

where

η = viscosity

n = number of pads

$P_0 = \dfrac{P\, h_{\min}^2}{\eta\, U\, l^2}$ = load number

P = load per unit width

f = power loss per unit load

$E_0 = \dfrac{E\, h_{\min}}{\eta\, U^2\, l}$ = power loss number

E = power loss per unit width

E_{tot} = total power loss for one pad

Q = oil flow for one pad

$Q_0 = \dfrac{Q}{U\, h_{\min}\, l}$ = oil flow number

Δt = average temperature rise

r = width-length ratio

c = specific heat of oil

ϱ = density of oil

If now the width, the length, and the mean radius of rotation are multiplied by a scale factor $\lambda > 1$, the new bearing quantities become

$$\eta_{II} = \frac{W h_{min}^2}{n \lambda b P_0 \lambda r \omega \lambda^2 l^2} = \frac{1}{\lambda^4} \cdot \eta_I$$

$$f_{II} = \frac{E_0}{P_0} \cdot \frac{\lambda r \omega h_{min}}{\lambda l} = f_I$$

$$n E_{tot_{II}} = f_{II} W = n E_{tot_I}$$

$$Q_{II} = Q_0 \lambda r \omega h_{min} \lambda l = \lambda^2 Q_I$$

$$\Delta t_{II} = \frac{\nu E_0}{Q_0 P_0} \cdot \frac{1}{c \varrho} \cdot \frac{W}{n \lambda b \lambda l} = \frac{1}{\lambda^2} \cdot \Delta t_I$$

The power loss is thus unchanged when the bearing area is increased. The viscosity decreases, the oil flow increases, and the average temperature rise is less.

3,3. Influence of Width-Length Ratio and Number of Pads

Consider now a thrust tilting-pad bearing with a given radius of rotation. The load, the mean surface velocity, and the minimum permissible oil film thickness are known. Study the influence of the number of pads and the width-length ratio on the power loss.

The power loss per unit load is

$$f = \frac{E_0}{P_0} \cdot \frac{U h_{min}}{l}$$

Thus the power loss for the thrust bearing is

$$n E_{tot} = \frac{E_0}{P_0} \cdot \frac{r \omega h_{min}}{l} \cdot W$$

This expression shall be minimum. As W, ω, and h_{min} are given constant values, the minimum for the function

$$\Phi = \frac{E_0}{P_0} \cdot \frac{r}{l}$$

shall be determined. E_0 and P_0 are functions of ν and k, r is constant and l is a function of n. ν is the ratio b/l and $1 + k$ is the oil film thickness ratio.

Thus there are three parameters to be determined, viz.

$$\nu \qquad k \qquad n$$

If optimum values of k are chosen, the minimum of E_0/P_0 as a function of ν can be separately determined. These values are given in the following table.

ν	0	0,5	0,75	1	1,5	2	∞
$\frac{E_0}{P_0}$	∞	18,7	11,9	9,18	7,08	6,29	4,62

Now the Φ-values as function of ν and n for optimum k-values are calculated for the ratio $b/r = 1$; 0,8; 0,6 and 0,4. They are given in table 11.1. Curves of Φ are given in fig. 12.1 as function of ν and n, and curves for the b/r-values are drawn in the same figure.

For a given width-radius ratio b/r the number of pads n and the width-length ratio ν shall be chosen to give the minimum of the

Table 11.1

b/r	n	2	3	4	6	8	12	16
	l/r	2,50	1,67	1,25	0,833	0,625	0,417	0,313
1	ν	0,40	0,60	0,80	1,20	1,60	2,40	3,20
	E_0/P_0	24	15,1	11,1	8,0	6,9	6,0	5,6
	Φ	9,6	9,0	8,9	9,6	11,0	14,4	17,9
0,8	ν	—	0,48	0,64	0,96	1,28	1,92	2,56
	E_0/P_0	—	19,5	14,1	9,5	7,7	6,4	5,9
	Φ	—	11,7	11,3	11,4	12,3	15,4	18,9
0,6	ν	—	0,36	0,48	0,72	0,96	1,44	1,92
	E_0/P_0	—	28	19,5	12,4	9,5	7,2	6,4
	Φ	—	16,8	15,6	14,9	15,2	17,3	20,4
0,4	ν	—	—	—	0,48	0,64	0,96	1,28
	E_0/P_0	—	—	—	19,5	14,1	9,5	7,7
	Φ	—	—	—	23,4	22,6	22,8	24,6

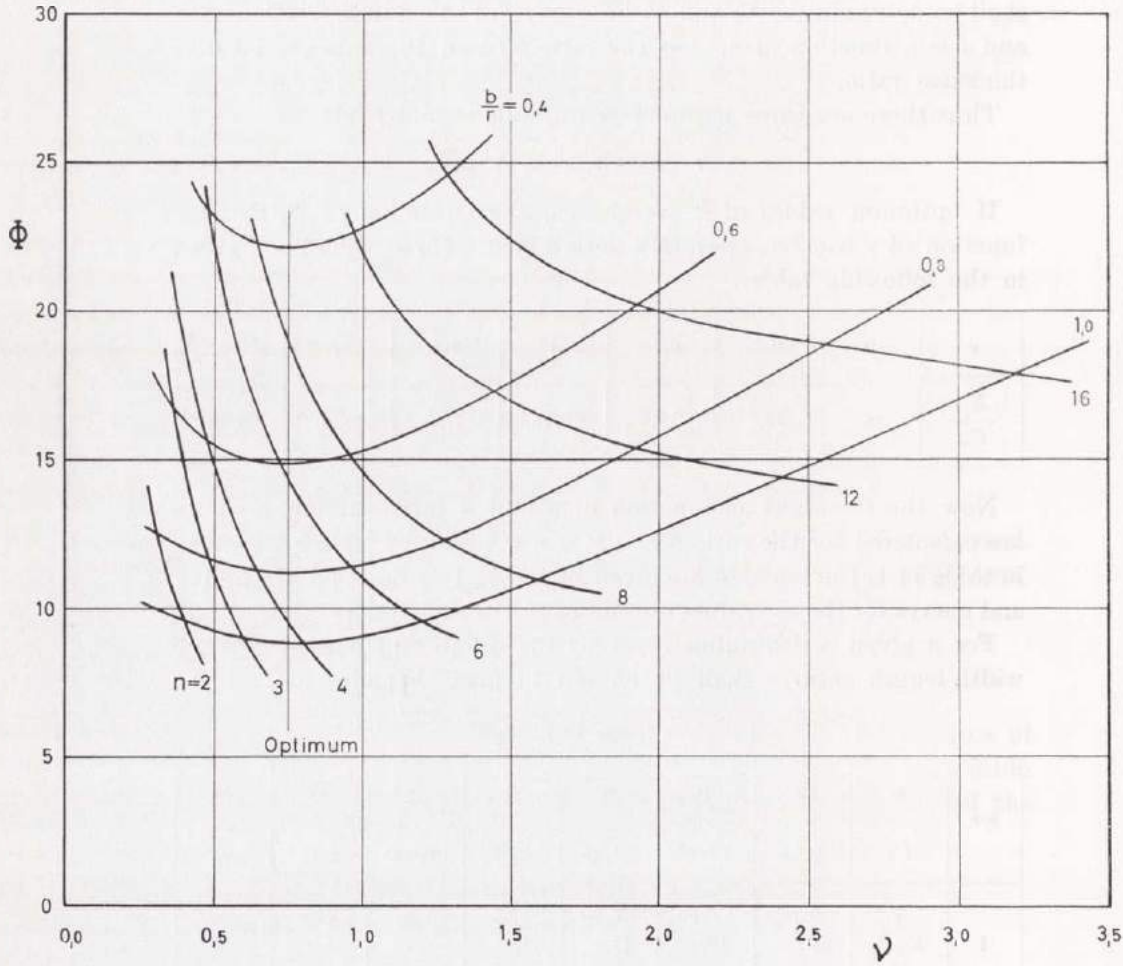

Fig. 12.1

Φ-value, which represents the power loss. It is interesting to note that for every b/r ratio, Φ is minimum at about $\nu = 3/4$. This gives a very simple design rule. Convenient oil film thickness ratios are 3 or 4, that means $k = 2$ or 3. Convenient number of pads at the different b/r ratios are as follows

b/r	1,0	0,8	0,6	0,4
n	3–4	4–6	6–8	8–10

The non-dimensional bearing quantities for the optimum values $r = 3/4$ and $k = 2$ are

P_0	ξ_P	q_0	E_0	$\frac{f\,l}{U\,h_{\min}}$
0,0498	0,636	1,25	0,599	12,0

where ξ_P = load location.

$$q_0 = \frac{q}{U\,h_{\min}} = \text{non-dimensional oil flow per unit width}$$

q = oil flow per unit width

Now we can outline the procedure for design calculation.

Known quantities are the load W, the angular velocity ω, and the minimum permissible oil film thickness $h_{\min}$. The radius of rotation does not influence the power loss as shown above; but the width of the pads shall be chosen as large as possible for design considerations.

From fig. 12.1 the optimum case is chosen. Then the geometri is known. The viscosity becomes

$$\eta = \frac{W\,h_{\min}^2}{n\,b\,P_0\,U\,l^2}$$

This viscosity is needed for the hydrodynamic lubrication. It must also be considered whether this viscosity compared with the surface roughness gives negligible wear at starts and stops of the machine. If the minimum oil film thickness is chosen large enough, this condition is automatically satisfied.

The maximum oil film thickness is

$$h_{\max} = (1 + k)\,h_{\min}$$

The power loss per unit load is

$$f = \frac{E_0}{P_0} \cdot \frac{r}{l} \cdot \omega\,h_{\min} = \Phi\,\omega\,h_{\min}$$

The power loss becomes

$$n\,E_{\mathrm{tot}} = f\,W = \Phi\,\omega\,h_{\min}\,W$$

The load location is

$$x_P = l\,\xi_P$$

The oil flow becomes

$$n\,Q = n\,Q_0\,U\,h_{\min}\,l = n\,b\,q_0\,U\,h_{\min}$$

The average temperature rise is

$$\Delta t = \frac{E_0}{q_0\,P_0} \cdot \frac{1}{c\,\varrho} \cdot \frac{W}{n\,b\,l} = \frac{(n\,E_{\mathrm{tot}})}{c\,\varrho\,(n\,Q)}$$

If the width-length ratio is approximately 3/4, the non-dimensional values given above may be used. If ν is chosen differently from 3/4, those values could be taken from the charts in chap. 4 or from the tables in the appendix.

3,4. Schedule for Calculation

The width b is chosen as large as is suitable for the design.

The optimum case of fig. 12.1 is chosen, i. e. when Φ has the minimum.

$$\eta = \frac{W\,h_{\min}^2}{n\,b\,P_0\,U\,l^2}$$

$$h_{\max} = (1 + k)\,h_{\min}$$

$$f = \frac{E_0}{P_0} \cdot \frac{r}{l} \cdot \omega\,h_{\min} = \Phi\,\omega\,h_{\min}$$

$$n\,E_{\mathrm{tot}} = f\,W = \Phi\,\omega\,h_{\min}\,W$$

$$x_P = l\,\xi_P$$

$$n\,Q = n\,b\,q_0\,U\,h_{\min}$$

$$\Delta t = \frac{(n\,E_{\mathrm{tot}})}{c\,\varrho\,(n\,Q)}$$

3,5. **Example**

Design an optimum thrust tilting-pad bearing for the load 30000 N, the rotational speed 1500 r/min, and the minimum permissible oil film thickness 0,050 mm. The radius of rotation is 100 mm and the pad width 60 mm. $c = 2000$ Nm/kg° C, $\varrho = 900$ kg/m³.

$$\frac{b}{r} = \frac{60}{100} = 0,6$$

From fig. 12.1 the optimum condition gives $r = 0,75$ and $n = 6$.

Thus

$$l = \frac{b}{r} = \frac{60}{0,75} = 80 \text{ mm}$$

and

$$\Phi = \frac{E_0}{P_0} \cdot \frac{r}{l} = 12,0 \cdot \frac{100}{80} = 15,0$$

The mean space between the pads is

$$\frac{2\pi\, 100 - 6 \cdot 80}{6} = 25 \text{ mm}$$

$$\eta = \frac{30000 \cdot 0,000050^2}{6 \cdot 0,060 \cdot 0,0498 \cdot 0,100 \cdot 157 \cdot 0,080^2} = 0,042 \text{ Ns/m}^2$$

$$h_{max} = (1 + 2)\, 0,050 = 0,150 \text{ mm}$$

$$f = 15,0 \cdot 157 \cdot 0,000050 = 0,118 \text{ m/s}$$

$$n\, E_{tot} = 0,118 \cdot 30000 = 3540 \text{ Nm/s} = 3,54 \text{ kW}$$

$$x_P = 80 \cdot 0,636 = 51 \text{ mm}$$

$$n\, Q = 6 \cdot 0,060 \cdot 1,25 \cdot 0,100 \cdot 157 \cdot 0,000050 = 0,000353 \text{ m}^3/\text{s} = 21 \text{ l/min}$$

$$\Delta t = \frac{3540}{2000 \cdot 900 \cdot 0,000353} = 5,6° \text{ C}$$

4. Charts of Bearing Quantities

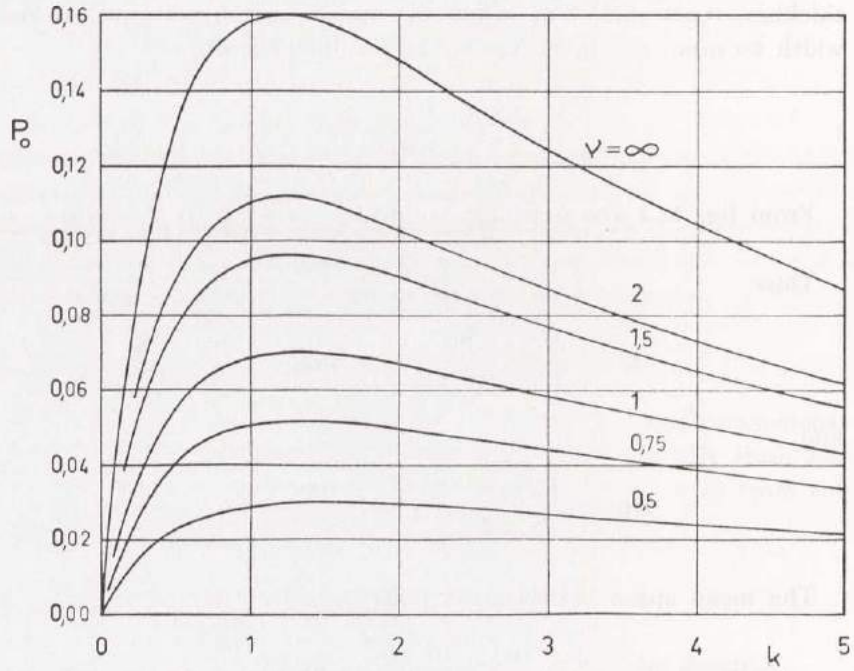

Chart 16.1. Load Capacity $\quad P_0 = \dfrac{P\, h_{\min}^2}{\eta\, U\, l^2}$

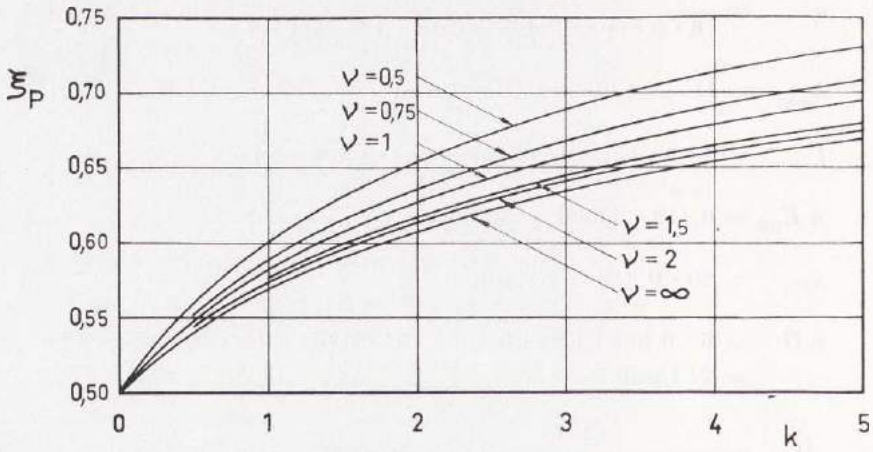

Chart 16.2. Load Location

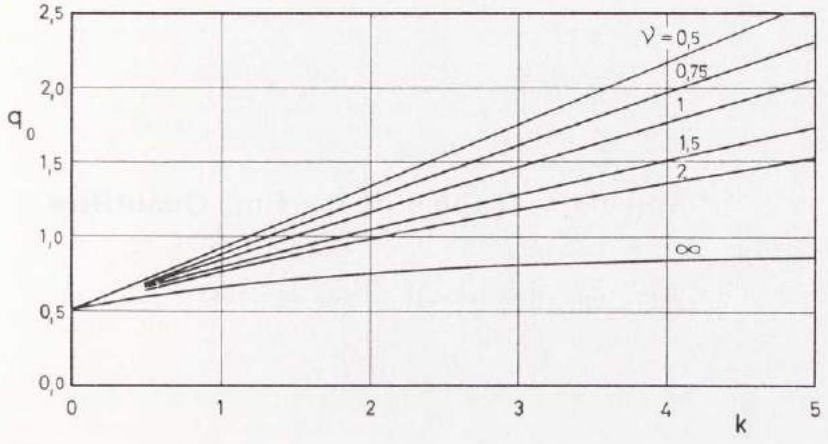

Chart 17.1. Oil Flow $\qquad q_0 = \dfrac{q}{U\, h_{\min}}$

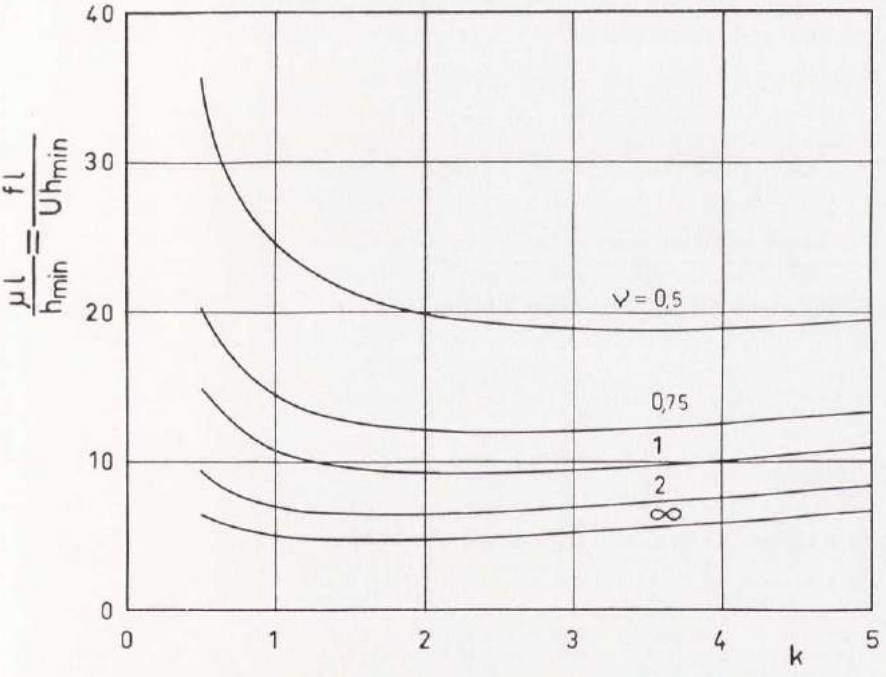

Chart 17.2. Coefficient of Friction and Relative Power Loss

5. Appendix: Tables of Bearing Quantities

The following non-dimensional values are used:

$$\nu = \frac{b}{l}$$

$$k = \frac{h_{max} - h_{min}}{h_{min}}$$

$$P_0 = \frac{P h_{min}^2}{\eta U l^2}$$

$$q_0 = \frac{q}{U h_{min}}$$

$$Q_0 = \frac{Q}{U h_{min} l}$$

$$E_0 = \frac{E h_{min}}{\eta U^2 l}$$

$$\Delta t_0 = c \varrho \cdot \frac{\Delta t h_{min}^2}{\eta U l}$$

$$\frac{\mu l}{h_{min}} = \frac{f l}{U h_{min}} = \frac{E_0}{P_0}$$

$\nu = \infty$

k	0	0,5	1	1,5	2	3	4	5
P_0	0	0,131	0,159	0,158	0,148	0,124	0,104	0,0872
ξ_P	0,500	0,540	0,569	0,590	0,607	0,634	0,654	0,669
q_0	0,500	0,600	0,667	0,714	0,750	0,800	0,833	0,857
E_0	1,00	0,844	0,773	0,729	0,697	0,648	0,609	0,576
Δt_0	2,00	1,41	1,16	1,02	0,930	0,811	0,731	0,672
$\frac{f\,l}{U\,h_{\min}}$	∞	6,43	4,86	4,62	4,71	5,22	5,89	6,61

$\nu = 2$

k	0	0,5	1	1,5	2	3	4	5
P_0	0	0,0900	0,110	0,110	0,103	0,0872	0,0729	0,0613
ξ_P	0,500	0,543	0,573	0,596	0,613	0,640	0,659	0,673
q_0	0,500	0,644	0,766	0,876	0,980	1,18	1,36	1,54
E_0	1,00	0,833	0,748	0,693	0,653	0,593	0,548	0,512
Δt_0	2,00	1,30	0,977	0,791	0,666	0,505	0,402	0,331
$\frac{f\,l}{U\,h_{\min}}$	∞	9,27	6,82	6,33	6,32	6,80	7,52	8,35

$\nu = 1{,}5$

k	0	0,5	1	1,5	2	3	4	5
P_0	0	0,0772	0,0946	0,0950	0,0900	0,0769	0,0649	0,0551
ξ_P	0,500	0,545	0,576	0,599	0,617	0,645	0,665	0,680
q_0	0,500	0,657	0,796	0,925	1,05	1,28	1,51	1,73
E_0	1,00	0,830	0,740	0,682	0,639	0,577	0,532	0,496
Δt_0	2,00	1,26	0,930	0,737	0,610	0,450	0,352	0,286
$\frac{f\,l}{U\,h_{\min}}$	∞	10,8	7,83	7,18	7,10	7,51	8,20	9,01

$\nu = 1$

k	0	0,5	1	1,5	2	3	4	5
P_0	0	0,0558	0,0689	0,0700	0,0670	0,0584	0,0501	0,0432
ξ_P	0,500	0,548	0,582	0,607	0,627	0,657	0,678	0,695
q_0	0,500	0,680	0,847	1,01	1,17	1,47	1,77	2,06
E_0	1,00	0,825	0,728	0,663	0,616	0,550	0,503	0,466
Δt_0	2,00	1,21	0,859	0,658	0,529	0,374	0,284	0,226
$\frac{f\,l}{U\,h_{\min}}$	∞	14,8	10,6	9,48	9,20	9,42	10,0	10,8

$\nu = 0{,}75$

k	0	0,5	1	1,5	2	3	4	5
P_0	0	0,0404	0,0504	0,0516	0,0498	0,0441	0,0384	0,0335
ξ_P	0,500	0,552	0,588	0,615	0,636	0,668	0,691	0,708
q_0	0,500	0,696	0,884	1,07	1,25	1,61	1,96	2,31
E_0	1,00	0,821	0,718	0,650	0,599	0,528	0,479	0,442
Δt_0	2,00	1,18	0,812	0,608	0,480	0,329	0,244	0,191
$\frac{f\,l}{U\,h_{\min}}$	∞	20,3	14,3	12,6	12,0	12,0	12,5	13,2

$\nu = 0{,}5$

k	0	0,5	1	1,5	2	3	4	5
P_0	0	0,0229	0,0289	0,0301	0,0295	0,0268	0,0238	0,0212
ξ_P	0,500	0,560	0,601	0,631	0,654	0,689	0,713	0,731
q_0	0,500	0,715	0,927	1,14	1,35	1,76	2,17	2,59
E_0	1,00	0,817	0,708	0,633	0,579	0,502	0,450	0,411
Δt_0	2,00	1,14	0,763	0,557	0,430	0,285	0,207	0,159
$\frac{f\,l}{U\,h_{\min}}$	∞	35,7	24,5	21,1	19,7	18,8	18,9	19,4

6. Conclusion

This paper treats optimum conditions for thrust tilting-pad bearings. Optimum means here minimum power loss. It is discussed how to choose the number of pads and the width-length ratio when the load capacity, the angular velocity and the minimum permissible oil film thickness are given. A schedule for design calculation is made. The viscosity is constant and the determination is based on values calculated for rectangular plane pads. Tables and charts of the bearing quantities are given.

7. References

1. Floberg, L.: The Infinite Journal Bearing, Considering Vaporization. Gothenburg, 1957.
2. Floberg, L.: Experimental Investigation of Power Loss in Journal Bearings, Considering Cavitation. Gothenburg, 1959.
3. Floberg, L.: Lubrication of a Rotating Cylinder on a Plane Surface, Considering Cavitation. Gothenburg, 1959.
4. Hays, D. F.: Plane Sliders of Finite Width. Trans. Am. Soc. Lubr. Engrs, Vol. 1, No. 2, 1958.
5. Jakobsson, B. and Floberg, L.: The Finite Journal Bearing, Considering Vaporization. Gothenburg, 1957.
6. Jakobsson, B. and Floberg, L.: The Partial Journal Bearing. Gothenburg, 1958.
7. Jakobsson, B. and Floberg, L.: The Rectangular Plane Pad Bearing. Gothenburg, 1958.
8. Jakobsson, B. and Floberg, L.: The Centrally Loaded Partial Journal Bearing. Gothenburg, 1959.
9. Michell, A. G. M.: The Lubrication of Plane Surfaces. Z. Math. Phys., vol. 52, p. 123, 1905.
10. Reynolds, O.: On the Theory of Lubrication . . . Phil. Trans. Roy. Soc., vol. 177, p. 157, 1886.

Forts. fr. omsl. 2:dra sida

178. OLVING, SVEN, *A new method for space charge wave interaction studies. I.* 12 s. 1956. Kr. 3: —. (Avd. Elektroteknik. 51.)
179. HANSBO, SVEN, *The critical load of rectangular frames analysed by convergence methods.* 47 s. 1956. Kr. 11: —. (Avd. Väg- och Vattenbyggnad. Byggnadsteknik. 25.)
180. WESTBERG, VIDOR, *Measurements of noise radiation at 10 cm from glow lamps. Preliminary report.* 14 s. 1956. Kr. 4: 50. (Avd. Elektroteknik. 52.)
181. SVENSSON, S. I., HELLGREN, G., AND PERERS, O., *The Swedish radioscientific solar eclipse expedition to Italy, 1952. Preliminary report.* 30 s. 1956. Kr. 8: —. (Avd. Elektroteknik. 53.)
182. WAX, NELSON, *A note on design considerations for a proposed auroral radar.* 16 s. 1957. Kr. 3: —. (Avd. Elektroteknik. 54.)
183. JOSHI, G. H., *The electromagnetic interaction between two crossing electron streams. I.* 31 s. 1957. Kr. 8 :—. (Avd. Elektroteknik. 55.)
184. SMITH, BENGT, *Dry methods for removing hydrogen sulphide from gases.* 65 s. 1957. Kr. 15: —. (Avd. Kemi och Kemisk Teknologi. 34.)
185. EKELÖF, S., BJÖRK, N., AND DAVIDSON, R., *Large signal behaviour of directly heated thermistors.* 31 s. 1957. Kr. 8 :—. (Avd. Elektroteknik. 56.)
186. CARLSSON, BENGT UND LARSSON, HANS, *Wirkungsgrad und Selbsthemmung einfacher umlaufgetriebe.* 48 s. 1957. Kr. 9 :—. (Avd. Maskinteknik. 8.)
187. AURELL, CARL G., *The equivalent transmission line of a linear four-terminal network. Calculations with cascade-connected four-terminal networks.* 39 s. 1957. Kr. 6: —. (Avd. Elektroteknik. 57.)
188. LUNDHOLM, R., *Induced overvoltage-surges on transmission lines and their bearing on the lightning performance at medium voltage networks.* 117 s. 1957. Kr. 19: —. (Avd. Elektroteknik. 58.)
189. FLOBERG, LEIF, *The infinite journal bearing, considering vaporization.* 83 s. 1957. Kr. 13: —. (Avd. Maskinteknik. 9.)
190. JAKOBSSON, BENGT, AND FLOBERG, LEIF, *The finite journal bearing, considering vaporization.* 117 s. 1957. Kr. 19: 50. (Avd. Maskinteknik. 10.)
191. CHAKO, NICHOLAS, *Characteristic curves on planes in the image space.* 49 s. 1957. Kr. 15: —. (Avd. Allmänna Vetenskaper. 12.)
192. EKELÖF, STIG, *The development and decay of the magnetic flux in a non-delayed telephone relay.* 50 s. 1957. Kr. 15: —. (Avd. Elektroteknik. 59.)
193. BJÖRKLUND, KJELL, *Bestämning av porslins draghållfasthet.* 78 s. 1958. Kr. 15: —. (Institutionen för Silikatkemisk Forskning. 39.)
194. GRANHOLM, PER, *Sound insulation of single leaf walls.* 48 s. 1958. Kr. 8: —. (Avd. Väg- och Vattenbyggnad. Byggnadsteknik. 26.)
195. GRANHOLM, HJALMAR, *Om vattengenomslag i murade väggar med särskild hänsyn till tegel som fasadmaterial.* 172 s. 1958. Kr. 16: —. (Avd. Väg- och Vattenbyggnad. Byggnadsteknik. 27.)
196. MEOS, JOHAN, AND OLVING, SVEN, *On the origin of radar echoes associated with auroral activity.* 20 s. 1958. Kr. 5: —. (Avd. Elektroteknik. 60.)
197. JOSHI, G. H., *The electromagnetic interaction between two crossing electron streams. II.* 10 s. 1958. Kr. 3: 50. (Avd. Elektroteknik. 61.)
198. WILHELMSSON, HANS, *The interaction between an obliquely incident plane electromagnetic wave and an electron beam. II.* 32 s. 1958. Kr. 7: —. (Avd. Elektroteknik. 62.)
199. KÄRRHOLM, GUNNAR, *A method of iteration applied to beams resting on springs.* 50 s. 1958. Kr. 12: —. (Avd. Allm. Vetenskaper. 13.)
200. JAKOBSSON, BENGT, AND FLOBERG, LEIF, *The partial journal bearing.* 60 s. 1958. Kr. 14: —. (Avd. Maskinteknik. 11.)
201. KÄRRHOLM, GUNNAR, *Influence functions of elastic plates divided in strips.* 18 s. 1958. Kr. 4: 50. (Avd. Väg- och Vattenbyggnad. Byggnadsteknik. 28.)
202. RÅDE, LENNART, *Sampling planes for acceptance sampling by variables using the range.* 34 s. 1958. Kr. 9: 50. (Avd. Allm. Vetenskaper. 14.)
203. JAKOBSSON, BENGT, AND FLOBERG, LEIF, *The rectangular plane pad bearing.* 44 s. 1958. Kr. 5: —. (Avd. Maskinteknik. 12.)
204. ASPLUND, SVEN OLOF, *Column-beams and suspension bridges analyzed by »Green's matrix».* 36 s. 1958. Kr 7: —. (Avd. Väg- och Vattenbyggnad. Byggnadsteknik. 29.)
205. WILHELMSSON, HANS, *On the properties of the electron beam in the presence of an axial magnetic field of arbitrary strength.* 32 s. 1958. Kr. 7: 50. (Avd. Elektroteknik. 63.)
206. WILHELMSSON, HANS, *The interaction between an obliquely incident plane electromagnetic wave and an electron beam. III.* 17 s. 1958. Kr. 5: —. (Avd. Elektroteknik. 64.)
207. HEDVALL, ARVID J., *On the influence of pre-treatment and transition processes on the adsorption capacity and the reactivity of various types of glass and silica.* 39 s. 1959. Kr. 8: —. (Institutionen för Silikatkemisk Forskning. 40.)

Forts. å omsl. 4:de sida

Forts. fr. omsl. 3:dje sida

208. KÄRRHOLM, GUNNAR, *A flow problem solved by strip method.* 22 s. 1959. Kr. 4: 50. (Avd. Allm. Vetenskaper. 15.)
209. GRANHOLM, HJALMAR, *Allmän teori för beräkning av armerad betong.* 228 s. 1959. Kr. 20: —. (Avd. Väg- och Vattenbyggnad. Byggnadsteknik. 30.)
210. LIDIN, LARS G., *On helical-springs suspension.* 75 s. 1959. Kr. 15: —. (Avd. Maskinteknik. 13.)
211. BJÖRK, NILS, *Theory of the indirectly heated thermistor.* 46 s. 1959. Kr. 10: —. (Avd. Elektroteknik. 65.)
212. CARLSSON, ORVAR, *The influence of submicroscopic pores on the resistance of bricks towards frost.* 13 s. 1959. Kr. 3: 50. (Institutionen för Silikatkemisk Forskning. 41.)
213. GRANHOLM, HJALMAR, *KAM 40, KAM 60 och KAM 90.* 41 s. 1959. Kr. 3: 50. (Avd. Väg- och Vattenbyggnad. Byggnadsteknik. 31.)
214. JAKOBSSON, BENGT, AND FLOBERG, LEIF, *The centrally loaded partial journal bearing.* 35 s. 1959. Kr. 7: 50. (Avd. Maskinteknik. 14.)
215. FLOBERG, LEIF, *Experimental investigation of power loss in journal bearings, considering cavitation.* 16 s. 1959. Kr. 3: 50. (Avd. Maskinteknik. 15.)
216. FLOBERG, LEIF, *Lubrication of a rotating cylinder on a plane surface, considering cavitation.* 40 s. 1959. Kr. 8: —. (Avd. Maskinteknik. 16.)
217. TROEDSSON, CARL BIRGER, *The growth of the Western city during the Middle Ages.* 125 s. 1959. Kr. 19: —. (Avd. Arkitektur. 4.)
218. HEDVALL, J. ARVID, *The importance of the reactivity of solids in geological-mineralogical processes.* 11 s. 1959. Kr. 2: 50. (Institutionen för Silikatkemisk Forskning. 42.)
219. CORNELL, ELIAS, *Humanistic inquiries into architecture. I—III.* 112 s. 1959. Kr. 17: —. (Avd. Arkitektur. 5.)
220. GRANHOLM, CARL-ADOLF, *Ekonomiska aluminiumprofiler.* 48 s. 1959. Kr. 5: 50. (Avd. Väg- och Vattenbyggnad. Byggnadsteknik. 32.)
221. LUNDÉN, ARNOLD, CHRISTOFFERSON, STINA, AND LODDING, ALEX, *The isotopic effect of lithium ions in countercurrent electromigration in molten lithium bromide and iodide.* 38 s. 1959. Kr. 7: 50. (Avd. Allm. Vetenskaper. 16.)
222. INGEMANSSON, STIG, AND KIHLMAN, TOR, *Sound insulation of frame walls.* 47 s. 1959. Kr. 8: 50. (Avd. Väg- och Vattenbyggnad. Byggnadsteknik. 33.)
223. HÖGLUND, B., and RADHAKRISHNAN, V., *A radiometer for the hydrogen line.* 25 s. 1959. Kr. 6:50. (Avd. Elektroteknik. 66.)
224. JAKOBSSON, BENGT, *Torque distribution, power flow, and zero output conditions of epicyclic gear trains.* 55 s. 1960. Kr. 12: —. (Avd. Maskinteknik. 17.)
225. OLVING, SVEN, *Electromagnetic and space charge waves in a sheath helix.* 91 s. 1960. Kr. 17: —. (Avd. Elektroteknik. 67.)
226. STRÖMBLAD, JOHN, *Beschleunigungsverlauf und Gleichgewichtsdrehzahlen einfacher Planetengetriebe nebst Selbsthemmungsversuche.* 80 s. 1960. Kr. 18: —. (Avd. Maskinteknik. 18.)
227. SANDFORD, FOLKE, *Some current problems concerning brick manufacture.* 20 s. 1960. Kr. 5: —. (Avd. Kemi och Kemisk Teknologi. 35.)
228. OLVING, SVEN, *A new method for space charge wave interaction studies. II.* 40 s. 1960. Kr. 8: —. (Avd. Elektroteknik. 68.)
229. GRANHOLM, HJALMAR, *Le problème de Boussinesq.* 15 s. 1960. Kr. 3: 50. (Avd. Väg- och Vattenbyggnad. Byggnadsteknik. 34.)
230. HIBA, MIODRAG ot CEDERWALL, KRISTER, *Flambement élastique d'une barre en bois lamellée et clouée avec le module de déplacement du moyen de liaison constant k.* 22 s. 1960. Kr. 5: —. (Avd. Väg- och Vattenbyggnad. Byggnadsteknik. 35.)

Pris kronor 5: —

ELANDERS BOKTRYCKERI AKTIEBOLAG
GÖTEBORG 1960

CHALMERS TEKNISKA HÖGSKOLAS HANDLINGAR
TRANSACTIONS OF CHALMERS UNIVERSITY OF TECHNOLOGY
GOTHENBURG, SWEDEN
Nr 232 (Avd. Maskinteknik 20) 1960

THE TWO-GROOVE JOURNAL BEARING, CONSIDERING CAVITATION

BY

LEIF FLOBERG

Report No. 13 from the Institute of Machine Elements
Chalmers University of Technology
Gothenburg, Sweden
1960

GUMPERTS FÖRLAG
GÖTEBORG

Av Chalmers Tekniska Högskolas Handlingar hava tidigare utkommit:

Fullständig förteckning över Chalmers Tekniska Högskolas Handlingar lämnas av Chalmers Tekniska Högskolas Bibliotek, Göteborg.

151. Hedvall, J. A., *Reactions with activated solids.* 23 s. 1954 Kr. 5: —. (Institutionen för Silikatkemisk Forskning. 32.)
152. Smith, Cyril Stanley, *The microstructure of polycrystalline materials.* 49 s. 1954. Kr. 9: 50 (Institutionen för Silikatkemisk Forskning. 33.)
153. Selberg, Arne, *Norske erfaringer fra bygging av små hengebroer.* 20 s. 1954. Kr. 4: —. (Avd. Väg- och Vattenbyggnad. Byggnadsteknik. 21.)
154. Granholm, Hjalmar, *Armerat trä.* 96 s. 1954. Kr. 9: — (Avd. Väg- och Vattenbyggnad. Byggnadsteknik. 22.)
155. Wilhelmsson, Hans, *The interaction between an obliquely incident plane electromagnetic wave and an electron beam. I.* 31 s. 1954. Kr. 7: —. (Avd. Elektroteknik. 42.)
156. Olving, Sven, *Electromagnetic wave propagation on helical conductors inbedded in dielectric medium.* 14 s. 1955. Kr. 3: —. (Avd. Elektroteknik. 43.)
157. Olving, Sven, *Amplification of the traveling wave tube at high beam current. I.* 11 s. 1955. Kr. 3: —. (Avd. Elektroteknik. 44.)
158. Hedvall, J. A., Nordengren, Sven, und Liljegren, B., *Über die thermische Zersetzung von Kalziumsulfat bei niedrigen Temperaturen.* 18 s. 1955. Kr. 5: — (Institutionen för Silikatkemisk Forskning. 34.)
159. Dahlgren, Sven-Eric, *On the break-down of thixotropic materials.* 18 s. 1955. Kr. 3: 50. (Institutionen för Silikatkemisk Forskning. 35.)
160. Sandford, Folke, och Liljegren, Berne, *Torkningen av råtegel och dennas inverkan på teglets frostbeständighet.* 22 s. 1955. Kr. 3: —. (Institutionen för Silikatkemisk Forskning. 36.)
161. Wallman, Henry, *Automatic noise-factor meter.* 17 s. 1955. Kr. 3: —. (Avd. Elektroteknik. 45.)
162. Sandford, Folke, and Fransson, Stig, *The refractoriness of some types of quartz and quartzite. II.* 24 s. 1955. Kr. 5: —. (Institutionen för Silikatkemisk Forskning. 37.)
163. Lindblad, Anders *Konstruktion av linjer för moderna handelsfartyg.* 176 s. 1955. Kr. 20: —. (Avd. Skeppsbyggeri. 6.)
164. Svartholm, Nils, *Two problems in the theory of the slowing down of neutrons by collisions with atomic nuclei.* 15 s. 1955. Kr. 5: —. (Avd. Allmänna Vetenskaper. 10.)
165. Persson, Per, *Bostadsvaneundersökning utförd i hyreslägenheter byggda 1947 i Göteborg, Torpaområdet.* 86 s. 1955. Kr. 12: —. (Avd. Arkitektur. 3.)
166. Hansson, P. R., *Undersökning av mullitbildning i keramiska produkter.* 29 s. 1955. Kr. 6: —. (Institutionen för Silikatkemisk Forskning. 38.)
167. Ekelöf, Stig, *Die Temperaturverteilung in einem gleichstromdurchflossenen langen Metallzylinder mit kreisförmigem Querschnitt.* 38 s. 1955. Kr. 10: —. (Avd. Elektroteknik. 46.)
168. Wilhelmsson, Hans, *On the reflection of electromagnetic waves from a dielectric cylinder.* 17 s. 1955. Kr. 4: 50. (Avd. Elektroteknik. 47.)
169. Björk, N., and Davidson, R., *Small signal behaviour of directly heated thermistors.* 43 s. 1955. Kr. 11: —. (Avd. Elektroteknik. 48.)
170. Forestier, H., *Tendances actuelles dans la formation de l'ingenieur chimiste: selection, orientation, specialisation; amelioration de son efficience.* 13 s. 1956. Kr. 2: 50. (Avd. Kemi och Kemisk Teknologi. 33.)
171. Wax, Nelson, *On the ring current hypothesis.* 32 s. 1956. Kr. 7: —. (Avd. Elektroteknik. 49.)
172. Elgeskog, Erik, *Photoformer analysis and design.* 40 s. 1956. Kr. 8:50. (Avd. Elektroteknik. 50.)
173. Anzelius, Adolf, *Bimolekulare Reaktion von zwei in Mischung vorliegenden Substanzen mit einer dritten Substanz.* 8 s. 1956. Kr. 5: —. (Avd. Allm. Vetenskaper. 11.)
174. Reinius, Erling, *Model studies for the extension of the harbour of Gothenburg.* 38 s. 1956. Kr. 6: —. (Avd. Väg- och Vattenbyggnad. Byggnadsteknik. 23.)
175. Zimen, K. E., *Diffusion von Edelgasatomen die durch Kernreaktion in festen Stoffen gebildet werden.* 7 s. 1956. Kr. 2: —. (Institutionen för Kärnkemi. 1.)
176. Inthoff, W., und Zimen, K. E., *Kinetik der Diffusion radioaktiver Edelgase aus festen Stoffen nach Bestrahlung.* 16 s. 1956. Kr. 4: —. (Institutionen för Kärnkemi. 2.)
177. Granholm, Hjalmar, *Puts och lättbetong.* 45 s. 1956. Kr. 3: —. (Avd. Väg- och Vattenbyggnad. Byggnadsteknik. 24.)

Forts. å omsl. 3:dje sida

CHALMERS TEKNISKA HÖGSKOLAS HANDLINGAR
TRANSACTIONS OF CHALMERS UNIVERSITY OF TECHNOLOGY
GOTHENBURG, SWEDEN
Nr 232 (Avd. Maskinteknik 20) 1960

THE TWO-GROOVE JOURNAL BEARING, CONSIDERING CAVITATION

BY

LEIF FLOBERG

Report No. 13 from the Institute of Machine Elements
Chalmers University of Technology
Gothenburg, Sweden
1960

GÖTEBORG 1960
ELANDERS BOKTRYCKERI AKTIEBOLAG

Manuscript received by the Publications Committee,
Chalmers University of Technology, Nov. 26th, 1959.

Preface

Since 1955, lubrication research has been carried out at the Institute of Machine Elements, Chalmers University of Technology, Sweden, under the leadership of the head of the Institute, Professor B. JAKOBSSON. Hydrodynamic lubrication and cavitation have been the main subjects. Regarding earlier works see ref. (1)—(8).

The purpose of this work is to give tables and charts for practical design of ring- or pressure-lubricated journal bearings.

I wish to express my gratitude to the Swedish Technical Research Council for their kind sponsorship.

Leif Floberg
Tekn. lic.

Contents

Page

Preface 3

1. Introduction 5

2. Notation 6

3. The Ring-lubricated Journal Bearing 8

3,1. Pressure Distribution and Load Capacity 8
3,2. Oil Flow 10
3,3. Power Loss and Average Temperature Rise 11
3,4. Coefficient of Friction and Relative Power Loss 13
3,5. Tables of Calculated Values at Ring-lubrication 14
3,6. Charts of Bearing Quantities at Ring-lubrication 16
3,7. Design of Ring-lubricated Journal Bearings 18
3,8. Schedule for Calculation 20
3,9. Example 20

4. The Pressure-lubricated Journal Bearing 22

4,1. Pressure Distribution and Load Capacity 22
4,2. Oil Flow 22
4,3. Power Loss and Average Temperature Rise 24
4,4. Coefficient of Friction and Relative Power Loss 25
4,5. Tables of Calculated Values at Pressure-lubrication 26
4,6. Charts of Bearing Quantities at Pressure-lubrication 28
4,7. Design of Pressure-lubricated Journal Bearings 30
4,8. Schedule for Calculation 30
4,9. Example 31

5. Conclusion 32

6. References 32

1. Introduction

There is a lack of works giving tables and charts for the design of journal bearings in which consideration of the influence of cavitation on load capacity and power loss is taken. This work is intended to give a contribution to this field.

In an earlier work ref. (8) the centrally loaded 180° journal bearing has been treated with regard to the air and oil strips in cavitation regions. That work was based on very accurate calculations by RAIMONDI-BOYD (9). Now an upper zero-pressure bearing half is added to give tables and charts for the design of ring- and pressure-lubricated 360° journal bearings. There are two axial oil grooves, 90° before and after the load, to permit rotation in both directions. It has been found convenient to refer the position of the oil grooves to the load direction and not to the varying location of the maximum oil film thickness. The viscosity is assumed to be constant.

An optimum analysis is made for the design of bearings with a minimum of power loss at given values of load capacity, angular velocity, and minimum permissible oil film thickness.

2. Notation

A = Area of the bearing housing

b = Bearing width

c = Specific heat of oil

E = Power loss per unit width

E_{tot} = Total power loss

$E_0 = \frac{E\,\psi}{\eta\,U^2}$ = Non-dimensional power loss per unit width

e = Eccentricity of journal relative to bearing

f = Relative power loss, i. e. power loss per unit load

$H = \frac{h}{\Delta r}$ = Non-dimensional oil film thickness

h = Oil film thickness

P = Load per unit width

P_{tot} = Total load capacity

$P_0 = \frac{P\,\psi^2}{\eta\,U}$ = Load number

Q = Oil flow

Q' = Side flow

q = Oil flow per unit width

q' = Side flow per unit bearing width

$q_0 = \frac{q}{U\,\Delta r}$ = Non-dimensional oil flow per unit width

$q_0' = \frac{q'}{U\,\Delta r}$ = Non-dimensional side flow per unit bearing width

r = Journal radius

Δr = Radial clearance

t_a = Average operation temperature of the bearing

t_r = Temperature of the oil in the reservoir

t_s = Temperature of the surroundings

Δt = Average temperature rise

$\Delta t_0 = c\,\varrho \cdot \dfrac{\Delta t\,\psi^2}{\eta\,\omega}$ = Non-dimensional temperature rise

U = Surface velocity

α = Coefficient of thermal transmittance by convection

β = Angle between load line and line of centres

γ = Angle

$\varepsilon = \dfrac{e}{\Delta r}$ = Eccentricity/radial clearance

η = Absolute viscosity

μ = Coefficient of friction

$\nu = \dfrac{b}{d}$ = Ratio width-diameter

ϱ = Density of oil

τ = Shear stress

φ = Angular coordinate

$\psi = \dfrac{\Delta r}{r}$ = Radial clearance/journal radius

ω = Angular velocity

3. The Ring-lubricated Journal Bearing

3,1. Pressure Distribution and Load Capacity

A 360° journal bearing of finite width is considered. The bearing has one oil groove 90° before the load line, and another 90° after the load. The oil is supplied by one or more suspended rings rotated by the shaft. The rings are wetted by oil in an oil reservoir below the shaft. Then the groove at the angle φ_1, see fig. 8.1, is filled with oil. The pressure in the groove is zero, i. e. atmospheric. It is assumed

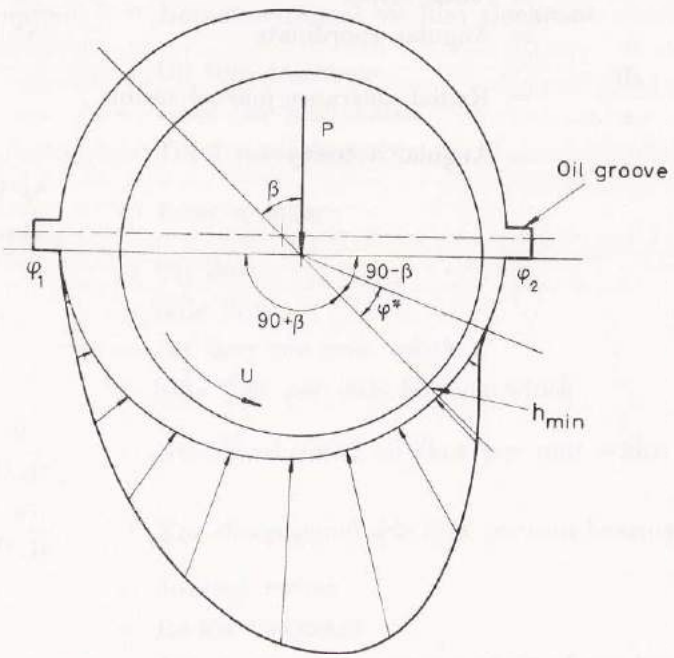

Fig. 8.1

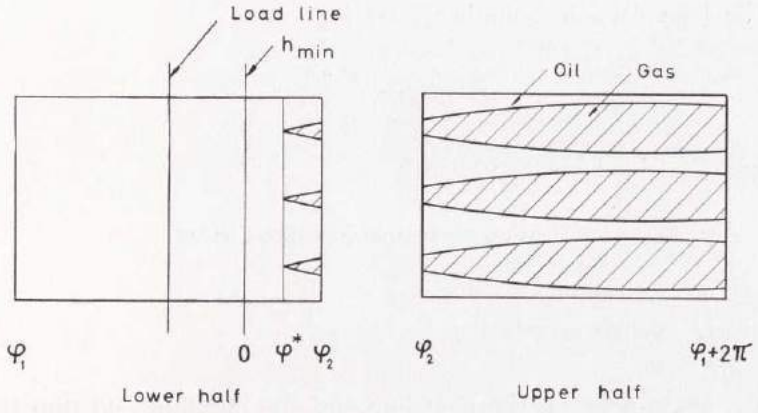

Fig. 9.1

that the oil supply is enough or more than what is needed for the intended operation of the bearing. There is no oil supply from the ring to the groove at the angle φ_2. Sometimes, however, the groove is filled with oil from the lower half of the bearing. In the calculations the grooves are assumed to have negligible extension in peripheral direction.

The pressure build-up begins at the angle φ_1. It ends at the angle φ_2 when the eccentricity is low, and within the lower half of the bearing with zero pressure derivative at higher eccentricities, see fig. 9.1. In the remaining part of the bearing there is a ruptured oil film with the pressure approximately zero. Thus the solution can be derived by adding a solution of an upper half with zero pressure to the centrally loaded 180° bearing solution. The latter case has already been treated in an earlier work, ref. (8), based on values calculated by RAIMONDI-BOYD (9). As they assume a full oil film in the cavitated region, they get somewhat too high power loss values at higher eccentricities. The case has also been treated by SASSENFELD-WALTHER (10). Unfortunately, there is a lack of oil flow values in their paper, and their power loss values are too low, as they assume that there is only air in the cavitated region. In ref. (8) the oil and air strips in the cavitation region are taken into account when calculating the power loss. The agreement of the load capacity values determined by RAIMONDI-BOYD with those of SASSENFELD-WALTHER is very good. The difference between them is about 1 % or less.

The load capacity number used is

$$P_0 = \frac{P\,\psi^2}{\eta\,U}$$

where P = load per unit width

$\psi = \frac{\Delta r}{r}$ = radial clearance/journal radius

η = absolut viscosity

U = surface velocity

The angle between the load line and the minimum oil film thickness is called β.

The calculated values are given in chap. 3,5 and charts in chap. 3,6. The relative eccentricity ε is the ratio eccentricity/radial clearance and ν is the width—diameter ratio.

3,2. Oil Flow

The oil is supplied to the groove located at φ_1 by the rings. This oil flow is equal to the side leakage. If more oil is supplied, it will go back to the reservoir without having been within the lubricating film. The side leakage from the lower half of the bearing thus attends to the cooling effect of the bearing. Oil flow values are taken from the very accurate calculations by RAIMONDI-BOYD (9), for the centrally loaded bearing case. The oil flow number used here is

$$q_0' = \frac{q'}{U\,\Delta r}$$

where q' = side leakage per unit bearing width.

At large bearing width the side leakage becomes small compared with the power loss, and the bearing will be very hot. It is advisable to control the temperature rise.

The total side flow is

$$Q' = b\,q',$$

which is equally divided on the two sides.

3,3. Power Loss and Average Temperature Rise

The power loss per unit width of the lower half of the bearing E_1 is taken from ref. (8), where due consideration is taken of the cavitation at the trailing edge.

In the whole upper half there is a cavitation region with oil and air strips. The mean shear stress is from ref. (1)

$$\tau = \frac{h^*}{h} \cdot \eta \cdot \frac{U}{h}$$

where h = oil film thickness

h^* = oil film thickness at beginning of film rupture. (In this case located in the lower half or at the lower eccentricities at the angle φ_2).

The power loss per unit width of the upper half of the bearing is

$$E_2 = \int_{\varphi_2}^{\varphi_1 + 2\pi} \tau \, U \, r \, d\varphi = \int_{\varphi_2}^{\varphi_1 + 2\pi} \frac{h^*}{h} \cdot \eta \cdot \frac{U}{h} \cdot U \, r \, d\varphi$$

Using the non-dimensional expressions

$$H = \frac{h}{\Delta r}$$

$$E_0 = \frac{E \psi}{\eta \, U^2}$$

the non-dimensional power loss per unit width for the upper bearing half is

$$E_{20} = \int_{\varphi_2}^{\varphi_1 + 2\pi} \frac{H^*}{H^2} \, d\varphi = H^* \int_{\varphi_2}^{\varphi_1 + 2\pi} \frac{d\varphi}{(1 - \varepsilon \cos \varphi)^2} =$$

$$= H^* \cdot \frac{(\gamma_1 + 2\pi - \gamma_2) + \varepsilon \left[\sin (\gamma_1 + 2\pi) - \sin \gamma_2\right]}{\sqrt{(1 - \varepsilon^2)^3}}$$

where $H^* = 1 - \varepsilon \cos \varphi^*$

$$\gamma = \arccos \frac{\cos \varphi - \varepsilon}{1 - \varepsilon \cos \varphi}$$

The values of E_{20} are given in table 12.1.

Table 12.1. Values of E_{20}

ε / ν	0	0,1	0,2	0,4	0,6	0,8	0,9	1,0
∞	3,14	2,78	2,41	1,87	1,20	0,518	0,217	0
1	3,14	2,80	2,46	1,82	1,15	0,492	0,208	0
0,5	3,14	2,81	2,49	1,79	1,09	0,456	0,192	0
0,25	3,14	2,82	2,48	1,78	1,06	0,427	0,178	0

Now it will be assumed that the effective width of the upper half is 2/3 of the bearing width because of the grooves for the oil rings. Thus the non-dimensional number of the power loss per unit width is

$$E_0 = \frac{E \psi}{\eta U^2} = E_{10} + \frac{2}{3} \cdot E_{20}$$

The total power loss is

$$E_{tot} = b E$$

From the continuity condition follows that the strips will go through the groove at φ_2. However, the groove will to some extent break the strips just after the groove, as the oil looses its grip to the bearing surface. The strips will then start later. This gives a small decrease of the power loss. The above described behaviour only takes place in the middle of the bearing. At the sides the oil is sucked into the bearing and there the strips are somewhat broader than the theoretical ones, which can be assumed to compensate the above decrease in power loss. The behaviour described above does only take place at higher eccentricities when cavitation starts in the lower half of the bearing, and the influence of this must be negligible. When the values of E_{20} are the same in the tables 12.1 and 24.1 there is no cavitation in the lower half of the bearing.

If all of the power loss heats the oil, the energy equation becomes

$$E = c\,\varrho\,q'\,\Delta t$$

where c = specific heat of oil

ϱ = density of oil

and the average temperature rise becomes

$$\Delta t = \frac{E}{c\,\varrho\,q'} = \frac{\eta\,U^2\,E_0}{\psi\,c\,\varrho\,U\,\Delta r\,q_0'}$$

or non-dimensionally

$$\Delta t_0 = c\,\varrho \cdot \frac{\Delta t\,\psi^2}{\eta\,\omega} = \frac{E_0}{q_0'}$$

The temperature calculation is based on the side leakage, which represents the oil circulation.

3,4. Coefficient of Friction and Relative Power Loss

The coefficient of friction μ is friction force per unit load, and the relative power loss f is defined as power loss per unit load. These two quantities written in the non-dimensional way are

$$\frac{\mu}{\psi} = \frac{f}{\omega\,\Delta r} = \frac{E_0}{P_0}$$

or

$$\frac{\mu\,r}{h_{\min}} = \frac{f}{\omega\,h_{\min}} = \frac{E_0}{P_0\,(1-\varepsilon)}$$

3,5. Tables of Calculated Values at Ring-lubrication

$\nu = \infty$

ε	0	0,1	0,2	0,4	0,6	0,8	0,9	1,0
P_0	0	0,917	1,78	3,55	6,09	12,6	24,9	∞
β	90,0	72,9	61,3	50,0	43,2	33,4	25,6	0
q_0'	0	0	0	0	0	0	0	0
E_0	5,23	5,11	5,18	5,82	7,17	10,6	15,6	∞
Δt_0	∞	∞	∞	∞	∞	∞	∞	∞
$\frac{f}{\omega\, \Delta r}$	∞	5,57	2,91	1,64	1,18	0,841	0,627	0
$\frac{f}{\omega\, h_{\min}}$	∞	6,19	3,64	2,73	2,95	4,21	6,27	∞

$\nu = 1$

ε	0	0,1	0,2	0,4	0,6	0,8	0,9	1,0
P_0	0	0,227	0,475	1,15	2,49	6,87	16,5	∞
β	90,0	78,5	68,9	55,9	44,7	32,3	24,1	0
q_0'	0	0,0739	0,139	0,236	0,296	0,302	0,279	—
E_0	5,23	5,08	5,04	5,38	6,36	9,25	13,3	∞
Δt_0	∞	68,7	36,3	22,8	21,5	30,6	47,7	∞
$\frac{f}{\omega\, \Delta r}$	∞	22,4	10,6	4,68	2,55	1,35	0,806	0
$\frac{f}{\omega\, h_{\min}}$	∞	24,9	13,3	7,80	6,38	6,75	8,06	∞

$\nu = 0{,}5$

ε	0	0,1	0,2	0,4	0,6	0,8	0,9	1,0
P_0	0	0,0727	0,155	0,401	0,992	3,46	10,1	∞
β	90,0	80,0	72,1	58,0	45,0	31,3	22,8	0
q_0'	0	0,0906	0,175	0,317	0,416	0,457	0,447	—
E_0	5,23	5,07	5,00	5,17	5,95	8,38	12,3	∞
Δt_0	∞	56,0	28,6	16,3	14,3	18,3	27,5	∞
$\frac{f}{\omega\, \Delta r}$	∞	69,7	32,3	12,9	6,00	2,42	1,22	0
$\frac{f}{\omega\, h_{\min}}$	∞	77,4	40,4	21,5	15,0	12,1	12,2	∞

$\nu = 0{,}25$

ε	0	0,1	0,2	0,4	0,6	0,8	0,9	1,0
P_0	0	0,0195	0,0419	0,112	0,295	1,21	4,32	∞
β	90,0	81,4	73,7	59,0	45,0	30,4	21,4	0
q_0'	0	0,0963	0,189	0,349	0,472	0,542	0,536	—
E_0	5,23	5,06	4,98	5,10	5,75	7,80	11,1	∞
Δt_0	∞	52,5	26,3	14,6	12,2	14,4	20,7	∞
$\frac{f}{\omega\, \Delta r}$	∞	259	119	45,5	19,5	6,45	2,57	0
$\frac{f}{\omega\, h_{\min}}$	∞	288	149	75,8	48,8	32,3	25,7	∞

3,6. Charts of Bearing Quantities at Ring-lubrication

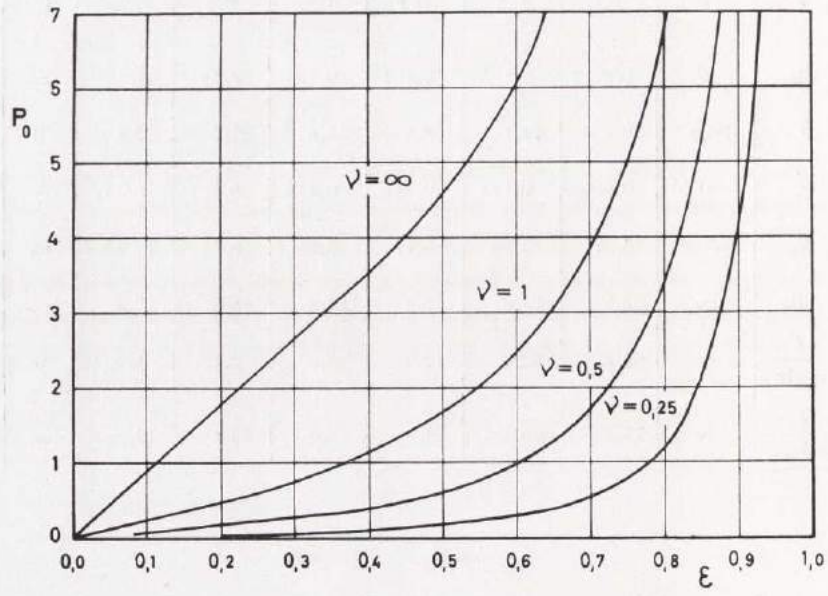

Chart 16.1. Load Capacity $P_0 = \dfrac{P\,\psi^2}{\eta\,U}$

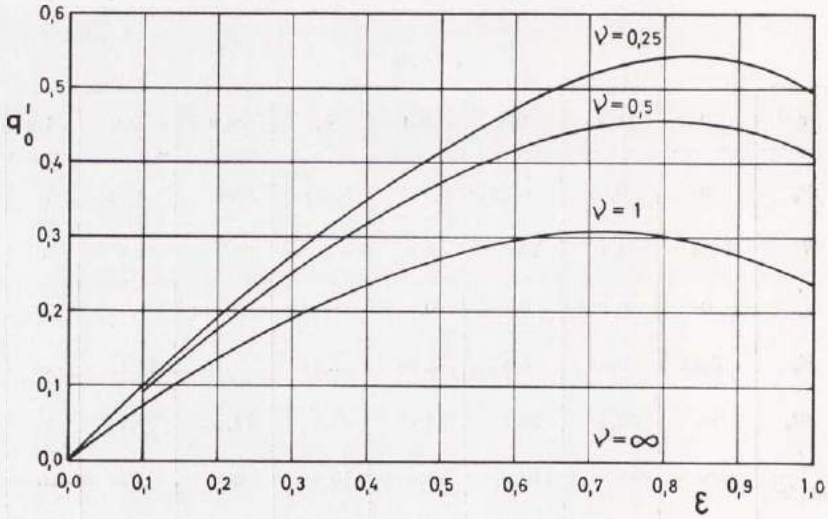

Chart 16.2. Oil Flow $q_0' = \dfrac{q}{U\,\Delta r}$

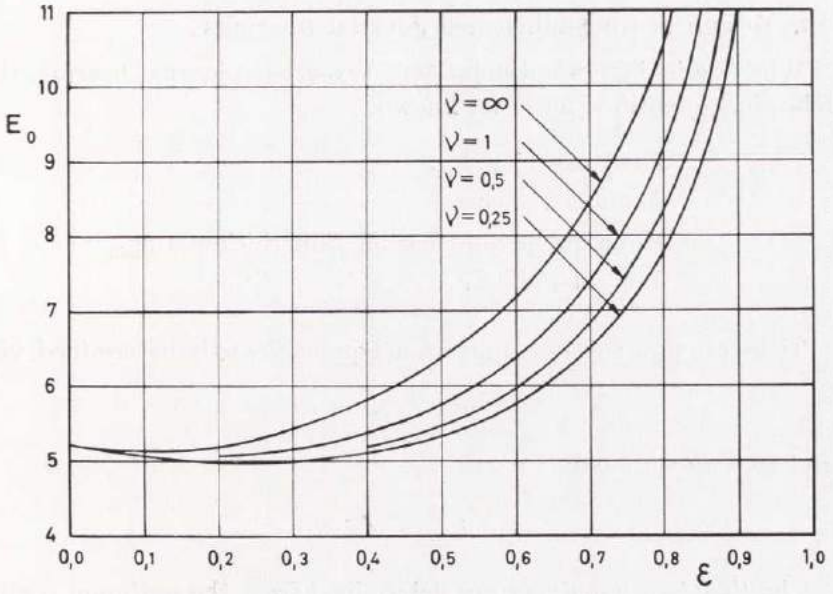

Chart 17.1. Power Loss $E_0 = \frac{E\,\psi}{\eta\,U^2}$

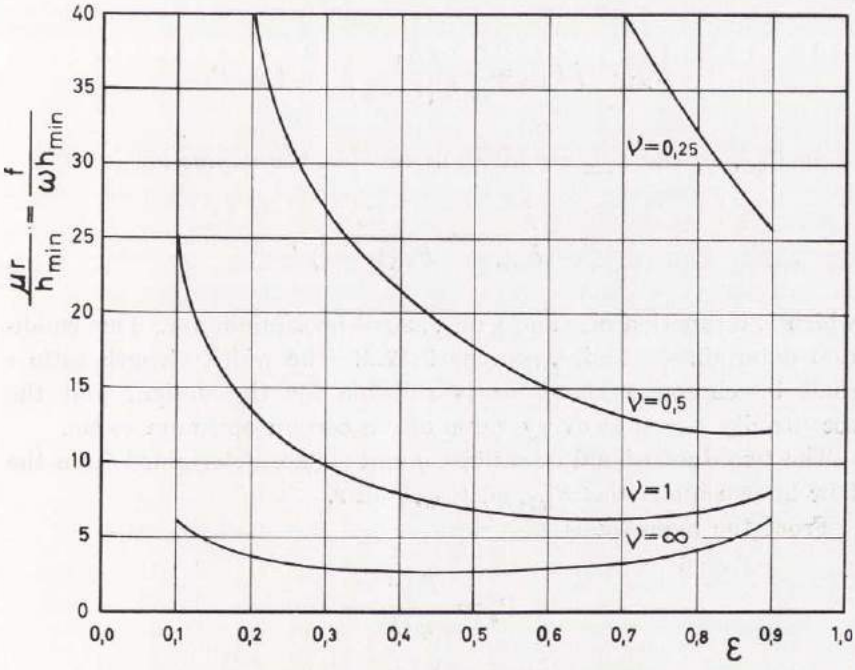

Chart 17.2. Coefficient of Friction and Relative Power Loss

3,7. Design of Ring-lubricated Journal Bearings

When designing an optimum 360° two-groove journal bearing, the following quantities must be known:

Load capacity P_{tot}
Angular velocity ω
Minimum permissible oil film thickness h_{min}
Journal radius r

There are now two non-dimensional quantities to be determined, viz.

$$\nu \qquad \varepsilon$$

and two dimensional

$$\eta \qquad \Delta r$$

The first two quantities are determined from the optimum condition that the power loss should be at a minimum. The total power loss is

$$E_{tot} = f P_{tot} = \frac{E_0}{P_0 (1 - \varepsilon)} \cdot \omega h_{min} P_{tot}$$

As P_{tot}, ω, and h_{min} are given quantities, the expression

$$\frac{f}{\omega h_{min}} = \frac{E_0}{P_0 (1 - \varepsilon)},$$

which is a function of ν and ε only, shall be a minimum. This condition determines ν and ε, see chart 17.2. The width—length ratio ν shall be chosen as large as is suitable for the design, and the eccentricity ε gets at every value of ν a certain optimum value.

The two dimensional quantities η and Δr are determined from the four known quantities P_{tot}, ω, h_{min}, and r.

From the expressions

$$P_0 = \frac{P \psi^2}{\eta U}$$

$$h_{min} = \Delta r (1 - \varepsilon)$$

we get

$$\eta = \frac{P_{tot}\, h_{min}^2}{b\, P_0\, \omega\, (1-\varepsilon)^2\, r^3}$$

$$\Delta r = \frac{h_{min}}{1-\varepsilon}$$

Study now the temperature conditions in the bearing. The oil chosen shall have the above calculated viscosity at the mean operation temperature of the bearing. A good value of this temperature is assumed to be the average temperature t_a of the side flow. The bearing thus operates at the temperature of the outlet oil. The temperature of the reservoir oil, which is supplied to the bearing, is called t_r, and the temperature of the surroundings is t_s. The heat equilibrium now gives

$$E_{tot} = c\, \varrho\, Q'\, (t_a - t_r) = \alpha\, A\, (t_r - t_s)$$

where α = coefficient of thermal transmittance by convection

A = area of the bearing housing

The average temperature rise in the bearing based on the side flow becomes

$$t_a - t_r = \Delta t = \frac{E_{tot}}{c\, \varrho\, Q'}$$

and the difference between the reservoir temperature and that of the surroundings is

$$t_r - t_s = \frac{E_{tot}}{\alpha\, A}$$

Thus

$$t_a - t_s = \frac{E_{tot}}{c\, \varrho\, Q'} + \frac{E_{tot}}{\alpha\, A}$$

3,8. Schedule for Calculation

ν is chosen in agreement with the design

ε is chosen so that $\dfrac{f}{\omega\, h_{\min}}$ is minimum

$$\eta = \frac{P_{\text{tot}}\, h_{\min}^2}{b\, P_0\, \omega\, (1-\varepsilon)^2\, r^3}$$

$$\Delta r = \frac{h_{\min}}{1-\varepsilon}$$

$$\psi = \frac{\Delta r}{r}$$

$$f = \frac{E_0}{P_0\,(1-\varepsilon)} \cdot \omega\, h_{\min}$$

$$E_{\text{tot}} = f\, P_{\text{tot}}$$

$$Q' = b\, q' = b\, q_0'\, U\, \Delta r$$

$$t_a - t_s = \frac{E_{\text{tot}}}{c\, \varrho\, Q'} + \frac{E_{\text{tot}}}{\alpha\, A}$$

3,9. Example

Design an optimum ring-lubricated two-groove journal bearing for the load capacity 5000 N, the rotational speed 1000 r/min, the minimum permissible oil film thickness 0,030 mm, and the shaft radius 5 cm. Suitable width is 10 cm. $c = 2000$ Nm/kg° C, $\varrho = 900$ kg/m³, and $\alpha = 10$ Nm/m²s° C. The area against the surroundings is $A = 0{,}25$ m².

$$\nu = 1$$

$$\varepsilon = 0{,}6$$

$$\eta = \frac{5000 \cdot 0{,}000030^2}{0{,}1 \cdot 2{,}49 \cdot 105 \cdot 0{,}4^2 \cdot 0{,}05^3} = 0{,}0086 \text{ Ns/m}^2$$

$$\Delta r = \frac{0{,}030}{0{,}4} = 0{,}075 \text{ mm}$$

$$\psi = \frac{0{,}075}{50} = 1{,}5\ ‰$$

$$f = 6{,}38 \cdot 105 \cdot 0{,}000030 = 0{,}0201\ \text{m/s}$$

$$E_{tot} = 0{,}0201 \cdot 5000 = 100\ \text{Nm/s} = 100\ \text{W} = 0{,}100\ \text{kW}$$

$$Q' = 0{,}1 \cdot 0{,}296 \cdot 0{,}05 \cdot 105 \cdot 0{,}000075 = 0{,}0000117\ \text{m}^3\text{/s} = 0{,}70\ \text{l/min}$$

$$t_a - t_s = \frac{100}{2000 \cdot 900 \cdot 0{,}0000117} + \frac{100}{10 \cdot 0{,}25} = 5 + 40 = 45^\circ\ \text{C}$$

If the air temperature is 25° C, the bearing operates at a temperature of 25 + 45 = 70° C. Thus the oil shall have the above calculated viscosity at the temperature 70° C.

A ring-lubricated bearing must have limited values of P_{tot}, ω, and h_{min}, if the bearing shall not get too hot.

4. The Pressure-lubricated Journal Bearing

4,1. Pressure Distribution and Load Capacity

Consider a 360° journal bearing of finite width with one oil groove 90° before, and another 90° after the load line. The lubricant is supplied to the two grooves by a pump, and it is assumed that the grooves are filled with oil of atmospheric pressure, or negligible pressure compared to the hydrodynamic pressures in the oil film, see fig. 8.1 and 23.1. The pressure distribution and the load capacity are the same as those of the ring-lubricated bearing, see chap. 3,1.

The calculated values of the pressure-lubricated bearing are given in chap. 4,5 and charts are given in chap. 4,6.

4,2. Oil Flow

In this case both grooves are filled with oil of atmospheric pressure and it is assumed that the groove oil is always kept cold through circulation. The oil flow per unit width entering the lower half of the bearing is called q_1 and given in tab. 23.2, and the flow entering the upper half is q_2 and given in tab. 23.3. For the lower half q_1 is calculated from the tables of RAIMONDI-BOYD (9). The flow in the upper half is

$$q_2 = \frac{U h_2}{2} = \frac{U \Delta r (1 - \varepsilon \cos \varphi_2)}{2}$$

or non-dimensionally

$$q_{20} = \frac{q_2}{U \Delta r} = \frac{1 - \varepsilon \cos \varphi_2}{2} = \frac{H_2}{2}$$

as there is a straight line velocity distribution of full width at the inlet oil groove.

The oil flow per unit width of the bearing is thus

$$q = q_1 + q_2$$

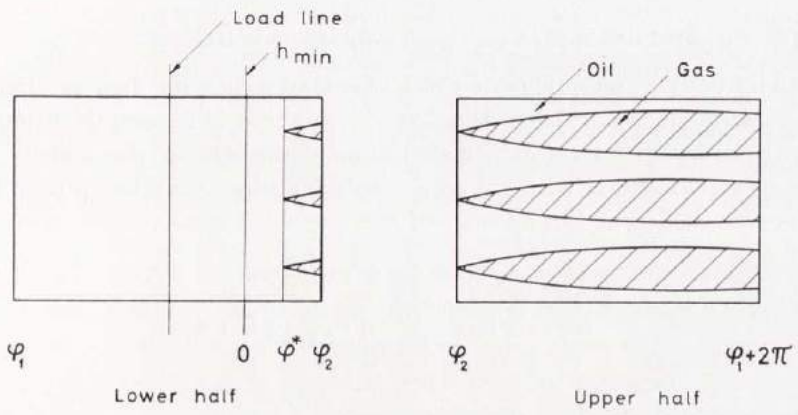

Fig. 23.1

and the non-dimensional group

$$q_0 = \frac{q}{U\,\Delta r} = q_{10} + q_{20}$$

Table 23.2. Values of q_{10}

ν \ ε	0	0,1	0,2	0,4	0,6	0,8	0,9	1,0
∞	0,500	0,484	0,446	0,350	0,242	0,122	0,0605	0
1	0,500	0,532	0,551	0,555	0,517	0,419	0,341	—
0,5	0,500	0,543	0,579	0,626	0,626	0,567	0,505	—
0,25	0,500	0,547	0,590	0,654	0,676	0,648	0,592	—

Table 23.3. Values of q_{20}

ν \ ε	0	0,1	0,2	0,4	0,6	0,8	0,9	1,0
∞	0,500	0,452	0,412	0,347	0,295	0,280	0,306	—
1	0,500	0,451	0,407	0,334	0,289	0,286	0,316	—
0,5	0,500	0,451	0,405	0,330	0,288	0,292	0,326	—
0,25	0,500	0,451	0,404	0,329	0,288	0,297	0,336	—

4,3. Power Loss and Average Temperature Rise

The power loss values of the lower loaded bearing half is already calculated in ref. (8). In the upper half there is a cavitation region with straight-line velocity distribution over part of the width. All the width is filled with oil at the leading edge; thus the power loss per unit width of the upper half is

$$E_2 = \int_{\varphi_2}^{\varphi_1 + 2\pi} \frac{h_2}{h} \cdot \eta \cdot \frac{U}{h} \cdot U \, r \, d\varphi$$

where h_2 is located at the angle φ_2.

Non-dimensionally

$$E_{20} = \frac{E_2 \psi}{\eta U^2} = H_2 \cdot \frac{(\gamma_1 + 2\pi - \gamma_2) + \varepsilon \left[\sin(\gamma_1 + 2\pi) - \sin \gamma_2\right]}{\sqrt{(1 - \varepsilon^2)^3}}$$

where H_2 is the non-dimensional oil film thickness at the angle φ_2. Values of E_{20} are given in table 24.1.

Now the non-dimensional power loss per unit width is

$$E_0 = \frac{E \psi}{\eta U^2} = E_{10} + E_{20}$$

Table 24.1. Values of E_{20}

ε / ν	0	0,1	0,2	0,4	0,6	0,8	0,9	1,0
∞	3,14	2,78	2,41	1,87	1,50	1,22	1,14	—
1	3,14	2,80	2,46	1,91	1,50	1,22	1,13	—
0,5	3,14	2,81	2,49	1,93	1,51	1,22	1,13	—
0,25	3,14	2,82	2,50	1,94	1,51	1,22	1,14	—

The power loss of a two-groove pressure-lubricated bearing has also been treated by WILCOCK-ROSENBLATT (11). However, they assume

that the oil film will rupture at the minimum space, and they neglect the influence of the pressure flow term in the oil region.

The average temperature rise calculation is based on the total oil flow entering the bearing halves from the grooves, assuming that all the oil entering the bearing is cold. The average temperature rise thus becomes

$$\Delta t = \frac{E}{c\,\varrho\,q}$$

or non-dimensionally

$$\Delta t_0 = c\,\varrho \cdot \frac{\Delta t\,\psi^2}{\eta\,\omega} = \frac{E_0}{q_0}$$

If the oil is not changed fully in the grooves, the temperature rise becomes higher than the above value. Is there no change at all in the grooves, but the oil is only supplied, the temperature rise must be based on the side leakage q', which then represents the circulation of oil and is given in chap. 3.

If there is an oil pressure in the grooves, the load, the oil flow, and the power loss will be somewhat influenced; but for practical cases the above given values still may be used.

4,4. Coefficient of Friction and Relative Power Loss

As in chap. 3,4

$$\frac{\mu}{\psi} = \frac{f}{\omega\,\Delta r} = \frac{E_0}{P_0}$$

or

$$\frac{\mu\,r}{h_{\min}} = \frac{f}{\omega\,h_{\min}} = \frac{E_0}{P_0\,(1-\varepsilon)}$$

4,5. Tables of Calculated Values at Pressure-lubrication

$\nu = \infty$

ε	0	0,1	0,2	0,4	0,6	0,8	0,9	1,0
P_0	0	0,917	1,78	3,55	6,09	12,6	24,9	∞
β	90,0	72,9	61,3	50,0	43,2	33,4	25,6	0
q_0	1,00	0,936	0,858	0,697	0,537	0,402	0,367	—
E_0	6,28	6,04	5,98	6,44	7,87	11,5	16,6	∞
Δt_0	6,28	6,45	6,97	9,24	14,7	28,6	45,2	∞
$\frac{f}{\omega\, \Delta r}$	∞	6,59	3,36	1,81	1,29	0,913	0,667	0
$\frac{f}{\omega\, h_{\min}}$	∞	7,32	4,20	3,02	3,23	4,57	6,67	∞

$\nu = 1$

ε	0	0,1	0,2	0,4	0,6	0,8	0,9	1,0
P_0	0	0,227	0,475	1,15	2,49	6,87	16,5	∞
β	90,0	78,5	68,9	55,9	44,7	32,3	24,1	0
q_0	1,00	0,983	0,958	0,889	0,806	0,705	0,657	—
E_0	6,28	6,01	5,86	6,08	7,09	10,1	14,3	∞
Δt_0	6,28	6,11	6,17	6,84	8,80	14,3	21,8	∞
$\frac{f}{\omega\, \Delta r}$	∞	26,5	12,3	5,29	2,85	1,47	0,867	0
$\frac{f}{\omega\, h_{\min}}$	∞	29,4	15,4	8,82	7,13	7,35	8,67	∞

$\nu = 0{,}5$

ε	0	0,1	0,2	0,4	0,6	0,8	0,9	1,0
P_0	0	0,0727	0,155	0,401	0,992	3,46	10,1	∞
β	90,0	80,0	72,1	58,0	45,0	31,3	22,8	0
q_0	1,00	0,994	0,984	0,956	0,914	0,859	0,831	—
E_0	6,28	6,01	5,83	5,91	6,73	9,30	13,3	∞
Δt_0	6,28	6,05	5,92	6,18	7,36	10,8	16,0	∞
$\frac{f}{\omega\, \Delta r}$	∞	82,7	37,6	14,7	6,78	2,69	1,31	0
$\frac{f}{\omega\, h_{\min}}$	∞	91,9	47,0	36,7	17,0	13,5	13,1	∞

$\nu = 0{,}25$

ε	0	0,1	0,2	0,4	0,6	0,8	0,9	1,0
P_0	0	0,0195	0,0419	0,112	0,295	1,21	4,32	∞
β	90,0	81,4	73,7	59,0	45,0	30,4	21,4	0
q_0	1,00	0,998	0,994	0,983	0,964	0,945	0,928	—
E_0	6,28	6,00	5,83	5,85	6,55	8,74	12,1	∞
Δt_0	6,28	6,01	5,87	5,95	6,79	9,25	13,0	∞
$\frac{f}{\omega\, \Delta r}$	∞	308	139	52,2	22,2	7,22	2,80	0
$\frac{f}{\omega\, h_{\min}}$	∞	342	174	87,0	55,5	36,1	28,0	∞

4,6. Charts of Bearing Quantities at Pressure-lubrication

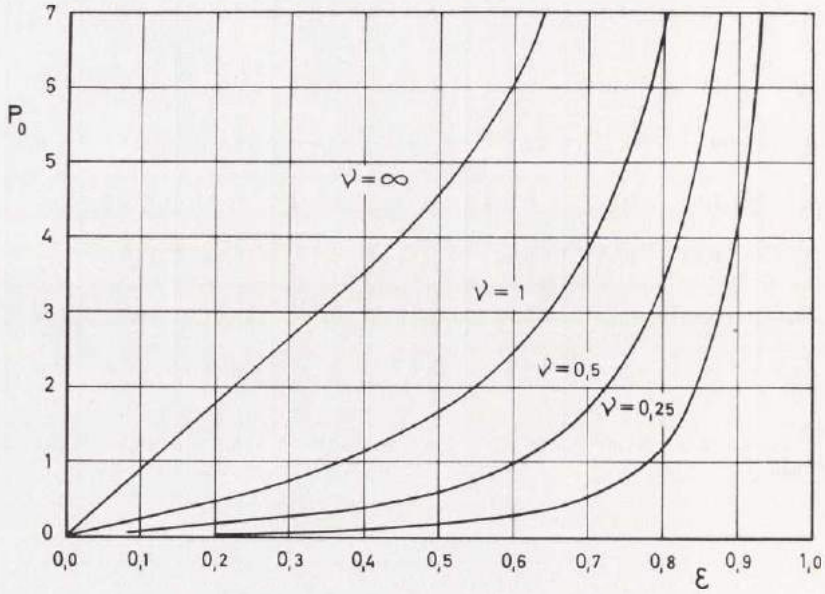

Chart 28.1. Load Capacity $P_0 = \dfrac{P\,\psi^2}{\eta\,U}$

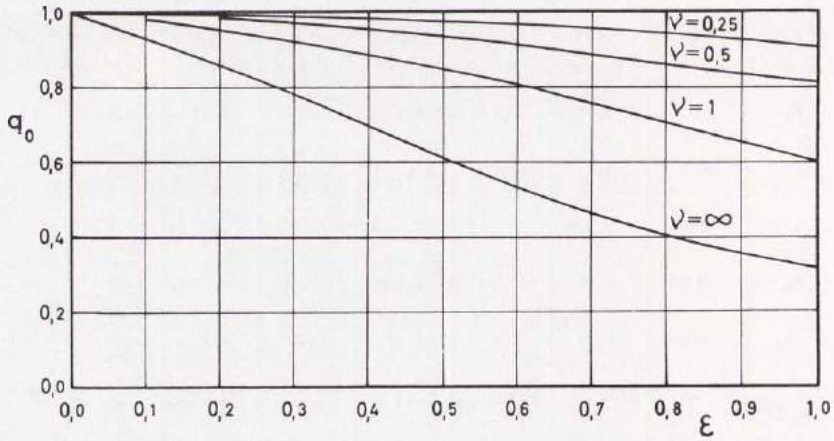

Chart 28.2. Oil Flow $q_0 = \dfrac{q}{U\,\Delta r}$

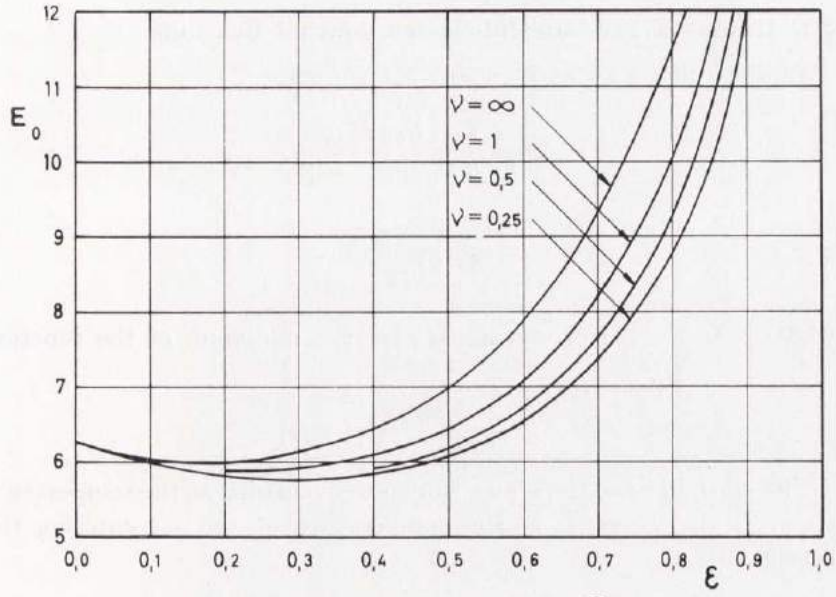

Chart 29.1. Power Loss $E_0 = \dfrac{E\,\psi}{\eta\,U^2}$

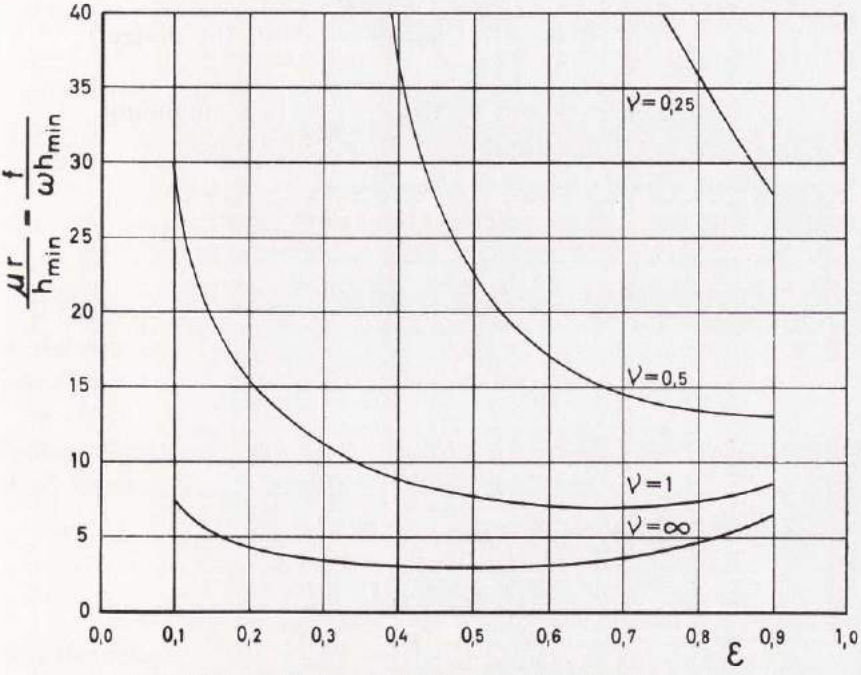

Chart 29.2. Coefficient of Friction and Relative Power Loss

4,7. Design of Pressure-lubricated Journal Bearings

In the same way as in chap. 3,7 we get

$$\eta = \frac{P_{tot}\, h_{min}^2}{b\, P_0\, \omega\, (1-\varepsilon)^2\, r^3}$$

and

$$\Delta r = \frac{h_{min}}{1-\varepsilon}$$

where ν and ε are chosen as to give the minimum of the function

$$\frac{f}{\omega\, h_{min}} = \frac{E_0}{P_0\,(1-\varepsilon)}$$

The oil shall have the above calculated viscosity at the temperature $t_a = t_r + \Delta t$, where t_r is the temperature of the oil entering the bearing.

4,8. Schedule for Calculation

ν is chosen in agreement with the design

ε is chosen so that $\dfrac{f}{\omega\, h_{min}}$ is a minimum

$$\eta = \frac{P_{tot}\, h_{min}^2}{b\, P_0\, \omega\, (1-\varepsilon)^2\, r^3}$$

$$\Delta r = \frac{h_{min}}{1-\varepsilon}$$

$$\psi = \frac{\Delta r}{r}$$

$$f = \frac{E_0}{P_0\,(1-\varepsilon)} \cdot \omega\, h_{min}$$

$$E_{tot} = f\, P_{tot}$$

$$Q = b\, q = b\, q_0\, U\, \Delta r$$

$$t_a - t_r = \Delta t = \frac{E_{tot}}{c\, \varrho\, Q}$$

4,9. **Example**

Design an optimum pressure-lubricated two-groove journal bearing for the load capacity 25000 N, the rotational speed 1500 r/min, the minimum permissible oil film thickness 0,040 mm, and the shaft radius 75 mm. The width is 75 mm. $c = 2000$ Nm/kg °C, $\varrho = 900$ kg/m³.

$$\nu = 0,5$$

$$\varepsilon = 0,8 \text{ is chosen}$$

$$\eta = \frac{25000 \cdot 0,000040^2}{0,075 \cdot 3,46 \cdot 157 \cdot 0,2^2 \cdot 0,075^3} = 0,058 \text{ Ns/m}^2$$

$$\Delta r = \frac{0,040}{0,2} = 0,200 \text{ mm}$$

$$\psi = \frac{0,200}{75} = 2,67 \text{ }^0/_{00}$$

$$f = 13,5 \cdot 157 \cdot 0,000040 = 0,0848 \text{ m/s}$$

$$E_{\text{tot}} = 0,0848 \cdot 25000 = 2120 \text{ Nm/s} = 2,12 \text{ kW}$$

$$Q = 0,075 \cdot 0,859 \cdot 0,075 \cdot 157 \cdot 0,000200 = 0,000152 \text{ m}^3/\text{s} = 9,1 \text{ l/min}$$

$$t_a - t_r = \frac{2120}{2000 \cdot 900 \cdot 0,000152} = 7,7 \text{ °C}$$

If the reservoir temperature t_r is 15° C higher than the temperature of the surroundings, which is $t_s = 25°$ C, the oil shall have the above calculated viscosity at the temperature $t_a = 25 + 15 + 8 = 48°$ C.

If there is no circulation of oil in the grooves and only the side leakage shall take care of the power generated, the value of $q_0 = 0,859$ shall be changed to $q_0' = 0,457$ from chap. 3,5. Then

$$Q = 4,8 \text{ l/min}$$

$$t_a - t_r = 14,5° \text{ C}$$

and the viscosity shall be chosen at the temperature $t_a = 25 + 15 + 15 = 55°$ C.

5. Conclusion

This work treats the 360° two-groove journal bearing with ring- or pressure-lubrication. It gives tables and charts for bearing design and schedules for calculation of the bearing quantities. Consideration is taken of cavitation of the oil when calculating the power loss. The viscosity is assumed to be constant. It is shown how to design bearings with a minimum of power loss at certain given conditions. Two optimum design examples are given.

6. References

1. Floberg, L.: The Infinite Journal Bearing, Considering Vaporization. Gothenburg, 1957.
2. Floberg, L.: Experimental Investigation of Power Loss in Journal Bearings, Considering Cavitation. Gothenburg, 1959.
3. Floberg, L.: Lubrication of a Rotating Cylinder on a Plane Surface, Considering Cavitation. Gothenburg, 1959.
4. Floberg, L.: The Optimum Thrust Tilting-Pad Bearing. Gothenburg, 1960.
5. Jakobsson, B. and Floberg, L.: The Finite Journal Bearing, Considering Vaporization. Gothenburg, 1957.
6. Jakobsson, B. and Floberg, L.: The Partial Journal Bearing. Gothenburg, 1958.
7. Jakobsson, B. and Floberg, L.: The Rectangular Plane Pad Bearing. Gothenburg, 1958.
8. Jakobsson, B. and Floberg, L.: The Centrally Loaded Partial Journal Bearing. Gothenburg, 1959.
9. Raimondi, A. A. and Boyd, J.: A Solution for the Finite Journal Bearing and its Application to Analysis and Design — III. Trans. Am. Soc. Lubr. Engrs, Vol. 1, No. 1, 1958.
10. Sassenfeld, H. and Walther, A.: Gleitlagerberechnungen. VDI-Forschungsheft 441, 1954.
11. Wilcock, D. F. and Rosenblatt, M.: Oil Flow, Key Factor in Sleeve Bearing Performance. Trans. Am. Soc. Mech. Engrs, vol. 74, p. 849, 1952.

Forts. fr. omsl. 2:dra sida

178. OLVING, SVEN, *A new method for space charge wave interaction studies. I.* 12 s. 1956. Kr. 3: —. (Avd. Elektroteknik. 51.)
179. HANSBO, SVEN, *The critical load of rectangular frames analysed by convergence methods.* 47 s. 1956. Kr. 11: —. (Avd. Väg- och Vattenbyggnad. Byggnadsteknik. 25.)
180. WESTBERG, VIDOR, *Measurements of noise radiation at 10 cm from glow lamps. Preliminary report.* 14 s. 1956. Kr. 4: 50. (Avd. Elektroteknik. 52.)
181. SVENSSON, S. I., HELLGREN, G., AND PERERS, O., *The Swedish radioscientific solar eclipse expedition to Italy, 1952. Preliminary report.* 30 s. 1956. Kr. 8: —. (Avd. Elektroteknik. 53.)
182. WAX, NELSON, *A note on design considerations for a proposed auroral radar.* 16 s. 1957. Kr. 3: —. (Avd. Elektroteknik. 54.)
183. JOSHI, G. H., *The electromagnetic interaction between two crossing electron streams. I.* 31 s. 1957. Kr. 8 :—. (Avd. Elektroteknik. 55.)
184. SMITH, BENGT, *Dry methods for removing hydrogen sulphide from gases.* 65 s. 1957. Kr. 15: —. (Avd. Kemi och Kemisk Teknologi. 34.)
185. EKELÖF, S., BJÖRK, N., AND DAVIDSON, R., *Large signal behaviour of directly heated thermistors.* 31 s. 1957. Kr. 8 :—. (Avd. Elektroteknik. 56.)
186. CARLSSON, BENGT UND LARSSON, HANS, *Wirkungsgrad und Selbsthemmung einfacher umlaufgetriebe.* 48 s. 1957. Kr. 9 :—. (Avd. Maskinteknik. 8.)
187. AURELL, CARL G., *The equivalent transmission line of a linear four-terminal network. Calculations with cascade-connected four-terminal networks.* 39 s. 1957. Kr. 6: —. (Avd. Elektroteknik. 57.)
188. LUNDHOLM, R., *Induced overvoltage-surges on transmission lines and their bearing on the lightning performance at medium voltage networks.* 117 s. 1957. Kr. 19: —. (Avd. Elektroteknik. 58.)
189. FLOBERG, LEIF, *The infinite journal bearing, considering vaporization.* 83 s. 1957. Kr. 13: —. (Avd. Maskinteknik. 9.)
190. JAKOBSSON, BENGT, AND FLOBERG, LEIF, *The finite journal bearing, considering vaporization.* 117 s. 1957. Kr. 19: 50. (Avd. Maskinteknik. 10.)
191. CHAKO, NICHOLAS, *Characteristic curves on planes in the image space.* 49 s. 1957. Kr. 15: —. (Avd. Allmänna Vetenskaper. 12.)
192. EKELÖF, STIG, *The development and decay of the magnetic flux in a non-delayed telephone relay.* 50 s. 1957. Kr. 15: —. (Avd. Elektroteknik. 59.)
193. BJÖRKLUND, KJELL, *Bestämning av porslins draghållfasthet.* 78 s. 1958. Kr. 15: —. (Institutionen för Silikatkemisk Forskning. 39.)
194. GRANHOLM, PER, *Sound insulation of single leaf walls.* 48 s. 1958. Kr. 8: —. (Avd. Väg- och Vattenbyggnad. Byggnadsteknik. 26.)
195. GRANHOLM, HJALMAR, *Om vattengenomslag i murade väggar med särskild hänsyn till tegel som fasadmaterial.* 172 s. 1958. Kr. 16: —. (Avd. Väg- och Vattenbyggnad. Byggnadsteknik. 27.)
196. MEOS, JOHAN, AND OLVING, SVEN, *On the origin of radar echoes associated with auroral activity.* 20 s. 1958. Kr. 5: —. (Avd. Elektroteknik. 60.)
197. JOSHI, G. H., *The electromagnetic interaction between two crossing electron streams. II.* 10 s. 1958. Kr. 3: 50. (Avd. Elektroteknik. 61.)
198. WILHELMSSON, HANS, *The interaction between an obliquely incident plane electromagnetic wave and an electron beam. II.* 32 s. 1958. Kr. 7: —. (Avd. Elektroteknik. 62.)
199. KÄRRHOLM, GUNNAR, *A method of iteration applied to beams resting on springs.* 50 s. 1958. Kr. 12: —. (Avd. Allm. Vetenskaper. 13.)
200. JAKOBSSON, BENGT, AND FLOBERG, LEIF, *The partial journal bearing.* 60 s. 1958. Kr. 14: —. (Avd. Maskinteknik. 11.)
201. KÄRRHOLM, GUNNAR, *Influence functions of elastic plates divided in strips.* 18 s. 1958. Kr. 4: 50. (Avd. Väg- och Vattenbyggnad. Byggnadsteknik. 28.)
202. RÅDE, LENNART, *Sampling planes for acceptance sampling by variables using the range.* 34 s. 1958. Kr. 9: 50. (Avd. Allm. Vetenskaper. 14.)
203. JAKOBSSON, BENGT, AND FLOBERG, LEIF, *The rectangular plane pad bearing.* 44 s. 1958. Kr. 5: —. (Avd. Maskinteknik. 12.)
204. ASPLUND, SVEN OLOF, *Column-beams and suspension bridges analyzed by »Green's matrix».* 36 s. 1958. Kr 7: —. (Avd. Väg- och Vattenbyggnad. Byggnadsteknik. 29.)
205. WILHELMSSON, HANS, *On the properties of the electron beam in the presence of an axial magnetic field of arbitrary strength.* 32 s. 1958. Kr. 7: 50. (Avd. Elektroteknik. 63.)
206. WILHELMSSON, HANS, *The interaction between an obliquely incident plane electromagnetic wave and an electron beam. III.* 17 s. 1958. Kr. 5: —. (Avd. Elektroteknik. 64.)
207. HEDVALL, ARVID J., *On the influence of pre-treatment and transition processes on the adsorption capacity and the reactivity of various types of glass and silica.* 39 s. 1959. Kr. 8: —. (Institutionen för Silikatkemisk Forskning. 40.)

Forts. å omsl. 4:de sida

Forts. fr. omsl. 3:dje sida

208. KÄRRHOLM, GUNNAR, *A flow problem solved by strip method.* 22 s. 1959. Kr. 4: 50. (Avd. Allm. Vetenskaper. 15.)
209. GRANHOLM, HJALMAR, *Allmän teori för beräkning av armerad betong.* 228 s. 1959. Kr. 20: —. (Avd. Väg- och Vattenbyggnad. Byggnadsteknik. 30.)
210. LIDIN, LARS G., *On helical-springs suspension.* 75 s. 1959. Kr. 15: —. (Avd. Maskinteknik. 13.)
211. BJÖRK, NILS, *Theory of the indirectly heated thermistor.* 46 s. 1959. Kr. 10: —. (Avd. Elektroteknik. 65.)
212. CARLSSON, ORVAR, *The influence of submicroscopic pores on the resistance of bricks towards frost.* 13 s. 1959. Kr. 3: 50. (Institutionen för Silikatkemisk Forskning. 41.)
213. GRANHOLM, HJALMAR, *KAM 40, KAM 60 och KAM 90.* 41 s. 1959. Kr. 3: 50. (Avd. Väg- och Vattenbyggnad. Byggnadsteknik. 31.)
214. JAKOBSSON, BENGT, AND FLOBERG, LEIF, *The centrally loaded partial journal bearing.* 35 s. 1959. Kr. 7: 50. (Avd. Maskinteknik. 14.)
215. FLOBERG, LEIF, *Experimental investigation of power loss in journal bearings, considering cavitation.* 16 s. 1959. Kr. 3: 50. (Avd. Maskinteknik. 15.)
216. FLOBERG, LEIF, *Lubrication of a rotating cylinder on a plane surface, considering cavitation.* 40 s. 1959. Kr. 8: —. (Avd. Maskinteknik. 16.)
217. TROEDSSON, CARL BIRGER, *The growth of the Western city during the Middle Ages.* 125 s. 1959. Kr. 19: —. (Avd. Arkitektur. 4.)
218. HEDVALL, J. ARVID, *The importance of the reactivity of solids in geological-mineralogical processes.* 11 s. 1959. Kr. 2: 50. (Institutionen för Silikatkemisk Forskning. 42.)
219. CORNELL, ELIAS, *Humanistic inquiries into architecture. I—III.* 112 s. 1959. Kr. 17: —. (Avd. Arkitektur. 5.)
220. GRANHOLM, CARL-ADOLF, *Ekonomiska aluminiumprofiler.* 48 s. 1959. Kr. 5: 50. (Avd. Väg- och Vattenbyggnad. Byggnadsteknik. 32.)
221. LUNDÉN, ARNOLD, CHRISTOFFERSON, STINA, AND LODDING, ALEX, *The isotopic effect of lithium ions in countercurrent electromigration in molten lithium bromide and iodide.* 38 s. 1959. Kr. 7: 50. (Avd. Allm. Vetenskaper. 16.)
222. INGEMANSSON, STIG, AND KIHLMAN, TOR, *Sound insulation of frame walls.* 47 s. 1959. Kr. 8: 50. (Avd. Väg- och Vattenbyggnad. Byggnadsteknik. 33.)
223. HÖGLUND, B., and RADHAKRISHNAN, V., *A radiometer for the hydrogen line.* 25 s. 1959. Kr. 6:50. (Avd. Elektroteknik. 66.)
224. JAKOBSSON, BENGT, *Torque distribution, power flow, and zero output conditions of epicyclic gear trains.* 55 s. 1960. Kr. 12: —. (Avd. Maskinteknik. 17.)
225. OLVING, SVEN, *Electromagnetic and space charge waves in a sheath helix.* 91 s. 1960. Kr. 17: —. (Avd. Elektroteknik. 67.)
226. STRÖMBLAD, JOHN, *Beschleunigungsverlauf und Gleichgewichtsdrehzahlen einfacher Planetengetriebe nebst Selbsthemmungsversuche.* 80 s. 1960. Kr. 18: —. (Avd. Maskinteknik. 18.)
227. SANDFORD, FOLKE, *Some current problems concerning brick manufacture.* 20 s. 1960. Kr. 5: —. (Avd. Kemi och Kemisk Teknologi. 35.)
228. OLVING, SVEN, *A new method for space charge wave interaction studies. II.* 40 s. 1960. Kr. 8: —. (Avd. Elektroteknik. 68.)
229. GRANHOLM, HJALMAR, *Le problème de Boussinesq.* 15 s. 1960. Kr. 3: 50. (Avd. Väg- och Vattenbyggnad. Byggnadsteknik. 34.)
230. HIBA, MIODRAG et CEDERWALL, KRISTER, *Flambement élastique d'une barre en bois lamellée et clouée avec le module de déplacement du moyen de liaison constant k.* 22 s. 1960. Kr. 5: —. (Avd. Väg- och Vattenbyggnad. Byggnadsteknik. 35.)
231. FLOBERG, LEIF, *The optimum thrust tilting-pad bearing.* 23 s. 1960. Kr. 5: —. (Avd. Maskinteknik. 19.)

Pris kronor 6: —

ELANDERS BOKTRYCKERI AKTIEBOLAG
GÖTEBORG 1960

CHALMERS TEKNISKA HÖGSKOLAS HANDLINGAR
TRANSACTIONS OF CHALMERS UNIVERSITY OF TECHNOLOGY
GOTHENBURG, SWEDEN
Nr 234 (Avd. Maskinteknik 21) 1961

LUBRICATION OF TWO CYLINDRICAL SURFACES, CONSIDERING CAVITATION

BY

LEIF FLOBERG

Report No. 14 from the Institute of Machine Elements
Chalmers University of Technology
Gothenburg, Sweden
1961

Av Chalmers Tekniska Högskolas Handlingar hava tidigare utkommit:

Fullständig förteckning över Chalmers Tekniska Högskolas Handlingar lämnas av Chalmers Tekniska Högskolas Bibliotek, Göteborg.

151. Hedvall, J. A., *Reactions with activated solids.* 23 s. 1954 Kr. 5: —. (Institutionen för Silikatkemisk Forskning. 32).
152. Smith, Cyril Stanley, *The microstructure of polycrystalline materials.* 49 s. 1954. Kr. 9: 50 (Institutionen för Silikatkemisk Forskning. 33.)
153. Selberg, Arne, *Norska erfaringer fra bygging av små hengebroer.* 20 s. 1954. Kr. 4: —. (Avd. Väg- och Vattenbyggnad. Byggnadsteknik. 21.)
154. Granholm, Hjalmar, *Armerat trä.* 96 s. 1954. Kr. 9: — (Avd. Väg- och Vattenbyggnad. Byggnadsteknik. 22).
155. Wilhelmsson, Hans, *The interaction between an obliquely incident plane electromagnetic wave and an electron beam. I.* 31 s. 1954. Kr. 7: —. (Avd. Elektroteknik. 42.)
156. Olving, Sven, *Electromagnetic wave propagation on helical conductors inbedded in dielectric medium.* 14 s. 1955. Kr. 3: —. (Avd. Elektroteknik. 43.)
157. Olving, Sven, *Amplification of the traveling wave tube at high beam current. I.* 11 s. 1955. Kr. 3: —. (Avd. Elektroteknik. 44.)
158. Hedvall, J. A., Nordengren, Sven, und Liljegren, B., *Über die thermische Zersetzung von Kalziumsulfat bei niedrigen Temperaturen.* 18 s. 1955. Kr. 5: — (Institutionen för Silikatkemisk Forskning. 34.)
159. Dahlgren, Sven-Eric, *On the break-down of thixotropic materials.* 18 s. 1955. Kr. 3: 50. (Institutionen för Silikatkemisk Forskning. 35.)
160. Sandford, Folke, och Liljegren, Berne, *Torkningen av råtegel och dennas inverkan på teglets frostbeständighet.* 22 s. 1955. Kr. 3: —. (Institutionen för Silikatkemisk Forskning. 36.)
161. Wallman, Henry, *Automatic noise-factor meter.* 17 s. 1955. Kr. 3: —. (Avd. Elektroteknik. 45.)
162. Sandford, Folke, and Fransson, Stig *The refractoriness of some types of quartz and quartzite. II.* 24 s. 1955. Kr. 5: —. (Institutionen för Silikatkemisk Forskning. 37).
163. Lindblad, Anders, *Konstruktion av linjer för moderna handelsfartyg.* 176 s. 1955. Kr. 20: —. (Avd. Skeppsbyggeri. 6.)
164. Svartholm, Nils, *Two problems in the theory of the slowing down of neutrons by collisions with atomic nuclei.* 15 s. 1955. Kr. 5: —. (Avd. Allmänna Vetenskaper. 10).
165. Persson, Per, *Bostadsvaneundersökning utförd i hyreslägenheter byggda 1947 i Göteborg, Torpaområdet.* 86 s. 1955. Kr. 12: —. (Avd. Arkitektur. 3.)
166. Hansson, P. R., *Undersökning av mullitbildning i keramiska produkter.* 29 s. 1955. Kr. 6: —. (Institutionen för Silikatkemisk Forskning. 38.)
167. Ekelöf, Stig, *Die Temperaturverteilung in einem gleichstromdurchflossenen langen Metallzylinder mit kreisförmigen Querschnitt.* 38 s. 1955. Kr. 10: —. (Avd. Elektroteknik. 46.)
168. Wilhelmsson, Hans, *On the reflection of electromagnetic waves from a dielectric cylinder.* 17 s. 1955. Kr. 4: 50. (Avd. Elektroteknik. 47.)
169. Björk, N., and Davidson, R., *Small signal behaviour of directly heated thermistors.* 43 s. 1955. Kr. 11: —. (Avd. Elektroteknik. 48.)
170. Forestier, H., *Tendances actuelles dans la formation de l'ingénieur chimiste: selection, orientation, spécialisation; amélioration de son efficience.* 13 s. 1956. Kr. 2: 50. (Avd. Kemi och Kemisk Teknologi 33.)
171. Wax, Nelson, *On the ring current hypothesis.* 32 s. 1956. Kr. 7: —. (Avd. Elektroteknik. 49.)
172. Elgeskog, Erik, *Photoformer analysis and design.* 40 s. 1956. Kr. 8: 50. (Avd. Elektroteknik. 50.)
173. Anzelius, Adolf, *Bimolekulare Reaktion von zwei in Mischung vorliegenden Substanzen mit einer dritten Substanz.* 8 s. 1956. Kr. 5 —. (Avd. Allm. Vetenskaper. 11.)
174. Reinius, Erling, *Model studies for the extension of the habour of Gothenburg.* 38 s. 1956. Kr. 6: —. (Avd. Väg- och Vattenbyggnad. Byggnadsteknik. 23.)
175. Zimen, K. E., *Diffusion von Edelgasatomen die durch Kernreaktion in festen Stoffen gebildet werden.* 7 s. 1956. Kr. 2: —. (Institutionen för Kärnkemi. 1.)
176. Inthoff, W., und Zimen, K. E., *Kinetik der Diffusion radioaktiver Edelgase aus festen Stoffen nach Bestrahlung.* 16 s. 1956. Kr. 4: —. (Institutionen för Kärnkemi. 2)
177. Granholm, Hjalmar, *Puts och lättbetong.* 45 s. 1956. Kr. 3: —. (Avd. Väg- och Vattenbyggnad. Byggnadsteknik. 24)

Forts. å omsl. 3:dje sida

CHALMERS TEKNISKA HÖGSKOLAS HANDLINGAR

TRANSACTIONS OF CHALMERS UNIVERSITY OF TECHNOLOGY
GOTHENBURG, SWEDEN

Nr 234 (Avd. Maskinteknik 21) 1961

LUBRICATION OF TWO CYLINDRICAL SURFACES, CONSIDERING CAVITATION

BY

LEIF FLOBERG

Report No. 14 from the Institute of Machine Elements
Chalmers University of Technology
Gothenburg, Sweden
1961

CHALMERS UNIVERSITY BOOKS / GUMPERTS, GÖTEBORG
GYLDENDALSKE BOGHANDEL / NORDISK FORLAG, KØBENHAVN
AKATEEMINEN KIRJAKAUPPA / AKADEMISKA BOKHANDELN, HELSINGFORS
WILLIAM HEINEMANN LTD, LONDON, MELBOURNE, TORONTO

SCANDINAVIAN UNIVERSITY BOOKS

Gyldendalske Boghandel / Nordisk Forlag, København
Svenska Bokförlaget / P. A. Norstedt & Söner — Albert Bonnier, Stockholm
Akademiförlaget / Gumperts, Göteborg
Akateeminen Kirjakauppa / Akademiska Bokhandeln, Helsingfors
William Heinemann Ltd, London, Melbourne, Toronto

Manuscript received by the Publications Committee,
Chalmers University of Technology, April 28th, 1960

GÖTEBORG 1961
ELANDERS BOKTRYCKERI AKTIEBOLAG

Preface

Since 1955 lubrication research has been carried out at the Institute of Machine Elements, Chalmers University of Technology, Göteborg, Sweden, under the leadership of the head of the Institute, Professor B. JAKOBSSON. Theoretical and experimental investigations have been made to study hydrodynamic lubrication and cavitation in journal bearings and rolling contacts. Nine reports have earlier been published, (1)—(5) and (8)—(11).

This work treats hydrodynamic lubrication of two rotating rigid cylinders. These are lightly loaded and the lubricant viscosity is constant.

I wish to express my sincere thanks to the Swedish Technical Research Council for their kind sponsorship.

Leif Floberg
Tekn. lic.

Contents

Page

Preface 3

1. Introduction 5

2. Notation 6

3. Lubrication of Two Cylindrical Surfaces 8

3,1. Hydrodynamic Pressure Distribution in the Oil Film 8

3,2. Load Capacity 13

3,3. Oil Flow 21

3,4. Power Loss 23

3,5. Temperature Rise 23

3,6. Relative Power Loss 24

3,7. Example 24

4. On the Accuracy of the Approximate Solution Method 28

5. Experimental Investigation 29

6. Conclusion 35

7. References 36

1. Introduction

This report is an extension of an earlier report, ref. (3), which treated the hydrodynamic oil film between a cylinder and a plane. In ref. (3) the behaviour of the oil with variable oil supply was discussed and the theoretical configurations of the oil strips in the cavitated region were shown. Infinite width was assumed. The same case has also been treated by KNESCHKE (12) and GATCOMBE (6). Their boundary condition with film break at the minimum space is, however, not correct as it violates the continuity condition, and the authors neglect the strips of oil in the ruptured zone. Their papers are discussed more in detail in ref. (3).

Here the circular cylinders are approximated to parabolic cylinder surfaces, which gives a more general calculation, as one parameter vanishes. In ref. (3) the exact circular cylinder was used. The parabola method represents a very good approximation. The calculation is made for rigid surfaces and constant viscosity, which holds for lightly loaded cylinders. The width is assumed to be infinite.

The problem treated here has also been studied by GRUBIN (7). He gives the pressure curve which holds for full oil supply, but does not show the influence of variable oil flow on the pressure build-up. GRUBIN neglects the oil strips in the cavitation region when calculating the friction forces, and he neglects the horizontal load components from pressure, which are necessary to give equilibrium of the oil.

2. Notation

A = Constant

c = Specific heat of oil

E = Power loss per unit width

$E_0 = \dfrac{E\sqrt{h_{\min}}}{\eta\,(U_1+U_2)^2\sqrt{r}}$ = Non-dimensional power loss per unit width

F = Shear force per unit width

$F_0 = \dfrac{F\sqrt{h_{\min}}}{\eta\,(U_1+U_2)\sqrt{r}}$ = Non-dimensional shear force per unit width

$f = \dfrac{E}{P_y}$ = Relative power loss

$H = \dfrac{h}{h_{\min}}$ = Non-dimensional oil film thickness

h = Oil film thickness

$h_{\min}$ = Minimum oil film thickness

$k = \dfrac{U_2}{U_1}$ = Velocity ratio

P_x = Force component from pressure in the x-direction per unit width

$P_{x0} = \dfrac{P_x\sqrt{h_{\min}}}{\eta\,(U_1+U_2)\sqrt{r}}$ = Non-dimensional force component from pressure in the x-direction per unit width

P_y = Load capacity per unit width

$P_{y0} = \dfrac{P_y\,h_{\min}}{\eta\,(U_1+U_2)\,r}$ = Non-dimensional load capacity per unit width

p = Oil film pressure

$p_0 = \dfrac{p\sqrt{h^3_{\min}}}{\eta\,(U_1+U_2)\sqrt{r}}$ = Non-dimensional oil film pressure

q = Oil flow per unit width

$q_0 = \dfrac{q}{(U_1 + U_2)\, h_{\min}}$ = Non-dimensional oil flow per unit width

$r = \dfrac{r_1\, r_2}{r_1 + r_2}$ = Equivalent curvature radius

r_1, r_2 = Cylinder radii

Δt = Temperature rise

$\Delta t_0 = c\, \varrho \cdot \dfrac{\Delta t \sqrt{h^3_{\min}}}{\eta\, (U_1 + U_2) \sqrt{r}}$ = Non-dimensional temperature rise

U_1, U_2 = Surface velocities

x, y = Coordinates

$x_0 = \dfrac{x}{\sqrt{r\, h_{\min}}}$ = Non-dimensional x-coordinate

η = Absolute viscosity

ϱ = Density of oil

τ = Shear stress

φ_1, φ_2 = Angular coordinates

3. Lubrication of Two Cylindrical Surfaces

3,1. Hydrodynamic Pressure Distribution in the Oil Film

Study the behaviour of a thin lubricating oil film between two rotating cylinders. The radii of the cylinders are r_1 and r_2, the rotational velocities U_1 and U_2, see fig. 9.1. The surfaces are assumed to be rigid and thus the theory holds for light loads. The calculations are made with the usual assumptions of laminar flow, constant viscosity, and negligible weight and acceleration forces. In theory the width is assumed to be infinite. This holds very well in most of the practical cases as the oil film thicknesses are so very small. For the pressure determination REYNOLDS' equation is used. The validity of this was discussed in an earlier report (3) where a rotating cylinder on a plane surface was treated. The pressure build-up is concentrated to the line of closest approach where REYNOLDS' equation, derived for a thin oil film, holds with good accuracy.

REYNOLDS' equation gives

$$\frac{d}{dx}\left(h^3 \frac{dp}{dx}\right) = 6\,\eta\,(U_1 + U_2)\,\frac{dh}{dx}$$

where x = coordinate

h = oil film thickness

p = oil film pressure

η = absolute viscosity

Integration gives

$$\frac{dp}{dx} = 6\,\eta\,(U_1 + U_2)\,\frac{h - h^*}{h^3} \quad \ldots\ldots\ldots\ldots \quad 8.1$$

if $$\frac{dp}{dx} = 0 \quad \text{at} \quad h = h^*.$$

The oil film thickness is

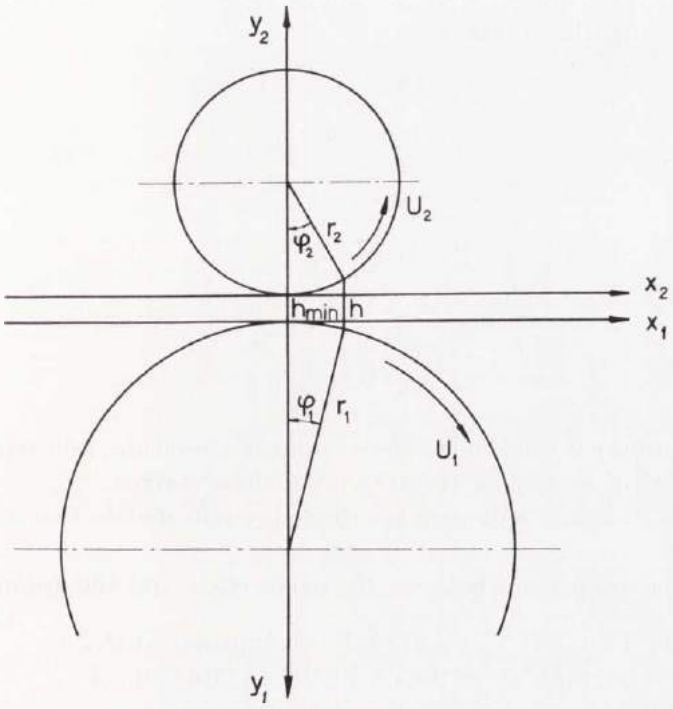

Fig. 9.1

$$h = h_{\min} + y_1 + y_2 = h_{\min} + r_1 (1 - \cos \varphi_1) + r_2 (1 - \cos \varphi_2)$$

Using the two first terms in the series

$$\cos \varphi = 1 - \frac{\varphi^2}{2!} + \frac{\varphi^4}{4!} \ldots\ldots$$

we get

$$h = h_{\min} + r_1 \cdot \frac{\varphi_1^2}{2} + r_2 \cdot \frac{\varphi_2^2}{2}$$

At small angles, where the pressure build-up occurs, we have

$$x = r_1 \varphi_1 = r_2 \varphi_2$$

and then

$$h = h_{\min} + \frac{x^2}{2 r_1} + \frac{x^2}{2 r_2} = h_{\min} + \frac{1}{2} \left(\frac{1}{r_1} + \frac{1}{r_2} \right) x^2$$

Introducing the notation

$$\frac{1}{r_1} + \frac{1}{r_2} = \frac{1}{r}$$

or

$$r = \frac{r_1 r_2}{r_1 + r_2}$$

we get

$$h = h_{\min} + \frac{x^2}{2r}$$

The radius r is called equivalent radius of curvature, as it represents the radius of a cylinder rotating on a plane surface.

The two circular cylinders are thus approximated to two parabolic cylinders.

Make a comparison between the exact circle and the approximate parabola. Then $r\,(1 - \cos\varphi)$ shall be compared to $x^2/2\,r = \frac{r \sin^2\varphi}{2}$. The following table gives the quantities as functions of φ.

$\varphi°$	1	2	3	5	10
$1-\cos\varphi$	0,0001523	0,0006092	0,001371	0,003805	0,01519
$\frac{\sin^2\varphi}{2}$	0,0001523	0,0006090	0,001370	0,003798	0,01508

At small angles, where the pressure has considerable values, the accuracy is quite good. At higher angles the accuracy is lost; but there the pressure has low values and the influence of the approximate height function on the calculated quantities can be neglected.

The non-dimensional oil film thickness

$$H = \frac{h}{h_{\min}} = 1 + \frac{x^2}{2\,r\,h_{\min}}$$

Introduce the notation

$$x_0^2 = \frac{x^2}{r\,h_{\min}}$$

or

$$x_0 = \frac{x}{\sqrt{r\, h_{\min}}}$$

which gives

$$H = 1 + \frac{x_0^2}{2}$$

By introduction of the non-dimensional coordinate x_0 and the non-dimensional oil film thickness H eq. 8.1 becomes

$$\frac{dp}{dx_0} \frac{1}{\sqrt{r\, h_{\min}}} = 6\, \eta\, (U_1 + U_2)\, \frac{H - H^*}{H^3} \cdot \frac{1}{h_{\min}^2} \quad \ldots\ldots \quad 11.1$$

where $H^* = 1 + \frac{(x_0^*)^2}{2}$

Introduce the non-dimensional pressure

$$p_0 = \frac{p \sqrt{h_{\min}^3}}{\eta\, (U_1 + U_2) \sqrt{r}}$$

Then from eq. 11.1

$$\frac{dp_0}{dx_0} = 6 \cdot \frac{H - H^*}{H^3} = \frac{6}{\left(1 + \frac{x_0^2}{2}\right)^2} - \frac{6\, H^*}{\left(1 + \frac{x_0^2}{2}\right)^3}$$

The non-dimensional pressure

$$p_0 = \int_{x_{01}}^{x_0} \left[\frac{6\, dx_0}{\left(1 + \frac{x_0^2}{2}\right)^2} - \frac{6\, H^*\, dx_0}{\left(1 + \frac{x_0^2}{2}\right)^3} \right] = 6 \int_{x_{01}}^{x_0} \left[\frac{1}{2} \cdot \frac{x_0}{1 + \frac{x_0^2}{2}} + \right.$$

$$+ \frac{1}{\sqrt{2}} \operatorname{arctg} \frac{x_0}{\sqrt{2}} \Bigg] - 6\, H^* \int_{x_{01}}^{x_0} \left[\frac{1}{4} \cdot \frac{x_0}{\left(1 + \frac{x_0^2}{2}\right)^2} + \right.$$

$$\left. + \frac{3}{4} \left(\frac{1}{2} \cdot \frac{x_0}{1 + \frac{x_0^2}{2}} + \frac{1}{\sqrt{2}} \operatorname{arctg} \frac{x_0}{\sqrt{2}} \right) \right] \quad \ldots\ldots\ldots\ldots \quad 11.2$$

Tab. 12.1. Theoretical Pressure Values

Curve No	x_{01}	$x_{02}=x_0^*$	x_0	p_0
			$-\infty$	0
			-10	0,00770
			-5	0,0552
			-4	0,0996
I	$-\infty$	0,6719	-3	0,201
			-2	0,458
			-1	0,983
			$-0,6719$	1,075
			0	0,538
			0,6719	0
			$-2,245$	0
			$-2,0$	0,0887
II	$-2,245$	0,6	$-1,0$	0,648
			$-0,6$	0,783
			0	0,391
			0,6	0
			$-1,380$	0
			$-1,0$	0,263
III	$-1,380$	0,5	$-0,5$	0,466
			0	0,233
			0,5	0
			$-0,9542$	0
IV	$-0,9542$	0,4	$-0,4$	0,245
			0	0,122
			0,4	0

If the oil adheres to the surfaces, the continuity of flow gives zero pressure derivative at the end of the pressure build-up. The start of the oil film is dependent upon the oil quantity supplied per unit time. If the oil flow is above a certain required amount and the gravity forces are neglected, the pressure build-up will start where the wedge between the two cylinders starts. With the approximate oil film thickness used that is at $x_{01} = -\infty$. It will end at $x_{02} = x_0^*$ with zero pressure derivative. If the oil flow is lower than that certain amount the oil wedge becomes shorter as x_0^* decreases and the value of x_{01} increases, see tab. 12.1 and fig. 13.1. One of the boundaries is chosen

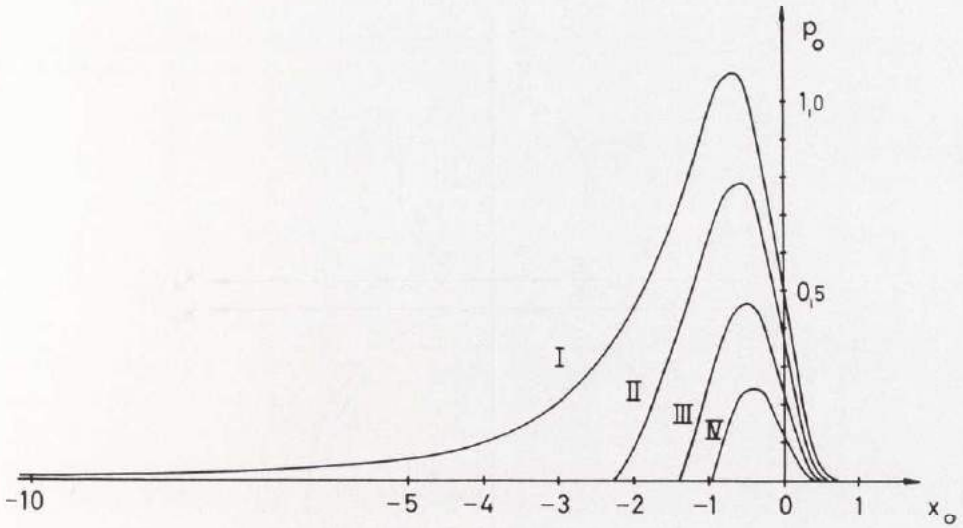

Fig. 13.1. Theoretical Pressure Curves

and the other one is determined by numerical calculation to get the pressure and the pressure derivative zero at the film break. Curve I represents full oil supply and the curves II—IV less oil supply.

3,2. **Load Capacity**

The load components from the pressure and from the shear stress in the oil are determined separately. The component in the y-direction of the shear stress can be neglected in comparison with the load component of the pressure in the same direction, see fig. 14.1. It is assumed that the pressure is constant across the oil film.

The load is

$$P_{1y} = P_{2y} = P_y = \int_{x_1}^{x^*} p\,dx = \prod_{x_1}^{x^*} p\,x - \int_{x_1}^{x^*} \frac{dp}{dx}\,x\,dx =$$

$$= -\int 6\,\eta\,(U_1 + U_2)\,\frac{h - h^*}{h^3}\cdot x\,dx =$$

$$= -\frac{\eta\,(U_1 + U_2)\,r}{h_{\min}} \cdot 6 \int_{x_{01}}^{x_0^*} \frac{H - H^*}{H^3} \cdot x_0\,dx_0$$

The non-dimensional load becomes

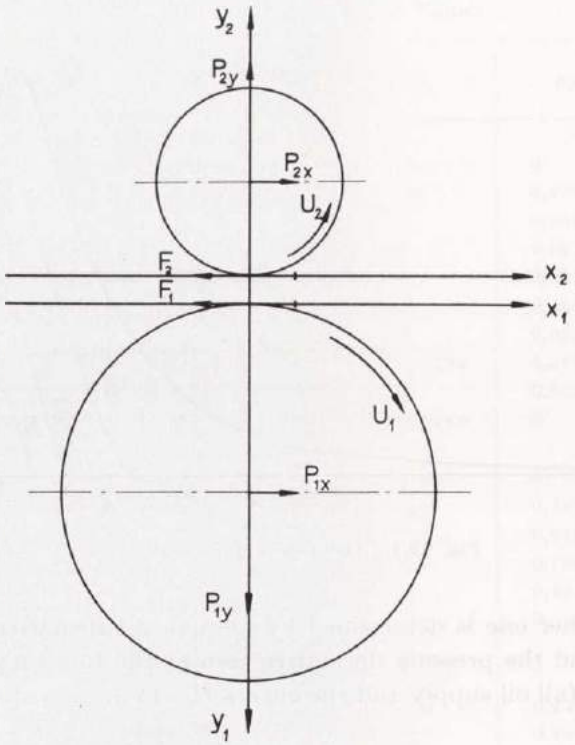

Fig. 14.1. Load Components from Pressure and Shear Stress in the Oil

$$P_{1y0} = P_{2y0} = P_{y0} = \frac{P_y h_{\min}}{\eta (U_1 + U_2) r} = -6 \int_{x_{01}}^{x_0^*} \frac{x_0 \, dx_0}{\left(1 + \frac{x_0^2}{2}\right)^2} +$$

$$+ 6 H^* \int_{x_{01}}^{x_0^*} \frac{x_0 \, dx_0}{\left(1 + \frac{x_0^2}{2}\right)^3} = 6 \left| \frac{1}{1 + \frac{x_0^2}{2}} \right|_{x_{01}}^{x_0^*} - 6 H^* \left| \frac{1}{2\left(1 + \frac{x_0^2}{2}\right)^2} \right|_{x_{01}}^{x_0^*}$$

Calculated values are given in tab. 20.1. The curve of P_{y0} as a function of x_0^* is shown in fig. 15.1.

The component from the pressure in the x-direction on cylinder 1 is

$$P_{1x} = -\int_{x_1}^{x^*} p \frac{dy_1}{dx} \, dx = -\int p \cdot \frac{x}{r_1} \, dx =$$

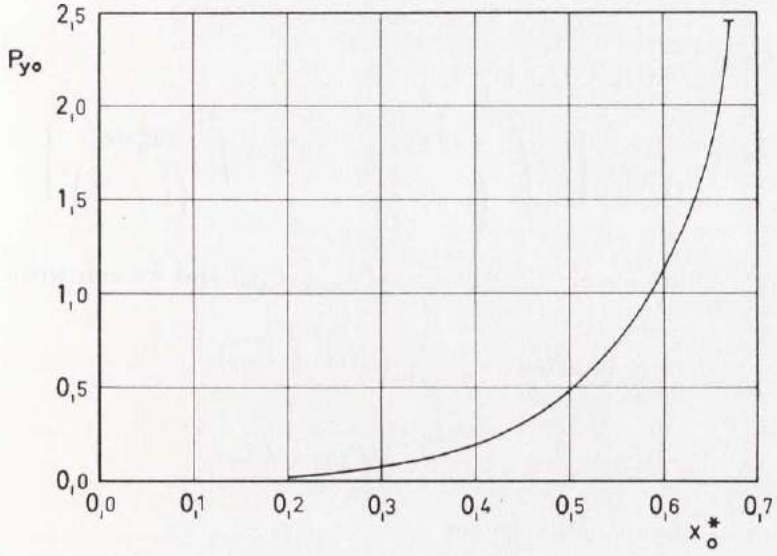

Fig. 15.1. Load Capacity

$$= -\int p \cdot \frac{x^2}{2 r_1} + \int \frac{dp}{dx} \cdot \frac{x^2}{2 r_1} dx =$$

$$= \int 6 \eta (U_1 + U_2) \frac{h - h^*}{h^3} \cdot \frac{x^2}{2 r_1} dx =$$

$$= \frac{\eta (U_1 + U_2)}{r_1 \sqrt{h_{\min}}} \sqrt{\left(\frac{r_1 r_2}{r_1 + r_2}\right)^3} \cdot 3 \int_{x_1}^{x^*} \frac{H - H^*}{H^3} \cdot x_0^2 \, dx_0$$

Non-dimensionally

$$P_{1x0} = \frac{P_{1x} \sqrt{h_{\min}}}{\eta (U_1 + U_2) \sqrt{r}} =$$

$$= \frac{r_2}{r_1 + r_2} \left[3 \int_{x_{01}}^{x_0^*} \frac{x_0^2 \, dx_0}{\left(1 + \frac{x_0^2}{2}\right)^2} - 3 H^* \int_{x_{01}}^{x_0^*} \frac{x_0^2 \, dx_0}{\left(1 + \frac{x_0^2}{2}\right)^3} \right]$$

In the same way

$$P_{2x0} = \frac{P_{2x}\sqrt{h_{\min}}}{\eta\,(U_1 + U_2)\sqrt{r}} =$$

$$= \frac{r_1}{r_1 + r_2}\left[3\int_{x_{01}}^{x_0^*} \frac{x_0^2\,dx_0}{\left(1 + \frac{x_0^2}{2}\right)^2} - 3\,H^*\int_{x_{01}}^{x_0^*} \frac{x_0^2\,dx_0}{\left(1 + \frac{x_0^2}{2}\right)^3}\right]$$

The parenthesis is thus equal to $(P_{1x0} + P_{2x0})$ and we can write

$$P_{1x0} = \frac{r_2}{r_1 + r_2}\,(P_{1x0} + P_{2x0})$$

$$P_{2x0} = \frac{r_1}{r_1 + r_2}\,(P_{1x0} + P_{2x0})$$

Solving the integrals we get

$$P_{1x0} + P_{2x0} = 3\int_{x_{01}}^{x_0^*}\left[-\frac{x_0}{1 + \frac{x_0^2}{2}} + \sqrt{2}\,\operatorname{arctg}\frac{x_0}{\sqrt{2}}\right] -$$

$$- 3\,H^*\int_{x_{01}}^{x_0^*}\left[-\frac{x_0}{2\left(1 + \frac{x_0^2}{2}\right)^2} + \frac{x_0}{4\left(1 + \frac{x_0^2}{2}\right)} + \frac{1}{2\sqrt{2}}\operatorname{arctg}\frac{x_0}{\sqrt{2}}\right]$$

If in eq. 11.2 the condition $p_0 = 0$ at $x_{02} = x_0^*$ is used, the expression is simplified to

$$P_{1x0} + P_{2x0} = 6\int_{x_{01}}^{x_0^*}\left[\sqrt{2}\,\operatorname{arctg}\frac{x_0}{\sqrt{2}} -\right.$$

$$\left. - H^*\left(\frac{x_0}{2\left(1 + \frac{x_0^2}{2}\right)} + \frac{1}{\sqrt{2}}\operatorname{arctg}\frac{x_0}{\sqrt{2}}\right)\right] \quad \ldots\ldots\ldots \quad 16.1$$

The curve of $(P_{1x0} + P_{2x0})$ is shown in fig. 17.1.

It should be pointed out that the non-dimensional groups for P_x and P_y are not the same.

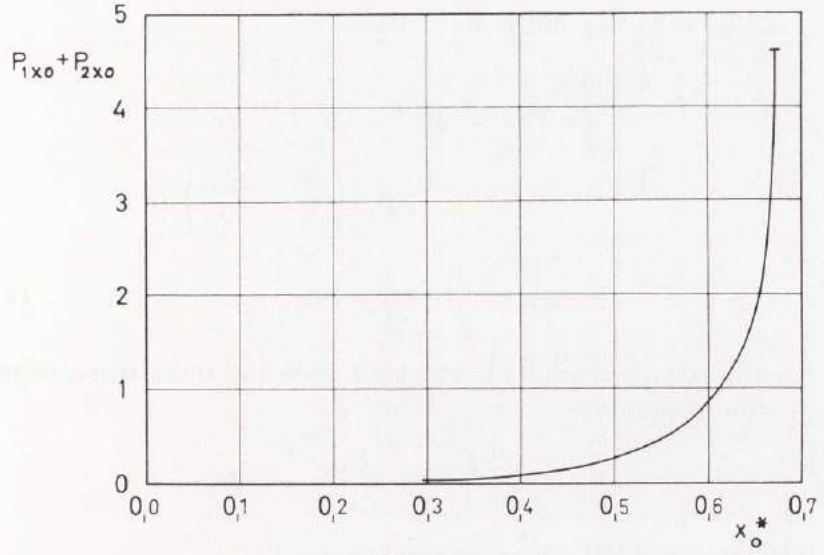

Fig. 17.1

In the oil region the shear stresses at the two surfaces are

$$\tau_1' = -\frac{h}{2}\cdot\frac{dp}{dx} - \eta\cdot\frac{U_1 - U_2}{h}$$

$$\tau_2' = \frac{h}{2}\cdot\frac{dp}{dx} - \eta\cdot\frac{U_1 - U_2}{h}$$

and in the cavitated region

$$\tau_1'' = \tau_2'' = -\frac{h^*}{h}\cdot\eta\cdot\frac{U_1 - U_2}{h}$$

The shear forces are

$$F_1 = -\int_{x_1}^{+\infty} \tau_1\, dx$$

$$F_2 = \int_{x_1}^{+\infty} \tau_2\, dx$$

The shear force acting on cylinder 1 from the shear stress in the oil region is

$$F_1' = \int_{x_1}^{x^*} \frac{h}{2}\cdot\frac{dp}{dx}\, dx + \int_{x_1}^{x^*} \eta\cdot\frac{U_1 - U_2}{h}\, dx$$

Transform the first integral as follows

$$\int_{x_1}^{x^*} \frac{h}{2} \cdot \frac{dp}{dx}\, dx = \left[\frac{h}{2} \cdot p\right] - \frac{1}{2} \int p \frac{dh}{dx}\, dx =$$

$$= -\frac{1}{2} \int p \left(\frac{dy_1}{dx} + \frac{dy_2}{dx}\right) dx =$$

$$= \frac{1}{2} (P_{1x} + P_{2x}) \quad \ldots\ldots\ldots\ldots\ldots\ldots \quad 18.1$$

The shear force acting on cylinder 1 from the shear stress in the cavitation region is

$$F_1'' = \int_{x^*}^{+\infty} \frac{h^*}{h} \cdot \eta \cdot \frac{U_1 - U_2}{h}\, dx$$

Thus the total shear force on cylinder 1 is

$$F_1 = F_1' + F_1'' = \frac{1}{2} (P_{1x} + P_{2x}) +$$

$$+ \frac{\eta (U_1 + U_2) \sqrt{r}}{\sqrt{h_{\min}}} \cdot \frac{1-k}{1+k} \left[\int_{x_{01}}^{x_0^*} \frac{dx_0}{1 + \frac{x_0^2}{2}} + H^* \int_{x_0^*}^{+\infty} \frac{dx_0}{\left(1 + \frac{x_0^2}{2}\right)^2}\right] =$$

$$= \frac{\eta (U_1 + U_2) \sqrt{r}}{\sqrt{h_{\min}}} \left\{\frac{1}{2} (P_{1x0} + P_{2x0}) +\right.$$

$$\left. + \frac{1-k}{1+k} \left[\left[\sqrt{2} \operatorname{arctg} \frac{x_0}{\sqrt{2}}\right]_{x_{01}}^{x_0^*} + H^* \left[\frac{x_0}{2\left(1 + \frac{x_0^2}{2}\right)} + \frac{1}{\sqrt{2}} \operatorname{arctg} \frac{x_0}{\sqrt{2}}\right]_{x_0^*}^{+\infty}\right]\right\}$$

where $k = \dfrac{U_2}{U_1}$.

Non-dimensionally

$$F_{10} = F_{10}' + F_{10}'' = \frac{F_1 \sqrt{h_{\min}}}{\eta (U_1 + U_2) \sqrt{r}} = \frac{1}{2} (P_{1x0} + P_{2x0}) + \frac{1-k}{1+k} \cdot A$$

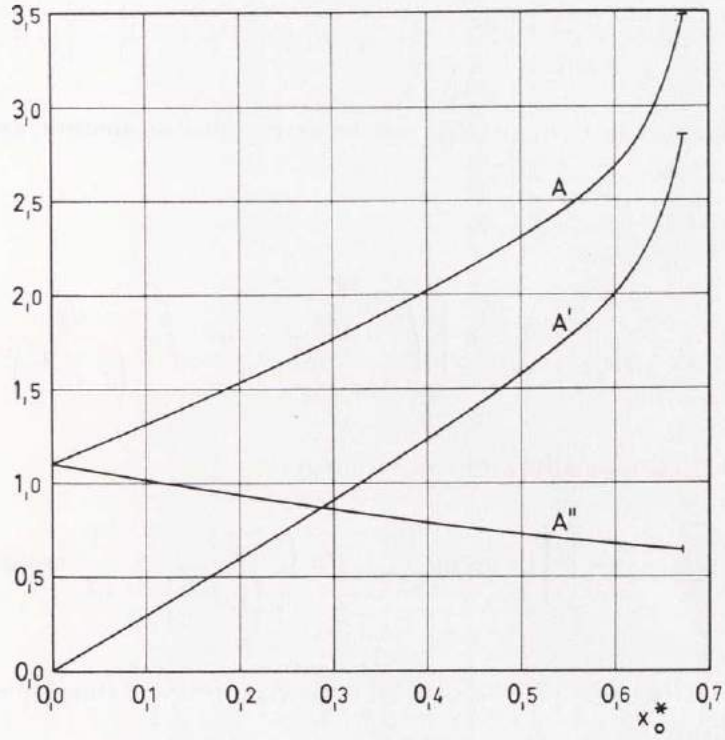

Fig. 19.1

where $A = A' + A''$

and $$A' = \int_{x_{01}}^{x_0^*} \sqrt{2} \operatorname{arctg} \frac{x_0}{\sqrt{2}}$$

$$A'' = H^* \int_{x_0^*}^{+\infty} \left[\frac{x_0}{2\left(1 + \frac{x_0^2}{2}\right)} + \frac{1}{\sqrt{2}} \operatorname{arctg} \frac{x_0}{\sqrt{2}} \right]$$

Curves of A, A' and A'' are shown in fig. 19.1. If the oil is still in contact with both the surfaces under no-load condition, $x_1 = x_2 = x^* = 0$, the value of $A = A'' = \frac{\pi}{2\sqrt{2}} = 1{,}111$. If the oil has lost its contact with one of the surfaces, this value is zero.

In the same way we get

$$F_{20} = \frac{F_2 \sqrt{h_{\min}}}{\eta (U_1 + U_2) \sqrt{r}} = \frac{1}{2} (P_{1x0} + P_{2x0}) - \frac{1-k}{1+k} \cdot A$$

Using eq. 18.1 $(P_{1x} + P_{2x})$ can be determined in another way.

$$P_{1x} + P_{2x} = \int_{x_1}^{x^*} h \frac{dp}{dx} dx =$$

$$= \frac{\eta (U_1 + U_2) \sqrt{r}}{\sqrt{h_{\min}}} \cdot 6 \left[\int_{x_{01}}^{x_0^*} \frac{dx_0}{1 + \frac{x_0^2}{2}} - H^* \int_{x_{01}}^{x_0^*} \frac{dx_0}{\left(1 + \frac{x_0^2}{2}\right)^2} \right]$$

or non-dimensionally with solved integrals

$$P_{1x0} + P_{2x0} = 6 \left[\sqrt{2} \operatorname{arctg} \frac{x_0}{\sqrt{2}} - H^* \left(\frac{x_0}{2\left(1 + \frac{x_0^2}{2}\right)} + \frac{1}{\sqrt{2}} \operatorname{arctg} \frac{x_0}{\sqrt{2}} \right) \right]_{x_{01}}^{x_0^*}$$

which is the same as the simplified expression 16.1 and thus represents a control.

Equilibrium of the oil film in fig. 14.1 gives

$$\begin{cases} P_{1y} = P_{2y} \\ P_{1x} + P_{2x} = F_1 + F_2 \end{cases}$$

These two equations are satisfied by the expressions determined above.

Tab. 20.1. Calculated Values

x_0^*	P_{y0}	$P_{1x0} + P_{2x0}$	A'	A''	A	q_0
0,6719	2,447	4,601	2,849	0,641	3,490	0,6129
0,65	1,777	1,824	2,317	0,651	2,968	0,6056
0,60	1,124	0,8473	1,994	0,676	2,670	0,5900
0,55	0,7367	0,4530	1,768	0,702	2,470	0,5756
0,50	0,4791	0,2465	1,574	0,729	2,303	0,5625
0,45	0,3035	0,1322	1,397	0,758	2,155	0,5506
0,40	0,1847	0,06822	1,229	0,789	2,018	0,5400

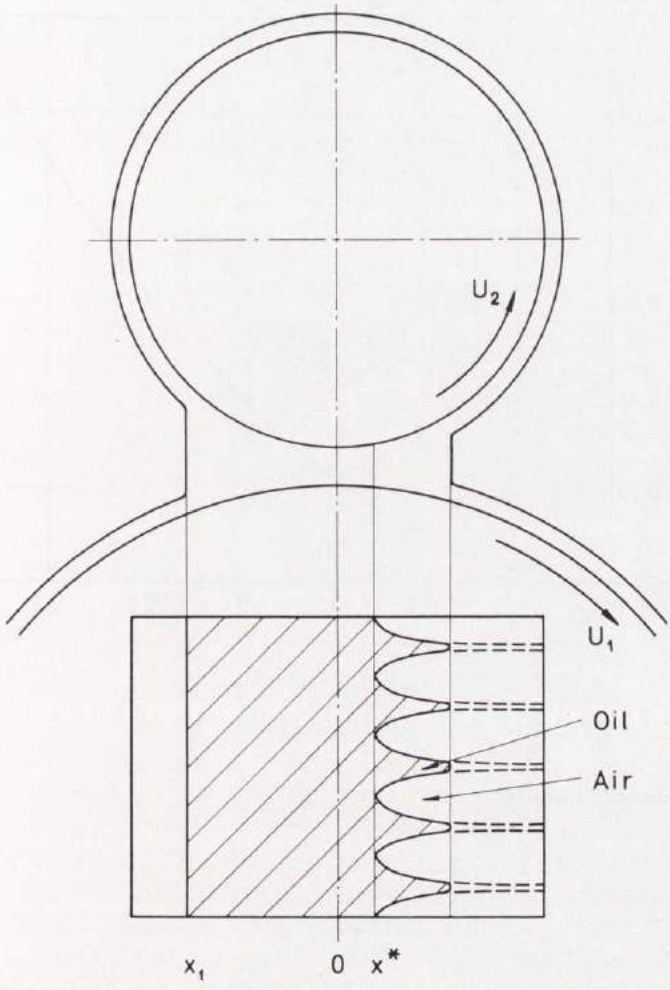

Fig. 21.1

3,3. **Oil Flow**

The oil flow is constant in every section of the wedge as the width is infinite. At $x = x^*$ and $h = h^*$ there is a straight line velocity distribution and thus the flow per unit width is

$$q = \frac{(U_1 + U_2)\, h^*}{2}$$

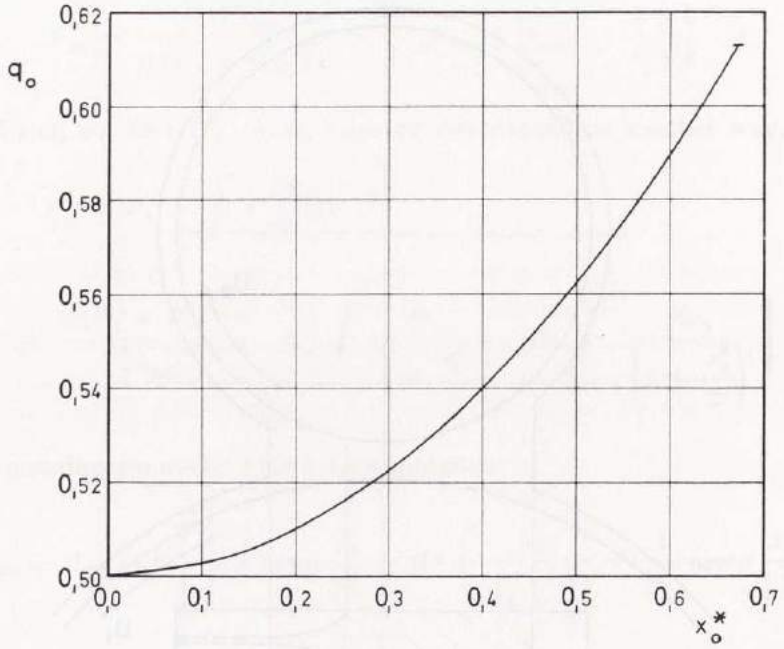

Fig. 22.1. Oil Flow

or non-dimensionally

$$q_0 = \frac{q}{(U_1 + U_2)\, h_{\min}} = \frac{H^*}{2} = \frac{1 + \frac{(x_0^*)^2}{2}}{2}$$

The oil flow values are given in tab. 20.1 and the curve is shown in fig. 22.1.

The oil film starts at $x = x_1$, see fig. 21.1. At $x = x^*$ the film will break into streamlets. It is assumed that these strips end where the wedge ends when calculating the friction forces. In practice they break earlier due to gravity forces and surface tension. However, the adhesion and cohesion forces in the oil are dominating in this case, so this has little influence on the calculated values.

The straight line velocity distribution is located close to the minimum space and thus the oil quantity per unit time needed for full film lubrication is very small.

3,4. Power Loss

The power loss per unit width is

$$E = F_1 U_1 + F_2 U_2 =$$

$$= \frac{\eta (U_1 + U_2) \sqrt{r}}{\sqrt{h_{\min}}} (F_{10} U_1 + F_{20} U_2) =$$

$$= \frac{\eta (U_1 + U_2)^2 \sqrt{r}}{\sqrt{h_{\min}}} \left[\frac{1}{1+k} \cdot F_{10} + \frac{k}{1+k} \cdot F_{20} \right]$$

or non-dimensionally

$$E_0 = \frac{E \sqrt{h_{\min}}}{\eta (U_1 + U_2)^2 \sqrt{r}} = \frac{1}{2} (P_{1x0} + P_{2x0}) + \left(\frac{1-k}{1+k} \right)^2 A$$

3,5. Temperature Rise

If it is assumed that all the power heats the oil, the energy equation becomes

$$E = c \varrho q \Delta t$$

where c = specific heat of oil

ϱ = density of oil

Δt = temperature rise

The temperature rise becomes

$$\Delta t = \frac{E}{c \varrho q} = \frac{\eta (U_1 + U_2)^2 \sqrt{r} E_0}{\sqrt{h_{\min}} c \varrho (U_1 + U_2) h_{\min} q_0}$$

or non-dimensionally

$$\Delta t_0 = c \varrho \cdot \frac{\Delta t \sqrt{h_{\min}^3}}{\eta (U_1 + U_2) \sqrt{r}} = \frac{E_0}{q_0}$$

3,6. Relative Power Loss

The relative power loss is

$$f = \frac{E}{P_y} = \frac{\eta\,(U_1 + U_2)^2\,\sqrt{r}\;E_0\,h_{\min}}{\sqrt{h_{\min}}\;\eta\,(U_1 + U_2)\;P_{y0}\,r}$$

In non-dimensional groups

$$\frac{f\sqrt{r}}{(U_1 + U_2)\sqrt{h_{\min}}} = \frac{E_0}{P_{y0}}$$

3,7. Example

Study the forces acting and the movement of a roller in an unloaded roller bearing with a given radial clearance. The outer ring is stationary and the inner ring is rotating with the angular speed $\omega_3 = 100$ 1/s. The radii are $r_1 = 25$ mm, $r_2 = 5$ mm and $r_3 = 15$ mm. The width of a roller is 10 mm and the radial clearance 10 μm. Calculate for the viscosities 0,1 and 1 Ns/m^2. Determine $h'_{\min}$, $h''_{\min}$, ω_c, ω_2, the forces acting on the roller, and the friction force on the inner ring. The notation is given in fig. 24.1.

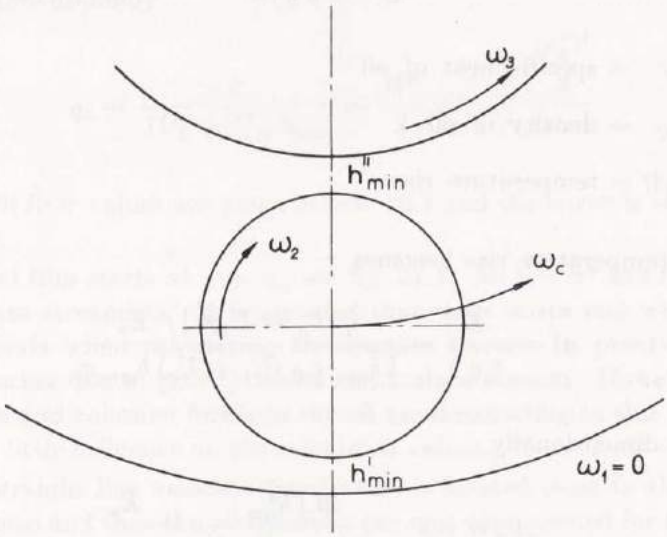

Fig. 24.1

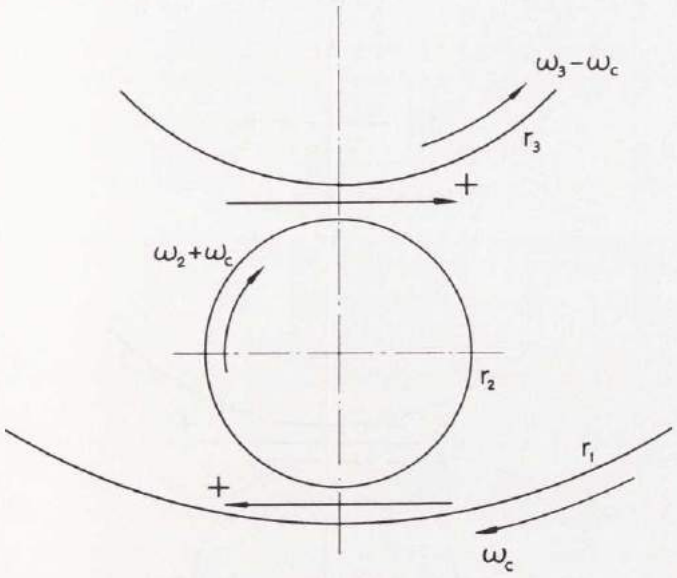

Fig. 25.1

In fig. 25.1 a rotation of ω_c is added to the system to get the speeds at the contact points.

The different forces acting on the three cylinder surfaces are shown in fig. 26.1. There are four unknown quantities: $h'_{\min}$, $h''_{\min}$, ω_c and ω_2. To determine these we need four equations. The geometry gives

$$h'_{\min} + h''_{\min} = C$$

where C = radial clearance.

The three equilibrium equations of the roller become

$$P'_{2x} + F''_2 - P''_{2x} - F'_2 = 0$$

$$P'_{2y} - P''_{2y} = m\,(r_2 + r_3)\,\omega_c^2$$

$$F'_2\,r_2 + F''_2\,r_2 = 0$$

where $m = \pi\,r_2^2\,\varrho$ = mass of the roller per unit width.

The expressions of the forces are

$$P'_{2x} = \frac{-r_1}{-r_1 + r_2}\,(P_{1x0} + P_{2x0})\,\frac{\eta\,[r_1\,\omega_c + r_2\,(\omega_2 + \omega_c)]}{\sqrt{h'_{\min}}}\,\sqrt{\frac{-r_1\,r_2}{-r_1 + r_2}}$$

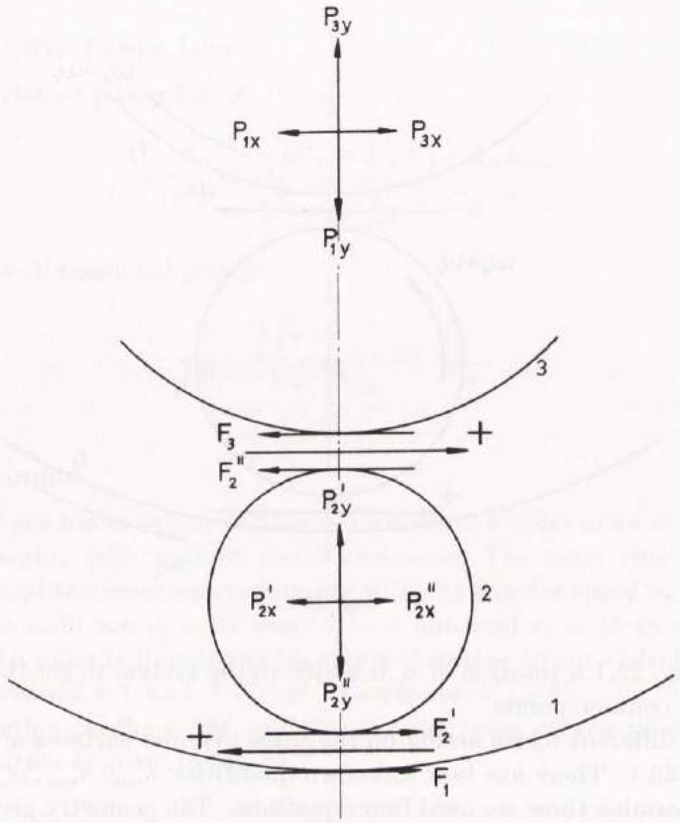

Fig. 26.1

$$P''_{2x} = \frac{r_3}{r_2 + r_3}\,(P_{1x0} + P_{2x0})\,\frac{\eta\,[r_2\,(\omega_2 + \omega_c) + r_3\,(\omega_3 - \omega_c)]}{\sqrt{h''_{\min}}}\,\sqrt{\frac{r_2\,r_3}{r_2 + r_3}}$$

$$P'_{2y} = P_{y0} \cdot \frac{\eta\,[r_1\,\omega_c + r_2\,(\omega_2 + \omega_c)]}{h'_{\min}} \cdot \frac{-r_1\,r_2}{-r_1 + r_2}$$

$$P''_{2y} = P_{y0} \cdot \frac{\eta\,[r_2\,(\omega_2 + \omega_c) + r_3\,(\omega_3 - \omega_c)]}{h''_{\min}} \cdot \frac{r_2\,r_3}{r_2 + r_3}$$

$$F'_2 = \left[\frac{1}{2}\,(P_{1x0} + P_{2x0}) - \frac{r_1\,\omega_c - r_2\,(\omega_2 + \omega_c)}{r_1\,\omega_c + r_2\,(\omega_2 + \omega_c)} \cdot A\right] \cdot$$

$$\cdot \frac{\eta\,[r_1\,\omega_c + r_2\,(\omega_2 + \omega_c)]}{\sqrt{h'_{\min}}}\,\sqrt{\frac{-r_1\,r_2}{-r_1 + r_2}}$$

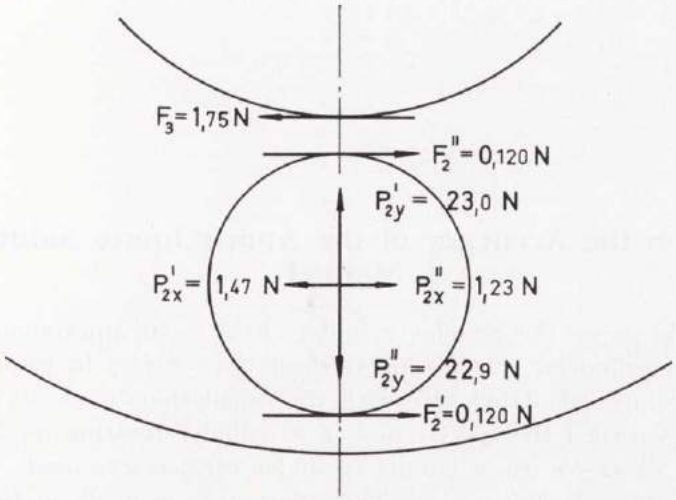

Fig. 27.1

$$F_2'' = \left[\frac{1}{2} (P_{1x0} + P_{2x0}) + \frac{r_2 (\omega_2 + \omega_c) - r_3 (\omega_3 - \omega_c)}{r_2 (\omega_2 + \omega_c) + r_3 (\omega_3 - \omega_c)} \cdot A \right] \cdot$$

$$\cdot \frac{\eta [r_2 (\omega_2 + \omega_c) + r_3 (\omega_3 - \omega_c)]}{\sqrt{h_{\min}''}} \sqrt{\frac{r_2 r_3}{r_2 + r_3}}$$

The four equations are solved and the results are given in the following table.

Case		1	2
η	Ns/m²	0,1	1,0
$h'_{\min}$	μm	4,52	4,60
$h''_{\min}$	μm	5,48	5,40
ω_c	1/s	20,8	21,1
ω_3	1/s	11,9	11,8
P'_{2x}	N/m	14,6	147
P''_{2x}	N/m	12,2	123
P'_{2y}	N/m	231	2300
P''_{2y}	N/m	226	2290
F'_2	N/m	1,22	12,0
F''_2	N/m	−1,22	−12,0
F_3	N/m	17,5	175

The forces acting on the roller are shown in fig. 27.1 for case 2.

4. On the Accuracy of the Approximate Solution Method

In this paper the circular cylinders have been approximated to parabolic cylinders. It is possible to check the accuracy by comparison of the values calculated here with the calculations made in ref. (3) which concerned the special case of a cylinder rotating on a plane surface, where an exact circular cylinder surface was used. In ref. (3) $r_1 = \infty$ and thus $r = r_2$. The comparison is made in the non-dimensional groups used in this treatise. Only the case with full oil supply is studied.

The comparison is made in tab. 28.1, where $\psi = r/h_{\min}$. The accuracy in x_0^*, P_{y0} and q_0 is very good. The values of $(P_{1x0} + P_{2x0})$ and A have satisfactory accuracy for practical use.

The non-dimensional groups for P_y and P_x are not the same so P_y in practice is much larger than P_x.

Tab. 28.1

Case	$\psi = \frac{r}{h_{\min}}$	x_0^*	P_{y0}	$P_{1x0} + P_{2x0}$	A	q_0
Circular cylinder	1 000	0,6711	2,411	4,133	3,409	0,6126
	5 000	0,6719	2,438	4,387	3,454	0,6129
	10 000	0,6720	2,442	4,449	3,464	0,6129
	20 000	0,6721	2,445	4,492	3,472	0,6129
	100 000	0,6722	2,446	4,551	3,482	0,6130
Parabolic cylinder		0,6719	2,447	4,601	3,490	0,6129

5. Experimental Investigation

In the papers by KNESCHKE (12), GATCOMBE (6) and GRUBIN (7) no consideration is taken to the oil strips in the ruptured part of the wedge. In ref. (3) by the present author the strips, derived from the continuity condition under the assumption that the oil adheres to both surfaces, were taken into account. The aim of the tests here was to confirm, if there were oil strips in the cavitated region or if the oil film ended with a straight line in axial direction.

The test apparatus consisted of a box in which a cylinder was mounted in ball bearings. The lid of the box was transparent, see fig. 29.1. The clearance between the cylinders and the plate was adjustable and the cylinder, rotated by a motor via a variator, was wetted by oil in the box.

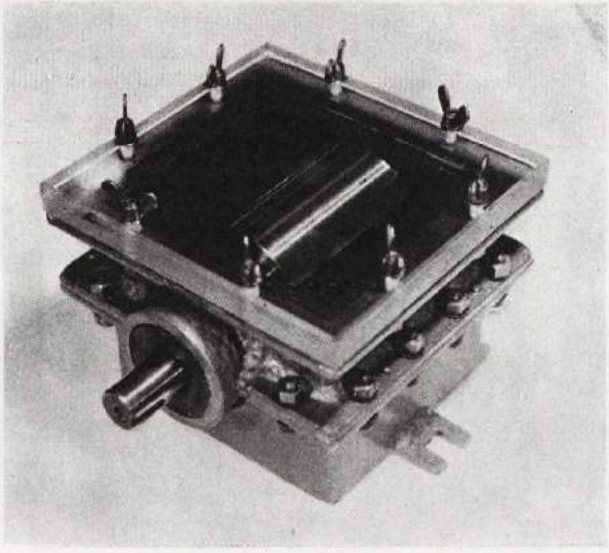

Fig. 29.1. The Test Apparatus

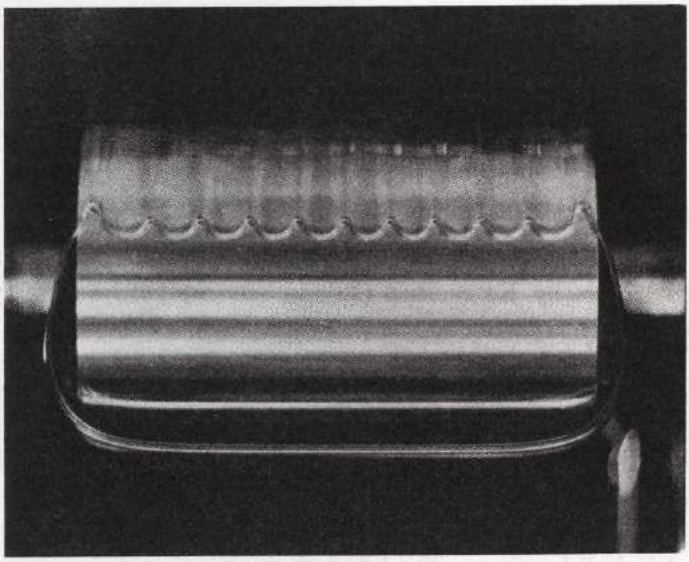

Fig. 30.1. Clearance 0,6 mm, rotational speed 25 r/m

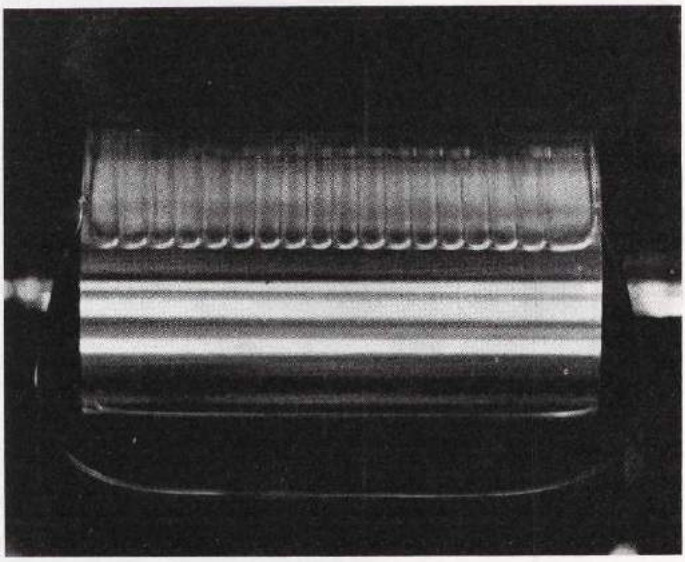

Fig. 30.2. Clearance 0,6 mm, rotational speed 100 r/m

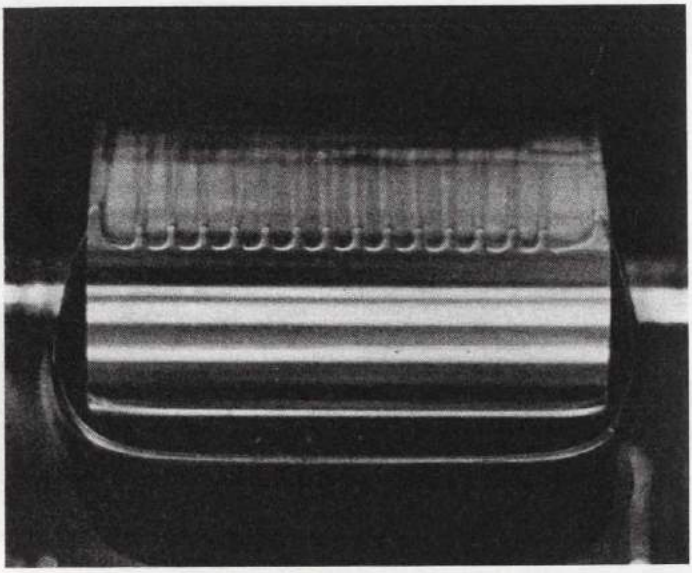

Fig. 31.1. Clearance 0,4 mm, rotational speed 25 r/m

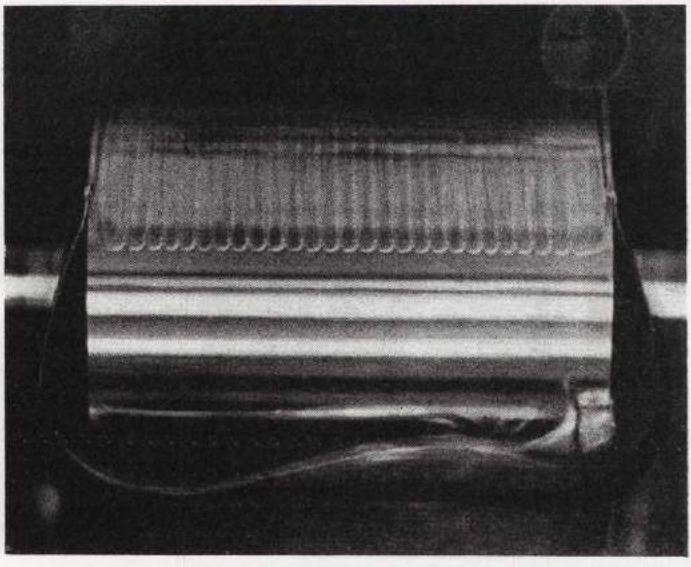

Fig. 31.2. Clearance 0,4 mm, rotational speed 100 r/m

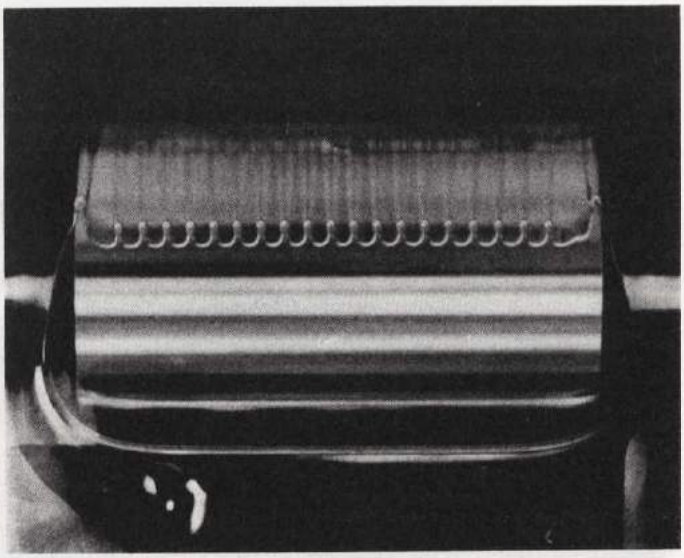

Fig. 32.1. Clearance 0,2 mm, rotational speed 25 r/m

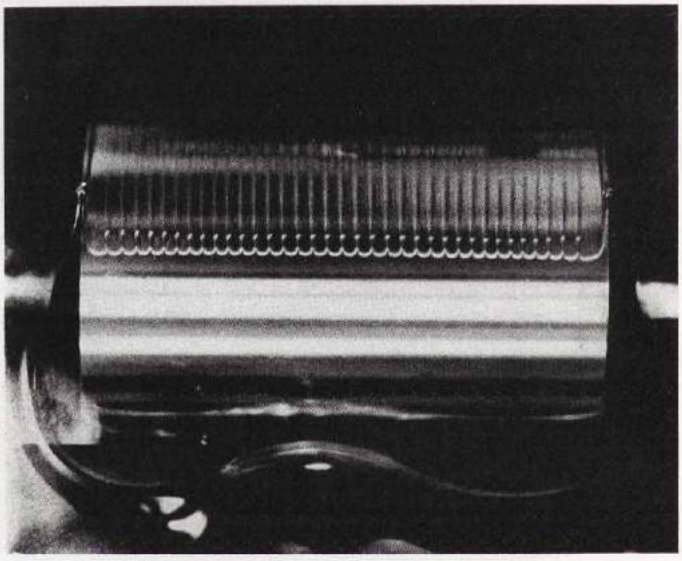

Fig. 32.2. Clearance 0,2 mm, rotational speed 100 r/m

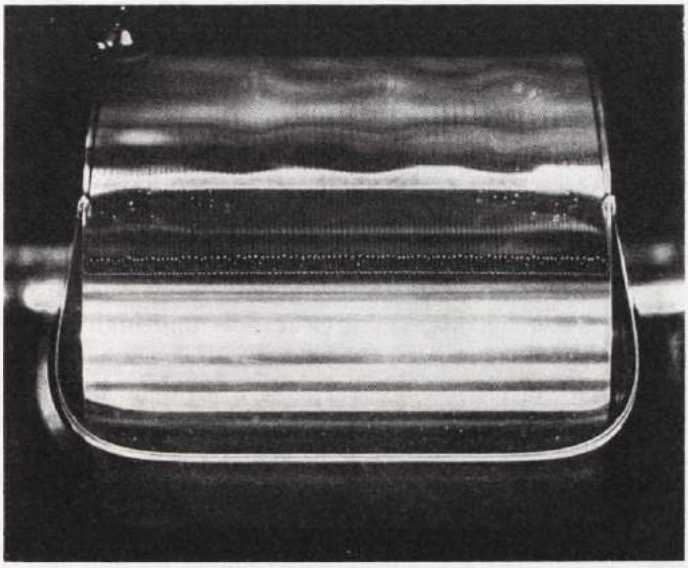

Fig. 33.1. Clearance 0,1 mm, rotational speed 25 r/m

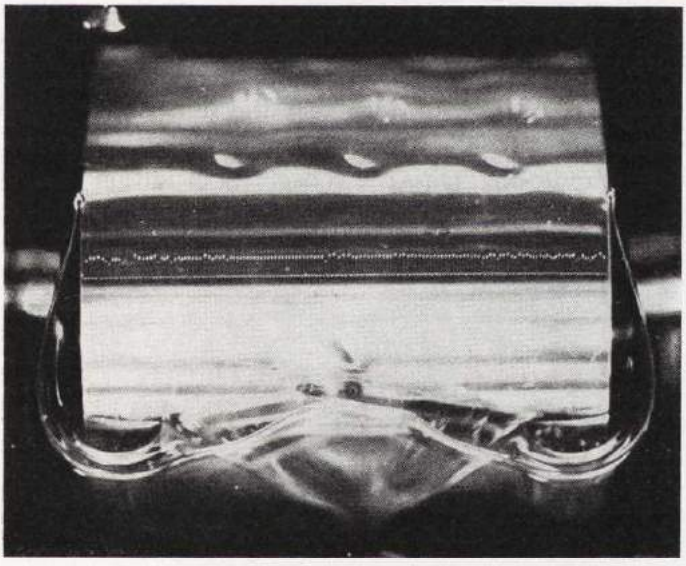

Fig. 33.2. Clearance 0,1 mm, rotational speed 100 r/m

The diameter of the cylinder was 80 mm and the width of it was equal to its diameter. Mobil Oil Vactra Extra Heavy lubricating oil was used. The temperature during the tests was 22° C.

The tests were made with different clearences and different speeds, see figs. 30.1—33.2. The first test, fig. 30.1, had a clearance 0,6 mm and the rotational speed 25 r/m. Here we have few oil tongues. In the last test, fig. 33.2, the clearance was 0,1 mm and the speed 100 r/m, which gave a large number of oil tongues. Their lengths in the peripheral direction are about the same. Large clearances and low speeds give few oil strips, small clearances and high speeds give a large number of strips.

In the tests the cavitation starts at a straight line in the axial direction. This confirms that the assumption of infinite width is correct.

With a clearance of 0,1 mm and a rotational speed of 200 r/m the distance between the minimum space and the start of cavitation is measured to 1,5 mm. The theoretical value is 1,3 mm and the agreement is thus good. At lower speeds the experimental x^* are somewhat higher than the theoretical values. Theoretically x^* is only dependent on r and h_{min}, not on the speed. The fact that the speed will influence can be explained by a slope in the pressure curve of small negative pressures just before the commencement of cavitation, which will exert influence at very low loads. In practical cases the maximum pressure is considerably higher than these small negative pressures and their influence on the pressure curve is completely negligible.

From the tests it is obvious that the film will not break at the minimum space, which is a usual assumption; but at a position which corresponds quite well with the continuity condition of zero pressure derivative.

6. Conclusion

In this paper the hydrodynamic theory of lubrication of the contact between two cylindrical surfaces has been treated. Tests have been made to study the oil film between a rotating cylinder and a stationary plane surface. There is a good agreement between theory and tests.

The treatise holds for light loads as the surfaces are assumed to be rigid and the viscosity to be constant. The calculations are made for variable oil supply and the different pressure curves are shown. Consideration is taken to the oil strips in the cavitation or air region. The width is assumed to be infinite.

Calculations are made for load capacity, oil flow, and friction forces. Curves of these quantities are given.

Photos of the oil film and the oil strips in the cavitation region are shown.

7. References

1. Floberg, L.: The Infinite Journal Bearing, Considering Vaporization. Göteborg, 1957.
2. Floberg, L.: Experimental Investigation of Power Loss in Journal Bearings, Considering Cavitation. Göteborg, 1959.
3. Floberg, L.: Lubrication of a Rotating Cylinder on a Plane Surface, Considering Cavitation. Göteborg, 1959.
4. Floberg, L.: The Optimum Thrust Tilting-pad Bearing. Göteborg, 1960.
5. Floberg, L.: The Two-groove Journal Bearing, Considering Cavitation. Göteborg, 1960.
6. Gatcombe, E. K.: Lubrication Characteristics of Involute Spur Gears. Trans. Am. Soc. Mech. Engrs, vol. 67, p. 177, 1945.
7. Grubin, A. N.: Fundamentals of the Hydrodynamic Theory of Lubrication of Heavily Loaded Cylindrical Surfaces. Moscow, 1949 (Translation from Russian).
8. Jakobsson, B. and Floberg, L.: The Finite Journal Bearing, Considering Vaporization. Göteborg, 1957.
9. Jakobsson, B. and Floberg, L.: The Partial Journal Bearing. Göteborg, 1958.
10. Jakobsson, B. and Floberg, L.: The Rectangular Plane Pad Bearing. Göteborg, 1958.
11. Jakobsson, B. and Floberg, L.: The Centrally Loaded Partial Journal Bearing. Göteborg, 1959.
12. Kneschke, A.: Rollreibung auf spurbildender Fahrbahn. Ingenieur-Archiv XXV. Band, 1957.
13. Reynolds, O.: On the Theory of Lubrication .... Phil. Trans. Roy. Soc., vol. 177, p. 157, 1886.

Forts. fr. omsl. 2:dra sida

178. OLVING, SVEN, *A new method for space charge wave interaction studies. I.* 12 s. 1956. Kr. 3: —. (Avd. Elektroteknik. 51.)
179. HANSBO, SVEN, *The critical load of rectangular frames analysed by convergence methods.* 47 s. 1956. Kr. 11: —. (Avd. Väg- och Vattenbyggnad. Byggnadsteknik. 25.)
180. WESTBERG, VIDOR, *Measurements of noise radiation at 10 cm from glow lamps. Preliminary report.* 14 s. 1956. Kr. 4: 50. (Avd. Elektroteknik. 52).
181. SVENSSON, S. I., HELLGREN, G., AND PERERS, O., *The Swedish radioscientific solar eclipse expedition to Italy, 1952. Preliminary report.* 30 s. 1956. Kr. 8: —. (Avd. Elektroteknik. 53.)
182. WAX, NELSON, *A note on design considerations for a proposed auroral radar.* 16 s. 1957. Kr. 3: —. (Avd. Elektroteknik. 54.)
183. JOSHI, G. H., *The electromagnetic interaction between two crossing electron streams. I.* 31 s. 1957. Kr. 8: —. (Avd. Elektroteknik. 55.)
184. SMITH, BENGT, *Dry methods for removing hydrogen sulphide from gases.* 65 s. 1957. Kr. 15: —. (Avd. Kemi och Kemisk Teknologi. 34.)
185. EKELÖF, S., BJÖRK, N., AND DAVIDSON, R., *Large signal behaviour of directly heated thermistors.* 31 s. 1957. Kr. 8: —. (Avd. Elektroteknik. 56.)
186. CARLSSON, BENGT, UND LARSSON, HANS, *Wirkungsgrad und Selbsthemmung einfacher Umlaufgetriebe.* 48 s. 1957. Kr. 9: —. (Avd. Maskinteknik. 8.)
187. AURELL, CARL G., *The equivalent transmission line of a linear four-terminal network. Calculations with cascade-connected four-terminal networks.* 39. s. 1957. Kr. 6: —. (Avd. Elektroteknik. 57.)
188. LUNDHOLM, R., *Induced overvoltage-surges on transmission lines and their bearing on the lightning performance at medium voltage networks.* 117 s. 1957. Kr. 19: —. (Avd. Elektroteknik. 58.)
189. FLOBERG, LEIF, *The infinite journal bearing, considering vaporization.* 83 s. 1957. Kr. 13: —. (Avd. Maskinteknik. 9.)
190. JAKOBSSON, BENGT, AND FLOBERG, LEIF, *The finite journal bearing, considering vaporization.* 117 s. 1957. Kr. 19: 50. (Avd. Maskinteknik. 10.)
191. CHAKO, NICHOLAS, *Characteristic curves on planes in the image space.* 49 s. 1957. Kr. 15: —. (Avd. Allmänna Vetenskaper. 12.)
192. EKELÖF, STIG, *The development and decay of the magnetic flux in a non-delayed telephone relay.* 50 s. 1957. Kr. 15: —. (Avd. Elektroteknik. 59.)
193. BJÖRKLUND, KJELL, *Bestämning av porslins draghållfasthet.* 78 s. 1958. Kr. 15: —. (Institutionen för Silikatkemisk Forskning. 39.)
194. GRANHOLM, PER, *Sound insulation of single leaf walls.* 48 s. 1958. Kr. 8:—. (Avd. Väg- och Vattenbyggnad. Byggnadsteknik. 26.)
195. GRANHOLM, HJALMAR, *Om vattengenomslag i murade väggar med särskild hänsyn till tegel som fasadmaterial.* 172 s. 1958. Kr. 16: —. (Avd. Väg- och Vattenbyggnad. Byggnadsteknik. 27.)
196. MEOS, JOHAN, AND OLVING, SVEN, *On the origin of radar echoes associated with auroral activity.* 20 s. 1958. Kr. 5: —. (Avd. Elektroteknik. 60.)
197. JOSHI, G. H., *The electromagnetic interaction between two crossing electron streams. II.* 10 s. 1958. Kr. 3: 50. (Avd. Elektroteknik. 61.)
198. WILHELMSSON, HANS, *The interaction between an obliquely incident plane electromagnetic wave and an electron beam. II.* 32 s. 1958. Kr. 7: —. (Avd. Elektroteknik. 62.)
199. KÄRRHOLM, GUNNAR, *A method of iteration applied to beams resting on springs.* 50 s. 1958. Kr. 12: —. (Avd. Allm. Vetenskaper. 13.)
200. JAKOBSSON, BENGT, AND FLOBERG, LEIF, *The partial journal bearing.* 60 s. 1958. Kr. 14: —. (Avd. Maskinteknik. 11.)
201. KÄRRHOLM, GUNNAR, *Influence functions of elastic plates divided in strips.* 18 s. 1958. Kr. 4: 50. (Avd. Väg- och Vattenbyggnad. Byggnadsteknik. 28.)
202. RÅDE, LENNART, *Sampling planes for acceptance sampling by variables using the range.* 34 s. 1958. Kr. 9: 50. (Avd. Allm. Vetenskaper. 14.)
203. JAKOBSSON, BENGT, AND FLOBERG, LEIF, *The rectangular plane pad bearing.* 44 s. 1958. Kr. 5: —. (Avd. Maskinteknik. 12.)
204. ASPLUND, SVEN OLOF, *Column-beams and suspension bridges analysed by »Green's matrix».* 36 s. 1958. Kr. 7: —. (Avd. Väg- och Vattenbyggnad. Byggnadsteknik. 29.)
205. WILHELMSSON, HANS, *On the properties of the electron beam in the presence of an axial magnetic field of abitrary strength.* 32 s. 1958. Kr. 7: 50. (Avd. Elektroteknik. 63.)
206. WILHELMSSON, HANS, *The interaction between an obliquely incident plane electromagnetic wave and an electron beam. III.* 17 s. 1958. Kr. 5: —. (Avd. Elektroteknik. 64.)
207. HEDVALL, ARVID J., *On the influence of pre-treatment and transition processes on the adsorption capacity and the reactivity of various types of glass and silica.* 39 s. 1959. Kr. 8: —. (Institutionen för Silikatkemisk Forskning. 40.)

Forts. å omsl. 4:de sida

Forts. fr. omsl. 3:dje sida

208. KÄRRHOLM, GUNNAR, *A flow problem solved by strip method.* 22 s. 1959. Kr. 4: 50. (Avd. Allm. Vetenskaper. 15.)
209. GRANHOLM, HJALMAR, *Allmän teori för beräkning av armerad betong.* 228 s. 1959. Kr. 20: —. (Avd. Väg- och Vattenbyggnad. Byggnadsteknik. 30.)
210. LIDIN, LARS G., *On helical-springs suspension.* 75 s. 1959. Kr. 15: —. (Avd. Maskinteknik. 13.)
211. BJÖRK, NILS, *Theory of the indirectly heated thermistor.* 46 s. 1959. Kr. 10: —. (Avd. Elektroteknik. 65.)
212. CARLSSON, ORVAR, *The influence of submicroscopic pores on the resistance of bricks towards frost.* 13 s. 1959. Kr. 3: 50. (Institutionen för Silikatkemisk Forskning. 41.)
213. GRANHOLM, HJALMAR, *KAM 40, KAM 60 och KAM 90.* 41 s. 1959. Kr. 3: 50. (Avd. Väg- och Vattenbyggnad, Byggnadsteknik. 31.)
214. JAKOBSSON, BENGT, AND FLOBERG, LEIF, *The centrally loaded partial journal bearing.* 35 s. 1959. Kr. 7: 50. (Avd. Maskinteknik. 14.)
215. FLOBERG, LEIF, *Experimental investigation of power loss in journal bearings, considering cavitation.* 16 s. 1959. Kr. 3: 50. (Avd. Maskinteknik. 15).
216. FLOBERG, LEIF, *Lubrication of a rotating cylinder on a plane surface, considering cavitation.* 40 s. 1959. Kr. 8: —. (Avd. Maskinteknik. 16.)
217. TROEDSSON, CARL BIRGER, *The growth of the Western city during the Middle Ages.* 125 s. 1959. Kr. 19: —. (Avd. Arkitektur. 4.)
218. HEDVALL, J. ARVID, *The importance of the reactivity of solids in geological-mineralogical processes.* 11 s. 1959. Kr. 2: 50. (Institutionen för Silikatkemisk Forskning. 42.)
219. CORNELL, ELIAS, *Humanistic inquiries into architecture. I—III.* 112 s. 1959. Kr. 17: —. (Avd. Arkitektur. 5.)
220. GRANHOLM, CARL-ADOLF, *Ekonomiska aluminiumprofiler.* 48 s. 1959. Kr. 5: 50. (Avd. Väg- och Vattenbyggnad. Byggnadsteknik. 32.)
221. LUNDÉN, ARNOLD, CHRISTOFFERSON, STINA, AND LODDING, ALEX, *The isotopic effect of lithium ions in countercurrent electromigration in molten lithium bromide and iodide.* 38 s. 1959. Kr. 7: 50. (Avd. Allm. Vetenskaper. 16.)
222. INGEMANSSON, STIG, AND KIHLMAN, TOR, *Sound insulation of frame walls.* 47 s. 1959. Kr. 8: 50. (Avd. Väg- och Vattenbyggnad, Byggnadsteknik. 33.)
223. HÖGLUND, B., AND RADHAKRISHNAN, V., *A radiometer for the hydrogen line.* 25 s. 1959. Kr. 6: 50. (Avd. Elektroteknik. 66.)
224. JAKOBSSON, BENGT, *Torque distribution, power flow, and zero output conditions of epicyclic gear trains.* 55 s. 1960. Kr. 12: —. (Avd. Maskinteknik. 17.)
225. OLVING, SVEN, *Electromagnetic and space charge waves in a sheath helix.* 91 s. 1960. Kr. 17: —. (Avd. Elektroteknik. 67.)
226. STRÖMBLAD, JOHN, *Beschleunigungsverlauf und Gleichgewichtsdrehzahlen einfacher Planetengetriebe nebst Selbsthemmungsversuche.* 80 s. 1960. Kr. 18:—. (Avd. Maskinteknik. 18.)
227. SANDFORD, FOLKE, *Some current problems concerning brick manufacture.* 20 s. 1960. Kr. 5: —. (Avd. Kemi och Kemisk Teknologi. 35.)
228. OLVING, SVEN, *A new method for space charge wave interaction studies. II.* 40 s. 1960. Kr. 8: —. (Avd. Elektroteknik. 68.)
229. GRANHOLM, HJALMAR, *Le problème de Boussinesq.* 15 s. 1960. Kr. 3: 50. (Avd. Väg- och Vattenbyggnad. Byggnadsteknik. 34.)
230. HIBA, MIODRAG et CEDERWALL, KRISTER, *Flambement élastique d'une barre en bois lamellée et clouée avec le module de déplacement du moyen de liaison constant k.* 22 s. 1960. Kr. 5: —. (Avd. Väg- och Vattenbyggnad. Byggnadsteknik. 35.)
231. FLOBERG, LEIF, *The optimum thrust tilting-pad bearing.* 23 s. 1960. Kr. 5: —. (Avd. Maskinteknik. 19.)
232. FLOBERG, LEIF, *The two-groove journal bearing, considering cavitation.* 32 s. 1960. Kr. 6: —. (Avd. Maskinteknik. 20.)
233. HEDVALL, ARVID J., *Heterogeneous catalysis, results and projects for research.* 18 s. 1961. Kr. 5: —. (Avd. Kemi och Kemisk Teknologi. 36.)

Pris kronor 10: —

ELANDERS BOKTRYCKERI AKTIEBOLAG
GÖTEBORG 1961

CHALMERS TEKNISKA HÖGSKOLAS HANDLINGAR
TRANSACTIONS OF CHALMERS UNIVERSITY OF TECHNOLOGY
GOTHENBURG, SWEDEN
Nr 235 (Avd. Maskinteknik 22) 1961

ATTITUDE-ECCENTRICITY CURVES AND STABILITY CONDITIONS OF THE INFINITE JOURNAL BEARING

BY

LEIF FLOBERG

Report No. 15 from the Institute of Machine Elements
Chalmers University of Technology
Gothenburg, Sweden
1961

Av Chalmers Tekniska Högskolas Handlingar hava tidigare utkommit:

Fullständig förteckning över Chalmers Tekniska Högskolas Handlingar
lämnas av Chalmers Tekniska Högskolas Bibliotek, Göteborg.

151. Hedvall, J. A., *Reactions with activated solids.* 23 s. 1954 Kr. 5: —. (Institutionen för Silikatkemisk Forskning. 32).
152. Smith, Cyril Stanley, *The microstructure of polycrystalline materials.* 49 s. 1954. Kr. 9: 50 (Institutionen för Silikatkemisk Forskning. 33.)
153. Selberg, Arne, *Norska erfaringer fra bygging av små hengebroer.* 20 s. 1954. Kr. 4: —. (Avd. Väg- och Vattenbyggnad. Byggnadsteknik. 21.)
154. Granholm, Hjalmar, *Armerat trä.* 96 s. 1954. Kr. 9: — (Avd. Väg- och Vattenbyggnad. Byggnadsteknik. 22).
155. Wilhelmsson, Hans, *The interaction between an obliquely incident plane electromagnetic wave and an electron beam. I.* 31 s. 1954. Kr. 7: —. (Avd. Elektroteknik. 42.)
156. Olving, Sven, *Electromagnetic wave propagation on helical conductors inbedded in dielectric medium.* 14 s. 1955. Kr. 3: —. (Avd. Elektroteknik. 43.)
157. Olving, Sven, *Amplification of the traveling wave tube at high beam current. I.* 11 s. 1955. Kr. 3: —. (Avd. Elektroteknik. 44.)
158. Hedvall, J. A., Nordengren, Sven, und Liljegren, B., *Über die thermische Zersetzung von Kalziumsulfat bei niedrigen Temperaturen.* 18 s. 1955. Kr. 5: — (Institutionen för Silikatkemisk Forskning. 34.)
159. Dahlgren, Sven-Eric, *On the break-down of thixotropic materials.* 18 s. 1955. Kr. 3: 50. (Institutionen för Silikatkemisk Forskning. 35.)
160. Sandford, Folke, och Liljegren, Berne, *Torkningen av råtegel och dennas inverkan på teglets frostbeständighet.* 22 s. 1955. Kr. 3: —. (Institutionen för Silikatkemisk Forskning. 36.)
161. Wallman, Henry, *Automatic noise-factor meter.* 17 s. 1955. Kr. 3: —. (Avd. Elektroteknik. 45.)
162. Sandford, Folke, and Fransson, Stig *The refractoriness of some types of quartz and quartzite. II.* 24 s. 1955. Kr. 5: —. (Institutionen för Silikatkemisk Forskning. 37).
163. Lindblad, Anders, *Konstruktion av linjer för moderna handelsfartyg.* 176 s. 1955. Kr. 20: —. (Avd. Skeppsbyggeri. 6.)
164. Svartholm, Nils, *Two problems in the theory of the slowing down of neutrons by collisions with atomic nuclei.* 15 s. 1955. Kr. 5: —. (Avd. Allmänna Vetenskaper. 10).
165. Persson, Per, *Bostadsvaneundersökning utförd i hyreslägenheter byggda 1947 i Göteborg, Torpaområdet.* 86 s. 1955. Kr. 12: —. (Avd. Arkitektur. 3.)
166. Hansson, P. R., *Undersökning av mullitbildning i keramiska produkter.* 29 s. 1955. Kr. 6: —. (Institutionen för Silikatkemisk Forskning. 38.)
167. Ekelöf, Stig, *Die Temperaturverteilung in einem gleichstromdurchflossenen langen Metallzylinder mit kreisförmigen Querschnitt.* 38 s. 1955. Kr. 10: —. (Avd. Elektroteknik. 46.)
168. Wilhelmsson, Hans, *On the reflection of electromagnetic waves from a dielectric cylinder.* 17 s. 1955. Kr. 4: 50. (Avd. Elektroteknik. 47.)
169. Björk, N., and Davidson, R., *Small signal behaviour of directly heated thermistors.* 43 s. 1955. Kr. 11: —. (Avd. Elektroteknik. 48.)
170. Forestier, H., *Tendances actuelles dans la formation de l'ingénieur chimiste: selection, orientation, spécialisation; amélioration de son efficience.* 13 s. 1956. Kr. 2: 50. (Avd. Kemi och Kemisk Teknologi 33.)
171. Wax, Nelson, *On the ring current hypothesis.* 32 s. 1956. Kr. 7: —. (Avd. Elektroteknik. 49.)
172. Elgeskog, Erik, *Photoformer analysis and design.* 40 s. 1956. Kr. 8: 50. (Avd. Elektroteknik. 50.)
173. Anzelius, Adolf, *Bimolekulare Reaktion von zwei in Mischung vorliegenden Substanzen mit einer dritten Substanz.* 8 s. 1956. Kr. 5 —. (Avd. Allm. Vetenskaper. 11.)
174. Reinius, Erling, *Model studies for the extension of the habour of Gothenburg.* 38 s. 1956. Kr. 6: —. (Avd. Väg- och Vattenbyggnad. Byggnadsteknik. 23.)
175. Zimen, K. E., *Diffusion von Edelgasatomen die durch Kernreaktion in festen Stoffen gebildet werden.* 7 s. 1956. Kr. 2: —. (Institutionen för Kärnkemi. 1.)
176. Inthoff, W., und Zimen, K. E., *Kinetik der Diffusion radioaktiver Edelgase aus festen Stoffen nach Bestrahlung.* 16 s. 1956. Kr. 4: —. (Institutionen för Kärnkemi. 2)
177. Granholm, Hjalmar, *Puts och lättbetong.* 45 s. 1956. Kr. 3: —. (Avd. Väg- och Vattenbyggnad. Byggnadsteknik. 24)

Forts. å omsl. 3:dje sida

CHALMERS TEKNISKA HÖGSKOLAS HANDLINGAR

TRANSACTIONS OF CHALMERS UNIVERSITY OF TECHNOLOGY
GOTHENBURG, SWEDEN

Nr 235 (Avd. Maskinteknik 22) 1961

ATTITUDE-ECCENTRICITY CURVES AND STABILITY CONDITIONS OF THE INFINITE JOURNAL BEARING

BY

LEIF FLOBERG

Report No. 15 from the Institute of Machine Elements
Chalmers University of Technology
Gothenburg, Sweden
1961

CHALMERS UNIVERSITY BOOKS / GUMPERTS, GÖTEBORG
GYLDENDALSKE BOGHANDEL / NORDISK FORLAG, KØBENHAVN
AKATEEMINEN KIRJAKAUPPA / AKADEMISKA BOKHANDELN, HELSINGFORS
WILLIAM HEINEMANN LTD, LONDON, MELBOURNE, TORONTO

SCANDINAVIAN UNIVERSITY BOOKS

Gyldendalske Boghandel / Nordisk Forlag, København
Svenska Bokförlaget / P. A. Norstedt & Söner — Albert Bonnier, Stockholm
Akademiförlaget / Gumperts, Göteborg
Akateeminen Kirjakauppa / Akademiska Bokhandeln, Helsingfors
William Heinemann Ltd, London, Melbourne, Toronto

Manuscript received by the Publications Committee,
Chalmers University of Technology, June 1st, 1960

GÖTEBORG 1961
ELANDERS BOKTRYCKERI AKTIEBOLAG

Preface

This report has been carried out during lubrication research at the Institute of Machine Elements, Chalmers University of Technology, Göteborg, Sweden, under the leadership of the head of the Institute, Professor B. JAKOBSSON. Hydrodynamic lubrication and cavitation in bearings have been studied theoretically and experimentally. Ten reports have earlier been published, refs. (1)—(10).

This paper is an extension of an earlier report ref. (1), which treated the oil flow continuity of the infinite journal bearing. Here the stability condition is treated.

I wish to express my sincere thanks to the Swedish Technical Research Council for their kind sponsorship. I also wish to thank Mr BENGT HÅKANSSON, M. Sc, who has made the program for the evaluations in the digital computer, Alwac III E.

Leif Floberg
Tekn. lic.

Contents

Page

Preface 3

1. Introduction 6

2. Notation 8

3. Theoretical Investigation 10

   3,1. Continuity and Boundary Conditions 10

   3,2. Attitude-Eccentricity Curves 12

   3,3. Stability Conditions 13

4. Experimental Investigation 22

   4,1. Test Apparatus 22

   4,2. Test Results 24

5. Conclusion 30

6. Appendix I: Tables of Calculated Values 31

7. Appendix II: Tables of Experimental Values 35

8. References 43

1. Introduction

Boundary conditions and attitude-eccentricity curves of the 360° infinite journal bearing with one axial oil groove are hitherto not fully solved and accepted in the bearing literature. In an earlier report (1) this problem was treated; but calculations were not made for the highest eccentricities, and it contained few experiments. Here the problem is discussed in more detail and several tests are made.

In the tests of ref. (1) the location of the shaft centre was evaluated from the shape of the measured pressure curve. Only the vertical location of the centre was controlled by measurement at the full SOMMERFELD conditions (12) and coincided with the horizontal attitude-eccentricity line. Here the location is measured mechanically in horizontal and vertical directions. It is assumed that the pressure curve will start or end at the groove. This holds, if the groove pressure is infinitesimally higher than the cavitation pressure. As the cavitation pressure is just below atmospheric the groove pressure then ought to be atmospheric in the tests.

The case studied in this paper has been theoretically treated by STIEBER (13) as early as 1933. He makes a very good and correct treatment of the infinite journal bearing. However, he does not check the stability of the derived attitude-eccentricity curves. His work seems to be forgotten as it is seldom referred to in literature, which perhaps is due to the lack of tests in his investigation. Today the full SOMMERFELD conditions are often assumed to be impossible in the bearing literature.

The infinite journal bearing has also been treated by SWIFT (14) in 1932. His paper is accepted in the literature notwithstanding the fact that he starts with an incorrect stability condition, which says that the shaft shall have as low location as possible choosing the pressure curves arbitrarily. By chance he gets the pressure curves, which end with zero pressure derivative and are the only curves satisfying the continuity of flow, and his calculation was made for the centrally loaded half-bearing, where all derived attitude-eccentri-

city curves are stable and the stability therefore need not be discussed. If the same condition of zero pressure derivative at the end of the pressure build-up is used for the 360° bearing, curves, which are not in accordance with the stability condition, are sometimes derived.

In theory the bearing quantities are determined for given positions of the shaft and the groove, and the continuity condition must be satisfied, when this calculation is made. In practice a certain load is applied at a certain angle and the calculated shaft centre position is only obtained, if it is stable. If it is not stable, the shaft will whirl or under certain conditions find another stable position.

As this work is an extension of ref. (1) the equations are not re-written; but the basic conditions, upon which the equations are built, are discussed in detail.

2. Notation

b = Bearing width

C = Diametral clearance

c = Specific heat of oil

D = Bearing diameter

d = Shaft diameter

E = Power loss per unit width

$E_0 = \dfrac{E\,\psi}{\eta\,U^2}$ = Non-dimensional power loss per unit width

e = Eccentricity of the shaft relative to the bearing

$f = \dfrac{E}{P}$ = Relative power loss

$h_{\min}$ = Minimum oil film thickness

m = Weight on the load scale

n = Rotational speed

P = Load per unit width

P_{tot} = Total load

$P_0 = \dfrac{P\,\psi^2}{\eta\,U}$ = Load number

q = Oil flow per unit width

$q_0 = \dfrac{q}{U\,\Delta r}$ = Non-dimensional oil flow per unit width

r = Radius of the shaft

Δr = Radial clearance

t = Temperature

Δt = Temperature rise

$\Delta t_0 = c\,\varrho \cdot \dfrac{\Delta t\,\psi^2}{\eta\,\omega}$ = Non-dimensional temperature rise

$U = r\omega$ = Velocity of the shaft surface

x, y = Coordinates of the shaft centre

β = Angle between load line and line of centres

$\varepsilon = \dfrac{e}{\Delta r}$ = Eccentricity/radial clearance

η = Viscosity of oil

ϱ = Density of oil

φ = Angular coordinate

$(\varphi_1 + \beta)$ = Angle between load line and start of oil film

$(\varphi_2 + \beta)$ = Angle between load line and end of oil film

$\psi = \frac{C}{d} = \frac{\Delta r}{r}$ = Relative clearance

ω = Angular speed

3. Theoretical Investigation

3,1. Continuity and Boundary Conditions

For a long time REYNOLDS' equation (11) for the pressure build-up in a thin lubricating oil film has been known and accepted. This continuity equation has got exact solutions for infinite bearing width, and for finite width exact solutions with infinite series and approximate solutions solving large systems of equations. However, there is still a discussion in literature about the boundary conditions and the continuity conditions when cavitation occurs; and cavitation practically always occurs in plain journal bearings.

If REYNOLDS' equation is solved for the boundary condition of zero pressure at the bearing boundaries both positive and negative pressures can be derived. If only positive pressures are derived, the solution is the correct one; but if there are negative pressure regions in the field, the solution must be rejected. As the oil cannot withstand tensile forces without cavitating, we then get cavitated constant pressure zones, the boundary conditions of which are given in ref. (1) for infinite width and in ref. (7) for finite width.

The cavitation pressure is negligibly lower than atmospheric. Theoretically it can be approximated to atmospheric pressure or to that reservoir or side pressure, where the oil is in contact with air. To confirm this behaviour some experiments where made with oil and air under pressure in a test-tube. The pressure in the tube was put at about 5 atm g during a long time to get the air dissolved in the oil. When then the pressure suddenly was dropped to atmospheric, cavitation started with small bubbles moving up to the surface. If then the pressure was increased to 4 atm g, the cavitation still went on. The aim with the rapid pressure drop was to start cavitation, when the oil is not moving. Photos of the test-tube with cavitating oil at atmospheric and at 3 atm g pressure are shown in fig. 11.1 and 11.2 respectively. The initial pressure was here 6 atm g. It is thus evident that the cavitation pressure is not tied to atmospheric; but to that pressure at which the air or the gases are dissolved in the

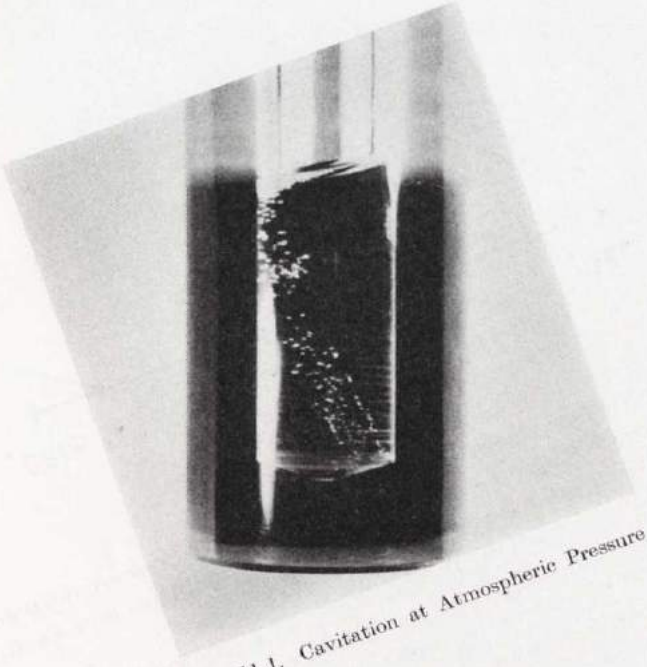

Fig. 11.1. Cavitation at Atmospheric Pressure

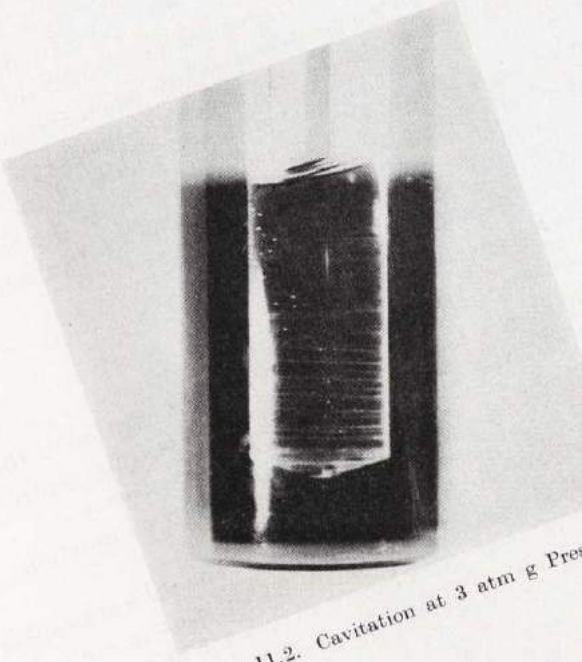

Fig. 11.2. Cavitation at 3 atm g Pre

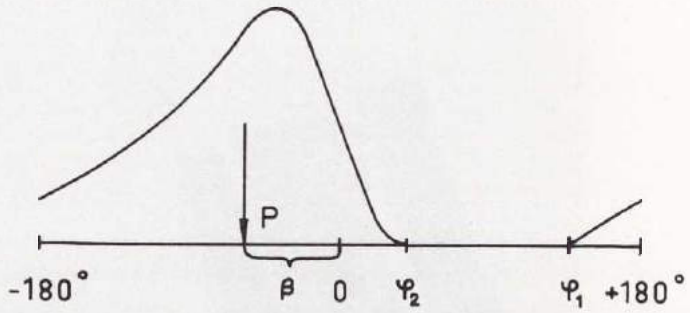

Fig. 12.1. Pressure Curve

oil, i. e. the pressure where we have air saturation. Pressure decreases from the pressure where we have oil-air contact will thus give cavitation. This pressure is mostly equal to atmospheric.

The continuity condition at the start of cavitation gives zero pressure derivative at the end of the pressure curve. This condition gives a multitude of curves for every eccentricity value as shown in ref. (1). One condition of a given pressure at a given angle determines which curve is derived. The notation is shown in fig. 12.1, where a pressure curve is drawn. The pressure build-up starts at φ_1 and ends at φ_2. These angles are prescribed to be positive, i. e. they are measured in the positive direction when drawing the diagrams. The angle between load line and minimum space is β.

The calculations are made for different values of the eccentricity ε and of the angle $\varphi_2 = \varphi^*$. φ_1 is determined from the condition that the pressure shall be zero at φ_1 and φ_2. The load capacity per unit width P and the load angle β are determined.

3,2. Attitude-Eccentricity Curves

The attitude-eccentricity curves represent the location of the shaft centre relative to the load direction and the bearing centre. The location is given by the load angle β and the eccentricity ε.

In the calculations φ_1, P and β were determined as functions of ε and $\varphi_2 = \varphi^*$.

As the cavitation pressure is negligibly smaller than the atmospheric groove pressure, the pressure build-up will either start or end at the groove. In order to get the shaft centre curves for different groove locations, the angles between the load line and the groove ($\varphi_1 + \beta$), and

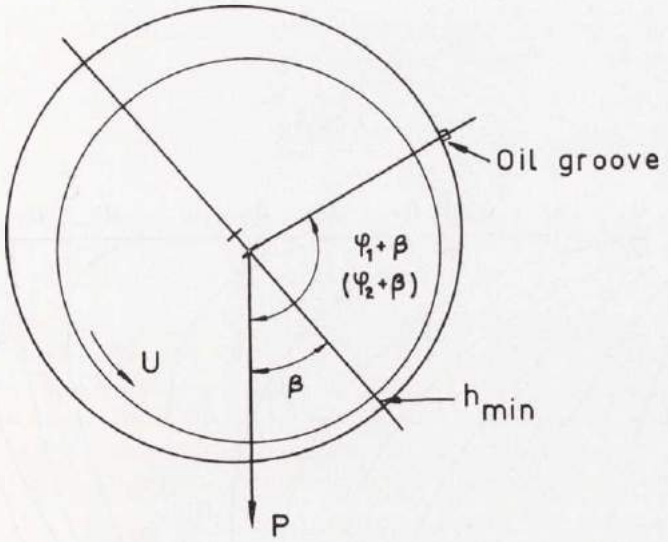

Fig. 13.1. Section of the Bearing

$(\varphi_2 + \beta)$, see fig. 13.1, are plotted against ε and β. Then curves for constant values of $(\varphi_1 + \beta)$ and $(\varphi_2 + \beta)$ are drawn, see figs. 14.1 and 15.1. In the same way a diagram to determine the non-dimensional load capacity P_0 as function of the shaft centre locus is made, see fig. 16.1. The non-dimensional group for the load number is

$$P_0 = \frac{P \psi^2}{\eta U}$$

In ref. (1) diagrams corresponding to 14.1, 15.1, and 16.1 were given. However, the calculations in that work were made only up to the eccentricity 0,8, why the curves for $(\varphi_1 + \beta) \leq 90$ in diagram 14.1 were not obtained. There was also an error in the calculation at $\varepsilon = 0{,}8$ in the same diagram, which is corrected here.

3,3. Stability Conditions

In theory the load capacity and the angle between the load and the groove $(\varphi + \beta)$ are calculated for given positions of the shaft centre. In practice a given load is applied at a given angle and the corresponding position of the shaft centre is only reached, if that

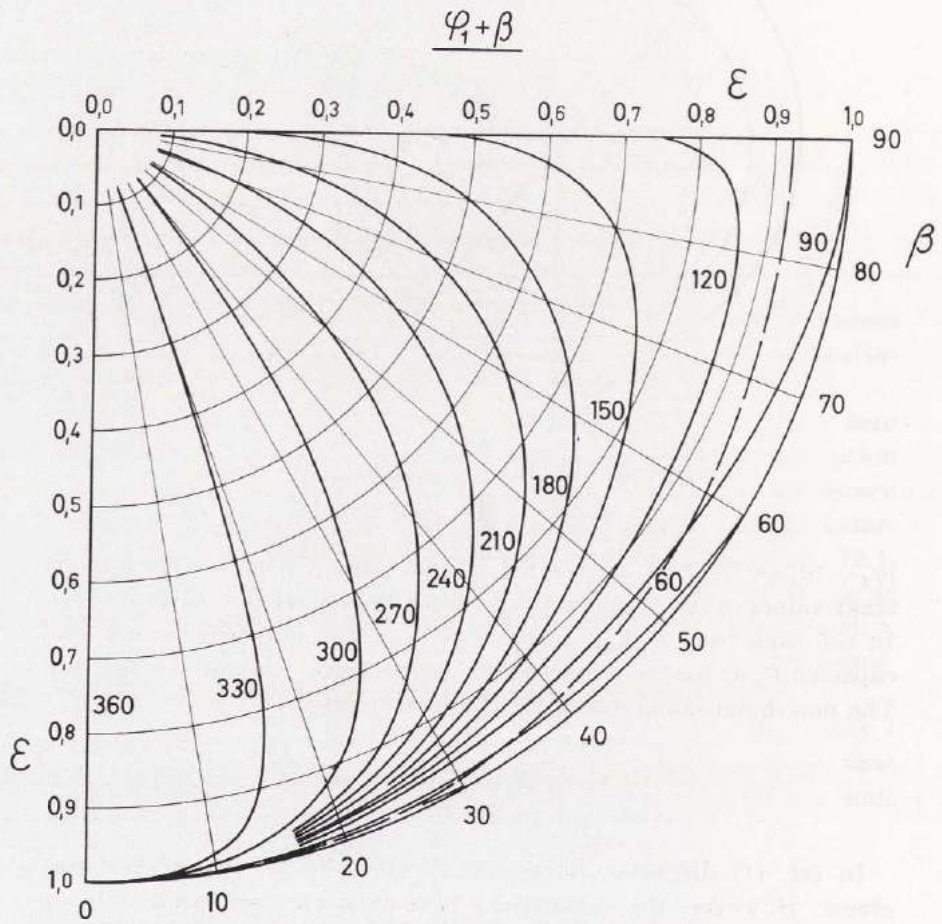

Fig. 14.1. Attitude-Eccentricity Curves for Different Groove Locations

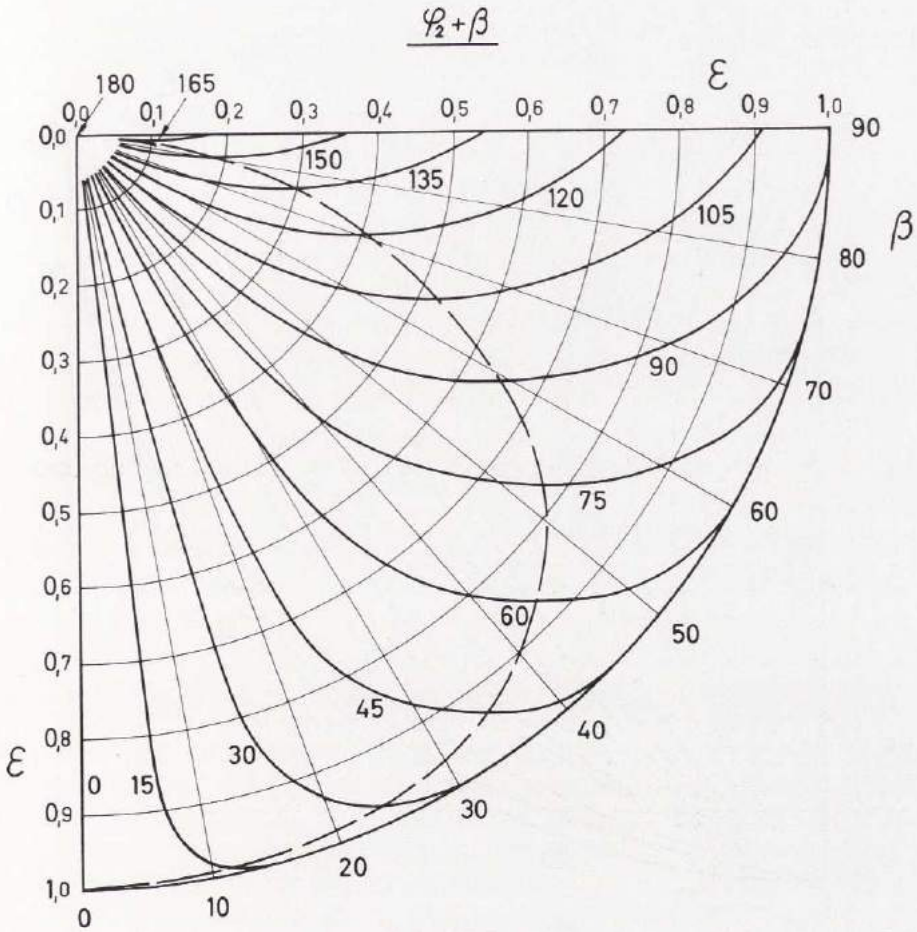

Fig. 15.1. Attitude-Eccentricity Curves for Different Groove Locations

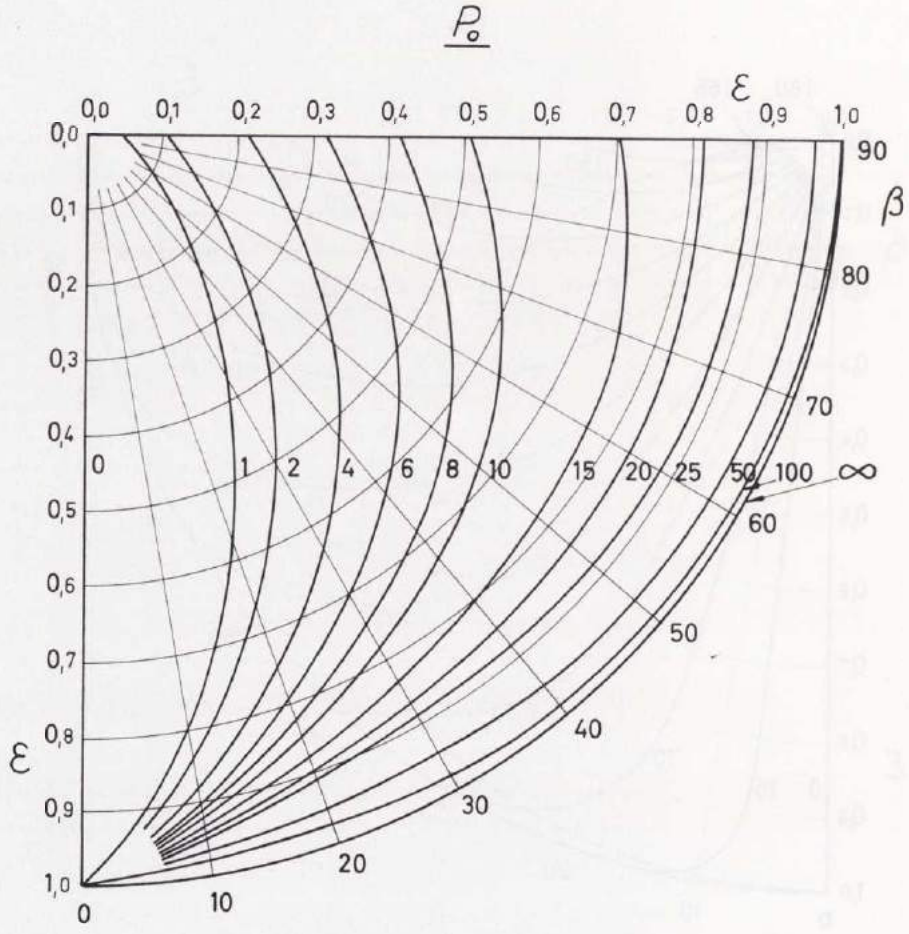

Fig. 16.1. Load Capacity

point is stable. If the point is not stable, the shaft will whirl or under certain conditions find another stable point. Thus stable solutions do not always exist.

The attitude-eccentricity curves derived here have also been derived by STIEBER (13). He has the continuity condition fully satisfied; but does not check that the curves are stable.

SWIFT (14) has treated a similar case of an infinitely wide centrally loaded half-bearing. He does not satisfy the continuity of flow and uses an incorrect stability condition.

To check if a point is stable or not small displacements are made in different directions. If the resultant force tends to bring the shaft centre closer to the equilibrium point after disturbances in all directions, the point is stable; but if it will remove the centre from the equilibrium point after a disturbance in one direction the point is unstable.

The stability condition can also be expressed thus: If work is needed to move the shaft a small distance in all directions the point is stable; but if the work is negative for a disturbance in one direction the point is unstable.

Thirdly, the equations of motion can be studied. If the solutions of these are periodical functions the position is stable, if not it is unstable.

The equations of motion are

$$\left.\begin{aligned} m\ddot{x} &= P_x \\ m\ddot{y} &= P_y \end{aligned}\right\} \quad \ldots\ldots\ldots\ldots\ldots\ldots \quad 17.1$$

where

m = mass

P_x = force component in the x-direction

P_y = force component in the y-direction

In the vicinity of a certain point the force components can be written linearized

$$P_x = k_1 x + k_2 y$$

$$P_y = k_3 x + k_4 y$$

and the solution of eqs. 17.1 is then

$$x = C_1 e^{\alpha t}$$

$$y = C_2 e^{\alpha t}$$

where

$$\alpha^2 = \frac{1}{2m}\left[k_1 + k_4 \pm \sqrt{k_1^2 + k_4^2 + 4k_2k_3 - 2k_1k_2}\right]$$

If the position shall be stable, α cannot have a positive real part, which means that α^2 must be real and negative. Curves for constant values of the load components P_x and P_y as functions of the eccentricity and the attitude relative to the groove are shown in fig. 19.1, where the groove is located at $x = r$. From this diagram the values of the coefficients k_1, k_2, k_3, and k_4 can be obtained.

Such an investigation shows that curves sloping down for increasing load capacity are stable and curves sloping upwards at increasing load are not stable. Thus the regions to the right of the dotted lines in the figs. 14.1 and 15.1 are unstable.

Consider a point in fig. 15.1 at an arbitrary curve to the right of the dotted line. If we get a disturbance to the right upwards the curve, we get a resultant force upwards and the shaft centre will move out from the equilibrium position. If we get a disturbance to the left down the curve, the resultant is directed down and the centre will also here move out from the point. Those points to the right of the dotted lines in figs. 14.1 and 15.1 can thus in a very simple way be established as unstable.

SWIFT does not satisfy the continuity condition of zero pressure derivative at the end of the pressure build-up. Here SWIFT must build upon an assumption that the oil will lose its grip to one of the surfaces, which is the only interpretation giving continuity of flow. The fact that SWIFT neglects the power loss in the cavitation region also speaks in favour of this supposed assumption of SWIFT's. As the oil does not behave in that way his solution method is not correct; but his results are true as his method only chooses curves with zero pressure derivative at the film rupture, and all the curves derived are stable.

SWIFT makes a discussion of SOMMERFELD's attitude-eccentricity curve derived for the centrally-loaded half bearing, see fig. 20.1, and

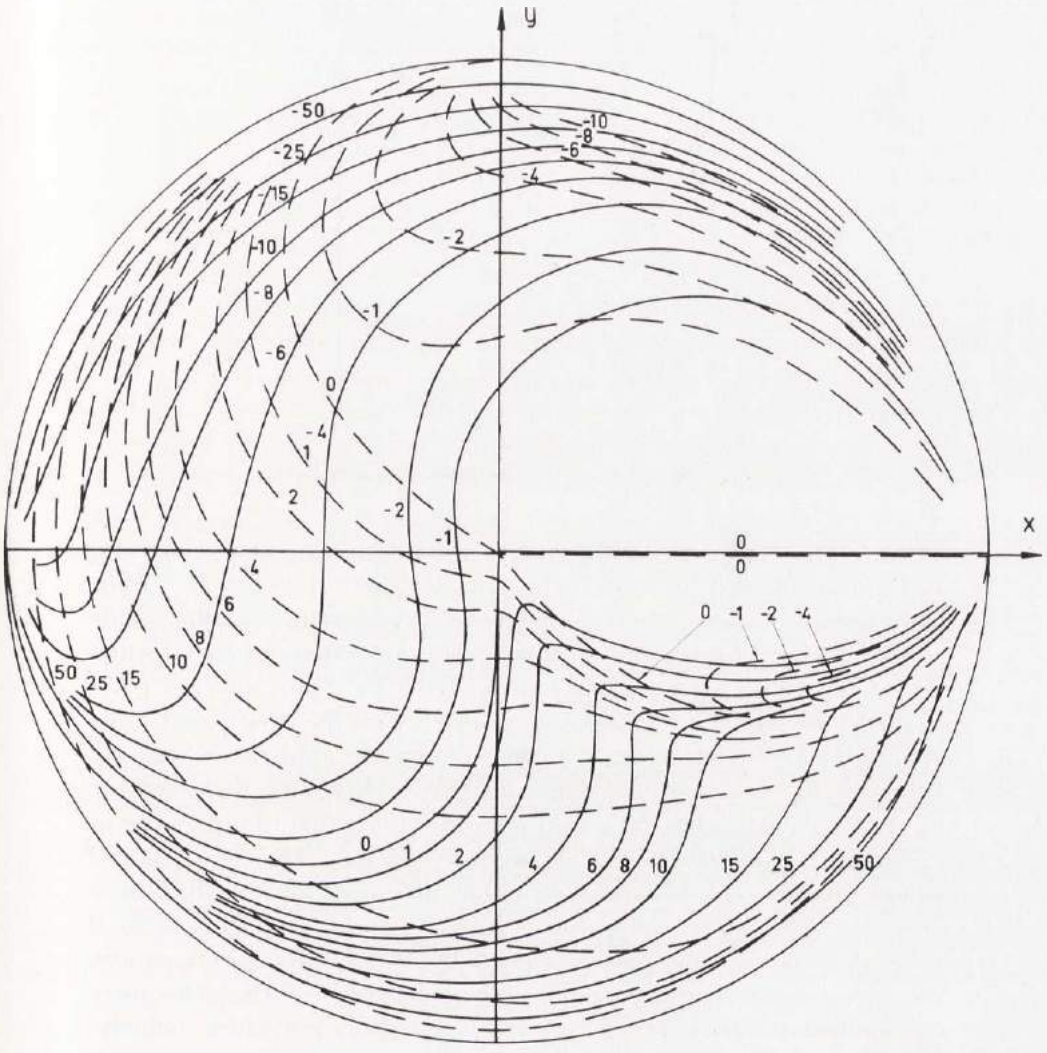

Fig. 19.1. Diagram of the Force Components with Groove Location on the x-axis at $x=r$. (The unbroken lines represent P_{x0} and the dotted lines P_{y0})

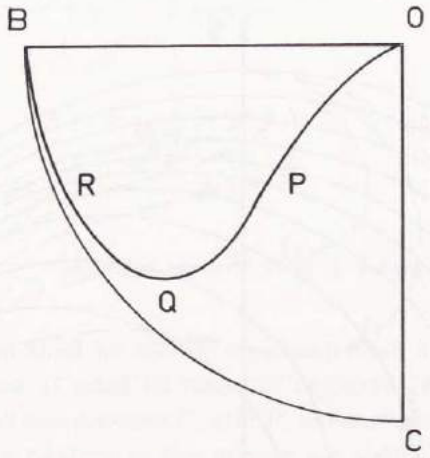

Fig. 20.1. Polar Diagram after SOMMERFELD

writes: "There are two serious objections to SOMMERFELD's diagram. In the first place it involves, over approximately the portion $PQRB$, the assumption that negative pressures may exist in the film. This is, of course, a physical impossibility, as was pointed out by GÜMBEL in 1914. In the second place it gives over the rising portion QRB a condition which is palpably unstable. Let the shaft centre be imagined running in a position such as R with the applied load exactly balanced by the resultant film pressure. Then any displacement upwards along the arc RB would produce an upward film pressure in excess of the applied load, while a downward displacement along RQ would produce a deficit; and in either direction the equilibrium is unstable. The whole of the rising portion of the locus from Q to B must therefore be rejected as impossible. These two objections are, of course, entirely independent of one another, so that the mere omission of negative pressures cannot by itself provide a remedy. The boundary and impressed conditions require fresh examination from the physical standpoint." The fact that negative pressures do not exist was pointed out by SOMMERFELD himself, when he gave the limit for his theory. After SWIFT has shown that part of SOMMERFELD's attitude-eccentricity curve of the half-bearing does not exist as the curve is not stable, he looks for new conditions to get a stable curve. Here, however, it is shown that if the continuity and boundary conditions are satisfied and the curve to some extent is unstable, stable solutions do not sometimes exist. However, the shaft will,

under certain conditions, find another stable position. The curve $P_0 = 50$ crosses the curve $\varphi + \beta = 90°$ at three points of which only the lowest one is stable.

About the stability SWIFT writes: "If, now, another eccentricity be chosen, then a similar range of corresponding values of Φ and P can be found, and ultimately a series of overlapping ranges of this kind will be developed and it will be found that the resultant pressure, attitude, and eccentricity are connected by some surface relationship which might, in theory be expressed in the form $P = f(\varepsilon, \Phi)$. It is not possible to find a value of P for every value of ε and Φ, owing to the fact that the pressure must fall to zero before the "off" point is reached, but in general there will be an infinity of combinations of ε, and Φ which will produce a given value of P. If, then, a certain load W were applied to the journal in the prescribed direction, the bearing would be able just to balance this load in any of a range of positions for which $P = W$; and clearly, from the physical nature of the problem, these positions lie on a continuous locus. The shaft will be in stable equilibrium only when it lies on that point on the locus which is farthest in the direction of action of the load W, and it is therefore this point which determines the running position of the journal under the load W. The displacement of the journal at any time in the direction of the load is given by $y = -r\varepsilon \cos \Phi$. Hence, of all its possible positions, that giving stable equilibrium for a given load W is the one for which $\varepsilon \cos \Phi$ has its greatest negative value." As pointed out above by the present author, SWIFT does not satisfy the continuity condition when he derives an infinity of positions carrying the same load in the same direction. Moreover the point, which is farthest in the direction of action of the load, on a locus with constant load carrying capacity is not stable, as all positions on such a curve are indifferent referring to motions along the curve. They may also be unstable depending on the conditions in other directions. If a certain position of the shaft centre shall exist, the continuity condition as well as the stability condition must be satisfied.

4. Experimental Investigation

4,1. Test Apparatus

The aim of the test apparatus was to determine the loci of the shaft centre at different loads and groove locations, and to determine where the shaft was stable and where it was not stable. The rig consisted of a stationary bearing and a shaft, mounted in spherical ball bearings and driven by a motor-variator. The bearing was tightened at the sides by two plates fastened to the shaft with a clearance of about 10 μm between the plates and the bearing. The bearing was covered inside and at the sides with bearing metal, and had an axial oil groove with oil inlet at one end and oil outlet at the other end for the cooling of the bearing. The location of the groove could be varied in peripheral direction. To supply the bearing with fresh oil a reservoir with oil-pump, oil-filter, and a cooling-system to keep the oil at desired temperature were used. A sketch of the test bearing is shown in fig. 22.1 and two photos in figs. 23.1 and 23.2.

The location of the bearing relative to the shaft was given in horizontal and vertical directions by two indicators graduated in microns. The bearing was loaded from above. The pressure in the groove was

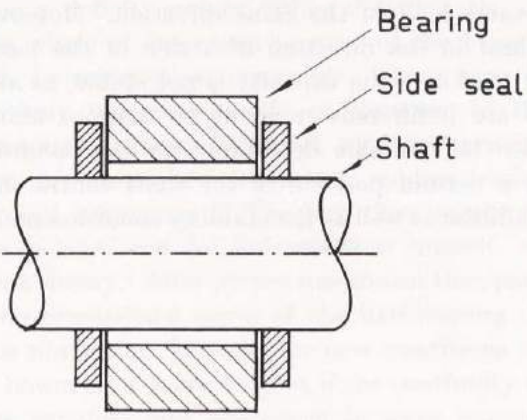

Fig. 22.1. The Principle of the Test Bearing

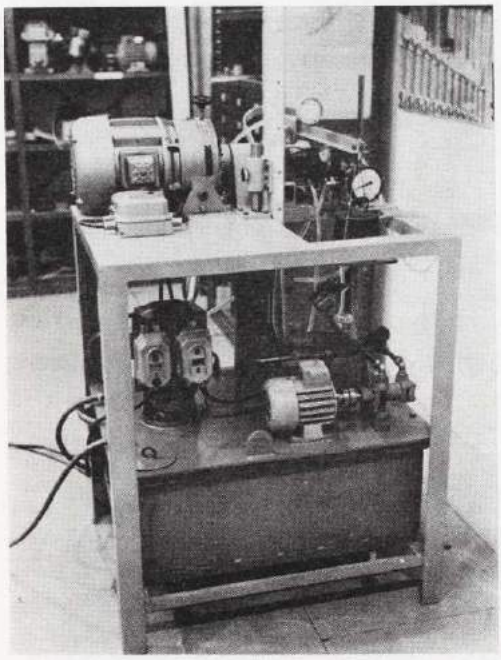

Fig. 23.1. The Test Rig

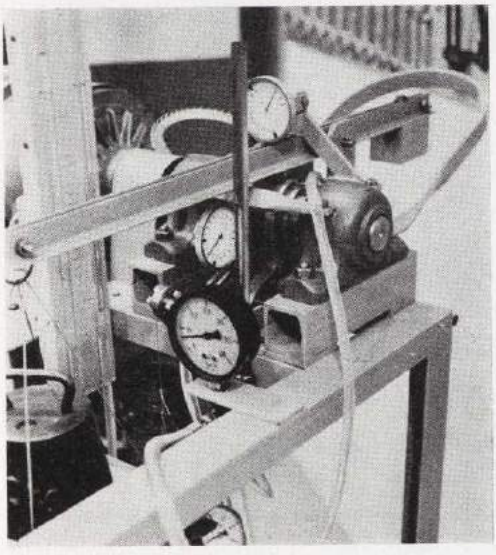

Fig. 23.2. The Test Bearing

measured by an oil manometer and adjusted to atmospheric. The temperature of the bearing was measured by a contact-thermometer and this temperature is very close to the oil temperature in the bearing.

Data of the test bearing:

Shaft diameter ..... $d = 49{,}999$ mm

Bearing diameter ..... $D = 50{,}439$ mm

Bearing width ..... $b = 75{,}0$ mm

Diametral clearance ..... $C = 440\ \mu$m

Relative clearance ..... $\psi = \frac{C}{d} = 8{,}80\ ^0/_{00}$

The weight of the bearing is 3,26 kg, which is thus the lowest possible load. If m is the mass put on the load-scale, we get 5 times as high load on the bearing and the total load is

$$P_{tot} = (5\,m + 3{,}26)\ 9{,}81\ \text{N}$$

4,2. Test Results

Tests are made to control the theoretical curves for constant values of $(\varphi_1 + \beta)$, $(\varphi_2 + \beta)$, and P_0. The angle $(\varphi_1 + \beta)$ exists between the boundaries 0° and 360° and tests are made for 270°, 180°, 120°, 90°, and 60°. The angle of $(\varphi_2 + \beta)$ exists between the boundaries 0° and 180° and tests are made for 120°, 90°, and 60°. A number of tests is also made with values of P_0 of 4, 10, and 20.

Tables of the test results are given in Appendix II,

where n = rotational speed

t = temperature of the bearing

x = horizontal eccentricity

y = vertical eccentricity

ω = angular velocity.

The figs. 26.1—29.2 show the comparisons between the theoretical curves and the experimental points. The agreement is quite satisfactory.

In theory the groove has infinitely small width in a peripheral direction. In the test apparatus its width is about 10°. As most of the tests are made for $(\varphi_1 + \beta)$ and it is only possible to test the $(\varphi_2 + \beta)$-curves to some small extent, the angle of $(\varphi + \beta)$ given in the test tables represents the angle between the load line and the beginning of the bearing surface to give somewhat higher accuracy.

The side seals give a torque on the bearing. This torque is taken up by a couple in order to get a correct loading of a single force in a well defined direction.

The relative eccentricity is determined from

$$\varepsilon = \frac{\sqrt{x^2 + y^2}}{\Delta r}$$

and the angle β from

$$\operatorname{tg} \beta = \frac{x}{y}$$

The tests coincide with the stability theory which says that the vertical eccentricity cannot decrease when the load is increased.

At lower eccentricities the shaft will vibrate even though the curves are stable, as the stiffness of the oil film there is very low.

For the groove location 120° the test points coincide with the horizontal attitude-eccentricity curve at lower eccentricities. This behaviour seems to be caused by small negative pressures giving full SOMMERFELD conditions at those low loads. At higher loads which correspond to higher speeds the small negative pressures will not influence and we get vibrations as predicted by the theory, see tab. 39.1.

When the groove is located 90° after the load, $(\varphi + \beta) = 90°$, the attitude-eccentricity curve does exist at low and high eccentricities but between those two curves there is an unstable region. This behaviour is verified by the tests, see tab. 39.2.

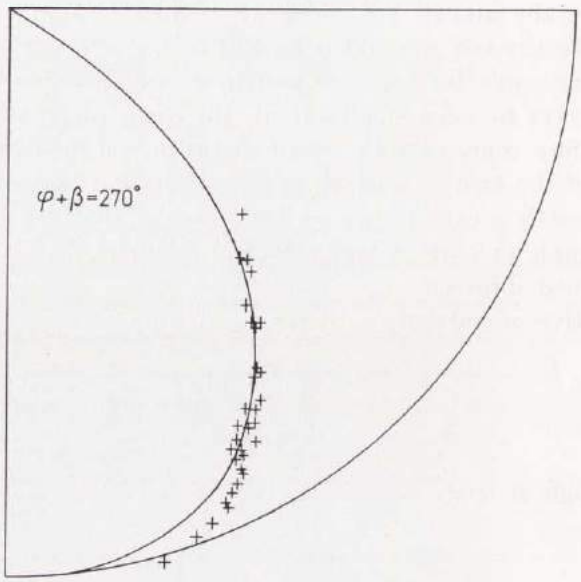

Fig. 26.1. Theoretical Curve and Test Points for $\varphi+\beta=270°$

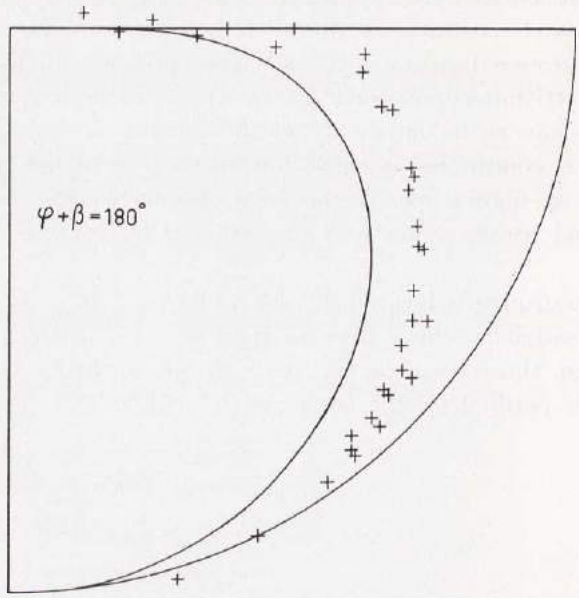

Fig. 26.2. Theoretical Curve and Test Points for $\varphi+\beta=180°$

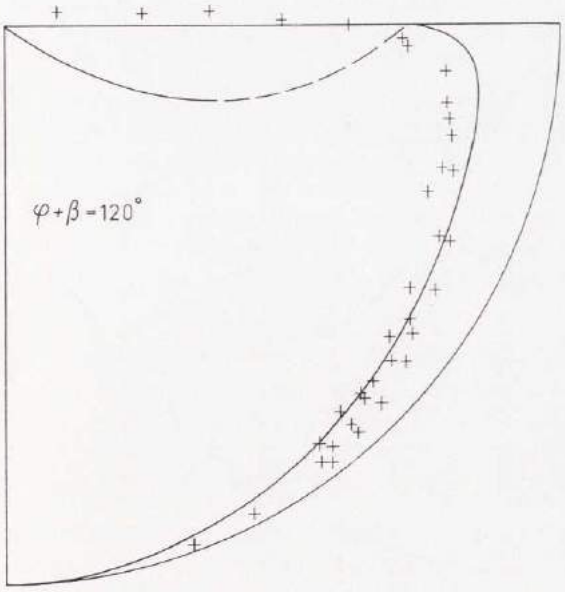

Fig. 27.1. Theoretical Curve and Test Points for $\varphi+\beta=120°$

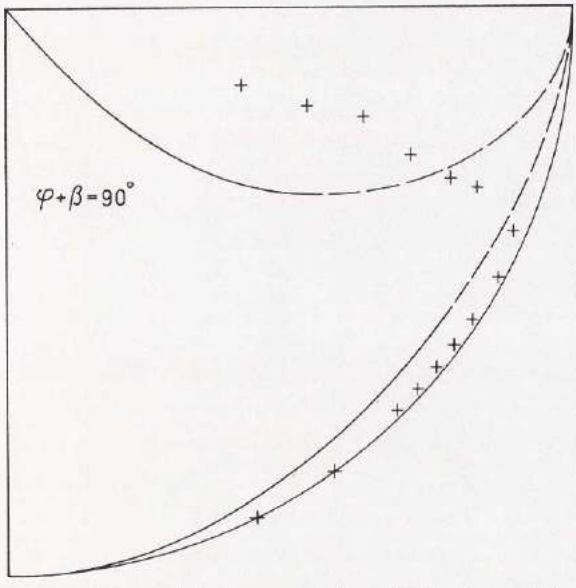

Fig. 27.2. Theoretical Curve and Test Points for $\varphi+\beta=90°$

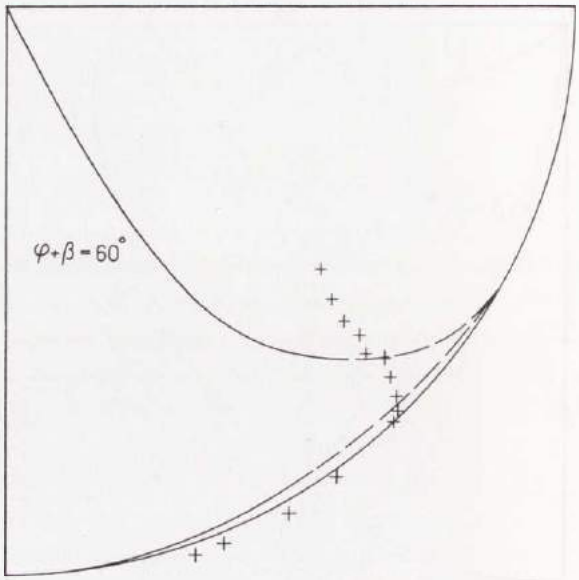

Fig. 28.1. Theoretical Curve and Test Points for $\varphi+\beta=60°$

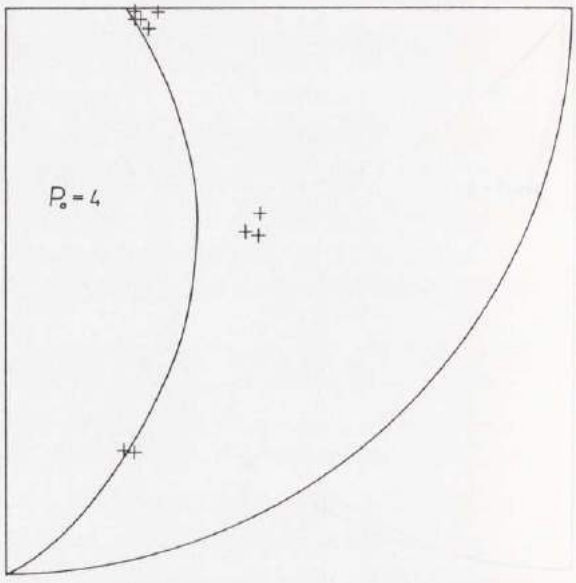

Fig. 28.2. Theoretical Curve and Test Points for $P_0=4$

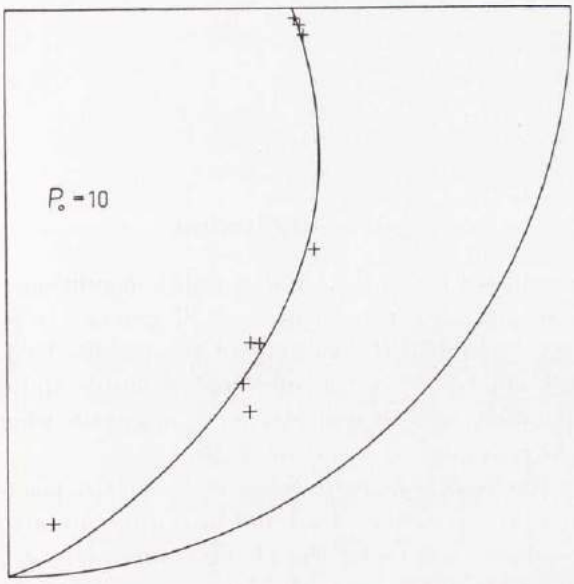

Fig. 29.1. Theoretical Curve and Test Points for $P_0 = 10$

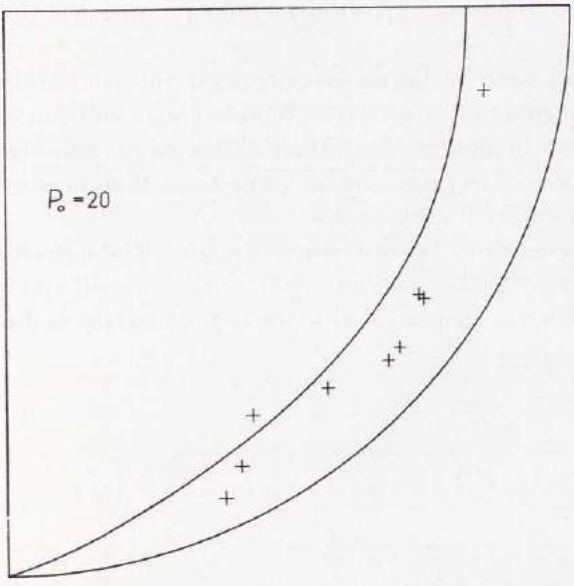

Fig. 29.2. Theoretical Curve and Test Points for $P_0 = 20$

5. Conclusion

This paper treats continuity and stability conditions of the 360° infinitely wide journal bearing with one oil groove. It is shown that it is necessary to control the validity of the results derived by using the continuity condition. Some solutions are stable and do exist; but others are not stable and those solutions do not exist, when in practice a certain load is applied at a certain angle.

In theory the shaft centre is fixed at a certain position and the corresponding pressure curve, load and load direction are determined. This solution does exist under the above assumption of a fixed shaft position. In practice, however, the load is applied at a given angle and it is not certain that the corresponding shaft position determined from the continuity condition is derived. If the location is stable, the solution is true; but if the point is unstable, the shaft will either vibrate or find another stable position. In the attitude-eccentricity diagrams the regions to the right of the dotted lines are unstable and ought to be avoided.

A test has been made to investigate if the cavitation pressure is tied to atmospheric or not. It is found that cavitation can very well take place at higher pressure than atmospheric and that cavitation occurs as soon as the pressure is lower than that pressure where the oil is in contact with air or gases.

A large number of bearing tests is made. The agreement between theory and tests is satisfactory. Tables of calculated and experimental values are given. Diagrams with theoretical curves and experimental points are shown.

6. Appendix I: Tables of Calculated Values

The following non-dimensional groups are used:

$$\varepsilon = \frac{e}{\Delta r}$$

$$P_0 = \frac{P\,\psi^2}{\eta\,U}$$

$$q_0 = \frac{q}{U\,\Delta r}$$

$$E_0 = \frac{E\,\psi}{\eta\,U^2}$$

$$\Delta t_0 = c\varrho \cdot \frac{\Delta t\,\psi^2}{\eta\,\omega}$$

$$\frac{f}{\omega\,\Delta r} = \frac{E_0}{P_0}$$

$$\frac{f}{\omega\,h_{\min}} = \frac{E_0}{P_0\,(1-\varepsilon)}$$

Tab. 31.1. Bearing Quantities at 360° Oil Film

ε	0	0,1	0,2	0,3	0,4	0,5	0,6	0,7	0,8	0,9	1,0
$\varphi_1 = \varphi_2 = \varphi^*$	90	81,42	72,90	64,49	56,25	48,19	40,30	32,50	24,62	16,09	0
P_0	0	1,885	3,772	5,673	7,617	9,674	11,98	14,84	19,04	27,70	∞
β	90	90	90	90	90	90	90	90	90	90	90
q_0	0,5000	0,4925	0,4706	0,4354	0,3889	0,3333	0,2712	0,2048	0,1364	0,06762	0
E_0	6,283	6,409	6,790	7,437	8,379	9,674	11,45	13,99	18,09	26,88	∞
Δt_0	12,57	13,01	14,43	17,08	21,55	29,02	42,22	68,32	132,6	397,5	∞
$\frac{f}{\omega\,\Delta r}$	∞	3,400	1,800	1,311	1,100	1,000	0,9556	0,9429	0,9500	0,9704	1
$\frac{f}{\omega\,h_{\min}}$	∞	3,778	2,250	1,873	1,833	2,000	2,389	3,143	4,750	9,704	∞

Tab. 32.1. Bearing Quantities at $\varepsilon = 0{,}2$

$\varphi_2 = \varphi^*$	70	65	60	50	40
φ_1	121,01	158,24	−172,83	−127,31	−92,70
P_0	3,586	3,032	2,407	1,302	0,5707
β	83,77	73,69	64,57	48,99	36,33
q_0	0,4658	0,4577	0,4500	0,4357	0,4234
E_0	6,698	6,503	6,302	5,952	5,702
Δt_0	14,38	14,21	14,00	13,66	13,47
$\frac{f}{\omega\, \Delta r}$	1,868	2,145	2,618	4,572	9,990
$\frac{f}{\omega\, h_{\min}}$	2,335	2,681	3,272	5,715	12,49

Tab. 32.2. Bearing Quantities at $\varepsilon = 0{,}4$

$\varphi_2 = \varphi^*$	54	50	40	20
φ_1	99,74	144,49	−124,81	−43,57
P_0	7,317	6,235	2,915	0,1848
β	83,81	71,77	45,33	17,21
q_0	0,3824	0,3714	0,3468	0,3121
E_0	8,182	7,642	6,213	5,108
Δt_0	21,39	20,57	17,92	16,37
$\frac{f}{\omega\, \Delta r}$	1,118	1,226	2,131	27,64
$\frac{f}{\omega\, h_{\min}}$	1,864	2,043	3,552	46,06

Tab. 33.1. Bearing Quantities at $\varepsilon = 0{,}6$

$\varphi_2 = \varphi^*$	38	35	30	20
φ_1	84,21	136,99	−121,44	−49,38
P_0	11,42	9,749	5,484	0,9795
β	80,79	65,06	40,25	18,99
q_0	0,2636	0,2543	0,2402	0,2181
E_0	10,98	9,776	7,312	5,480
Δt_0	41,64	38,45	30,44	25,13
$\frac{f}{\omega\, \Delta r}$	0,9616	1,003	1,333	5,595
$\frac{f}{\omega\, h_{\min}}$	2,404	2,507	3,334	13,99

Tab. 33.2. Bearing Quantities at $\varepsilon = 0{,}8$

$\varphi_2 = \varphi^*$	22	20	15	10
φ_1	76,22	−164,24	−43,35	−22,73
P_0	17,90	14,51	3,580	0,6507
β	67,91	39,71	15,96	8,89
q_0	0,1291	0,1241	0,1136	0,1061
E_0	16,36	12,17	7,136	6,225
Δt_0	126,7	98,02	62,80	58,68
$\frac{f}{\omega\, \Delta r}$	0,9138	0,8383	1,993	9,567
$\frac{f}{\omega\, h_{\min}}$	4,569	4,191	9,967	47,83

Tab. 34.1. Bearing Angles and Load Capacity at $\varepsilon = 0{,}85$

$\varphi_2 = \varphi^*$	20	18	16	14	10	8	5
φ_1	32,85	73,05	−93,00	−47,65	−24,29	−17,93	−10,42
P_0	22,22	21,47	14,60	7,316	1,682	0,6698	0,09980
β	86,03	61,54	25,93	16,63	9,37	7,04	4,14

Tab. 34.2. Bearing Angles and Load Capacity at $\varepsilon = 0{,}90$

$\varphi_2 = \varphi^*$	15	14	13	12	10	8	5	2
φ_1	36,02	60,93	−119,39	−51,74	−28,97	−19,51	−10,69	−4,04
P_0	27,47	28,20	25,19	15,46	6,459	2,475	0,3600	0,009048
β	75,47	55,95	25,91	16,45	10,65	7,51	4,23	1,62

Tab. 34.3. Bearing Angles and Load Capacity at $\varepsilon = 0{,}95$

$\varphi_2 = \varphi^*$	10,5	10,0	9,5	9,0	8,0	7,0	5,0	2,0
φ_1	19,41	27,11	39,95	135,74	−31,04	−20,73	−11,69	−4,09
P_0	39,55	41,00	45,24	52,79	25,16	13,29	3,146	0,07669
β	80,64	66,07	49,21	25,88	10,29	7,57	4,54	1,63

Tab. 34.4. Bearing Angles and Load Capacity at $\varepsilon = 0{,}98$

$\varphi_2 = \varphi^*$	6,20	5,90	5,70	5,60	5,58	5,56	5,54	5,53	5,52	5,50	4,00
φ_1	15,95	22,57	32,69	48,83	57,21	73,97	135,92	−139,26	−93,75	−64,44	−10.81
P_0	70,34	86,33	103,9	117,0	119,6	123,0	125,8	124,9	122,1	116,8	22,09
β	58,70	40,49	29,18	22,53	21,17	19,18	15,82	14,05	12,76	11,48	4,05

7. Appendix II: Tables of Experimental Values

Tab. 35.1. Test Values at $\varphi+\beta=270°$

m	n	t	x	y	P_{tot}	ω	ε	β
kg	r/m	°C	μm	μm	N	l/s		
20,0	310	25,3	62	214	1010	32,5	1,01	16
9,0	312	27,2	75	204	473	32,7	0,99	20
7,0	311	27,0	82	200	375	32,6	0,98	22
3,5	304	27,4	90	175	204	31,8	0,89	27
3,0	302	27,6	91	170	179	31,6	0,88	28
2,5	302	27,9	93	163	155	31,6	0,85	30
2,0	302	27,9	95	155	130	31,6	0,83	32
1,5	303	27,8	97	141	106	31,7	0,78	35
1,0	303	28,2	96	122	81	31,7	0,70	38
0,8	303	28,4	94	115	71	31,7	0,67	39
0,6	303	28,4	94	96	61	31,7	0,61	44
0,5	303	28,4	91	80	57	31,7	0,55	49

Tab. 35.2. Test Values at $\varphi+\beta=270°$

m	n	t	x	y	P_{tot}	ω	ε	β
kg	r/m	°C	μm	μm	N	l/s		
8	599	23,2	86	172	424	62,7	0,87	27
7	600	23,7	88	168	375	62,8	0,86	28
6	599	24,2	91	162	326	62,7	0,84	29
5	599	24,3	93	154	277	62,7	0,82	31
4	600	24,4	95	142	228	62,8	0,78	34
3	600	25,2	96	124	179	62,8	0,71	38
2	600	25,2	91	96	130	62,8	0,60	43
1	600	25,8	Vibr.	Vibr.	81	62,8	Vibr.	Vibr.

Tab. 36.1. Test Values at $\varphi+\beta=270°$

m	n	t	x	y	P_{tot}	ω	ε	β
kg	r/m	°C	μm	μm	N	l/s		
15	899	27,2	85	193	768	94,1	0,96	24
14	898	27,3	86	190	719	94,0	0,95	24
13	898	27,6	87	187	670	94,0	0,94	25
12	898	28,1	89	184	621	94,0	0,93	26
11	898	28,2	91	181	572	94,0	0,92	27
10	898	28,2	92	177	522	94,0	0,91	27
9	900	28,6	93	173	473	94,2	0,89	28
8	898	28,7	96	167	424	94,0	0,88	30
7	900	28,8	97	160	375	94,2	0,85	31
6	900	28,4	98	152	326	94,2	0,82	33
5	900	28,7	99	139	277	94,2	0,77	35
4	900	28,8	98	122	228	94,2	0,71	39
3	900	28,9	94	102	179	94,2	0,63	43
2	898	29,2	Vibr.	Vibr.	130	94,0	Vibr.	Vibr.

Tab. 36.2. Test Values at $\varphi+\beta=180°$

m	n	t	x	y	P_{tot}	ω	ε	β
kg	r/m	°C	μm	μm	N	l/s		
20,0	312	28,0	66	214	1010	32,7	1,02	17
10,0	312	27,0	96	198	522	32,7	1,00	26
3,5	310	28,1	146	139	204	32,5	0,92	46
3,0	313	28,2	152	123	179	32,8	0,89	51
2,5	313	28,7	157	102	155	32,8	0,85	57
2,2	315	28,8	157	78	140	33,0	0,80	64
2,0	312	29,0	156	55	130	32,7	0,75	71
1,8	313	29,1	149	32	120	32,8	0,69	78
1,6	313	29,2	137	17	110	32,8	0,63	83
1,0	312	29,3	103	7	81	32,7	0,47	86
0,5	313	29,4	73	2	57	32,8	0,33	88
0	312	29,4	42	1	32	32,7	0,19	89

Tab. 37.1. Test Values at $\varphi+\beta=180°$

m	n	t	x	y	P_{tot}	ω	ε	β
kg	r/m	°C	μm	μm	N	1/s		
12	600	24,2	132	165	621	62,8	0,96	39
11	600	25,3	132	158	572	62,8	0,94	40
10	600	25,0	142	151	522	62,8	0,94	43
9	600	24,8	148	142	473	62,8	0,93	46
8	600	25,0	153	132	424	62,8	0,92	49
7	600	25,0	157	115	375	62,8	0,88	54
6	600	25,2	159	86	326	62,8	0,82	62
5	600	25,4	157	57	277	62,8	0,76	70
4	600	26,2	138	10	228	62,8	0,63	86
3	600	26,2	111	2	179	62,8	0,50	90
2	600	26,3	84	−1	130	62,8	0,38	90
1	600	26,4	56	−3	81	62,8	0,25	93
0	600	26,6	27	−6	32	62,8	0,13	102

Tab. 37.2. Test Values at $\varphi+\beta=180°$

m	n	t	x	y	P_{tot}	ω	ε	β
kg	r/m	°C	μm	μm	N	1/s		
18	900	26,8	125	174	915	94,2	0,98	35
16	903	26,7	135	165	817	94,5	0,97	39
14	899	26,7	145	153	719	94,1	0,96	43
12	899	26,6	155	136	621	94,1	0,94	49
10	901	26,9	162	113	522	94,3	0,90	55
8	902	27,2	161	86	424	94,4	0,83	62
7	898	27,6	156	63	375	94,0	0,76	68
6	900	28,2	145	32	326	94,2	0,67	78
5	900	28,2	Vibr.	Vibr.	277	94,2	Vibr.	Vibr.
4	900	28,2	Vibr.	Vibr.	228	94,2	Vibr.	Vibr.
3	900	28,2	Vibr.	Vibr.	179	94,2	Vibr.	Vibr.
2	900	28,2	Vibr.	Vibr.	130	94,2	Vibr.	Vibr.
1	900	28,2	Vibr.	Vibr.	81	94,2	Vibr.	Vibr.

Tab. 38.1. Test Values at $\varphi+\beta=120°$

m	n	t	x	y	P_{tot}	ω	ε	β
kg	r/m	°C	μm	μm	N	l/s		
20,0	312	27,7	73	206	1010	32,7	0,99	20
12,0	312	27,8	100	192	621	32,7	0,98	27
7,0	310	25,2	125	165	375	32,5	0,94	37
6,0	310	25,2	133	153	326	32,5	0,92	41
5,5	311	25,2	140	145	302	32,6	0,92	44
5,0	312	25,4	145	140	277	32,7	0,92	46
4,5	311	25,4	152	125	253	32,6	0,89	51
4,0	312	25,5	159	105	228	32,7	0,87	57
3,5	312	26,0	167	68	204	32,7	0,82	68
3,3	312	25,6	174	57	193	32,7	0,83	72
3,1	312	25,8	175	32	184	32,7	0,81	80
2,5	312	26,2	159	4	155	32,7	0,72	88

Tab. 38.2. Test Values at $\varphi+\beta=120°$

m	n	t	x	y	P_{tot}	ω	ε	β
kg	r/m	°C	μm	μm	N	l/s		
13	602	26,9	125	172	670	63,0	0,97	36
12	602	26,7	131	165	621	63,0	0,96	38
11	602	27,0	137	158	572	63,0	0,95	41
10	602	26,7	144	147	522	63,0	0,93	44
9	602	26,8	152	134	473	63,0	0,92	49
8	601	26,8	160	117	424	62,9	0,90	54
7	602	26,8	171	85	375	63,0	0,87	64
6	602	27,3	176	37	326	63,0	0,82	78
5	602	27,3	160	9	277	63,0	0,73	87
4	602	27,4	137	1	228	63,0	0,62	90
3	602	27,6	111	−2	179	63,0	0,50	91
2	603	27,6	82	−5	130	63,1	0,37	94
1	603	27,5	54	−5	81	63,1	0,25	95
0	603	27,6	22	−6	32	63,1	0,10	105

Tab. 39.1. The Values at $\varphi+\beta=120°$

m	n	t	x	y	P_{tot}	ω	ε	β
kg	r/m	°C	μm	μm	N	1/s		
19	901	27,0	129	173	964	94,3	0,98	37
17	900	27,2	140	163	866	94,2	0,97	41
15	901	27,7	148	151	768	94,3	0,96	45
13	901	27,6	158	133	670	94,3	0,94	50
12	900	28,0	163	121	621	94,2	0,92	53
11	901	28,1	170	106	572	94,3	0,91	58
10	902	28,3	175	85	522	94,4	0,89	64
9	901	28,7	177	58	473	94,3	0,85	72
8,5	902	28,9	177	43	449	94,4	0,83	76
8	901	29,6	175	18	424	94,3	0,80	84
7	902	29,9	Vibr.	Vibr.	375	94,4	Vibr.	Vibr.
6	903	29,2	Vibr.	Vibr.	326	94,5	Vibr.	Vibr.
5	903	29,2	Vibr.	Vibr.	277	94,5	Vibr.	Vibr.
0	903	29,2	Vibr.	Vibr.	32	94,5	Vibr.	Vibr.

Tab. 39.2. Test Values at $\varphi+\beta=90°$

m	n	t	x	y	P_{tot}	ω	ε	β
kg	r/m	°C	μm	μm	N	1/s		
30	602	26,7	95	198	1500	63,0	1,00	26
20	602	26,6	125	180	1010	63,0	1,00	35
16	602	28,0	152	156	817	63,0	0,99	44
15	602	28,5	159	149	768	63,0	0,99	47
14	602	28,6	167	141	719	63,0	0,99	50
13	603	28,8	174	131	670	63,1	0,99	53
12	602	28,9	181	121	621	63,0	0,99	56
11	602	29,1	109	105	572	63,0	0,99	61
10	603	29,2	198	88	522	63,1	0,98	66
9	603	29,7	Vibr.	Vibr.	473	63,1	Vibr.	Vibr.
8	603	29,7	Vibr.	Vibr.	424	63,1	Vibr.	Vibr.
7	603	29,7	Vibr.	Vibr.	375	63,1	Vibr.	Vibr.
6	603	29,7	182	71	326	63,1	0,89	69
5	603	29,7	172	66	277	63,1	0,84	69
4	603	29,7	158	58	228	63,1	0,76	70
3	603	29,7	138	42	179	63,1	0,66	73
2	603	29,8	116	38	130	63,1	0,56	72
1	603	29,8	91	30	81	63,1	0,44	72

Tab. 40.1. Test Values at $\varphi+\beta=60°$

m	n	t	x	y	P_{tot}	ω	ε	β
kg	r/m	°C	μm	μm	N	l/s		
30,0	311	26,0	74	212	1500	32,6	1,02	19
25,0	311	26,0	83	210	1260	32,6	1,02	22
15,0	312	26,0	108	198	768	32,7	1,02	29
10,0	312	26,0	127	183	522	32,7	1,01	35
7,0	311	27,6	150	161	375	32,6	1,00	43
6,0	311	27,5	151	156	326	32,6	0,99	44
5,0	311	27,4	151	150	277	32,6	0,97	45
4,0	311	27,4	149	143	228	32,6	0,94	46
3,0	312	27,4	145	137	179	32,7	0,91	47
2,5	311	26,9	140	133	155	32,6	0,88	46
2,0	311	27,0	136	127	130	32,6	0,85	47
1,5	312	26,7	131	122	106	32,7	0,81	47
1,0	312	26,4	126	114	81	32,7	0,77	48
0,4	312	26,4	122	102	52	32,7	0,72	50

Tab. 40.2. Test Values at $P_0=4$

m	n	t	x	y	$\varphi_1+\beta$	P_{tot}	ω	η	ε	β
kg	r/m	°C	μm	μm		N	l/s	Ns/m²		
1	672	28,2	47	172	330	81	70,4	0,0119	0,81	15
1	666	28,0	50	174	330	81	69,7	0,0120	0,82	16
1	666	28,0	92	87	300	81	69,7	0,0120	0,58	47
1	649	27,5	98	88	300	81	68,0	0,0123	0,60	48
1	664	28,0	99	80	300	81	69,5	0,0120	0,58	51
1	665	28,0	57	8	270	81	69,6	0,0120	0,26	82
1	650	27,5	50	2	240	81	68,1	0,0123	0,23	89
1	639	27,0	60	2	210	81	66,9	0,0125	0,27	89
1	613	26,0	52	6	180	81	64,2	0,0130	0,24	85
1	588	24,8	50	6	180	81	61,6	0,0136	0,23	85

Tab. 41.1. Test Values at $P_0 = 10$

m	n	t	x	y	$\varphi_1+\beta$	P_{tot}	ω	η	ε	β
kg	r/m	°C	μm	μm		N	l/s	Ns/m²		
3	582	27,6	17	200	330	179	60,9	0,0122	0,91	5
3	592	28,0	94	156	300	179	62,0	0,0120	0,83	31
3	546	26,0	91	145	300	179	57,1	0,0130	0,78	32
3	526	25,0	95	130	270	179	55,1	0,0135	0,73	36
3	555	26,5	98	131	270	179	58,1	0,0128	0,74	37
3	542	25,8	121	93	240	179	56,7	0,0131	0,69	52
3	542	25,8	117	10	210	179	56,7	0,0131	0,53	85
3	547	26,0	112	4	180	179	57,3	0,0130	0,51	88
3	564	26,9	114	5	180	179	59,1	0,0126	0,52	87

Tab. 41.2. Test Values at $P_0 = 20$

m	n	t	x	y	$\varphi_1+\beta$	P_{tot}	ω	η	ε	β
kg	r/m	°C	μm	μm		N	l/s	Ns/m²		
6	480	25,2	84	191	300	326	50,2	0,0134	0,95	24
6	491	25,8	84	191	300	326	51,4	0,0131	0,95	24
6	487	25,6	91	178	270	326	51,0	0,0132	0,91	27
6	495	26,0	92	178	270	326	51,8	0,0130	0,91	27
6	498	26,2	95	159	240	326	52,2	0,0129	0,84	31
6	502	26,5	94	159	240	326	52,6	0,0128	0,84	31
6	498	26,2	124	149	210	326	52,2	0,0129	0,88	40
6	502	26,5	123	149	210	326	52,6	0,0128	0,88	40
6	495	26,0	153	132	180	326	51,8	0,0130	0,92	49
6	495	26,0	149	137	180	326	51,8	0,0130	0,92	47
6	502	26,4	165	108	150	326	52,6	0,0128	0,90	57
6	441	23,4	164	107	150	326	46,2	0,0145	0,89	57
6	455	24,0	186	33	120	326	47,6	0,0141	0,86	80

8. References

1. Floberg, L.: The Infinite Journal Bearing, Considering Vaporization. Göteborg, 1957.
2. Floberg, L.: Experimental Investigation of Power Loss in Journal Bearings, Considering Cavitation. Göteborg, 1959.
3. Floberg, L.: Lubrication of a Rotating Cylinder on a Plane Surface, Considering Cavitation. Göteborg, 1959.
4. Floberg, L.: The Optimum Thrust Tilting-pad Bearing. Göteborg, 1960.
5. Floberg, L.: The Two-groove Journal Bearing, Considering Cavitation. Göteborg, 1960.
6. Floberg, L.: Lubrication of Two Cylindrical Surfaces, Considering Cavitation. Göteborg, 1961.
7. Jakobsson, B. and Floberg, L.: The Finite Journal Bearing, Considering Vaporization. Göteborg, 1957.
8. Jakobsson, B. and Floberg, L.: The Partial Journal Bearing. Göteborg, 1958.
9. Jakobsson, B. and Floberg, L.: The Rectangular Plane Pad Bearing. Göteborg, 1958.
10. Jakobsson, B. and Floberg, L.: The Centrally Loaded Partial Journal Bearing. Göteborg, 1959.
11. Reynolds, O.: On the Theory of Lubrication .... Phil. Trans. Roy. Soc., vol. 177, p. 157, 1886.
12. Sommerfeld, A.: Zur hydrodynamischen Theorie der Schmiermittelreibung. Zeitschrift für Mathematik und Physik, vol. 50, p. 97, 1904.
13. Stieber, W.: Das Schwimmlager. Hydrodynamische Theorie des Gleitlagers. Berlin, 1933.
14. Swift, H. W.: "The Stability of Lubricating Films in Journal Bearings". Proc. Inst. Civ. Engrs, vol. 233, p. 267, 1932.

Forts. fr. omsl. 2:dra sida

178. OLVING, SVEN, *A new method for space charge wave interaction studies. I.* 12 s. 1956. Kr. 3: —. (Avd. Elektroteknik. 51.)
179. HANSBO, SVEN, *The critical load of rectangular frames analysed by convergence methods.* 47 s. 1956. Kr. 11: —. (Avd. Väg- och Vattenbyggnad. Byggnadsteknik. 25.)
180. WESTBERG, VIDOR, *Measurements of noise radiation at 10 cm from glow lamps. Preliminary report.* 14 s. 1956. Kr. 4: 50. (Avd. Elektroteknik. 52).
181. SVENSSON, S. I., HELLGREN, G., AND PERERS, O., *The Swedish radioscientific solar eclipse expedition to Italy, 1952. Preliminary report.* 30 s. 1956. Kr. 8: —. (Avd. Elektroteknik. 53.)
182. WAX, NELSON, *A note on design considerations for a proposed auroral radar.* 16 s. 1957. Kr. 3: —. (Avd. Elektroteknik. 54.)
183. JOSHI, G. H., *The electromagnetic interaction between two crossing electron streams. I.* 31 s. 1957. Kr. 8: —. (Avd. Elektroteknik. 55.)
184. SMITH, BENGT, *Dry methods for removing hydrogen sulphide from gases.* 65 s. 1957. Kr. 15: —. (Avd. Kemi och Kemisk Teknologi. 34.)
185. EKELÖF, S., BJÖRK, N., AND DAVIDSON, R., *Large signal behaviour of directly heated thermistors.* 31 s. 1957. Kr. 8: —. (Avd. Elektroteknik. 56.)
186. CARLSSON, BENGT, UND LARSSON, HANS, *Wirkungsgrad und Selbsthemmung einfacher Umlaufgetriebe.* 48 s. 1957. Kr. 9: —. (Avd. Maskinteknik. 8.)
187. AURELL, CARL G., *The equivalent transmission line of a linear four-terminal network. Calculations with cascade-connected four-terminal networks.* 39. s. 1957. Kr. 6: —. (Avd. Elektroteknik. 57.)
188. LUNDHOLM, R., *Induced overvoltage-surges on transmission lines and their bearing on the lightning performance at medium voltage networks.* 117 s. 1957. Kr. 19: —. (Avd. Elektroteknik. 58.)
189. FLOBERG, LEIF, *The infinite journal bearing, considering vaporization.* 83 s. 1957. Kr. 13: —. (Avd. Maskinteknik. 9.)
190. JAKOBSSON, BENGT, AND FLOBERG, LEIF, *The finite journal bearing, considering vaporization.* 117 s. 1957. Kr. 19: 50. (Avd. Maskinteknik. 10.)
191. CHAKO, NICHOLAS, *Characteristic curves on planes in the image space.* 49 s. 1957. Kr. 15: —. (Avd. Allmänna Vetenskaper. 12.)
192. EKELÖF, STIG, *The development and decay of the magnetic flux in a non-delayed telephone relay.* 50 s. 1957. Kr. 15: —. (Avd. Elektroteknik. 59.)
193. BJÖRKLUND, KJELL, *Bestämning av porslins draghållfasthet.* 78 s. 1958. Kr. 15: —. (Institutionen för Silikatkemisk Forskning. 39.)
194. GRANHOLM, PER, *Sound insulation of single leaf walls.* 48 s. 1958. Kr. 8:—. (Avd. Väg- och Vattenbyggnad. Byggnadsteknik. 26.)
195. GRANHOLM, HJALMAR, *Om vattengenomslag i murade väggar med särskild hänsyn till tegel som fasadmaterial.* 172 s. 1958. Kr. 16: —. (Avd. Väg- och Vattenbyggnad. Byggnadsteknik. 27.)
196. MEOS, JOHAN, AND OLVING, SVEN, *On the origin of radar echoes associated with auroral activity.* 20 s. 1958. Kr. 5: —. (Avd. Elektroteknik. 60.)
197. JOSHI, G. H., *The electromagnetic interaction between two crossing electron streams. II.* 10 s. 1958. Kr. 3: 50. (Avd. Elektroteknik. 61.)
198. WILHELMSSON, HANS, *The interaction between an obliquely incident plane electromagnetic wave and an electron beam. II.* 32 s. 1958. Kr. 7: —. (Avd. Elektroteknik. 62.)
199. KÄRRHOLM, GUNNAR, *A method of iteration applied to beams resting on springs.* 50 s. 1958. Kr. 12: —. (Avd. Allm. Vetenskaper. 13.)
200. JAKOBSSON, BENGT, AND FLOBERG, LEIF, *The partial journal bearing.* 60 s. 1958. Kr. 14: —. (Avd. Maskinteknik. 11.)
201. KÄRRHOLM, GUNNAR, *Influence functions of elastic plates divided in strips.* 18 s. 1958. Kr. 4: 50. (Avd. Väg- och Vattenbyggnad. Byggnadsteknik. 28.)
202. RÅDE, LENNART, *Sampling planes for acceptance sampling by variables using the range.* 34 s. 1958. Kr. 9: 50. (Avd. Allm. Vetenskaper. 14.)
203. JAKOBSSON, BENGT, AND FLOBERG, LEIF, *The rectangular plane pad bearing.* 44 s. 1958. Kr. 5: —. (Avd. Maskinteknik. 12.)
204. ASPLUND, SVEN OLOF, *Column-beams and suspension bridges analysed by »Green's matrix».* 36 s. 1958. Kr. 7: —. (Avd. Väg- och Vattenbyggnad. Byggnadsteknik. 29.)
205. WILHELMSSON, HANS, *On the properties of the electron beam in the presence of an axial magnetic field of abitrary strength.* 32 s. 1958. Kr. 7: 50. (Avd. Elektroteknik. 63.)
206. WILHELMSSON, HANS, *The interaction between an obliquely incident plane electromagnetic wave and an electron beam. III.* 17 s. 1958. Kr. 5: —. (Avd. Elektroteknik. 64.)
207. HEDVALL, ARVID J., *On the influence of pre-treatment and transition processes on the adsorption capacity and the reactivity of various types of glass and silica.* 39 s. 1959. Kr. 8: —. (Institutionen för Silikatkemisk Forskning. 40.)

Forts. å omsl. 4:de sida

Forts. fr. omsl. 3:dje sida

208. KÄRRHOLM, GUNNAR, *A flow problem solved by strip method.* 22 s. 1959. Kr. 4: 50. (Avd. Allm. Vetenskaper. 15.)
209. GRANHOLM, HJALMAR, *Allmän teori för beräkning av armerad betong.* 228 s. 1959. Kr. 20: —. (Avd. Väg- och Vattenbyggnad. Byggnadsteknik. 30.)
210. LIDIN, LARS G., *On helical-springs suspension.* 75 s. 1959. Kr. 15: —. (Avd. Maskinteknik. 13.)
211. BJÖRK, NILS, *Theory of the indirectly heated thermistor.* 46 s. 1959. Kr. 10: —. (Avd. Elektroteknik. 65.)
212. CARLSSON, ORVAR, *The influence of submicroscopic pores on the resistance of bricks towards frost.* 13 s. 1959. Kr. 3: 50. (Institutionen för Silikatkemisk Forskning. 41.)
213. GRANHOLM, HJALMAR, *KAM 40, KAM 60 och KAM 90.* 41 s. 1959. Kr. 3: 50. (Avd. Väg- och Vattenbyggnad, Byggnadsteknik. 31.)
214. JAKOBSSON, BENGT, AND FLOBERG, LEIF, *The centrally loaded partial journal bearing.* 35 s. 1959. Kr. 7: 50. (Avd. Maskinteknik. 14.)
215. FLOBERG, LEIF, *Experimental investigation of power loss in journal bearings, considering cavitation.* 16 s. 1959. Kr. 3: 50. (Avd. Maskinteknik. 15).
216. FLOBERG, LEIF, *Lubrication of a rotating cylinder on a plane surface, considering cavitation.* 40 s. 1959. Kr. 8: —. (Avd. Maskinteknik. 16.)
217. TROEDSSON, CARL BIRGER, *The growth of the Western city during the Middle Ages.* 125 s. 1959. Kr. 19: —. (Avd. Arkitektur. 4.)
218. HEDVALL, J. ARVID, *The importance of the reactivity of solids in geological-mineralogical processes.* 11 s. 1959. Kr. 2: 50. (Institutionen för Silikatkemisk Forskning. 42.)
219. CORNELL, ELIAS, *Humanistic inquiries into architecture. I—III.* 112 s. 1959. Kr. 17: —. (Avd. Arkitektur. 5.)
220. GRANHOLM, CARL-ADOLF, *Ekonomiska aluminiumprofiler.* 48 s. 1959. Kr. 5: 50. (Avd. Väg- och Vattenbyggnad. Byggnadsteknik. 32.)
221. LUNDÉN, ARNOLD, CHRISTOFFERSON, STINA, AND LODDING, ALEX, *The isotopic effect of lithium ions in countercurrent electromigration in molten lithium bromide and iodide.* 38 s. 1959. Kr. 7: 50. (Avd. Allm. Vetenskaper. 16.)
222. INGEMANSSON, STIG, AND KIHLMAN, TOR, *Sound insulation of frame walls.* 47 s. 1959. Kr. 8: 50. (Avd. Väg- och Vattenbyggnad, Byggnadsteknik. 33.)
223. HÖGLUND, B., AND RADHAKRISHNAN, V., *A radiometer for the hydrogen line.* 25 s. 1959. Kr. 6: 50. (Avd. Elektroteknik. 66.)
224. JAKOBSSON, BENGT, *Torque distribution, power flow, and zero output conditions of epicyclic gear trains.* 55 s. 1960. Kr. 12: —. (Avd. Maskinteknik. 17.)
225. OLVING, SVEN, *Electromagnetic and space charge waves in a sheath helix.* 91 s. 1960. Kr. 17: —. (Avd. Elektroteknik. 67.)
226. STRÖMBLAD, JOHN, *Beschleunigungsverlauf und Gleichgewichtsdrehzahlen einfacher Planetengetriebe nebst Selbsthemmungsversuche.* 80 s. 1960. Kr. 18:—. (Avd. Maskinteknik. 18.)
227. SANDFORD, FOLKE, *Some current problems concerning brick manufacture.* 20 s. 1960. Kr. 5: —. (Avd. Kemi och Kemisk Teknologi. 35.)
228. OLVING, SVEN, *A new method for space charge wave interaction studies. II.* 40 s. 1960. Kr. 8: —. (Avd. Elektroteknik. 68.)
229. GRANHOLM, HJALMAR, *Le problème de Boussinesq.* 15 s. 1960. Kr. 3: 50. (Avd. Väg- och Vattenbyggnad. Byggnadsteknik. 34.)
230. HIBA, MIODRAG et CEDERWALL, KRISTER, *Flambement élastique d'une barre en bois lamellée et clouée avec le module de déplacement du moyen de liaison constant k.* 22 s. 1960. Kr. 5: —. (Avd. Väg- och Vattenbyggnad. Byggnadsteknik. 35.)
231. FLOBERG, LEIF, *The optimum thrust tilting-pad bearing.* 23 s. 1960. Kr. 5: —. (Avd. Maskinteknik. 19.)
232. FLOBERG, LEIF, *The two-groove journal bearing, considering cavitation.* 32 s. 1960. Kr. 6: —. (Avd. Maskinteknik. 20.)
233. HEDVALL, ARVID J., *Heterogeneous catalysis, results and projects for research.* 18 s. 1961. Kr. 5: —. (Avd. Kemi och Kemisk Teknologi. 36.)
234. FLOBERG, LEIF, *Lubrication of two cylindrical surfaces, considering cavitation.* 36 s. 1961. Kr. 10: —. (Avd. Maskinteknik. 21.)

Pris kronor 11: —

ELANDERS BOKTRYCKERI AKTIEBOLAG
GÖTEBORG 1961

CHALMERS TEKNISKA HÖGSKOLAS HANDLINGAR
TRANSACTIONS OF CHALMERS UNIVERSITY OF TECHNOLOGY
GOTHENBURG, SWEDEN
Nr 238 (Avd. Maskinteknik 23) 1961

EXPERIMENTAL INVESTIGATION OF CAVITATION REGIONS IN JOURNAL BEARINGS

BY

LEIF FLOBERG

Report No. 16 from the Institute of Machine Elements
Chalmers University of Technology
Gothenburg, Sweden
1961

Av Chalmers Tekniska Högskolas Handlingar hava tidigare utkommit:

Fullständig förteckning över Chalmers Tekniska Högskolas Handlingar
lämnas av Chalmers Tekniska Högskolas Bibliotek, Göteborg.

151. HEDVALL, J. A., *Reactions with activated solids.* 23 s. 1954 Kr. 5: —. (Institutionen för Silikatkemisk Forskning. 32).
152. SMITH, CYRIL STANLEY, *The microstructure of polycrystalline materials.* 49 s. 1954. Kr. 9: 50 (Institutionen för Silikatkemisk Forskning. 33.)
153. SELBERG, ARNE, *Norska erfaringer fra bygging av små hengebroer.* 20 s. 1954. Kr. 4: —. (Avd. Väg- och Vattenbyggnad. Byggnadsteknik. 21.)
154. GRANHOLM, HJALMAR, *Armerat trä.* 96 s. 1954. Kr. 9: — (Avd. Väg- och Vattenbyggnad. Byggnadsteknik. 22).
155. WILHELMSSON, HANS, *The interaction between an obliquely incident plane electromagnetic wave and an electron beam. I.* 31 s. 1954. Kr. 7: —. (Avd. Elektroteknik. 42.)
156. OLVING, SVEN, *Electromagnetic wave propagation on helical conductors inbedded in dielectric medium.* 14 s. 1955. Kr. 3: —. (Avd. Elektroteknik. 43.)
157. OLVING, SVEN, *Amplification of the traveling wave tube at high beam current. I.* 11 s. 1955. Kr. 3: —. (Avd. Elektroteknik. 44.)
158. HEDVALL, J. A., NORDENGREN, SVEN, UND LILJEGREN, B., *Über die thermische Zersetzung von Kalziumsulfat bei niedrigen Temperaturen.* 18 s. 1955. Kr. 5: — (Institutionen för Silikatkemisk Forskning. 34.)
159. DAHLGREN, SVEN-ERIC, *On the break-down of thixotropic materials.* 18 s. 1955. Kr. 3: 50. (Institutionen för Silikatkemisk Forskning. 35.)
160. SANDFORD, FOLKE, OCH LILJEGREN, BERNE, *Torkningen av råtegel och dennas inverkan på teglets frostbeständighet.* 22 s. 1955. Kr. 3: —. (Institutionen för Silikatkemisk Forskning. 36.)
161. WALLMAN, HENRY, *Automatic noise-factor meter.* 17 s. 1955. Kr. 3: —. (Avd. Elektroteknik. 45.)
162. SANDFORD, FOLKE, AND FRANSSON, STIG *The refractoriness of some types of quartz and quartzite. II.* 24 s. 1955. Kr. 5: —. (Institutionen för Silikatkemisk Forskning. 37).
163. LINDBLAD, ANDERS, *Konstruktion av linjer för moderna handelsfartyg.* 176 s. 1955. Kr. 20: —. (Avd. Skeppsbyggeri. 6.)
164. SVARTHOLM, NILS, *Two problems in the theory of the slowing down of neutrons by collisions with atomic nuclei.* 15 s. 1955. Kr. 5: —. (Avd. Allmänna Vetenskaper. 10).
165. PERSSON, PER, *Bostadsvaneundersökning utförd i hyreslägenheter byggda 1947 i Göteborg, Torpaområdet.* 86 s. 1955. Kr. 12: —. (Avd. Arkitektur. 3.)
166. HANSSON, P. R., *Undersökning av mullitbildning i keramiska produkter.* 29 s. 1955. Kr. 6: —. (Institutionen för Silikatkemisk Forskning. 38.)
167. EKELÖF, STIG, *Die Temperaturverteilung in einem gleichstromdurchflossenen langen Metallzylinder mit kreisförmigen Querschnitt.* 38 s. 1955. Kr. 10: —. (Avd. Elektroteknik. 46.)
168. WILHELMSSON, HANS, *On the reflection of electromagnetic waves from a dielectric cylinder.* 17 s. 1955. Kr. 4: 50. (Avd. Elektroteknik. 47.)
169. BJÖRK, N., AND DAVIDSON, R., *Small signal behaviour of directly heated thermistors.* 43 s. 1955. Kr. 11: —. (Avd. Elektroteknik. 48.)
170. FORESTIER, H., *Tendances actuelles dans la formation de l'ingénieur chimiste: selection, orientation, spécialisation; amélioration de son efficience.* 13 s. 1956. Kr. 2: 50. (Avd. Kemi och Kemisk Teknologi 33.)
171. WAX, NELSON, *On the ring current hypothesis.* 32 s. 1956. Kr. 7: —. (Avd. Elektroteknik. 49.)
172. ELGESKOG, ERIK, *Photoformer analysis and design.* 40 s. 1956. Kr. 8: 50. (Avd. Elektroteknik. 50.)
173. ANZELIUS, ADOLF, *Bimolekulare Reaktion von zwei in Mischung vorliegenden Substanzen mit einer dritten Substanz.* 8 s. 1956. Kr. 5 —. (Avd. Allm. Vetenskaper. 11.)
174. REINIUS, ERLING, *Model studies for the extension of the habour of Gothenburg.* 38 s. 1956. Kr. 6: —. (Avd. Väg- och Vattenbyggnad. Byggnadsteknik. 23.)
175. ZIMEN, K. E., *Diffusion von Edelgasatomen die durch Kernreaktion in festen Stoffen gebildet werden.* 7 s. 1956. Kr. 2: —. (Institutionen för Kärnkemi. 1.)
176. INTHOFF, W., UND ZIMEN, K. E., *Kinetik der Diffusion radioaktiver Edelgase aus festen Stoffen nach Bestrahlung.* 16 s. 1956. Kr. 4: —. (Institutionen för Kärnkemi. 2)
177. GRANHOLM, HJALMAR, *Puts och lättbetong.* 45 s. 1956. Kr. 3: —. (Avd. Väg- och Vattenbyggnad. Byggnadsteknik. 24)

Forts. å omsl. 3:dje sida

CHALMERS TEKNISKA HÖGSKOLAS HANDLINGAR
TRANSACTIONS OF CHALMERS UNIVERSITY OF TECHNOLOGY
GOTHENBURG, SWEDEN
Nr 238 (Avd. Maskinteknik 23) 1961

EXPERIMENTAL INVESTIGATION OF CAVITATION REGIONS IN JOURNAL BEARINGS

BY

LEIF FLOBERG

Report No. 16 from the Institute of Machine Elements
Chalmers University of Technology
Gothenburg, Sweden
1961

CHALMERS UNIVERSITY BOOKS / GUMPERTS, GÖTEBORG
AKATEEMINEN KIRJAKAUPPA / AKADEMISKA BOKHANDELN, HELSINGFORS
GYLDENDALSKE BOGHANDEL / NORDISK FORLAG, KØBENHAVN
WILLIAM HEINEMANN LTD, LONDON, MELBOURNE, TORONTO

SCANDINAVIAN UNIVERSITY BOOKS

Gyldendalske Boghandel / Nordisk Forlag, København
Svenska Bokförlaget / P. A. Norstedt & Söner — Albert Bonnier, Stockholm
Akademiförlaget / Gumperts, Göteborg
Akateeminen Kirjakauppa / Akademiska Bokhandeln, Helsingfors
William Heinemann Ltd, London, Melbourne, Toronto

Manuscript received by the Publications Committee,
Chalmers University of Technology, Nov. 1st, 1960

GÖTEBORG 1961
ELANDERS BOKTRYCKERI AKTIEBOLAG

Preface

Since 1955 lubrication research has been carried out at the Institute of Machine Elements, Chalmers University of Technology, Göteborg, Sweden, under the leadership of the head of the Institute, Professor B. JAKOBSSON. Theoretical and experimental investigations have been made to study hydrodynamic lubrication and cavitation in journal bearings and rolling contacts. Eleven reports have been published earlier, (4)—(10) and (13)—(16).

Here an experimental investigation is made to show cavitation regions in transparent bearings. The classical case of the grooveless journal bearing with oil at the bearing sides and the bearing with an axial oil groove 90° before the load are studied.

I wish to express my sincere thanks to the Swedish Technical Research Council for their kind sponsorship.

Leif Floberg
Tekn. lic.

Contents

Preface 3

1. Introduction 5

2. Notation 9

3. Theory of Hydrodynamic Lubrication and Cavitation 11

4. Test Apparatus 13

5. Test Results 14

5,1. Journal Bearing without Oil Grooves 14

5,2. Journal Bearing with an Oil Groove 90° before the Load 20

6. Conclusion 26

7. References 27

1. Introduction

Since REYNOLDS (19) 1886 gave the basic equation for hydrodynamic lubrication the cavitation problem has been discussed in literature; but not until recent years does this problem seem to have been solved. REYNOLDS' equation itself is difficult to solve and the boundary conditions are even more difficult.

SOMMERFELD (21) mentions the problem in his work of 1904 when he discusses the validity of his theory. He writes: "Sehr bedenklich muss für die Stickhaltichkeit unserer Theorie das Auftreten negativen Druckes erscheinen. Eine Flüssigkeit kann keinen nennenswerten negativen Druck (d. h. Zug) ertragen; sie würde unter dessen Einfluss zerreissen. Wenn wir nun auch annehmen wollen, dass der mittlere Druck p_0, der bei uns unbestimmt blieb, für jeden bestimmten Querschnitt des Lagers einen gewissen positiven Wert besitzt (wobei derselbe übrigens von Querschnitt zu Querschnitt veränderlich sein wird), so gibt es nach Fig. 15 jedenfalls eine untere Grenze für die Geschwindigkeit, nach deren Unterschreitung der variable Bestandteil p_1 des Druckes in der Nähe der Stelle N den positiven Druck p_0 im negativen Sinne überwiegen würde. Unsere Theorie reicht dann nur bis an diese untere Geschwindigkeitsgrenze heran, nicht bis über dieselbe hinaus. Zerreisst nämlich die Ölschicht an der Stelle beginnenden negativen Druckes, so werden die Voraussetzungen hinfällig, aus denen wir die Gleichgewichtslage des Zapfens, die Grösse des Reibungsmomentes usw. früher bestimmten." SOMMERFELD thus gives a very clear limitation of his theory considering the appearance of negative pressures which cause film rupture. Authors often criticize SOMMERFELD's theory and results without noticing the limitation, cited above.

GÜMBEL (12) showed in 1925 experimentally that negative pressures do not appear in a journal bearing and that the tests appear to be in favour of the boundary condition of zero pressure and zero pressure derivative at the end of the pressure build-up.

In 1932 an experimental investigation was made by NÜCKER (17) to study the pressure build-up in a journal bearing. His tests show

small negative pressures in the unloaded half. However, most of the interest is paid to the loaded half and very few pressure measurements are made in the unloaded half of the bearing.

VOGELPOHL (22) studied the cavitation problem in 1937. He showed that there were gases dissolved in the oil, which were released when the oil was submitted to tensile forces. VOGELPOHL also shows photographs of cavitation regions. He makes no theoretical treatise of the behaviour of the oil in connection with cavitation; but assumes that the film will start at the maximum space and break at the minimum space.

FRÄNKEL (11) treats the journal bearing in a work of 1944. He writes: "Für endlich breite Lager lassen sich die negativen Drücke, wie sie die Rechnung fordert, nicht erzielen, weil Luft eintritt und das Öl verdampft, wodurch das Ölband zerreisst. Deshalb ist die gesperrt angeführte SOMMERFELD'sche Voraussetzung nicht erfüllt und damit fallen seine Folgerungen dahin. Da SOMMERFELD seine Berechnungen unter Berücksichtigung dieser negativen Drücke durchführte, hat er Ergebnisse erhalten, welche mit der Wirklichkeit nicht übereinstimmten (z. B. horizontale Verlagerungskurve des Wellenmittelpunktes), und deshalb wenig beachtet wurden." As oil has air or gases dissolved in it, the oil will cavitate not vaporize. FRÄNKEL has not understood SOMMERFELD's solution when he thinks that it needs negative pressures, and he has not noticed SOMMERFELD's limiting criterion for the validity of the theory. FRÄNKEL writes that SOMMERFELD's solution is not true. However, it is theoretically possible to get the full SOMMERFELD conditions for an infinitely wide journal bearing with an oil groove at the lowest pressure, which also was shown experimentally in ref. (4). As the behaviour of the oil is so different in a bearing of finite width compared to an infinitely wide bearing, it is suitable to differentiate those two cases from one another. FRÄNKEL writes further: "Gümbel hat bekanntlich als Randbedingungen $p=0$ für $\varphi=0$ (also im weitesten Spaltquerschnitt) und $p=0$ für die Stelle, wo $\frac{dp}{d\varphi}=0$, angenommen. Seine Überlegung erscheint zwar physikalisch nicht unbedingt zwingend, da nicht einzusehen ist, warum der Druck mit stetiger Tangente in den drucklosen Teil übergehen sollte, wenn es sich um ein plötzliches Abreissen des Ölfilms handelt." The condition of zero pressure derivative at the end of the pressure build-up is the only condition which satisfies the continuity of flow, if there are no pressures lower than the cavitation pressure.

FRÄNKEL thinks that the film break is so sudden that the pressure derivative should not be zero. However, the gases are continuously expelled from the oil until a cavitation pressure of about atmospheric is reached and the gas is not rotating with the shaft; but it collects in bubbles at the sides passed by streamlets of oil. FRÄNKEL assumes in his calculations that the film starts at the maximum space and ends at the minimum space.

CAMERON and WOOD (1), made a calculation in 1949 on the full journal bearing of finite width assuming film start at maximum space and with zero pressure derivative at the film break. They assume a full oil film in the cavitated part of the bearing when calculating the power loss.

In 1956 COLE and HUGHES (2) showed photos of oil strips in a cavitation region. However, they use an oil hole for the lubricant supply, which case has not been treated hitherto in theory and therefore a comparison between theory and test cannot be made; but the photos give a good view of the behaviour of the oil in a cavitation region.

DOWSON (3) has in 1957 studied cavitation between a lens and a plane surface. He shows photos of the bubbles and gives measured pressure fields and finds that cavitation does not start where the pressure derivative is zero but further on downstream. At very low loads it is possible to do experiments for the full SOMMERFELD case with positive pressure in the convergent part and negative pressure in the divergent part of the bearing, if the negative pressure does not reach that level where cavitation starts. As the cavitation pressure is some hundredths of an atm this case represents very low loads and is very far from practical bearings. Before a cavitation zone there is a slope of negative pressures lower than the cavitation pressure. This slope will influence the shape of the pressure curve in cases close to the full SOMMERFELD condition and with low loads; but when the slope pressure is small compared with the maximum pressure the influence is fully negligible. That was shown experimentally in ref. (9), where the oil film between a transparent plate and a rotating cylinder was studied. At higher speeds, which give higher loads, the agreement is quite good; but at lower speeds the slope will influence and cause commencement of cavitation further on downstream. This behaviour is also shown by DOWSON's own experiments. His highest loaded test gives the best agreement with theory; but even there the

load is very low and if he had gone further on, the agreement would have been still better.

RAIMONDI and BOYD (18) published in 1958 tables and charts of journal bearing quantities based on zero pressure derivative at the end of the pressure build-up. They assume a full oil film in the cavitation region when calculating power loss, to be on the safe side.

In 1957 the continuity condition at the downstream boundary of a cavitation region was given by JAKOBSSON-FLOBERG (13). This condition makes it possible to determine the location of the cavitation region in a bearing under given conditions at the bearing boundaries. When this location is known the bearing quantities can be determined.

2. Notation

b	Bearing width
c	Specific heat of oil
D	Bearing diameter
d	Journal diameter
Δd	Diametral clearance
e	Eccentricity
g	Acceleration due to gravity
H	Height of oil column
h	Oil film thickness
n	Rotational speed
P	Load capacity per unit width
P_{tot}	Total load
$P_0 = \frac{P \psi^2}{\eta U}$	Non-dimensional load capacity per unit width
p	Oil film pressure
$p_0 = \frac{p \psi^2}{\eta \omega}$	Non-dimensional oil film pressure
p_c	Cavitation pressure
$p_{c0} = \frac{p_c \psi^2}{\eta \omega}$	Non-dimensional cavitation pressure
r	Journal radius
Δr	Radial clearance
t	Temperature
U	Surface velocity
x, z	Coordinates
β	Angle between load line and minimum space
$\varepsilon = \frac{e}{\Delta r}$	Relative eccentricity

η	Absolute viscosity
$\nu = \frac{b}{d}$	Width-diameter ratio
ϱ	Density of oil
φ_2	Angle between minimum space and film rupture
$\psi = \frac{\Delta r}{r} = \frac{\Delta d}{d}$	Relative clearance
ω	Angular speed

3. Theory of Hydrodynamic Lubrication and Cavitation

The pressure build-up in the full oil film is determined by REYNOLDS' equation

$$\frac{\partial}{\partial x}\left(h^3 \frac{\partial p}{\partial x}\right) + \frac{\partial}{\partial z}\left(h^3 \frac{\partial p}{\partial z}\right) = 6\,\eta\, U \frac{\partial h}{\partial x}$$

In a cavitation region the pressure is constant and approximately equal to that pressure where the oil is in contact with air or gases. The oil within the region will divide into streamlets.

The continuity condition at the upstream boundary of a cavitation region is

$$\frac{\partial p}{\partial x} = 0$$

The continuity condition at the downstream boundary of the region is, see fig. 11.1

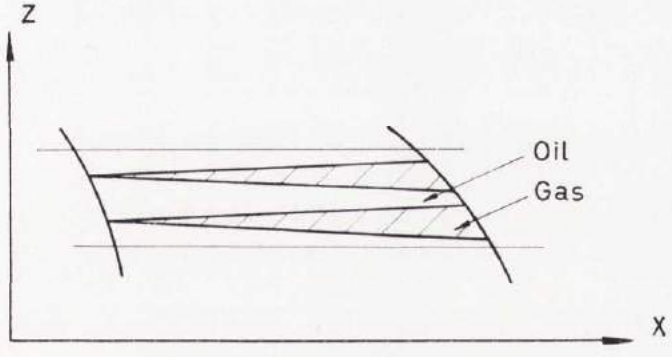

Fig. 11.1

$$\frac{Uh_1}{2} = \frac{Uh_2}{2} - \frac{h_2^3}{12\eta}\left[\frac{\partial p}{\partial x} - \frac{\partial p}{\partial z}\cdot\frac{dx}{dz}\right]$$

where h_1=oil film thickness at the upstream boundary

h_2=oil film thickness at the downstream boundary

In the cavitation region there is only oil flow in the x-direction. The continuity conditions were treated more in detail in ref. (13).

4. Test Apparatus

The test bearings are made from transparent material. The shaft is made of steel and it is mounted in two bearings. The shaft is driven by a motor via a variator and a universal joint shaft.

The tests are made to get photos of the cavitation regions and to compare the theoretical and experimental boundaries of them. To give good photos of the behaviour of the oil at cavitation the transparent bearing ought to be thin in order not to give light refraction. However, a thin plastic bearing will deform, so that it is then not possible to carry out correct measurements of the boundary locations. For boundary location measurements the bearing ought to be thick. Because of this every test is made with two different bearings, a thin bearing with a wall thickness of about 4 mm for the photos and a thicker bearing of about 14 mm for the measurements of the locations of the regions. A photo of the test rig is given in fig. 13.1.

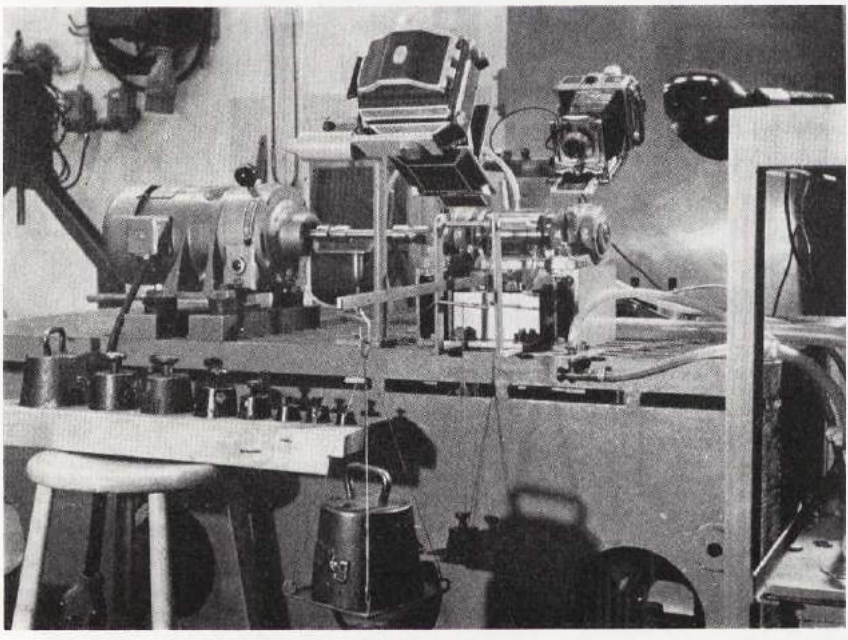

Fig. 13.1. Photo of the Test Rig

5. Test Results

5,1. Journal Bearing without Oil Grooves

In this case the bearing was submerged in oil which means two peripheral grooves filled with oil at the bearing sides. The bearing surface had no grooves. This case corresponds to that treated in ref. (13), chap. 5. The oil is sucked into the bearing where the pressure is lower than the side pressure, and there is oil flow out from the bearing where the pressure is higher than the oil pressure at the bearing sides. The bearing operates quite well if there is a difference large enough between the side pressure and the cavitation pressure. In practice, however, it is difficult to guarantee this difference, why it is safer to use one or more grooves for the oil supply.

In the test apparatus the pressure was measured at the bearing side and in the cavitation region with oil manometers. Due to the air volume in the manometer, the cavitation pressure was at once very close to atmospheric and remained at that value during the test. The groove pressure could thus easily be put to that value giving the desired pressure difference.

The bearing load was applied from beneath to give cavitation in the upper part of the bearing.

The torque from the side seals was balanced by a couple in order to give a correct loading.

The load number is

$$P_0 = \frac{P \psi^2}{\eta U}$$

from which the desired speed under certain given conditions is

$$\omega = \frac{P_{tot} \psi^2}{b P_0 \eta r}$$

The non-dimensional group for the pressure is

$$p_0 = \frac{p\,\psi^2}{\eta\,\omega}$$

and the pressure measured by an oil manometer is

$$p = H \varrho\, g$$

where H=height of the oil column

ϱ=density of the oil

g=acceleration due to gravity

Thus

$$H = \frac{p_0\,\eta\,\omega}{\psi^2\,\varrho\,g} = \frac{p_0\,P_{tot}}{b\,P_0\,r\varrho\,g}$$

Tests were made at the eccentricities $\varepsilon = 0{,}4$ and $0{,}6$ with a non-dimensional cavitation pressure of $p_{co} = -0{,}1$. The eccentricities were not measured, but the theoretical load corresponding to a certain eccentricity was applied.

Data of the thin test bearing:

Diameter of the shaft $d = 50{,}992$ mm

Diameter of the bearing $D = 51{,}390$ mm

Diametral clearance $\Delta d = 398\ \mu$m

Relative clearance $\psi = \frac{\Delta d}{d} = 7{,}80\ ^0/_{00}$

Bearing width $b = 51{,}0$ mm

Mobil Vactra Oil Heavy was used. The density of the oil was $\varrho = 910$ kg/m³.

Data of the tests with the thin bearing are given in tab. 18.1 and the photos of the cavitation regions are shown in figs. 16.1, 16.2, 17.1 and 17.2.

Data of the thick test bearing:

Diameter of the shaft $d = 50{,}992$ mm

Diameter of the bearing $D = 51{,}156$ mm

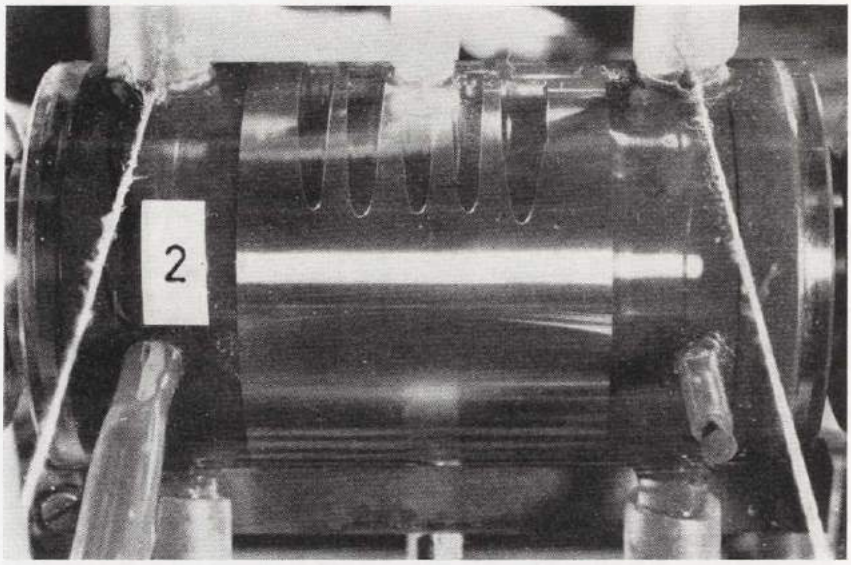

Fig. 16.1. Upstream Part of the Cavitation Region
($v=1$, $\varepsilon=0,4$ and $p_{c0}=-0,1$)

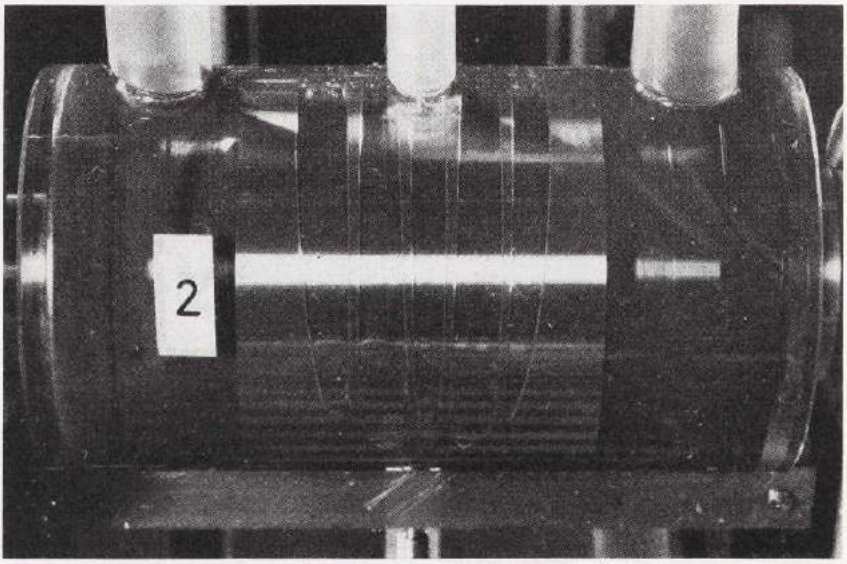

Fig. 16.2. Downstream Part of the Cavitation Region
($v=1$, $\varepsilon=0,4$ and $p_{c0}=-0,1$)

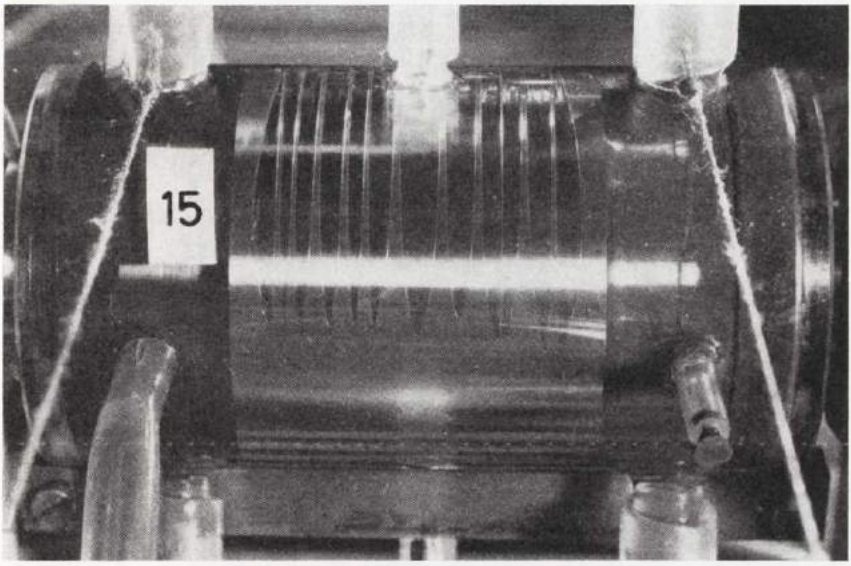

Fig. 17.1. Upstream Part of the Cavitation Region
($v=1$, $\varepsilon=0{,}6$ and $p_{c0}=-0{,}1$)

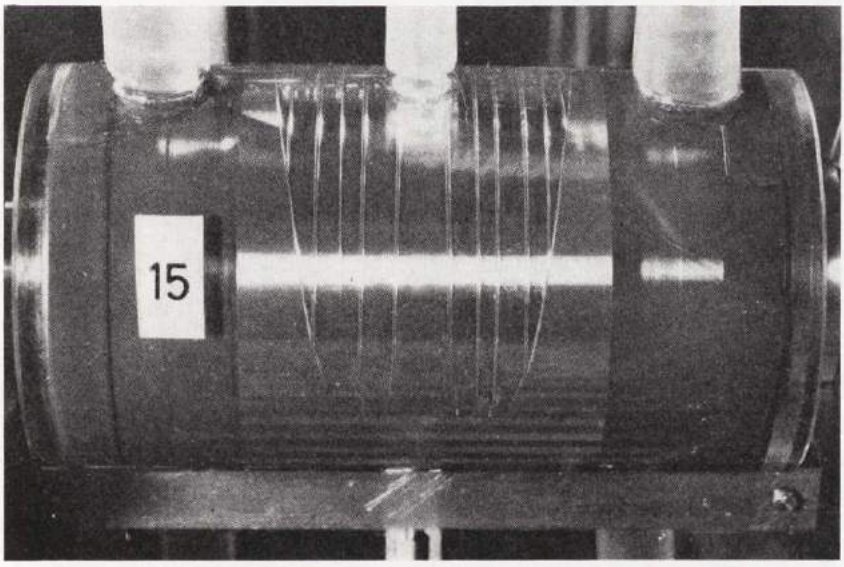

Fig. 17.2. Downstream Part of the Cavitation Region
($v=1$, $\varepsilon=0{,}6$ and $p_{c0}=-0{,}1$)

Tab. 18.1. Data of the Thin-bearing Tests

Test No		2	15
ε		0,4	0,6
P_0		0,960	2,26
P_{tot}	N	196	392
t	°C	34	32
η	Ns/m²	0,095	0,108
ω	1/s	101	75,1
H	m	1,76	1,49

Diametral clearance $\Delta d = 164\ \mu$m

Relative clearance $\psi = \frac{\Delta d}{d} = 3,22\ ^0/_{00}$

Bearing width $b = 51,0$ mm

Mobil Vactra Oil Light was used. The density of the oil was $\varrho = 900$ kg/m³.

Tab. 18.2. Data of the Thick-bearing Tests

Test No		111	112
ε		0,4	0,6
P_0		0,960	2,26
P_{tot}	N	392	687
t	°C	31	28
η	Ns/m²	0,040	0,046
ω	1/s	81,6	52,9
H	m	3,52	2,62

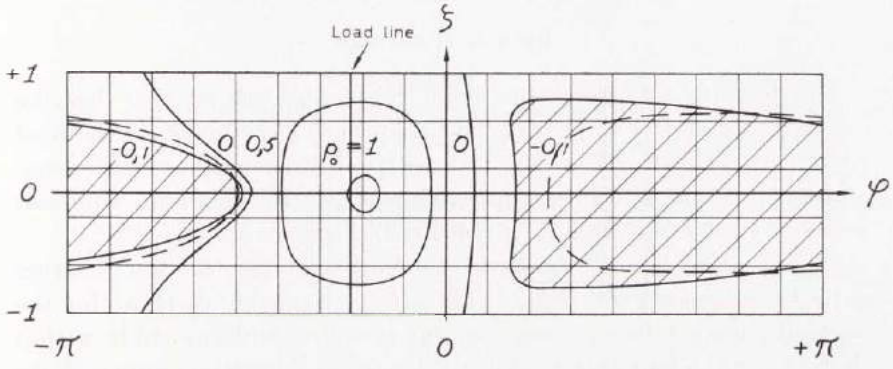

Fig. 19.1. Theoretical Cavitation Region for
$\nu=1$, $\varepsilon=0{,}4$ and $p_{co}=-0{,}1$
The dotted line represents the experimental boundary

Data of the tests with the thick bearing are given in table 18.2 and comparisons between the theoretical and experimental boundaries of the cavitation region are given in the figs. 19.1 and 19.2. The agreement between theory and test is quite satisfactory.

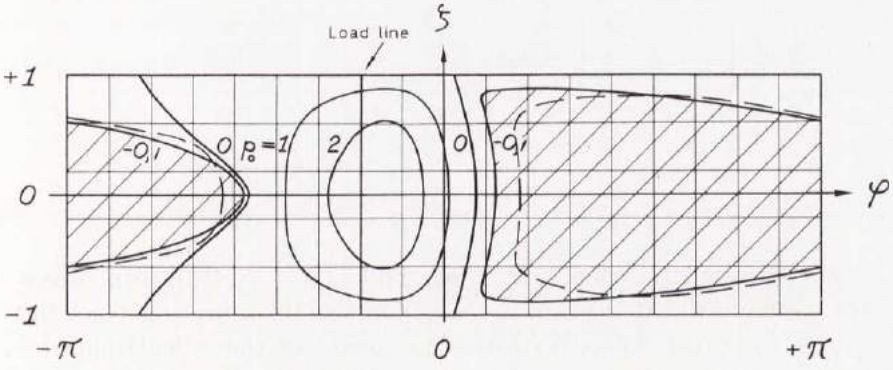

Fig. 19.2. Theoretical Cavitation Region for
$\nu=1$, $\varepsilon=0{,}6$ and $p_{co}=-0{,}1$
The dotted line represents the experimental boundary

5,2. Journal Bearing with an Oil Groove 90° before the Load

The test rig was the same as in chap. 5,1; but another bearing case was studied. The bearing had an oil groove 90° before the load which, in the tests, was supplied with oil at atmospheric pressure, and the pressure at the bearing sides was also atmospheric. This case corresponds to that treated in ref. (13), chap. 9.

The pressure build-up and the load capacity for the 360° bearing with an oil groove 90° before the load are the same as those for the centrally loaded half-bearing, if the pressure build-up ends within that bearing. The latter case has been treated by SASSENFELD-WALTHER (20) and RAIMONDI-BOYD (18), whose values are given in the following tables, where $(\varphi_2+\beta)$ is the angle between the load and the start of film rupture, which is approximated to a straight line.

Values by Sassenfeld-Walther

ε	0,4	0,5	0,6	0,7	0,8
P_0	1,14	1,67	2,47	3,90	6,89
$(\varphi_2+\beta)$	82	76	69	61	51

Values by Raimondi-Boyd

ε	0,4	0,6	0,8
P_0	1,15	2,49	6,87
$(\varphi_2+\beta)$	80,8	66,8	48,5

The agreement is thus very good. The values by RAIMONDI-BOYD are used for the thin-bearing tests. For the thick-bearing tests the values by SASSENFELD-WALTHER are used, as the calculations by RAIMONDI-BOYD do not contain the eccentricities 0,5 and 0,7.

In the tests the pressure was measured in the groove and in the cavitation region with oil manometers and it was held to atmospheric.

Tab. 21.1. Data of the Thin-bearing Tests

Test No		18	23
ε		0,4	0,6
P_0		1,15	2,49
P_{tot}	N	245	441
t	°C	32	33
η	Ns/m²	0,108	0,101
ω	1/s	90,2	80,1

Data of the thin test bearing:

Shaft diameter $d=50{,}992$ mm

Bearing diameter $D=51{,}385$ mm

Diametral clearance $\Delta d=393\ \mu$m

Relative clearance $\psi=\frac{\Delta d}{d}=7{,}71\ ‰$

Bearing width $b=51{,}0$ mm

Mobil Vactra Oil Heavy was used. The density of the oil was $\varrho=910$ kg/m³.

Data of the tests with the thin bearing are given in tab. 21.1 and photos of the cavitation regions are shown in figs. 22.1, 22.2, 23.1 and 23.2.

Data of the thick test bearing:

Shaft diameter $d=50{,}992$ mm

Bearing diameter $D=51{,}156$ mm

Diametral clearance $\Delta d=164\ \mu$m

Relative clearance $\psi=3{,}22\ ‰$

Bearing width $b=51{,}0$ mm

Mobil Vactra Oil Light was used. The density of the oil was $\varrho=900$ kg/m³.

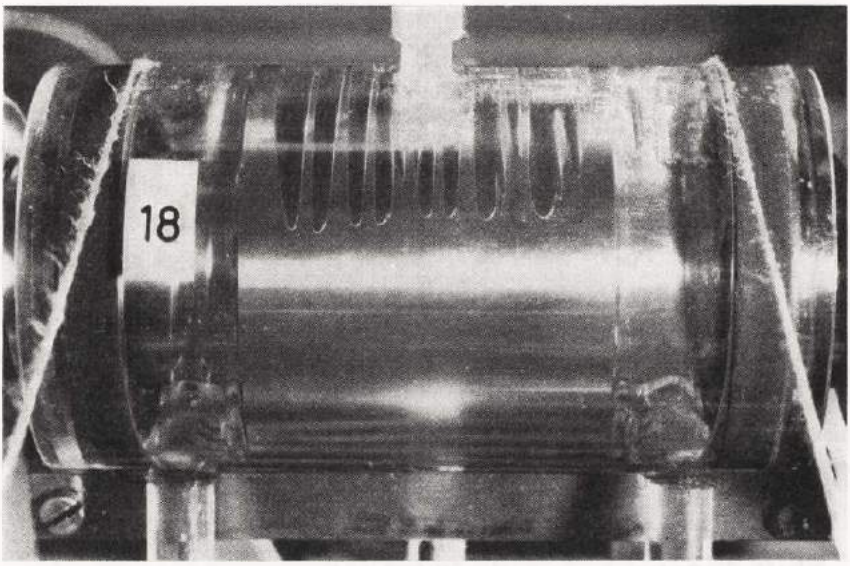

Fig. 22.1. Upstream Part of the Cavitation Region
($\nu=1$ and $\varepsilon=0,4$)

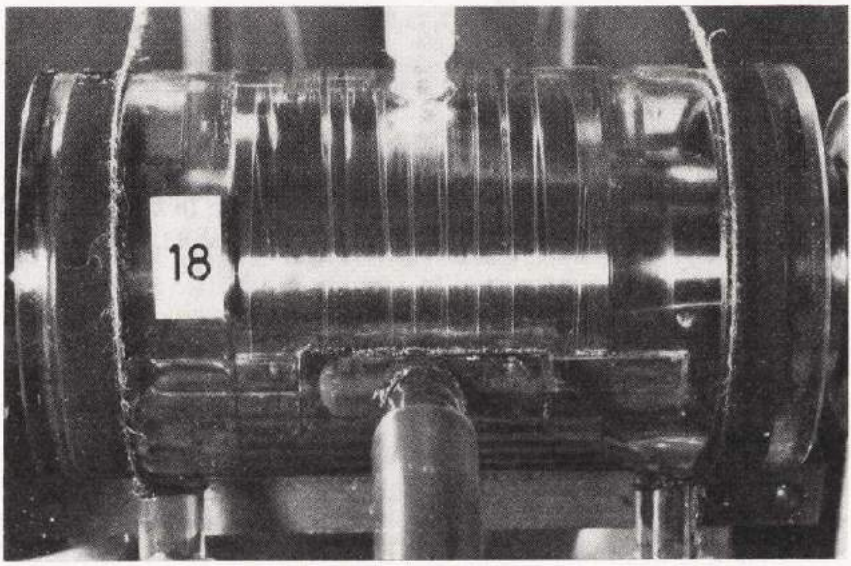

Fig. 22.2. Downstream Part of the Cavitation Region
($\nu=1$ and $\varepsilon=0,4$)

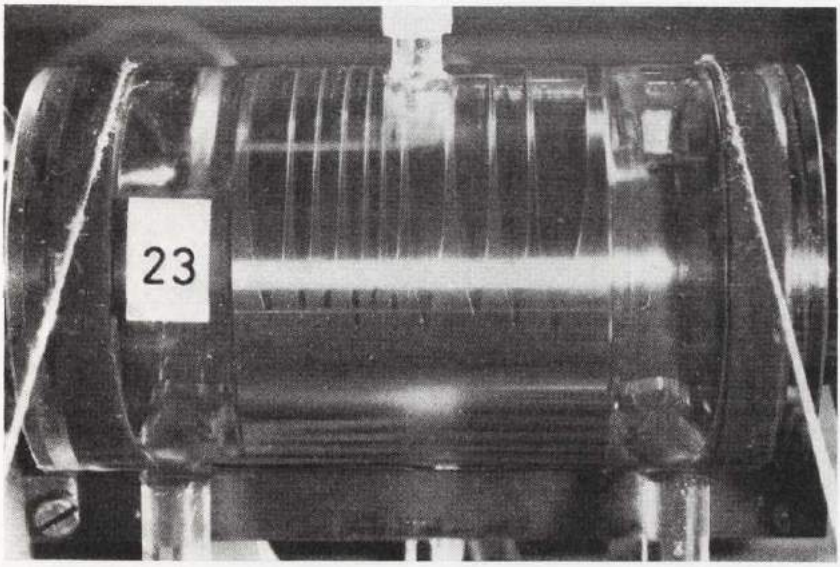

Fig. 23.1. Upstream Part of the Cavitation Region
($\nu=1$ and $\varepsilon=0,6$)

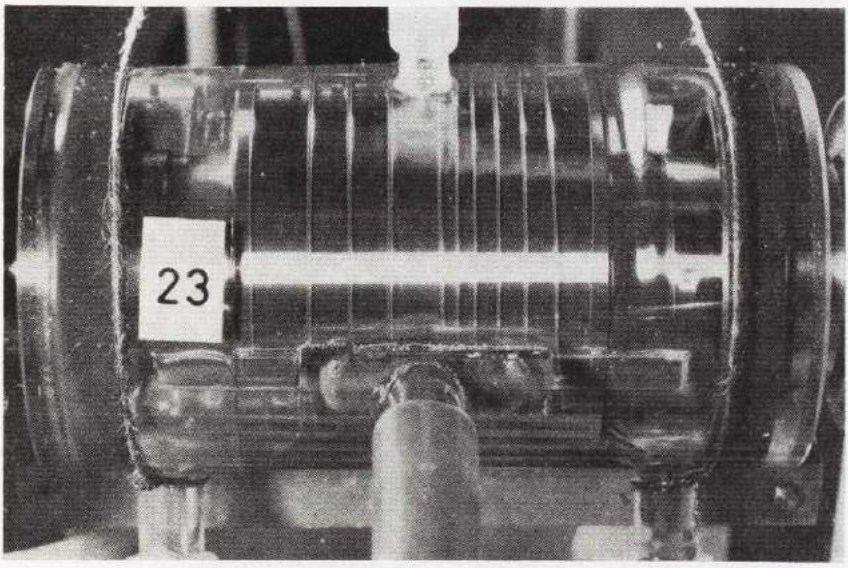

Fig. 23.2. Downstream Part of the Cavitation Region
($\nu=1$ and $\varepsilon=0,6$)

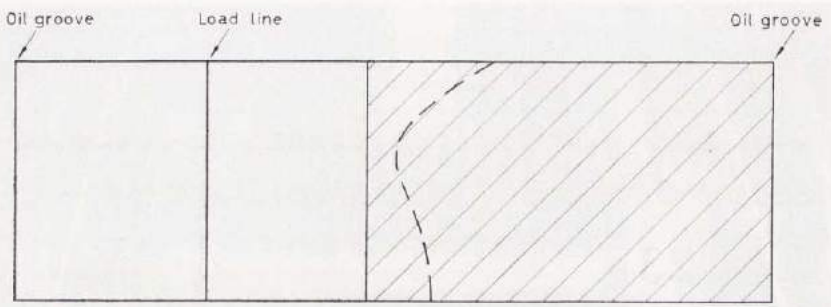

Fig. 24.1. Theoretical Cavitation Region for
$\nu = 1$ and $\varepsilon = 0{,}5$
The dotted line represents the experimental boundary

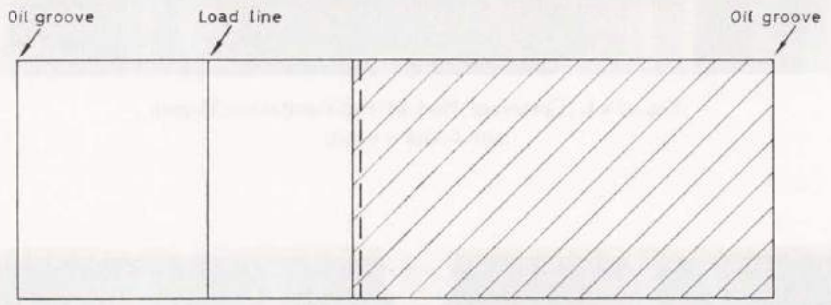

Fig. 24.2. Theoretical Cavitation Region for
$\nu = 1$ and $\varepsilon = 0{,}6$
The dotted line represents the experimental boundary

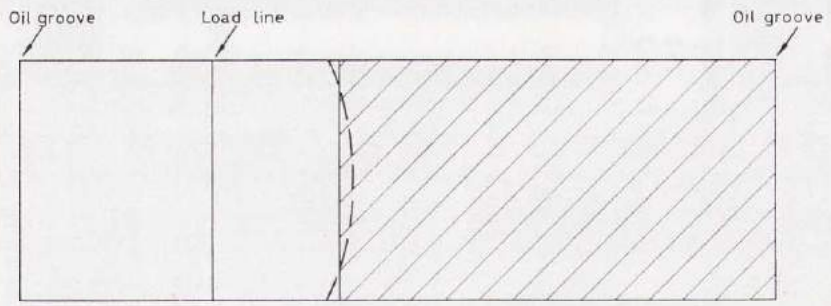

Fig. 24.3. Theoretical Cavitation Region for
$\nu = 1$ and $\varepsilon = 0{,}7$
The dotted line represents the experimental boundary

Tab. 25.1. Data of the Thick-bearing Tests

Test No		103	101	104
ε		0,5	0,6	0,7
P_0		1,67	2,47	3,90
P_{tot}	N	540	736	1180
t	°C	30	29	29
η	Ns/m²	0,042	0,044	0,044
ω	1/s	61,3	54,0	54,7

Data of the tests with the thick bearing are given in tab. 25.1 and comparisons between the theoretical and experimental areas of the cavitation regions are given in figs. 24.1, 24.2, and 24.3. The eccentricities are $\varepsilon = 0,5$; 0,6 and 0,7. The figs. 24.2 and 24.3 show a very good agreement between theory and tests. In the test, fig. 24.1, the bearing was vibrating and the result is not fully satisfactory.

In theory the cavitation boundary is approximated to a straight line. A correct calculation gives a curved boundary, when the agreement between theory and tests may be even better.

6. Conclusion

This report represents an experimental investigation of the behaviour of the oil in a cavitation region. Photos show how the oil flows in streamlets through the region. Comparisons between theory and tests are made and the agreement is satisfactory. Bearings without and with oil grooves are tested.

Boundary conditions of cavitation regions are discussed and the experiments show that a theory assuming a constant cavitation pressure zone with the continuity of flow satisfied all around the boundary is quite satisfactory. The continuity conditions of a cavitation region say that the pressure derivative should be zero at the upstream boundary and that the oil flow entering the region at the upstream boundary must leave at the downstream boundary.

In fig. 16.1 the strips are rounded at the upstream boundary of the cavitation region. This is due to a slope of subcavity pressures upstream from that boundary, which will exert influence at low loads. The average oil film pressure was here 0,8 atm g. In fig. 17.1 the average pressure is 1,6 atm g and the strips are here sharper. For practical bearings the influence of the subcavity pressure slope is fully negligible, which is shown by the very good agreement between theory and tests. The number of streamlets will not influence the results. However, it was shown in ref. (9) that higher speed and smaller clearance give a larger number of strips.

7. References

1. Cameron, A. and Wood, W. L.: The Full Journal Bearing. Proc. Instn Mech. Engrs, vol. 161, p. 59, 1949.
2. Cole, J. A. and Hughes, C. J.: Oil Flow and Film Extent in Complete Journal Bearings. Proc. Instn Mech. Engrs, vol. 170, p. 499, 1956.
3. Dowson, D.: Investigation of Cavitation in Lubricating Films Supporting Small Loads. Proceedings of The Conference on Lubrication and Wear, held by The Institution of Mechanical Engineers in London, 1957.
4. Floberg, L.: The Infinite Journal Bearing, Considering Vaporization. Göteborg, 1957.
5. Floberg, L.: Experimental Investigation of Power Loss in Journal Bearings, Considering Cavitation. Göteborg, 1959.
6. Floberg, L.: Lubrication of a Rotating Cylinder on a Plane Surface, Considering Cavitation. Göteborg, 1959.
7. Floberg, L.: The Optimum Thrust Tilting-pad Bearing. Göteborg, 1960.
8. Floberg, L.: The Two-groove Journal Bearing, Considering Cavitation. Göteborg, 1960.
9. Floberg, L.: Lubrication of Two Cylindical Surfaces, Considering Cavitation. Göteborg, 1961.
10. Floberg, L.: Attitude-Eccentricity Curves and Stability Conditions of the Infinite Journal Bearing. Göteborg, 1961.
11. Fränkel, A.: Berechnung von zylindrischen Gleitlagern. Zürich und Leipzig, 1944.
12. Gümbel, L. and Everling, E.: Reibung und Schmierung im Maschinenbau. Berlin, 1925.
13. Jakobsson, B. and Floberg, L.: The Finite Journal Bearing, Considering Vaporization. Göteborg, 1957.
14. Jakobsson, B. and Floberg, L.: The Partial Journal Bearing. Göteborg, 1958.
15. Jakobsson, B. and Floberg, L.: The Rectangular Plane Pad Bearing. Göteborg, 1958.
16. Jakobsson, B. and Floberg, L.: The Centrally Loaded Partial Journal Bearing. Göteborg, 1959.
17. Nücker, W.: Über den Schmiervorgang im Gleitlager. VDI-Forschungsheft 352, 1932.
18. Raimondi, A. A. and Boyd, J.: A Solution for the Finite Journal Bearing and its Application to Analysis and Design: III. Trans. Am. Soc. Lubr. Engrs, Vol. 1, No. 1, 1958.
19. Reynolds, O.: On the Theory of Lubrication and its Application to Mr. Beauchamp Tower's Experiments, including an Experimental Determination of the Viscosity of Olive Oil. Phil. Trans. Roy. Soc., vol. 177, p. 157, 1886.

20. Sassenfeld, H. and Walther, A.: Gleitlagerberechnungen. VDI-Forschungsheft 441, 1954.
21. Sommerfeld, A.: Zur hydrodynamischen Theorie der Schmiermittelreibung. Z. Math. Phys. vol. 50, p. 97, 1904.
22. Vogelpohl, G.: Beiträge zur Kenntnis der Gleitlagerreibung. VDI-Forschungsheft 386, 1937.

Forts. fr. omsl. 2:dra sida

178. Olving, Sven, *A new method for space charge wave interaction studies. I.* 12 s. 1956. Kr. 3: —. (Avd. Elektroteknik. 51.)
179. Hansbo, Sven, *The critical load of rectangular frames analysed by convergence methods.* 47 s. 1956. Kr. 11: —. (Avd. Väg- och Vattenbyggnad. Byggnadsteknik. 25.)
180. Westberg, Vidor, *Measurements of noise radiation at 10 cm from glow lamps. Preliminary report.* 14 s. 1956. Kr. 4: 50. (Avd. Elektroteknik. 52).
181. Svensson, S. I., Hellgren, G., and Perers, O., *The Swedish radioscientific solar eclipse expedition to Italy, 1952. Preliminary report.* 30 s. 1956. Kr. 8: —. (Avd. Elektroteknik. 53.)
182. Wax, Nelson, *A note on design considerations for a proposed auroral radar.* 16 s. 1957. Kr. 3: —. (Avd. Elektroteknik. 54.)
183. Joshi, G. H., *The electromagnetic interaction between two crossing electron streams. I.* 31 s. 1957. Kr. 8: —. (Avd. Elektroteknik. 55.)
184. Smith, Bengt, *Dry methods for removing hydrogen sulphide from gases.* 65 s. 1957. Kr. 15: —. (Avd. Kemi och Kemisk Teknologi. 34.)
185. Ekelöf, S., Björk, N., and Davidson, R., *Large signal behaviour of directly heated thermistors.* 31 s. 1957. Kr. 8: —. (Avd. Elektroteknik. 56.)
186. Carlsson, Bengt, und Larsson, Hans, *Wirkungsgrad und Selbsthemmung einfacher Umlaufgetriebe.* 48 s. 1957. Kr. 9: —. (Avd. Maskinteknik. 8.)
187. Aurell, Carl G., *The equivalent transmission line of a linear four-terminal network. Calculations with cascade-connected four-terminal networks.* 39. s. 1957. Kr. 6: —. (Avd. Elektroteknik. 57.)
188. Lundholm, R., *Induced overvoltage-surges on transmission lines and their bearing on the lightning performance at medium voltage networks.* 117 s. 1957. Kr. 19: —. (Avd. Elektroteknik. 58.)
189. Floberg, Leif, *The infinite journal bearing, considering vaporization.* 83 s. 1957. Kr. 13: —. (Avd. Maskinteknik. 9.)
190. Jakobsson, Bengt, and Floberg, Leif, *The finite journal bearing, considering vaporization.* 117 s. 1957. Kr. 19: 50. (Avd. Maskinteknik. 10.)
191. Chako, Nicholas, *Characteristic curves on planes in the image space.* 49 s. 1957. Kr. 15: —. (Avd. Allmänna Vetenskaper. 12.)
192. Ekelöf, Stig, *The development and decay of the magnetic flux in a non-delayed telephone relay.* 50 s. 1957. Kr. 15: —. (Avd. Elektroteknik. 59.)
193. Björklund, Kjell, *Bestämning av porslins draghållfasthet.* 78 s. 1958. Kr. 15: —. (Institutionen för Silikatkemisk Forskning. 39.)
194. Granholm, Per, *Sound insulation of single leaf walls.* 48 s. 1958. Kr. 8:—. (Avd. Väg- och Vattenbyggnad. Byggnadsteknik. 26.)
195. Granholm, Hjalmar, *Om vattengenomslag i murade väggar med särskild hänsyn till tegel som fasadmaterial.* 172 s. 1958. Kr. 16: —. (Avd. Väg- och Vattenbyggnad. Byggnadsteknik. 27.)
196. Meos, Johan, and Olving, Sven, *On the origin of radar echoes associated with auroral activity.* 20 s. 1958. Kr. 5: —. (Avd. Elektroteknik. 60.)
197. Joshi, G. H., *The electromagnetic interaction between two crossing electron streams. II.* 10 s. 1958. Kr. 3: 50. (Avd. Elektroteknik. 61.)
198. Wilhelmsson, Hans, *The interaction between an obliquely incident plane electromagnetic wave and an electron beam. II.* 32 s. 1958. Kr. 7: —. (Avd. Elektroteknik. 62.)
199. Kärrholm, Gunnar, *A method of iteration applied to beams resting on springs.* 50 s. 1958. Kr. 12: —. (Avd. Allm. Vetenskaper. 13.)
200. Jakobsson, Bengt, and Floberg, Leif, *The partial journal bearing.* 60 s. 1958. Kr. 14: —. (Avd. Maskinteknik. 11.)
201. Kärrholm, Gunnar, *Influence functions of elastic plates divided in strips.* 18 s. 1958. Kr. 4: 50. (Avd. Väg- och Vattenbyggnad. Byggnadsteknik. 28.)
202. Råde, Lennart, *Sampling plans for acceptance sampling by variables using the range.* 34 s. 1958. Kr. 9: 50. (Avd. Allm. Vetenskaper. 14.)
203. Jakobsson, Bengt, and Floberg, Leif, *The rectangular plane pad bearing.* 44 s. 1958. Kr. 5: —. (Avd. Maskinteknik. 12.)
204. Asplund, Sven Olof, *Column-beams and suspension bridges analysed by »Green's matrix».* 36 s. 1958. Kr. 7: —. (Avd. Väg- och Vattenbyggnad. Byggnadsteknik. 29.)
205. Wilhelmsson, Hans, *On the properties of the electron beam in the presence of an axial magnetic field of abitrary strength.* 32 s. 1958. Kr. 7: 50. (Avd. Elektroteknik. 63.)
206. Wilhelmsson, Hans, *The interaction between an obliquely incident plane electromagnetic wave and an electron beam. III.* 17 s. 1958. Kr. 5: —. (Avd. Elektroteknik. 64.)
207. Hedvall, Arvid J., *On the influence of pre-treatment and transition processes on the adsorption capacity and the reactivity of various types of glass and silica.* 39 s. 1959. Kr. 8: —. (Institutionen för Silikatkemisk Forskning. 40.)

Forts. å omsl. 4:de sida

Forts. fr. omsl. 3:dje sida

208. KÄRRHOLM, GUNNAR, *A flow problem solved by strip method.* 22 s. 1959. Kr. 4: 50. (Avd. Allm. Vetenskaper. 15.)
209. GRANHOLM, HJALMAR, *Allmän teori för beräkning av armerad betong.* 228 s. 1959. Kr. 20: —. (Avd. Väg- och Vattenbyggnad. Byggnadsteknik. 30.)
210. LIDIN, LARS G., *On helical-springs suspension.* 75 s. 1959. Kr. 15: —. (Avd. Maskinteknik. 13.)
211. BJÖRK, NILS, *Theory of the indirectly heated thermistor.* 46 s. 1959. Kr. 10: —. (Avd. Elektroteknik. 65.)
212. CARLSSON, ORVAR, *The influence of submicroscopic pores on the resistance of bricks towards frost.* 13 s. 1959. Kr. 3: 50. (Institutionen för Silikatkemisk Forskning. 41.)
213. GRANHOLM, HJALMAR, *KAM 40, KAM 60 och KAM 90.* 41 s. 1959. Kr. 3: 50. (Avd. Väg- och Vattenbyggnad, Byggnadsteknik. 31.)
214. JAKOBSSON, BENGT, AND FLOBERG, LEIF, *The centrally loaded partial journal bearing.* 35 s. 1959. Kr. 7: 50. (Avd. Maskinteknik. 14.)
215. FLOBERG, LEIF, *Experimental investigation of power loss in journal bearings, considering cavitation.* 16 s. 1959. Kr. 3: 50. (Avd. Maskinteknik. 15).
216. FLOBERG, LEIF, *Lubrication of a rotating cylinder on a plane surface, considering cavitation.* 40 s. 1959. Kr. 8: —. (Avd. Maskinteknik. 16.)
217. TROEDSSON, CARL BIRGER, *The growth of the Western city during the Middle Ages.* 125 s. 1959. Kr. 19: —. (Avd. Arkitektur. 4.)
218. HEDVALL, J. ARVID, *The importance of the reactivity of solids in geological-mineralogical processes.* 11 s. 1959. Kr. 2: 50. (Institutionen för Silikatkemisk Forskning. 42.)
219. CORNELL, ELIAS, *Humanistic inquiries into architecture. I—III.* 112 s. 1959. Kr. 17: —. (Avd. Arkitektur. 5.)
220. GRANHOLM, CARL-ADOLF, *Ekonomiska aluminiumprofiler.* 48 s. 1959. Kr. 5: 50. (Avd. Väg- och Vattenbyggnad. Byggnadsteknik. 32.)
221. LUNDÉN, ARNOLD, CHRISTOFFERSON, STINA, AND LODDING, ALEX, *The isotopic effect of lithium ions in countercurrent electromigration in molten lithium bromide and iodide.* 38 s. 1959. Kr. 7: 50. (Avd. Allm. Vetenskaper. 16.)
222. INGEMANSSON, STIG, AND KIHLMAN, TOR, *Sound insulation of frame walls.* 47 s. 1959. Kr. 8: 50. (Avd. Väg- och Vattenbyggnad, Byggnadsteknik. 33.)
223. HÖGLUND, B., AND RADHAKRISHNAN, V., *A radiometer for the hydrogen line.* 25 s. 1959. Kr. 6: 50. (Avd. Elektroteknik. 66.)
224. JAKOBSSON, BENGT, *Torque distribution, power flow, and zero output conditions of epicyclic gear trains.* 55 s. 1960. Kr. 12: —. (Avd. Maskinteknik. 17.)
225. OLVING, SVEN, *Electromagnetic and space charge waves in a sheath helix.* 91 s. 1960. Kr. 17: —. (Avd. Elektroteknik. 67.)
226. STRÖMBLAD, JOHN, *Beschleunigungsverlauf und Gleichgewichtsdrehzahlen einfacher Planetengetriebe nebst Selbsthemmungsversuche.* 80 s. 1960. Kr. 18:—. (Avd. Maskinteknik. 18.)
227. SANDFORD, FOLKE, *Some current problems concerning brick manufacture.* 20 s. 1960. Kr. 5: —. (Avd. Kemi och Kemisk Teknologi. 35.)
228. OLVING, SVEN, *A new method for space charge wave interaction studies. II.* 40 s. 1960. Kr. 8: —. (Avd. Elektroteknik. 68.)
229. GRANHOLM, HJALMAR, *Le problème de Boussinesq.* 15 s. 1960. Kr. 3: 50. (Avd. Väg- och Vattenbyggnad. Byggnadsteknik. 34.)
230. HIBA, MIODRAG et CEDERWALL, KRISTER, *Flambement élastique d'une barre en bois lamellée et clouée avec le module de déplacement du moyen de liaison constant k.* 22 s. 1960. Kr. 5: —. (Avd. Väg- och Vattenbyggnad. Byggnadsteknik. 35.)
231. FLOBERG, LEIF, *The optimum thrust tilling-pad bearing.* 23 s. 1960. Kr. 5: —. (Avd. Maskinteknik. 19.)
232. FLOBERG, LEIF, *The two-groove journal bearing, considering cavitation.* 32 s. 1960. Kr. 6: —. (Avd. Maskinteknik. 20.)
233. HEDVALL, ARVID J., *Heterogeneous catalysis, results and projects for research.* 18 s. 1961. Kr. 5: —. (Avd. Kemi och Kemisk Teknologi. 36.)
234. FLOBERG, LEIF, *Lubrication of two cylindrical surfaces, considering cavitation.* 36 s. 1961. Kr. 10: —. (Avd. Maskinteknik. 21.)
235. FLOBERG, LEIF, *Attitude-eccentricity curves and stability conditions of the infinite journal bearing.* 43 s. 1961. Kr. 11:—. (Avd. Maskinteknik. 22.)
236. BEN-YAIR, M. P., *Thermometric titrations of zinc, cadmium and mercuric salts.* 11 s. 1961. Kr. 3:—. (Avd. Kemi och Kemisk Teknologi. 37.)
237. SANDFORD, F., LILJEGREN, B., and JONSSON, B., *The resistance of bricks towards frost experiments and considerations.* 20 s. 1961. Kr. 5: —. (Avd. Kemi och Kemisk Teknologi. 38.)

Pris kronor 6: —

ELANDERS BOKTRYCKERI AKTIEBOLAG
GÖTEBORG 1961